NASA Contractor Report 159166

Development of a Low-Risk Augmentation System for an Energy-Efficient Transport Having Relaxed Static Stability

T. R. Sizlo, R. A. Berg, and D. L. Gilles

McDonnell Douglas Corporation
Douglas Aircraft Company
Long Beach, California 90846

CONTRACT NAS1-14744
DECEMBER 1979

National Aeronautics and
Space Administration

Langley Research Center
Hampton, Virginia 23665
AC 804 827-3966

NASA CONTRACTOR REPORT 159166

DEVELOPMENT OF A LOW-RISK AUGMENTATION SYSTEM FOR AN ENERGY-EFFICIENT TRANSPORT HAVING RELAXED STATIC STABILITY

December 1979

Prepared Under Contract NAS1-14744

for

National Aeronautics and Space Administration

Aircraft Energy Efficiency Program

Langley Research Center

Hampton, Virginia

by

Douglas Aircraft Company

McDonnell Douglas Corporation

Long Beach, California

FOREWORD

This document presents the results of a contract study performed for the National Aeronautics and Space Administration (NASA) by the Douglas Aircraft Company, McDonnell Douglas Corporation. This work was part of the Energy Efficient Transport (EET) project of the Aircraft Energy Efficiency (ACEE) program. Specifically, the study was one task in the contract — Selected Advanced Aerodynamic and Active Control Concepts Development. The reported study includes the formulation and evaluation of control laws and system architectures with respect to reliability, flying qualities, and aircraft flightpath tracking performance.

ACKNOWLEDGEMENTS

Primary contributions to this study were made by the following at Douglas Aircraft Company. Their effort is gratefully acknowledged.

B. P. Benton — Flying Qualities Analysis

P. L. Jernigan — MBS Programming and Operation

D. L. Jester — Simulation Development and Control Law Verification

J. T. Halbert — Safety Analysis Model and Programming

H. W. Kuehne — Control Law Synthesis

W. L. Mason — RSSAS Performance Analysis and Augmented MBS Testing

G. L. Nichols — Candidate System Architecture Formulation

W. W. Rickard — Aerodynamic Data and Closed-Loop Flying Qualities Analysis

R. E. Schenbeck — Actuation Configuration Formulation

J. T. Slama — RSSAS Performance Analysis

A. B. Taylor — Technical Editorial Assistance

CONTENTS

CONTENTS (Continued)

CONTENTS (Continued)

ILLUSTRATIONS

ILLUSTRATIONS (Continued)

ILLUSTRATIONS (Continued)

ILLUSTRATIONS (Continued)

ILLUSTRATIONS (Continued)

ILLUSTRATIONS (Continued

TABLES

A/D	analog to digital
A_N	aircraft normal acceleration
Augcom	sum of autopilot/pilot and RSSAS elevator commands
A_x	aircraft longitudinal acceleration
C	confidence factor of ability to detect and isolate failures
CAA	British Civil Aviation Authority
CADC	central air data computer
CL, CON	control law
CLF	control law failure flag
CPU	digital computer central processing unit and associated electronics except SCDP
D/A	digital to analog
DETAC	Digital Equipment Technology Analysis Center
DT	simulation integration step size
Elecom	autopilot or pilot elevator command
ELF	artificial elevator load feel
EHV, CV	electrohydraulic valve
FAC	flight augmentation computer
FAR	Federal Aviation Regulations
FL	flap lineator
FMEA	Failure Modes and Effects Analysis
I/O	input/output
JAR	European Joint Aeronautical Regulations
LFE	large flight envelope
LI	left inboard
LO	left outboard
LVDT	linear voltage differential transformer

M	mach number
MAC	mean aerodynamic chord
MTBUR	mean time between unscheduled removals
N_1	engine fan speed (measure of engine thrust)
Q, q	failure probability
R	reliability (probability of not failing)
RI	right inboard
RO	right outboard
RSSAS	relaxed static stability augmentation system
SCDP	signal conditioner/data processor of a digital computer
SCL	selected system control law
S/H	sample and hold
TD	time delay
THRUST	aircraft thrust normalized by $\frac{1}{qS}$ where q is dynamic pressure and S is wing area (dimensionless)
T_2	time to double amplitude
UCL	individual EAC unit control law
VCK	variable camber Krueger leading-edge flap
V_{TRIM}	aircraft initial velocity approach — 73.09 m/s cruise — 237.2 m/s
V_e	equivalent airspeed
$d\gamma/dV$	flight path stability parameter
h	altitude
$\dot{h}$	altitude rate
$j\omega$	imaginary root
n	load factor
u, VIAS, V	aircraft velocity

x	longitudinal displacement from runway threshold
y	lateral displacement from runway centerline
α, AOA	aircraft angle-of-attack
Δ	change in value
$\delta_{A/P}$	autopilot elevator input
δ_{APT}	autopilot stabilizes trim
δ_{PT}	pilot stabilizes trim
δ_{ST}	augmentation stabilizes displacement
δ_{TC}	augmentation trim command
δ_{WO}	trim elevator reachout command
δ_c	augmentation elevator command
δ_e	elevator deflection
$\dot{\delta}_e$	elevator rate
δ_{ep}	pilot elevator input
δ_{es}	series augmentation elevator input
η/α	acceleration sensitivity
γ	flight path angle
λ	failure rate
ω_N	natural frequency
$\omega_{n_{PH}}$	phugoid frequency
$\omega_{n_{SP}}$	short-period frequency
$\dot{\psi}$	aircraft yaw rate

σ	real root (Sections 2 and 3) standard deviation (Section 5)
σ_w	RMS gust velocity
θ	aircraft pitch angle
$\dot{\theta}$	aircraft pitch rate
θ/θ_c	closed-loop resonance
ζ	damping ratio
ζ_{PH}	phugoid damping ratio
ζ_{SP}	short-period damping ratio

SUBSCRIPTS

PH	phugoid
SP	short period
c	command
o	initial conditions

SECTION 1
INTRODUCTION, SUMMARY, AND CONCLUSIONS

Introduction

It has long been recognized that penalties in weight and trim drag, along with the resultant increase in energy usage, are incurred by utilizing the conventional solution to provide adequate longitudinal stability in aircraft. These penalties could be reduced somewhat by incorporating artificial stability through an active control system. However, it is difficult to determine the best combination of aircraft configuration and control system design because the process involves an interrelationship of flying qualities, reliability and safety, and the design and development of the control system. The design must be governed also by certification and cost factors.

Anticipating that a significant gain could be realized in the next generation of aircraft, it was proposed to consolidate into one study the principal considerations that would guide the selection of an acceptable standard. It would seem logical that the flight integrity of the next generation of aircraft would not be allowed to depend completely upon the augmentation system. Accordingly, in the event of any failure of the system, the aircraft should be so configured as to permit the pilot to fly and land safely. In this sense, the augmentation system is described as having "low risk."

The aircraft configuration chosen as the basis for this study is representative of a family of commercial transports which, being the largest, is therefore the greatest user of fuel. The aircraft is the Douglas DC-X-200 — a major derivative of the DC-10 — designed for a nominal seat capacity of 230, with a design range of 5844 km (2620 n mi); the study evaluation mission, typical of a large class of operations, has a block distance of 1389 km (750 n mi). The aircraft has a shortened DC-10 fuselage, with twin engines mounted conventionally under a high-aspect-ratio wing with supercritical sections. An advanced high-lift system is included, consisting of a full-span variable Krueger leading-edge flap and an 80-percent-span, high-extension, two-segment flap. Because preliminary design studies for this aircraft revealed a benefit for relaxed static stability, the configuration was arranged with a design minimum aerodynamic center margin of zero. This baseline aircraft is subsequently referred to as the Energy-Efficient Transport (EET).

The objective of this study is the development of the system required to augment the aircraft's relaxed static stability. This system is referred to as the RSSAS (relaxed static stability augmentation system). The study comprises three distinct elements. The first element includes the definition of the design constraints related to the aircraft flying qualities and reliability/safety criteria. Flying qualities criteria were established and verified primarily with an evaluation of the unaugmented EET on a six-degree-of-freedom motion-base simulator. System reliability requirements are based on the existing capabilities of the DC-10. The safety criterion is an interpretation of the various commercial transport regulatory requirements. The second study element is the system design. From control law synthesis and verification, the RSSAS was architecturally constructed and analyzed at the individual component and system level. In the third element of the study, selected systems were established for evaluation. Using the motion-base simulator, the flying qualities of the augmented aircraft were demonstrated. Quantitative system performance was analyzed and compliance with the established reliability and safety criteria was shown. Finally, the anticipated impact of relaxed static stability on certification of the aircraft was determined.

Summary and Conclusions

An aircraft parametric study which analyzed the effect of decreasing levels of stability provided a prime motivation for the development of an RSSAS for the EET. In this study, the same basic aircraft configuration was sized for three different center-of-gravity operating ranges, with the aerodynamic center margin at the aft limit in these cases being +10, 0, and -14.3 percent of MAC (mean aerodynamic chord). The positive case represents current practice. Fuel usage was then determined for a fixed, average mission length of 750 nautical miles, assuming realistic profiles and loading conditions. As the stability went from the conventional level to neutral, a 2-percent fuel savings was projected. For longer missions, the savings would be greater. The actual stability level to be recommended was developed from the RSSAS flying-qualities evaluation.

The first phase of the flying-qualities evaluation was conducted using the unaugmented aircraft on the Douglas six-degree-of-freedom motion-base simulator. Various center-of-gravity locations, flight conditions, aircraft

configuration changes, and environmental conditions were demonstrated. The results of the solicited pilot ratings established a relationship of flying qualities -- in terms of Cooper-Harper ratings -- to aircraft static margin for the approach condition, and to maneuver margin for the cruise case. These parameters were chosen because of their strong association with center-of-gravity location and relaxed stability. These margins were converted to aerodynamic center margin for determination of fuel savings. To achieve the maximum acceptable mean pilot rating of 6.5, the corresponding aerodynamic center margin was determined to be:

- In the approach phase, an aerodynamic center margin more than -3.1 percent MAC.
- In the nonterminal phase, an aerodynamic center margin more than -4.5 percent MAC.

It was determined, by virtue of the critical tail-sizing requirements, that the nonterminal phase was critical, thus establishing a potential fuel savings for the evaluation mission of 2.8 percent.

The pilot rating results reflect an interpretation of the pilot opinions that weigh the results to the worst mean ratings in the array of tests. This interpretation recognizes that the worst means are probably representative of a significant proportion of the pilot population and that a safety-related requirement should take this factor into consideration. The severity of the interpretation has a significant effect on the allowable stability margin. It is concluded that future studies in this area should carefully evaluate pilot ratings in the stability area of interest.

Using existing Douglas modern control analysis and simulation programs, augmentation control laws were developed, employing an implicit-model-following technique with the conventionally stable DC-10 aircraft as the flying-qualities model. The neutrally stable EET 40 percent MAC center-of-gravity configuration was augmented with several different control laws using various combinations of aircraft dynamic feedbacks representing existing DC-10 sensor arrays. The static margin of the EET configuration was approximately zero while the static margin of the DC-10 model was about 20 percent MAC. With these multiple control laws, it was shown that:

- Performance of the DC-10 "model" was duplicated by the augmented EET.
- Control law redundancy provided a technique to increase the system functional availability.

A flying-qualities evaluation of three of these control laws ($\theta\dot{\theta}u\alpha, \theta\dot{\theta}\alpha, \alpha$) was performed on the motion-base simulator. The pilot ratings achieved with the augmented EET showed a significant flying-qualities improvement, with the augmented 40-percent MAC center-of-gravity, neutrally stable aircraft duplicating approximately the ratings of the unaugmented 25-percent MAC center-of-gravity EET. The augmentation system was additionally evaluated for a negative statically stable center-of-gravity location, compensation of the pitching moment characteristics resulting from thrust changes, and failure-reversion configurations. It was successfully demonstrated that:

- The proposed control laws provided equally satisfactory augmentation for neutral (design point) and negative static stability, and
- Thrust pitching moments were adequately controlled for all flight maneuvers.

The total RSSAS functional design was accomplished, including definition of the major system elements: the sensors, computers, actuation, and interfaces. Then, based upon the Douglas interpretation of the regulatory reliability and safety requirements, plus the Douglas requirements, candidate architectures were formulated and evaluated. Two augmentation system configurations were selected which differ only in the computer redundancy. One has two computers; the other has three computers. Both use existing aircraft sensors (three vertical gyros, two air-data computers, and two angle-of-attack transducers), and both achieve control through the two inboard elevator actuators which are modified to accept dual-series augmentation commands. The computers are either dual- or triple-redundant, depending upon the dispatch-inoperable capability desired.

A complete reliability analysis was performed on the selected systems. The functional reliability was calculated for the normal system configurations and for the worst-case dispatch-inoperable configurations. Significantly, compliance with the regulatory requirements was verified for both the dual- and triple-redundant system configurations. For the system requirements that the EET RSSAS must meet, compliance was interpreted to mandate a probability

of function loss of less than 1×10^{-5} per flight hour. Also, the total EET flight control system with the RSSAS was found to equal the established reliability standard of the DC-10 flight control system.

Finally, to provide some insight as to the impact of incorporating an RSSAS into a commercial transport, the pertinent FAA regulations were listed, a validation plan proposed, and a typical airframe manufacturer's cost (including RSSAS hardware) estimated.

SECTION 2
AIRCRAFT CONFIGURATION, CRITERIA, FLYING QUALITIES, AND EVALUATION

2.1 Stability and Control Considerations

Relaxed static stability offers some of the more significant benefits that may be derived from active control technology. For a transport aircraft, the primary benefit is reduced aircraft drag and weight for a given payload and mission, arising from a reduction in tail volume.

Relaxed static stability is accomplished through a more aft center-of-gravity location and/or a smaller horizontal tail size. The reduced stability results from the decreased aerodynamic restoring-moment with respect to angle of attack. This alteration of static stability naturally has a substantial impact on the aircraft longitudinal dynamics, affecting both the short-period and phugoid modes. As the inherent stability is reduced, flying qualities tend to degrade. Therefore the deficiencies, both in static and dynamic stability, must be compensated for by a relaxed static stability augmentation system (RSSAS). While, for the next generation of commercial transports, it might be possible to devise an RSSAS reliable enough to maintain the flight integrity of an inherently unstable aircraft, such a system was not considered in the present study. The aircraft that was considered would allow the pilot to fly and land safely if the system failed. The study did, in fact, conclude that a negatively stable aircraft could provide these qualities.

Basic design considerations influencing wing location, center-of-gravity range and limits, and horizontal tail size are affected by the requirements of both augmented and unaugmented modes of flight. The considerations germane to this study are discussed below.

Tail area requirements for the forward center-of-gravity limit typically have been set by trim capability or by the degree of control required to develop maximum lift in the landing configuration. The critical condition depends on the type of control system selected, i.e., separate trim and control surfaces, or a single surface providing both control and trim. Aft center-of-gravity limit requirements have generally been set by minimum levels of static longitudinal stability. For the active-control relaxed stability design, the horizontal tail area may be set

by one or more of the following: the landing case, the pitching moment required for takeoff rotation at forward center-of-gravity locations, the reduced level of stability, the pitching acceleration required for control in the presence of gusts, or high angles of attack at aft center-of-gravity locations. These points are illustrated in Figure 2-1, which shows the typical active-controlled aircraft rebalanced with a farther-aft center-of-gravity range and a smaller horizontal tail. The dashed lines in the figure show requirements not yet critical for the reduced tail size. Further reduction and a more aft rebalancing may emphasize these requirements. Other requirements may also become critical. An example from the nonflight mode, where aerodynamic controls become ineffective, is the requirement for ground stability and control. This condition determines criteria for nose-wheel steering and for tipback stability, and in turn leads to requirements determining location of the main landing gear. The landing gear location is closely interrelated with the aerodynamic and structural design of the wing, unless the penalties associated with a fuselage-mounted gear are accepted.

The typical variation of airplane drag with center-of-gravity position is illustrated in Figure 2-2. This variation results from an interchange between the tail-induced drag, the drag component of the tail lift vector, and the wing-induced/compressibility drag characteristics (i.e., the basic components of the trim drag formulation). As the center of gravity is moved aft, the tail load required to trim (download) is reduced until it finally reaches zero and then becomes an upload. The trim drag is not necessarily a minimum at the point where the tail load goes to zero, since an upload on the tail will help the wing-induced/compressibility drag, thus continuing to reduce the trim drag until the tail contribution begins to dominate. The exact center-of-gravity location for minimum trim drag is largely dependent upon the aircraft configuration.

Three areas of interest must be examined to determine the acceptable longitudinal stability characteristics of the unaugmented aircraft. The first is where the stability is measured by "static margin." Static margin relates the neutral point to the center of gravity. The neutral point is the center-of-gravity location at which the static stability is neutral and the elevator deflection per knot of speed is zero. All three longitudinal degrees of freedom — speed, attitude, and angle of attack — are involved.

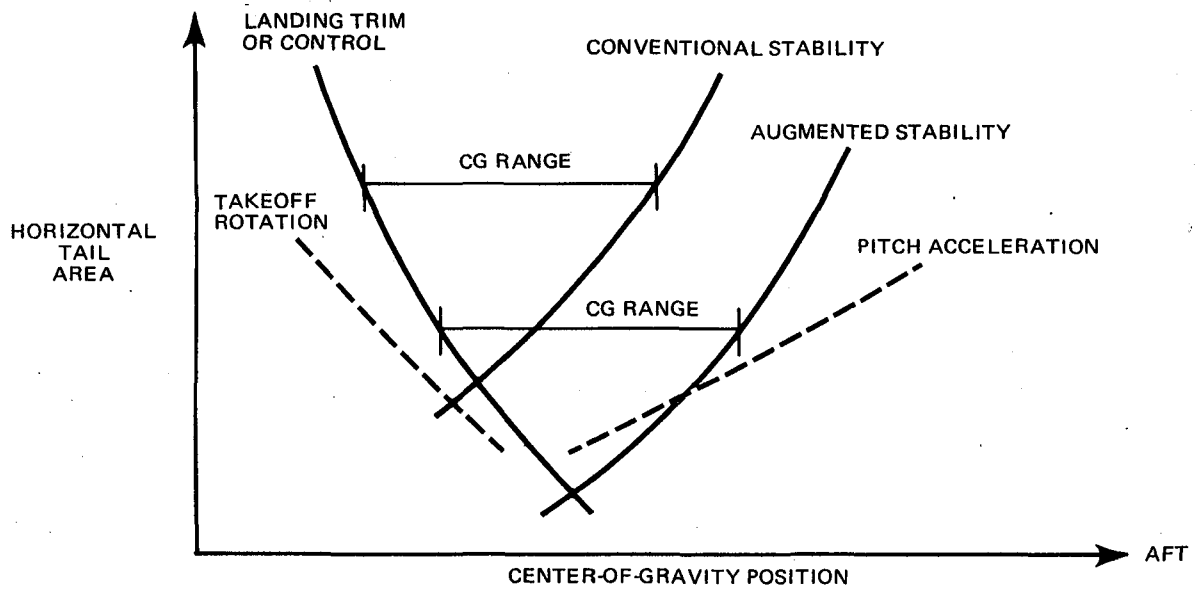

FIGURE 2-1. HORIZONTAL TAIL AREA REQUIREMENTS

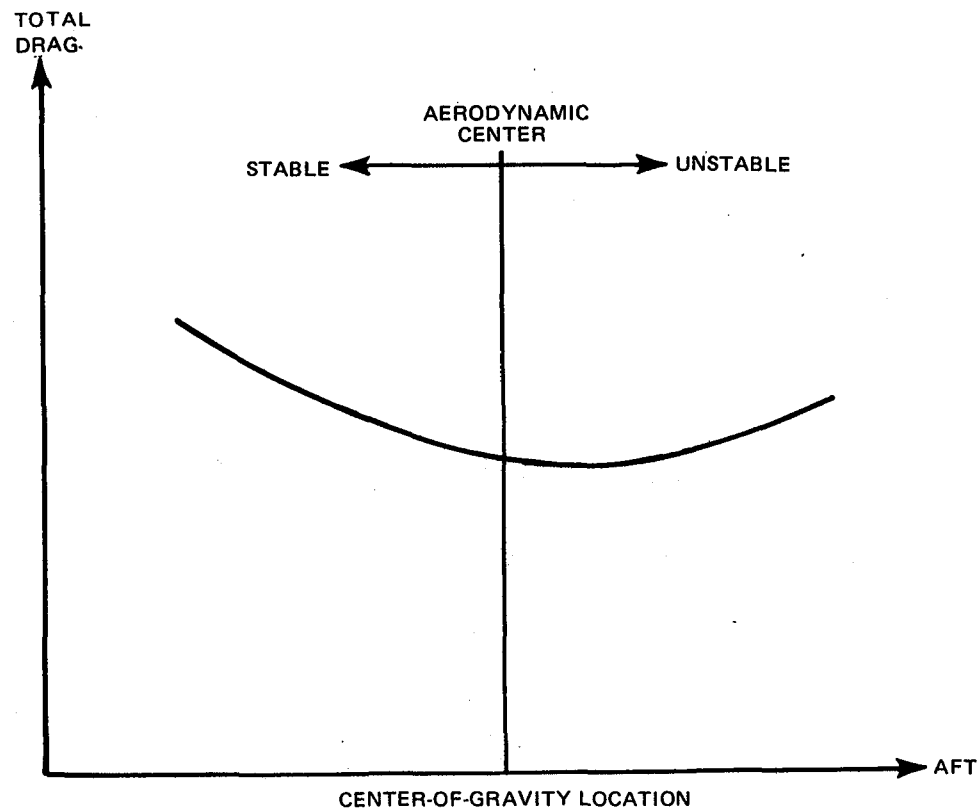

FIGURE 2-2. TRIMMED DRAG VARIATION WITH CENTER-OF-GRAVITY LOCATION

This form of stability is of importance in determining pilot opinion of flying qualities. The second area of interest is the "aerodynamic center." The aerodynamic center is the point about which pitching moments are invariant with angle of attack. It is not the same as the neutral point. No other degrees of freedom are involved; it is a single degree-of-freedom parameter. There is no commonly accepted term describing the distance between the center of gravity and the aerodynamic center, but in this report, the term "aerodynamic center margin" will be used. Similarly, the term "aerodynamic center stability" will be used when referring to this type of stability. It is this area of stability which is of importance in determining fuel savings due to the relaxed-static stability concept. The third type of stability of interest in this study is "maneuvering stability," measured by elevator angle per load factor. Like aerodynamic center stability, maneuvering stability is determined at constant speed. The difference between the two arises from pitch damping effects, which cause the maneuver point to fall aft of the aerodynamic center. This type of stability is of particular interest for flight conditions in which load factor changes provide important cues to the pilot.

2.2 Aircraft Configuation Studies and Baseline Definition

2.2.1 Initial Investigations. - The explorations giving rise to the aircraft baseline for this study centered on a major derivative of the DC-10. The guideline for this derivative defined a nominal seat capacity of 230, with a design range of 5844 km (2620 n.mi.). The range capacity encompasses a fleet class which has the largest number of commercial transports. This class is therefore the greatest user of fuel.

The aircraft mission design requirements are shown in Table 2-1. For the class of aircraft described, the most representative operation has a block distance of 1389 km (750 n.mi.), and this was chosen for the study evaluation. The mission rules are defined in Table 2-2.

The aircraft family which resulted from the guidelines and requirements was generically known as the DC-X-200, subsequently referred to in this report as the Energy Efficient Transport (EET). The family is characterized by a shortened DC-10 fuselage, and twin engines mounted conventionally under a high-aspect-ratio wing with supercritical sections.

TABLE 2-1
AIRCRAFT MISSION REQUIREMENTS

Payload	21,390 kilograms (47,150 pounds) (230 passengers and baggage)
Range	5844 kilometers (2620 nautical miles) equivalent still air distance
Initial Cruise Altitude	10,363 meters (34,000 feet)
Initial Cruise Mach No.	0.80
Approach Speed	76 m/s (148 knots)

TABLE 2-2
EVALUATION MISSION PROFILE

Flight Segment	Requirements
Taxi Out	5 minutes at taxi thrust
Takeoff	Climb to 457 meters (1500 feet)
Climb	Maximum climb thrust, long-range climb schedule to initial cruise altitude
Cruise	Constant Mach number, step cruise technique (31,000, 35,000, 39,000 feet) 1389-kilometer (750-nautical-mile) mission at best constant odd altitude
Descent	Employ long-range speed schedule to sea level
Approach	4 minutes at approach thrust
Taxi in	3 minutes at taxi thrust

Reserve fuel based on FAR 121.639 as follows:

Climb from sea level to 9144 meters (30,000 feet) using maximum-climb thrust and long-range speed schedule, cruise at 9144 meters (30,000 feet) at 99-percent maximum specific range, descent to sea level for total distance to alternate of 370.4 kilometers (200 nautical miles), and cruise for 45 minutes at 9144 meters (30,000 feet) at 99-percent maximum specific range.

Prior to the definition of the EET baseline aircraft, a parametric study was conducted to assess the configuration characteristics of EET family aircraft as a function of aerodynamic center margin. Three aircraft of this family were sized and configured to reflect an aerodynamic center margin at aft center of gravity of 10 percent, 0 percent, and -14.3 percent. The 10 percent margin aircraft represented an aircraft of currently conventional levels of natural longitudinal stability, for example, the DC-10. The 0 percent margin aircraft, having neutral stability at the aft limit, represented a class which the current pace of technology development might make acceptable for the next generation. The -14.3 percent margin aircraft represented an aircraft with natural instability, the margin value being an arbitrary product of other design requirements. Each parametric design was checked for realistic design conditions and layout. Payload arrangement and fuel usage effects on the flight center of gravity were included in the definition of the mission aircraft.

The characteristics of the three configurations are shown in Table 2-3, together with the block fuel required for the evaluation mission defined in Table 2-1.

The fuel savings due to relaxed static stability relative to the inherently stable aircraft have been plotted as a function of aerodynamic center margin in Figure 2-3. The neutrally stable aircraft would save 2 percent of fuel. The inherently unstable aircraft would save just over 4 percent. For missions longer than the evaluation mission, the fuel savings would be greater.

The data shown in Figure 2-3 indicate that further fuel savings will accrue with an even more unstable configuration. In order to pursue such savings, a number of design conditions would have to be altered, and a new family of configurations would emerge. For example, as explained in Paragraph 2.1, difficulties are apparent with the more unstable aircraft in the installation of a wing-mounted landing gear. A different wing having a thicker airfoil with more conventional sections might be justified to house the required gear. A lower design cruise Mach number, allowing a wing with less sweep or more thickness, might also help if market requirements permitted. No such changes were considered in this report.

TABLE 2-3
COMPARISON OF PARAMETRIC CONFIGURATIONS

AERODYNAMIC CENTER MARGIN AT AFT CG LIMIT	+10 PERCENT	+0 PERCENT	−14.3 PERCENT
ENGINE SLST RATING KN (LB)	209.73 (45,950)	200.17 (45,000)	195.68 (43,990)
PASSENGERS	230	230	230
PAYLOAD, KG (LB)	21,387 (47,150)	21,387 (47,150)	21,387 (47,150)
RANGE, KM (N MI)	4,854 (2,621)	4,854 (2,621)	4,854 (2,621)
CRUISE MACH	0.80	0.80	0.80
ASPECT RATIO	10.85	10.85	10.85
TRAPEZOIDAL WING AREA M^2 (SQ FT)	213.2 (2,295)	208.1 (2,240)	201.1 (2,165)
HORIZONTAL TAIL AREA M^2 (SQ FT)	75.5 (813)	63.5 (684)	49.0 (527)
MAX TAKEOFF WEIGHT KG (LB)	135,669 (299,100)	133,809 (295,000)	131,768 (290,500)
OPERATING EMPTY WEIGHT KG (LB)	80,256 (176,930)	79,239 (174,690)	77,997 (171,950)
BLOCK FUEL FOR 1,389 KM (750 N MI) MISSION, KG (LB)	8,447 (18,623)	8,276 (18,245)	8,096 (17,849)

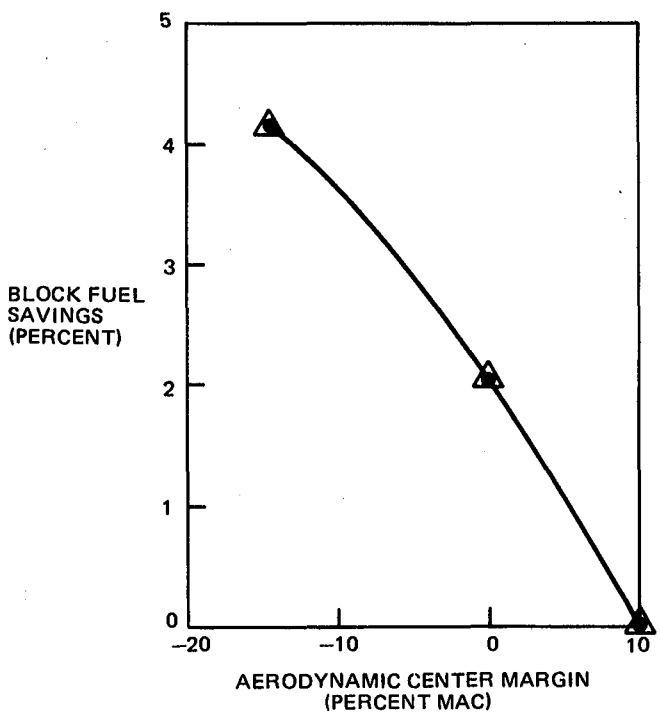

FIGURE 2-3. FUEL SAVINGS FROM PARAMETRIC STUDY

After consideration of the initial studies, it was determined that the EET baseline should be configured with zero aerodynamic center margin until any recommendation to the contrary could be made.

2.2.2 Baseline Definition. - The EET baseline aircraft is shown in Figure 2-4, with its principal geometry summarized in the tabular inset of the figure. The aircraft conformed to the family characteristics previously described, but is the product of further study and refinement. The wing includes an advanced high lift system consisting of a full-span variable Krueger leading edge flap and an 80 percent span, high-extension, two-segment trailing-edge flap.

2.3 Development of Aerodynamic Data

Aerodynamic data for the study were developed in two phases. In the first phase, data were generated and put in the form of linear small-perturbation equations of motion for application to control system design. In the second phase, more complete large-flight-envelope (LFE) characteristics were developed for use in programming the motion-base simulator. The LFE data were presented as functions of such parameters as Mach number, altitude, and angle of attack. The methods used for both forms of estimation were normal for preliminary design, e.g., DATCOM procedures and references to DC-10, limited DC-X-200 wind tunnel data, and other empirical data. A comparison was made of the LFE with the equations of motion previously written and only negligible differences were noted. The LFE data were then programmed on the motion-base simulator host computer. Concurrently, a second set of equations of motion were developed for the control system design effort using the LFE data in a linearized form.

The aircraft mass used for the bulk of the study was 115,666 kg (255,000 lb). This is representative of high weights in cruise. As a result of past experience and judgment, two flight conditions were selected for use in the design effort: a low-speed (72 m/s (140-kn) landing approach case, and a cruise flight case. It may be noted that the approach and cruise flight phases were subsequently judged to be of critical interest in the piloted simulations (see Paragraph 3.1). A description of the design cases is tabulated below:

Landing		Cruise	
V_e	= 72 m/s (140 kn)	M	= 0.8
Sea Level		h	= 10,668 m (35,000 ft)
Center-of-Gravity Location	= 40 percent MAC	Center-of-Gravity Location	= 40 percent MAC
ω_{nSP}	= 0.509 rad/s	ω_{nSP}	= 0.967 rad/s
ζ_{SP}	= 0.969	ζ_{SP}	= 0.533
ω_{nPH}	= 0.051 rad/s	ω_{nPH}	= 0.226 rad/s
ζ_{PH}	= -0.092	ζ_{PH}	= 0.250
n/α	= 3.79 g/rad	n/α	= 11.82 g/rad
$d\gamma/dV$	= 0.0088 rad/m/s (0.260 deg/kn)	$d\gamma/dV$	= 0.0020 rad/m/s (0.059 deg/kn)

Data for other conditions were generated for use in the flying qualities analysis and for motion-base simulation. Fifteen combinations of five center-of-gravity locations (25-, 35-, 40-, 45-, and 50-percent MAC) and three horizontal tail sizes (100, 85, and 70 percent of basic) were selected. The 100 percent of basic tail area size corresponds to the baseline configuration.

While both center-of-gravity location and horizontal tail size have a direct effect on the static stability of the aircraft, variations in tail size were included in the test matrix with the idea of identifying problems that might be attributed to deficient pitch control at different stability levels. However, tail size has a significant effect also on pitch damping, thereby complicating the task of identifying potential control problems.

Linearized equations of motion were developed from the LFE data for the combinations of center-of-gravity and tail-size cases at the cruise flight condition and a normal landing approach condition [V_e = 76 m/s (148 kn)]. The effect of center-of-gravity location and tail size on aircraft stability for the landing approach case is shown in Figure 2-5a. A similar presentation for the cruise condition is given in Figure 2-5b, except that maneuver margin is used for the stability metric. A tabulation of the flying qualities characteristics of these 30 cases is presented in Tables 2-4 and 2-5. Root locus diagrams for variations of center-of-gravity location are presented for the three tail sizes in Figures 2-6, 2-7, and 2-8 for the landing approach condition. Similar presentations are made in Figures 2-9, 2-10, and 2-11 for the cruise condition.

CHARACTERISTICS DATA			
ITEM	WING TRAPEZOIDAL	HORIZONTAL TAIL	VERTICAL TAIL
AREA, SQ. FT	1790	641	550
ASPECT RATIO	12.0	3.8	1.6
TAPER RATIO	0.35	0.35	0.35
SWEEP, °C/4	33°	30°	35°
DIHEDRAL, C/4	4°	+10°	
TAIL VOLUME	~	1.60	.118

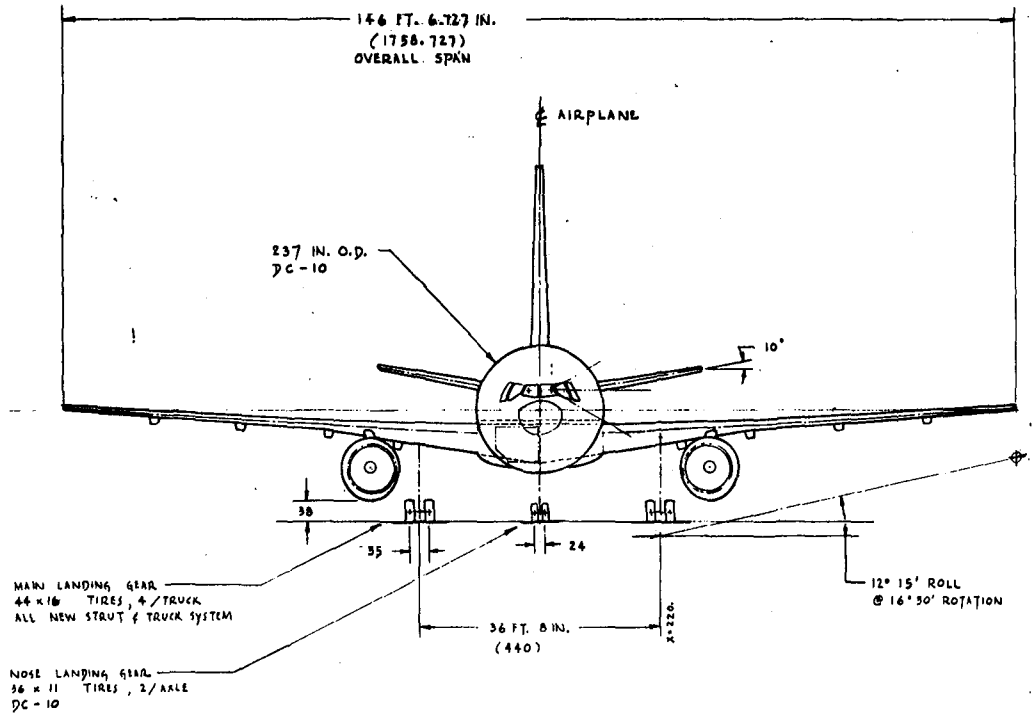

FIGURE 2-4. GENERAL ARRANGEMENT – EET BASELINE

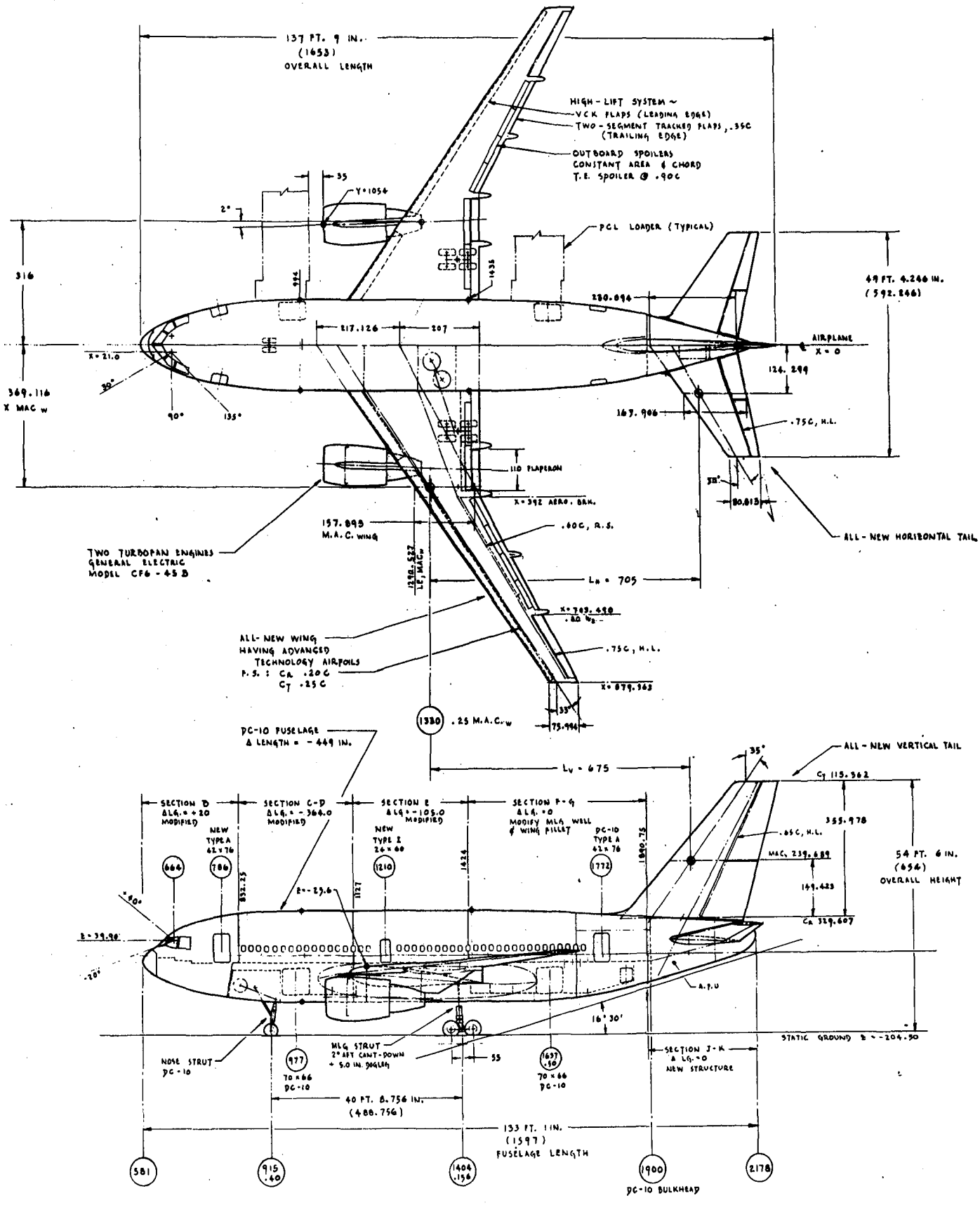

FIGURE 2-4. GENERAL ARRANGEMENT – EET BASELINE (CONTINUED)

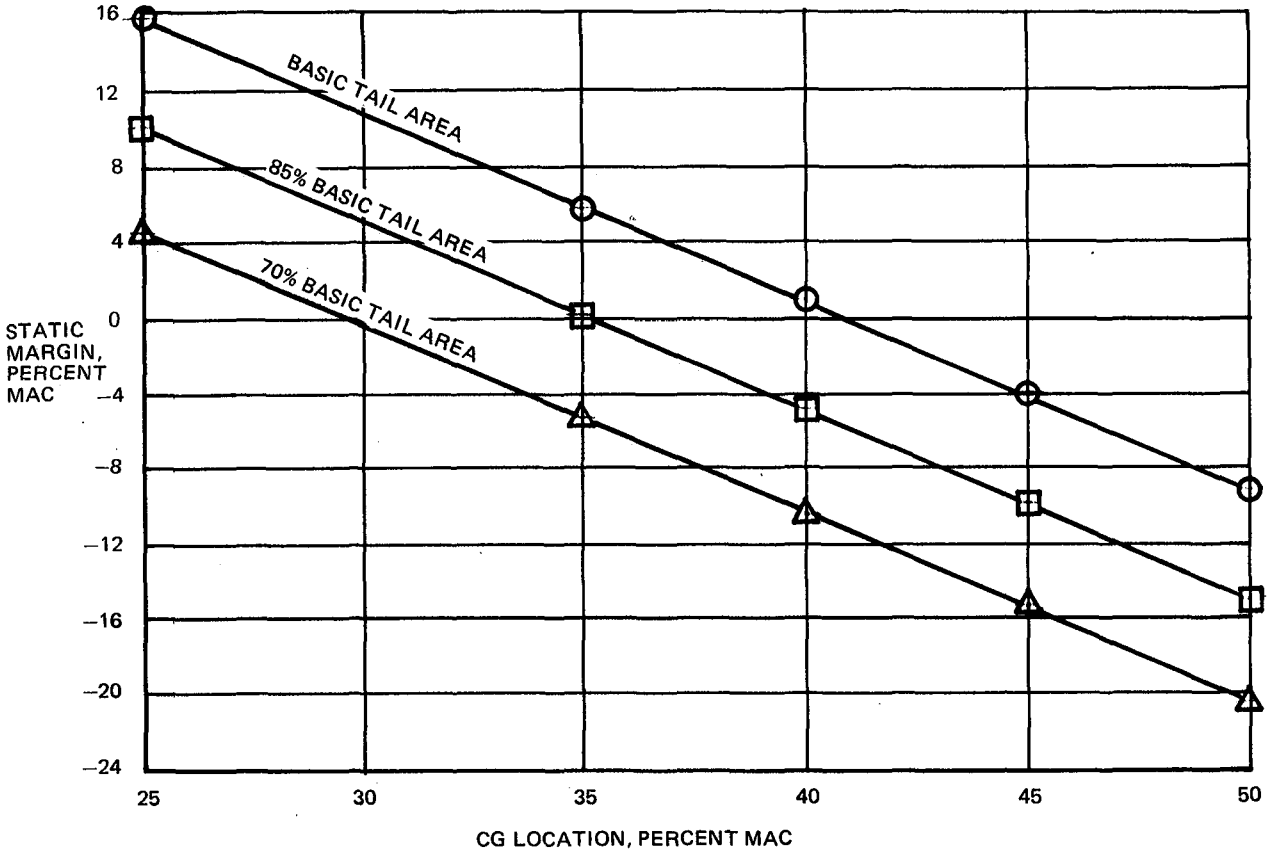

FIGURE 2-5a. VARIATION OF STATIC MARGIN WITH CG LOCATION AND TAIL AREA – LANDING APPROACH

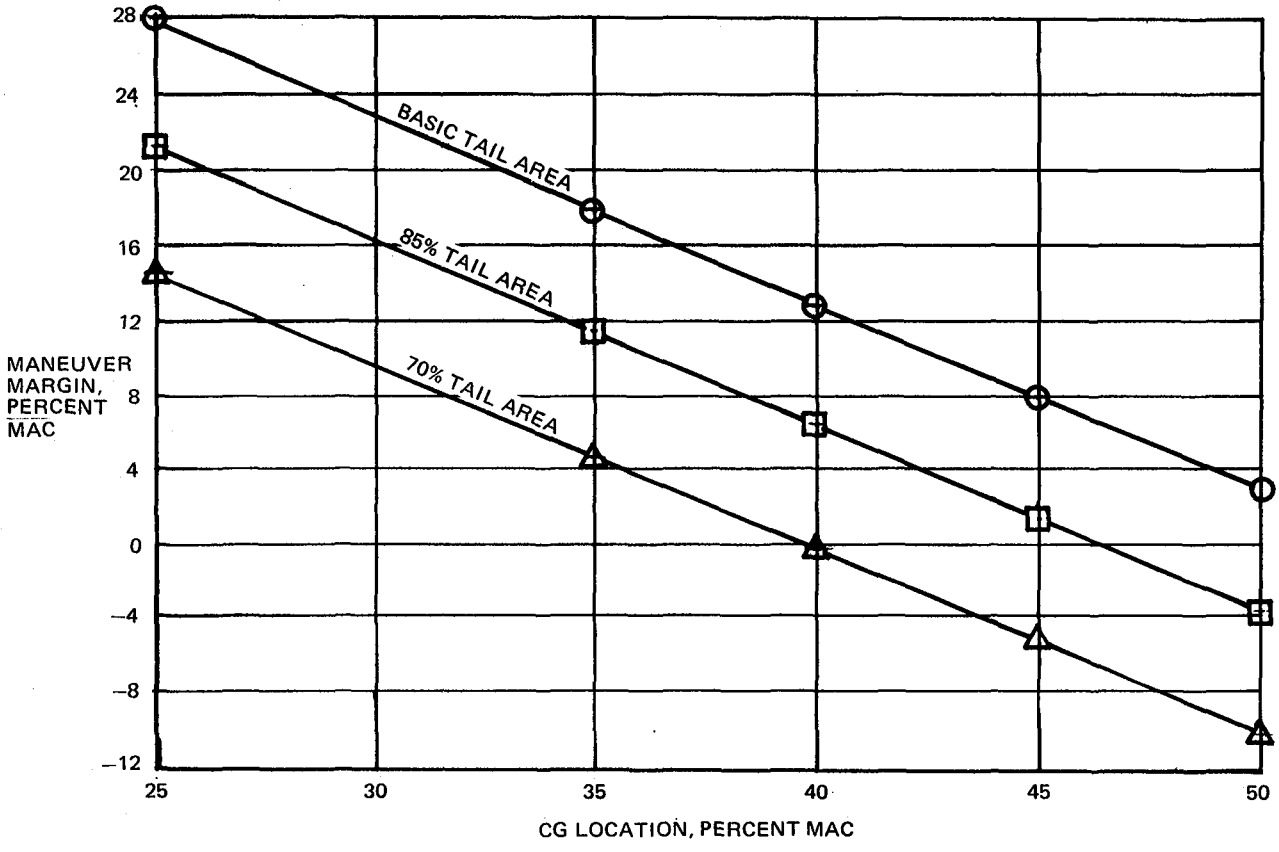

FIGURE 2-5b. VARIATION OF MANEUVER MARGIN WITH CG LOCATION AND TAIL AREA – CRUISE

TABLE 2-4

SUMMARY OF FLYING QUALITIES CHARACTERISTICS IN LANDING APPROACH
– UNAUGMENTED AIRCRAFT –

CENTER-OF-GRAVITY LOCATION	TAIL AREA	$\omega_{n_{SP}}$	ζ_{SP}	$\omega_{n_{PH}}$	ζ_{PH}	T_2	STATIC MARGIN	n/α	$d\gamma/dV$
(% MAC)	(% OF BASIC)	(RAD/S)		(RAD/S)		(SEC)	(% MAC)	(g/RAD)	(DEG/KN)
25	100	0.849	0.641	0.146	-0.028	—	15.8	4.02	0.178
35	100	0.657	0.813	0.114	-0.065	—	5.8	4.11	0.174
40	100	0.524	0.992	0.051	-0.007	—	0.8	4.16	0.172
45	100	—	—	0.191	0.695	5.41	-4.2	4.21	0.170
50	100	—	—	0.202	0.460	3.25	-9.2	4.25	0.168
25	85	0.722	0.705	0.137	-0.052	—	10.2	4.02	0.178
35	85	—	—	0.030	0.090	—	0.2	4.11	0.174
40	85	—	—	0.189	0.603	4.77	-4.8	4.16	0.172
45	85	—	—	0.198	0.407	2.96	-9.8	4.21	0.170
50	85	—	—	0.198	0.311	2.17	-14.8	4.25	0.168
25	70	0.568	0.833	0.114	-0.085	—	4.6	4.02	0.178
35	70	—	—	0.187	0.510	4.12	-5.4	4.11	0.174
40	70	—	—	0.193	0.355	2.65	-10.4	4.16	0.172
45	70	—	—	0.193	0.277	1.99	-15.4	4.21	0.170
50	70	—	—	0.192	0.231	1.60	-20.4	4.25	0.168

TABLE 2-5

SUMMARY OF FLYING QUALITIES CHARACTERISTICS IN CRUISE FLIGHT
– UNAUGMENTED AIRCRAFT –

CENTER-OF-GRAVITY LOCATION	TAIL AREA	ω_{nSP}	ζ_{SP}	ω_{nPH}	ζ_{PH}	MANEUVER MARGIN	AERO CENTER	n/α
(% MAC)	(% OF BASIC)	(RAD/S)		(RAD/S)		(% MAC)	(% MAC)	(g/RAD)
25	100	1.509	0.377	0.156	0.192	27.8	49.3	10.91
35	100	1.181	0.455	0.190	0.229	17.8	49.3	11.14
40	100	0.967	0.533	0.226	0.250	12.8	49.3	11.27
45	100	0.676	0.741	0.315	0.199	7.8	49.3	11.40
50	100	—	—	0.392	-0.175	2.8	49.3	11.52
25	85	1.303	0.397	0.160	0.191	21.3	43.3	10.90
35	85	0.899	0.536	0.218	0.232	11.3	43.3	11.14
40	85	0.600	0.807	0.316	0.128	6.3	43.3	11.27
45	85	—	—	0.374	-0.276	1.3	43.3	11.39
50	85	—	—	0.384	-0.579	-3.7	43.3	11.52
25	70	1.055	0.441	0.168	0.189	14.5	36.8	10.90
35	70	0.526	0.909	0.310	0.017	4.5	36.8	11.14
40	70	—	—	0.348	-0.404	-0.5	36.8	11.27
45	70	—	—	0.353	-0.718	-5.5	36.8	11.39
50	70	—	—	0.351	-0.989	-10.5	36.8	11.53

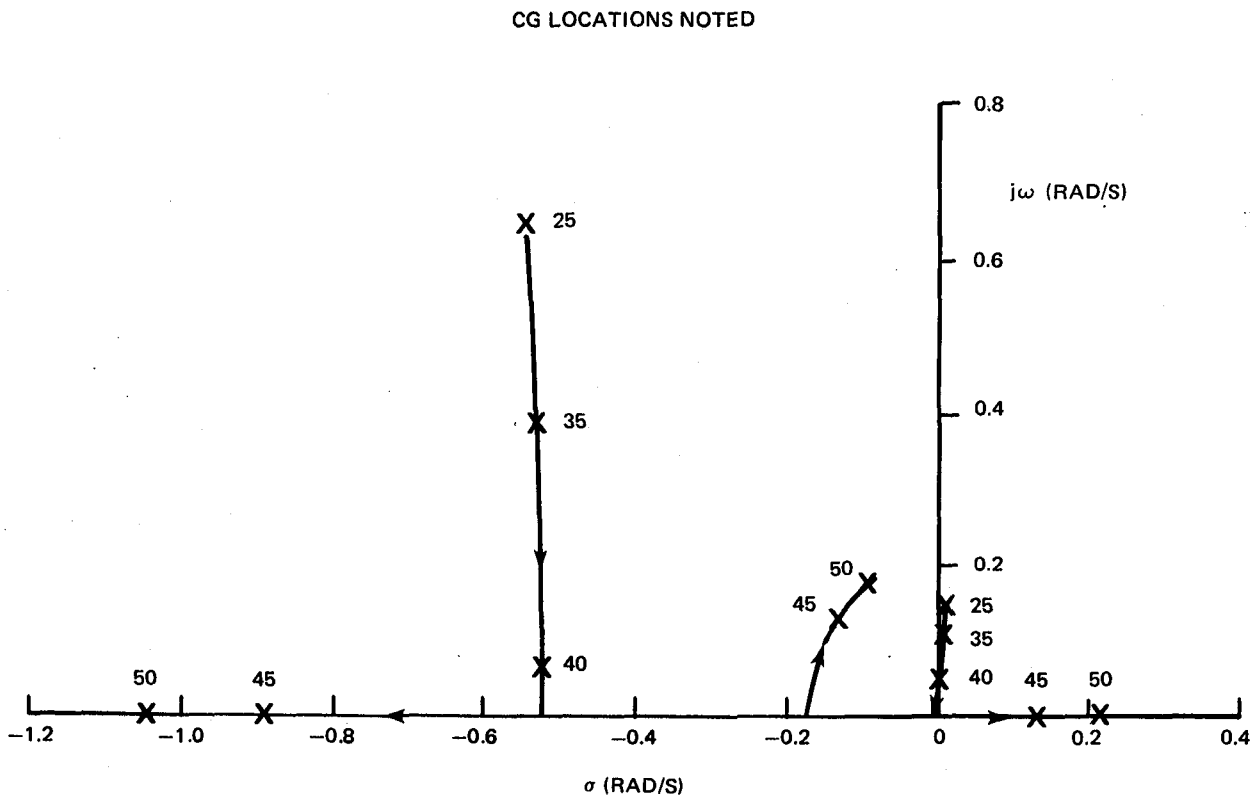

FIGURE 2-6. LOCUS OF ROOTS AS CG IS MOVED AFT, IN LANDING APPROACH – BASIC TAIL AREA

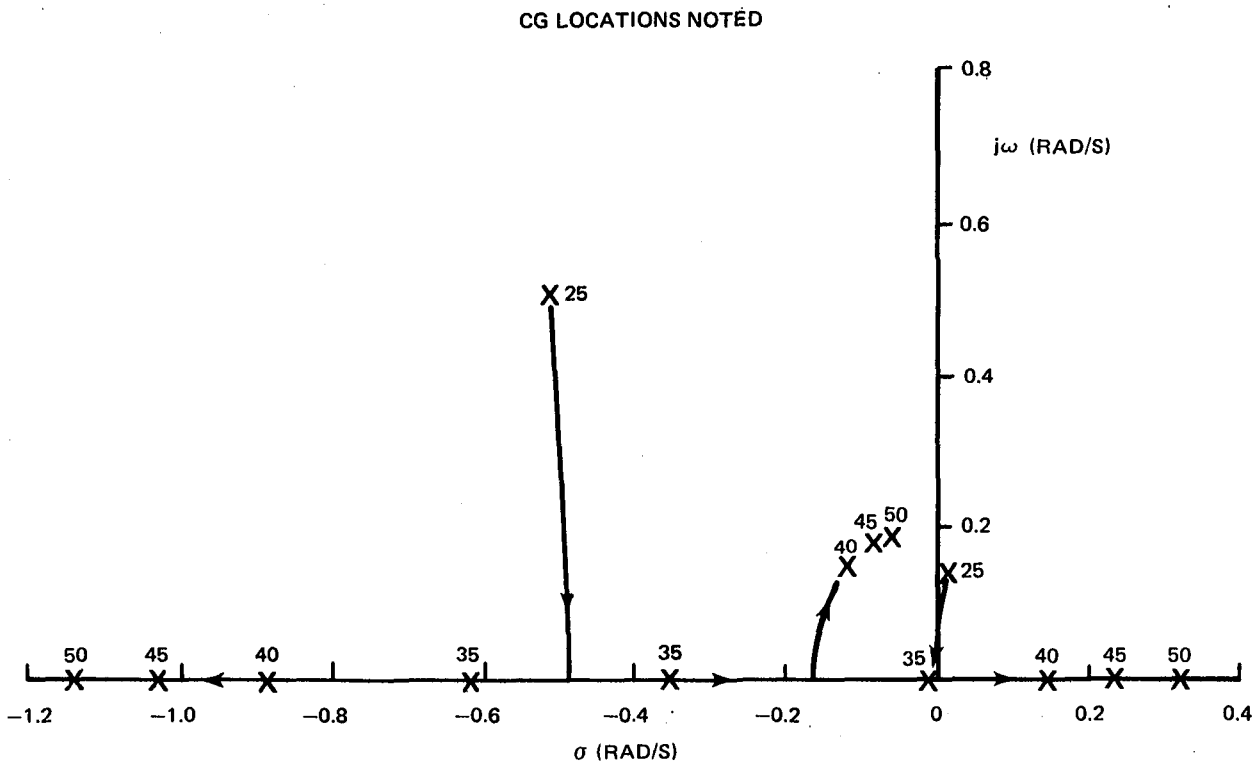

FIGURE 2-7. LOCUS OF ROOTS AS CG IS MOVED AFT, IN LANDING APPROACH – 85 PERCENT OF BASIC TAIL AREA

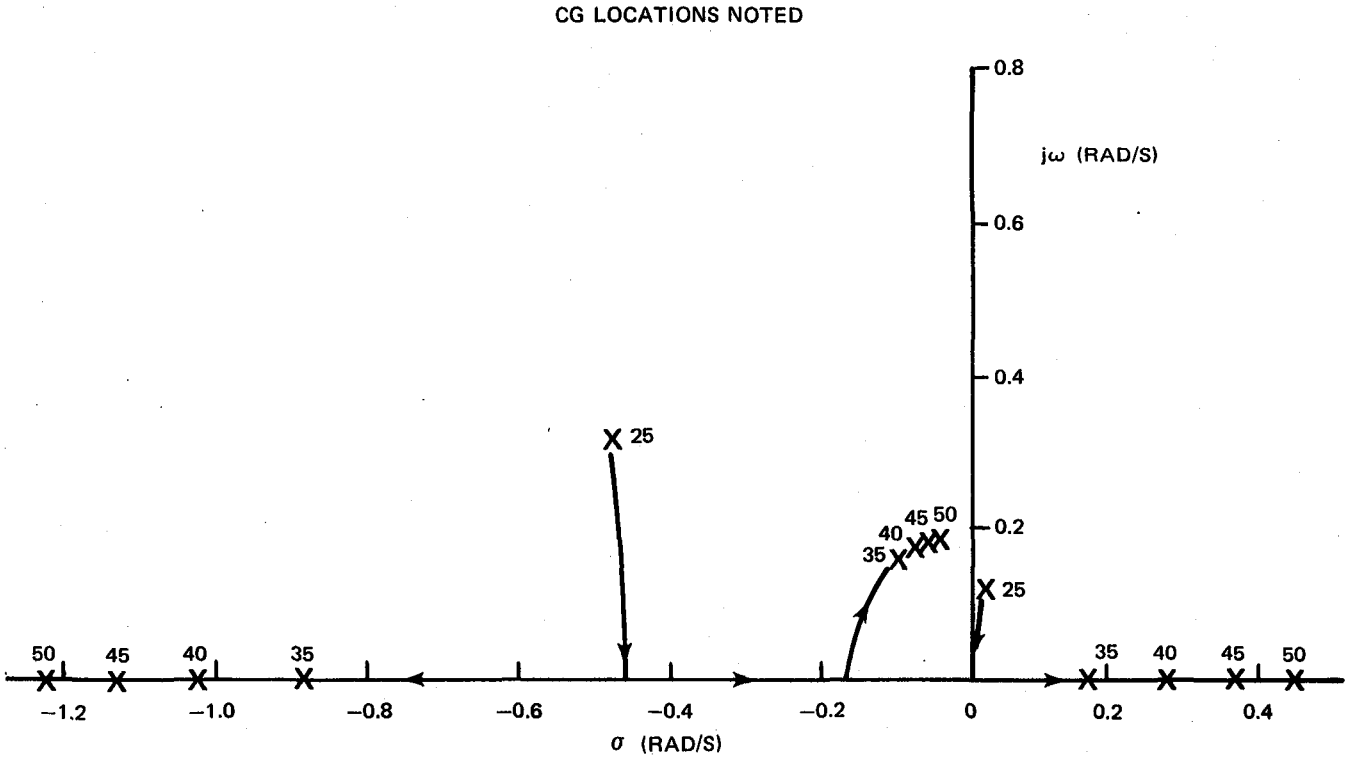

FIGURE 2-8. LOCUS OF ROOTS AS CG IS MOVED AFT IN LANDING APPROACH – 70 PERCENT OF BASIC TAIL AREA

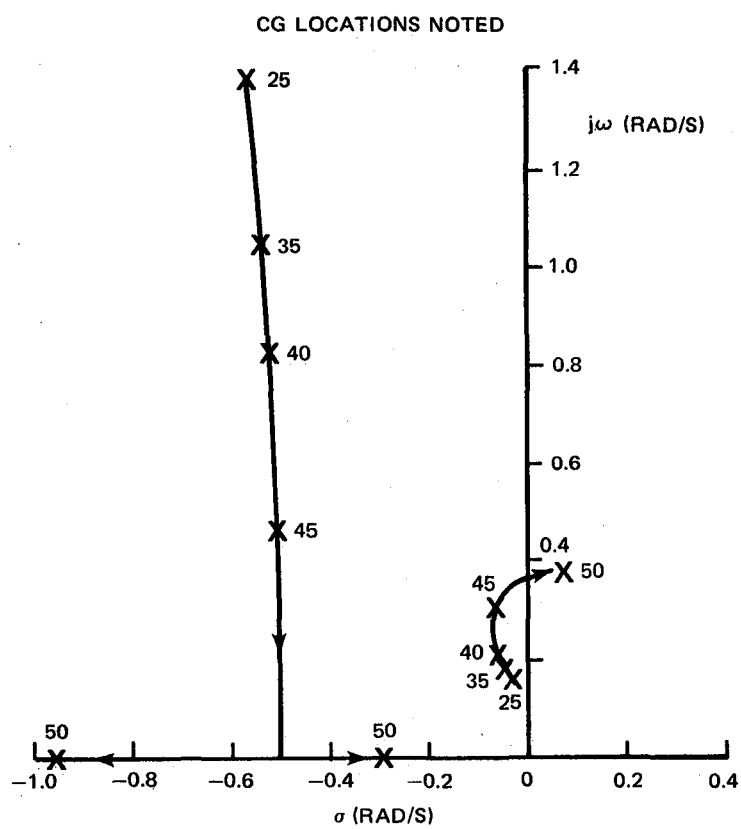

FIGURE 2-9. LOCUS OF ROOTS AS CG IS MOVED AFT IN CRUISE FLIGHT – BASIC TAIL AREA

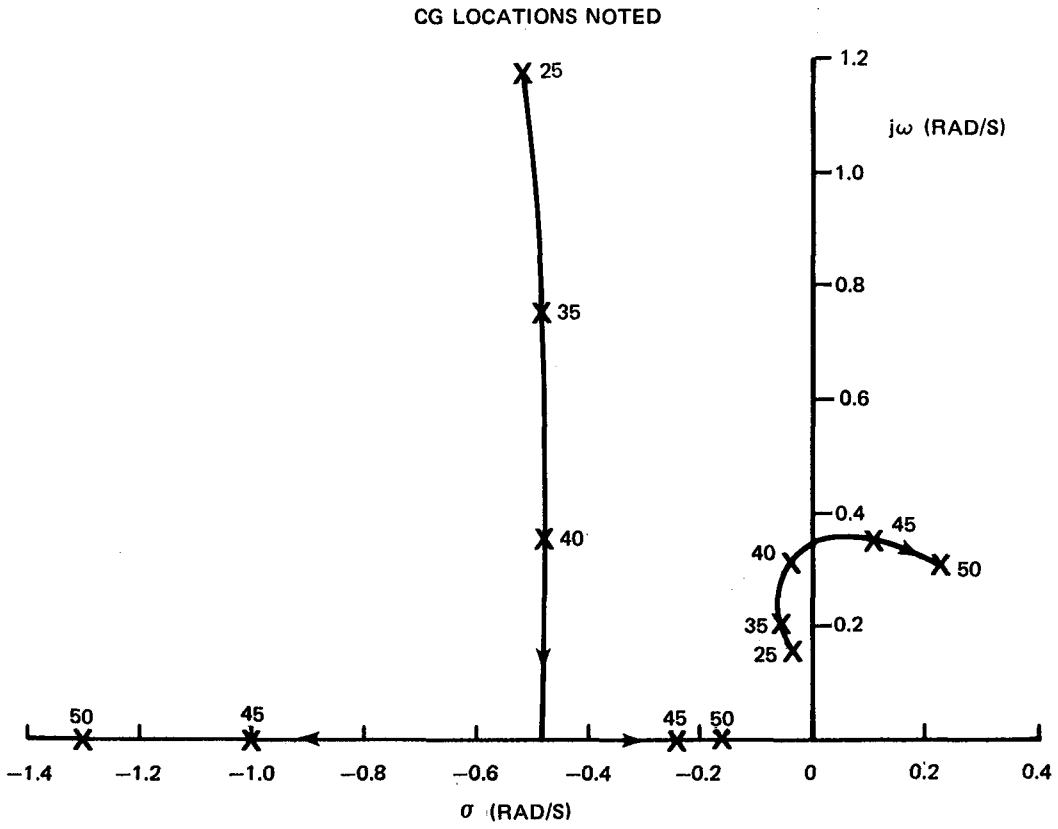

FIGURE 2-10. LOCUS OF ROOTS AS CG IS MOVED AFT, IN CRUISE FLIGHT – 85 PERCENT OF BASIC TAIL AREA

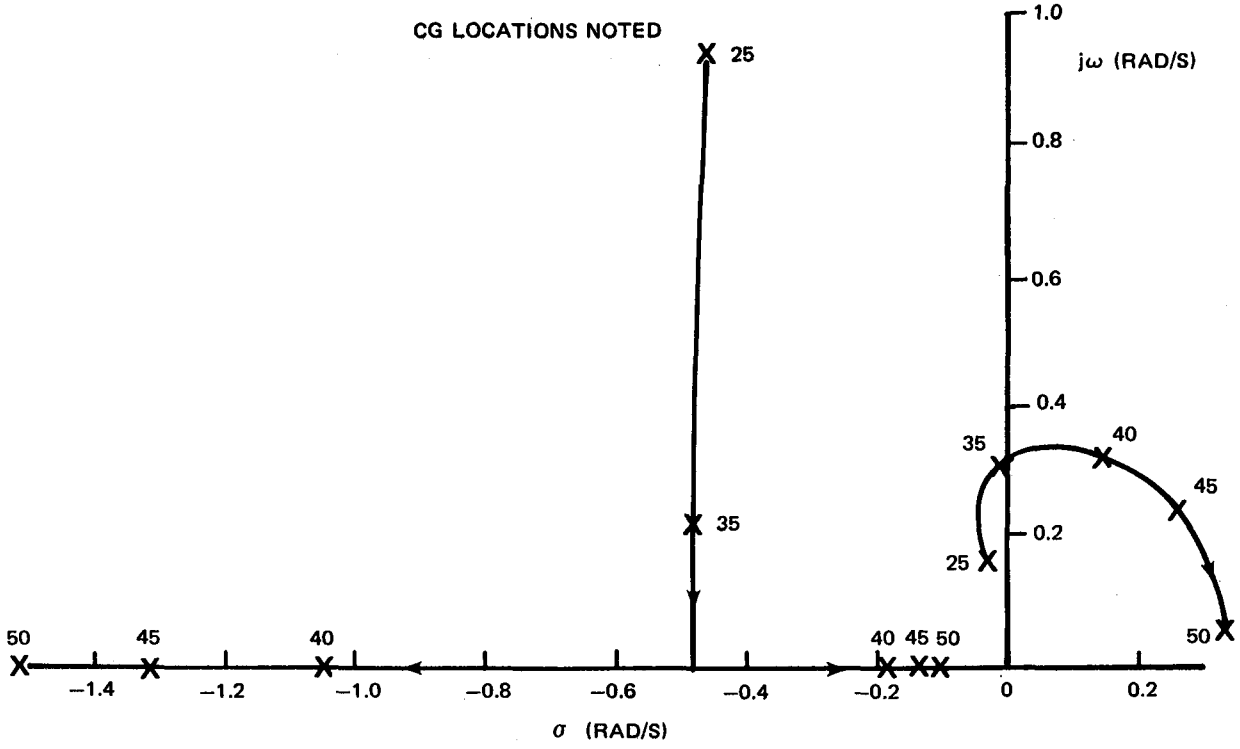

FIGURE 2-11. LOCUS OF ROOTS AS CG IS MOVED AFT, IN CRUISE FLIGHT – 70 PERCENT OF BASIC TAIL AREA

2.4 Flying Qualities Criteria

In this study, flying qualities criteria were required for two purposes. First, there was the need to specify the flying qualities that would be acceptable in the event of total augmentation system failure, i.e., flying qualities of the unaugmented vehicle in the most critical condition. The second purpose was to establish the flying qualities desired with the augmentation system in normal operation.

In the first case, acceptable unaugmented aircraft flying qualities were determined on the basis of safety considerations. It is usual for flying qualities to be described in terms of either Cooper-Harper pilot rating values (Figure 2-12 and Reference 1) and/or the military flying qualities "Levels" (Reference 2). Safety considerations for commercial transport aircraft dictate a maximum acceptable pilot rating of 6.5, which corresponds approximately to the boundary for Level 2 from the military specification. In the second case, the desired flying qualities of the normal augmented aircraft are those of military Level 1, which corresponds to a pilot rating of 3.5 or better.

At the outset of the program it was decided that satisfactory (Level 1) flying qualities for the augmented vehicle could be ensured by requiring the augmentation system to provide a match with the proven good flying qualities of the DC-10 in terms of phugoid-mode time histories and short-period characteristics measured by the "Bandwidth Model." In addition, other criteria were considered for application to this task to furnish confidence in the final characteristics. The "Bandwidth Model" is a pitch-tracking criterion originally developed by Calspan (Reference 3) which has been modified and adopted by Douglas for use in transport design work. The Douglas work is reported in Reference 4, and briefly described in Appendix 1, and the criterion is depicted in Figure 2-13. The criterion considers the amount of compensation, lead or lag, that the pilot must apply to achieve a given level of pitch-tracking performance without encountering pilot-induced-oscillation tendencies. The types of aircraft response expected from pilot commands are noted in each section of the chart. While this criterion may be used for both landing approach and cruise flight conditions, there is less confidence when it is applied to cruise cases, particularly in the left side of the diagram. In developing the criterion, there were relatively few data available to construct the boundaries in this area.

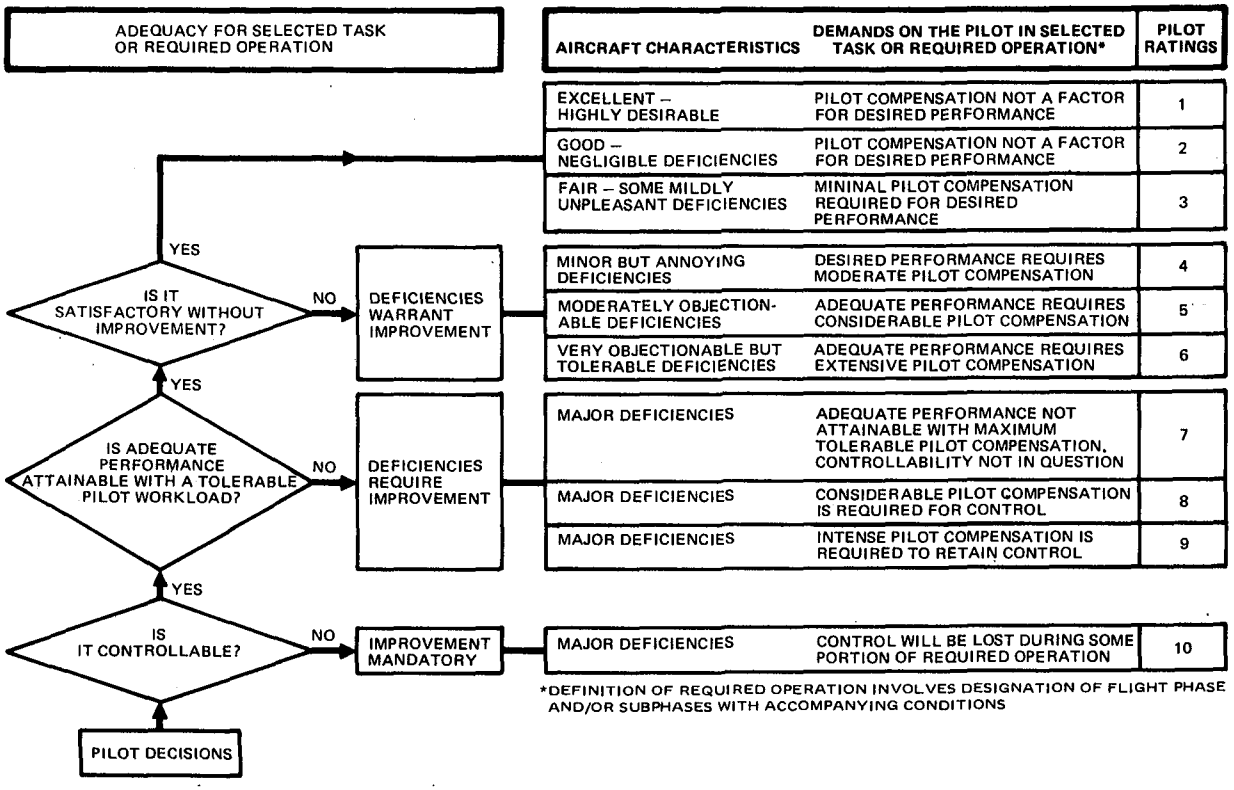

FIGURE 2-12. HANDLING QUALITIES RATING SCALE

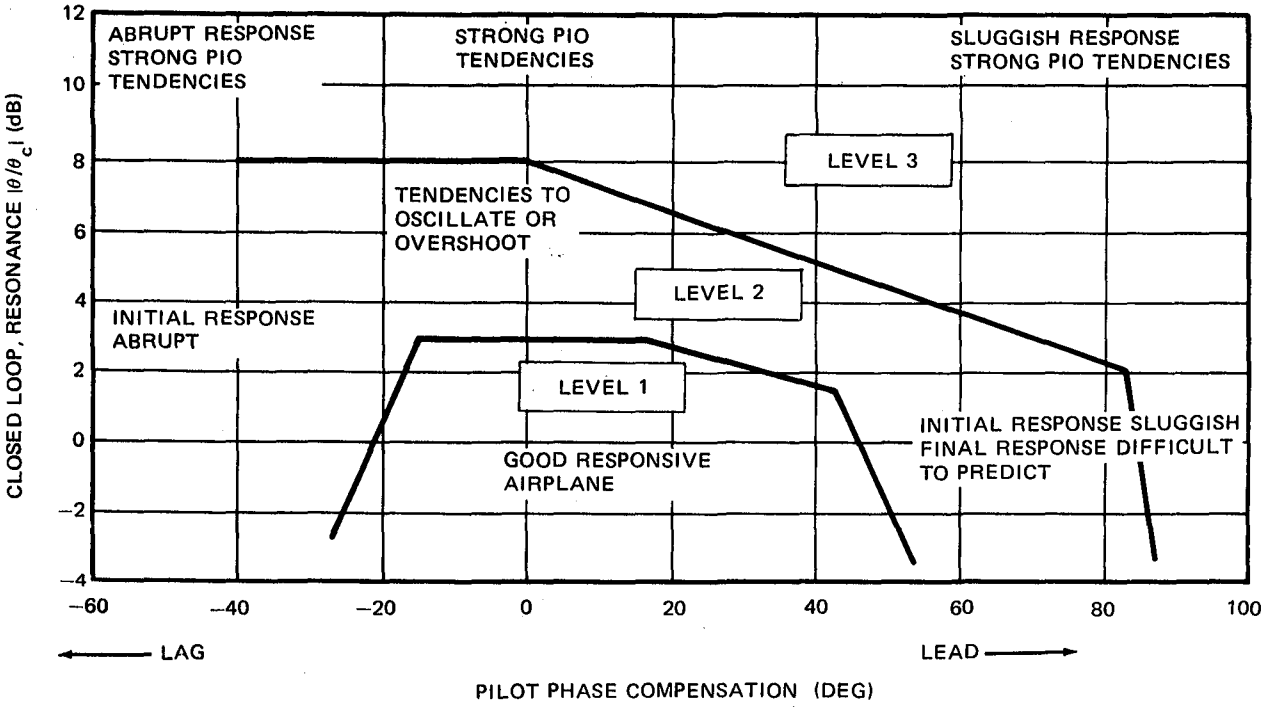

FIGURE 2-13. PITCH-TRACKING CRITERION

A criterion often mentioned for application to unstable aircraft involves the time-to-double-amplitude of the most unstable first-order root of the longitudinal characteristic equation. For example, Reference 5, which reported an inflight simulation of a supersonic transport configuration, cites a minimum acceptable time-to-double-amplitude of 2.5 seconds in light turbulence and 4.25 seconds in moderate turbulence, for the landing approach task. The configurations of this study have been used in Figure 2-14 to show the effect of static margin (as varied by center-of-gravity location and horizontal tail size) on time-to-double-amplitude. If the times indicated above are used to enter the chart, a minimum static margin of about minus 11 or minus 12 percent MAC is indicated for the light turbulence case and about minus 6 percent MAC for the moderate turbulence case. It should be noted,however, that in Reference 5 the authors cautioned about effects of pitch-control sensitivity, pitching-moment nonlinearities, pilot training, and visibility conditions.

The military flying qualities specification, Reference 2, sets down requirements for longitudinal short-period dynamics. The short-period frequency requirement is given as a function of the acceleration sensitivity, n/α, which is not dependent upon center-of-gravity location. The Level 2 boundaries are shown in Figures 2-15 and 2-16 for the landing approach and cruise flight cases, respectively. It is seen in Figure 2-15 that in the landing approach case the Level 2 frequency requirement is not met at centers of gravity aft of approximately 35 percent MAC. The most aft center-of-gravity location for compliance with the Level 2 frequency requirement in cruise flight is about 43 percent MAC, as shown in Figure 2-16.

2.5 Flying Qualities Analysis of Candidate Augmentors

Section 5 contains description of the control-law development process which in the early stages involved more than 25 laws. This section contains an evaluation of those control laws which were selected in Section 5.

Satisfactory long-period, or phugoid, characteristics were obtained by matching the time response to that of the DC-10. Short-period dynamics were investigated through use of the "Bandwidth Model." Because it was found that the selected control laws (augmentors) provide the same short-period characteristics, they are discussed collectively in this paragraph.

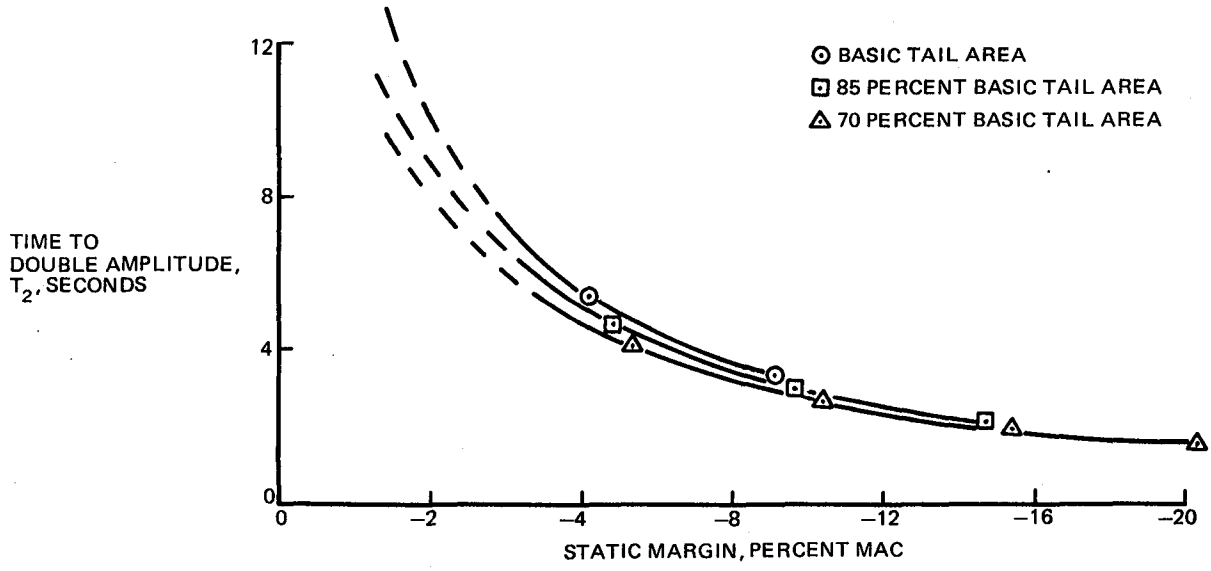

FIGURE 2-14. VARIATION OF TIME TO DOUBLE AMPLITUDE WITH STATIC MARGIN AND TAIL AREA – LANDING APPROACH

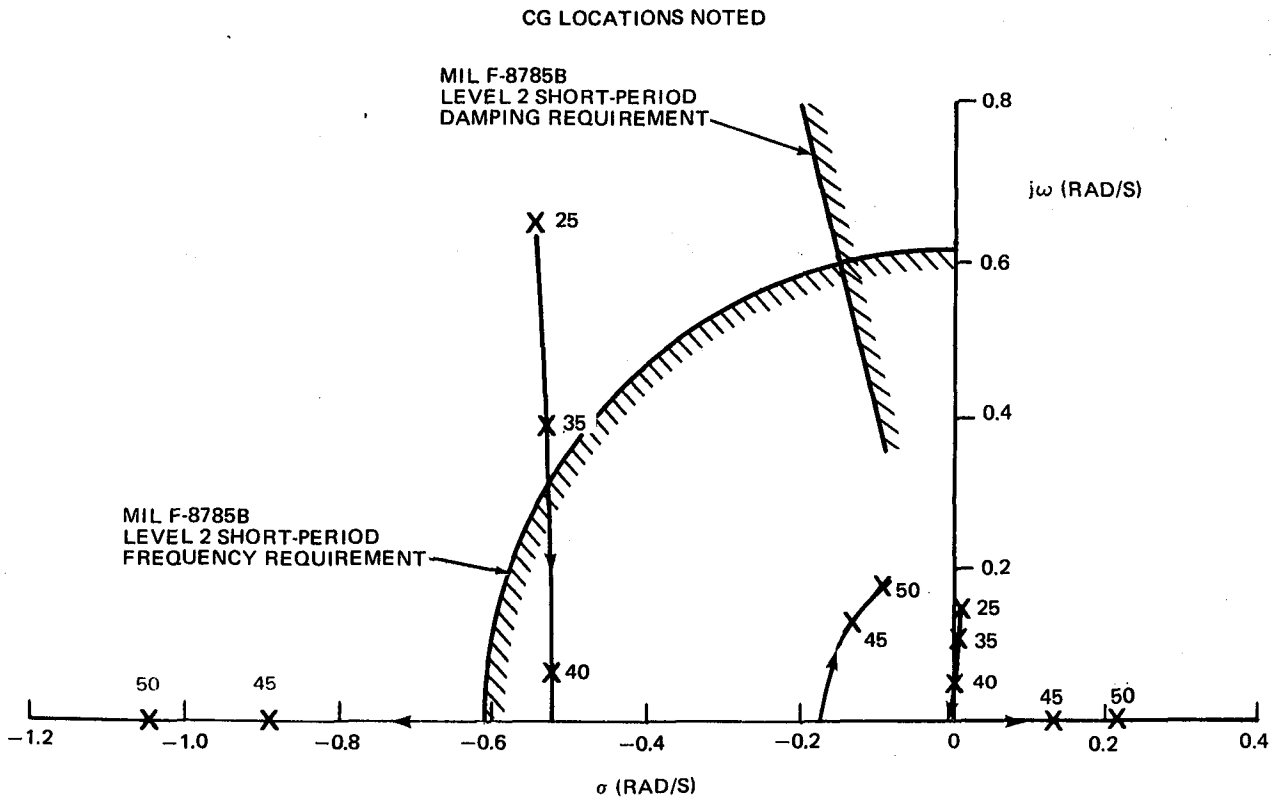

FIGURE 2-15. LOCUS OF ROOTS AS CG IS MOVED AFT, LANDING APPROACH – BASIC TAIL AREA

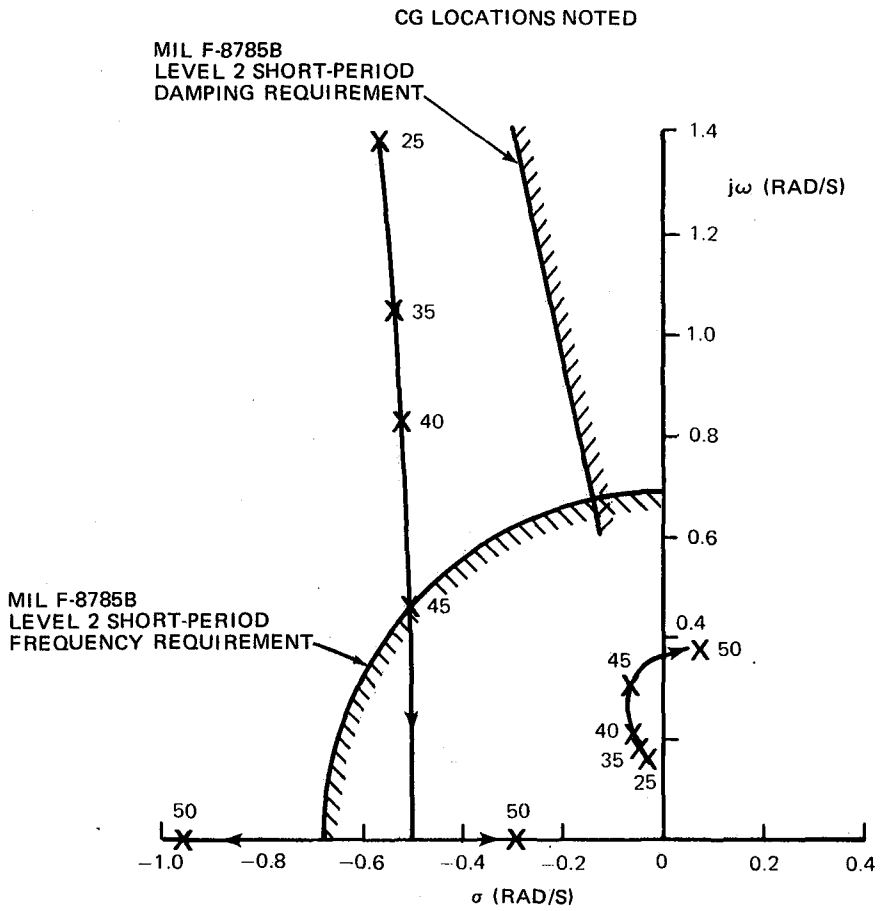

FIGURE 2-16. LOCUS OF ROOTS AS CG IS MOVED AFT, CRUISE FLIGHT – BASIC TAIL AREA

In Figure 2-17 the effect of augmentor operation on pitch-tracking is shown for the landing approach case with the center of gravity located at 40 percent MAC. The unaugmented aircraft is well in the Level 2 area, and in fact received a mean pilot rating of 5.4 in the first simulator test. With the RSSAS in operation, the predicted flying qualities fall into Level 1. Further validation of the short-period characteristics is furnished by reference to the frequency and damping requirements given in the military flying qualities specification, Reference 2. In this case, the minimum frequencies are specified in terms of the normal acceleration sensitivity, n/α. However, because the augmentation system has no direct lift controller, n/α is fixed for each flight condition (see Tables 2-4 and 2-5). It should be noted that frequency requirement is regarded as unduly strict with respect to large aircraft. Many such aircraft with demonstrated good flying qualities have difficulty meeting this requirement. In Figure 2-18 the effect of augmentation system operation on the aircraft in landing approach is shown

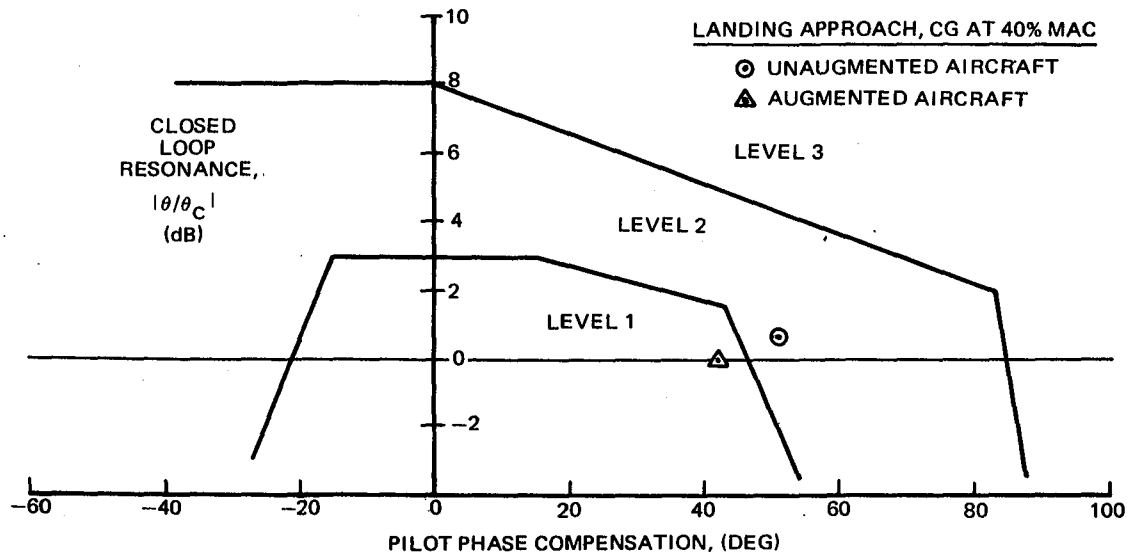

FIGURE 2-17. EFFECT OF AUGMENTATION SYSTEM ON PITCH TRACKING CONTROL

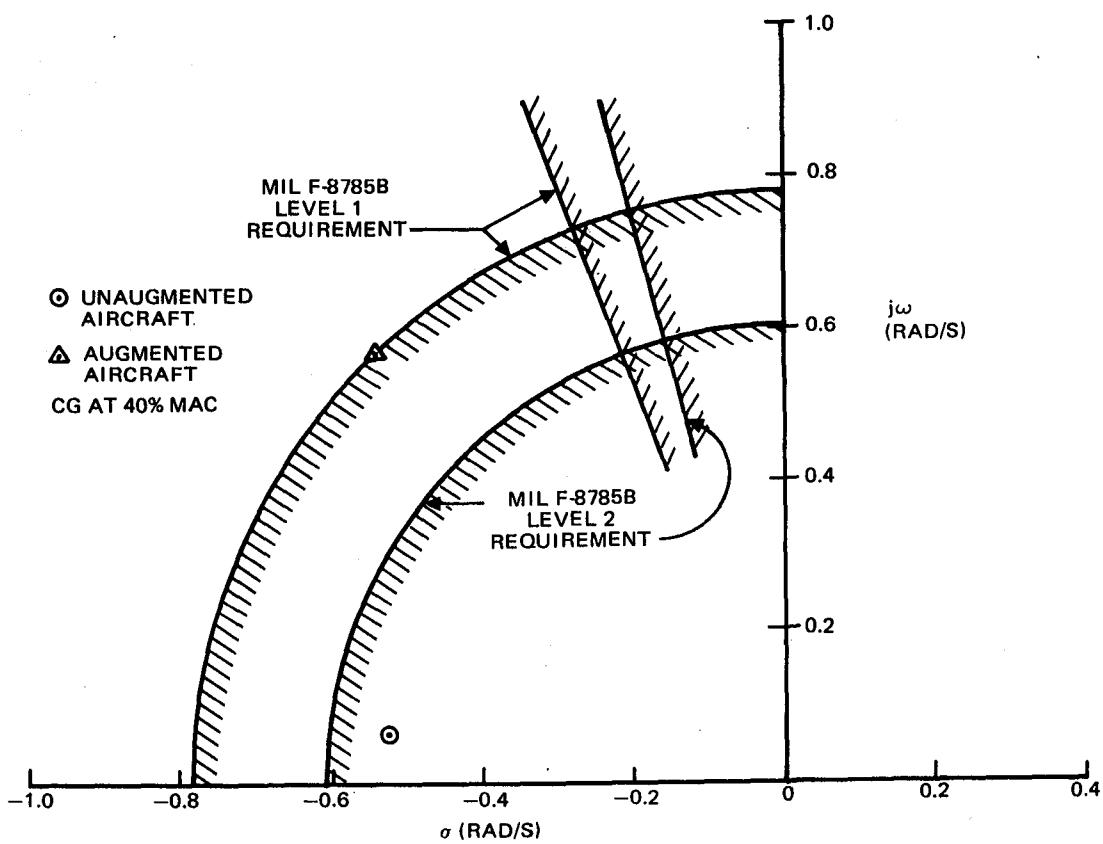

FIGURE 2-18. MILITARY SHORT-PERIOD REQUIREMENTS – LANDING APPROACH

for the design center-of-gravity location of 40 percent MAC. The augmented aircraft is marginally Level 1, using this criterion. In the less critical cruise flight condition, use of the augmentor brings the frequency well into the Level 1 area, as shown in Figure 2-19.

While all of the control laws provided satisfactory performance in terms of response to elevator inputs, there was concern regarding the response to other inputs. There was particular concern about thrust inputs because of the large thrust-moment arm associated with the wing-mounted engines (see Figure 2-3). To illustrate the effect, Figure 2-20 is presented showing the response of the unaugmented aircraft (solid line) to a sudden thrust reduction while

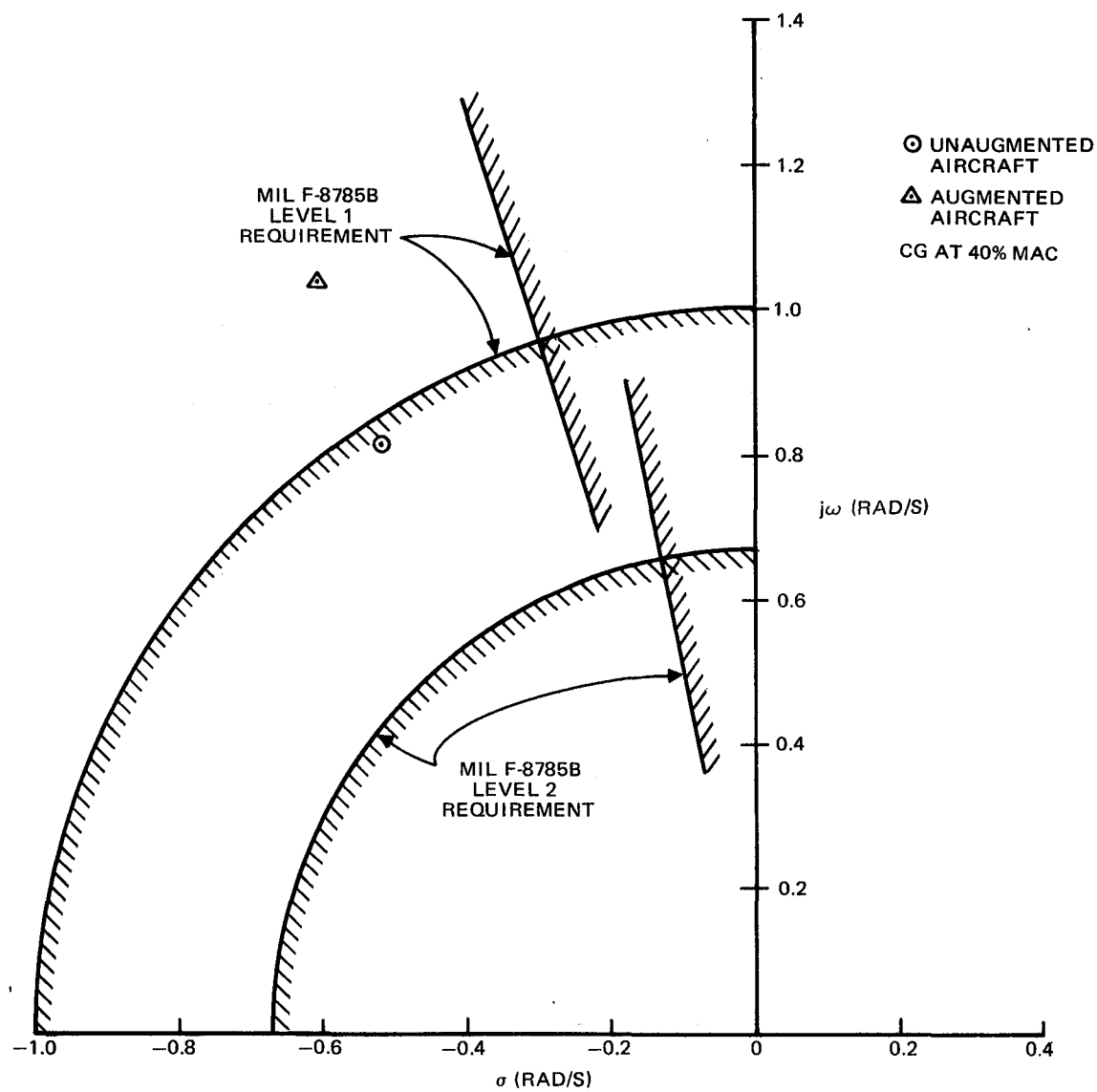

FIGURE 2-19. MILITARY SHORT-PERIOD REQUIREMENTS – CRUISE FLIGHT

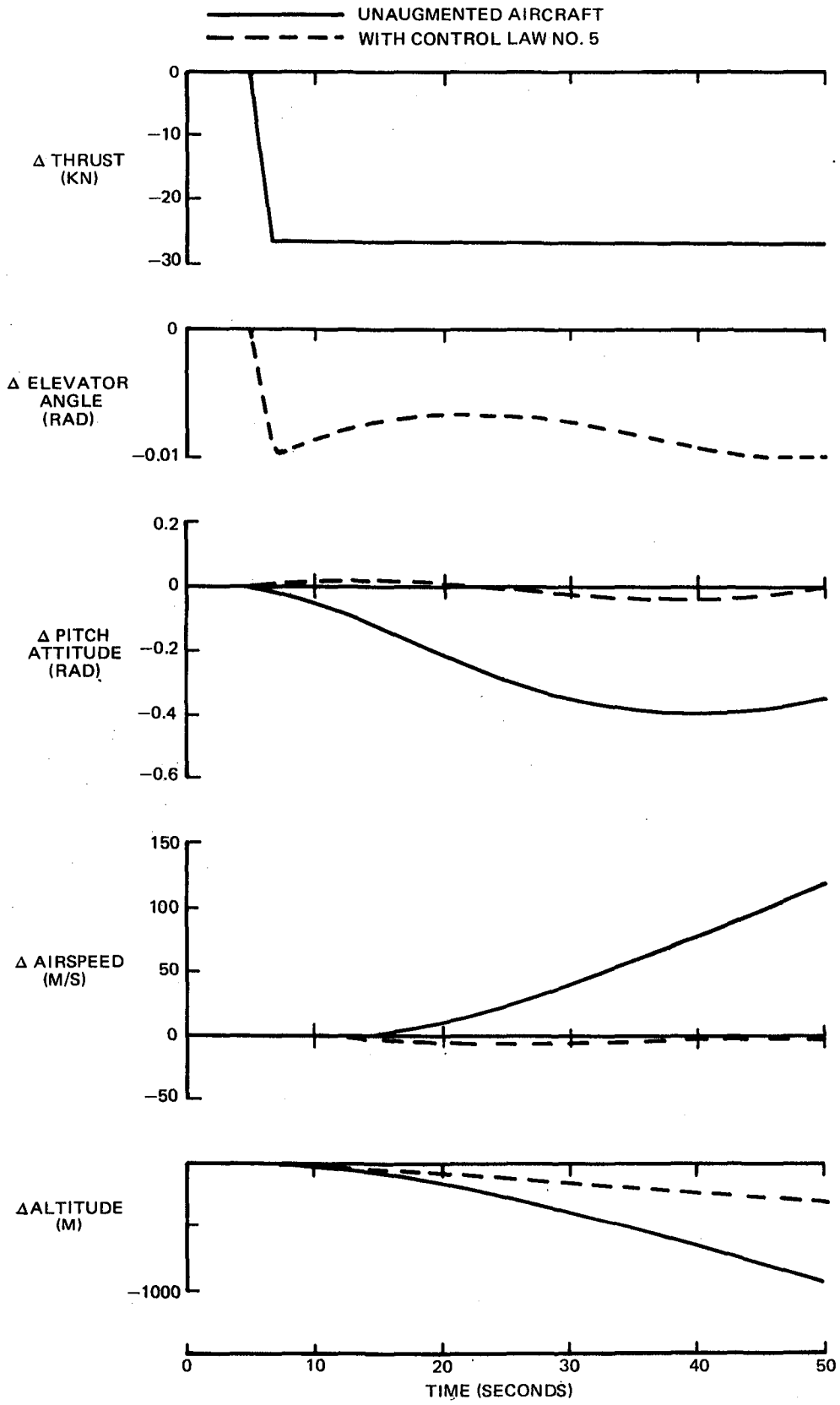

FIGURE 2-20. EFFECT OF THRUST CHANGE ON AIRCRAFT RESPONSE

in the landing approach. The thrust reduction amounts to approximately half of the thrust required for the landing approach. The most obvious effect is the immediate pitch-down and loss of altitude that occurs. The incorporation of a thrust compensation feature in the augmentors effectively controls the thrust pitching moments as shown by the dashed line in Figure 2-20. The response for control law Number 5 is shown in this figure, but the other control laws are similarly effective.

2.6 Summary of Aerodynamic Center Margin Results from the Motion-Base Tests

The results of the motion-base simulator tests discussed in Section 3 are summarized below. The results reflect an interpretation of the pilot opinions that weigh the results to the worst mean ratings in the array of tests. This interpretation recognizes that the worst means are probably representative of a significant portion of the line pilot population, and that a safety-related requirement should consider this portion of the population. The severity of the interpretation has a significant effect on the allowable stability margin. For example, in the landing approach, the use of mean pilot ratings would allow a negative 6-percent static margin compared to a negative 2.5 percent based on the worst mean ratings.

From the simulation, the minimum acceptable aerodynamic center margin for landing approach was determined to be a negative 3.1 percent MAC. The aerodynamic center margin is determined by subtracting from the static margin the difference between the neutral point and aerodynamic center, defined by the distances from the aft limit of the aircraft center of gravity. The static margin as determined from the simulator was negative 2.5 percent MAC; the difference between the neutral point and aerodynamic center was negative 0.6 percent MAC. For the nonterminal flight phases, the minimum acceptable aerodynamic center margin is a negative 4.5-percent MAC. Although less instability can be tolerated during landing approach, it is not necessarily the critical condition for tail sizing and setting the aft center-of-gravity limit. For a fixed tail size and center-of-gravity position, an aircraft has more static stability (or less instability if unstable) at landing speeds than it does at high-speed conditions. The reduction in static stability as airspeed is increased is caused by the variation in aeroelastic effects

with variations in airspeed. As a result, the critical condition for tail sizing is determined by how the stability level naturally varies with flight phase, as well as how the requirement for stability varies with flight phase. This is shown graphically and in a typical fashion in Figure 2-21. In this figure, the decrease in aerodynamic center margin – as speed is increased from the landing-approach range to the high-speed end of the nonterminal range – is greater than the change in the allowable margin. In this typical case, the critical tail sizing condition would be at high speed in the nonterminal flight phase, even though the actual level of required stability is not as great.

As previously mentioned, the minimum allowable aerodynamic center margin is a negative 3.1-percent MAC for landing approach and a negative 4.5-percent MAC for the nonterminal flight phases, a difference of 2.6-percent MAC. The normal variation of the actual margin with airspeed for a subsonic jet transport is orders-of-magnitude greater than 2.6-percent MAC, when the extremes of

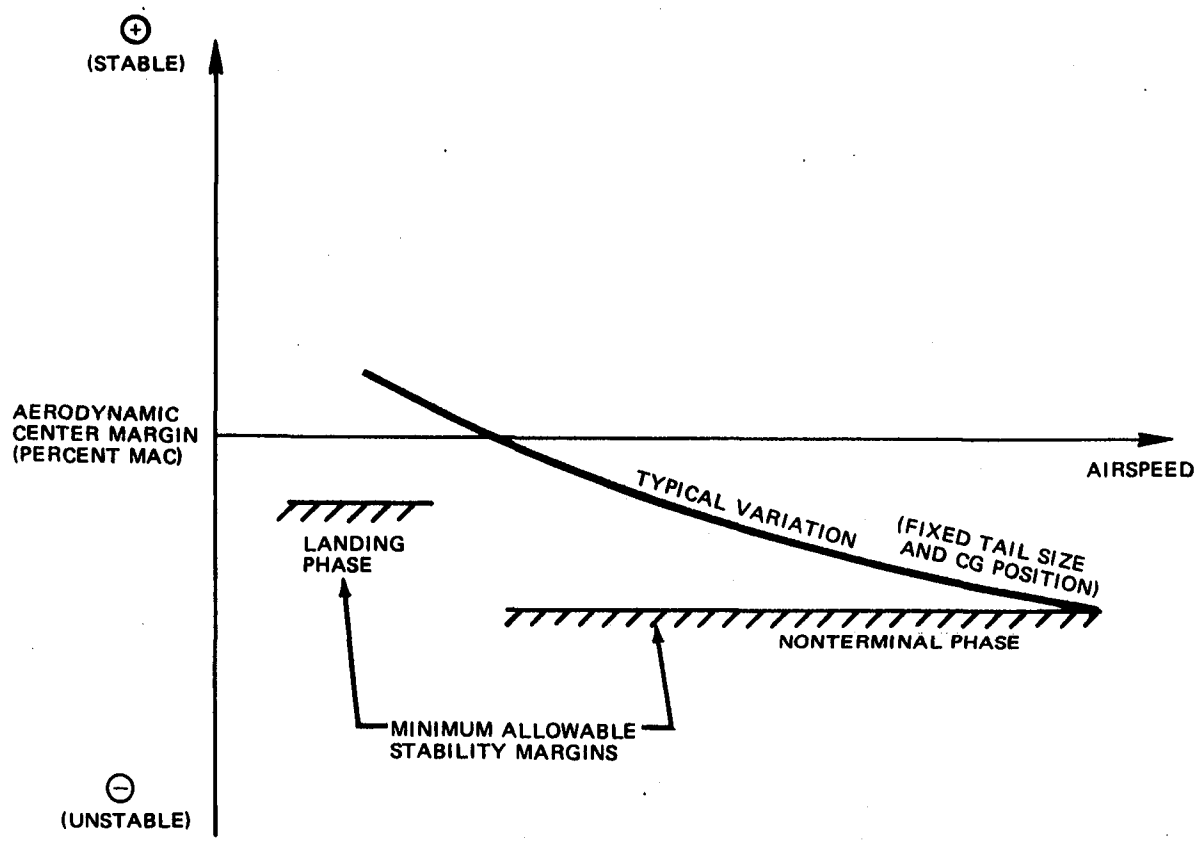

FIGURE 2-21. TYPICAL RELATIONSHIP OF AERODYNAMIC CENTER MARGIN VARIATIONS WITH SPEED

the speed range are considered. Therefore, the critical condition for tail sizing in actual practice is high speed in the nonterminal flight phase. Within this phase, the most critical point occurs at the highest equivalent airspeed/dynamic pressure within the operating envelope where aeroelastic losses are great, and at relatively low altitudes and Mach number where stability has not increased significantly due to compressibility effects.

2.7 Fuel Savings

The fuel savings relative to an EET-type aircraft configured with current levels of inherent stability can be determined from Figure 2-22. This figure uses data from the study described in Paragraph 2.2. The fuel savings are based on the tail size which provides the required aerodynamic center margins at the critical condition of high airspeed and relatively low altitude.

Using the aerodynamic center margin recommendation from Paragraph 2.6 of minus 4.5 percent, the fuel savings are 2.8 percent. Relative to the EET baseline described in Paragraph 2.1, the fuel savings would be three-quarters of one percent. The savings are significant.

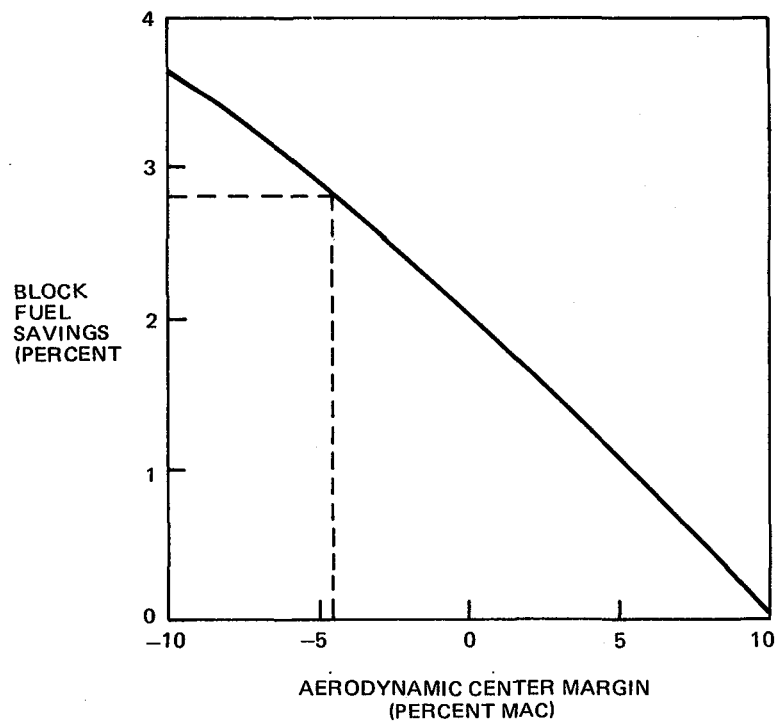

FIGURE 2-22. EFFECT OF AERODYNAMIC CENTER MARGIN ON FUEL SAVINGS

SECTION 3
MOTION-BASE SIMULATOR TESTS

3.1 Test Facility and Methodology

Simulations of the aircraft and of the system were conducted in order to explore the relationship of flying qualities and aircraft characteristics with and without the RSSAS.

The tests were conducted on the Douglas six-degree-of-freedom motion simulator. The mechanism supports a complete simulated transport cockpit and provides realistic motion cues. Visual simulation for the cockpit is available from a Redifon visual flight attachment. A detailed description of the simulator facility is given in Appendix 2.

In the first simulation, flying qualities of the unaugmented aircraft were examined through most of the flight envelope. This examination led to emphasis being placed on the cruise flight and landing approach conditions. Pilot ratings were obtained for a number of configuration variations and in conditions of turbulence or calm. Five test pilots, experienced in DC-10 and other transport handling evaluations, participated in the experiment.

In the second simulation, flying qualities of the augmented aircraft were examined in landing approach and cruise flight. Some reversion conditions were examined, together with configuration variations and turbulence. Six test pilots took part in the test.

The programming for the simulation utilized the large-flight-envelope data previously developed, thereby permitting simulated flight through most of the flight envelope as well as permitting flap, leading-edge-device, and landing gear extension and retraction. In this way, representation of a realistic transport flight was attempted. The scope of the study did not permit investigations to revise the aircraft configuration. However, relatively minor improvements in the aerodynamic characteristics were made through the program in response to adverse comment.

In analyzing the test results, it was necessary to use mean (average) pilot ratings to define the trends of the data. All the data points describing the pilot rating results represent the mean of a number of

individual pilots. One interpretation of a curve fairing through these points weights the data equally. However, it has been argued that, for the purpose of establishing stability limits or boundaries, the worst averages should be used to fair the interpretive curve. The argument states that each of the "worst" points in the sample represents a significant portion of the airline pilot population, and that the boundary should consider these pilots. Such an interpretation is also included in the presentations of pilot ratings, and is used for the final evaluation of fuel savings. The presentations which follow indicate "mean" curves with solid lines and "worst mean" curves with dashed lines.

3.2 Tests of the Unaugmented Aircraft

3.2.1 Test Description. — The pupose of the first test was to determine the longitudinal condition which met the minimum standard of flying qualities laid down for the unaugmented aircraft.

In the initial procedure, each evaluation pilot became familiar with the basic configuration (center of gravity at 25 percent MAC) by performing approaches, landings, go-arounds, climbs to altitude, maneuvers at altitude, descents, and stalls. Additional familiarization was provided by having the pilots repeat the process for an aft center-of-gravity case (center of gravity at 40 percent MAC). No pilot ratings were taken during this portion of the experiment, but pilot comments were solicited. From the commentary it was determined that the remainder of the test should concentrate on the landing approach and the cruise flight conditions. The lateral-directional characteristics were recognized as unsatisfactory during this period but time did not permit the problem to be pinpointed and corrections to be made. The problem was later indentified as being due to improper spoiler -- aileron mixing. The result was low lateral control sensitivity for small wheel deflections.

All configurations were evaluated in both a calm air environment and in the presence of simulated atmospheric turbulence. The turbulence model used is in the Dryden form and is a slightly modified version of that described in Reference 6. For the landing approach cases, the RMS vertical gust intensity was 2.13 m/s (7.0 ft/sec). Pilots described this level as "moder-

ate," or "moderate to heavy," but their opinion is probably based to a large extent on motion cues, and in any ground-based simulator there is necessarily considerable motion attenuation. It is believed that this intensity of turbulence would be more accurately described as "heavy" or "severe" if full motion cues were felt by the pilot. In fact, the proposed revision (Reference 7) to the military flying qualities specification suggests that a RMS vertical gust component of 2.3 m/s (7.6 ft/sec) be used for the threshold of "severe" turbulence for low altitude flight. For the cruise condition, the RMS turbulence value was 1.5 m/s (5.0 ft/sec). This was generally described as "moderate" which corresponds to the "moderate" stated in Reference 7.

Following the familiarization stage, the formal evaluations commenced. Five Douglas pilots participated. The configurations tested were the 15 combinations of center-of-gravity location and tail size previously described. Variations in tail size were included in the matrix to identify problems that might be attributed to deficient pitch control at various stability levels. As mentioned previously, a listing of the more pertinent flying qualities parameters for the 15 test configurations, for landing approach and for cruise, is presented in Table 2-4.

A description of the pilot task for the landing approach condition is presented in Figure 3-1. The conditions for the cruise flight evaluations are: altitude = 10,668 m (35,000 ft), Mach number = 0.80, in the clean configuration. In the cruise condition, pilots were asked to make altitude changes of 457 m (1500 ft), speed changes of ±10 m/s (20 kn), and steep turns using about 0.785 rad (45 degrees) of bank. The evaluations were made with both smooth air and with a moderate turbulence level [σ_w = 1.5 m/s (5.0 ft/sec)].

During the experiment, three pilots evaluated all of the 15 configurations, one evaluated 13 of the configurations, and one evaluated 7 of the configurations. An evaluation consisted of flight at the cruise condition, with calm air and with turbulence, and landing approaches, with and without turbulence. Several approaches could be made if the pilot felt it necessary. At the conclusion of each run, the pilot was interrogated by the test engineer who recorded the comments on a debriefing form. Pilot ratings were given for each of the

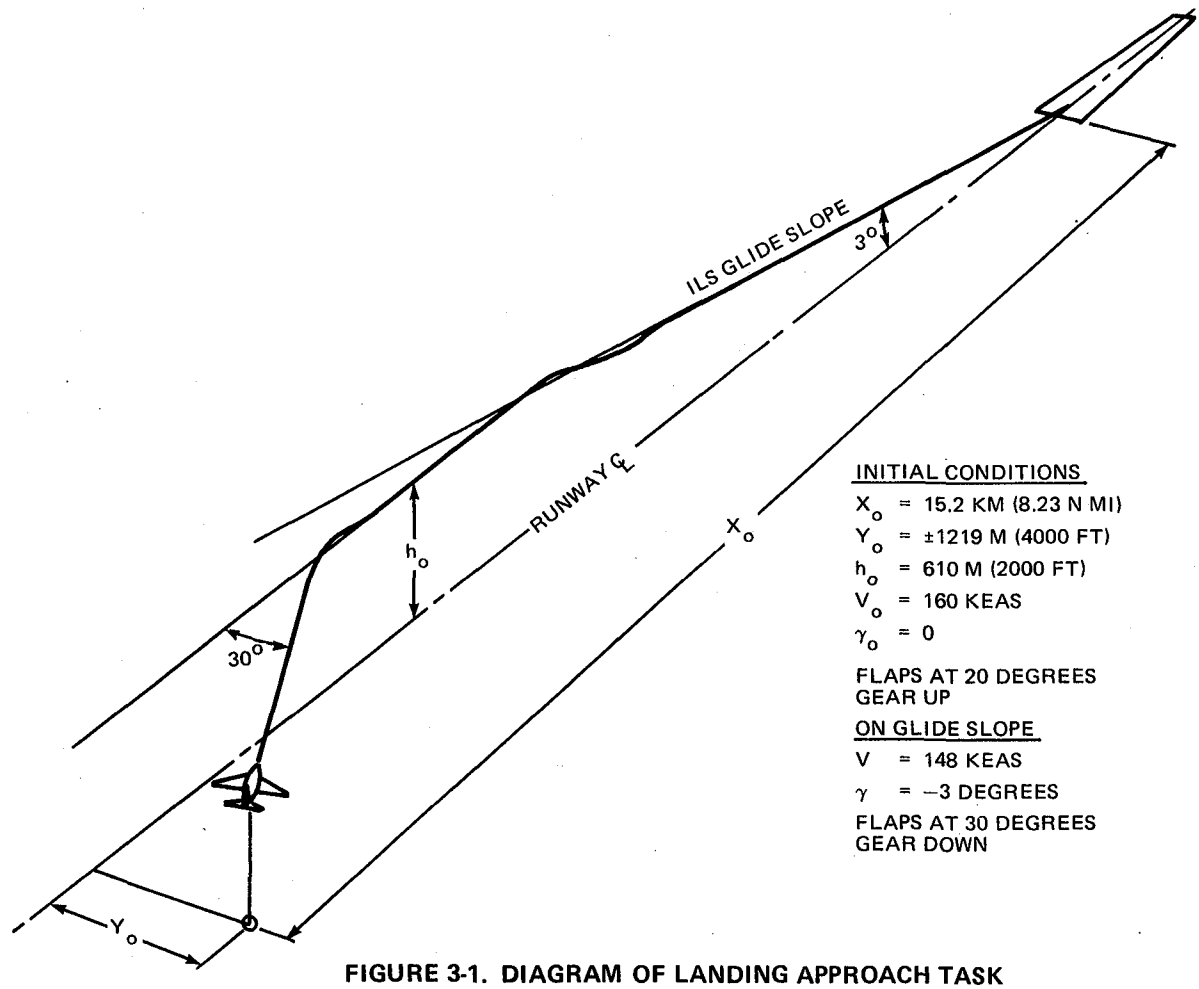

FIGURE 3-1. DIAGRAM OF LANDING APPROACH TASK

configurations and turbulence conditions. The Cooper-Harper scale was used (see Figure 2-12 and Reference 1).

3.2.2 Flying Qualities Evaluation. — Figure 3-2 shows the effect of static margin on mean pilot rating for the landing approach task in turbulence. The data represent the mean of five individual pilots. As previously explained, two fairings through the data have been made: one considering all the means (solid line), and the other considering only the worst of the means (dashed line). Reading the dashed curve at a mean pilot rating of 6.5 establishes the minimum acceptable static margin at minus 2.5 percent MAC. The corresponding minimum time-to-double-amplitude, T_2, is found from Figure 2-14 to be approximately 7 or 8 seconds, depending on the tail area. It will be noticed that the curve in the area of interest (where pilot rating is approximately 6.5) is relatively flat. This flatness causes the acceptable limit to be very sensitive to the manner in which the curve is faired.

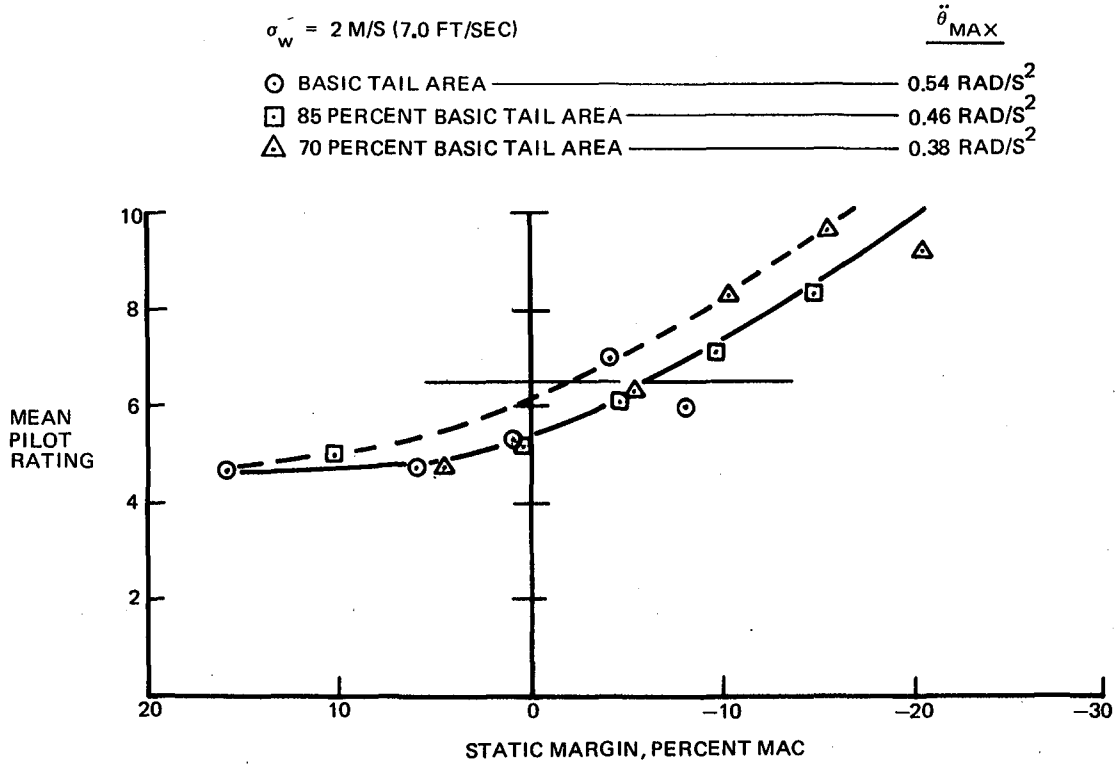

FIGURE 3-2. EFFECT OF LONGITUDINAL STABILITY ON MEAN PILOT RATING – LANDING APPROACH

In the landing approach condition, the aerodynamic center is only 0.6 percent MAC forward of the neutral point. Therefore, the acceptable aerodynamic center margin for landing approach is minus 3.1 percent MAC [(−2.5) + (−0.6)].

No firm conclusions can be drawn regarding the effect of horizontal tail size, although there is some indication that the smallest tail tested (70 percent of basic) develops too little control power for the very unstable cases. It should be noted however, that the values of maximum pitch acceleration which each of the tails can produce, noted in Figure 3-2, are not particularly low by transport aircraft standards. Pitch acceleration capability is seldom critical for transport aircraft in which the tail is sized by stability considerations. Therefore, the few pilot comments relating to poor controllability may have had more to do with decreased pitch control sensitivity than with inadequate maximum control power. This sensitivity is of no concern for the stability range of interest in this study. The reduced tail area also provided less pitch damping, which possibly contributes to degraded pilot ratings. However, no pilot comments related to this specific effect.

The effect of turbulence on pilot rating is shown in Figure 3-3 where the two curve fairings have been constructed using equally weighted data points (the upper curve corresponds to the solid curve in Figure 3-2). The turbulence effect for the stable cases is approximately one pilot rating unit while the increment for the unstable cases is about two units.

In Figure 3-4 the pilot rating data for the landing approach case in turbulence is shown on the pitch-tracking criterion chart. The agreement between the ratings and the boundaries of the criterion is generally good, particularly near the Level 2 boundary. The ratings near the Level 1 boundary are somewhat worse than expected, probably because of the poor lateral-directional characteristics.

For the cruise flight condition, maneuver margin was chosen as the metric of stability rather than static margin. Maneuver margin is more appropriate for this condition, in which load factor changes provide important cues for the pilot. In Figure 3-5 the effect of maneuver margin on mean pilot rating is shown for flight in turbulent air. As before, two fairings have been drawn through the data. Using the upper (dashed) line, which weights the poor ratings more heavily, the minimum acceptable maneuver margin for a pilot rating of 6.5 is found to be approximately minus 1 percent MAC.

The effect of turbulence on pilot opinion of maneuver margin is presented in Figure 3-6 for the cruise flight condition. The effect is quite small, with the stable cases indicating an incremental pilot rating of less than half a unit and increasing to nearly one unit for the unstable cases. This small effect is attributed to the rather low precision required in the cruise piloting task.

Knowledge of the minimum acceptable aerodynamic center stability is necessary to determine fuel savings due to relaxed stability from the parametric data of Paragraph 2.6. In Figure 3-7, the effect of aerodynamic center margin on the mean pilot rating is presented for cruise flight in turbulent air. Using the curve faired through the poorer mean ratings yields a minimum acceptable aerodynamic center stability level of about minus 4-1/2 percent MAC. While these ratings are for a piloting task involving cruise flight at 10,668 meters (35,000 feet), the limit of minus 4-1/2 percent

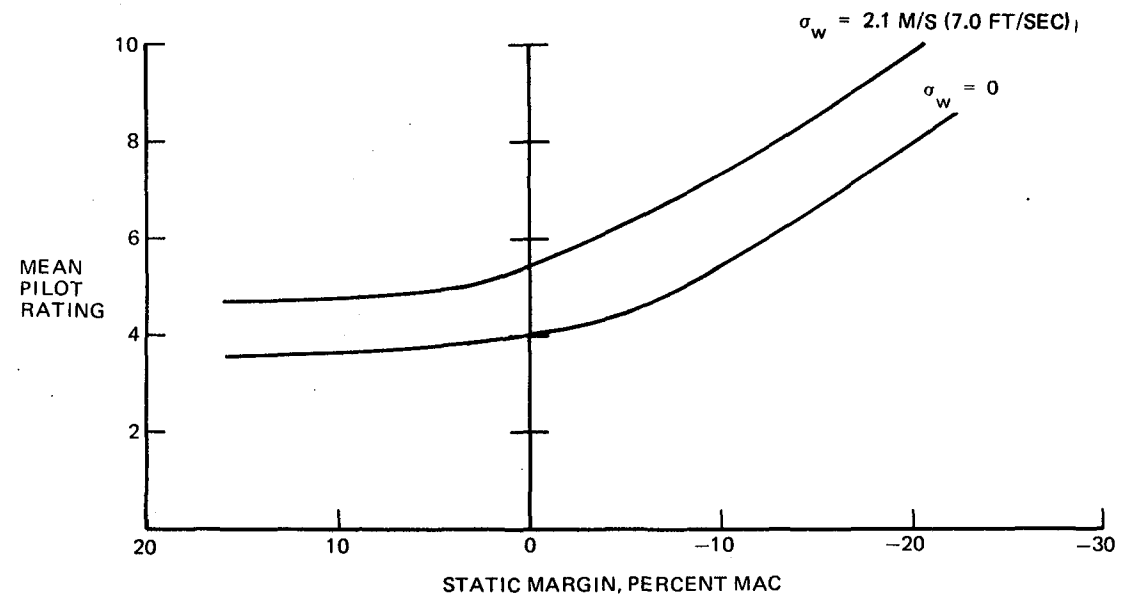

FIGURE 3-3. EFFECT OF TURBULENCE AND STABILITY ON MEAN PILOT RATING – LANDING APPROACH

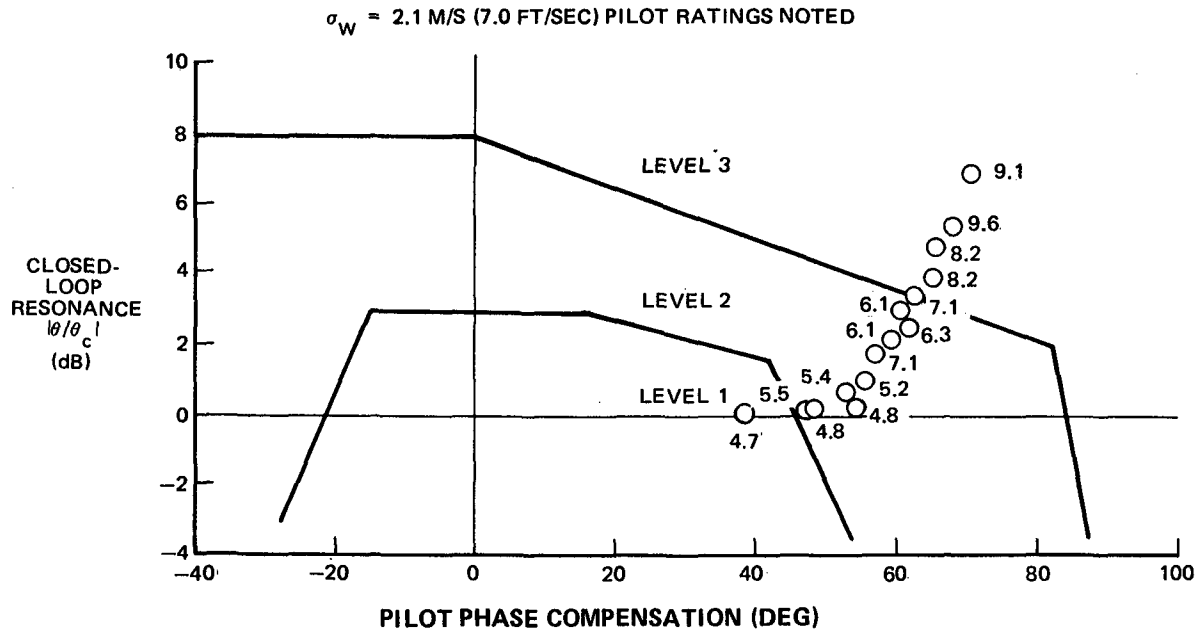

FIGURE 3-4. PITCH-TRACKING CRITERION – LANDING APPROACH

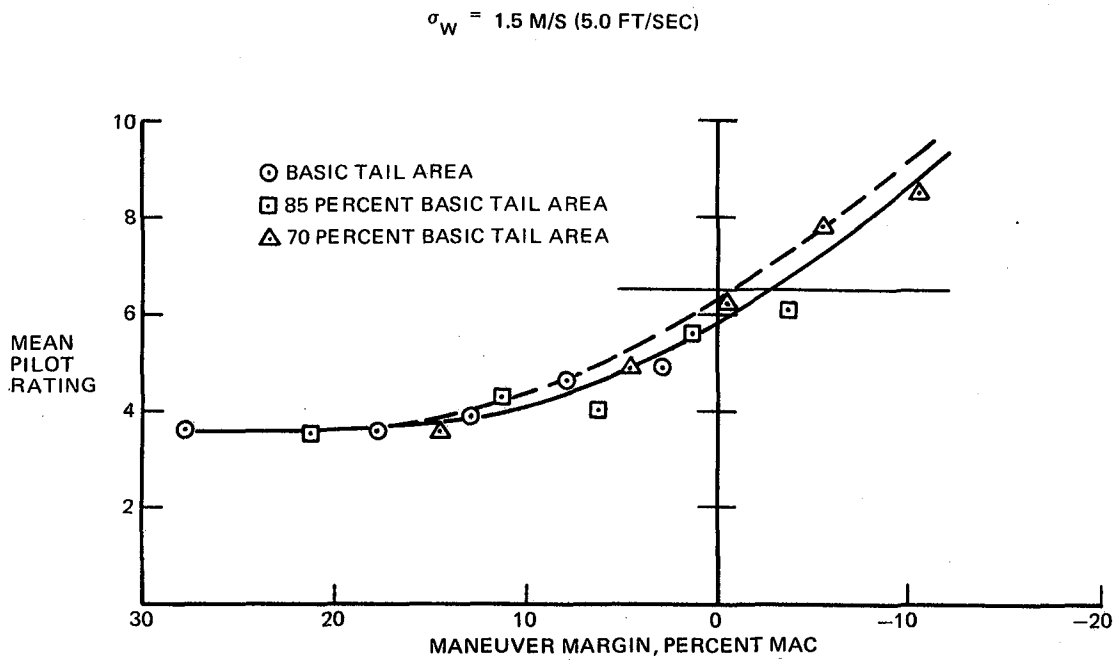

FIGURE 3-5. EFFECT OF LONGITUDINAL STABILITY ON MEAN PILOT RATING – CRUISE FLIGHT

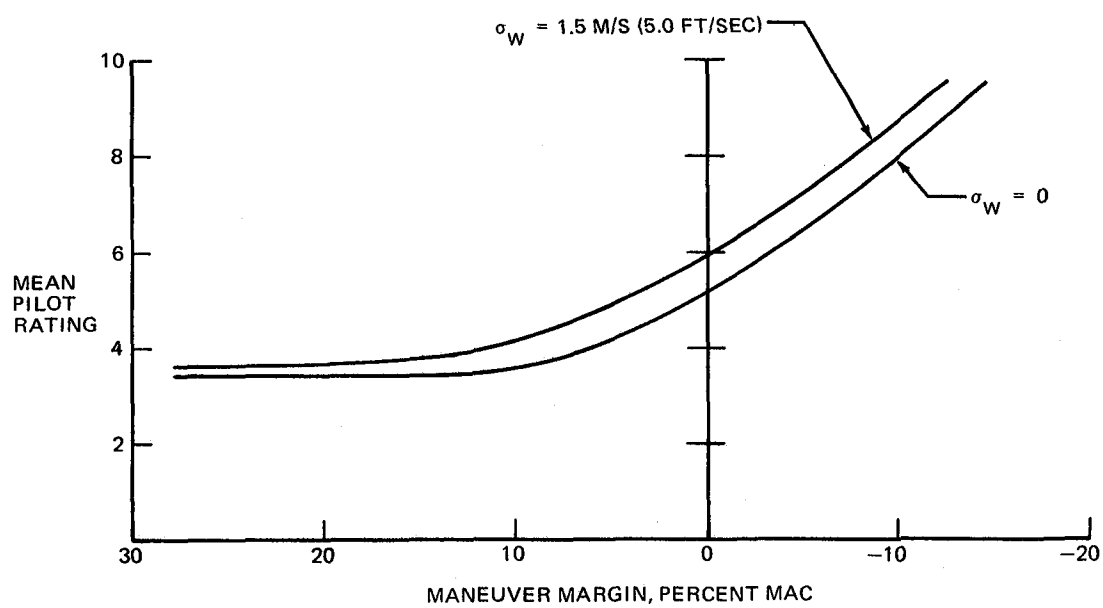

FIGURE 3-6. EFFECT OF TURBULENCE AND STABILITY ON MEAN PILOT RATING – CRUISE FLIGHT

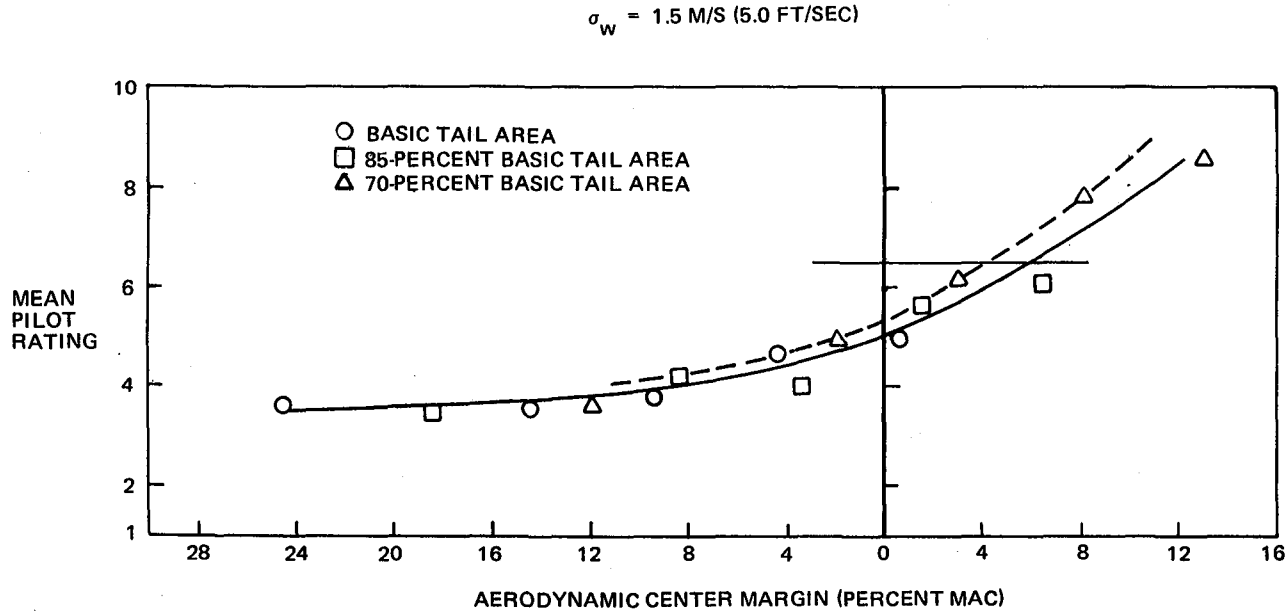

FIGURE 3-7. EFFECT OF AERODYNAMIC CENTER STABILITY ON MEAN PILOT RATING CRUISE FLIGHT

MAC also is judged appropriate for other nonterminal flight phase tasks in commercial transport operations.

3.3 Tests of the Augmented Aircraft

3.3.1 Test Description. — A second motion-base simulator test was conducted with the purpose of examining the flying qualities and pilot evaluations of three control laws, certain augmentation system features, and several reversion conditions. The control laws tested were $\theta\dot{\theta}u\alpha$, $\theta\dot{\theta}\alpha$, and α in landing approach and α in cruise flight. Evaluations were made of the augmentor performance with varying levels of augmentor elevator authority: full, 0.087 rad (5 degrees), and 0.035 rad (2 degrees). (A limited augmentation elevator authority is normally desirable to minimize the consequences of augmentor failure. The primary pilot elevator authority was not limited during these tests.) Tests were conducted in which the pilots evaluated a simulated auto trim failure, i.e., the pilot was forced to manually trim the aircraft during large trim change maneuvers. Failure of the thrust compensation feature of the augmentor (θ/thrust damper off) was also simulated with the critical case being the go-around maneuver. Other failure conditions which were evaluated included passive total failure of each of the augmentors and augmentor failures in which a reversion from one control

law to another occurred. During individual test runs, the pilot was not aware of which sensor had been failed.

Evaluations of the unaugmented aircraft were made at two center-of-gravity locations: 25 percent MAC and 40 percent MAC, except for a brief look at an off-design case with the center of gravity at 50 percent MAC. The basic horizontal tail was used in all cases.

The simulated aircraft was the same as used in the first simulation, except that the troublesome lateral-directional characteristics were improved by an increase in lateral control sensitivity for small deflections. Most of the evaluations were made in the presence of turbulence as described for the first test. The flight conditions used in this experiment were, again, landing approach and cruise, but some additional conditions were investigated. Several emergency descents with speed brakes extended were made and approaches to stalls at an intermediate altitude were performed. Six Douglas pilots participated in the evaluations.

Table 3-1 lists the minimum test configurations sequence that was provided for each of the evaluation pilots.

3.3.2 MBS RSSAS Configuration. — The RSSAS simulation for the augmented motion-base flying qualities evaluation was a single computational channel configuration as shown in the simplified block diagram of Figure 3-8. This included: (1) control law computation and elevator control to provide aircraft static stability and to compensate for the pitching moment resulting from engine thrust changes, and (2) trim commands, both automatic and manual, to offload steady-state elevator augmentation commands. Three different control laws, $\theta\ \dot{\theta}\ u\ \alpha$ (control law No. 1), $\theta\ \dot{\theta}\ \alpha$ (control law No. 3) and α (control law No. 5), were implemented from the $\theta\dot{\theta}u\alpha$ control law family. They represent a progression of sensor failures starting with a full-up array, then airspeed (u) failed and finally the attitude sources ($\theta\dot{\theta}$) failed, leaving the single type, angle-of-attack (α) control law. Effects of variations in sensor characteristics were not evaluated on the MBS, but have been studied during the DETAC analysis (Reference 5.5.3). To present the status of the system in the cockpit, a combined RSSAS caution/warning annunciator and trim director indicator, as shown in Figure 3-9, was installed on the left side of the pilot's forward instrument panel.

TABLE 3-1
MBS TEST SEQUENCE

I. Landing Approach/Go-Around (if noted)

	Augmentor	Center of Gravity	Turbulence	Control Law	Other
1.	Off	25%	σ_w = 0	-	-
2.	Off	40%	σ_w = 0	-	-
3.	Off	40%	σ_w = 2.3 (7)	-	-
4.	On	40%	σ_w = 2.3 (7)	1	-
5.	On	40%	σ_w = 2.3 (7)	3	-
6.	On	40%	σ_w = 2.3 (7)	5	-
7.	On	40%	σ_w = 2.3 (7)	5	RSSAS off @ 91m (300 ft)
8.	On	40%	σ_w = 2.3 (7)	3→5 @ 137M (450 ft)	GA
9.	On	40%	σ_w = 2.3 (7)	5→1 @ 137M (450 ft)	GA, 0.087 rad (5^o) Auth
10.	On	40%	σ_w = 2.3 (7)	5*	GA, 0.035 rad (2^o) Auth
11.	On	40%	σ_w = 2.3 (7)	5*	θ/Thrust damper off
12.	On	40%	σ_w = 2.3 (7)	5*	Trim INOP
13.	On	40%	σ_w = 2.3 (7)	5*	Trim INOP, GA
14.	On	50%	σ_w = 2.3 (7)	5*	-

II. Cruise

1.	Off	40%	σ_w = 1.5 (5)	-	-
2.	On	40%	σ_w = 1.5 (5)	5	-
3.	On	40%	σ_w = 1.5 (5)	5	Emer. Desc.
4.	On	40%	σ_w = 1.5 (5)	5	Clean Stall. 4.6km (15K ft)
5.	On	40%	σ_w = 1.5 (5)	5	Approach Config. Stall

*or option of test pilot

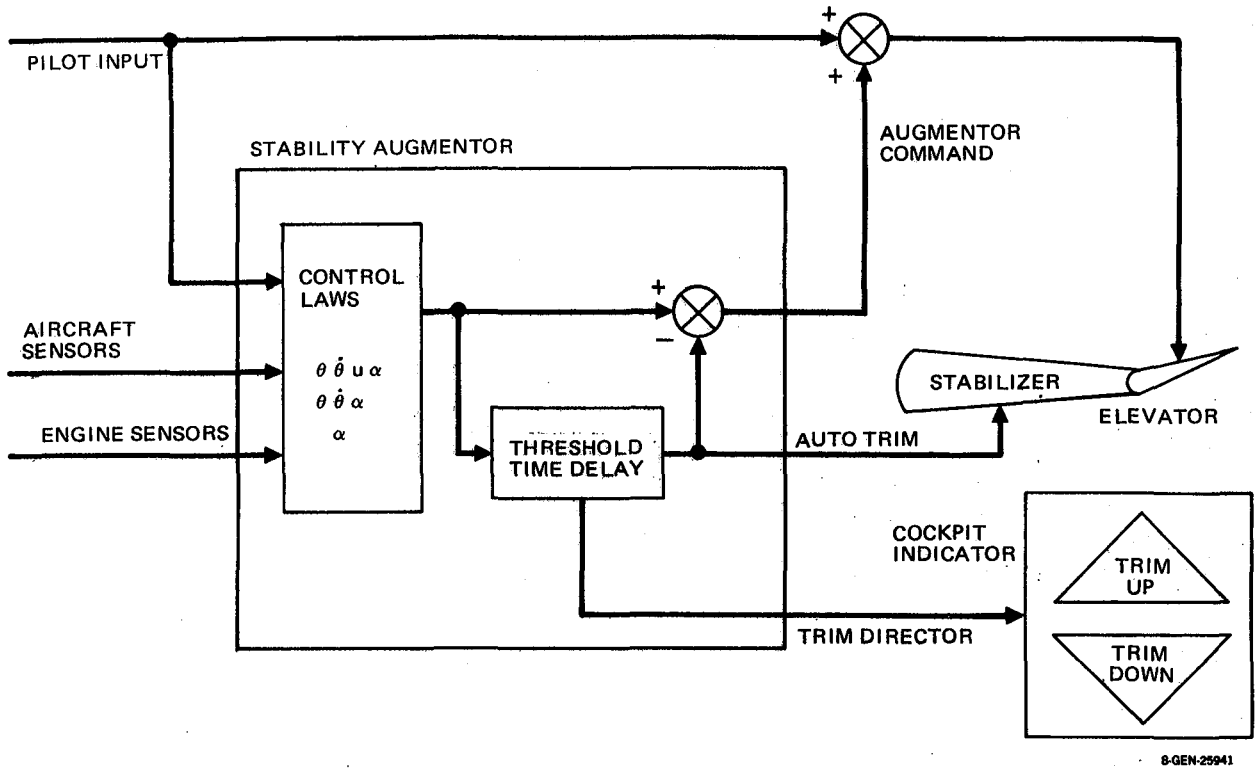

FIGURE 3-8. SINGLE-CHANNEL RSSAS BLOCK DIAGRAM – MBS CONFIGURATION

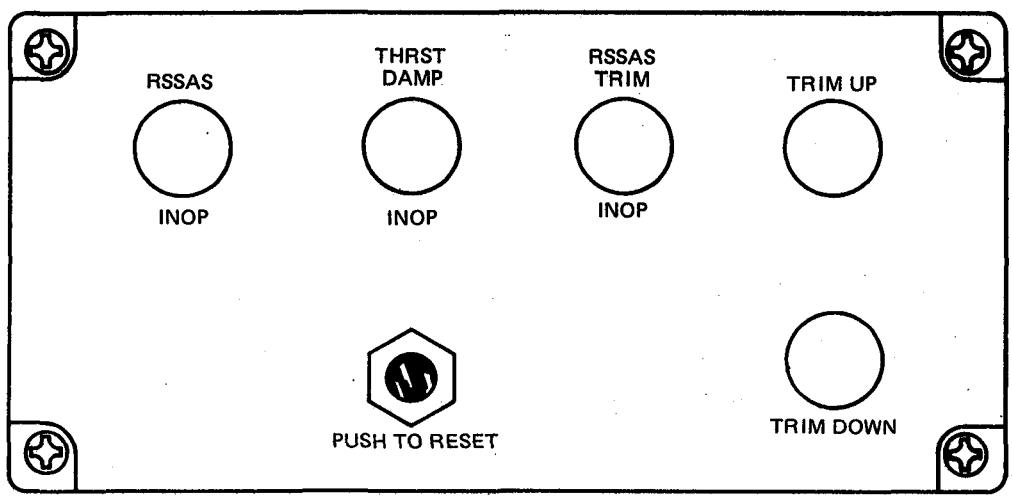

FIGURE 3-9. RSSAS CAUTION/WARNING AND TRIM DIRECTOR INDICATOR

Control of the RSSAS configuration was accomplished by means of a programmable test operator panel shown in Figure 3-10. The configurations evaluated and the control unit-augmentor interface are described with the aid of the RSSAS diagram shown in Figure 3-11. (This diagram is developed in Section 6 of this report.) Selection of the augmentor control law was accomplished by pushing one of the top three control panels' pushbuttons, which in turn provided an input to the select logic (Point A, Figure 3-11) corresponding to the sensor validities necessary for the desired control law. With the use of the thumbwheels, the maximum augmentor series elevator command authority at point B could be set to 0.035 rad (2^{o}), 0.087 rad (5^{o}), 0.1745 rad (10^{o}) or full authority.

The toggle switches along the left side of the control unit inserted failure conditions. The top switch input corresponded to a series actuator failure by opening the signal path at point C. This resulted in an "RSASS inop" light on the RSSAS caution/warning panel. The middle toggle switch opened the thrust input to the augmentor at point D. The augmentor responds to this by "holding" the last N_1 value in the pitch/thrust compensation calculation and provides a "Thrust Damper Inop" warning. The bottom switch opens the horizontal stabilizer position feedback at point E, which is detected by the trim actuator failure detection circuit. This provides an RSSAS Trim Inop warning and activates the manual trim director indicator.

The toggle switches on the right side of the controller were used to make minor changes to the augmentor configuration. The top switch opened the horizontal stabilizer signal path at the feedforward input to the observer at point F. This configuration was examined in an attempt to simplify the RSSAS-horizontal stabilizer interface. This is desirable, since not all stabilizer movement (only pilot-initiated)should be input to the observer and it may be difficult to extract the necessary data with the accuracy needed, especially during failure conditions. All pilot ratings were, however, taken with the stabilizer input in its normal position. The middle switch was used to change the feedforward gain at point G from the

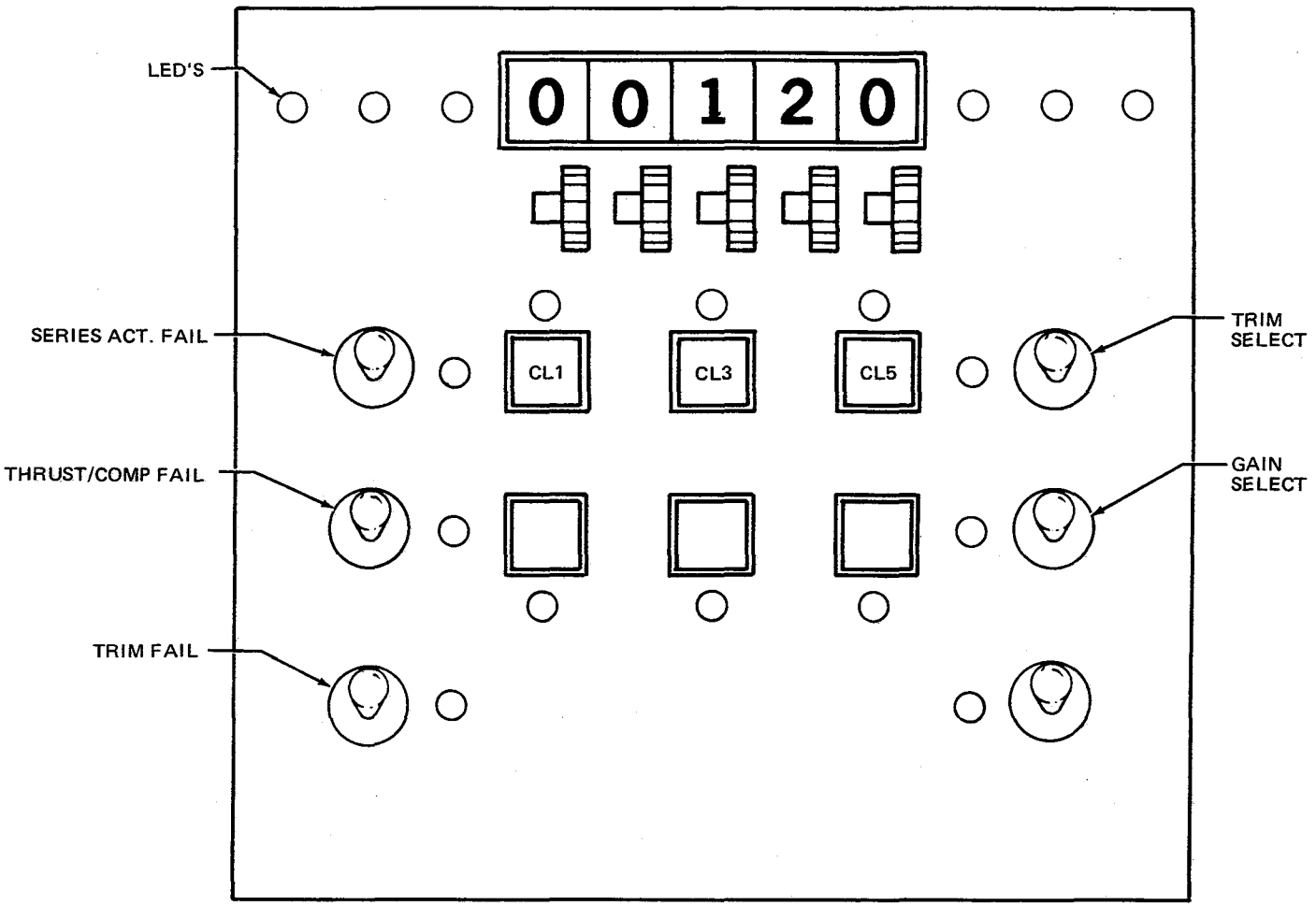

FIGURE 3-10. TEST OPERATOR PANEL

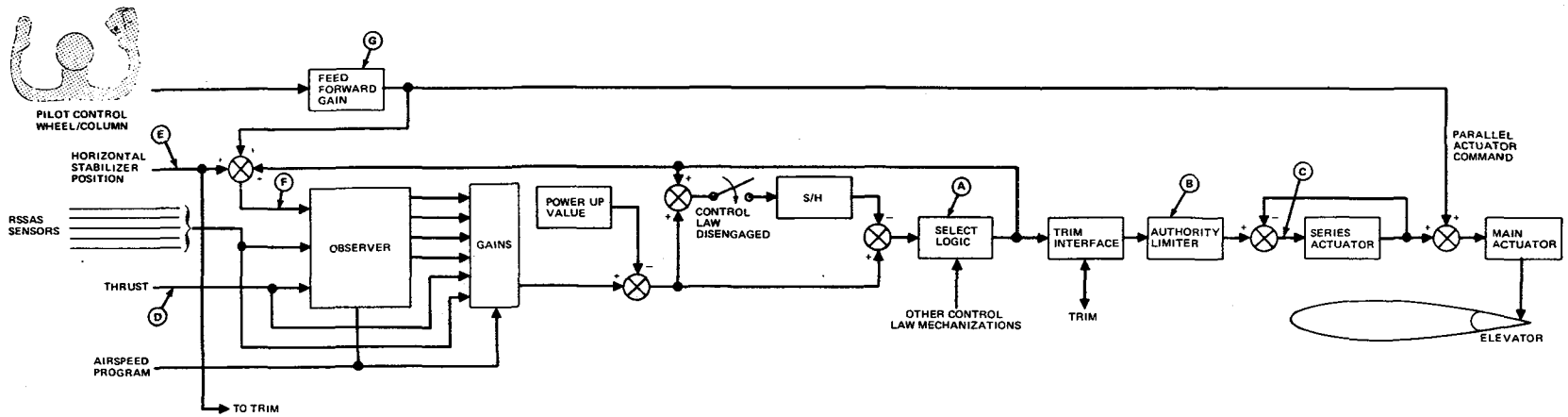

FIGURE 3-11. RSSAS BLOCK DIAGRAM

value calculated by the augmentor, to a fixed value of 1. The augmentor gain is selected to provide the DC-10 pitch rate to control column deflection while the unity gain results in the normal EET pitch rate to control column deflection. Pilot evaluation indicated a preference for the EET response and most tests were flown with the gain set to 1..

3.3.3 Flying Qualities Evaluation. — In Figure 3-12, pilot ratings obtained in the second simulator test are shown together with data from the first test. The data are for the landing approach case in the presence of turbulence.

Although the pilot commentary indicated that the lateral control characteristics were considerably improved over those used in the first test, the pilot ratings did not reflect a significant change for the two center-of-gravity locations which were evaluated. It is believed that although the lateral characteristics during the first test were objectionable, because longitudinal properties were the major concern the pilots attempted to overlook the deficiencies when assigning pilot ratings. The slightly higher (worse) mean pilot rating that was obtained for the near neutral stability case tends to support the upper, more conservative, curve fairing that was used to establish the minimum acceptable stability level at 2-1/2 percent MAC (pilot rating of 6.5). A similar presentation is made for the calm air case in Figure 3-13. Again the task is the landing approach. The curve from the first test is based on equal weighting of the data points and shows good correlation with the two data points from the second test.

In the cruise flight condition, only a brief evaluation of the unaugmented aircraft was conducted. With the center of gravity located at 40 percent MAC, this case represents an augmentor failure during a prolonged flight, and the question asked of the pilots was, "Would you continue to your destination or land as soon as possible?" Of the five pilots who evaluated this condition, only one had doubts that the flight should be continued. He commented that some pilots might want to discontinue the flight if the conditions persisted (moderate turbulence and the center of gravity located at the aft limit, 40 percent MAC). The other four evaluation pilots felt that there would be no problem. Opinions

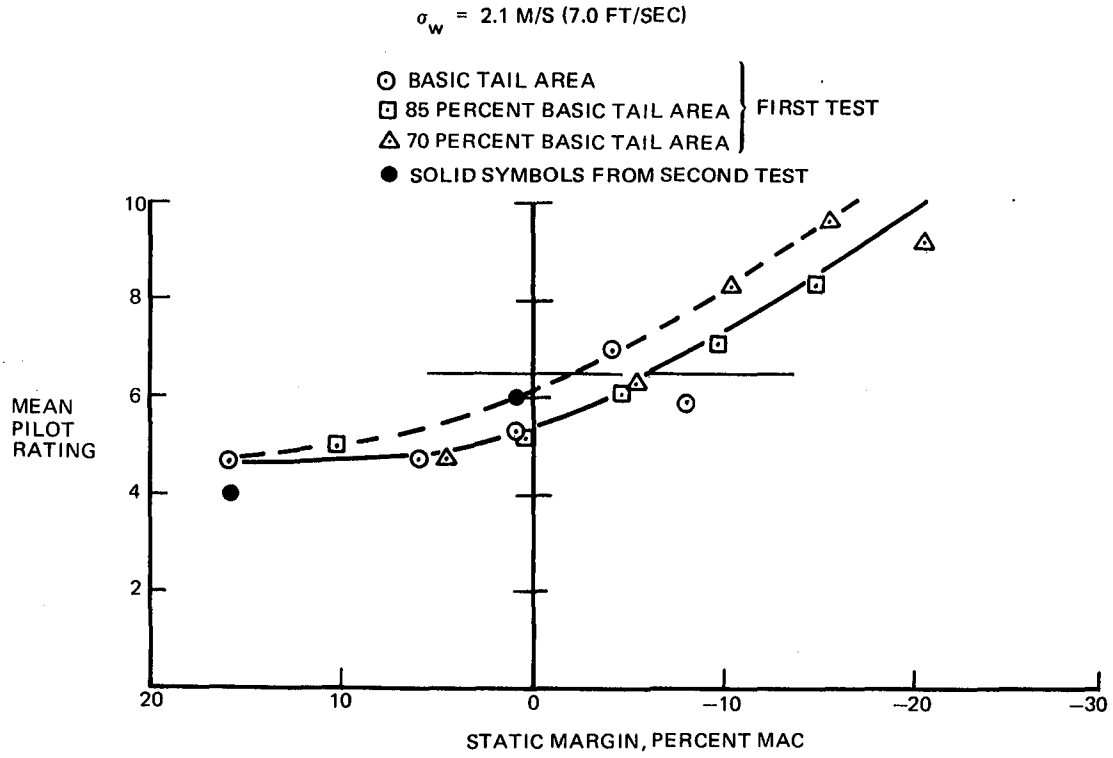

FIGURE 3-12. EFFECT OF LONGITUDINAL STABILITY ON MEAN PILOT RATING – LANDING APPROACH (COMPARISON OF DATA FROM FIRST AND SECOND TESTS)

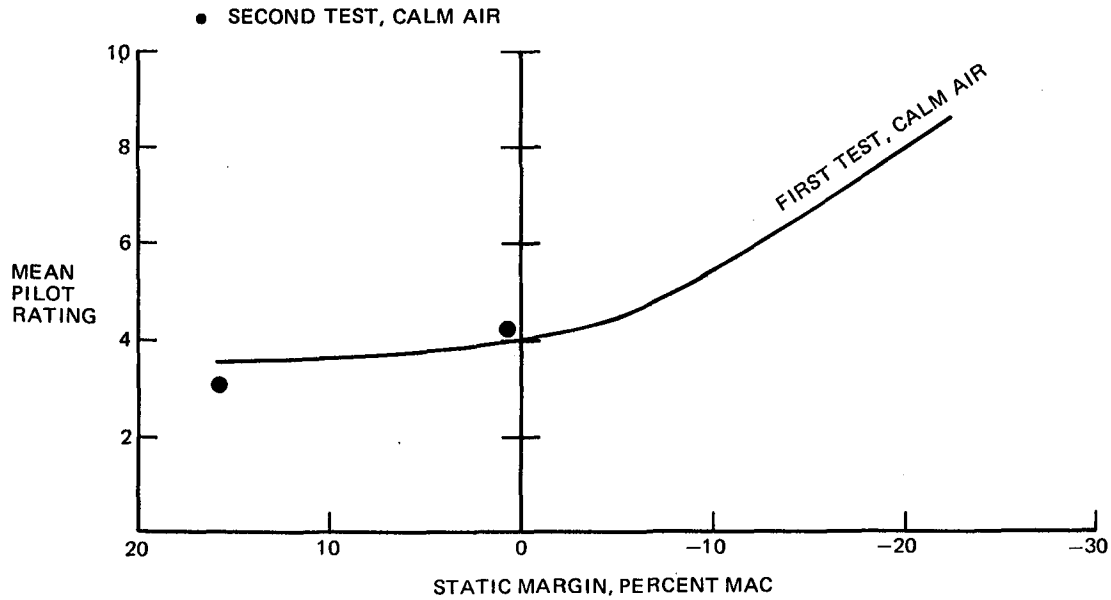

FIGURE 3-13. EFFECT OF TURBULENCE AND STABILITY ON MEAN PILOT RATING – LANDING APPROACH (COMPARISON OF DATA FROM FIRST AND SECOND TESTS)

varied from "not bad," to "OK", and "flies great." Actually, no problems should be expected since the maneuver margin at this center-of-gravity location is nearly 13 percent MAC. In Figure 3-5, the results of the first test showed a mean pilot rating of less (better) than 4.0 for the same center-of-gravity location and flight condition.

Three augmentors, No. 1, No. 3, and No. 5, were evaluated in the landing approach in the presence of turbulence. These are described in Section 5. It is interesting that although several of the evaluation pilots indicated a clear preference for one augmentor over another, the pilot ratings for each of the three averaged 3.8. For a similar center-of-gravity location and flight condition, it was shown in Figure 3-12 that the mean pilot rating for the unaugmented aircraft was 6.0. In the same figure, the mean pilot rating for a center-of-gravity location of 25 percent MAC is 4.0, about the same as the 3.8 given for the augmented aircraft for a center-of-gravity location of 40 percent MAC.

In cruise flight, only augmentor No. 5 was evaluated. Because the unaugmented aircraft was rated satisfactory in this flight condition, there was little room for improvement, and none was observed. The pilot who expressed slight doubts about the unaugmented aircraft in cruise, observed the same weakly damped oscillation with the augmentor in operation.

Simulated stalls were performed at about 4600 m (15,000 ft) altitude in clean and landing configurations, both with augmentor No. 5 in operation and unaugmented. All of the stalls were easily recoverable (no lateral-directional separation effects were simulated). The only problems encountered involved the addition of thrust when recovering from power-off stalls with the unaugmented aircraft. Unless the thrust was added carefully, the nose-up thrust pitching moment made it difficult to get the nose down.

For the test involving simulated autotrim failure, the manual RSSAS trim director (see Paragraph 3.3.2) was used. The manual RSSAS trim director was activated whenever the autotrim system could not properly off-load the augmentor series elevator displacement. The command display can present an unusual situation for the pilot, since the RSSAS trim requirement may be in direct conflict with the pilot's primary trim

requirement. As an example, while the pilot may be holding nose-up elevator with the control column, the RSSAS trim director could command nose-down trim to off-load a steady-state nose-down-series elevator deflection.

The trim director was evaluated in several approaches. The pilot was instructed to (a) respond to the trim command, but immediate action was not necessary, and (b) if the trim command was in opposition to the desired primary trim requirement, satisfy both in any order that was comfortable. The test demonstrated the following: (a) trim commands are a new idea and not immediately natural to respond to, (b) the pilot should first satisfy primary trim requirements and then the RSSAS trim command, (c) the trim director threshold must be carefully selected to minimize nuisance or reversing-trim commands, and (d) a manual trim director could increase the pilot's workload. It is concluded that development is needed in this area.

3.3.4 Other Results. — Besides establishing levels of flying quality for the augmented aircraft, the following significant conclusions resulted from the tests.

Required Elevator Deflection — Figure 3-14 is a bar chart reflecting the nominal and maximum observed pilot elevator control required to perform specified piloting tasks with and without the RSSAS. All data were observed in a moderate level of turbulence. The effect of the augmentation was to significantly reduce the magnitude of the required pilot elevator command during the landing/approach and go-around maneuvers. The large deflections in go-around are required because of the pitching moment resulting from the engine thrust change. These elevator deflections are trimmed out if unaugmented, or satisfied by the augmentor if the RSSAS is engaged. During this testing, it was observed also that the augmentation provided control for all higher frequency aircraft disturbances; therefore, the higher-frequency pilot elevator response to the turbulence was eliminated with the RSSAS.

Authority-Limiting — The maximum observed augmentor elevator command did not exceed 0.07 radian (4^o) except during the thrust change of the go-around maneuver. With the authority limit set to 0.035 radian (2^o),

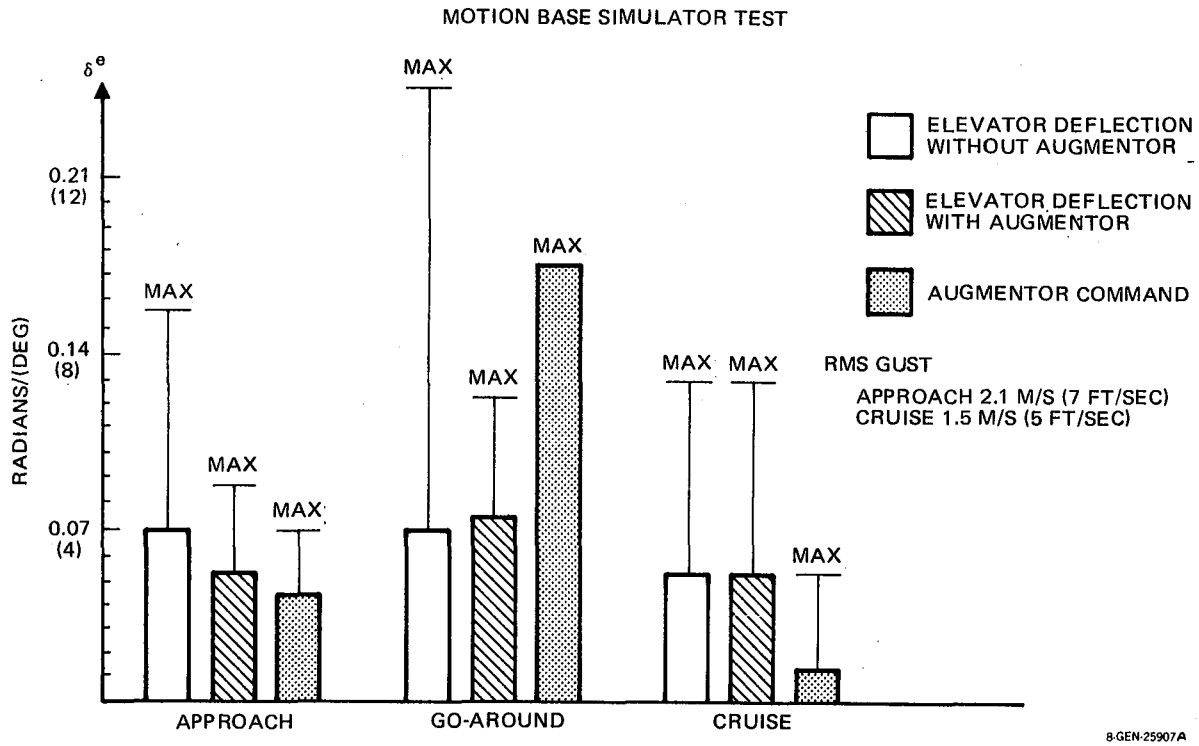

FIGURE 3-14. ELEVATOR DEFLECTION IN MODERATE TURBULENCE

no noticeable degradation in performance was observed and the pilot flying qualities ratings were unchanged. Authority-limiting during go-around had the effect of allowing more of the natural pitching moment due to the thrust change. At the 0.035-radian (2^o) limit, the pitch-up during go-around was significant but not objectionable. Some pilots, in fact, preferred the positive pitch-up in this situation. With no augmentation, however, the go-around pitch-up requires immediate and constant pilot attention. This would indicate that the amount of lead in the initial augmentation command is more important than its authority for this condition.

Ground-Air Transition — One of the "point" design conditions to be evaluated was the ground-air transition. This is of interest since it is a situation where the augmentation system may not have sufficient aerodynamic data with which to make its necessary calculations. This is due to the fact that the augmentation system, upon engagement, has synchronized to the conditions of a trimmed aircraft. The aircraft, however, makes a large positional and dynamic change in order to establish a trimmed flight path.

The ground-air transition was accomplished by making a touch-and-go maneuver out of a landing sequence. During the first test, the augmentor was allowed to continuously compute and control during the landing, ground roll, and liftoff. The result was a large nose-down elevator command out of the augmentor after rotation. What had actually happened was that the RSSAS autotrim had continuously run nose-down during the ground roll in response in the augmentor elevator command to maintain the approach trim conditions.

The solution to this problem was to synchronize the augmentor during the ground roll and then again allow control at landing gear liftoff. With this mechanization, the augmentor provided the proper control for all subsequent ground-to-air tests. No additional time delays after liftoff were judged necessary in order to allow the aircraft time to settle on a trimmed condition.

SECTION 4
RELIABILITY AND SAFETY CRITERIA AND ANALYSIS

4.1 Baseline and Criteria

4.1.1 System Definition

DC-10 Baseline. — The reliability goals established for the EET stability augmentation system are based on comparable DC-10 systems capability. The addition of a totally new and somewhat complex system impacts the aircraft flight control system and it is on this level that the goals and comparisons have been made. The flight control system evaluated includes the primary control components (surfaces, actuators, cables and controllers), the flight guidance systems (automatic controls, dampers and limiters) and primary sensor systems (attitude, air data, etc.). Simplified schematics of the DC-10 system components are presented in Figures 4-1, 4-2, and 4-3.

Items Considered. — Using the DC-10 master component list, more than 240 components were identified as significant to consider in the reliability study. Appendix 3 provides a list of these items identified by name and ATA Code number. The EET components are in most cases similar to or identical to those used on the DC-10.

Major Differences. — The major differences are in (1) the flight guidance system where a greater degree of functional integration is used, (2) the primary control elevator and stabilizer trim actuation, and (3) the addition of the augmentation system.

4.1.2 Reliability Data Source. — The quantitative DC-10 reliability has been determined using in-service data recorded by Douglas. The Douglas DC-10 data base includes over 2-1/2 million flight hours by major domestic and foreign airlines. All operational and maintenance actions are recorded and itemized to the specific aircraft component. The specific desired system and component reliability data may be manipulated and extracted with the use of the Douglas computer program THESYS.

THESYS is a computerized data management system. It has been specifically tailored for storage and retrieval of component failure data gathered from

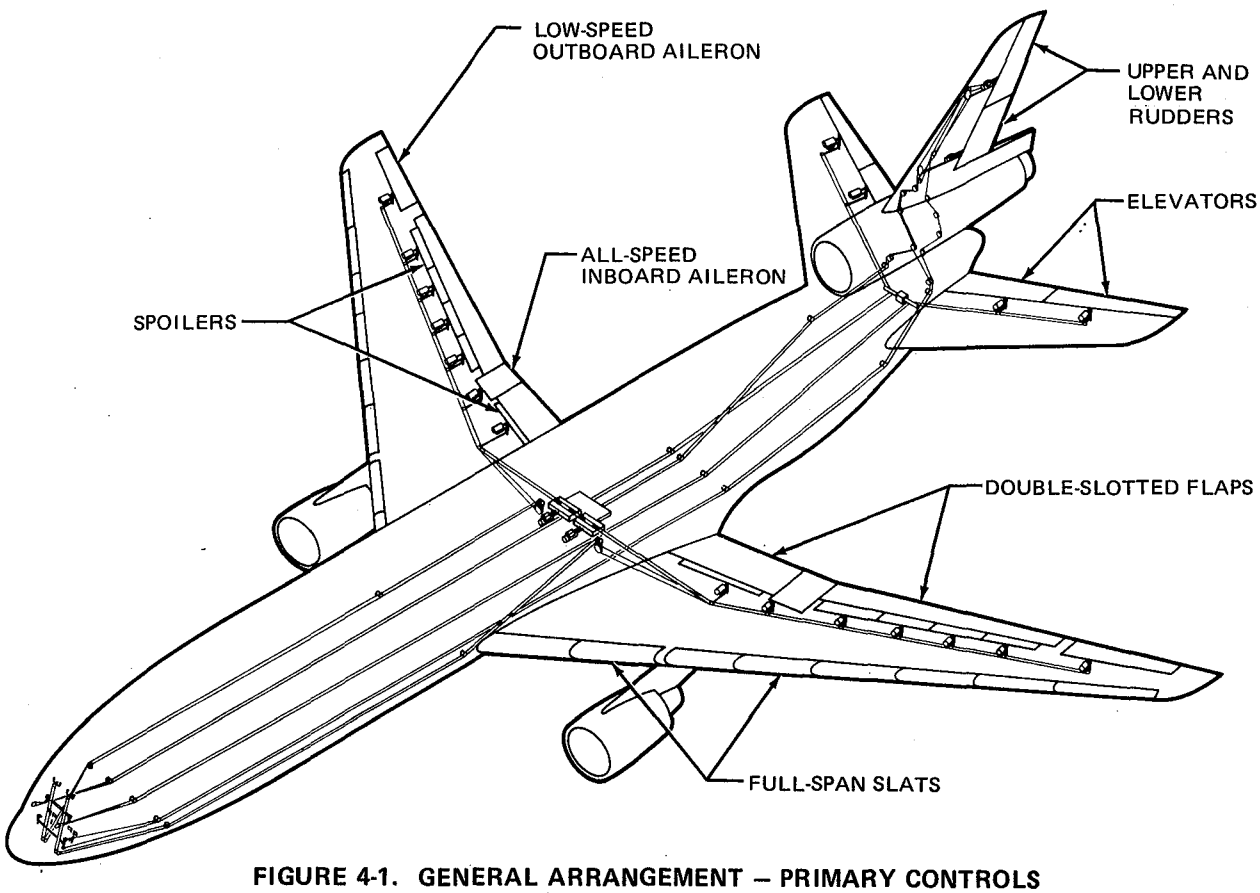

FIGURE 4-1. GENERAL ARRANGEMENT – PRIMARY CONTROLS

commercial airline service. More than a file maintenance program, THESYS is a complete software package providing the create, update, and query functions, report generation programs, and special purpose programs necessary to support our data requirements. THESYS was written exclusively in FORTRAN IV to provide for easy modification, updating, and to preclude obsolescence. Because comparative information is often desired on other than Douglas airplanes, THESYS was designed to provide a repository for data obtained on any commercial aircraft.

The THESYS Flow Chart (Figure 4-4) shows the path that data follows from the raw airline reports through the data system and subsequently to various output programs.

The bulk of data input to THESYS comes from monthly airline removal reports. To facilitate the processing of this data, an airline data conversion program was written. This program, when combined with airline data reformatting programs (each tailored to a particular airline's unique reporting practices), is designed to process the removal reports and update the master file with a minimum of clerical intervention.

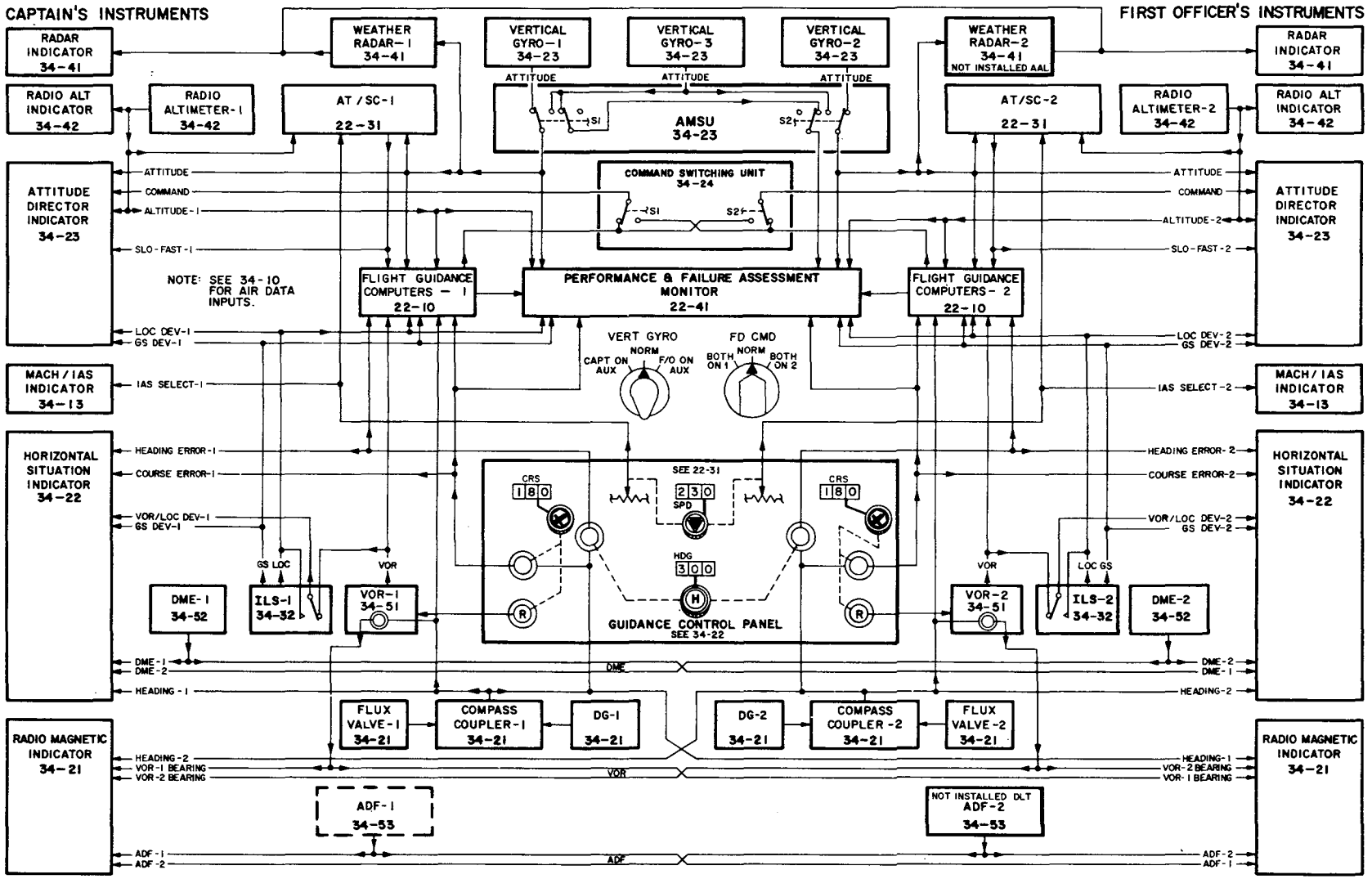

FIGURE 4-2. DC-10 FLIGHT GUIDANCE SYSTEM

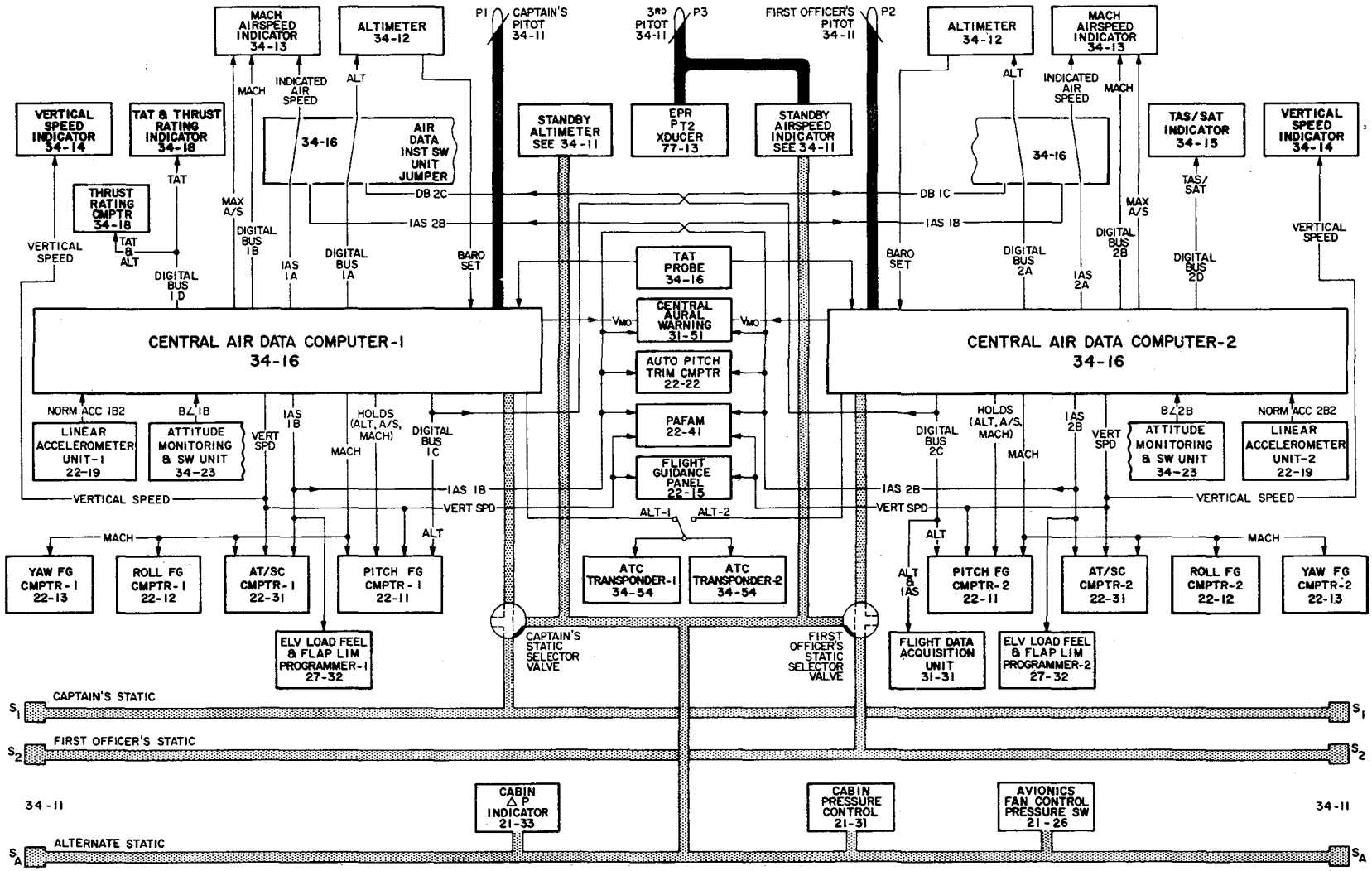

FIGURE 4-3. DC-10 FLIGHT ENVIRONMENTAL DATA

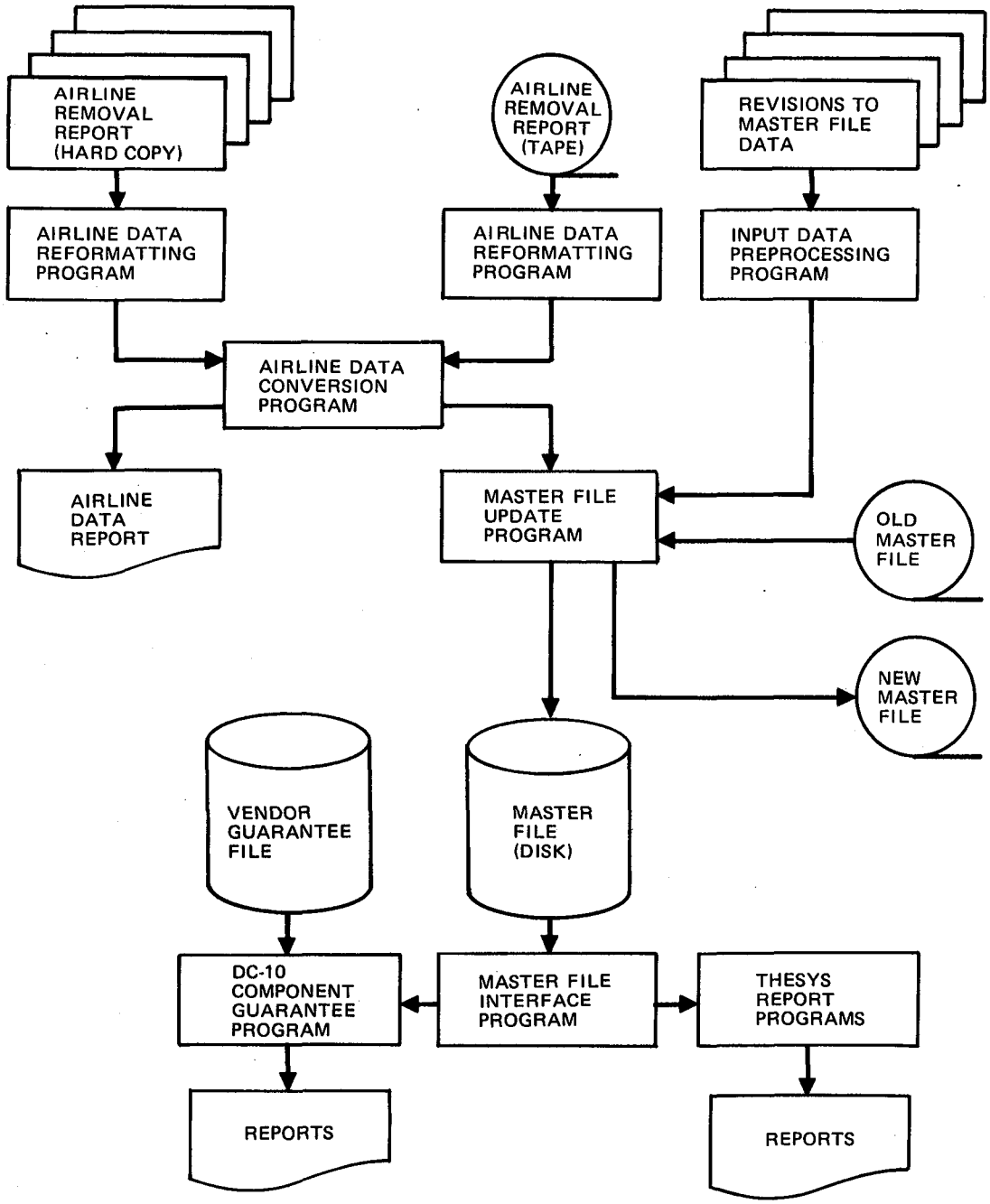

FIGURE 4-4. THESYS FLOWCHART

An example of one of the many report formats available from THESYS is shown in Figures 4-5 and 4-6 for the DC-10 Yaw Computer and Auto Throttle Speed Computer. This report provides the Mean Time Between Unscheduled Removals (MTBUR) for a selected component by airline and total fleet for a calendar year. For each month and airline, the component flight hours and removals are printed so the user is aware of the sample size and any gaps that may exist in the reports received from the airlines. The fleet MTBUR in the far right column is a three-month moving average. The component MTBUR for each airline for the year and from initial use to date is given across the bottom row. In the examples shown, these two values are the same because only one year's data was interrogated.

4.1.3 Reliability Factors of Interest. — There are primarily three reliability terms of interest in specifying the required system capability. The first is Dispatchability — the minimum capability required to begin a mission. The next is Mission Reliability — the probability the system will not cause an abort in flight. The third is Economic Reliability — the frequency of maintenance actions on the system components.

4.1.3.1 Dispatchability. — Dispatchability, the probability that a scheduled flight will not be delayed or cancelled due to equipment malfunctions, is a relatively complex conditional probability with many influencing parameters. Somewhat oversimplified, it is the combined probability of one or more faults occurring between the last takeoff and the next, and the probability these faults will be repaired in time, given that the next flight cannot dispatch with the fault existing. If it can, this changes the probability that the next succeeding flight will be delayed.

The probability a fault will occur is influenced by the length of the previous flight, condition of the aircraft system, weather, and other factors. The probability of repair in the alloted time is influenced by such things as the type of station, type of flight, ground time available, spares availability, maintenance policy and staffing. Each of these factors has a unique distribution pattern and these patterns vary from airline to airline.

To establish an average condition for this study, the Dispatchability goal was determined using a one-year data sample from 1 October 1975 through

DOUGLAS AIRCRAFT COMPANY — RELIABILITY AND SAFETY ENGRG

THESYS COMPONENT RELIABILITY REPORT

SUPPLIER	BENDIX CORP, NAV DIV	MTBUR LAST 3 MONTHS	2200
COMPONENT	COMPUTER,FLT GDNC YAW	MTBUR LAST 12 MONTHS	2355
PART NUMBER	1954094	MTBUR THROUGH DEC 1977	2355

COMPONENT FLIGHT HOURS AND UNSCHEDULED REMOVALS

AIRLINE QTY/AC	AAL 2	UAL 2	ANZ 2	ATL 2	JAL 2	KSS 2	NWA 2	VAR 2	FLEET MTBUR
JAN 77	10912 9	16866 9	5652 0	16540 7	1714 3	26708 9	10068 1	2054 0	
FEB 77	9088 7	15464 16	4880 0	15006 3	1828 1	22556 6	8670 4	1926 0	
MAR 77	9854 7	17282 5	5338 0	16530 1	2006 1	25882 16	10154 8	2044 0	2292
APR 77	9736 4	16494 7	5016 0	17630 5	2620 2	27060 6	9470 3	1784 0	2532
MAY 77	10856 12	17220 9	5114 0	18600 5	2966 2	26408 10	9026 3	1942 1	2533
JUN 77	13680 7	18632 12	4824 0	18462 1	2840 1	28634 16	9056 3	1914 1	2545
JUL 77	15374 8	20800 14	4948 4	20512 4	2384 0	30744 9	9102 2	2162 2	2350
AUG 77	15382 12	21096 17	4980 3	20026 5	2798 1	28750 3	9286 13	1986 2	2202
SEPT77	15382 8	18972 10	5108 0	19584 2	2658 0	30312 5	8732 5	2184 1	2409
OCT 77	12630 14	19108 5	5242 2	18400 6	2888 2	26594 11	8718 9	2204 0	2228
NOV 77	11394 4	18508 4	5194 2	17440 4	2626 4	32474 16	8262 9	2216 0	2413
DEC 77	12988 3	18994 8	5638 1	16750 6	2446 1	30300 13	9524 6	2104 3	2200
YRLY MTBUR	1550	1891	5161	4397	1654	2803	1667	2452	
TO DATE	1550	1891	5161	4397	1654	2803	1667	2452	

MCL 22-13-01 — DC-10-10 — RUN DATE 02/02/79

FIGURE 4-5. TYPICAL THESYS OUTPUT (FLIGHT GUIDANCE COMPUTER)

DOUGLAS AIRCRAFT COMPANY — RELIABILITY AND SAFETY ENGRG

THESYS COMPONENT RELIABILITY REPORT

SUPPLIER	SPERRY, PHOENIX	MTBUR LAST 3 MONTHS	1939
COMPONENT	COMPUTER,A/T SPEED CONT	MTBUR LAST 12 MONTHS	2427
PART NUMBER	2593342	MTBUR THROUGH DEC 1977	2427

COMPONENT FLIGHT HOURS AND UNSCHEDULED REMOVALS

AIRLINE QTY/AC	AAL 2	ANZ 2	ATL 2	JAL 2	KSS 2	NWA 2	UAL 2	VAR 2	FLEET MTBUR
JAN 77	10912 8	5652 2	16540 6	1714 2	26706 9	10068 3	16866 0	2054 1	
FEB 77	9088 3	4880 2	15006 5	1828 4	22556 6	8670 7	15464 0	1926 0	
MAR 77	9654 9	5336 1	16530 3	2006 4	25882 19	10154 9	17282 0	2044 0	2514
APR 77	9736 10	5016 2	17630 3	2620 3	27060 15	9470 9	16494 0	1784 0	2265
MAY 77	10856 5	5114 2	18600 8	2966 6	26408 10	9026 5	17220 1	1942 0	2185
JUN 77	13680 9	4824 0	18462 4	2840 8	28634 13	9056 2	18632 2	1914 0	2393
JUL 77	15374 11	4948 0	20512 6	2384 1	30744 12	9102 4	20800 3	2162 2	2598
AUG 77	15382 8	4980 2	20026 1	2798 1	28750 8	9286 1	21096 5	1986 4	2881
SEPT77	15382 5	5108 0	19564 1	2658 5	30312 8	8732 2		2184 1	3097
OCT 77	12630 6	5242 0	18400 1	2688 0	26594 19	8718 8		2204 0	2649
NOV 77	11394 3	5194 3	17440 6	2626 2	32474 11	8262 6	18508 9	2216 0	2352
DEC 77	12988 7	5638 2	16750 3	2446 1	30300 24	9524 8	18994 9	2104 3	1939
YRLY MTBUR	1712	3870	4584	804	2184	1719	4423	2229	
TO DATE	1712	3870	4584	804	2184	1719	4423	2229	

MCL 22-31-07 — DC-10-10 — RUN DATE 02/02/79

FIGURE 4-6. TYPICAL THESYS OUTPUT (AUTOTHROTTLE)

30 September 1976 which included 217,535 revenue DC-10 departures. The following data represent all events affecting departures and flights attributed to the aircraft systems being compared.

CONSEQUENCE		NUMBER	RATE x 10^{-3}
Delays	0-15 minutes	159	0.73
Delays	> 15 minutes	458	2.11
Cancellations		27	0.12
Aborts		11	0.05
Out of Service		5	0.02
TOTAL		660	3.03 x 10^{-3}

This total corresponds to approximately one event per 330 departures. A goal of $3x10^{-3}$ was thus established as a maximum acceptable delay or cancellation probability for a new configuration including the addition of RSSAS functions.

4.1.3.2 Mission Reliability. — Mission Reliability is the probability that a flight after takeoff will continue to its planned destination. It is the complement of abort probability. For the systems of interest, the DC-10 value for the probability of inflight abort is shown in the preceding table. A review of the individual aborts, however, indicates that none of the recorded aborts can be justified as required by the aircraft system or hardware state but were based on pilot judgment of the situation. The eleven aborts included in the data sample are itemized in Table 4-1. A review of these descriptions shows that a truly critical flight safety issue was not involved. Although pilot judgment will continue to produce aborts of the type listed for any new aircraft, it is anticipated that improved fault detection and monitoring should reduce the frequency by providing the crew with better information. Therefore, for the Mission Reliability we have used the goal of one abort in 100,000 flights, or a single flight abort probability of $1x10^{-5}$. This number is an interpretation of the regulatory requirements and is more stringent than the five in 100,000 derived from the data. For a further discussion on flight safety see Paragraph 4.1.4.

TABLE 4-1
REASONS FOR ABORTS

1.	BOTH ATSC COMPUTERS MALFUNCTIONED SHORTLY AFTER TAKEOFF. CAUSED STALL WARNING AND AUTO SLAT TRIP.
2.	ONE ATSC FAILED DURING OR SHORTLY AFTER TAKEOFF. CAUSED STICK SHAKER TO ACTUATE AND SLAT DISAGREE LIGHT TO COME ON WHEN FLAPS WERE RETRACTED. PULLED CIRCUIT BREAKER AND REDISPATCHED FLIGHT.
3.	RETURNED AFTER TAKEOFF BECAUSE OF ANGLE-OF-ATTACK SENSOR PROBLEM. UNABLE TO REPAIR LOCALLY SO AIRCRAFT DISPATCHED AND SENSOR REPLACED AT MAIN BASE.
4.	RETURNED AFTER TAKEOFF DUE TO ATSC FAULT WHICH ACTUATED STICK SHAKER. ATSC CIRCUIT BREAKER PULLED AND FLIGHT REDISPATCHED.
5.	NUMBER 3 HYDRAULIC SYSTEM LOST FLUID DUE TO LEAK AT A HORIZONTAL STABILIZER TRIM MOTOR.
6.	NUMBER 1 HYDRAULIC SYSTEM LOST FLUID DUE TO LEAK IN A HORIZONTAL STABILIZER TRIM MOTOR.
7.	RETURNED AFTER TAKEOFF BECAUSE HORIZONTAL STABILIZER TRIM WAS INOPERATIVE. COUPLING HAD COME LOOSE, ALLOWING QUILL SHAFT TO DISENGAGE.
8.	AFTER TAKEOFF AND FLAP RETRACTION, SELECT FLAP-LIMIT OVERRIDE LIGHT CAME ON. REPLACED ACTUATOR.
9.	NUMBER 1 HYDRAULIC SYSTEM LEAKING. FOUND LEAK AT A SPOILER SERVO.
10.	RETURNED AFTER TAKEOFF DUE TO A VIBRATION IN LEFT WING AREA. FOUND INBOARD SLAT TRAILING EDGE RUBBING ON WING SURFACE AREA. REPOSITIONED SLAT AND AIRCRAFT CHECKED OK.
11.	MACH AIRSPEED INDICATOR FAILED. AFTER INFLIGHT CONSULTATION WITH COMPANY, AIRCRAFT RETURNED AND INDICATOR WAS REPLACED.

4.1.3.3 Economic Reliability. — MTBUR is often used as an indicator of economic reliability because it indicates the frequency of maintenance actions performed on a system, and suggests the level of spares, staffing, skills, etc., required to support the system.

All of the items listed in Appendix 3 were interrogated through THESYS to determine the contribution their overall combined MTBUR has on DC-10 economic reliability. Based on this evaluation, an MTBUR of close to 70 hours was established. This means that one of the listed items is removed from a DC-10 on the average of once every 70 flight hours. Using the DC-10 as the baseline for acceptable economic reliability, the goal for the systems considered in this study was set at a total MTBUR of no less than 70 hours. The additions, deletions, and changes to the DC-10 components resulting from the study configurations were tabulated and researched to provide an estimate of the equivalent EET MTBUR.

4.1.4 Definition of Safety Factors. — Various approaches are in use among civil and military agencies for controlling the safety level of active

or augmented primary control systems. These approaches have required evaluation and reconciliation. Generally, the current status of these approaches is as follows:

(a) No special civil regulations or advisory circulars currently exist that are directed specifically at relaxed stability designs. FAR 25.671 and 25.672, together with the prevailing interpretation of 25.1309, must be extrapolated to cover relaxed stability designs with active controls.

(b) Civil regulatory agencies do not define flying qualities in the detail that MIL-F-8785 and MIL-F-9490D do, but rather relate the allowable degradation to the effect on the outcome of the flight. For example, FAR 25.671 states the airplane must be "capable of continued safe flight and landing . . . within the normal flight envelope, without requiring exceptional piloting skill or strength." This condition must prevail after any single failure or combination of failures not shown to be extremely improbable. Likewise, FAR 25.672 states that after any single failure of a stability augmentation system or other powered control system the airplane must be "safely controllable" and its basic flight characteristics must not be "impaired below a level needed to permit continued safe flight and landing."

(c) The British Civil Aviation Authority (CAA) and the European Joint Aeronautical Regulations (JAR) have published quantitative probability requirements for use in analytical safety assessment of systems. The FAA philosophy is basically in agreement with CAA Paper No. 670 and JAR 25.1309, but no official publication quantifying the probability expressions found in various FAR's has yet been issued. Figure 4-7 depicts the apparent consensus of the three organizations. The FAA is currently endorsing the view that the approximate 1×10^{-9} probability of catastrophic loss is "per flight or flight-hour."* This means that if the aircraft is exposed to the hazard for a flight

*Occasionally this has been expressed as "For each trial or hour of exposure." The interpretation is the same for both.

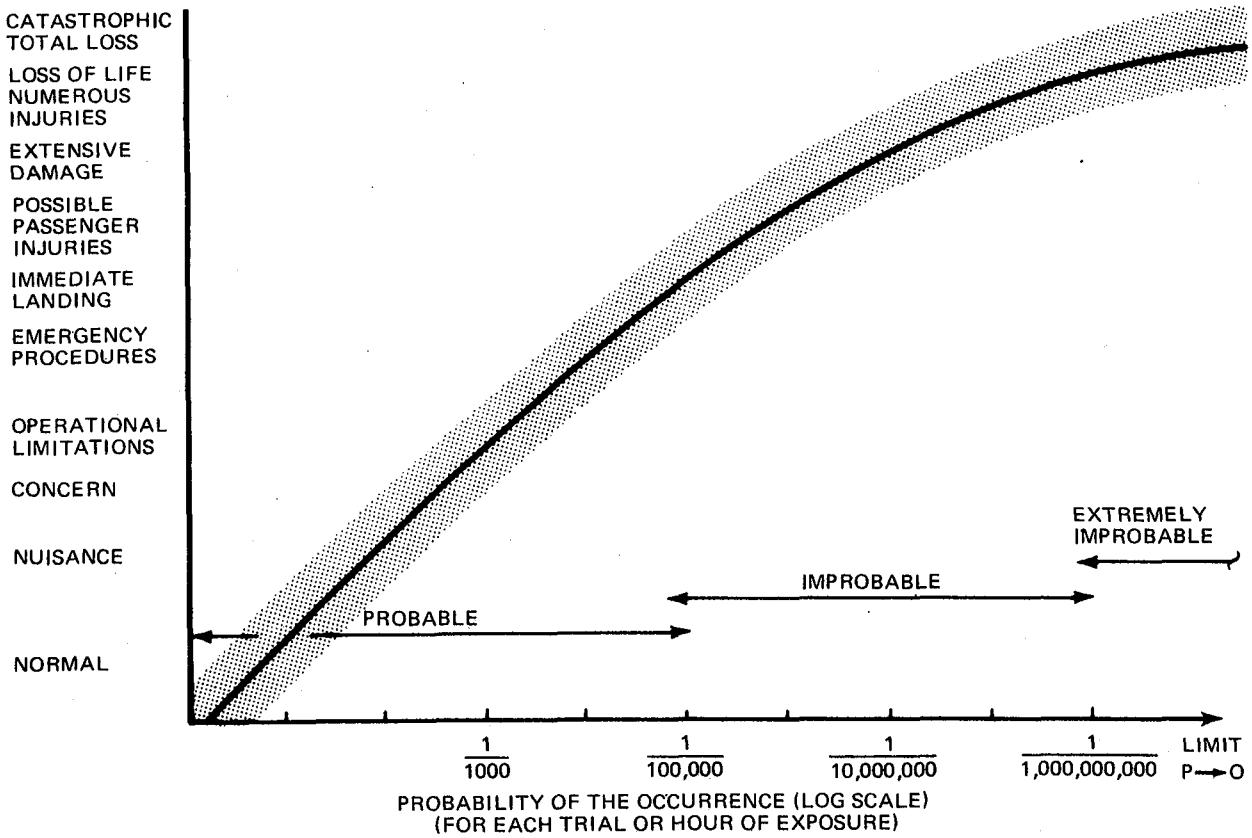

FIGURE 4-7. RELATIONSHIP BETWEEN THE CONSEQUENCE OF FAILURE AND THE PROBABILITY OF THE OCCURRENCE

duration longer than one hour, the event risk probability for a flight may be greater than $1x10^{-9}$. For additional discussion on this subject, see Appendix 4.

(d) In contrast to (a) through (c) above, the two military specifications are relatively precise in relating specific quantitative probability requirements to subjective flying quality criteria such as the Cooper Rating Scale. The military is also, understandably, somewhat more lenient in their quantitative requirements for the probability of undesired events.

4.1.5 Formulation of Safety Factors. — Figure 4-8 illustrates the various measures for rating aircraft safety as they relate to flight control systems and handling qualities. The figure attempts to correlate the civil and military quantitative risks with a suitable qualitative measure of flying quality such as the levels defined in MIL-F-9490D. The Cooper-Harper Rating, as evolved from NASA TN-D-5153 dated April 1969, is also correlated.

COOPER HARPER RATING	MIL-F-8785B FLYING QUALITIES LEVEL	MIL-F-9490D FCS OPERATIONAL STATES	JAR-25 AND CAA PAPER NO. 670 OCCURRENCE EFFECTS	PROBABILITY OF ENCOUNTERING (TRANSPORT AIRCRAFT)				LIKELY OUTCOMES
						CURRENT APPARENT OUTLOOK		
				MIL-F-8785B	MIL-F-9490D	FAA	CAA/JAR	
1 TO 3.5	1 NORMAL STATE FOR OPERATIONAL ENVELOPE	I (OPERATIONAL ENVELOPE)	NORMAL	NORMAL	NORMAL	NORMAL	NORMAL	FLIGHT PLAN OR MISSION COMPLETED
3.5 TO 6.5	2 NORMAL STATE FOR SERVICE ENVELOPE	I (SERVICE ENVELOPE) II (OPERATIONAL ENVELOPE)	MINOR	$<1 \times 10^{-2}$ PER FLIGHT	$\leq 1 \times 10^{-3}$ PER FLIGHT (FCS ONLY)	UNDEFINED	$>1 \times 10^{-5}$ PER FLIGHT OR FLIGHT HOUR	FLIGHT PLAN OR MISSION COMPLETED
6.5 TO 9	3	II (SERVICE ENVELOPE) III	MAJOR SIGNIFICANT	$<1 \times 10^{-4}$ PER FLIGHT	NOT SPECIFIED	$\leq 1 \times 10^{-5}$ PER FLIGHT OR FLIGHT HOUR	1×10^{-5} TO 1×10^{-7} PER FLIGHT OR FLIGHT HOUR	FLIGHT PLAN ABORTED; POSSIBLE INCIDENT
10	WORSE THAN 3	IV (EMERGENCY LANDING POSSIBLE)	MAJOR HAZARDOUS	NOT SPECIFIED	NOT SPECIFIED	UNDEFINED	1×10^{-7} TO 1×10^{-9} PER FLIGHT OR FLIGHT HOUR	INCIDENT OP ACCIDENT; INJURIES POSSIBLE LOSS OF LIFE
WORSE THAN 10	WORSE THAN 3	V (AIRCRAFT LOST)	CATASTROPHIC	NOT SPECIFIED	$\leq 5 \times 10^{-7}$ PER FLIGHT (FCS ONLY)	$\sim 1 \times 10^{-9}$ PER FLIGHT OR FLIGHT HOUR	$<1 \times 10^{-9}$ PER FLIGHT OR FLIGHT HOUR	TOTALLY DESTROYED; MULTIPLE DEATHS

OPERATIONAL ENVELOPE (MIL-F-8785B)

THE BOUNDARIES IN TERMS OF SPEED, ALTITUDE AND LOAD FACTOR WITHIN WHICH THE DEFINED MISSION FOR EACH FLIGHT PHASE MAY BE ACCOMPLISHED.

SERVICE ENVELOPE (MIL-F-8785B)

THE BOUNDARIES IN TERMS OF COMBINATIONS OF SPEED, ALTITUDE, AND NORMAL ACCELERATION DERIVED FROM AIRPLANE LIMITS.

FIGURE 4-8. FLIGHT SAFETY CRITERIA, COMPARISON OF CURRENT GOVERNMENT STANDARDS

Figure 4-8 is intended to stimulate discussion and generate comments from interested parties. It illustrates several points that must be reconciled in the near future. The civil agencies are, understandably, more conservative in the quantified risk probabilities for undesired events than the military. The military does, however, correlate handling qualities and envelope restrictions to quantified risk probabilities. This the civil agencies have not as yet done. Some "force fitting" of civil scales to military scales was necessary to establish an initial handling qualities scale which correlates with the civil quantified risk scale. Guidance for the correlation of the Cooper-Harper scale with the two military specifications, and the two specifications with each other, was taken from the user's guides for these two specifications.

It was necessary to identify "worse than 10" and "worse than 3" conditions because both 10 on the Cooper-Harper Scale and 3 in MIL-F-8785B are conditions from which the aircraft may be recovered to at least an emergency landing. The civil risk probability of $1x10^{-9}$ applies to catastrophic loss, which is postulated to be even worse than 10 or 3. MIL-F-9490D, State V, also implies conditions worse than 10 or 3.

Although the comparison of standards in Figure 4-8 is somewhat subjective, it does reveal uniformity of philosophy among agencies. Variations are encountered in such specifics as the level of risk, and the descriptors of a particular condition or event. Therefore it is possible to judge design configurations being considered in this study in an orderly, unambiguous manner. The quantitative scale selected is that of the more conservative civil agency, specifically the CAA/JAR scale. This is defined in more detail than the FAA scale, and aligns both with the Cooper-Harper Rating and the well-defined flying qualities scales of the two military specifications. An example of the use of the data may be offered. Since the unaugmented EET was designed to exhibit Level 2 or better flying qualities for all flight regimes, the probability of functional failure of the augmentation system should be in the area of $1x10^{-5}$ for one hour of flight.

4.2 Selected System Reliability Analysis

The RSSAS function and architecture are developed in Section 6 of this report. In this section, the reliability of those selected architectures is

analyzed with a Flight Augmentation Computer (FAC) configuration which performs only the RSSAS function and another which integrates several augmentation functions including the RSSAS. The probability of individual function loss will be shown for various mission lengths assuming a fully operative system at dispatch and then again for a minimum equipment dispatch. Compliance with safety criteria established in Paragraph 4.1.5 will be verified. Finally, the reliability of the total EET flight control system including integrated flight augmentation functions and two versions of the flight guidance system to be defined, is compared with the DC-10 reliability criteria of Paragraph 4.1.3.

4.2.1 Definition of the EET Augmentation System

4.2.1.1 Selected RSSAS Architecture. — Two candidate RSSAS architectures were selected as a result of the evaluation studies described in Section 6. They differ only in the redundancy of the Flight Augmentation Computer (FAC), one using three computers and the other only two. The triple redundant FAC configuration is shown in Figure 4-9. The dual configuration would eliminate

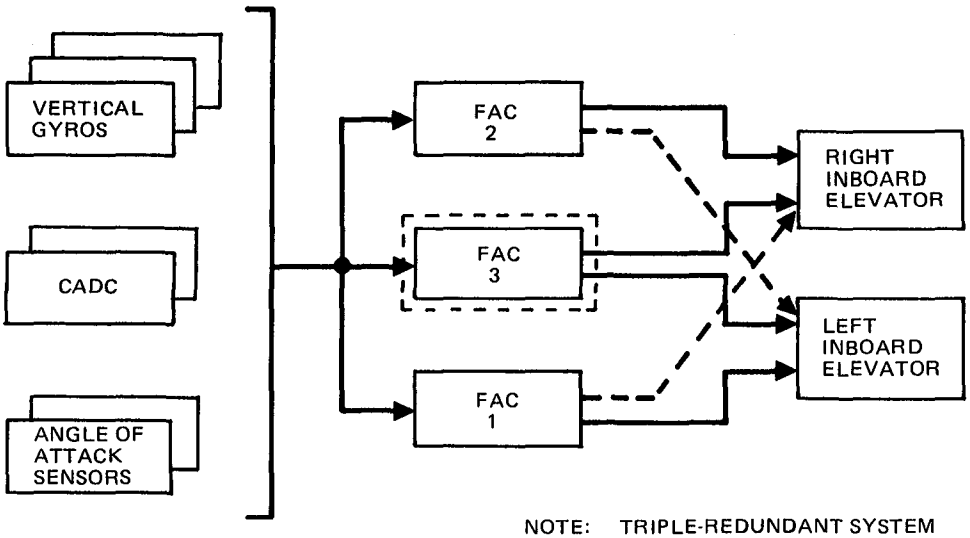

FIGURE 4-9. SELECTED RSSAS BLOCK DIAGRAM

the No. 3 FAC and rewire the elevator interface so that both inboard elevators received an input from both FACs.

The required sensor array is based upon the selection of the control law family. Pitch attitude (θ) is provided the the vertical gyros, pitch rate ($\dot{\theta}$) is obtained by differentiating the pitch signal, airspeed (u) by the air data computer, and angle of attack (α) from the angle of attack sensors.

4.2.1.2 Additional Augmentation Functions. — Additional augmentation functions were considered for integration into the FAC. These include yaw damping, elevator load feel programming, flap limiting, and stall warning. On the DC-10 these functions are spread out among several different computers as shown in Figure 4-10. Yaw damping is performed by the yaw computer which also provides the autoland flight guidance function of runway alignment and rollout guidance. Elevator load feel programming and flap limiting computation is performed by two, dual ELF/FL computers. The two Autothrottle/Speed Control (AT/SC) computers provide the stall warning calculations.

Figure 4-11 shows the integrated triple redundant flight augmentation system proposed for the EET. This configuration is expanded in Figure 4-12 to identify the individual elements to be considered in this reliability analysis.

4.2.1.3 Flight Guidance Systems. — The automatic flight control functions on the DC-10 are performed by a large complement of computers as shown in Figure 4-13. These computers are all analog and represent the state-of-the-art technology for the time period in which the system was designed. For the EET, digital technology will be used to integrate and perform these automatic control functions. As shown in Figure 4-14, two digital Flight Control Computers will replace the 10 analog computers required for the DC-10.

Reliability comparisons of the EET flight control system with that of the DC-10 baseline will consider:

(a) An EET with a DC-10 type automatic flight guidance system to establish the individual effect of the revised flight augmentation functions, and

(b) An EET with a new digital automatic flight control system to evaluate the actual expect configurations.

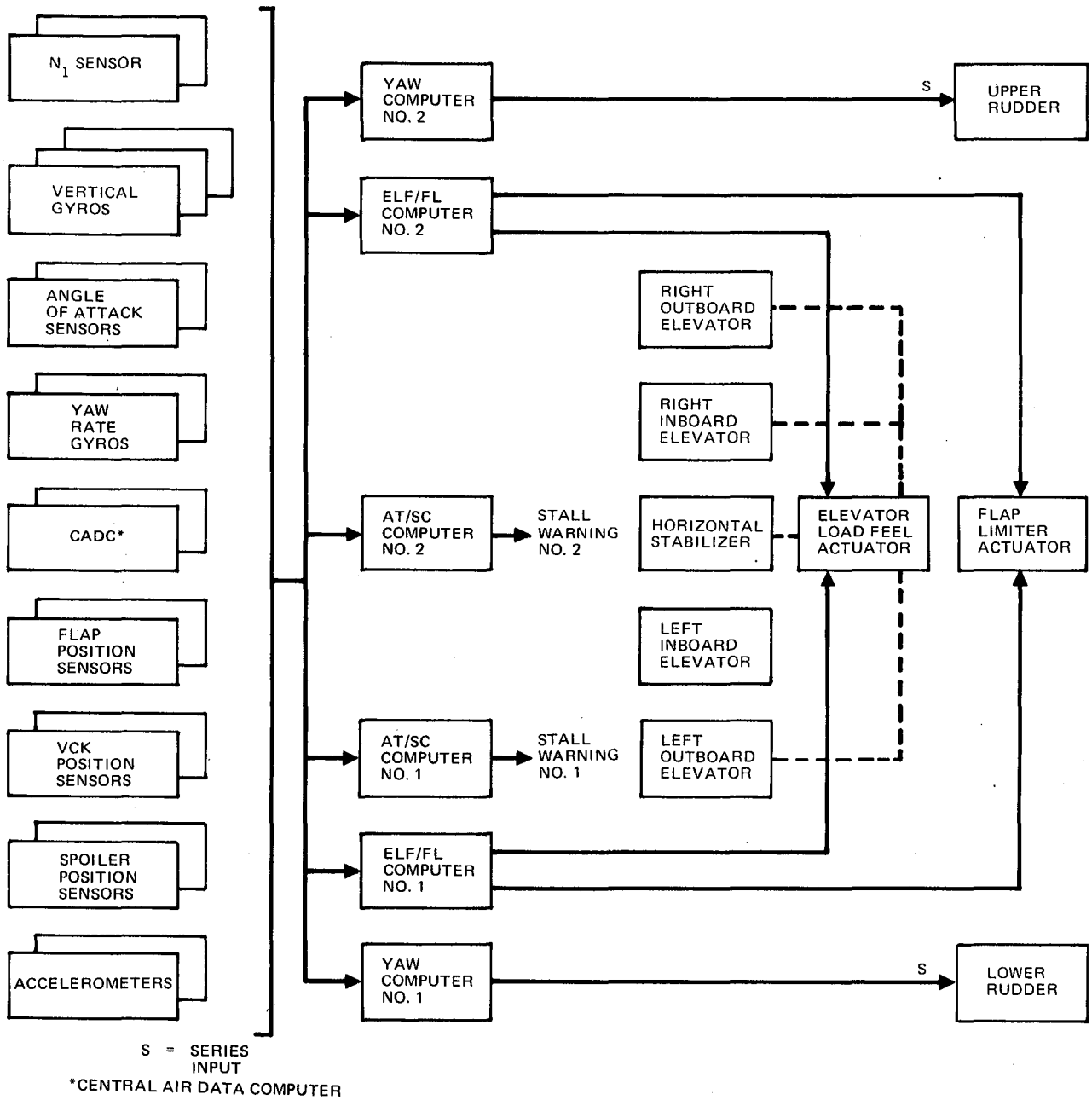

FIGURE 4-10. DC-10 FLIGHT AUGMENTATION SYSTEM BLOCK DIAGRAM

4.2.1.4 Failure Rate Data For Selected Systems. — To enable a quantitative reliability analysis of the selected configurations, failure rates are required at the appropriate level to be used in a math model of the system. Table 4-2 summarizes the failure rates derived for the 34 identified elements included in the analyses discussed in the next section. With the exception of the computer, the values were taken from current operational aircraft experience or were adjusted for changes at the element or piece-part level where

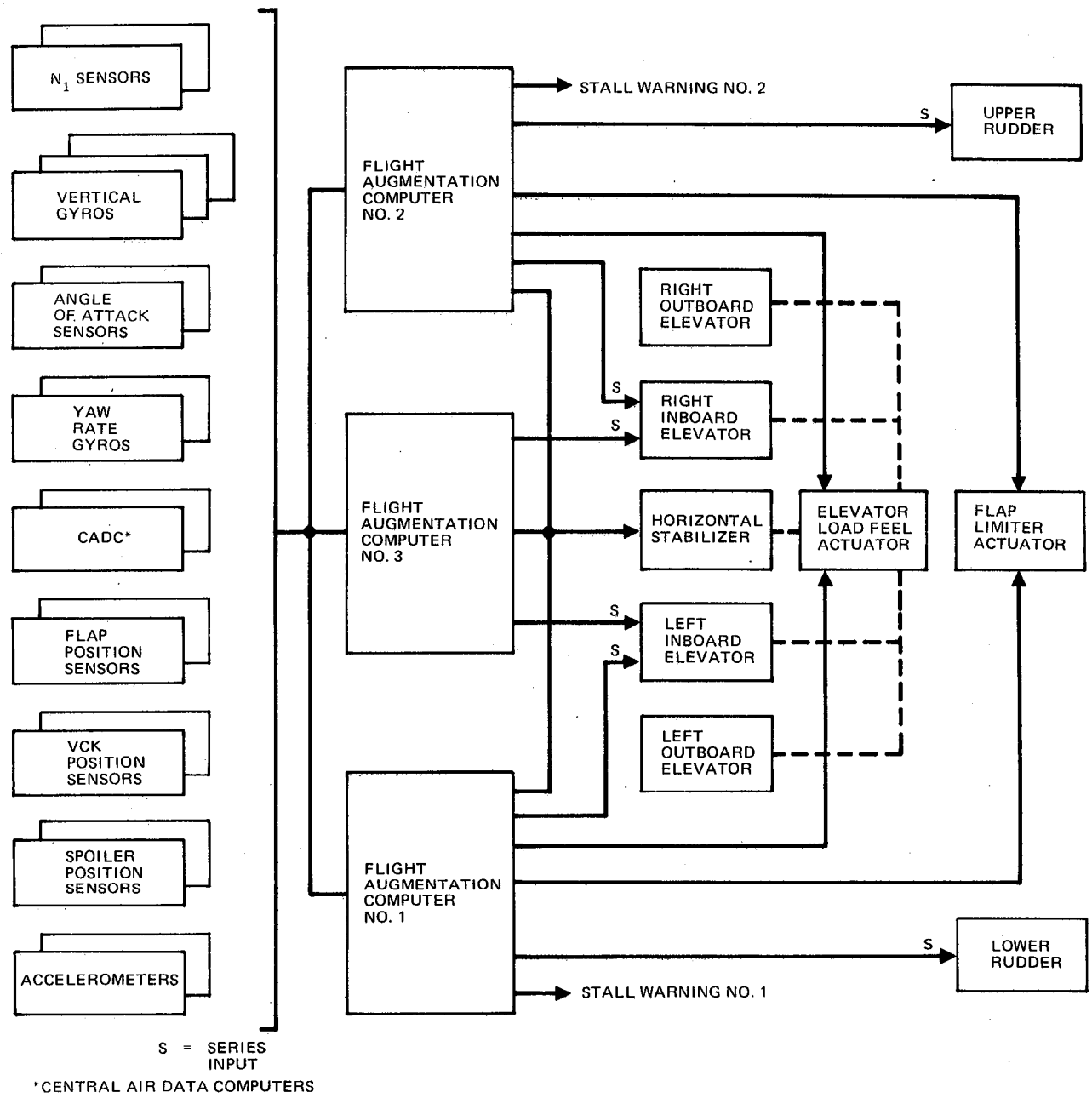

FIGURE 4-11. EET FLIGHT AUGMENTATION SYSTEM BLOCK DIAGRAM

design changes were deemed necessary for the RSSAS function or because the new computer performs the function differently from current systems.

The computer failure rates are derived from a study of digital systems currently under development such as the DC-9 Super 80 autopilot, and design level estimates provided by vendors based largely on generic sources such as MIL-STD-217B. Two sets of failure rates were used for the SCDP and CPU to account for performing only the RSSAS function or to incorporate all the other functions also. The analyses considered both cases.

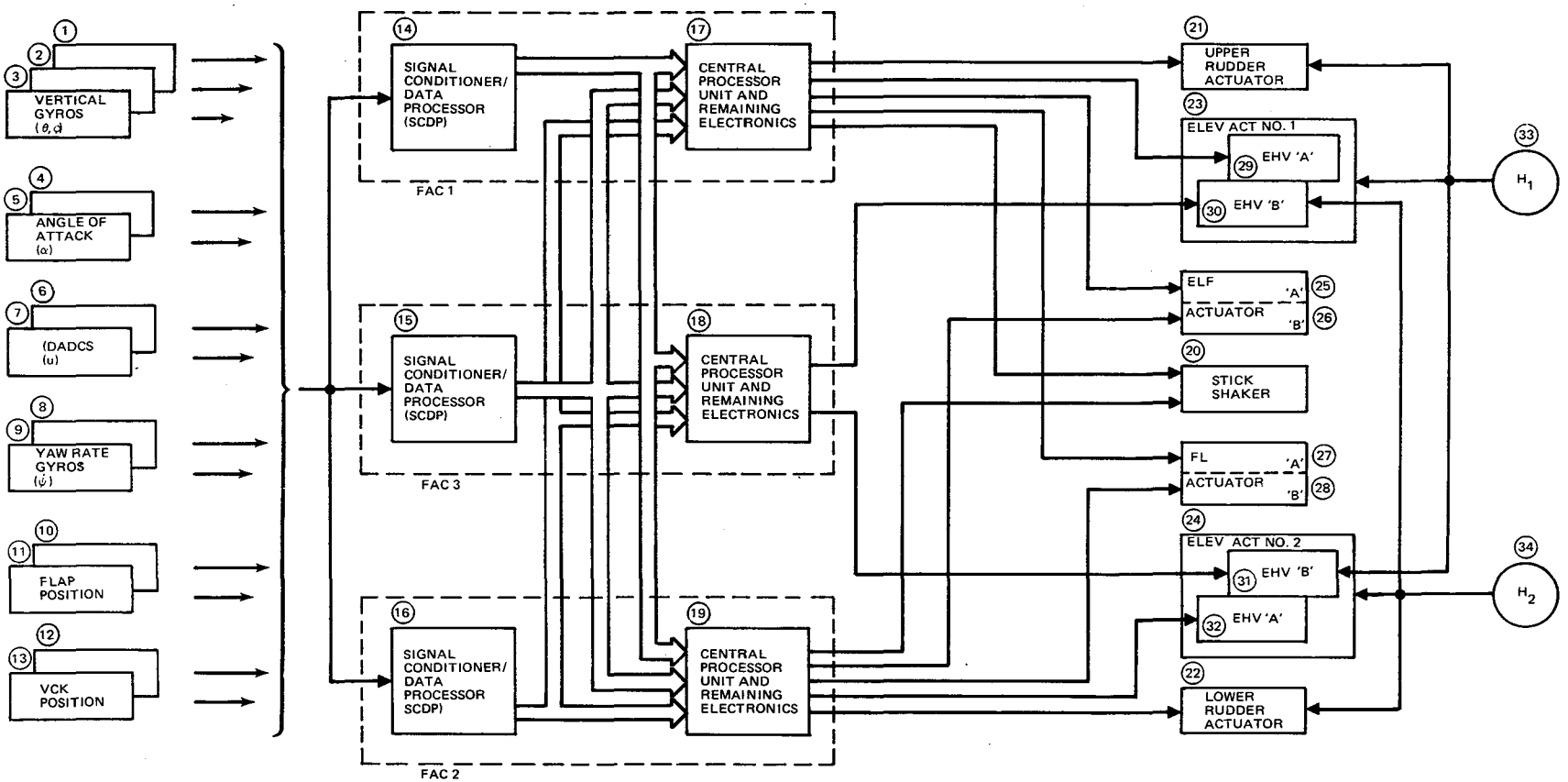

FIGURE 4-12. DETAILED INTEGRATED FLIGHT AUGMENTATION BLOCK DIAGRAM

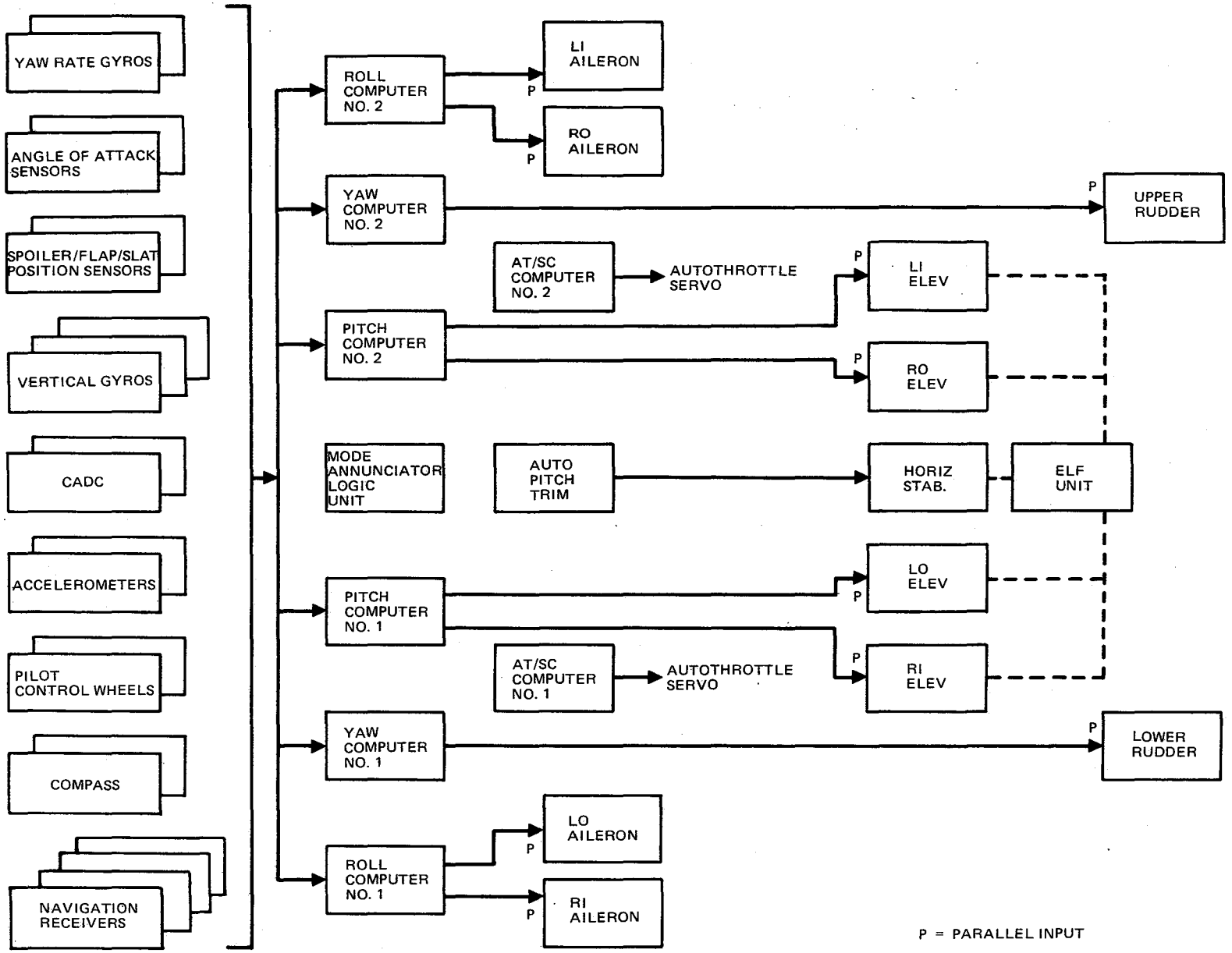

FIGURE 4-13. DC-10 AUTOMATIC FLIGHT CONTROL SYSTEM BLOCK DIAGRAM

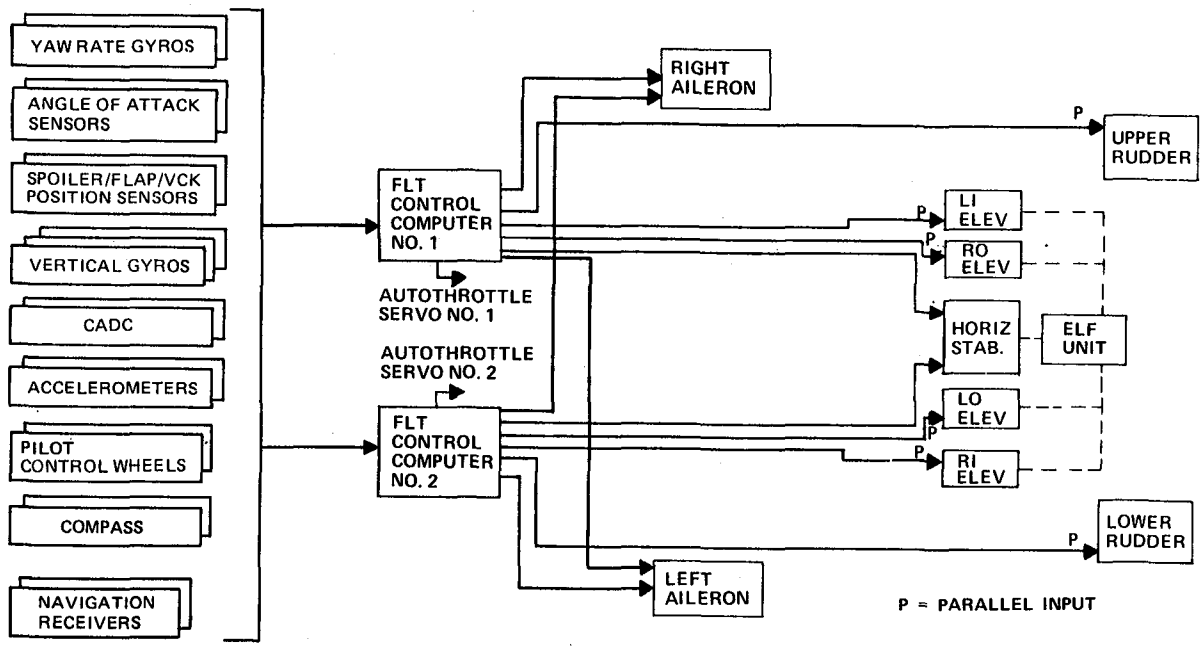

FIGURE 4-14. EET AUTOMATIC FLIGHT CONTROL SYSTEM BLOCK DIAGRAM

TABLE 4-2
FAILURE RATES FOR SELECTED SYSTEM ELEMENTS

ANALYSIS CODE NUMBER	NAME	FAILURE RATE IN FAILURES/HR	FAILURE RATE SOURCE
X1, X2, X3	VERTICAL GYROS	510×10^{-6}	CURRENT AIRCRAFT
X4, X5	AOA SENSORS	330×10^{-6}	CURRENT AIRCRAFT
X6, X7	AIR DATA COMPUTER	100×10^{-6}	IMPROVED DC-10 TYPE
X8, X9	YAW RATE GYRO	86×10^{-6}	CURRENT AIRCRAFT
X10, X11	FLAP-POSITION SENSING	2×10^{-6}	DERIVED FROM DC-10 ELEMENTS
X12, X13	SLAT-POSITION SENSING	61×10^{-6}	DERIVED FROM DC-10 ELEMENTS
X14, X15, X16	SCDP WITH ALL FUNCTIONS	80×10^{-6}	GENERICALLY DERIVED FROM STUDIES AND SYSTEMS UNDER DEVELOPMENT
Y14, Y15, Y16	SCDP FOR RSSAS ONLY	62.5×10^{-6}	
X17, X18, X19	CPU WITH ALL FUNCTIONS	260×10^{-6}	
Y17, Y18, Y19	CPU FOR RSSAS ONLY	188×10^{-6}	
X20	STICK SHAKER	2.4×10^{-6}	DERIVED FROM DC-10 ELEMENTS
X21, X22	RUDDER ACTUATION	5×10^{-6}	MODIFIED DC-10
X23, X24	ELEVATOR ACTUATION	5×10^{-6}	MODIFIED DC-10
X25, X26	ELEVATOR-LOAD FEEL	35×10^{-6}	DERIVED FROM DC-10 ELEMENTS
X27, X28	FLAP-LIMITING	35×10^{-6}	DERIVED FROM DC-10 ELEMENTS
X29, X30, X31, X32	EHV, MOD, LVDT, AND VALVES COMBINED	9×10^{-6}	DERIVED FROM DC-10 AND VENDOR'S DESIGN DATA
X33, X34	INFLIGHT HYDRAULIC SYSTEM LOSS	15×10^{-6}	CURRENT AIRCRAFT

4.2.2 Reliability Analysis

4.2.2.1 Program Description. — The Network Reliability Analysis Model (RAM) is a computer program designed to calculate the reliability of complex systems. The program, written in Fortran IV for the IBM 370 computer, is capable of analyzing any system that can be described by a reliability logic diagram.

The inputs required to run the program include:

(a) Mission time (and total exposure time, if different)

(b) Component failure rates

(c) System success criteria.

With this information RAM systematically "fails" different combinations of components, utilizing the success criteria to determine which combinations cause system failure. The probability of each such combination is then computed (using the product rule for independent events) and these are added together to produce the total probability of system failure. To ensure that the calculations are "mutually exclusive and exhaustive" a binomial expansion method is used. That is, the model first examines all "one failure" combinations, then all combinations of exactly two component failures, and so on until all probable combinations have been examined. A simplified flow chart of RAM is given in Figure 4-15.

The success criteria are entered by means of logic equations. The use of this method is best explained by giving some examples.

Table 4-3 shows some typical system networks and the logic equations that describe the successful operation of the networks. An "and" condition is symbolized by the character "*" and an "or" condition by the symbol "+."

RAM is capable of analyzing one or several systems or system functions during the same run by entering a set of logic equations for each system function to be analyzed. This feature is of value in evaluating alternative systems and determining the effect of varying component failure rates.

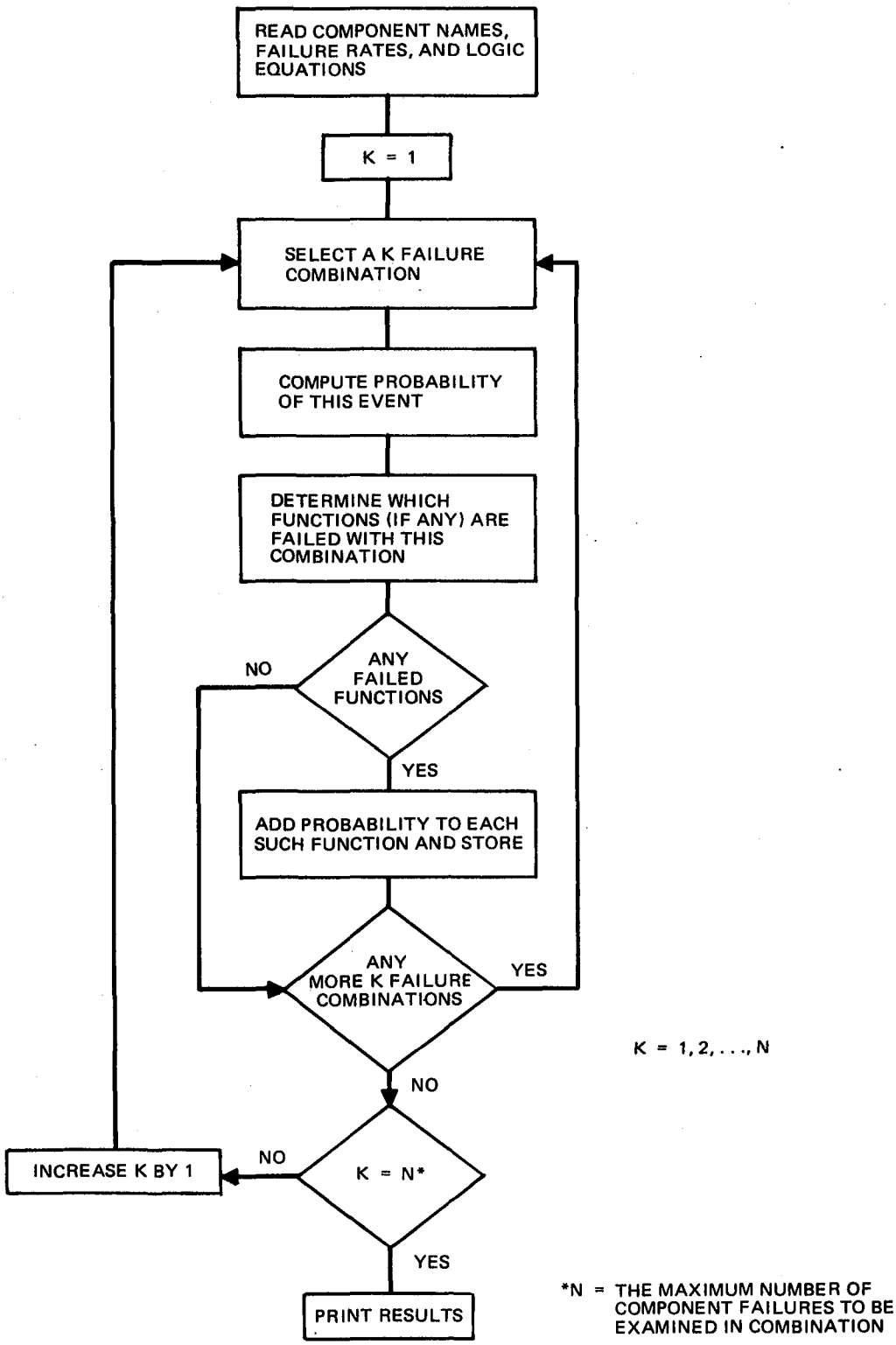

FIGURE 4-15. RAM FLOWCHART

TABLE 4-3
EXAMPLES OF RAM LOGIC EQUATIONS

LOGIC DIAGRAM	LOGIC EQUATION	ENGLISH EQUIVALENT
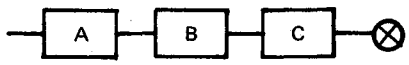 (SERIES)	S = A * B * C	THE SYSTEM(S) WORKS IF A AND B AND C WORK
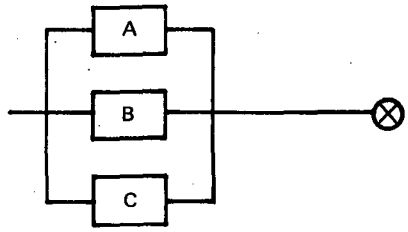 (PARALLEL)	S = A + B + C	THE SYSTEM(S) WORKS IF A OR B OR C WORKS
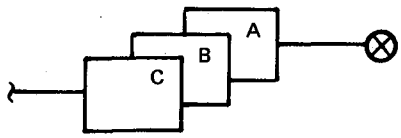 (TWO OF THREE REQUIRED)	S = A * (B + C) + (B * C)	THE SYSTEM(S) WORKS IF A WORKS AND EITHER B OR C WORKS, OR BOTH B AND C WORK
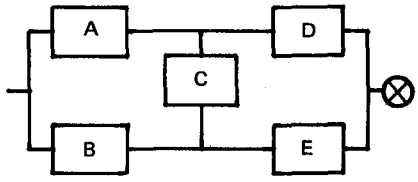 (CROSSTIE)	S = C * (A + B) * (D + E) + (A * D) + (B * E)	THE SYSTEM(S) WORKS IF THE CROSSTIE (C) WORKS AND EITHER A OR B WORKS AND EITHER D OR E WORKS, OR (IN CASE C FAILS) EITHER A AND D MUST WORK OR B AND E MUST WORK

The output from the model includes a listing of the components with their associated failure rates, and the probability of failure for each function requested. Appendix 5 provides these for some of the runs conducted in this study.

4.2.2.2 Reliability Logic Diagrams. — The reliability logic diagrams in Figures 4-16 through 4-19 are for the triple- and dual-redundant architectures discussed in Paragraph 4.2.1. The numbers in the blocks correspond to the elements listed in Table 4-2.

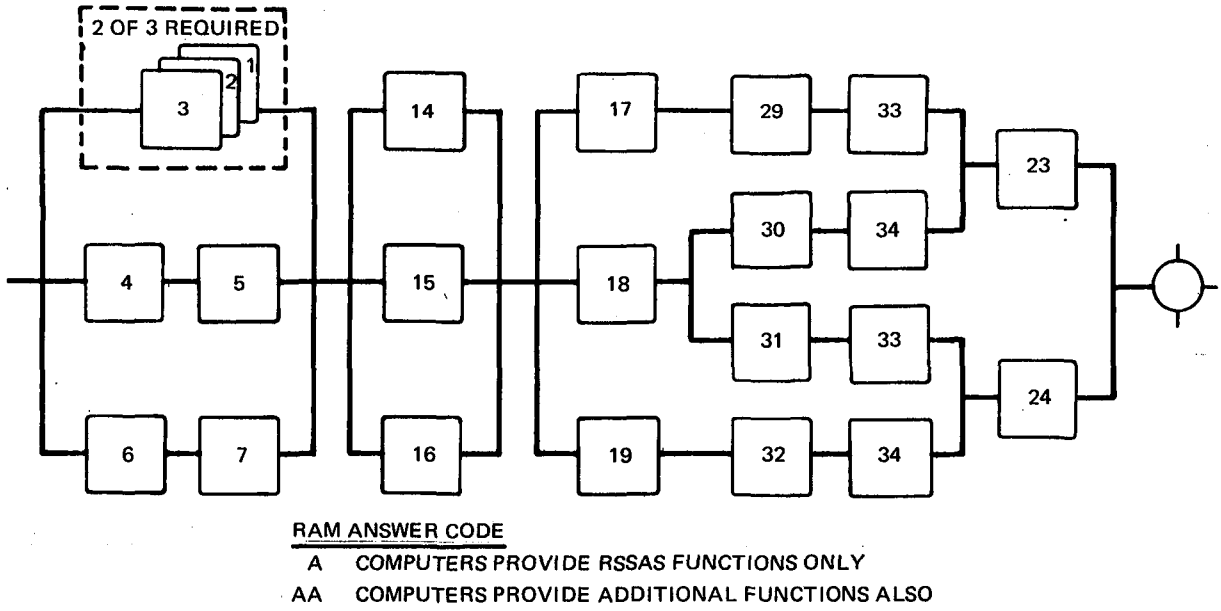

FIGURE 4-16. RELIABILITY LOGIC DIAGRAM FOR RSSAS TRIPLE-REDUNDANT COMPUTERS

Reliability logic diagrams are used to provide visual insight into the mathematical calculations performed by RAM. They illustrate the various paths available for successful performance of the function of interest as determined by the system architecture. In this sense they are usually clearer and less ambiguous than system schematics.

Each function of interest is diagramed separately although many elements are common to several functions. Wherever the same number appears in more than one block it represents the same physical element, not another like it. When identical elements are physically duplicated each is uniquely identified as indicated in Table 4-2. Thus, if an element bearing a particular identification number fails, that failure affects every location where that number is used. The RAM answer code is merely to aid correlating the computer printouts provided in Appendix 5 to the proper logic diagrams.

4.2.2.3 Functional Reliability Calculations. — The logic equations for each of the diagramed functions were entered in RAM as previously discussed. Failure rates from Table 4-2 were used and probability calculations were made for exposure times of one, two, and five hours for each of the configurations. Complete computer printouts for these runs are provided in Appendix 5.

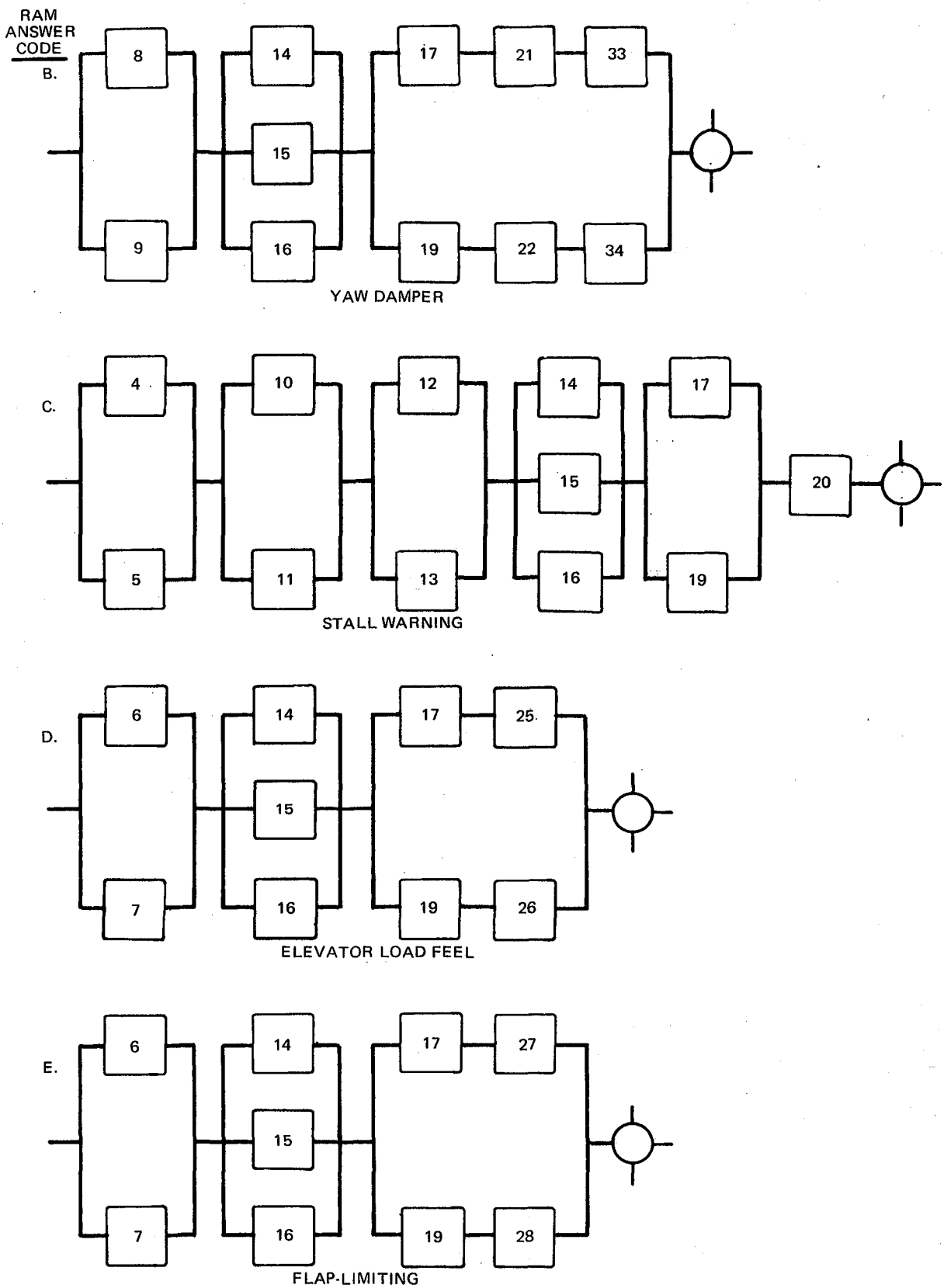

FIGURE 4-17. RELIABILITY LOGIC DIAGRAM FOR NOTED FUNCTIONS – TRIPLE-REDUNDANT COMPUTERS

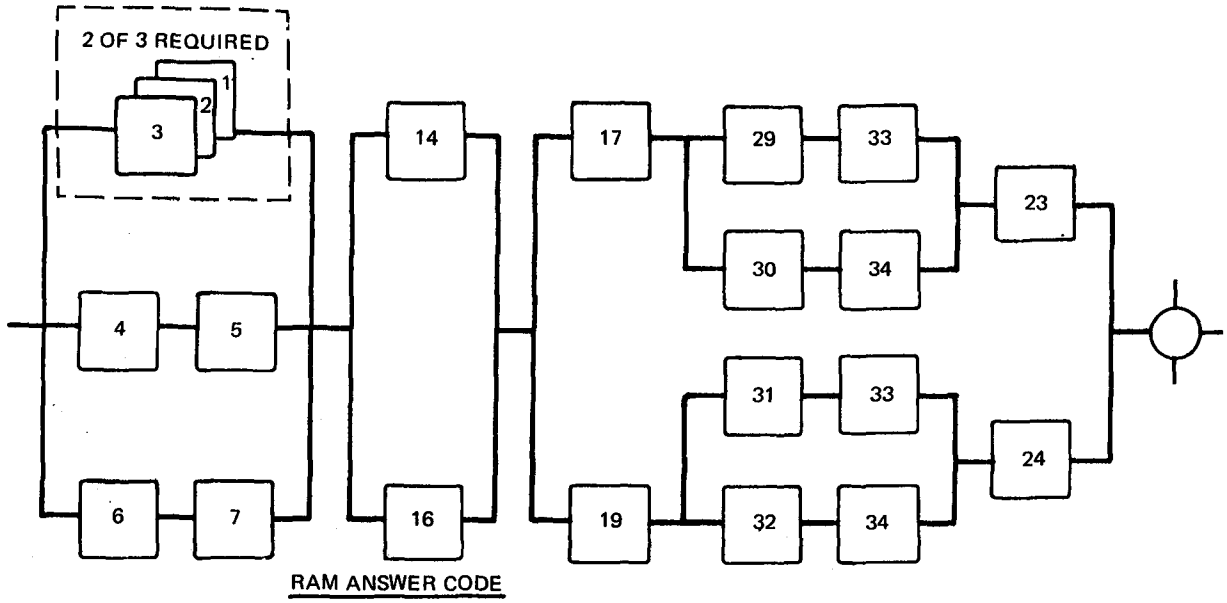

FIGURE 4-18. RELIABILITY LOGIC DIAGRAM FOR RSSAS DUAL-REDUNDANT COMPUTERS

Additionally, calculations were made for a postulated worst case minimum equipment dispatch. The aircraft was presumed to depart with all of the items listed below inoperative at the start of the flight.

One of three vertical gyros
One of two angle-of-attack sensors
One of two yaw rate gyros
One of two flap position monitors
One of two slat position monitors
One of three computers (SCDP and CPU)
One of two rudder actuators
One of two ELF actuators

Table 4-4 is a tabulation of some of the results of these analyses. Figure 4-20 is a plot of the RSSAS function failure probability versus exposure time. It illustrates the sensitivity of the configurations considered in this study to the one-hour standard discussed in Paragraph 4.1.4. Even for the worst case minimum equipment dispatch, the goal of $1x10^{-5}$ failure probability is not exceeded.

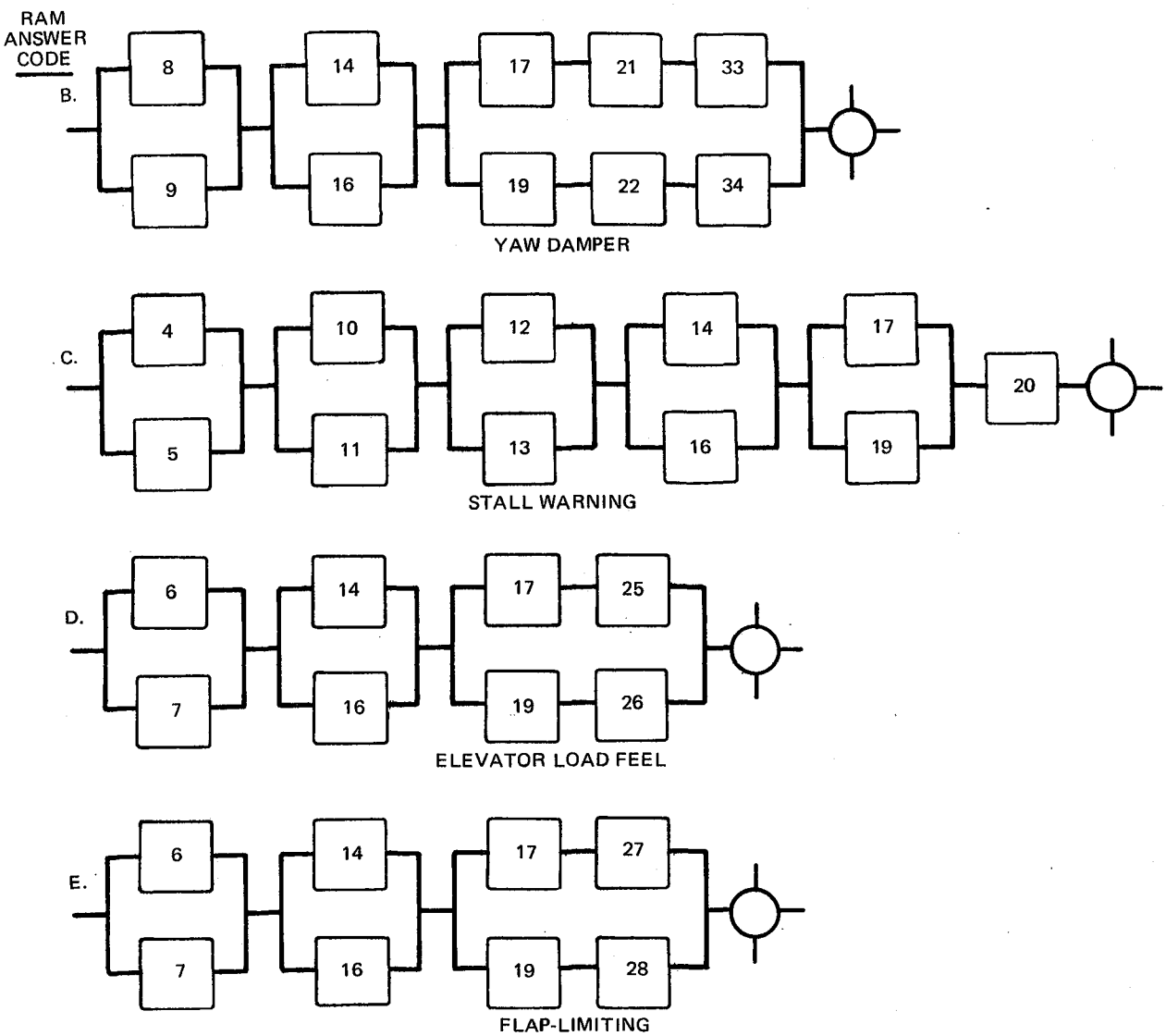

FIGURE 4-19. RELIABILITY LOGIC DIAGRAMS FOR NOTED FUNCTIONS – DUAL-REDUNDANT COMPUTERS

A further analysis was conducted to determine the reliability sensitivity of the functions with a single-selected element inoperative at dispatch. Tables 4-5 and 4-6 show the results of this analysis in terms of a multiplier to the loss probabilities calculated for "all up" dispatches shown in Table 4-4.

Finally, an analysis of the impact on dispatch delays and economic reliability was conducted. Two possibilities were considered. First, that RSSAS would be added but the baseline DC-10 flight guidance system would remain. Second, the new computers would integrate both RSSAS and FGS functions. The basis for this analysis is the components listed in Appendix 3. Those compo-

TABLE 4-4
PROBABILITY OF FUNCTION LOSS
DURING ONE-, TWO-, AND FIVE-HOUR EXPOSURES

		3-COMP CONFIGURATION				2-COMP CONFIGURATION		
RAM CODE	FUNCTION	1 HR	2 HR	5 HR	1 HR MIN DISP	1 HR	2 HR	5 HR
A	RSSAS (ONLY)	0.259×10^{-9}	1.07×10^{-9}	7.37×10^{-9}	255×10^{-9}	41.4×10^{-9}	166×10^{-9}	1030×10^{-9}
AA	RSSAS (ALL FUNCTIONS)	0.272×10^{-9}	1.18×10^{-9}	8.98×10^{-9}	294×10^{-9}	76.8×10^{-9}	307×10^{-9}	1920×10^{-9}
B	YAW DAMPER	0.858×10^{-7}	3.43×10^{-7}	21.4×10^{-7}	3660×10^{-7}	0.922×10^{-7}	3.69×10^{-7}	23×10^{-7}
C	STALL WARNING	0.258×10^{-5}	0.552×10^{-5}	1.65×10^{-5}	39.5×10^{-5}	0.259×10^{-5}	0.555×10^{-5}	1.67×10^{-5}
D	ELF	0.970×10^{-7}	3.88×10^{-7}	24.2×10^{-7}	2950×10^{-7}	1.03×10^{-7}	4.14×10^{-7}	25.8×10^{-7}
E	FLAP LIMITING	0.970×10^{-7}	3.88×10^{-7}	24.2×10^{-7}	2950×10^{-7}	1.03×10^{-7}	4.14×10^{-7}	25.8×10^{-7}
ALL	ALL FUNCTIONS	0.018×10^{-9}	0.144×10^{-9}	2.22×10^{-9}	74×10^{-9}	74×10^{-9}	296×10^{-9}	1850×10^{-9}
AAB	RSSAS AND YAW DAMPER	0.245×10^{-9}	1.06×10^{-9}	8.10×10^{-9}	85.9×10^{-9}	74.2×10^{-9}	297×10^{-9}	1860×10^{-9}

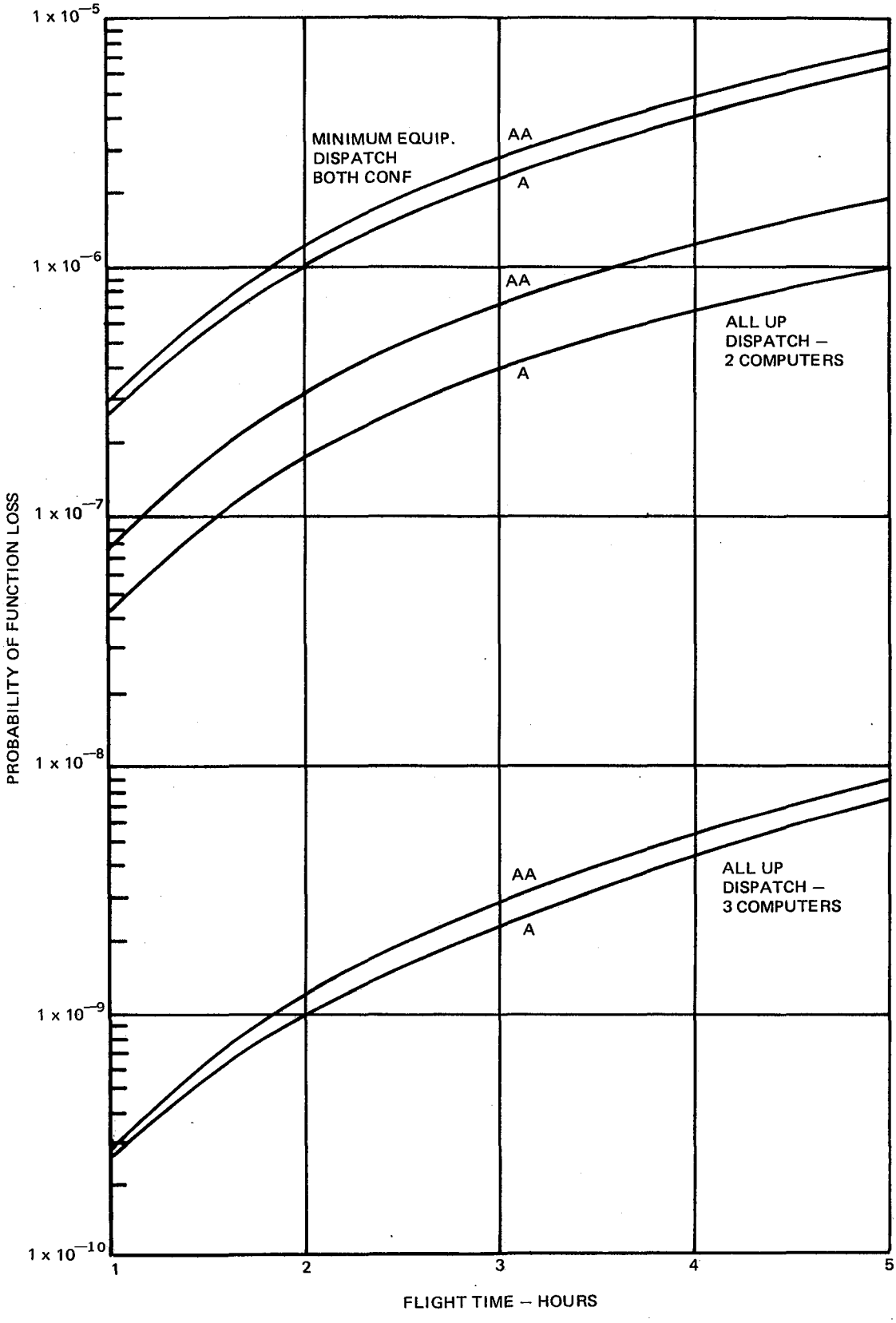

FIGURE 4-20. RSSAS FAILURE PROBABILITY VERSUS EXPOSURE TIME

TABLE 4-5
EFFECT OF VARIOUS SINGLE COMPONENTS INOPERATIVE – 3-COMPUTER CONFIGURATION

SINGLE-COMPONENT TYPE INOPERATIVE	INFLIGHT FAILURE PROBABILITY IMPACT ON:				
	ONLY RSSAS (A)	YAW DAMPER (B)	STALL WARN (C)	ELF (D)	FL (E)
VERTICAL GYRO	INSIG	NONE	NONE	NONE	NONE
A OF A	INSIG	NONE	127 TIMES WORSE	NONE	NONE
AIR DATA COMPUTER	INSIG	NONE	NONE	1030 TIMES WORSE	1030 TIMES WORSE
YAW RATE GYRO	NONE	1000 TIMES WORSE	NONE	NONE	NONE
FLAP POSITION	NONE	NONE	1.8 TIMES WORSE	NONE	NONE
SLAT POSITION	NONE	NONE	24 TIMES WORSE	NONE	NONE
SCDP AND CPU (1 OR 3)	173 TIMES WORSE	3255 TIMES WORSE	100 TIMES WORSE	3093 TIMES WORSE	3093 TIMES WORSE
SCDP AND CPU (2)	158 TIMES WORSE	INSIG	INSIG	INSIG	INSIG
STICK SHAKER	NONE	NONE	CRITICAL	NONE	NONE
RUDDER ACTUATION	NONE	3255 TIMES WORSE	NONE	NONE	NONE
ELEVATOR ACTUATION	20,000 TIMES WORSE	NONE	NONE	NONE	NONE
ELEVATOR LOAD FEEL ACTUATION	NONE	NONE	NONE	3093 TIMES WORSE	NONE
FLAP LIMITER ACTUATION	NONE	NONE	NONE	NONE	3093 TIMES WORSE
EHV, MOD, LVDT AND SOV (COMP 2)	16 TIMES WORSE	NONE	NONE	NONE	NONE
HYDRAULIC SYSTEM	60,000 TIMES WORSE	3255 TIMES WORSE	NONE	NONE	NONE
EHV, MOD, LVDT AND SOV (COMP 1 OR 3)	157 TIMES WORSE	NONE	NONE	NONE	NONE

THIS TABLE ILLUSTRATES THE FAILURE PROBABILITY SENSITIVITY OF FUNCTIONS WITH SELECTED COMPONENTS INOPERATIVE FOR THE TOTAL FLIGHT. IT REFLECTS THE RELATIVE IMPORTANCE OF THESE COMPONENTS TO THE FUNCTIONAL CONFIGURATIONS ANALYZED. IT SHOULD NOT BE CONSTRUED TO ENDORSE ANY SPECIFIC DISPATCH-INOPERATIVE CRITERIA.

TABLE 4-6
EFFECT OF VARIOUS SINGLE COMPONENTS INOPERATIVE – 2-COMPUTER CONFIGURATION

SINGLE-COMPONENT TYPE INOPERATIVE	INFLIGHT FAILURE PROBABILITY IMPACT ON:				
	RSSAS (A)	YAW DAMPER (B)	STALL WARN (C)	ELF (D)	FL (E)
VERTICAL GYRO	INSIG	NONE	NONE	NONE	NONE
A OF A	INSIG	NONE	127 TIMES WORSE	NONE	NONE
AIR DATA COMPUTER	INSIG	NONE	NONE	1000 TIMES WORSE	1000 TIMES WORSE
YAW RATE GYRO	NONE	934 TIMES WORSE	NONE	NONE	NONE
FLAP POSITION	NONE	NONE	1.7 TIMES WORSE	NONE	NONE
SLAT POSITION	NONE	NONE	24 TIMES WORSE	NONE	NONE
SCDP AND DPU	6038 TIMES WORSE	3913 TIMES WORSE	130 TIMES WORSE	3800 TIMES WORSE	3800 TIMES WORSE
STICK SHAKER	NONE	NONE	CRITICAL	NONE	NONE
RUDDER ACTUATION	NONE	3043 TIMES WORSE	NONE	NONE	NONE
ELEVATOR ACTUATION	120 TIMES WORSE	NONE	NONE	NONE	NONE
ELEVATOR LOAD FEEL ACTUATION	NONE	NONE	NONE	3000 TIMES WORSE	NONE
FLAP LIMITER ACTUATION	NONE	NONE	NONE	NONE	3000 TIMES WORSE
EHV, MOD, LVDT AND SOV	INSIG	NONE	NONE	NONE	NONE
HYDRAULIC SYSTEM	362 TIMES WORSE	3043 TIMES WORSE	NONE	NONE	NONE

THIS TABLE ILLUSTRATES THE FAILURE PROBABILITY SENSITIVITY OF FUNCTIONS WITH SELECTED COMPONENTS INOPERATIVE FOR THE TOTAL FLIGHT. IT REFLECTS THE RELATIVE IMPORTANCE OF THESE COMPONENTS TO THE FUNCTIONAL CONFIGURATIONS ANALYZED. IT SHOULD NOT BE CONSTRUED TO ENDORSE ANY SPECIFIC DISPATCH-INOPERATIVE CRITERIA.

nents that are replaced by new items were deleted and replaced by the appropriate items from Table 4-2. The net difference was then calculated by comparing item by item the cause for each delay in the baseline sample of 660 occurrences discussed in Paragraph 4.1.3.1, and adjusting the overall probabilities by the relative reliability of the old and new elements. Two computers were assumed required for dispatch in all four cases analyzed.

A similar approach was used to estimate the net effect on economic reliability in terms of MTBUR. The components replaced from the list in Appendix 3 by new elements had their contribution to the MTBUR subtracted out. The failure rates of the selected new items from Table 4-2 were increased by 20 percent to allow for less than perfect troubleshooting at the line level and factored into the remaining list to calculate the new total MTBUR for each configuration. The results of the delay analysis and the MTBUR analysis are given on Table 4-7.

TABLE 4-7
RESULTS OF DISPATCH DELAY AND ECONOMIC RELIABILITY ANALYSES

EVENT	BASE DC-10	*RSSAS ADDED 3-COMP CONF	*RSSAS ADDED 2-COMP CONF	*RSSAS AND NEW FGS FUNCTION ADDED	
				3-COMP CONF	2-COMP CONF
DELAYS					
0-15 MIN	0.73×10^{-3}	0.66×10^{-3}	0.89×10^{-3}	0.57×10^{-3}	0.76×10^{-3}
> 15 MIN	2.11×10^{-3}	1.99×10^{-3}	2.38×10^{-3}	1.73×10^{-3}	2.18×10^{-3}
CANCELLATIONS	0.12×10^{-3}	0.11×10^{-3}	0.14×10^{-3}	0.11×10^{-3}	0.13×10^{-3}
ABORTS	0.05×10^{-3}**	———	———	———	———
OUT OF SERVICE	0.02×10^{-3}	0.02×10^{-3}	0.02×10^{-3}	0.02×10^{-3}	0.03×10^{-3}
TOTAL	3.03×10^{-3}	2.79×10^{-3}	3.43×10^{-3}	2.43×10^{-3}	3.10×10^{-3}
MTBUR	(STUDY GOAL) 70 HOURS	76 HOURS	78 HOURS	116 HOURS	122 HOURS

*VALUES BASED ON 1-HOUR FLIGHT; NO CREDIT FOR GROUND REPAIR TIME; TWO COMPUTERS REQUIRED FOR DISPATCH.

**PILOT ELECTIVE ABORTS, NO CRITICAL FUNCTIONS LOST.

SECTION 5
CONTROL LAW DEVELOPMENT

The aerodynamic performance of the EET aircraft requires two unique control functions: relaxed longitudinal static stability augmentation, and compensation for pitch coupling to variations in engine thrust. The primary objective of this study is the development of a longitudinal control system to restore the classic commercial transport flying qualities to an aircraft with approximately zero static margin. The system referred to as the Relaxed Static Stability Augmentation System (RSSAS) must perform this task by sensing the primary control inputs and aircraft response and providing supplementary aircraft control commands. Since the EET is a derivative of the DC-10 with anticipated common airline operators, commonality of hardware, function, and flying qualities are goals of the aircraft system design. Specifically, the RSSAS control law development has been based upon (1) use of the sensor types presently available on the DC-10, and (2) duplication of the DC-10 flying qualities with regard to aircraft response to pilot control inputs. RSSAS aircraft control is accomplished primarily through the elevator surfaces. Control laws have also been developed for joint elevator and throttle control, but the added complexity of an automatic throttle augmentor will not be permitted, since elevator-only control has been successfully demonstrated.

The basic EET exhibits significant pitching moments due to thrust changes on the wing-mounted engines. While this characteristic is not a result of relaxed stability, it has a degrading effect on both the aircraft static stability and the pilots ability to stabilize the aircraft velocity. The augmentor has been developed also to provide the necessary elevator control to compensate for this pitch-thrust coupling. Two methods were identified as solutions. The first was to develop relaxed stability augmentation control laws with integral thrust-sensing and automatic throttle control. This would have a significant impact on the required system components, interfaces, and total functional availability. The second approach (which was followed) assumed that a simple thrust-to-elevator compensation could be determined for all control laws and flight conditions. This control is functionally independent of the relaxed static stability augmentation.

It is very important that large displacement or long-term elevator deflections be transferred to the horizontal stabilizer to restore the elevator authority and trim. The existing DC-10 type horizontal stabilizer trim system has been modified to provide this feature and the autotrim mechanization is discussed in detail in Section 6 of this report.

5.1 Modern Control Theory Technique

5.1.1 General Discussion. — The modern control analysis and simulation program J8QN, previously developed at Douglas, has been used to generate full-state feedback RSSAS control laws based upon EET equations of motion for six flight conditions. These control laws were developed using an implicit-model-following technique (Reference 8) in which selected feedforward and feedback gains cause the aircraft to follow a specified model as closely as possible. Figure 5-1 is an example of this model-following technique. In this example, the aircraft equations are for the cruise aft center of gravity with the EET (40 percent mean aerodynamic chord (MAC)), and the model equations are the aft center of gravity DC-10 (30.3 percent MAC). The gain matrix, M, is the resultant required gains for u,α,θ, and $\dot{\theta}$ for the elevator and throttle controls. The F matrix is the required gains for elevator and throttle commands.

5.1.2 Optimization Constraints. — Results obtained from this implicit-model-following synthesis method depend heavily upon the designer-selected weighting factor matrices, Q and R. Past experience with the method has shown that the best model-following is obtained when R is taken as a null matrix. Selecting R to be null could, in principle, lead to excessively high gain matrices. This possible problem can always be avoided in practice by realistic model selection. No problems of this sort have been encountered in the EET studies. Past experience has also shown that choosing Q to be simply a diagonal matrix, as is usually done in application of theory, leads to a matching of the high-frequency response of the model. This choice can result in totally unacceptable low-frequency-matching in some cases. A method was previously developed at Douglas which automatically selects the weighting matrix Q so that all frequencies are reasonably matched. This is done when equating the aircraft and model by multiplying by the inverse

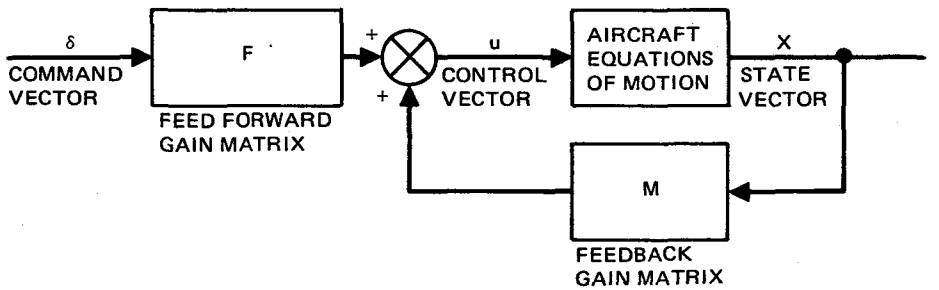

AIRCRAFT EQUATIONS

$$\dot{X} = AX + BU$$

MODEL EQUATIONS

$$\dot{X}_m = LX_m + N\delta$$

COST FUNCTION MINIMIZED

$$\int_0^\infty [(\dot{X} - \dot{X}_m)^t Q(\dot{X} - \dot{X}_m) + U^t RU]\, dt$$

NUMERICAL EXAMPLE

$$A = \begin{bmatrix} -0.004 & 0.006 & -0.0724 & -0.0412 \\ -0.247 & -0.494 & 0.986 & -0.003 \\ 2.031 & -0.64 & -0.646 & 0.0 \\ 0.0 & 0.0 & 1.0 & 0.0 \end{bmatrix} \quad B = \begin{bmatrix} 0.004 & 0.1298 \\ -0.049 & -0.003 \\ -3.925 & 1.142 \\ 0.0 & 0.0 \end{bmatrix}$$

$$L = \begin{bmatrix} -0.008 & 0.029 & -0.024 & -0.040 \\ -0.105 & -0.607 & 0.973 & -0.001 \\ -0.051 & -1.412 & -0.723 & -0.001 \\ 0.0 & 0.0 & 1.0 & 0.0 \end{bmatrix} \quad N = \begin{bmatrix} 0.001 & 0.287 \\ -0.053 & -0.006 \\ -2.387 & 0.0 \\ 0.0 & 0.0 \end{bmatrix}$$

$$X = \begin{bmatrix} u \\ \alpha \\ \dot{\theta} \\ \theta \end{bmatrix} \begin{matrix} \text{VELOCITY ERROR} \\ \text{ANGLE OF ATTACK} \\ \text{PITCH RATE} \\ \text{PITCH ATTITUDE} \end{matrix}$$

$$U = \begin{bmatrix} \delta_e \\ \delta_t \end{bmatrix} \begin{matrix} \text{ELEVATOR DEFLECTION} \\ \text{THROTTLE DEFLECTION} \end{matrix}$$

$$\delta = \begin{bmatrix} \delta_{e_c} \\ \delta_{t_c} \end{bmatrix} \begin{matrix} \text{ELEVATOR COMMAND} \\ \text{THROTTLE COMMAND} \end{matrix}$$

$$M = \begin{bmatrix} 0.075 & 0.306 & -0.025 & 0.129 \\ -0.919 & -0.022 & 0.091 & 0.020 \end{bmatrix} \quad F = \begin{bmatrix} 0.767 & 0.66 \\ 0.408 & 2.123 \end{bmatrix}$$

FIGURE 5-1. IMPLICIT-MODEL-FOLLOWING CONTROL

of L $[(L)^{-1}]$. In practice, this is done by setting $Q = (L\,L^T)^{-1}\ (|L|L^T)^{1/2}$ Modern control analysis program J8QN has incorporated these weighting factor selection features. Thus, in the present synthesis studies, the full-state feedback solutions were determined uniquely in terms of the aircraft equations of motion and the desired model equations. This method has proved to be highly successful in producing high-quality solutions for all frequencies.

5.1.3 Real-Model Following. — Although most of the EET control law synthesis studies performed have involved the implicit-model-following approach, some preliminary work has been done using a new real-model-following synthesis procedure. This real-model-following approach, shown in Figure 5-2, first generates a full-state feedback gain matrix, M, by means of a Linear-Quadratic-Gaussian (LQG) regulation synthesis. The weighting factors, Q and R, are selected by the designer so that reasonable feedback gains and closed-loop natural frequencies are obtained. These gains will usually be higher than the gains generated by the implicit-model-following approach. The new features in this approach involve the subsequent determination of a compensator model and a feedforward gain matrix which cause the command response of the system to track the desired model response. The command response tracking of this system is similar to that of the system based on implicit-model-following. Real-model-following is suggested when a reduction is required in sensitivity of the response to changes or uncertainties in aircraft parameters. In the analysis performed to date, a need for this approach has not been demonstrated; therefore, work in this area has been discontinued. Subsequent studies based on flight data may result in a renewed interest in real-model-following.

5.2 Control Law Formulation

5.2.1 Full-State Control Law Development. — The implicit-model-following synthesis technique has been employed in the current EET studies to develop full-state feedback control laws for approach and cruise flight conditions. The aircraft equations of motion employed were EET linearized three-degrees-of-freedom longitudinal equations for center-of-gravity

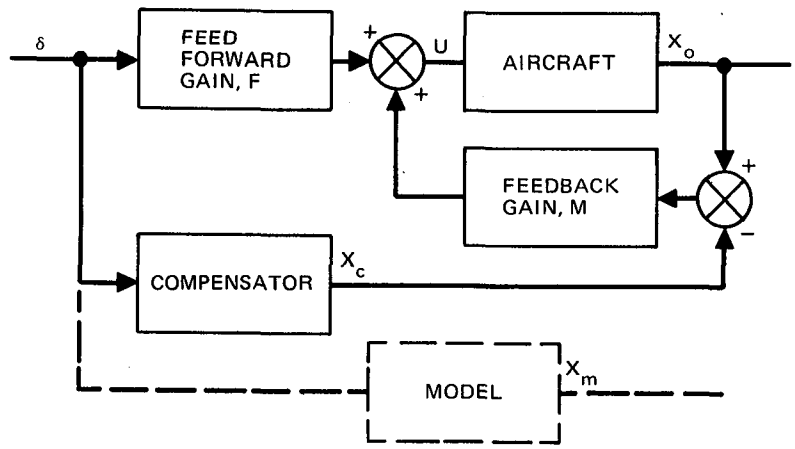

AIRCRAFT EQUATIONS

$\dot{X} = AX + BU$

MODEL EQUATIONS

$\dot{X}_m = LX_m + N\delta$

CONTROL EQUATIONS

$U = M(X - X_c) + F\delta$

COMPENSATOR EQUATIONS

$\dot{X}_c = CX_c + D\delta$

COST FUNCTION MINIMIZED

$$\int_0^\infty [X^T QX + U^T RU]\, dt$$

FIGURE 5-2. REAL-MODEL-FOLLOWING CONTROL

locations at 40- and 50-percent aft mean aerodynamic chord described with data established November 1977. The model equations employed were the DC-10 equations for comparable flight conditions, except that a center-of-gravity location of 30-percent MAC was used in all cases. Various configurations were investigated for elevator and throttle commands. Satisfactory model-tracking for elevator commands was obtained, using only elevator surface control. It was necessary to introduce a crosstie between thrust and elevator to obtain acceptable throttle command model-tracking. Thus, implicit-model-following synthesis cases were run for elevator-only control, and elevator and throttle command and control. The latter cases produced full-state feedbacks to both elevator and throttle as well as a complete command crosscoupling feedforward matrix.

5.2.2 Reduced States Control Law Development. — State-transformation and transfer-function-generating techniques previously developed at Douglas were employed to generate alternative control laws with many different sensor arrays for several approach and cruise flight conditions. These control laws were based upon the corresponding full-state implicit-model-following

synthesis. It will be shown later in this report that these control laws produce approximately the same aircraft command response. A total of 32 sensor combinations have been considered (see Table 5-1). Most of these have yielded acceptable control laws.

In the initial control law development phase, a transfer-function-generating technique was used which expressed the elevator and throttle commands in terms of transfer functions that shape the state feedbacks and pilot commands. Fewer feedbacks were required than for full-state feedback; thus, sensor configuration simplification occurred at the expense of filter complexity. Quite often the filters generated by the theory were reduced by pole-zero cancellation, and the resulting configurations were somewhat simpler than the original full-state feedbacks. A block diagram of an initial angle-of-attack control law (Law No. 5) is shown in Figure 5-3 for the approach and cruise cases. An acceptable thrust crossfeed was not obtained for the cruise cases. Block diagrams for all of these initial control laws, excluding those containing longitudinal acceleration, are presented in Appendix 6.

TABLE 5-1
CONTROL LAWS INVESTIGATED

1.	$\theta\ \dot{\theta}\ u\ \alpha$	12.	$\theta\ \dot{\theta}\ A_N\ \dot{h}$	23.	$A_X\ A_N\ \alpha$
2.	$\theta\ \dot{\theta}$	13.	$\theta\ \dot{\theta}\ A_N\ \alpha$	24.	$A_X\ A_N$
3.	$\theta\ \dot{\theta}\ \alpha$	14.	$\theta\ \dot{\theta}\ A_N\ u$	25.	A_X
4.	$\theta\ \dot{\theta}\ u$	15.	$\theta\ \dot{\theta}\ \dot{h}\ u$	26.	A_N
5.	α	16.	$\theta\ \dot{\theta}\ \dot{h}$	27.	$u\ \dot{\theta}$
6	$u\ \alpha$	17.	$A_X A_N\ \dot{h}\ u$	28.	$\alpha\ \dot{\theta}$
7.	u	18.	$A_X\ A_N\ \dot{h}$	29.	$\theta\ \dot{\theta}\ A_N$
8.	$\theta\ \dot{\theta}\ A_X\ A_N$	19.	$\dot{h}\ u$	30.	$A_N\ U$
9.	$\theta\ \dot{\theta}\ A_X\ \alpha$	20.	$\dot{h}$	31.	$A_N\ \dot{h}$
10.	$\theta\ \dot{\theta}\ A_X\ u$	21.	$A_X\ A_N\ u$	32.	$A_N\ \alpha$
11.	$\theta\ \dot{\theta}\ A_X\ \dot{h}$	22.	$A_X\ A_N\ u\ \alpha$		

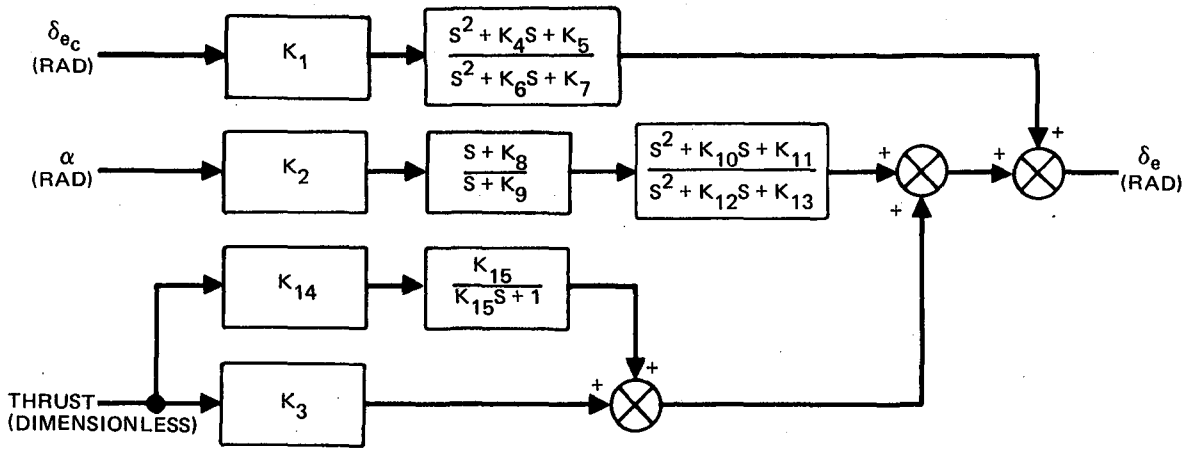

APPROACH

$K_1 = 0.6457$	$K_6 = 0.07758$	$K_{11} = -0.0008052$
$K_2 = 0.3816$	$K_7 = 0.0227$	$K_{12} = 0.07758$
$K_3 = 0.20$	$K_8 = 1.385$	$K_{13} = 0.0227$
$K_4 = 0.0356$	$K_9 = 1.80$	$K_{14} = 0.0024$
$K_5 = 0.000318$	$K_{10} = 0.0478$	$K_{15} = 50.0$

CRUISE

$K_1 = 0.51035$	$K_6 = 0.02$	$K_{11} = -0.02793$
$K_2 = 0.1195$	$K_7 = 0.004709$	$K_{12} = 0.02$
$K_3 = 0.0$	$K_8 = 1.138$	$K_{13} = 0.004709$
$K_4 = 0.05$	$K_9 = 1.64$	$K_{14} = 0.0$
$K_5 = 0.03338$	$K_{10} = -0.2198$	$K_{15} = 50.0$

FIGURE 5-3. CONTROL LAW NO. 5 (α)

Two problems that occurred with the transfer-function method are: (1) the generation of control laws that lead to unstable closed-loop poles which are cancelled by unstable zeros in the feedforward transfer function, and (2) the generation of control-transfer functions with unstable poles. The command responses still match that of the full-state configuration from which these transfer-function forms were derived, but these unstable configurations cannot be employed in a practical control system.

5.2.3 Elimination of Several Initial Control Laws. — Prior to solving the unstable pole problem, the number of control laws being investigated was reduced. Based on simulation studies, all control laws involving longitudinal acceleration (Ax) were eliminated. The Ax control laws provided acceptable response to elevator inputs but quite unacceptable response for throttle inputs. The throttle response could be made acceptable but required high-gain crossfeeds with destabilizing signs (i.e., positive feedback). With the number of acceptable control laws not requiring this high-gain crossfeed, no system degradation was obtained by the elimination of the Ax sensor. Control

laws containing altitude rate ($\dot{h}$) were eliminated, based on the statistical evaluation of the control law performance in turbulence which will be discussed later in Paragraph 5.5.1. Two control laws, 27 and 28, utilizing pitch rate but not pitch, were eliminated due to similarity of sensor source with control laws 3 and 4. Finally, control laws 13 and 32 were eliminated by the configuration studies reported in Section 6 of this report, since the selected sensor sets did not provide these combinations of sensors in the failure-reversion paths.

5.2.4 Pole Placement Synthesis. — With the number of control laws reduced from 32 to 11, an attempt was made to eliminate the unstable elements of the control laws. The transfer-function forms required placement of the shaping network closed-loop poles and also placement of open-loop transfer-function poles. All control laws were stabilized by performing a multiple-pole placement synthesis in which both sets of poles were simultaneously moved to new locations. While this method was able to eliminate the unstable elements, it did not have enough independent physical parameters which could be varied so that all poles could be place at will.

Two sets of perturbation equations (cruise and approach) were used to develop the control laws with this new technique and when the same control law forms were compared for the two flight conditions, it was noted that the filters were radically different. The combined filters were the same order, but the individual components were different. A third-order filter for approach might consist of a second-order and a first-order while the same law for cruise would be three first-order filters. Simplification and approximations for the filters was attempted, to determine if the control law would perform satisfactorily over the flight envelope. Of the eleven control laws, three were acceptable over the flight regime. Two of these were full state control laws (θ, $\dot{\theta}$, u, α, and θ, $\dot{\theta}$, u, a_n) requiring no filters and the other (θ $\dot{\theta}$ u), by coincidence, had the same filter for the two flight conditions. Unfortunately, the pole-placement synthesis could not place the poles in the same location for the two flight conditions.

5.2.5 State Space Form. — It was assumed at the beginning of the control law development that when transfer functions are used, it is undesirable to have the surface control fed back to the observer, as Luenberg's form requires

(Reference 8). This is due to noise generally present on the position feedback, as well as the consideration that a single computation may drive more than one surface and thus require some type of signal-averaging before use in the observer. The disadvantage of this form, however, is that the observer poles are distinct from the extra closed-loop poles, due to the observer. A re-examination of the control laws showed that the transfer function method expressed in state space form was closely related to Luenberger's reduced-order observer. A control form was then adopted which essentially replaced the requirement for surface-position feedback, with the control command fed back to the observer. This is a simple mechanization, since the control command is singular and totally contained within the RSSAS computer. Having adopted this form, the closed-loop poles added by the observer are the same as the observer poles. This new form requires only a single pole placement, and there are enough free parameters to permit pole location of all observer poles to desired values.

Since the control laws were now being developed in state space form rather than transfer functions, a reduction was also possible in the amount of computation required to implement the control laws. There was no reason that the observer had to generate physical states; therefore, much computation was eliminated by employing normal states instead of physical states. A computer program was then written which takes the basic Luenberger observer matrices, and a matrix which contains the observer pole placement synthesis transformation matrix, and generates all the elements needed for a difference-equation control law formulation. This program was used to generate control laws for nine configurations at both cruise and approach. The full-state feedback control laws are unaffected by the change of form. A block diagram of the control laws is shown in Figure 5-4, with the gains used for the angle-of-attack law given in Figure 5-5. Figure 5-4 applies for all control laws. Numbers for the remaining 10 control laws are given in Appendix 7.

An advantage of the present control law formulation is that the feed-forward and throttle cross-tie blocks are the same for all nominally equivalent control laws. Also, in the state space form, the filters are not only the same throughout the flight envelope, but they are also the same from control law to control law.

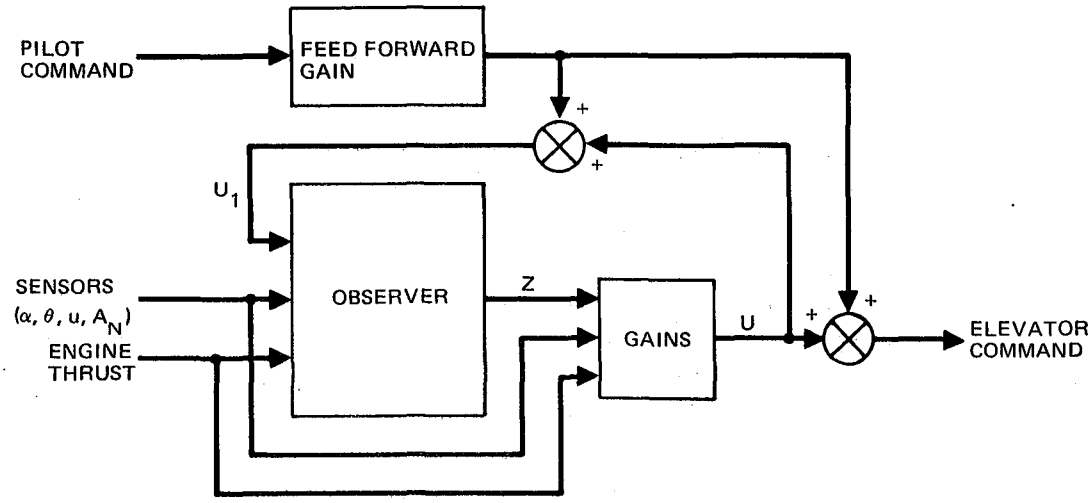

FIGURE 5-4. RSSAS CONTROL LAW BLOCK DIAGRAM

PX1 = EXP (−10.0 * DT)
PX2 = EXP (−0.8 * DT)
PX3 = EXP (−0.25 * DT)
PX4 = EXP (−0.2 * DT)

CRUISE
U1 = 0.5 * PILOT COMMAND + U
Z1 = Z1 * PX1 + U1 * (1 − PX1)
Z2 = Z2 * PX2 + (−10.8726 * U1 + 2.05745 * THRUST − 1.83644 * α) * (1 − PX2)
Z3 = Z3 * PX3 + (−79.918 * U1 + 4.31615 * THRUST − 18.297 * α) * (1 − PX3)
Z4 = Z4 * PX4 + (79.777 * U1 − 1.38494 * THRUST + 22.18449 * α) * (1 − PX4)
U = 0.01501 * Z1 + 0.15802 * Z2 − 0.1778 * Z3 − 0.14585 * Z4 + 0.21952 * α + 0.29 * THRUST
FEED FORWARD = 0.5

APPROACH
U1 = 0.674 * PILOT COMMAND + U
Z1 = Z1 * PX1 + U1 * (1 − PX1)
Z2 = Z2 * PX2 + (−7.4035 * U1 + 2.0827 * THRUST − 0.71526 * α) * (1 − PX2)
Z3 = Z3 * PX3 + (−147.064 * U1 + 46.4056 * THRUST − 7.395 * α) * (1 − PX3)
Z4 = Z4 * PX4 + (157.61 * U1 − 50.7887 * THRUST + 9.20378 * α) * (1 − PX4)
U = 0.01519 * Z1 + 0.12673 * Z2 − 0.07174 * Z3 − 0.06469 * Z4 + 0.5598 * α + 0.31 * THRUST
FEED FORWARD = 0.674

FIGURE 5-5. EET CONTROL EQUATIONS – LAW NO. 5

5.2.6 Gain Programming. — With the control laws expressed in state space form, it becomes quite simple to write programs for the numbers as a function of velocity. However, each number in the matrix has to have its own program. Some of the gains increase with velocity, while others will decrease with increasing velocity. Also, the number of gain programs per control law varies. The full-state feedback requires only six gain programs, while the angle-of-attack control law requires seventeen. The gain programming schedules for control laws 1-7 are provided in Appendix 7.

5.3 Simulation Configuration

The RSSAS control law validation and performance analysis was conducted in the Douglas DETAC (Digital Equipment Technology Analysis Center). In this facility a simulation was developed to represent the aircraft, augmenter, and necessary interfacing systems. Both perturbation and LFE (large flight envelope) aircraft aerodynamics were used, depending upon the intent of the various RSSAS evaluations.

5.3.1 Facility. — A digital computer simulation of the EET aircraft and augmentor was used to evaluate the dynamic performance of the system. The simulation was developed in FORTRAN IV, for the DETAC facility (Figure 5-6). The facility consists of:

- Central digital computer with a real-time operating system FORTRAN IV software package, 96K words of memory-mapping, cache, and floating-point hardware, plus three satellite computers, each with 32K words of memory, all connected by a high-speed communication link.
- Three interactive graphics units, one with color displays.
- Cockpit mockup.

The relationships among the major elements of DETAC are shown in the block diagram of Figure 5-7. The Sperry Univac V76 minicomputer is general-purpose and microprogrammable. A cache enhances memory access for faster operation. Three Sperry Univac V73 minicomputers provide computations and simulation support for the central computer. Peripheral support equipment includes a DEC-writer III terminal, card reader, magnetic tape, cassette tape,

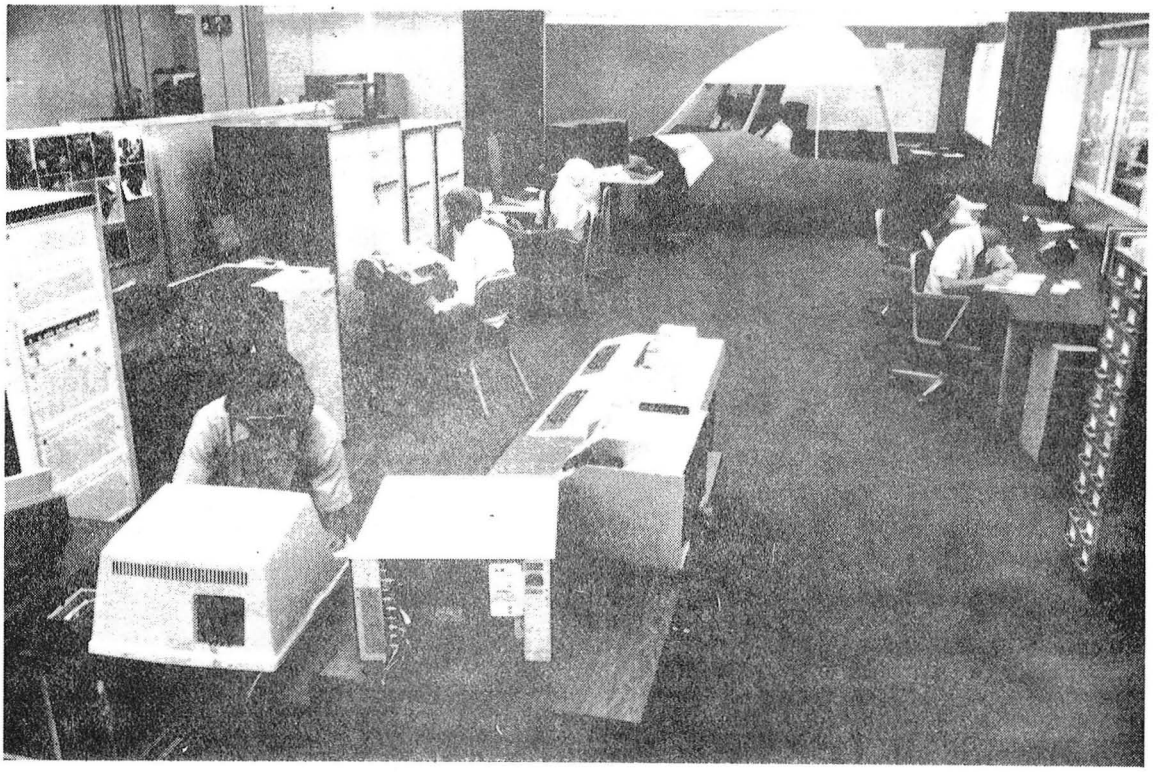

FIGURE 5-6. DETAC FACILITY

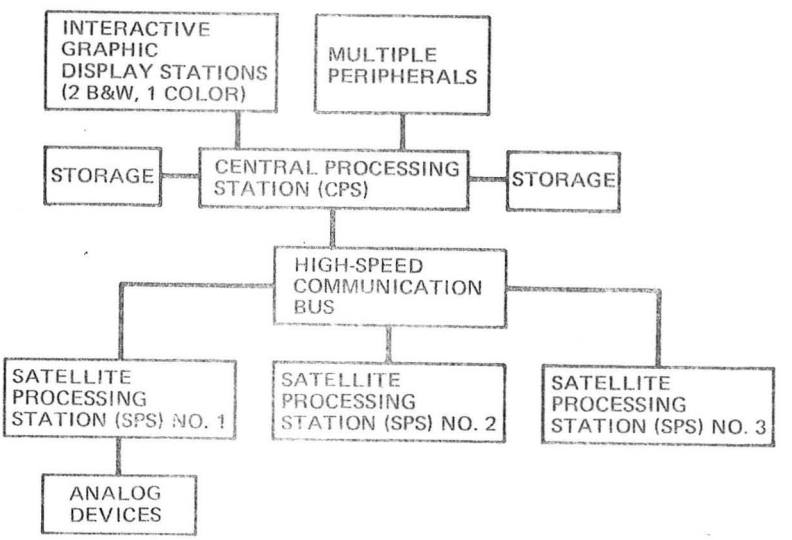

FIGURE 5-7. DETAC HARDWARE BLOCK DIAGRAM

Century Data CDS-114 disc, Infotron Vistar/GT Alphanumeric display terminal, and Varian Statos-31 printer/plotter.

The Vector General display system interacts in real time with the central computer. The graphic system has a hardware two-dimensional, rotatable-coordinate transformation generator driving two display stations, each with a 53-cm (21-inch) CRT, light pen, function-switch keyboard, and alphanumeric keyboard. The displays can be driven independently or in parallel.

Equipment for interfacing with avionics devices includes analog-to-digital and digital-to-analog converters, digital-to-synchro converters, and digital input/output modules.

5.3.2 Computer Setup. — The simulation is separated into three separate and distinct jobs: problem setup, execution, and analysis. The setup task consists of modifying the system gains, initial conditions, type of upsets, wind conditions, and other related items. Each of these inputs is easily modified by means of the light pen and alphanumeric keyboard at the graphics system. This program runs exclusively in the main machine.

The simulation task is broken down into three subtasks. Each of these tasks is then solved in one of the three computers used and any data needed by the other machines are transferred via a high-speed data link. The machines run in an asynchronous mode with the data being transferred when available. The data from the other machines are buffered so all solutions are solved with data obtained at the same time. The main machine schedules the other two machines, but after that no machine is master. The main machine solves the display portion of the problem, samples autopilot and augmentor mode switching, and transfers the time history data points from the other two computers to the disk storage device. The second computer solves the aircraft equations, generates sensor information, develops the environment, and solves the engine dynamics. The third computer interfaces with the pilot inputs, solves the autopilot, autothrottle, and augmentor equations, and simulates the actuator dynamics. The main computer completes its task 10 times per second while the other two machines run 20 times per second. Time-history data are stored twice per second. A flow chart of the simulation task is shown in Figure 5-8.

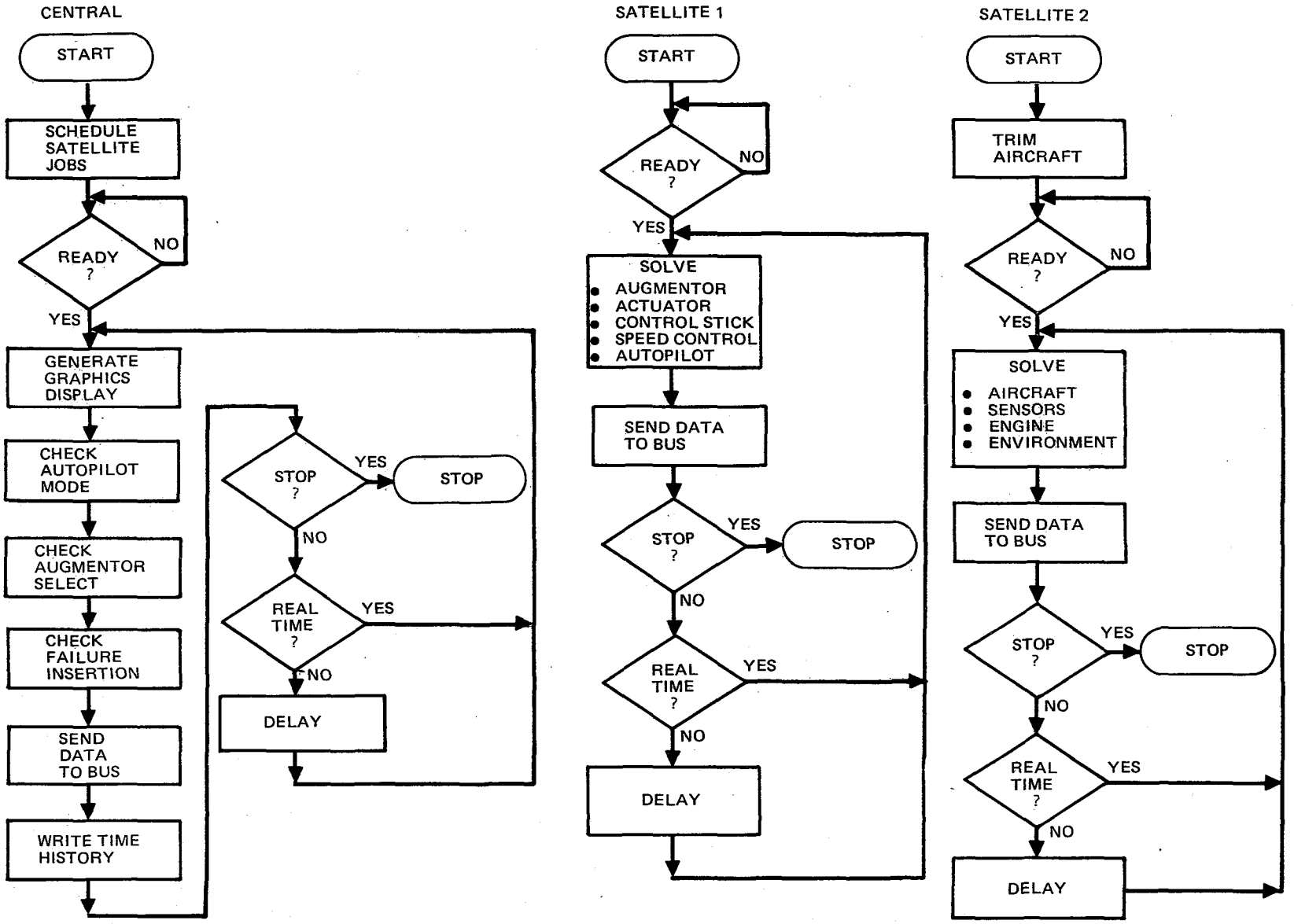

FIGURE 5-8. MULTICOMPUTER SIMULATION

While the simulation task is being solved, time-history data are written to the disk. These data are sent to the disk as rapidly as possible in whatever order and form available. The first section of the analysis task reads the data into the computer to reorder and process the data for plotting purposes. The plot program allows the analyst great flexibility. He or she has the option of plotting any of 60 parameters with any of the remaining 59 from any of four cases. Up to two parameters can be plotted on the same curve with a maximum of six curves per page. If only a section of the curve is desired, a zoom feature is supplied. Hard copy of any desirable data, of report quality, is instantaneously available. Tabulation of the data is also available.

5.3.3 System Descriptions

5.3.3.1 Aircraft. — Two aircraft simulations were developed — a perturbation aircraft and a large-flight-envelope aircraft. The perturbation aircraft is simulated as two sets of three-degree-of-freedom equations with cross-coupling terms between the sets of equations. The longitudinal equations are based upon the aerodynamic description of the EET aircraft. The lateral equations are those of the DC-10 Series 10 for a corresponding flight condition at a 30 percent center-of-gravity case. The cross-coupling terms are those of the EET. The perturbation equations are valid for large pitch changes, but allow only small changes in airspeed and angle of attack. These equations utilize linear fixed coefficients for the aircraft description. The large-flight-envelope equations were the same equations used for the motion base studies. These equations allow for large airspeed and angle-of-attack variations, valid from takeoff to landing.

5.3.3.2 Sensors.— No system lags were simulated for the aircraft sensors. The sensors were located at the proper station number for the DC-10 aircraft. Gains other than unity could be introduced for the sensors used by the augmentor, but these gain-varied signals were not utilized by the autopilot or speed command system. Multiple sensors of the same signal were not simulated.

5.3.3.3 Engines. — Two engine simulations were developed — one for the perturbed aircraft equations and one for the large-flight-envelope equations. The engine for the perturbed aircraft was simulated as a first-order lag

(time constant of 0.5 seconds) and a fixed gradient (183.5 kilonewtons per radian of throttle). The maximum thrust is limited to 169 kilonewtons per engine while the minimum thrust is 6.2 kilonewtons per engine. The large-flight-envelope engine simulation is basically the same engine with the gradient, and limits a function of the aerodynamics.

5.3.3.4 Environment. — The wind model used for the turbulence is the standard Dryden wind model. In addition to turbulence, steady-state winds or winds as a function of altitude can be added in all axes. Even though the ILS beam signals are not used for the data runs discussed in this report, nonlinear centerline representations are available for several CAT I and CAT II airports.

5.3.3.5 Actuators. — The elevator actuators (four independent actuators) were simulated as a first-order lag (time constant of 0.1 seconds) with rate (1 radian per second) and position (0.44 radians) limits. At this stage of control law verification, the hysteresis and dead-zone characteristics have been eliminated. Also eliminated were the mechanical cross-ties between surfaces. The aileron actuators (two only) were simulated the same except with different rate (0.44 radians per second) and position (0.35 radians) limits. Only one rudder actuator was simulated with the same time-constant as the other actuator, but once again different rate (0.44 radians per second) and position (0.17 radians) limits.

5.3.3.6 Pilot Interface. — The pilot interface with the simulation is by one of two methods. Either the pilot can use the soft cockpit in the DETAC facility or he may use a small joystick. The graphics provides ADI-type information plus a plan view of aircraft path for pilot interface and the augmentor monitor. Both the joystick box and the cockpit provide for elevator and aileron inputs, flap movement, pilot trim switches, gear extension, and speed brake deployment. The pilot also has control of augmentor control law select, autopilot mode, speed control engage, and failure insertion by means of the control keys connected to the graphics system. Vertical speed knob of the autopilot vertical speed mode is simulated on the joystick box.

5.3.3.7 Speed Control. — Automatic speed control is provided by means of a simulation of the standard DC-10 speed command system (see Figure 5-9).

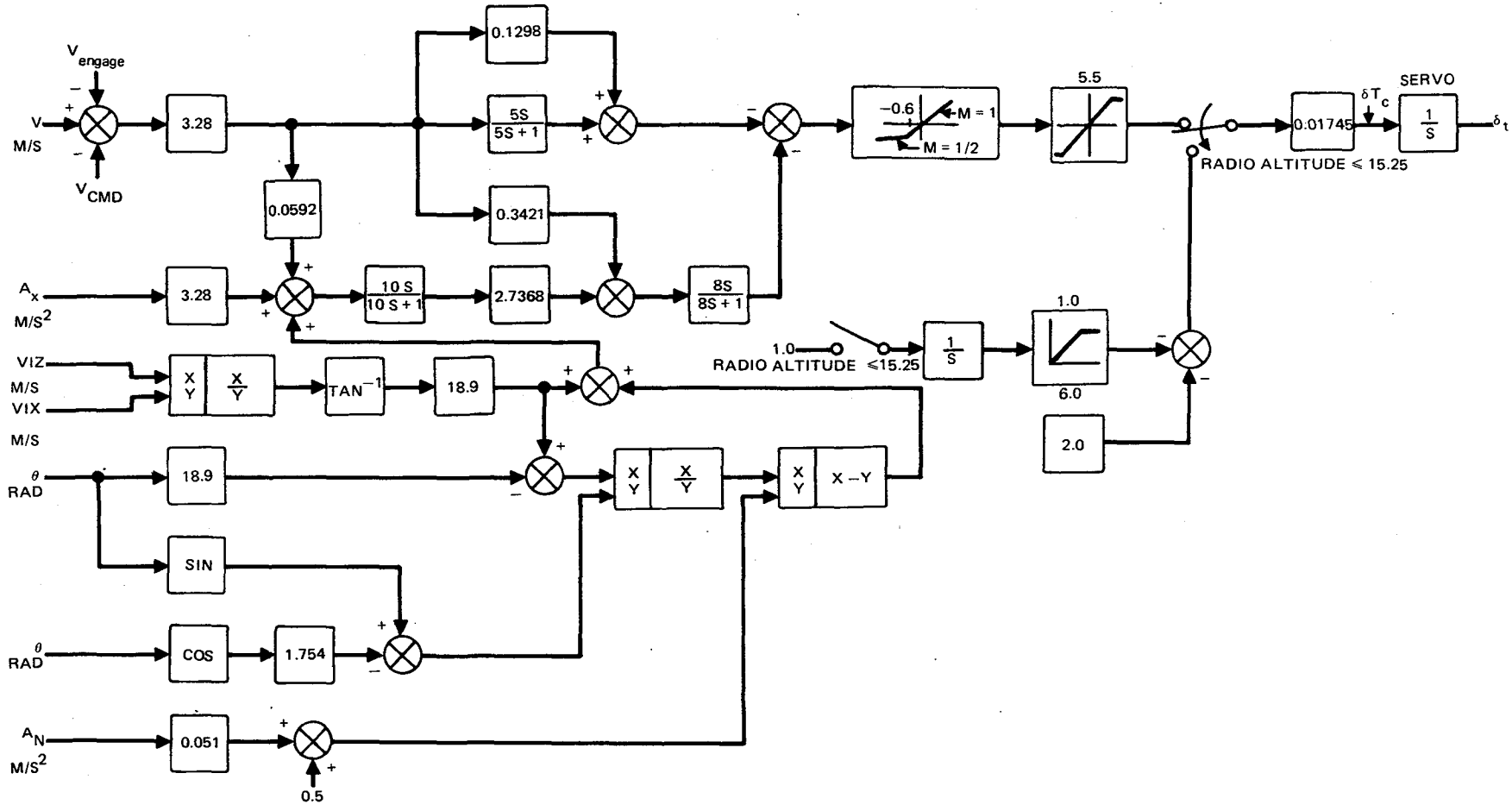

FIGURE 5-9. EET SPEED COMMAND SYSTEM

No changes have been made to the system to make it compatible with the EET aircraft. An autothrottle servo is simulated for the system and no parallel input to the joystick or soft cockpit is provided (i.e., throttle levers do not move when automatic system is engaged). The automatic system can be engaged or disengaged at any time during the simulation run.

5.3.3.8 Autopilot. — The autopilot used for this study was an experimental system developed by Douglas IRAD for the DC-10. This autopilot is valid throughout the flight regime and includes such modes as pitch hold, vertical speed, altitude preselect, altitude hold, glideslope capture, glideslope track, flare, heading hold, heading select, localizer capture, localizer track, and align.

5.3.3.9 Augmentor. — During the development of the augmentor design, each version of the augmentor was simulated. The augmentor simulated now is the final version of the design described in Section 6 of this report.

5.4 Control Law Verification

All control laws formulated were initially verified in the DETAC where time histories of the aircraft response to elevator and thrust upsets were obtained, using the perturbation aerodynamic equations. The two upsets were an elevator pulse of 0.0175 radians (1°) for one second and a step thrust change of 6.3 kilonewtons (1430 lb). The time histories were obtained at both approach and cruise flight conditions. Each of the time histories was then compared with the responses of the DC-10 which was used as a model in the control law synthesis. Each control law response was also compared with every other control law. Although all 32 original and 11 final control laws were evaluated, only the seven control laws of $\theta\dot{\theta}u\alpha$ family ($\theta\dot{\theta}u\alpha$,$\theta\dot{\theta}$,$\theta\dot{\theta}\alpha$,$\theta\dot{\theta}u$, α,$\mu\alpha$,μ) will be discussed in this section.

Figures 5-10 through 5-13 provide an insight to the basic DC-10 and unaugmented EET airframe responses to the pitch and thrust upsets. The 25 percent center-of-gravity EET is a mid center-of-gravity position and is statically stable while the 40 percent center-of-gravity EET is approximately at zero static margin. As shown, these configurations display significantly different characteristics for short-period damping, phugoid, and stability. Figure 5-14 provides a comparison of the DC-10 and augmented ($\theta\dot{\theta}u\alpha$ control

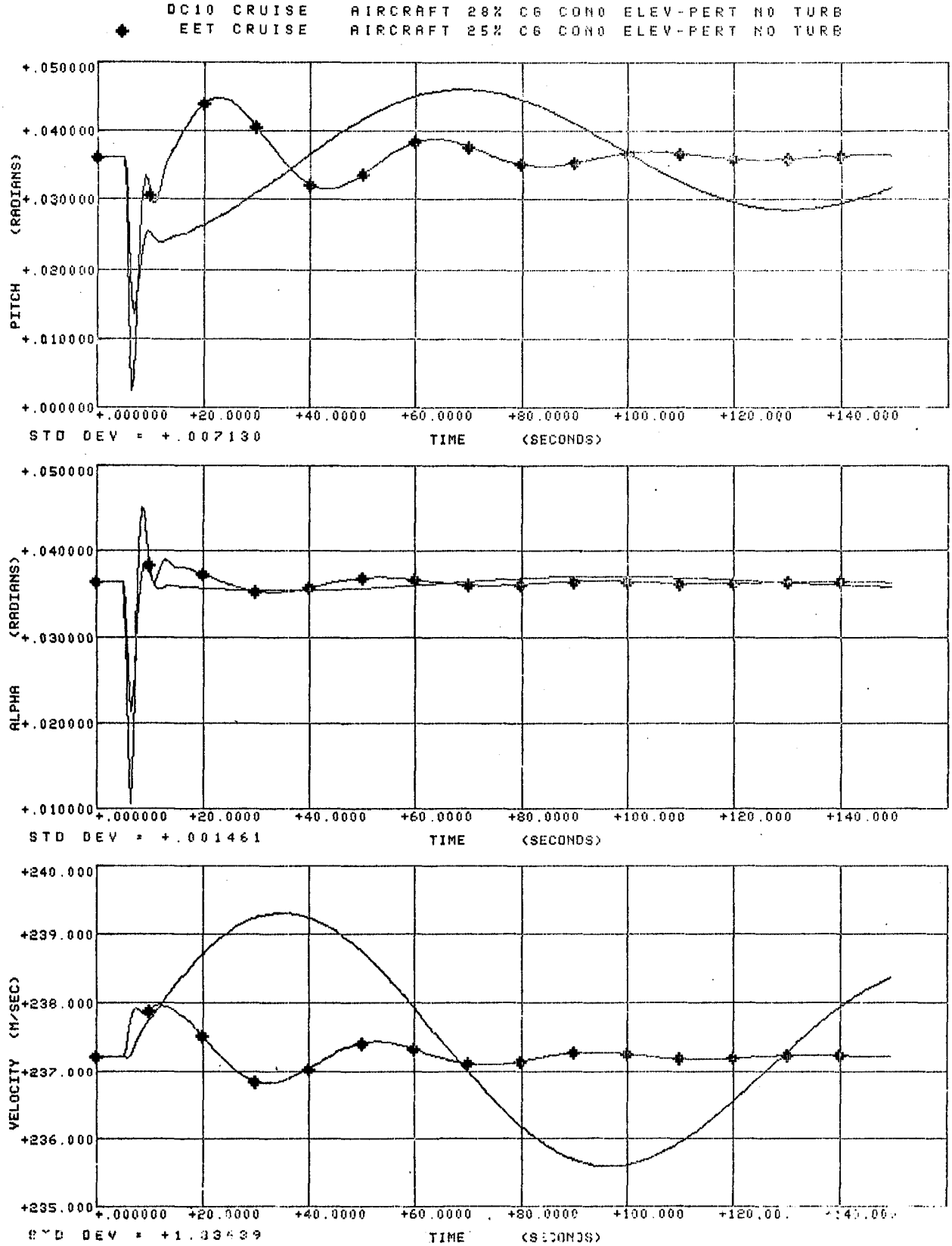

FIGURE 5-10a. COMPARISON OF DC-10 AND UNAUGMENTED EET IN CRUISE, 25 PERCENT CG — ELEVATOR PERTURBATION

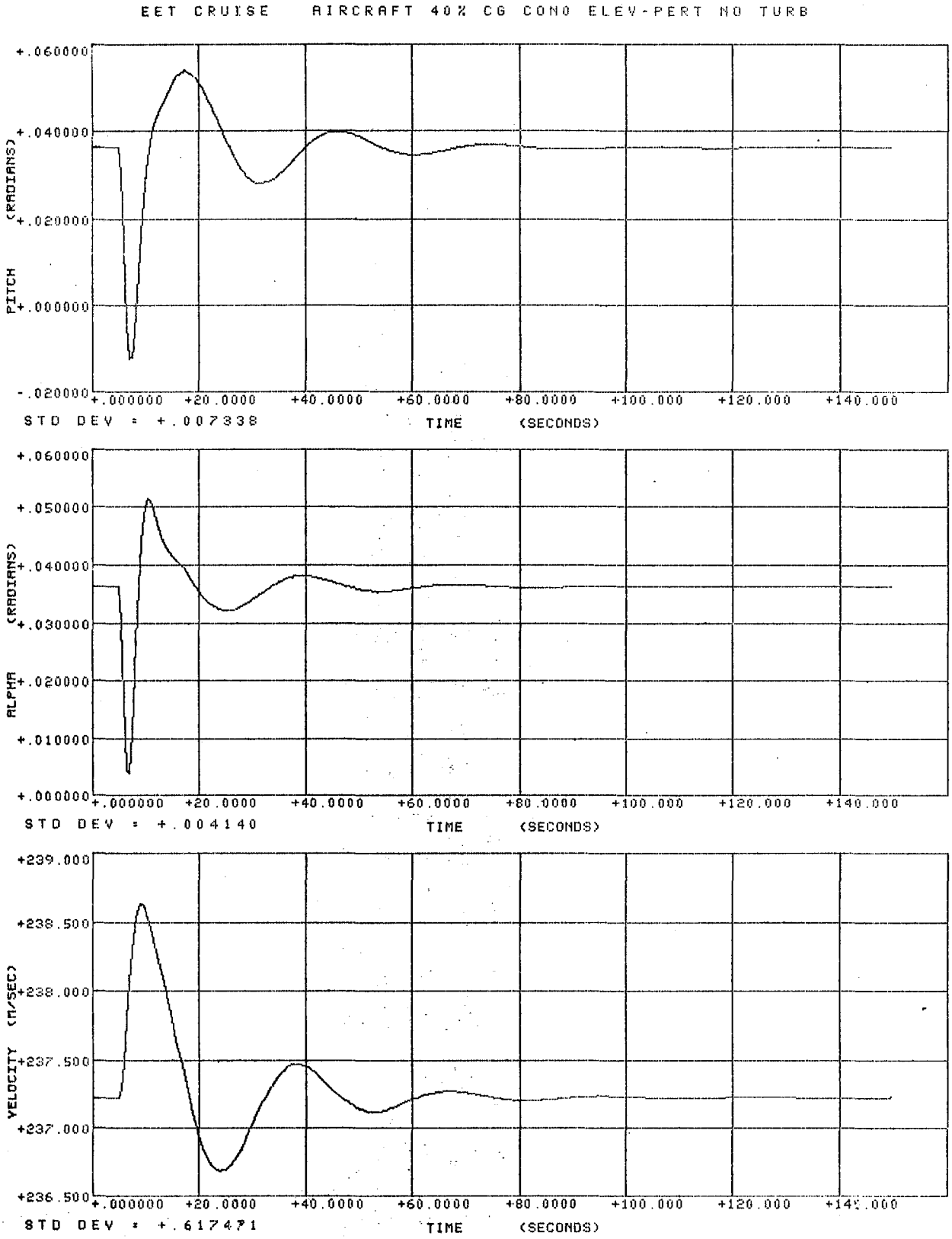

FIGURE 5-10b. UNAUGMENTED EET IN CRUISE, 40 PERCENT CG – ELEVATOR PERTURBATION

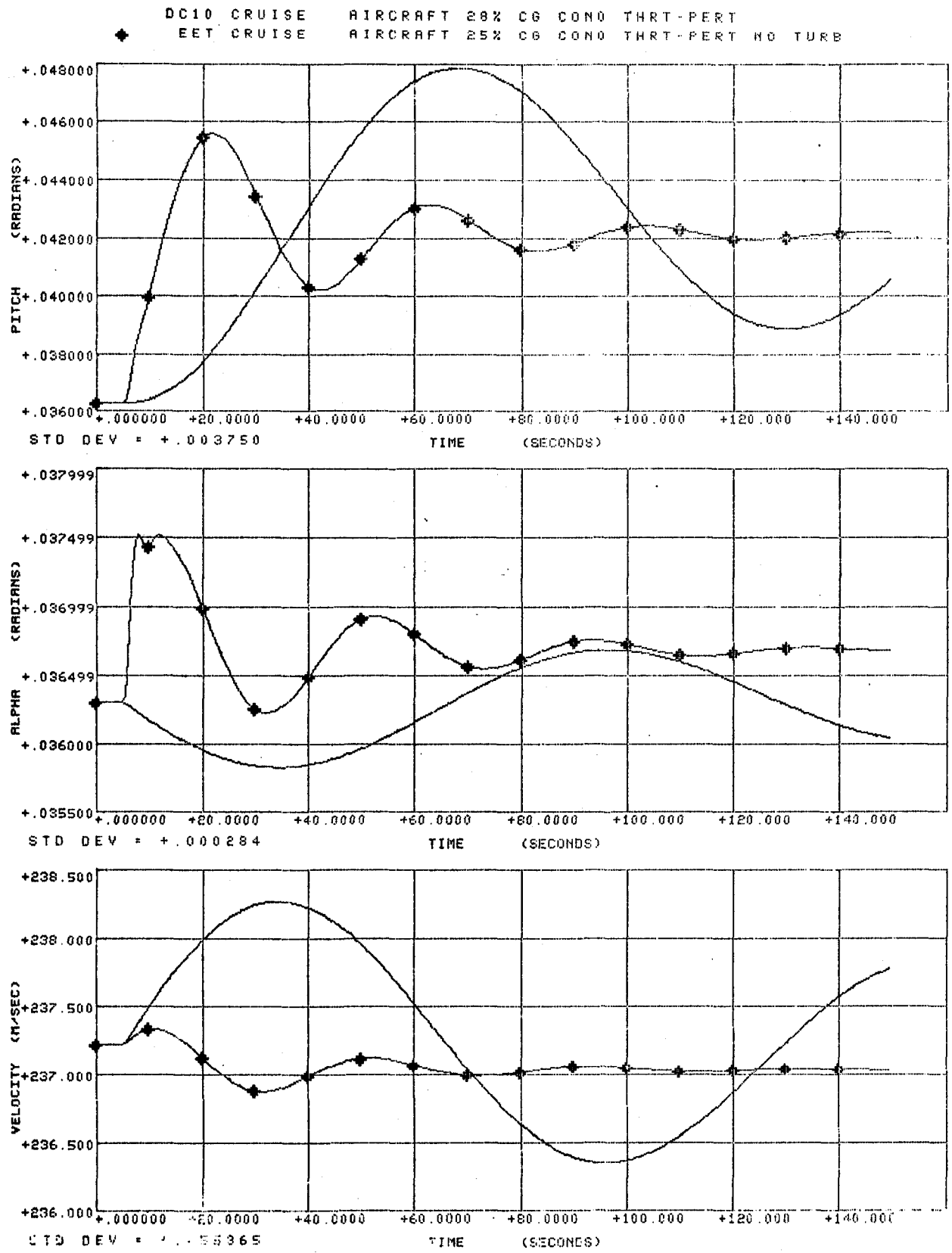

FIGURE 5-11a. COMPARISON OF DC-10 AND UNAUGMENTED EET IN CRUISE, 25 PERCENT CG – THRUST PERTURBATION

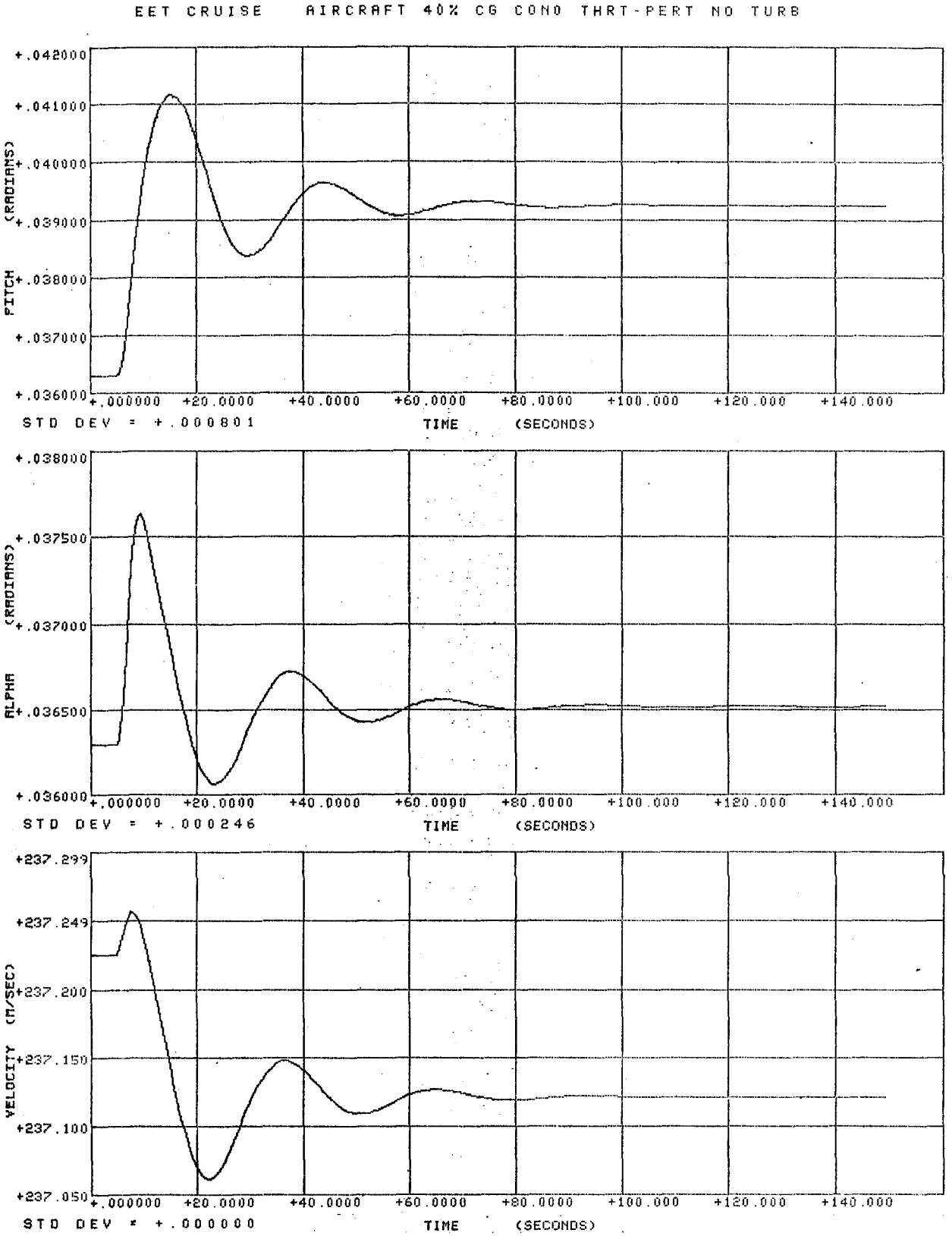

FIGURE 5-11b. UNAUGMENTED EET IN CRUISE, 40 PERCENT CG – THRUST PERTURBATION

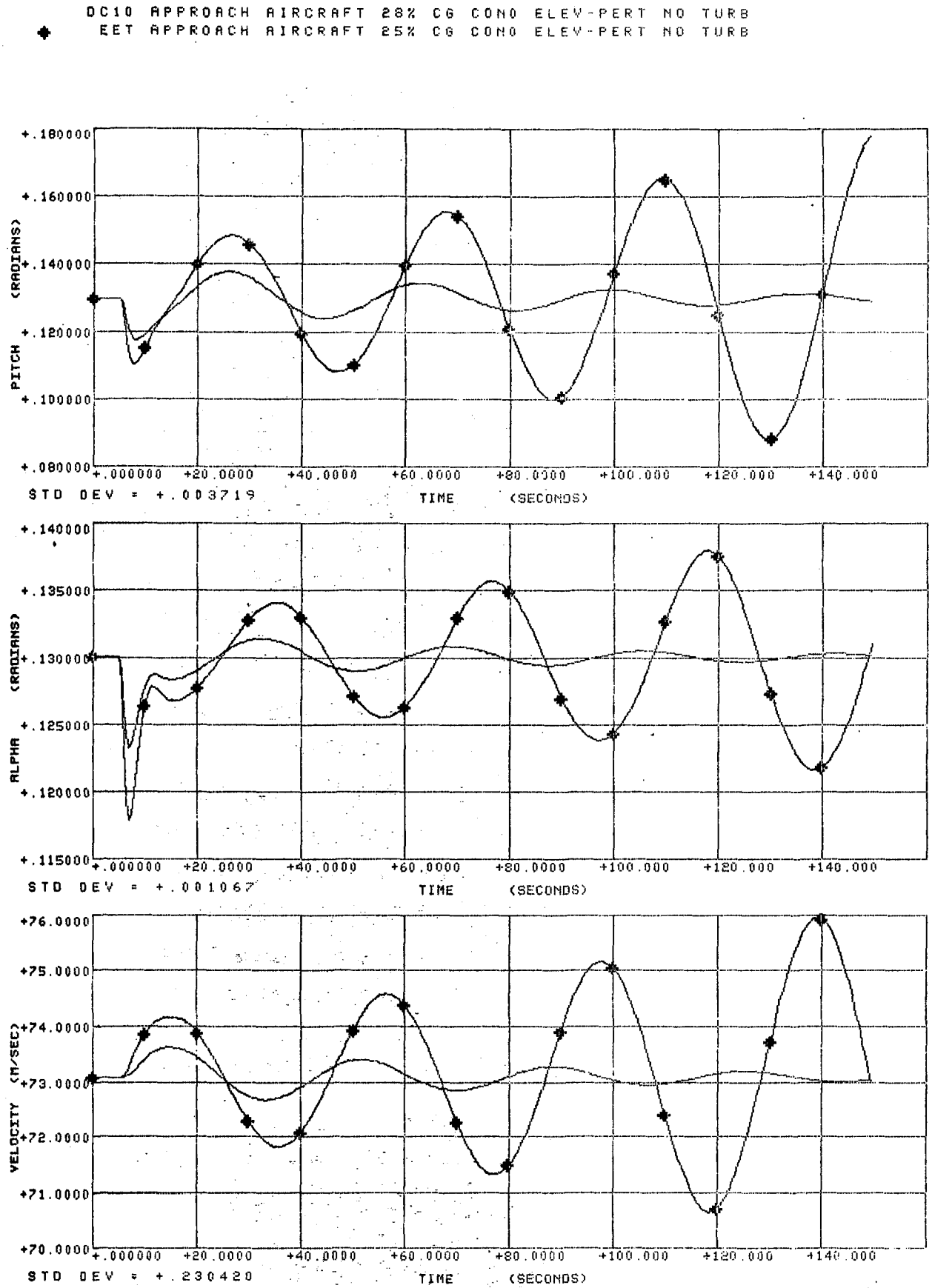

FIGURE 5-12a. COMPARISON OF DC-10 AND UNAUGMENTED EET IN APPROACH – ELEVATOR PERTURBATION

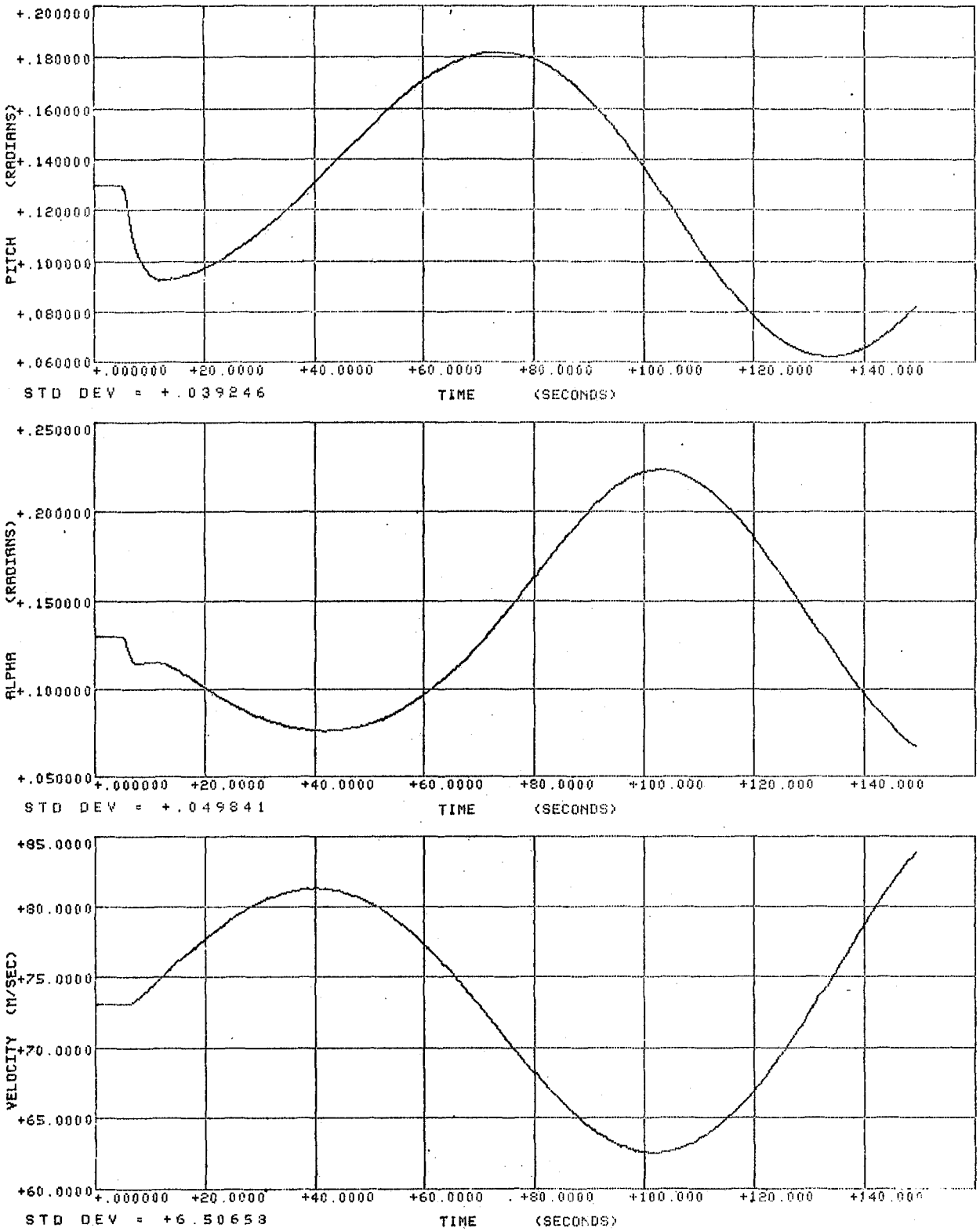

FIGURE 5-12b. COMPARISON OF DC-10 AND UNAUGMENTED EET IN APPROACH – ELEVATOR PERTURBATION

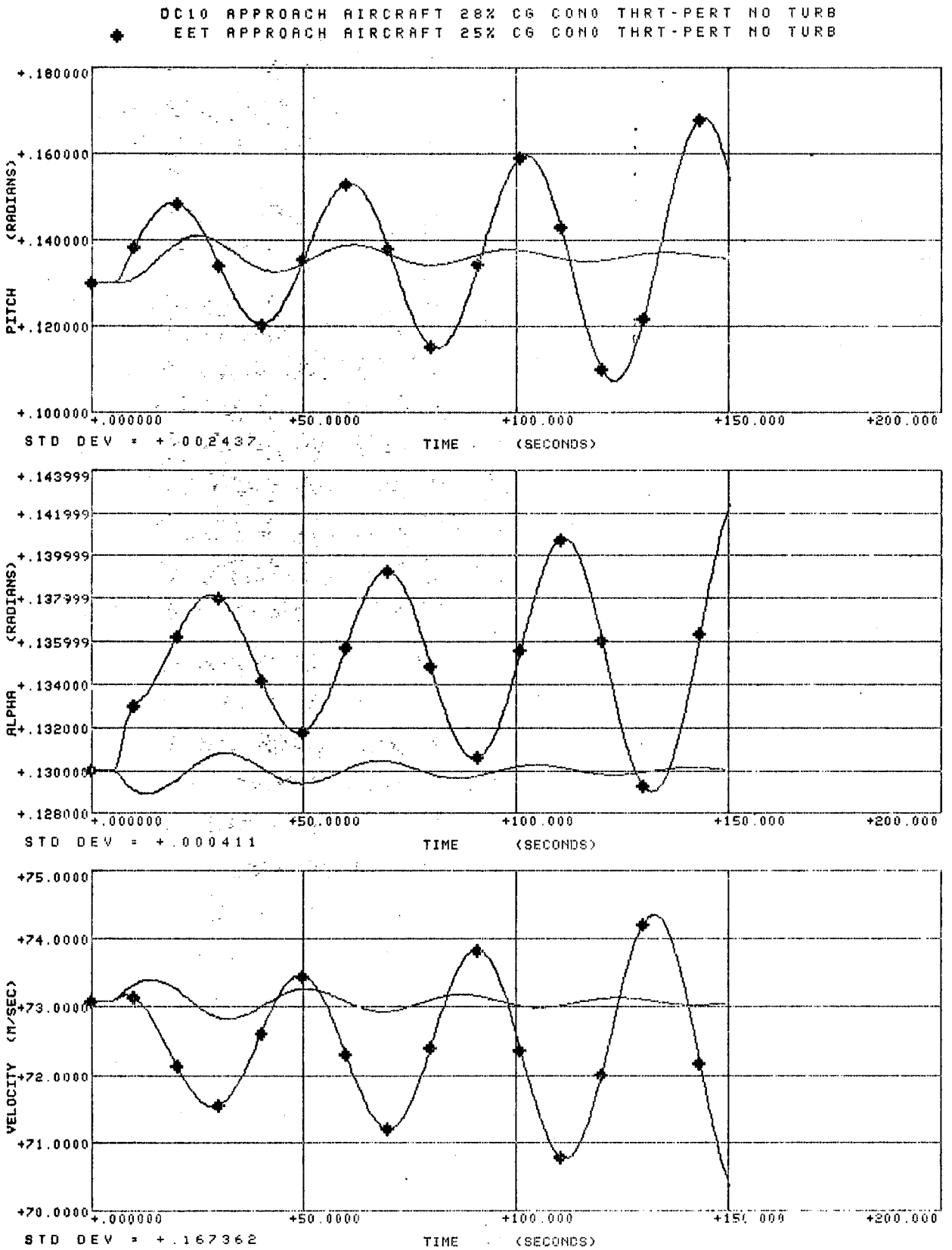

FIGURE 5-13a. COMPARISON OF DC-10 AND UNAUGMENTED EET IN APPROACH, 25 PERCENT CG — THRUST PERTURBATION

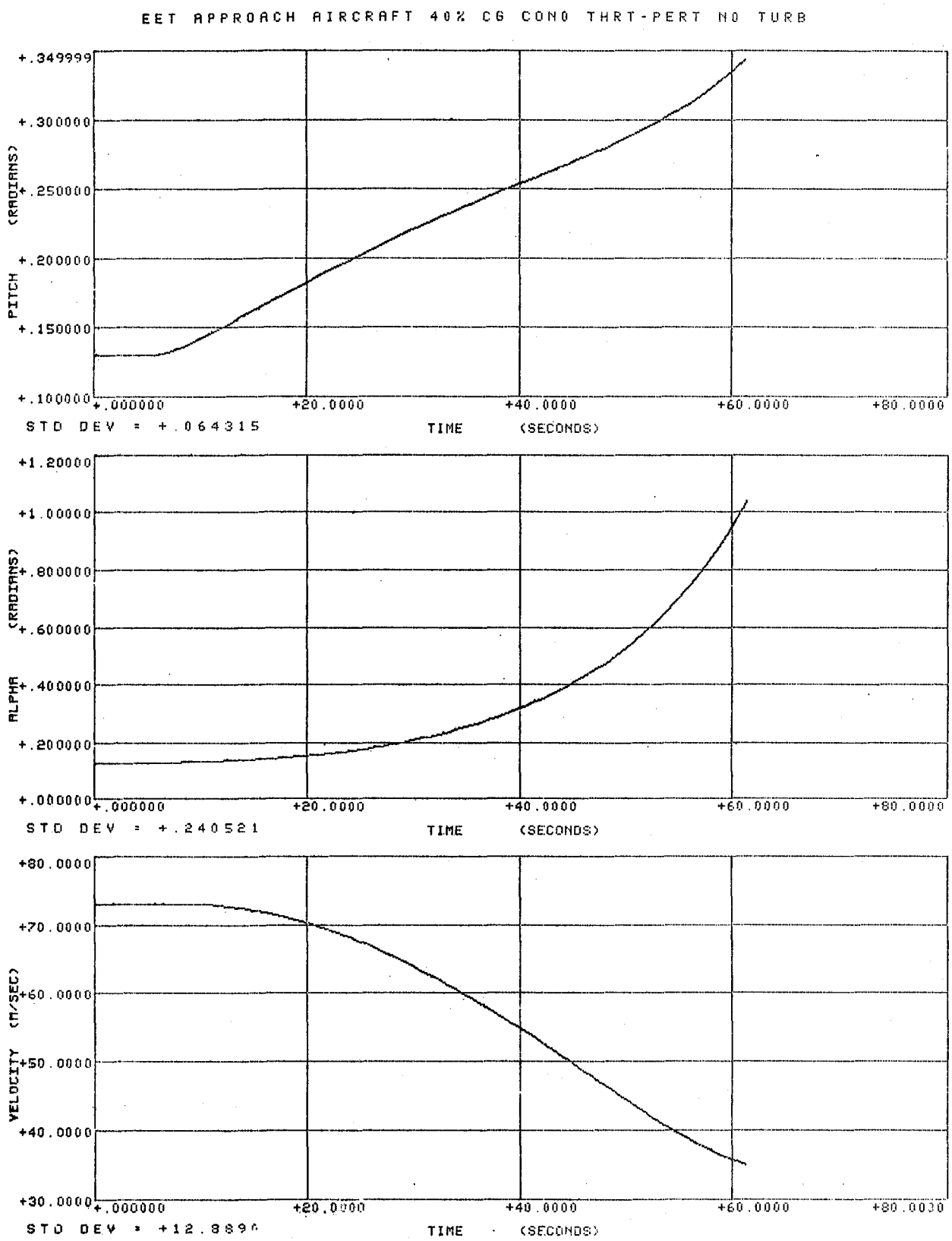

FIGURE 5-13b. UNAUGMENTED EET IN APPROACH, 40 PERCENT CG – THRUST PERTURBATION

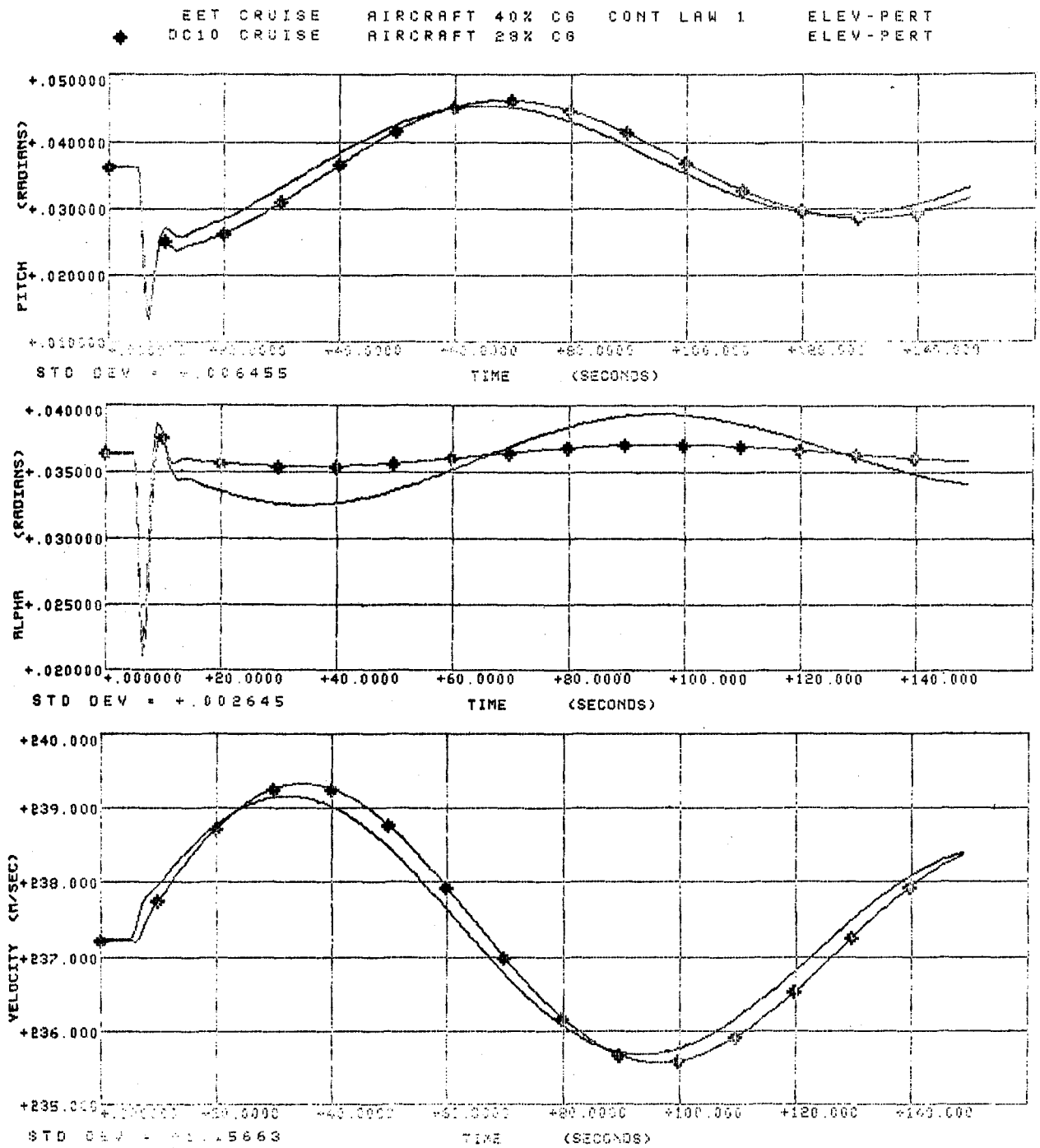

FIGURE 5-14. COMPARISON OF DC-10 AND AUGMENTED EET IN CRUISE, 40 PERCENT CG – ELEVATOR PERTURBATION

law) 40 percent center-of-gravity EET responses to the elevator upset for the cruise flight condition. These time histories for pitch and velocity are almost identical. It is these two parameters that the RSSAS attempts to match at the expense of α, since they are the physical characteristics that the flight crew observes. Comparisons of all seven control laws with the DC-10 for cruise and approach flight conditions are presented in Appendix 8. Figure 5-15 shows control law ($\theta\dot{\theta}u\alpha$) to control law ($\theta\dot{\theta}u$) tracking for this same upset. All control laws demonstrate this close comparison.

The RSSAS without thrust-to-pitch compensation cannot provide the DC-10 characteristics for the thrust upset. Figure 5-16 shows the two responses to be quite different. Adding the thrust/pitch compensation to the augmentor provides the satisfactory response shown in Figure 5-17. Comparisons of all seven control laws with the DC-10 for cruise and approach flight conditions have demonstrated this correlation.

5.5 Performance Analyses

Several analyses have been conducted to evaluate the RSSAS performance for various aircraft, environment, and system conditions. The intent of the individual analyses is discussed below.

Statistical Performance — A statistical evaluation of the performance of each control law was conducted in a turbulent air environment. For the initial control laws, this analysis was used to eliminate configurations which did not add to the RSSAS capability. The final selected control laws were analyzed to provide an insight into the flying qualities to be exhibited during the motion base simulator tests.

Aircraft Configuration Changes — The augmented aircraft response to flap and landing gear extensions was evaluated to compare the capabilities of various control laws when no special aircraft configuration intelligence is provided.

Control Law Sensor Sensitivities — Each control law was evaluated to determine its sensitivity to sensor signal variations. This analysis was performed to establish the allowable sensor tolerances and/or sensor comparison monitor thresholds.

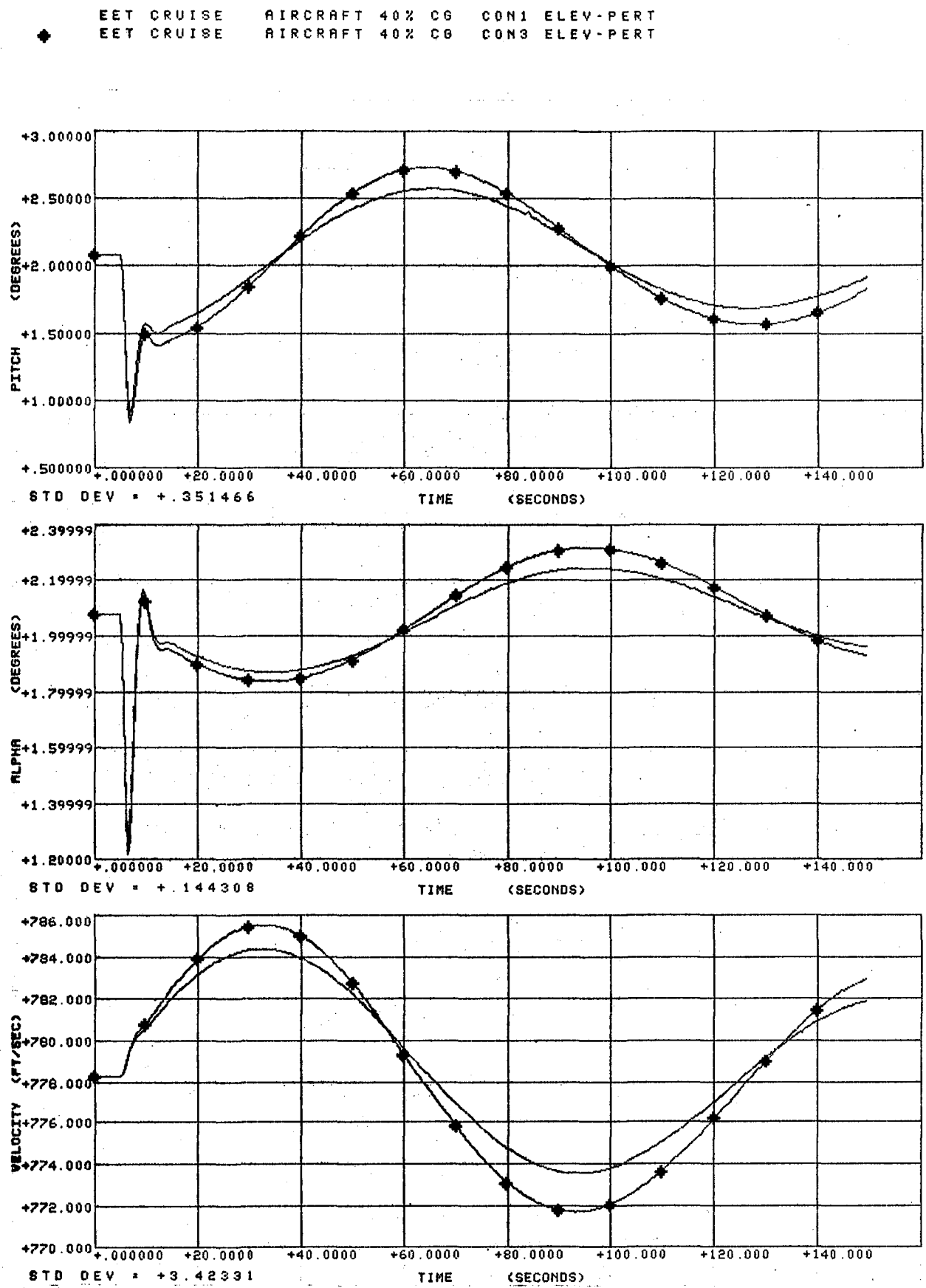

FIGURE 5-15. COMPARISON OF TWO DIFFERENT AUGMENTATION CONTROL LAWS – CRUISE ELEVATOR PERTURBATION

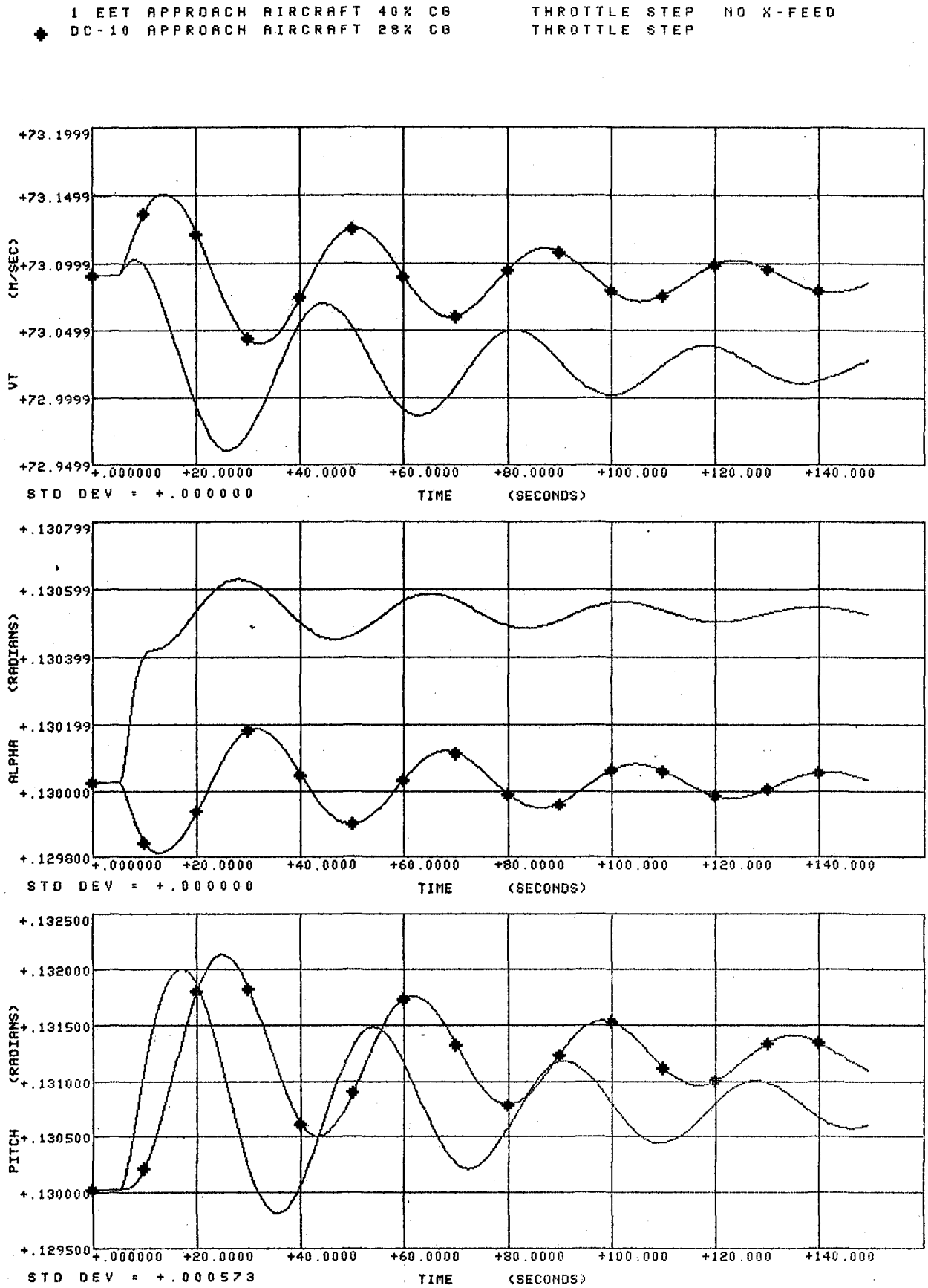

FIGURE 5-16. COMPARISON OF DC-10 AND AUGMENTED EET WITHOUT PITCH/THRUST COMPENSATION – APPROACH THRUST PERTURBATION

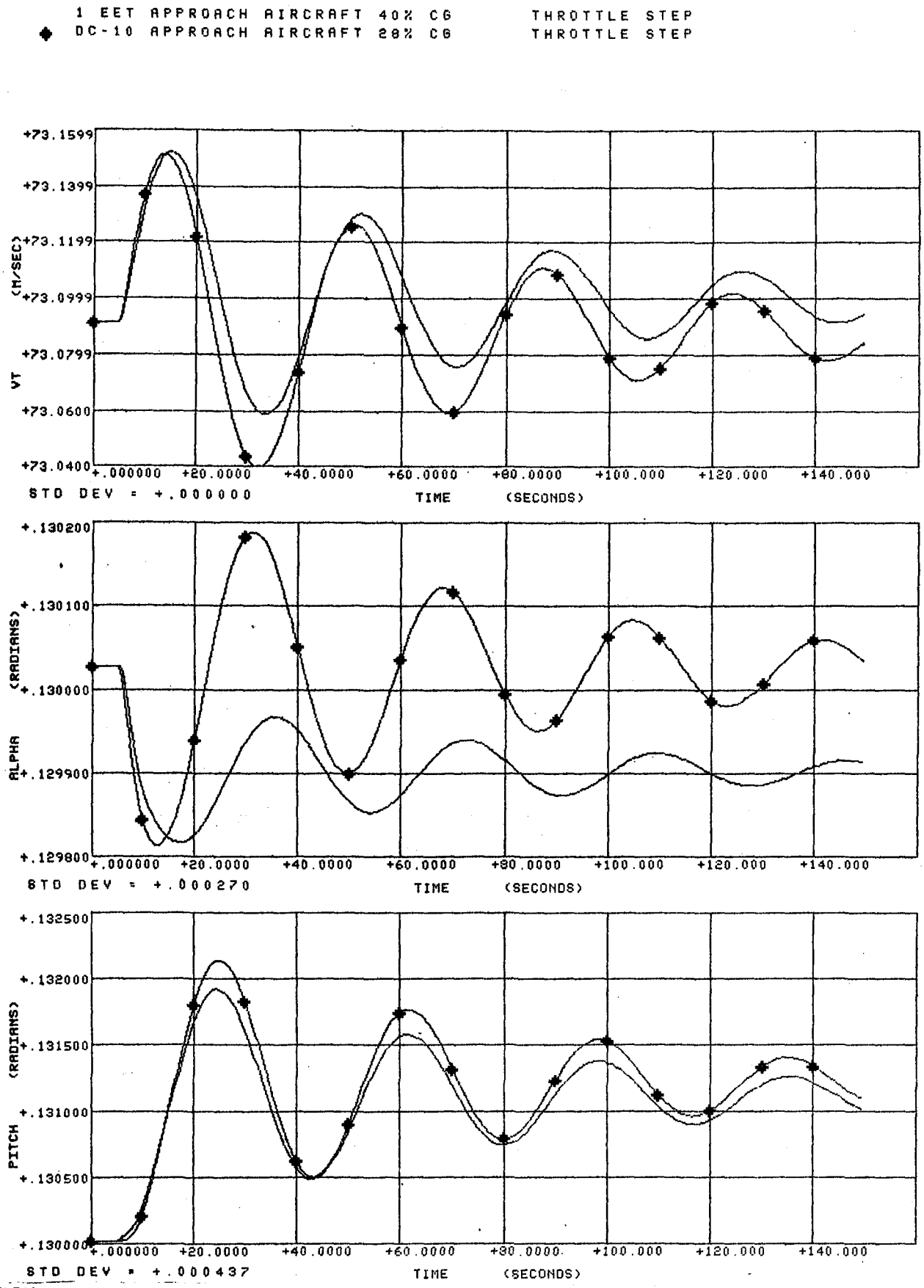

FIGURE 5-17. COMPARISON OF DC-10 AND AUGMENTED EET WITH PITCH/THRUST COMPENSATION – APPROACH THRUST PERTURBATION

Control Law Tracking — For a given flight patch tracking maneuver, each control law was monitored to evaluate the relative differences in control commands. This establishes the level of synchronization necessary for control laws in standby. Control-law-to-control-law comparison capability is also determined.

FGS/RSSAS Interaction/Operation — This analysis establishes the inherent static stability augmentation capability of various combinations of the flight guidance system autopilot and autothrottle. Flight guidance system performance with and without the RSSAS is also evaluated. Although automatic flight control is demonstrated, several performance characteristics may be valid for manual pilot control.

5.5.1 Statistical Performance Analysis. — An existing general-purpose linear control system analysis computer program was adapted for use in statistically evaluating the response of the proposed control laws in a turbulent air environment. As shown in Figure 5-18, the analysis was affected by subjecting the closed loop linearly modeled system to simultaneous longitudinal and vertical wind gusts, input through aerodynamic coupling as well as through the appropriate sensors. The Dryden wind gust models for angle-of-attack and forward-velocity gusts, as defined in MIL 8785-B, were used. The standard deviations of the aircraft variables were computed by solving for the steady-state matrix variance equation for the linear system driven by white noise. The aircraft variables observed include: pitch attitude (θ), pitch rate ($\dot{\theta}$), angle of attack (α), velocity (u), altitude rate ($\dot{h}$), normal acceleration (A_N), and elevator deflection (δe).

Of the initial 32 control law configurations, 11 were eliminated by excluding longitudinal acceleration, A_X, as a feedback parameter prior to this analysis. Statistical gust responses for the remaining 21 control laws have been computed and bar diagrams drawn. Figures 5-19 and 5-23 shows the relative θ, α, A_N and δe performance between each of the control law configurations for a cruise flight condition. Based on this evaluation, altitude rate ($\dot{h}$) was eliminated as a feedback parameter. This was due to its degrading effect on some sensor combinations and its consistently lower level of performance compared with airspeed (u), the other air data computer parameter.

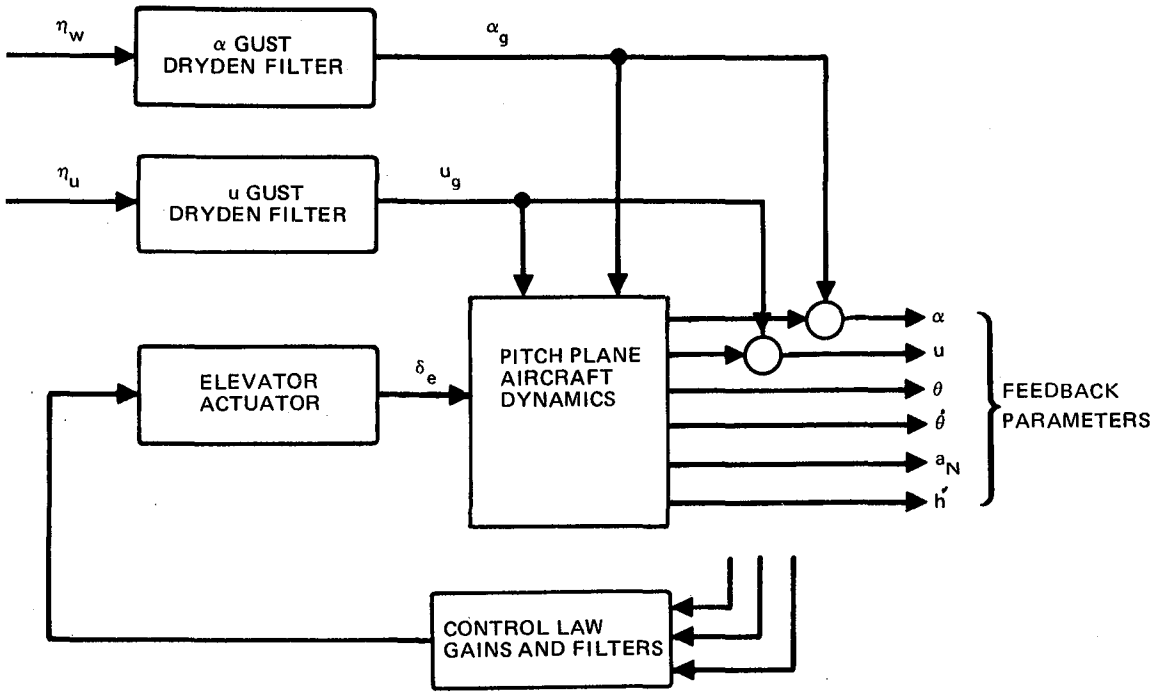

FIGURE 5-18. MODELED SYSTEM BLOCK DIAGRAM

As a result of this and concurrent studies, the original 32 control laws have been reduced to the $\theta\dot{\theta}u\alpha$ family of seven ($\theta\dot{\theta}u\alpha$,$\theta\dot{\theta}$,$\theta\dot{\theta}\alpha$,$\theta\dot{\theta}u$,$u\alpha$,$u$,$\alpha$) configurations. The remaining seven have been revised (gains and filter changes), new statistical gust responses were computed, and bar charts drawn. Figures 5-20 and 5-21 show the new gust responses for the cruise and approach flight conditions. An evaluation of these responses can provide an insight into comparative system/aircraft performance. $\sigma\delta_e$ and $\sigma_{\dot{\delta}_e}$ are indications of control law sensitivity to gusts, and $\sigma_{\dot{\theta}}$,σA_N and $\sigma_{\dot{h}}$ relate to passenger ride comfort. Tight augmentor control is reflected in σ_θ and σ_α, while σ_u indicates possible coupling to the aircraft thrust control. Three control laws, No. 1 ($\theta\dot{\theta}u\alpha$), No. 3 ($\theta\ddot{\theta}\alpha$), and No. 5 ($\alpha$) were demonstrated on the motion base simulator (MBS). During the MBS tests, the higher values of θ and A_N for the No. 5, α, control law manifested themselves with pilot opinions of a more active aircraft. The No. 1, $\theta\dot{\theta}u\alpha$, control law has the tightest θ control which also agrees with several pilot comments during the tests.

5.5.2 Aircraft Configuration Changes. — No special intelligence has been added to the RSSAS to sense and compensate for aircraft configuration changes. The RSSAS control laws do, of course, respond to the perturbed aircraft parameters in such a manner as to maintain the previous trimmed aircraft flight path. Figures 5-22 and 5-23, provide comparisons of the

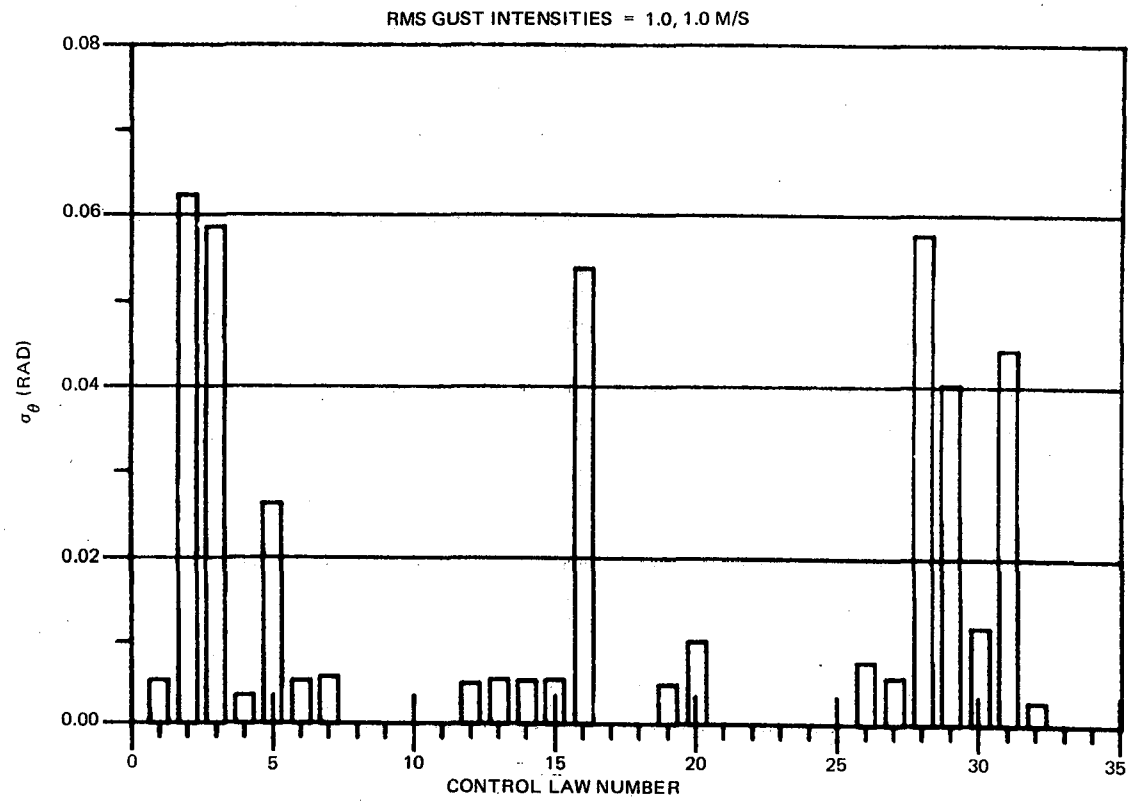

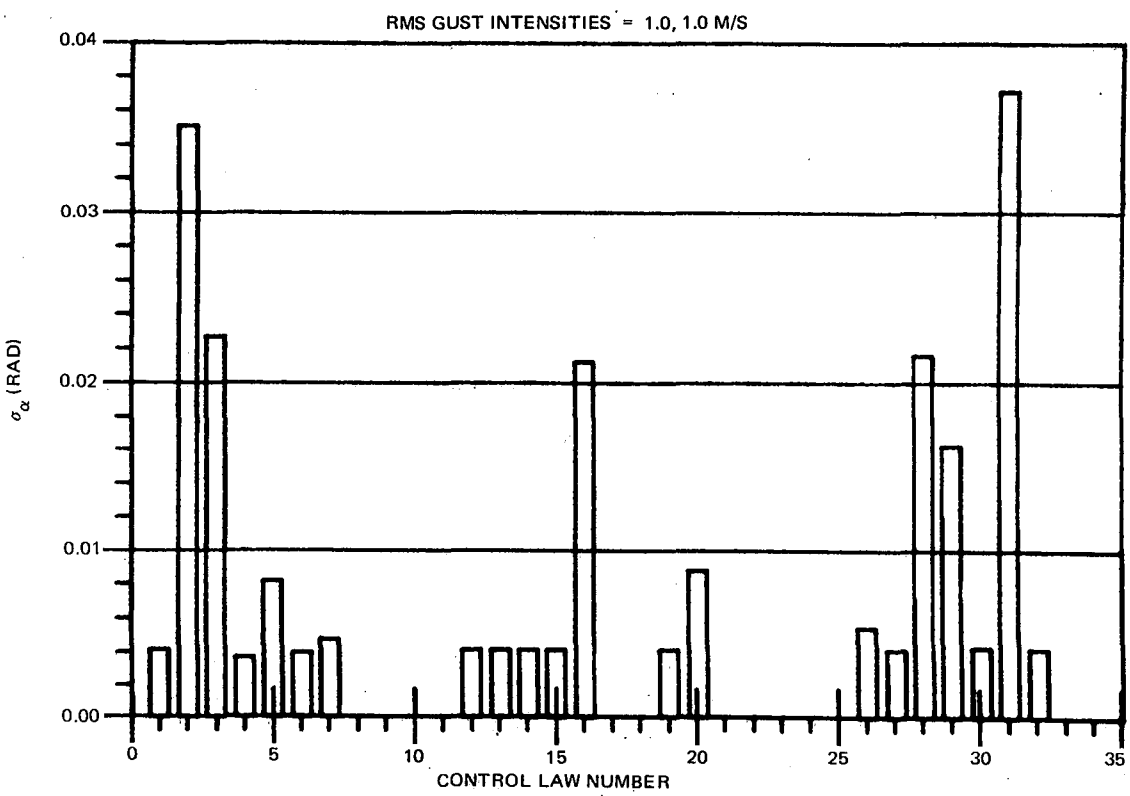

FIGURE 5-19. PRELIMINARY STATISTICAL PERFORMANCE – CRUISE

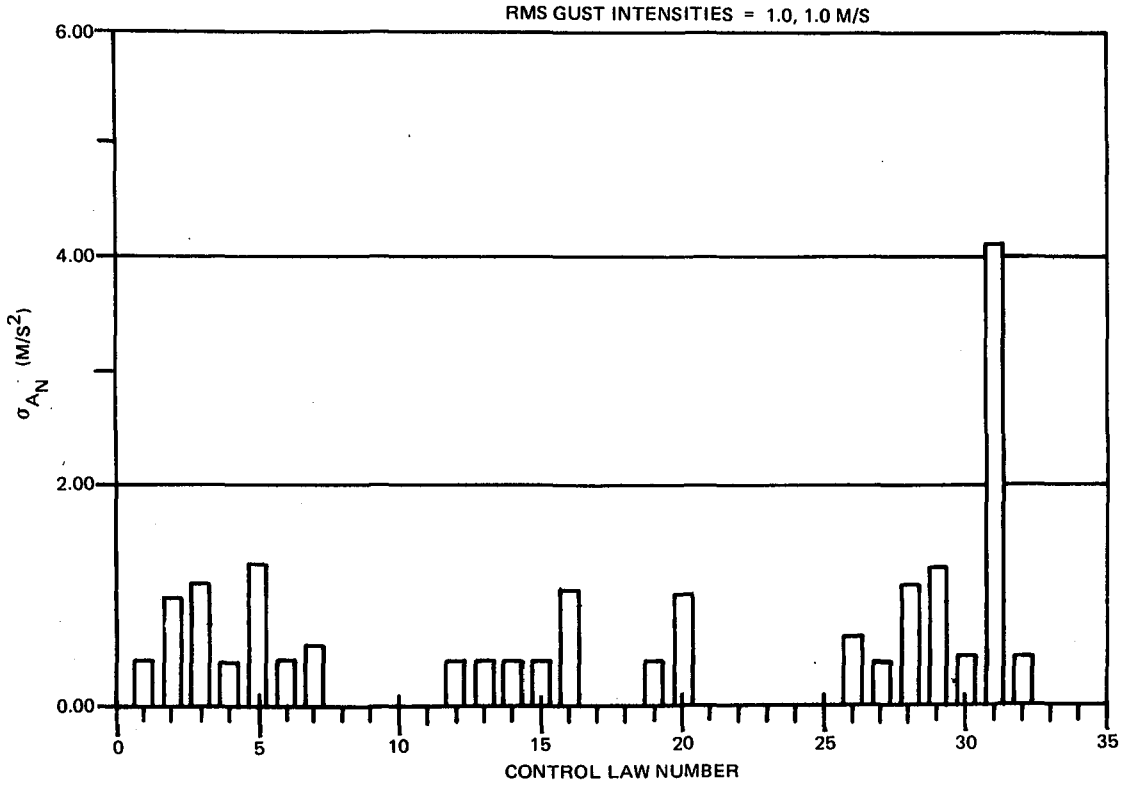

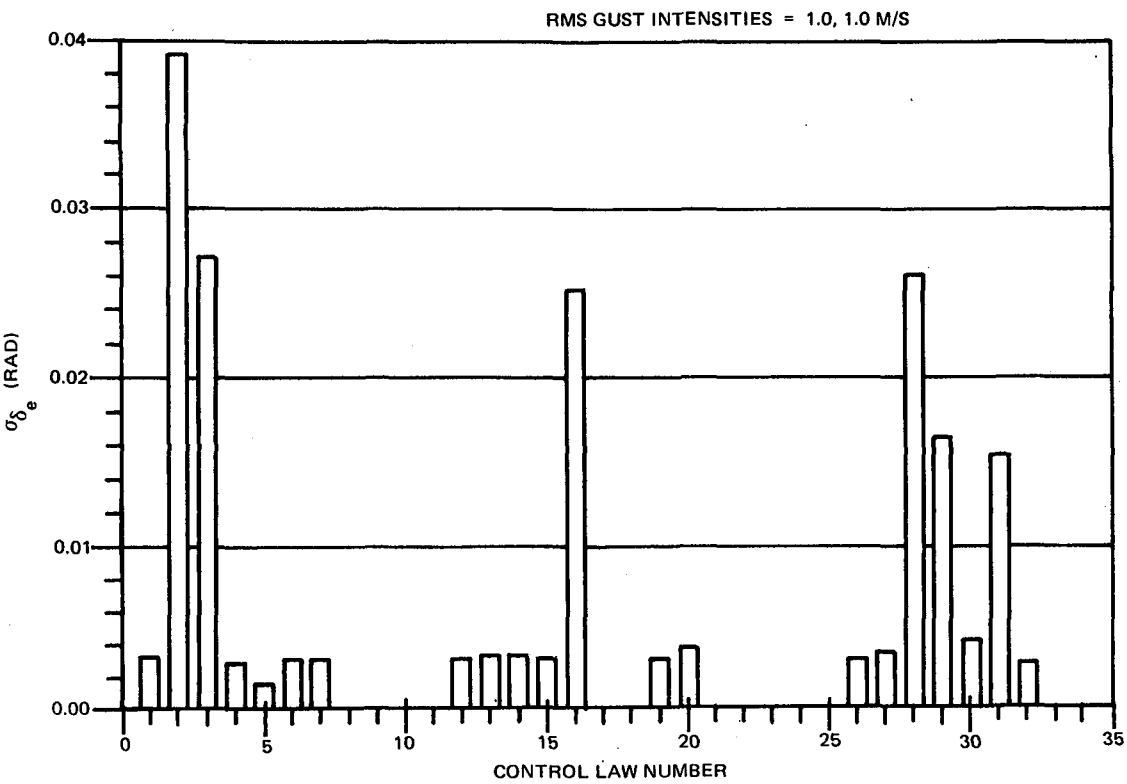

FIGURE 5-19. PRELIMINARY STATISTICAL PERFORMANCE – CRUISE (CONTINUED)

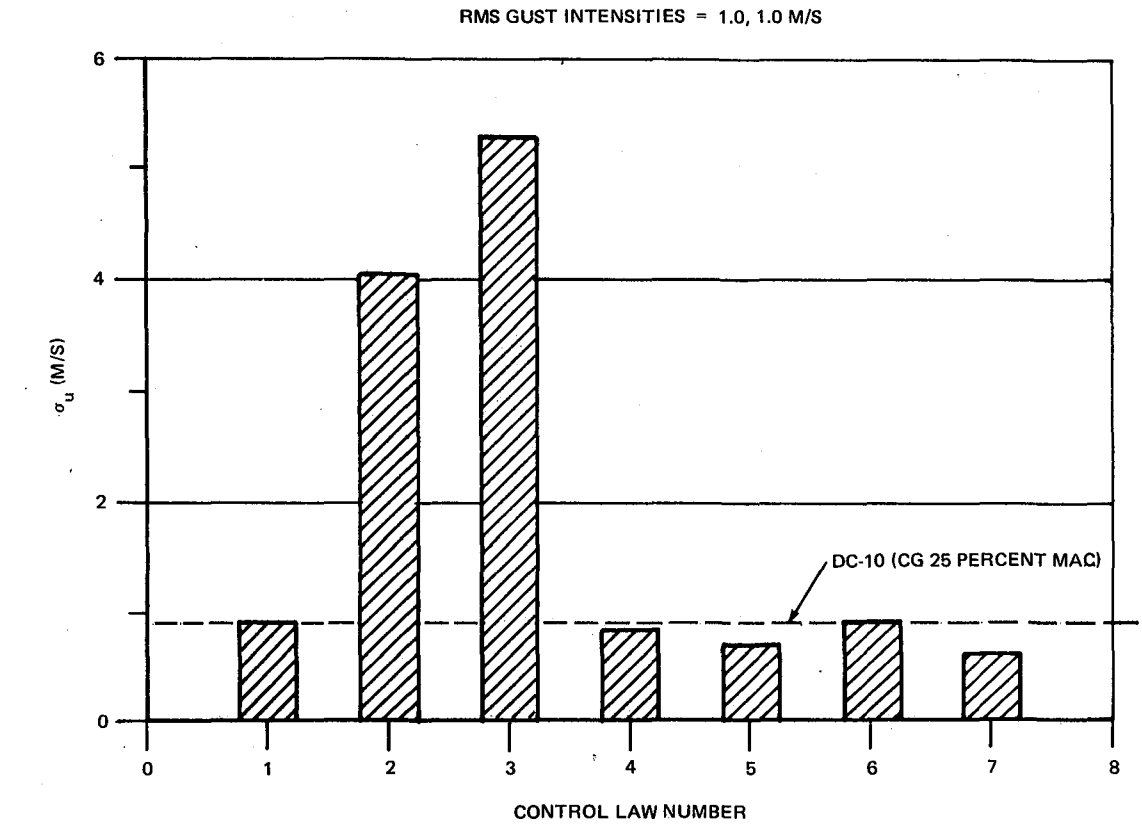

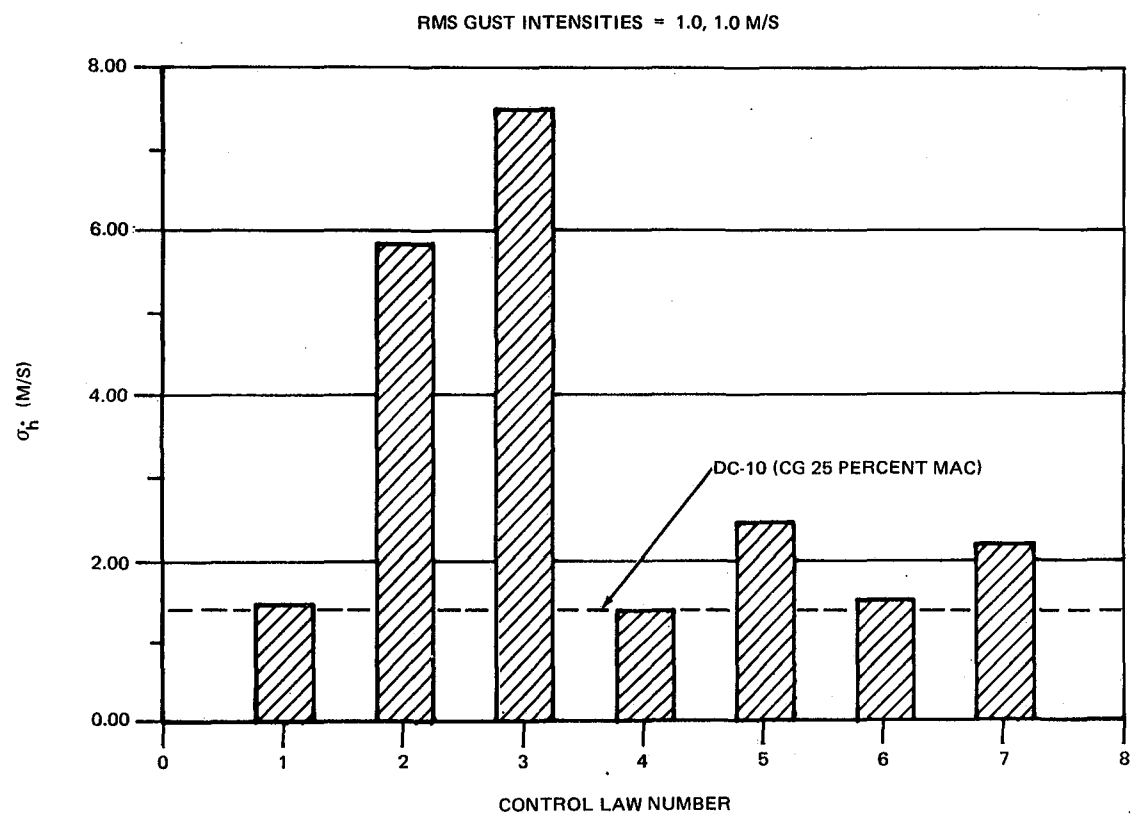

FIGURE 5-20. STATISTICAL PERFORMANCE – CRUISE

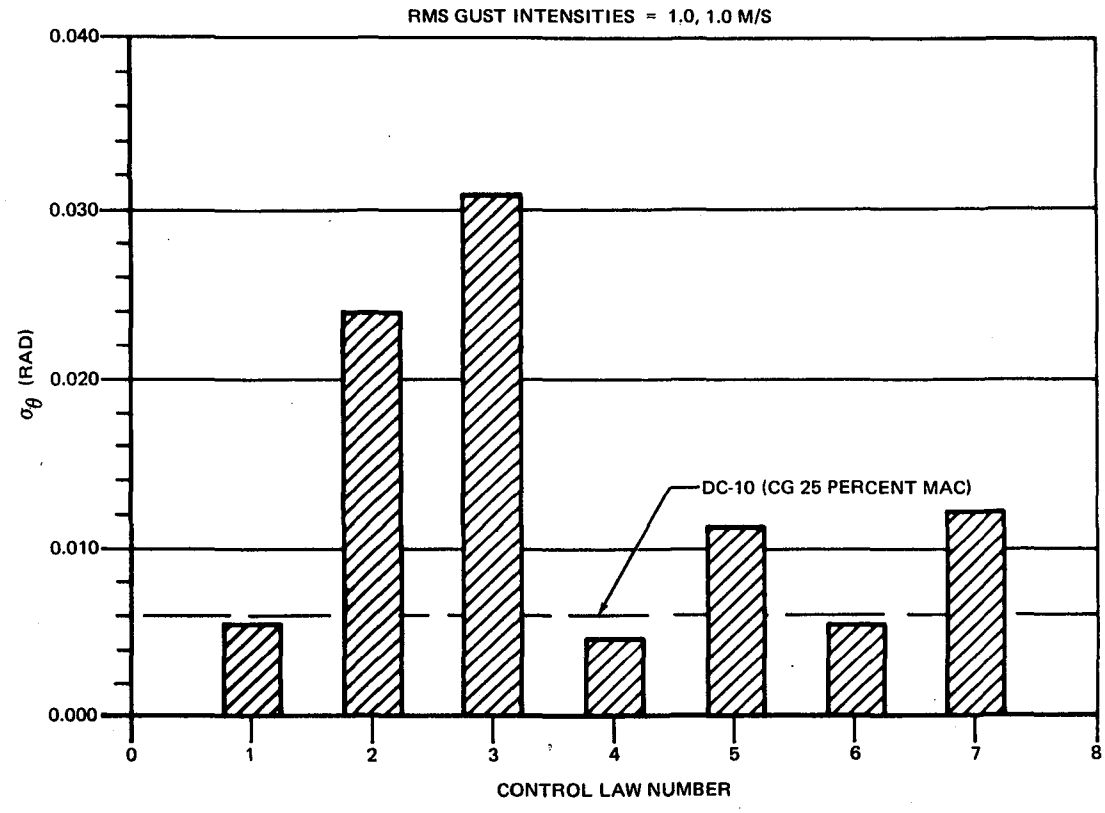

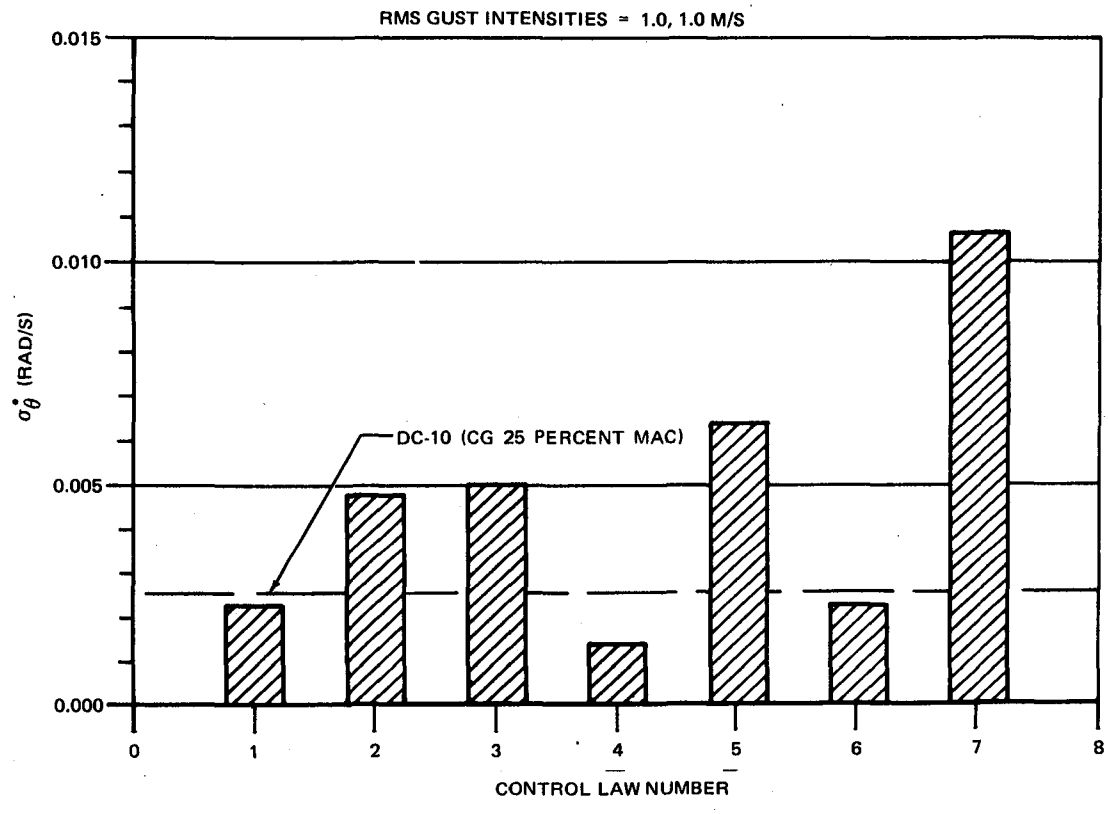

FIGURE 5-20. STATISTICAL PERFORMANCE – CRUISE (CONTINUED)

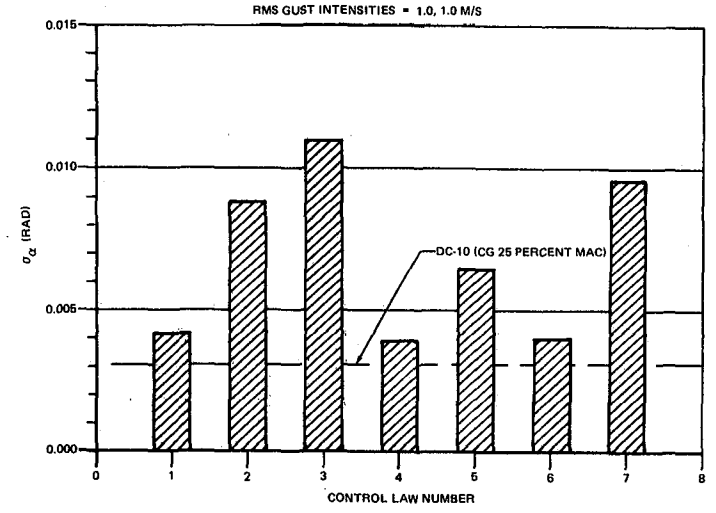

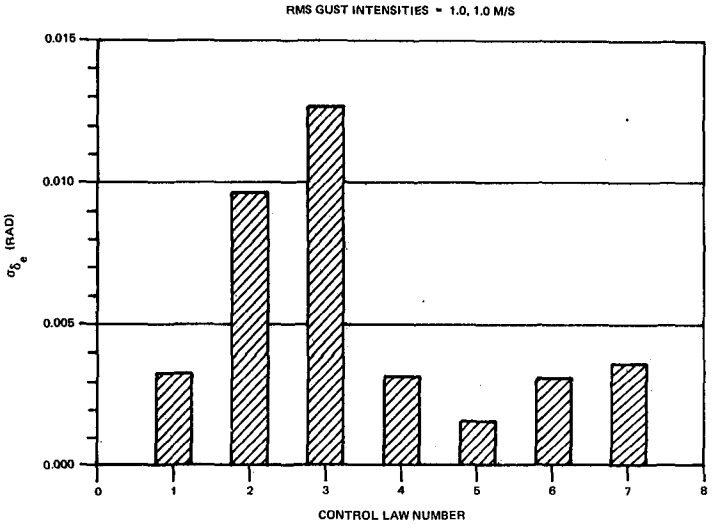

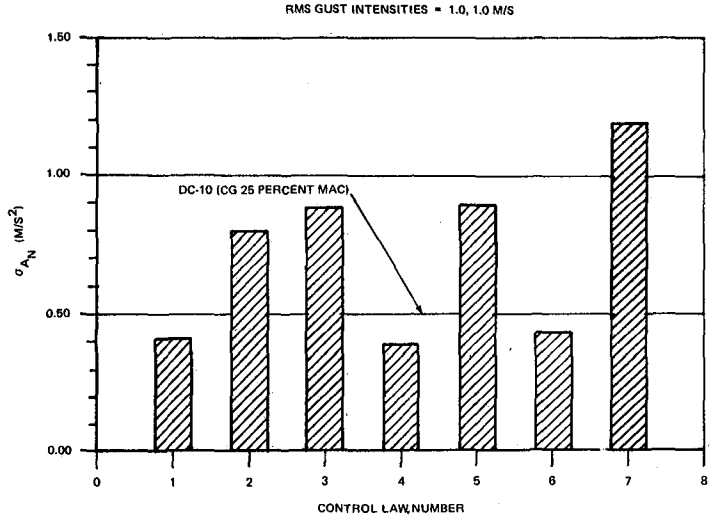

FIGURE 5-20. STATISTICAL PERFORMANCE – CRUISE (CONTINUED)

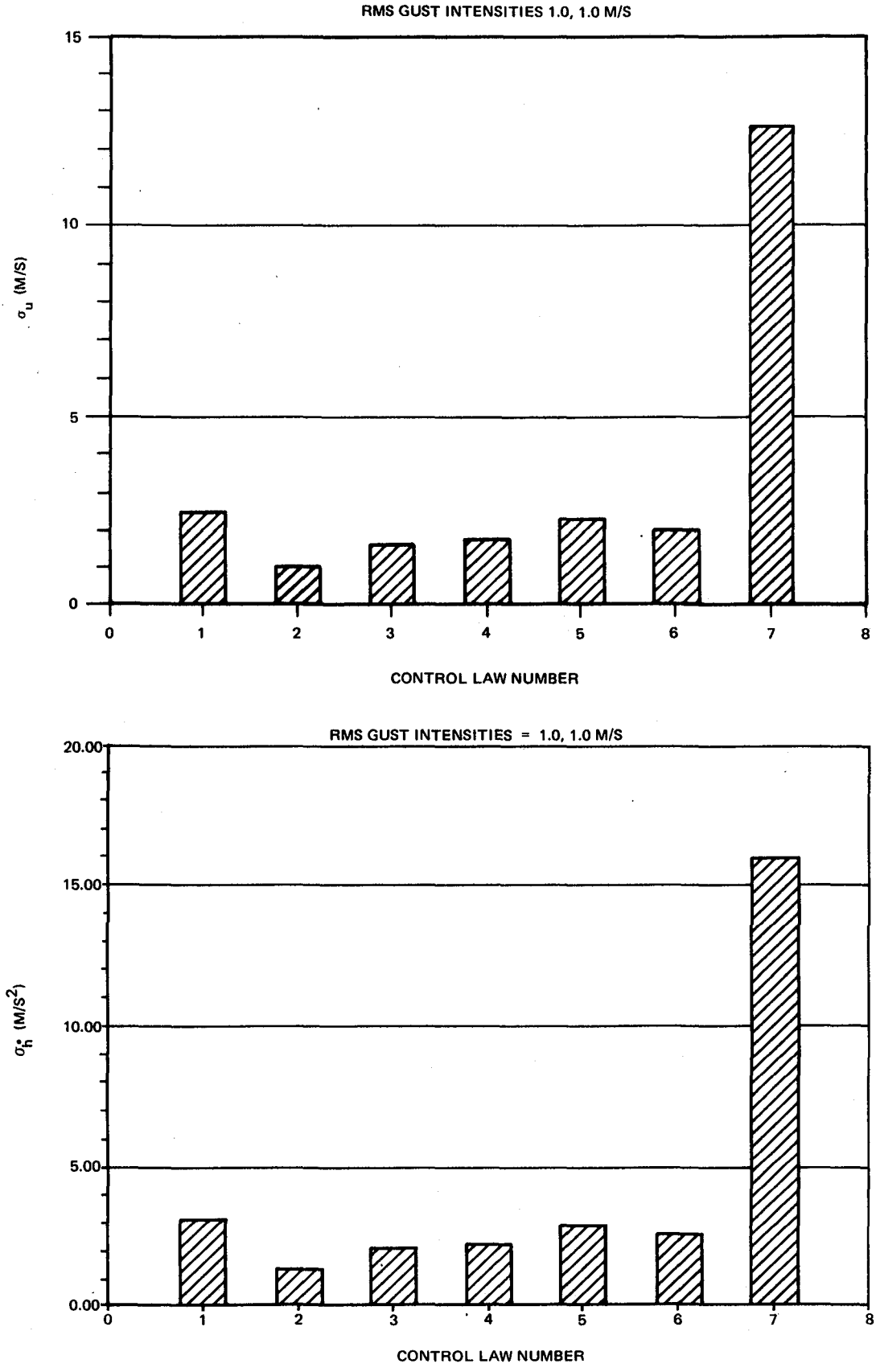

FIGURE 5-21. STATISTICAL PERFORMANCE – APPROACH

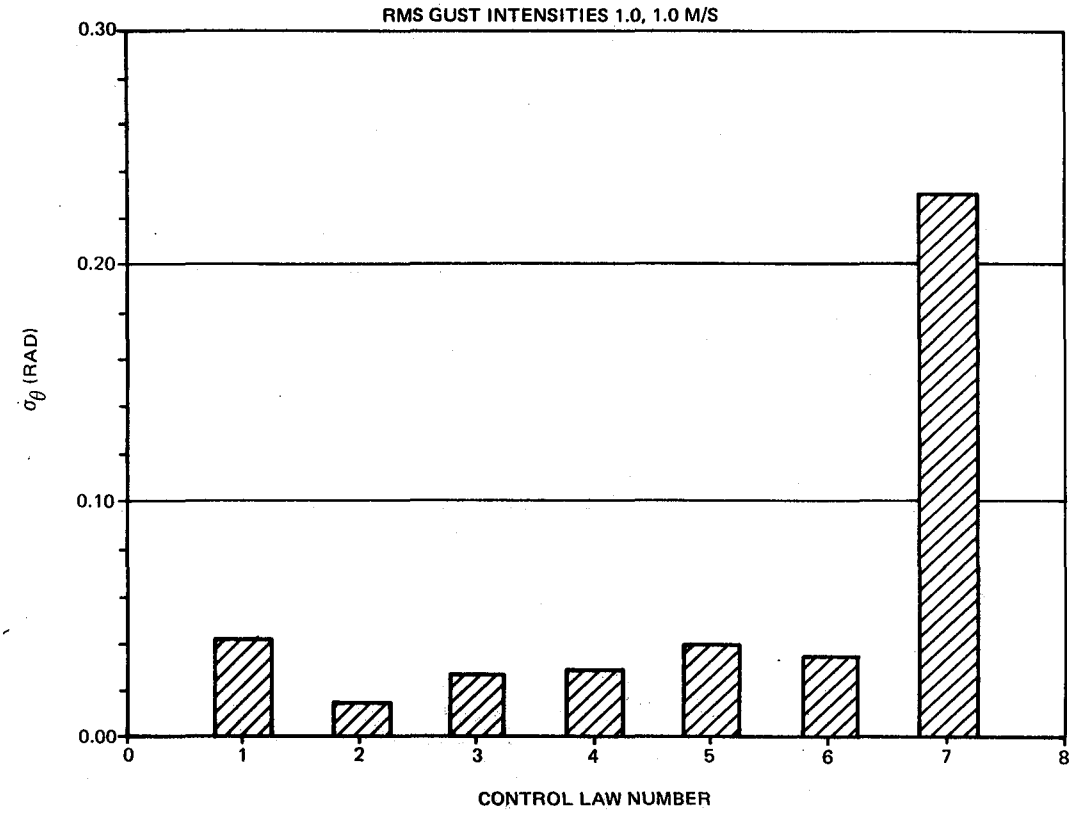

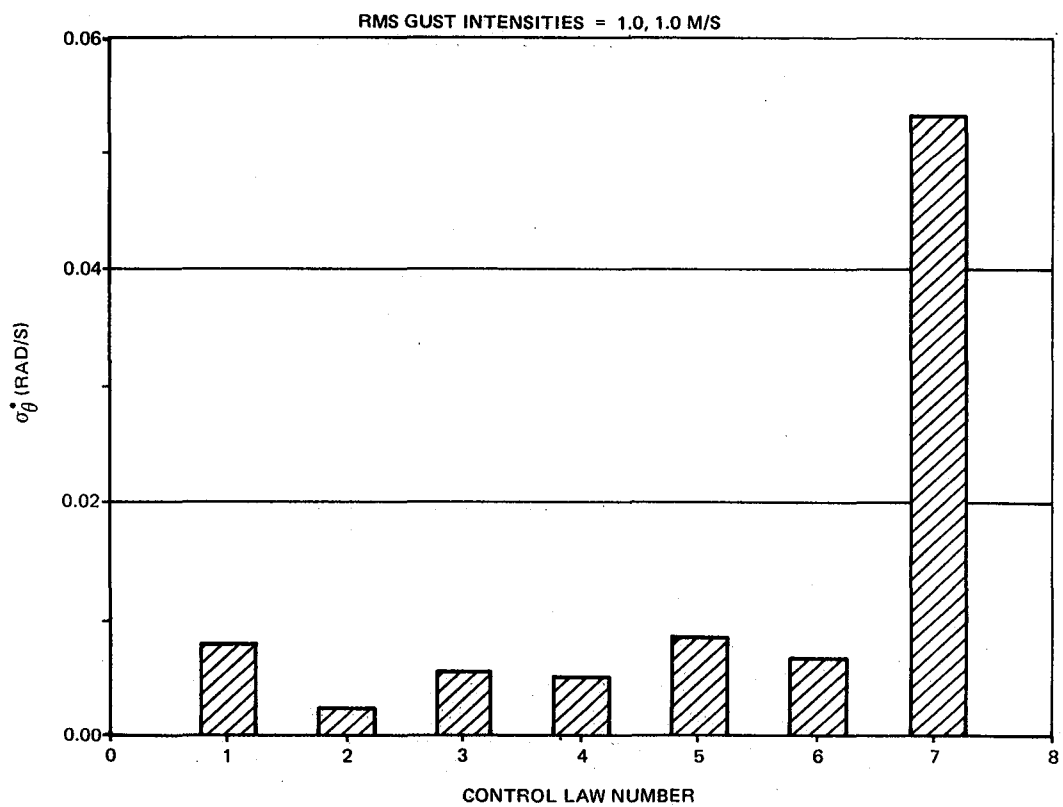

FIGURE 5-21. STATISTICAL PERFORMANCE – APPROACH (CONTINUED)

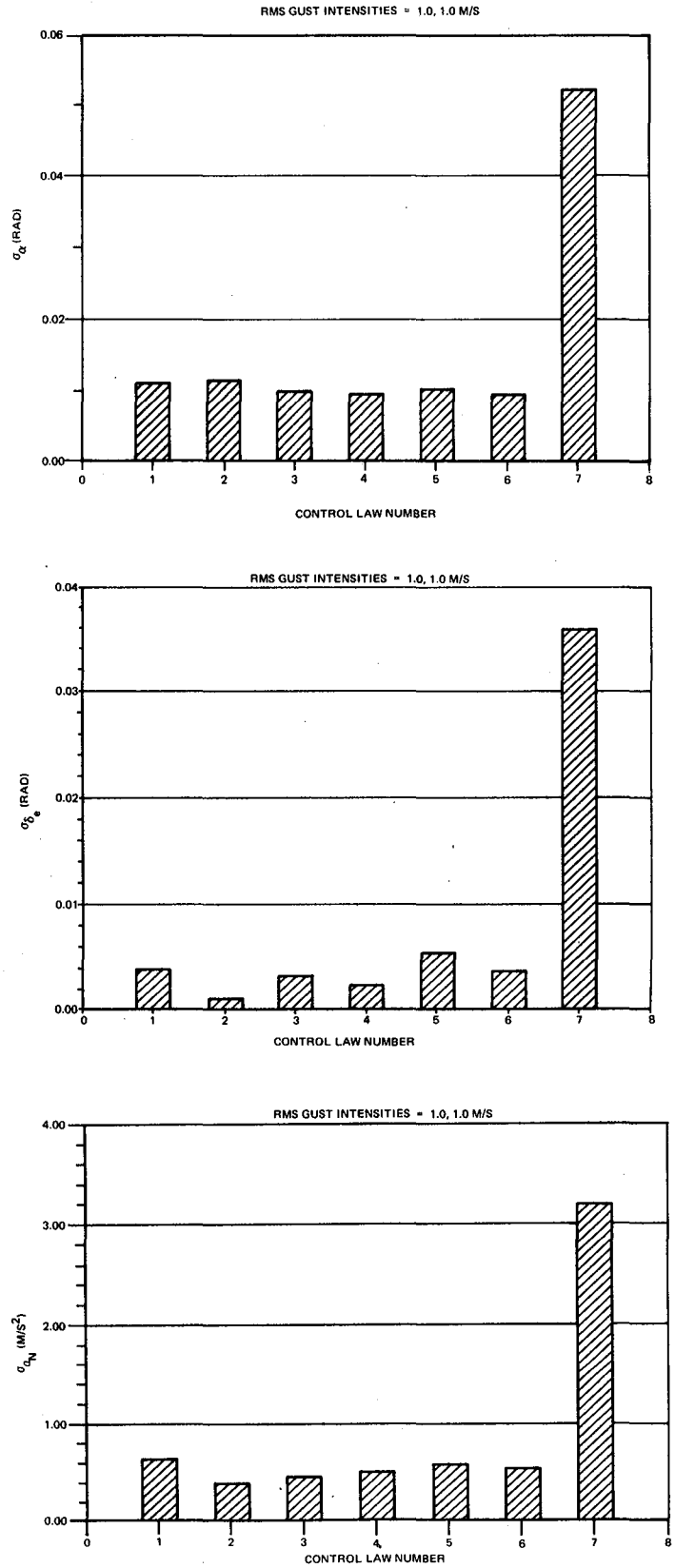

FIGURE 5-21. STATISTICAL PERFORMANCE – APPROACH (CONTINUED)

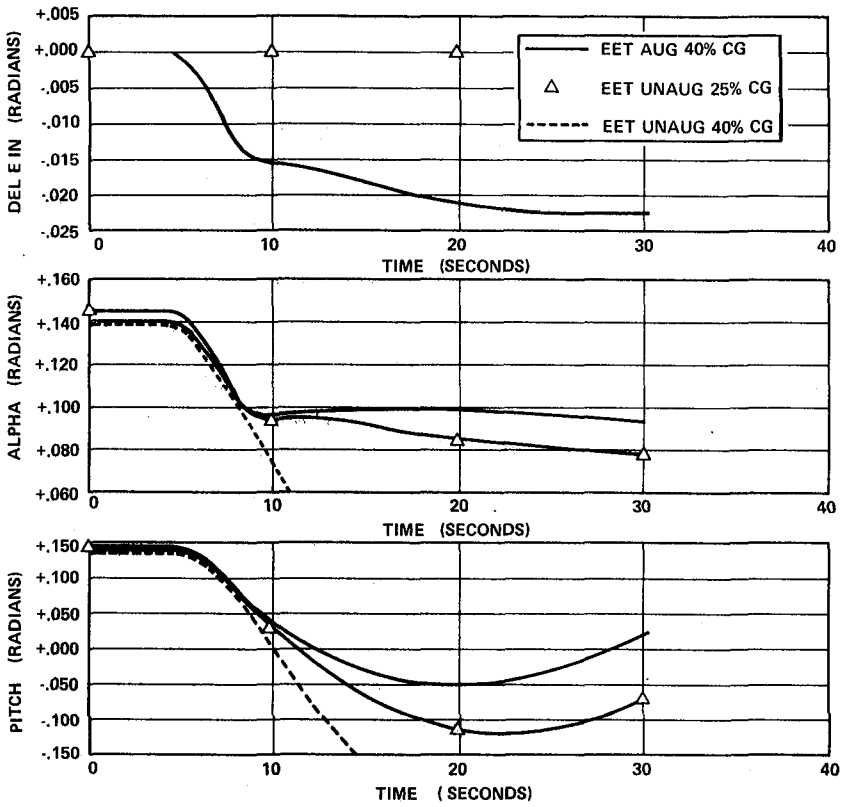

FIGURE 5-22. COMPARISON OF AUGMENTED AND AUGMENTED EET IN APPROACH – GEAR EXTENSION

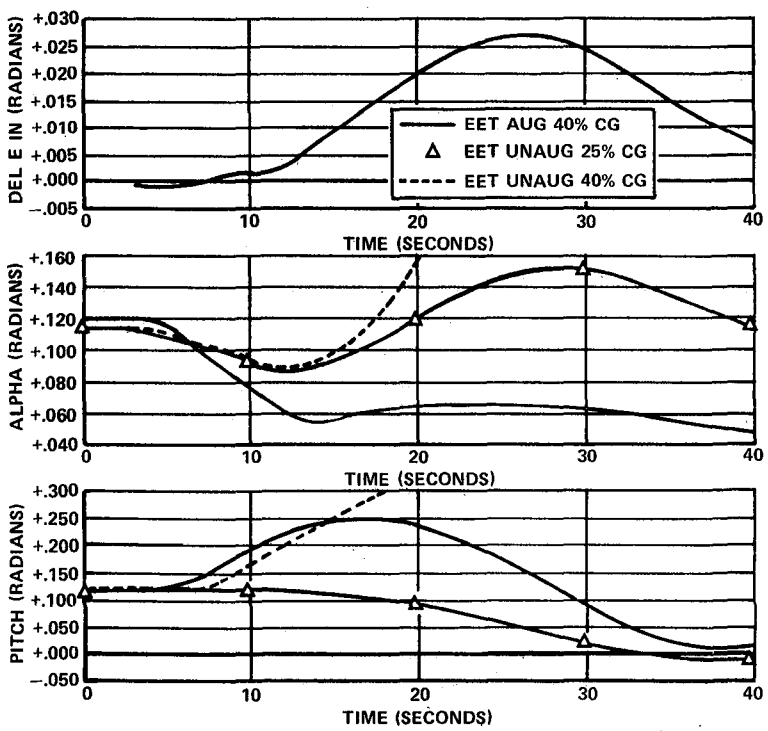

FIGURE 5-23. COMPARISON OF UNAUGMENTED AND AUGMENTED EET (APPROACH FLIGHT CONDITION – FLAP EXTENSION 10 TO 30 DEGREES)

unaugmented 25 percent center-of-gravity EET, unaugmented 40 percent center-of-gravity EET and augmented (control law No. 5, α,) 40 percent center of-gravity EET responses to landing gear and flap extensions. In all cases shown, no correcting pilot control has been applied, but during actual flight conditions, the pilot or autopilot would immediately compensate for the normal aircraft responses.

The landing gear responses in Figure 5-22 shows that the neutrally stable 40 percent center-of-gravity EET responds to this maneuver with an undamped pitch-down. Both the unaugmented 25 percent center-of-gravity and augmented 40 percent center-of-gravity EET respond to the gear extension with a conventional pitch-down, decreasing the angle of attack, and increasing airspeed. All of the augmentation configurations will attempt to maintain the trimmed condition. As shown in Figure 5-22, the augmentor provides nose-up elevator (negative sign) and the aircraft demonstrates the least landing gear effect.

Figure 5-23 shows the aircraft responses to the flap extension. (The low-drag flap design of the EET does not need a significant increase in thrust to maintain the approach airspeed for this configuration change.) The unaugmented 25 percent center-of-gravity EET response is similar to that of a conventional aircraft with an immediate angle-of-attack reduction and pitch-up, followed by an increased angle-of-attack and a reduced steady-state pitch altitude as the aircraft slows down and descends. The unaugmented 40 percent center-of-gravity EET responds to the configuration change with a continuous pitch-up maneuver. The augmented 40 percent center-of-gravity EET responds immediately to the change in angle of attack and pitch, and applies nose-down elevator (positive), which improves the 40 percent center-of-gravity response. The 0.027 radians (1.5 degrees) of elevator is not sufficient, however, and the resulting 0.25 radians (15 degrees) is considerably greater than the mid 25 percent center-of-gravity response.

5.5.3 Control Law Sensor Sensitivity. — An evaluation of the control law sensitivity to variations in sensor signals was performed by establishing representative sensor errors, inserting these tolerances in the RSSAS DETAC simulation, and then comparing the resultant responses to the elevator and thrust upsets with those of the nominal system. The sensor tolerances were obtained from a composite of the specification values, results from accept-

ance testing, and from the DC-10 in-service experience. They are presented in Table 5-2. The greatest deviation from nominal, whether empirically evidenced in the specifications or statistically obtained, was set as the maximum allowable tolerance.

Testing was conducted using the $\theta\dot{\theta}u\alpha$ control law family (No. 1 through No. 7) with the 40 percent center-of-gravity EET for both the cruise and approach flight conditions without turbulence effects. Upsets were introduced in the form of a 0.01745-radian (one-degree), one-second elevator step and a steady-state thrust increase of approximately 6300 newtons (1430 lb). Runs were made using nominal sensor values and then repeated with sensor gains set to the maximum positive tolerance and again with gains set to maximum negative tolerance as shown in Table 5-3. Comparison of the data presented in Appendix 9 shows good correlation between the nominal value runs and the maximum tolerance runs, except for control law No. 3 ($\theta\dot{\theta}\alpha$) in the cruise case.

As will be noted in the data package for these runs, several combinations of off-nominal values for the pitch and angle-of-attack sensor signal inputs to control law No. 3 were demonstrated. The data show that large excursions of the pitch sensor gain result in unstable — possibly divergent — response, whereas similar excursions of the angle-of-attack sensor gain result in heavily over-damped response characteristics.

With the exception of some necessary refinements to control law No. 3 gain terms, the data demonstrate that the control laws are adequately insensitive to anticipated levels of sensor-tolerance variations. This allows setting the sensor comparator levels at a value sufficiently high to eliminate nuisance warning, yet assure adequate performance capability.

5.5.4 Control Law Tracking. — Control-law-to-control-law tracking for the $\theta\dot{\theta}\mu\alpha$ control law family (No. 1 through No. 7) has been evaluated with the 40 percent center-of-gravity EET in a moderate turbulence with RMS level of 2.3 meters/sec. The test runs were made for the approach and cruise flight conditions, and initiated with an upset of 0.0175 radian (1°) of elevator for one second. Each of the seven control laws was allowed to augment the aircraft and the instantaneous commands of the other six control laws were compared to the active control. Excellent correlation was observed between the active and standby control laws. Figure 5-24 shows the precise

TABLE 5-2
SENSOR TOLERANCES

SENSOR	COMPONENT SPECIFICATION			INFLIGHT PERFORMANCE DEVIATIONS	MANUFACTURE OR MAINTENANCE ACCEPTANCE
	ACCURACY	BIAS	NOISE		
ANGLE OF ATTACK (α) DUAL OUTPUT MOUNTING	±0.0044 RAD (±0.25 DEG)	 ±0.0018 RAD (±0.1 DEG) ±0.0044 RAD (±0.25 DEG)		NO DATA AVAILABLE	±0.0044 RAD (±0 25 DEG)
NORMAL ACCELERATION (A_n) MOUNTING	±0.01g_n	±0.002g_n ±0.0044 (±0.25)	±0.002g_n	1σ = ±0.06g_n	±0.0075g_n
AIR DATA COMPUTER				1σ = ±0.22 M/S (±0.54 KN)	
1. AIRSPEED (u)	±2.57 M/S (±5 KN) AT 30.87 M/S (60 KN) ±1.03 M/S (±2 KN) AT 51.44 M/S (100 KN) ±1.03 M/S (±2 KN) AT 102.89 M/S (200 KN) ±2.06 M/S (±4 KN) AT 231.5 M/S (450 KN)				AS IN ACCURACY SPECIFICATION AS IN ACCURACY SPECIFICATION AS IN ACCURACY SPECIFICATION AS IN ACCURACY SPECIFICATION
2. ALTITUDE RATE ($\dot{h}$)	±5 PERCENT OR 0.15 M/S (30 FPM), WHICHEVER IS GREATER			1σ = ±0.22 M/S (±0 707 FT/SEC)	
VERTICAL GYRO PITCH ATTITUDE (θ) MOUNTING	TAKEOFF ±0.021 RAD (±1.18 DEG) CRUISE ±0.006 RAD (±0.35 DEG) DESCENT AND LANDING ±0.020 RAD (±1.15 DEG)	 ±0.0018 RAD (±0.10 DEG)		1σ = ±0.00134 RAD (±0.077 DEG)	±0.0087 RAD (±0.5 DEG – STATIC CHECK)

TABLE 5-3
MAXIMUM TOLERANCE RUNS

SENSOR SIGNAL	TOLERANCE	
	Cruise	Approach
Velocity	± 1%	± 2%
Pitch	±10%	±15%
Alpha	±10%	± 5%
Pitch Rate	± 1%	± 1%

correlation of the comparisons with control law No. 1 ($\theta\dot{\theta}u\alpha$) as the active control. The results of this analysis assure that minimal command synchronization is necessary for the control law in standby. Also demonstrated is a possible application of control-law-to-control-law comparison for system monitoring.

5.5.5 Flight Guidance System/RSSAS Interaction-Operation. — The Flight Guidance System (FGS) performance with the 40 percent center-of-gravity EET was evaluated for a flightpath tracking task consisting of control to a selected positive rate of climb and then a transition to a fixed altitude. In Figure 5-25, the FGS autopilot performs the specified maneuver with a fixed throttle setting which allows an increasing velocity as the aircraft levels to hold altitude. Approximately 0.007 radians (0.5 degrees) of elevator is required for a satisfactory altitude capture. With the autothrottles engaged, Figure 5-26 shows that the reduction in thrust to maintain airspeed results in a significant nose-down pitching moment which causes the aircraft to deviate from the selected altitude. (Elecom is the autopilot elevator command and Augcom is the sum of the autopilot and RSSAS commands.) The autopilot responds to the pitch-down but is limited at approximately 0.044 radians (2.5 degrees) of elevator authority for this flight condition. In Figure 5-27 the autopilot, autothrottle, and RSSAS are all engaged, and once again a satisfactory altitude capture is performed. During the capture maneuver, the autopilot applies 0.012 radians (0.69 degrees) of nose-down

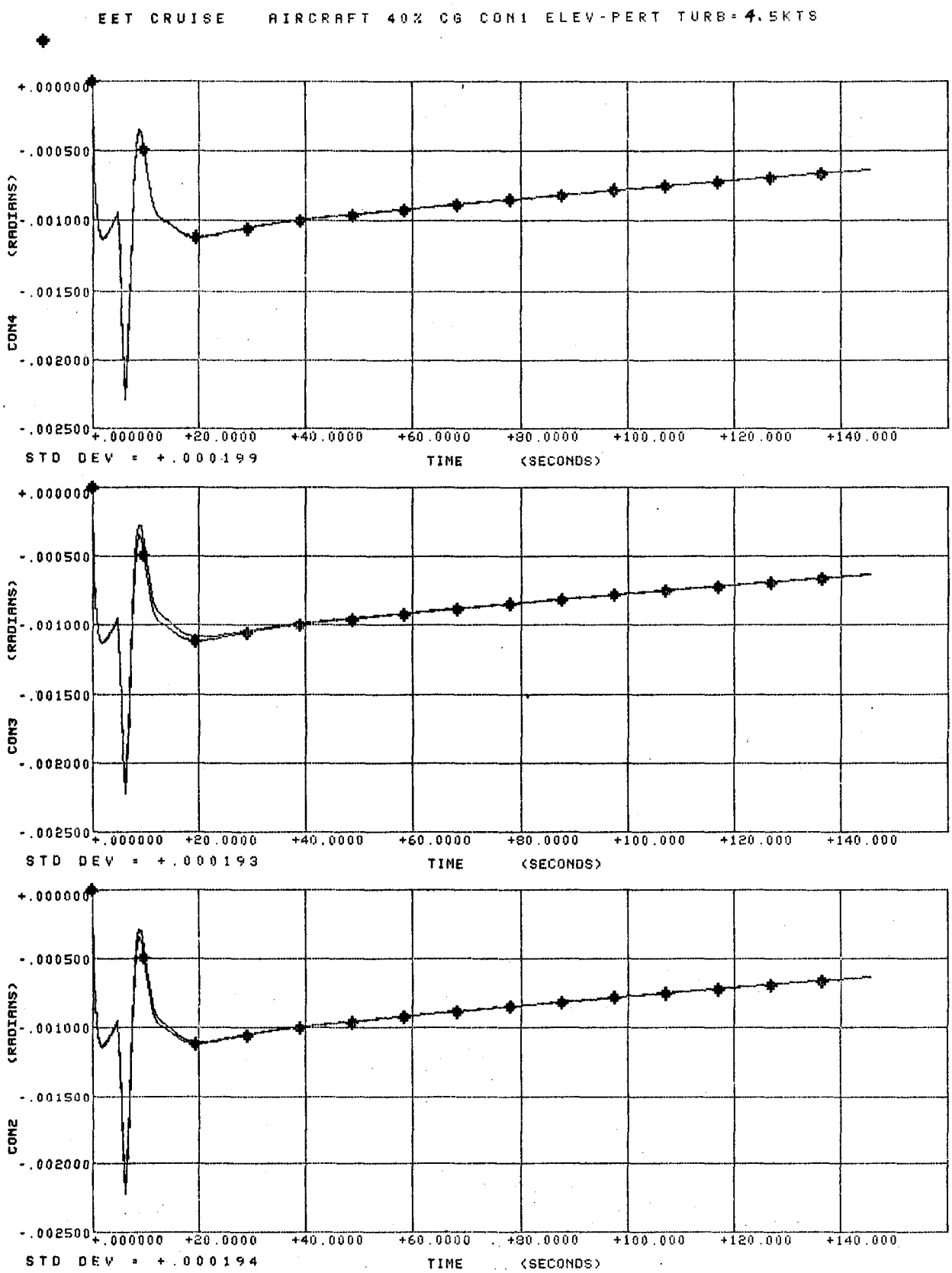

FIGURE 5-24a. COMPARISON OF CONTROL LAW NO. 1 WITH OTHER CONTROL LAWS – CRUISE CONFIGURATION -- CONTROL LAW NO. 1 ACTIVE

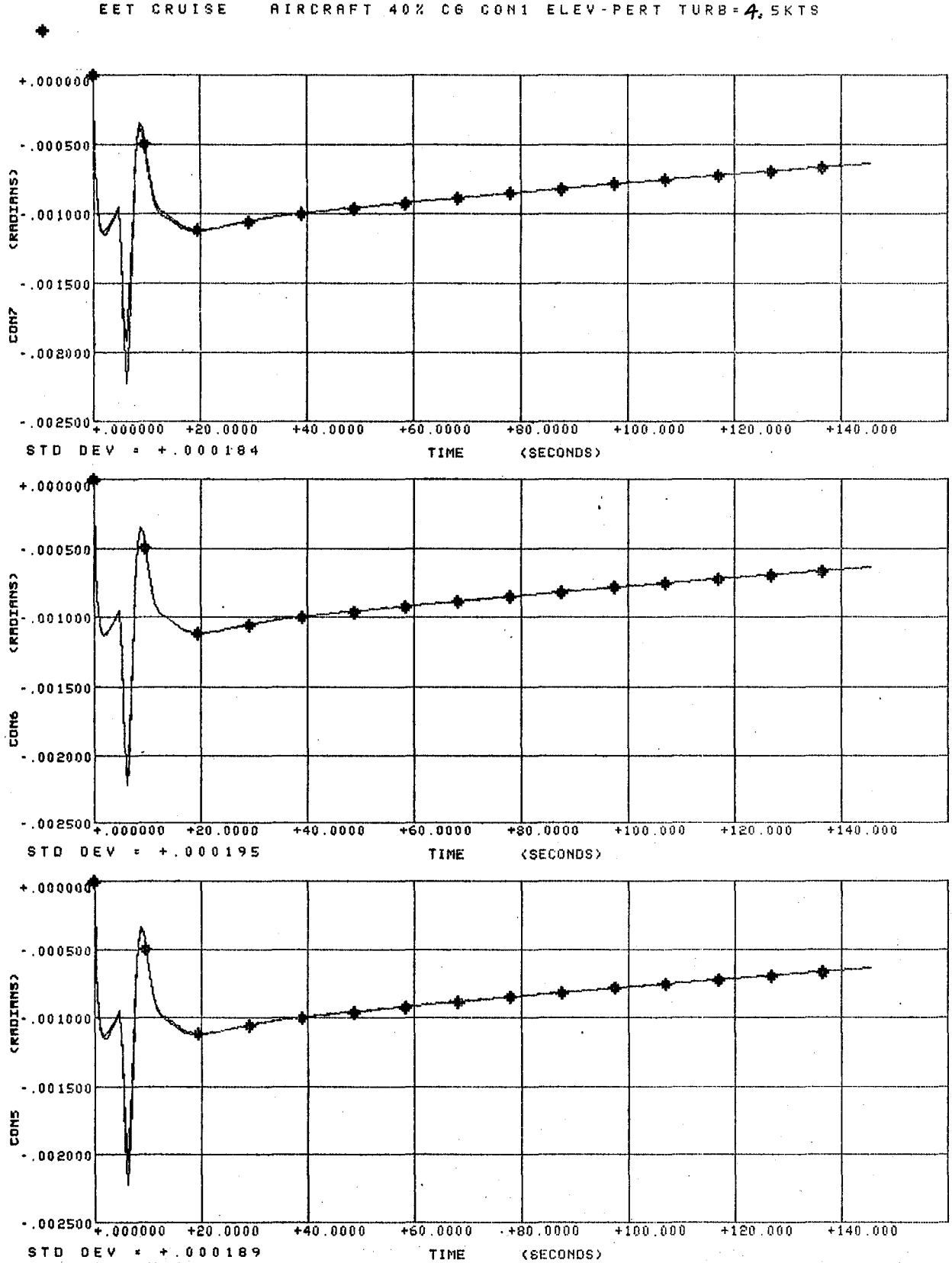

FIGURE 5-24b. COMPARISON OF CONTROL LAW NO. 1 WITH OTHER CONTROL LAWS – CRUISE CONFIGURATION – CONTROL LAW NO. 1 ACTIVE

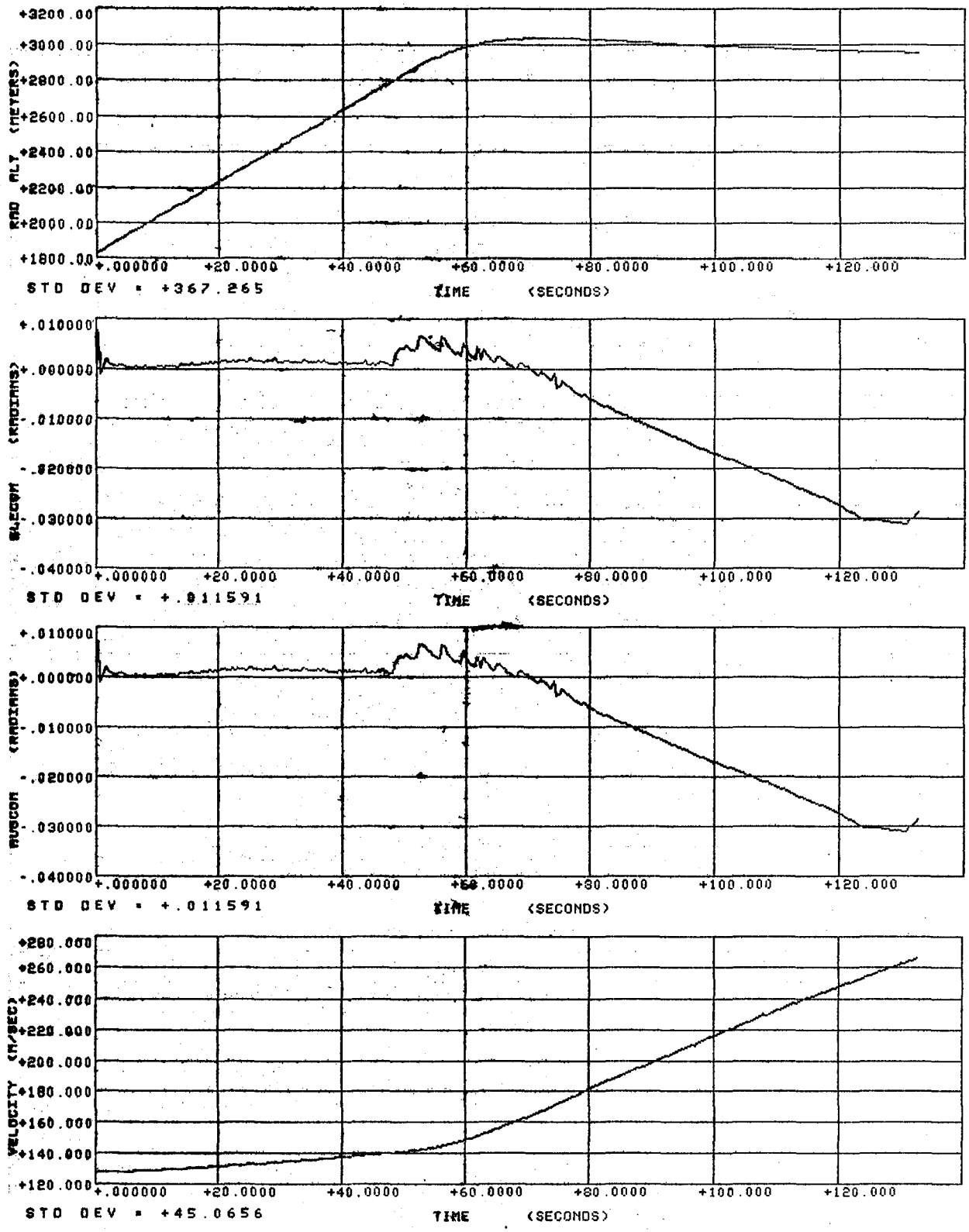

FIGURE 5-25. AUTOPILOT ALTITUDE CAPTURE WITHOUT AUTOTHROTTLES – UNAUGMENTED, 40% CG

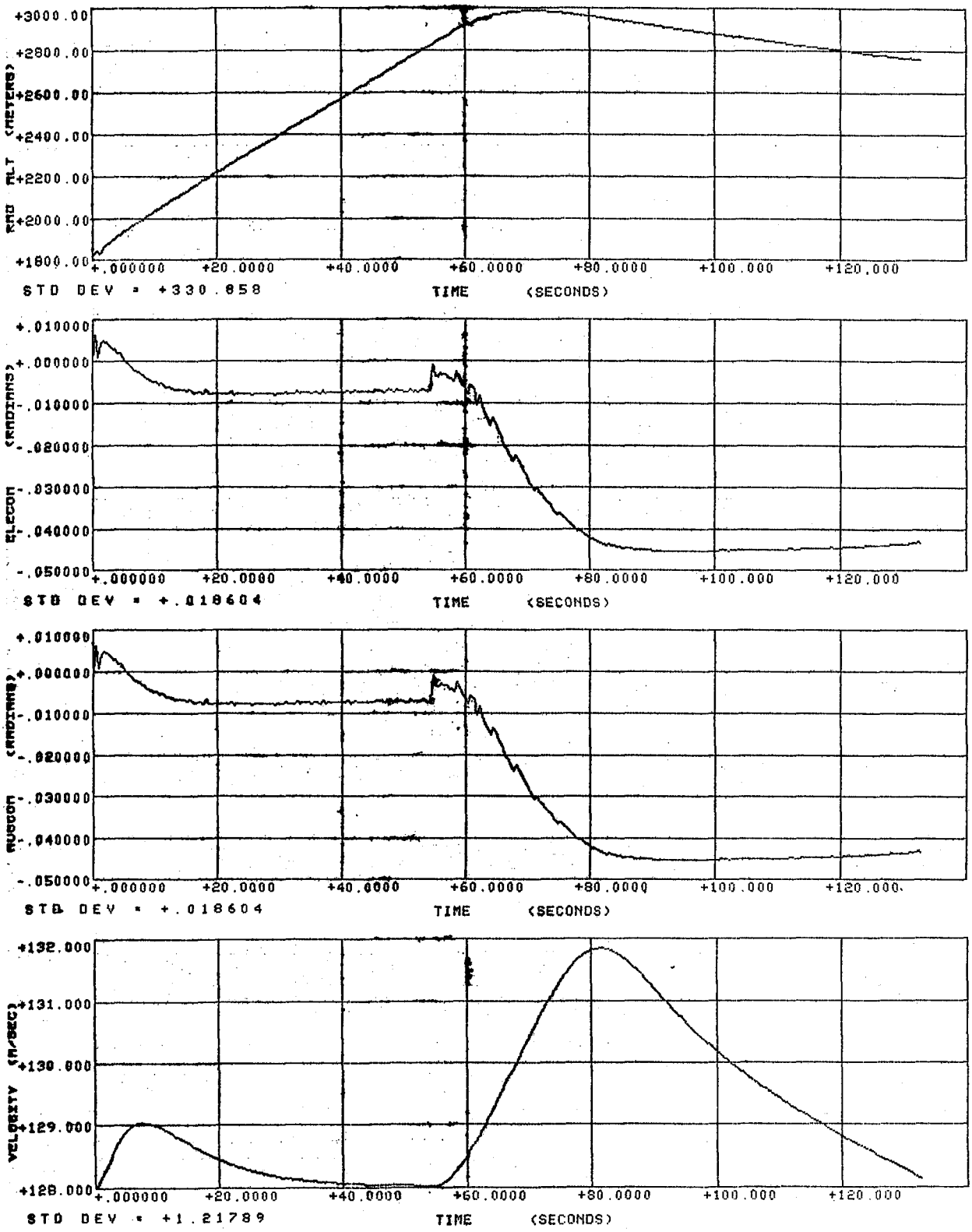

FIGURE 5-26. AUTOPILOT ALTITUDE CAPTURE WITH AUTOTHROTTLES – UNAUGMENTED, 40% CG

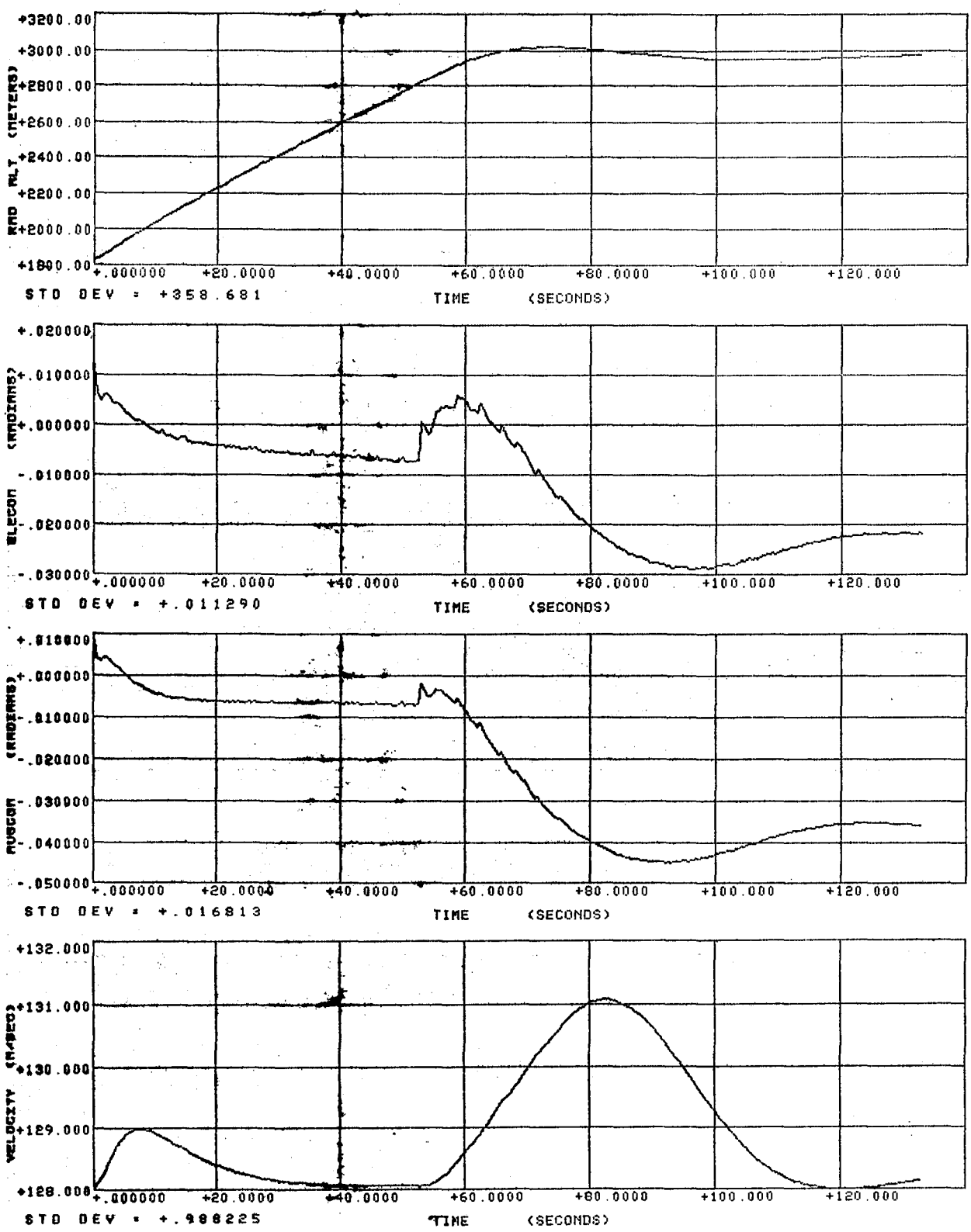

FIGURE 5-27. AUTOPILOT ALTITUDE CAPTURE WITH AUTOTHROTTLES – AUGMENTED, 40% CG

(positive) elevator and the RSSAS provides 0.008 radians (0.46 degree) of nose-up (negative) elevator for a total command (Augcom) of 0.004 radians (0.23 degree) of nose-down (positive) elevator. Then, as the autothrottles reduce the thrust and the aircraft pitches nose-down, the autopilot applies 0.028 radian (1.6 degrees) of nose-up elevator and the RSSAS provides 0.017 radian (0.97 degree) of nose-up elevator, for a total of 0.045 radian (2.58 degrees) of nose-up elevator.

The results of these tests indicate that the conventional autopilot can easily handle the aircraft's relaxed static stability, but when coupled to a significant pitch/thrust coupling, it does not provide the necessary elevator response. Also observed in the fixed-throttle maneuver of Figure 5-25 were several large command reversals during the capture. When the RSSAS was engaged, these reversals were significantly reduced, as was the frequency of the autopilot command input.

SECTION 6
SYSTEM ARCHITECTURE DEVELOPMENT

The RSSAS is a multichannel avionics system consisting of the appropriate sensors to describe the aircraft response, Flight Augmentation Computers (FAC) to perform the control calculations to achieve the desired flight response, an actuation system which transforms the computations into longitudinal aircraft control, and hydraulic and electrical systems to provide the necessary power for the other elements. Figure 6-1 is a diagram of the major RSSAS elements. Operationally, the RSSAS is independent of other normal aircraft flight controls and will function continuously in conjunction with either pilot or automatic pilot control. RSSAS aircraft control is accomplished through the elevator surfaces wherein augmentation commands are summed with the primary flightpath commands to provide a total surface deflection. Unlike the primary control commands which are reflected back to the control column, the RSSAS control is performed by a series actuator, the displacement of which will not be reflected back into the primary flight control system.

The elements in developing the system include (1) the system design requirements, (2) the formulation of proposed configurations, and (3) the evaluation of several selected candidates. Figure 6-2 shows the relationship of these elements. The system design requirements are obtained from the initial study constraints and the results of other study tasks. They define the fixed hardware requirements or hardware flexibility, the existing and desired flying qualities, the necessary functional reliability and safety, and the augmentation control requirements. The architectural formulation tasks then define: (1) the individual system components, (2) their level of redundancy, (3) their functional capability, (4) the interconnection of the devices, and (5) the characteristics of the architecture which could impact the design of the system/aircraft. Finally, the evaluation task determines the merit of the proposed systems with regard to the established requirements and also compares the satisfactory systems in order to select the most promising candidates for further consideration.

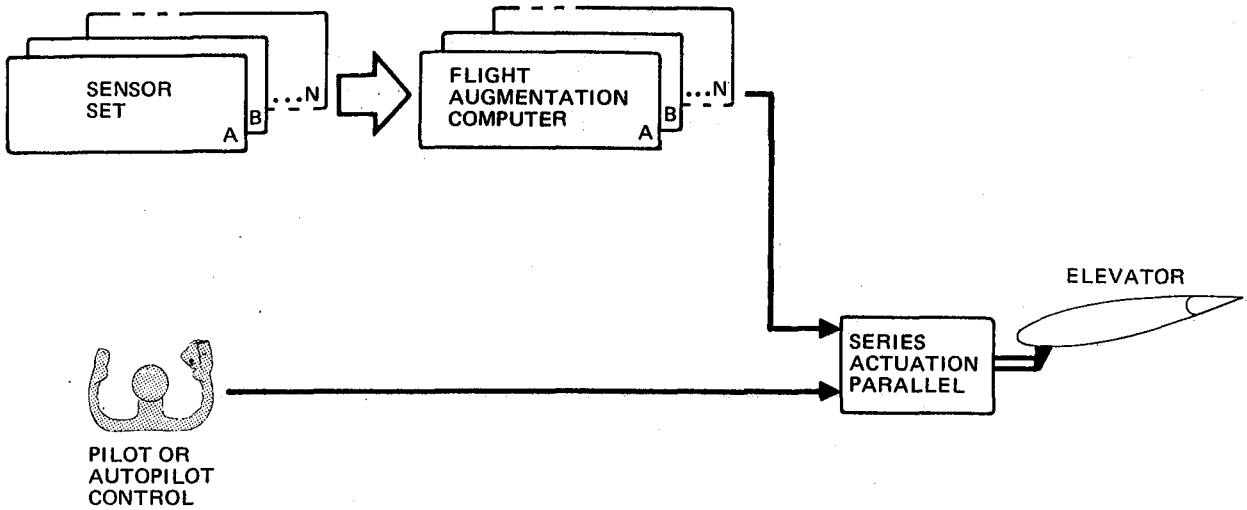

FIGURE 6-1. MAJOR RSSAS ELEMENTS

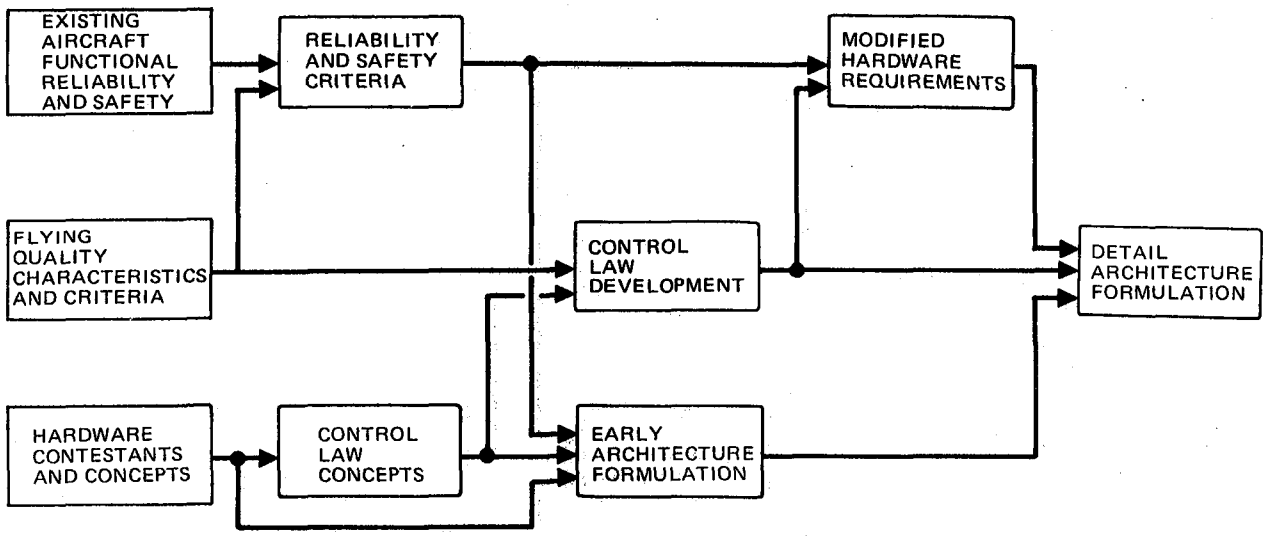

FIGURE 6-2. RELATIONSHIP OF THE SYSTEM DESIGN TASKS

6.1 System Design

6.1.1 Sensors. — The sensors considered for the relaxed static stability computation consist of all devices whose combination of parameters provides sufficient dynamic aircraft data to be used in the calculation of the augmentation control laws. The candidate parameter list includes: pitch attitude (θ), pitch attitude rate ($\dot{\theta}$), angle of attack (α), airspeed (u), altitude rate ($\dot{h}$), longitudinal acceleration (A_X) and normal acceleration (A_N). The baseline equivalent DC-10 sensor arrays which provide these data are:

- Three vertical gyros for θ and $\dot{\theta}$
- Two angle-of-attack vanes for α
- Two air data computers for u and $\dot{h}$
- Two accelerometer units for A_X and A_N.

The vertical gyros provide θ as an analog two-wire output and the FAC must derive $\dot{\theta}$ from this signal. α as used for the RSSAS is actually the average value of the two wing-mounted (one on each wing) dual transducer vanes, which have been calibrated for induced-flow effects. Each digital air data computer provides both u and $\dot{h}$ on a common serial digital data bus. The accelerometer units provide both A_X and A_N as two-wire analog signals with an additional 28 VDC discrete validity for A_N which is determined by comparing dual A_N accelerometers. The pitch/thrust compensation calculations are based upon the N_1 thrust parameter of each engine. The N_1 signal is provided as a two-wire analog signal from the engine indicator system.

A strapdown Attitude and Heading Reference System (AHRS) was considered as a variation to the baseline DC-10 sensors. Three AHRS units replaced the vertical gyros and accelerometer units supplying θ, $\dot{\theta}$, A_X and A_N on a common serial digital data bus. Resulting reliability calculations were essentially identical to the DC-10 sensors, so the tabulations are not repeated.

6.1.2 Flight Augmentation Computers (FAC). — A specification of the FAC includes both the definition of the internal hardware mechanization and a detailed description of its functional operation. The system analysis and simulation of this study require a rather extensive development of the

functional operation but a detailed hardware architecture is not necessary nor will it be established. It is assumed, however, that the hardware mechanization will be digital and that the individual computers will be capable of full internal failure detection. This and several other hardware characteristics will be discussed in general.

6.1.2.1 Hardware Architecture. — The main hardware elements within a digital computer are the input/output (I/O) circuits, memory, and central processing unit (CPU). The I/O is required to provide the interface with all external components of the system which include the sensors, actuators, control and annunciation units, and the other RSSAS computers. The computer memory stores the data required for the system calculations performed by arithmetic operations and logic decisions of the CPU. Using these elements, several different architectures may be constructed to satisfy the system requirements. The following configuration summaries are the primary near-term concepts which are intended to provide full internal fault-detection capability.

The single-path, dual-processor architecture shown in Figure 6-3 includes two central processors while most of the other elements are single-string. It is argued that if the processors themselves can be guaranteed to be functioning properly by comparing their outputs, the rest of the machine can be shown to function by various error-detection schemes. It is felt by the advocates of this architecture that one may be able to avoid a detailed Failure Modes and Effects Analysis (FMEA) of the processor since the second processor (which may be dissimilar) is always watching the first processor.

The dual-path, single-processor architecture shown in Figure 6-4 consists of dual paths (i.e., dual memory, I/O) within the machine but uses a single processor to operate on the data. After the A and B sensor sources are converted to data words in separate memory locations, the data values are compared. The data are then averaged and control laws are computed twice and compared. If the control law computations are valid, the data are sent out to the servo-amplifiers through the digital to analog converters. The outputs of the D to A converters are sent back through the input analog to digital converters and compared with what their value should be. If the

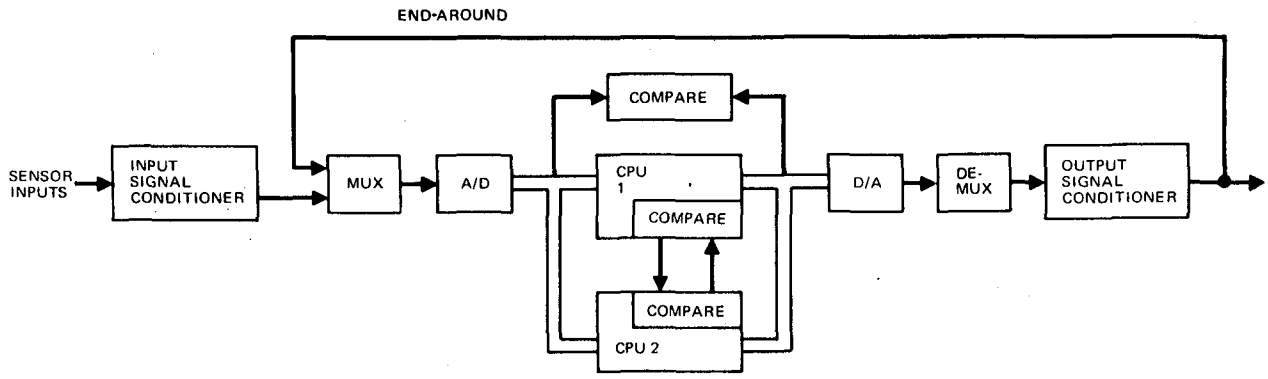

FIGURE 6-3. SINGLE-PATH, DUAL-PROCESSOR ARCHITECTURE

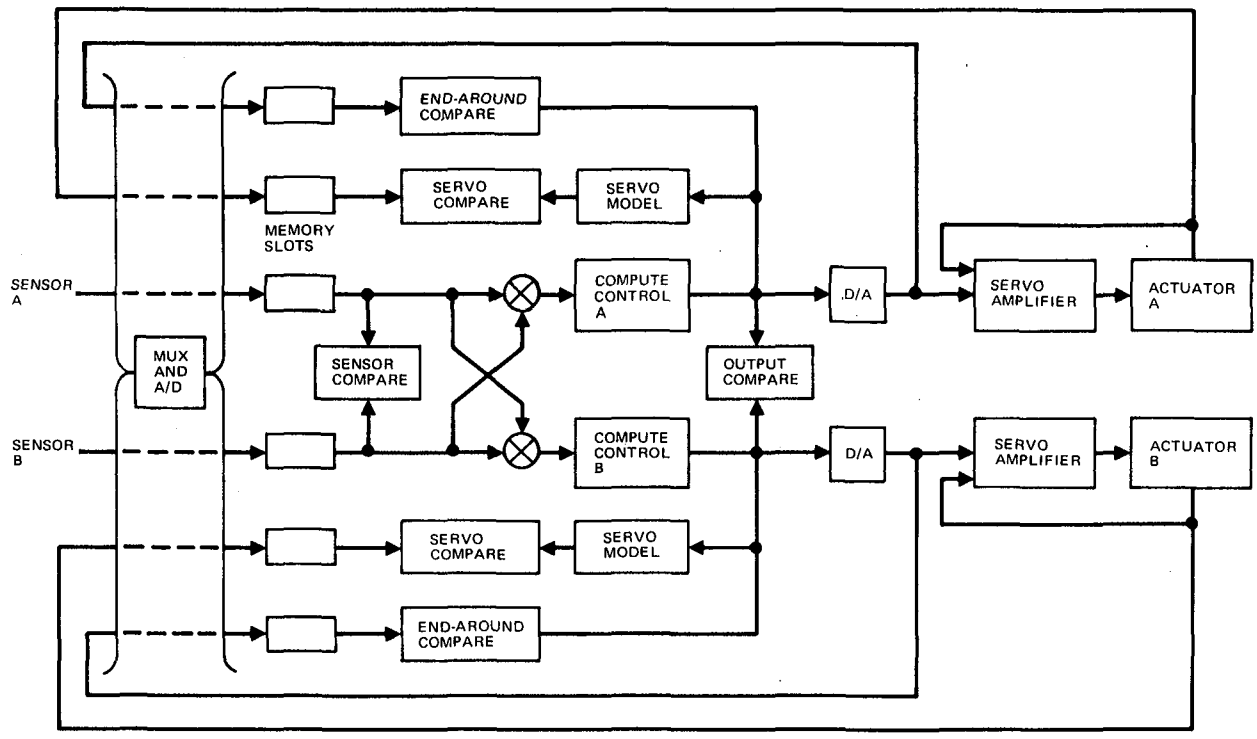

FIGURE 6-4. DUAL-PATH, SINGLE-PROCESSOR COMPUTER

output is valid, servo response must be checked. The servo position is sent back through the input and compared with what its response should be. In this way the entire system is monitored.

The key to the whole process is the integrity of the processor itself. It must be fully monitored. Several techniques for ensuring proper functioning of the processor will be discussed later in this report.

The dual-path, dual-processor architecture is essentially the packaging of two completely independent computers in one line-replaceable unit (LRU). This is the direct equivalent of today's analog dual-channel fully monitored computers, and many of the cross-comparison techniques described above are applicable. Manufacturers differ in the details with regard to frame synchronization, I/O handling, etc. In general, the internal comparators are set a little wider since each channel is either not operating on the same data or receives the same data through different I/O devices. Time skewing and data freshness affect channel-tracking tolerances also.

6.1.2.2 Functional Architecture. — The functional requirements of a FAC are shown in Figure 6-5 and consist of: (1) processing data between the computer and the external system components; (2) performing the control computations; (3) maintaining executive control of the internal functions, and external actuation control and communications, and (4) monitoring the system functions. Each computer within the RSSAS performs these functions identically and independently except that such operations may be pre-programmed decisions based upon the other computer data transfer.

(a) Data Processing. The computer must interface with three different types of signals: Analog, 28-VDC discrete, and serial digital data. The largest anticipated interface list for the RSSAS function is itemized below:

Inputs

Analog (2-wire)

*3 - Pitch Attitude

*2 - Vertical Acceleration

4 - Angle of Attack

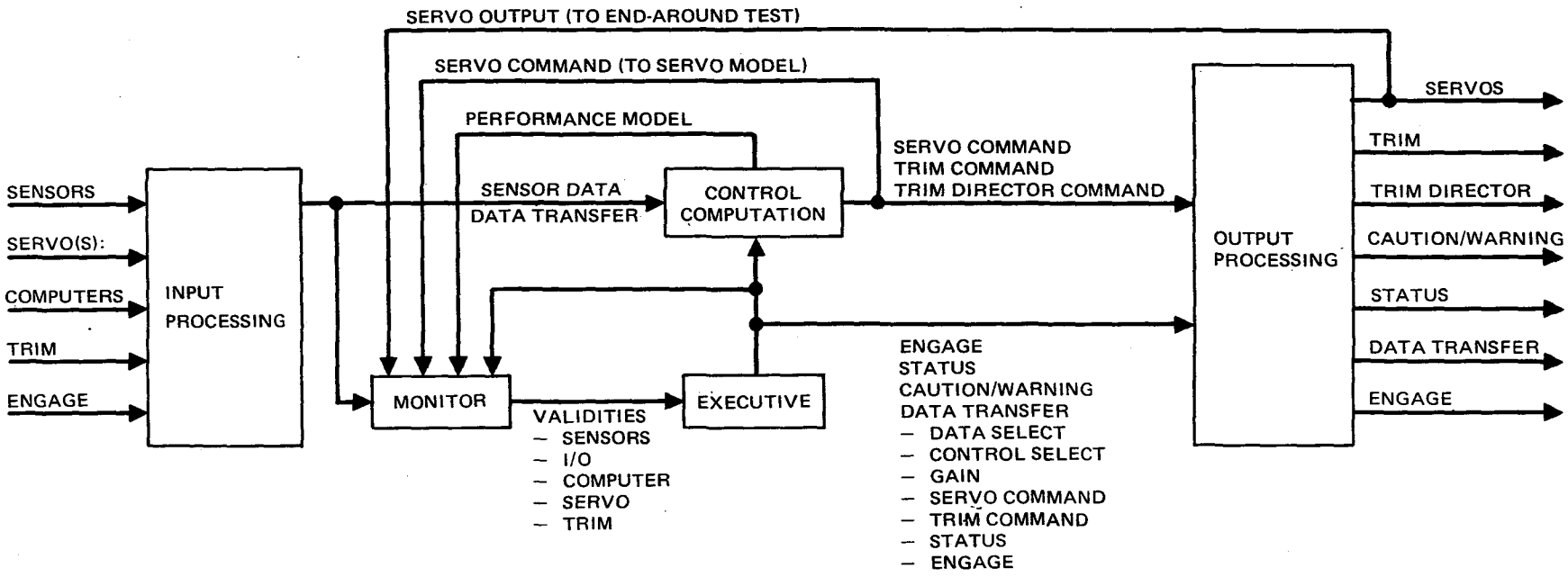

FIGURE 6-5. FLIGHT AUGMENTATION COMPUTER FUNCTIONAL DIAGRAM

2 - N_1 (Engine Thrust)
2 - Series Elevator Actuator Position
2 - Horizontal Stabilizer Position
2 - Primary Elevator Control Position
1 - Manual Airspeed Slew

28-VDC Discrete (1-wire)
*2 - Vertical Acceleration Validity
1 - System Engage Logic
1 - Test Initiate Logic

Serial Digital Data Bus (2-wire)
2 - Airspeed
2 - Computer Intercommunication
1 - Maintenance System

*May be replaced by 3 - Attitude Heading Reference System, 2-wire serial digital data buses.

Outputs

Analog (2-wire)
2 - Series Elevator Actuator Command

28-VDC Discrete (1-wire)
4 - Trim Command
2 - Trim Director Command
2 - Series Elevator Actuator Engage
1 - System Warning
1 - Pitch/Thrust Warning

Serial Digital Data Bus
1 - Intersystem Communications

Figure 6-6 is a typical hardware mechanization which shows the required data-processing interfaces. At the input, the analog signals are conditioned and multiplexed, then converted to digital and impressed onto the input data bus. The 28-VDC discretes are packed into digital words with each input typically representing a

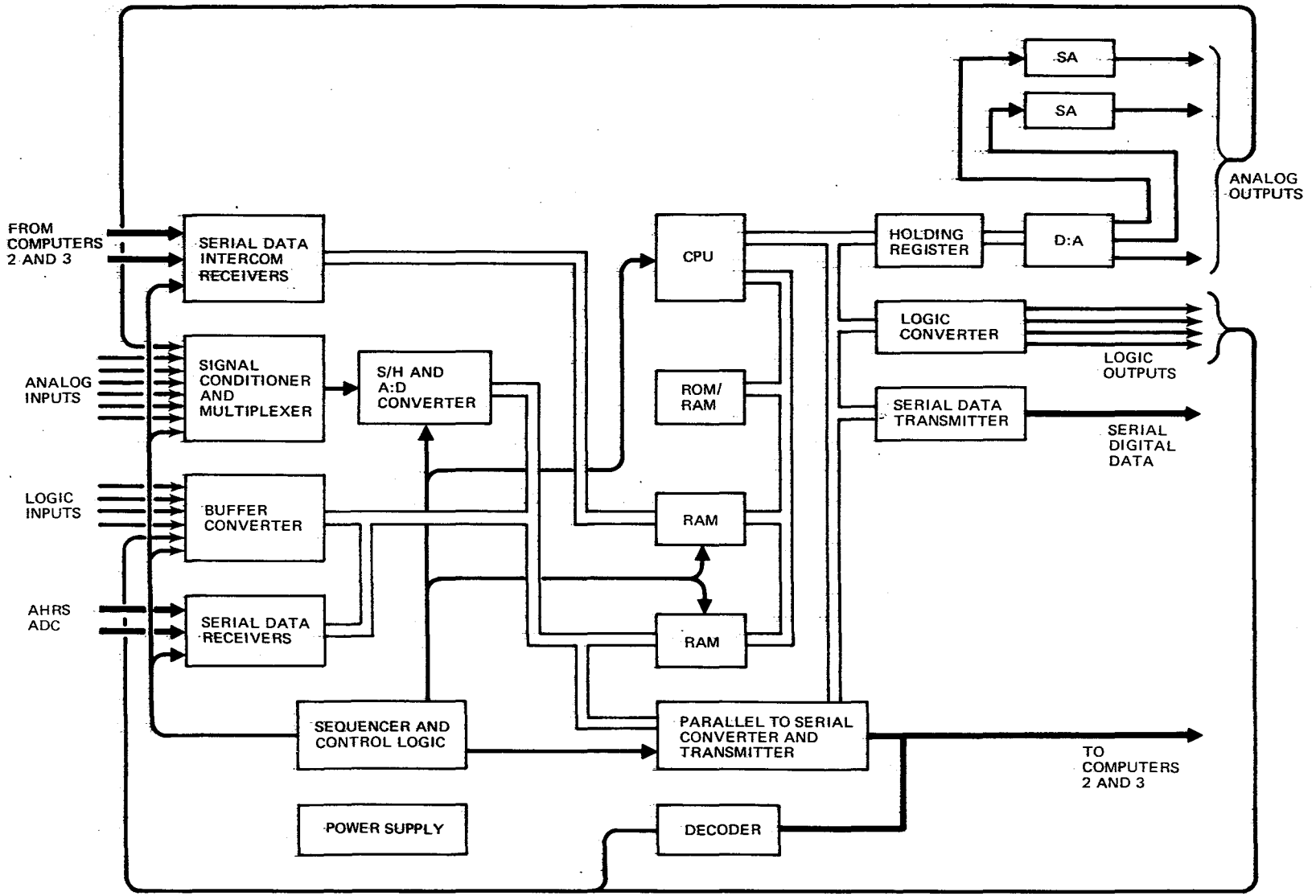

FIGURE 6-6. COMPUTER BLOCK DIAGRAM, MONITORED PLUS INTERCOM

single bit of the word and sequenced onto the input bus. The serial digital data buses require a serial-to-parallel conversion prior to interface with the data input bus. The output data are provided by picking the appropriate data of the CPU output data bus and reversing the operations performed at the input.

(b) Control Computation. The control computation function performs the necessary operations, as shown in the flow diagram of Figure 6-7, to select or synchronize the appropriate control laws, compute the selected control law, and provide the corresponding series elevator actuator and horizontal stabilizer commands. The control logic is provided by the executive function and the command outputs are fed back to the monitor as part of the validation process. Figure 6-8 shows the computer mechanization of the control law forms shown in Section 5, Figure 5-3.

A single control law is represented in the figure showing the system pre-engage synchronization (power-up value), and control law in standby synchronization (sample and hold, S/H), The pre-engage synchronization essentially establishes the existing aircraft inputs as the trim condition at engagement. The standby synchronization is active whenever the associated actuator is engaged but that control law is not active. This will assure that at the moment of transfer between control laws, identical servo commands are present; therefore, a surface transient will not result. Also, since the pilot can maneuver the aircraft with the primary horizontal stabilizer trim, the pilot command input to each control law is a combination of these two commands. The stabilizer position has, however, been converted to equivalent elevator by the gain factor K_2 which is approximately a constant 1.613 over the flight envelope of interest.

Each control law mechanization has a unique sensor input array, observer, and gain matrix. Selection of the appropriate control law is performed in accordance with the logic from the executive function. The selected control law command is then output to the series elevator actuator. The automatic series elevator trim function

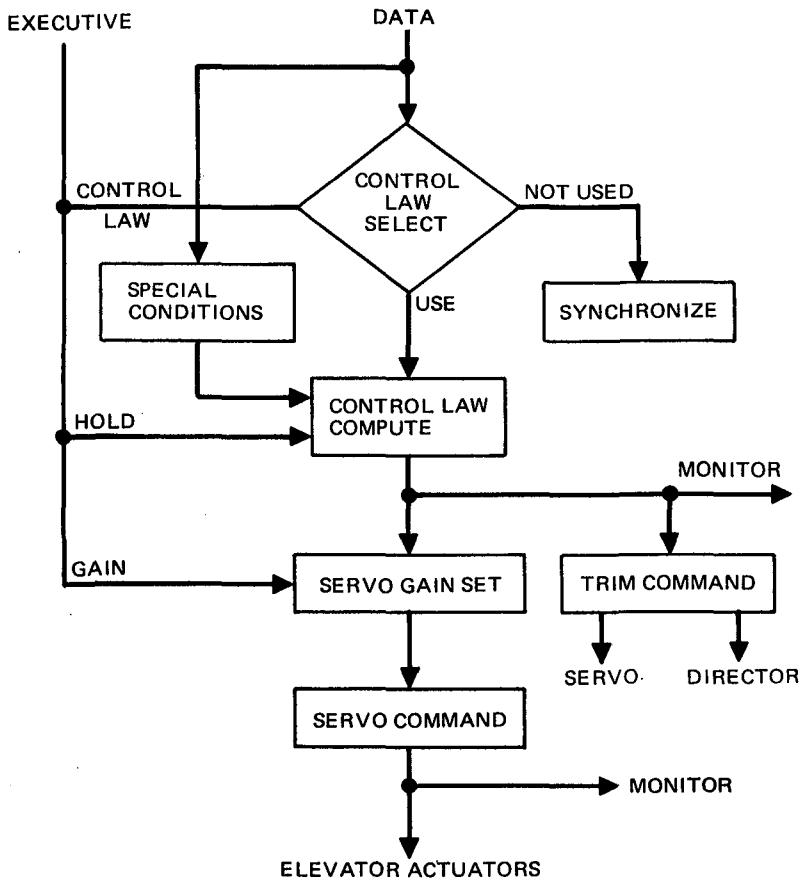

FIGURE 6-7. CONTROL COMPUTATION FLOW DIAGRAM

interfaces at this point and this feature will be discussed in detail in Paragraph 6.1.4.

Gain programming of the control laws is accomplished using the airspeed input from the air data computer. Should both air data computers fail, the gain programming reverts to the input from the manual airspeed slew switch on the overhead instrument panel, which is activated by the flight crew.

(c) Executive Control. The executive function determines and controls the actuator engagement, control law selection, and status/warning data transfer. The flow diagram in Figure 6-9 shows that the executive decision process is initiated with an input from the monitor function. Based on the validity of the computer and actuator, and provided an engage logic from the RSSAS controller is present, the associated actuator will be supplied an engage command. The validity of the sensor array is used to determine the available control laws

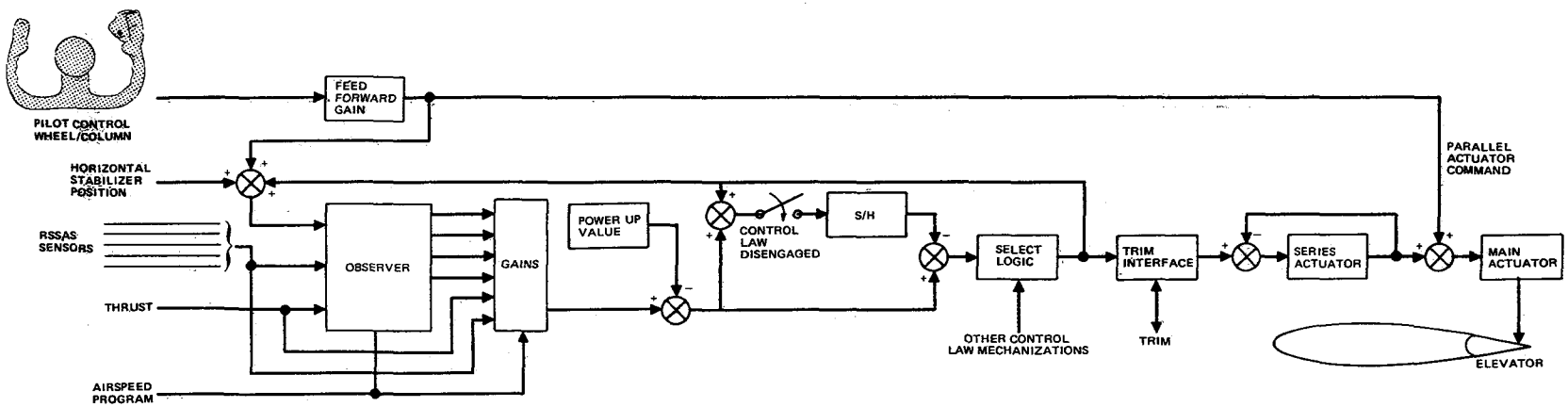

FIGURE 6-8. RSSAS CONTROL COMPUTATION BLOCK DIAGRAM

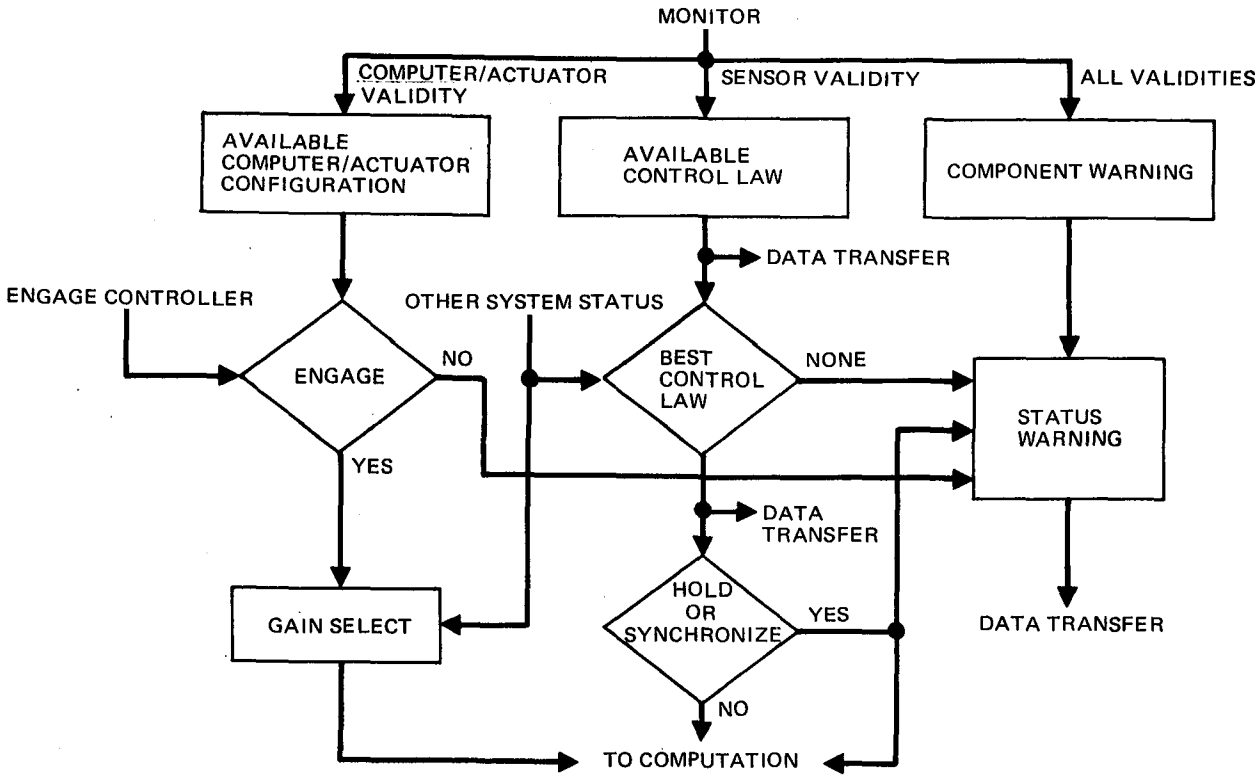

FIGURE 6-9. EXECUTIVE FUNCTION FLOW DIAGRAM

and then, in conjunction with the status of the other computers and the actuator engagement, the best control law is selected for control and the others are synchronized. Appropriate logic functions are picked off for status/warning annunciation and for data transfer to the other RSSAS computers.

A more detailed flow diagram of the actuator engage and system warning is shown in Figure 6-10. The computer first determines if the associated engage switch has been selected. If not, the warning light output is reset and the actuator is not engaged. With the switch on, the computer validity must be present and a control law available (unit control law not in standby) to continue the logic process for actuator engagement. If not, the system warning is set. Next, with the computer configured for the control of two actuators, the validity of the first is checked and if present, the actuator is armed. Now, if a satisfactory total system control law is available (one which agrees with the other computers or gives best performance available), the actuator is engaged. This sequence is then performed on the second actuator (note that a warning will be provided if either actuator is armed and a control law is not available).

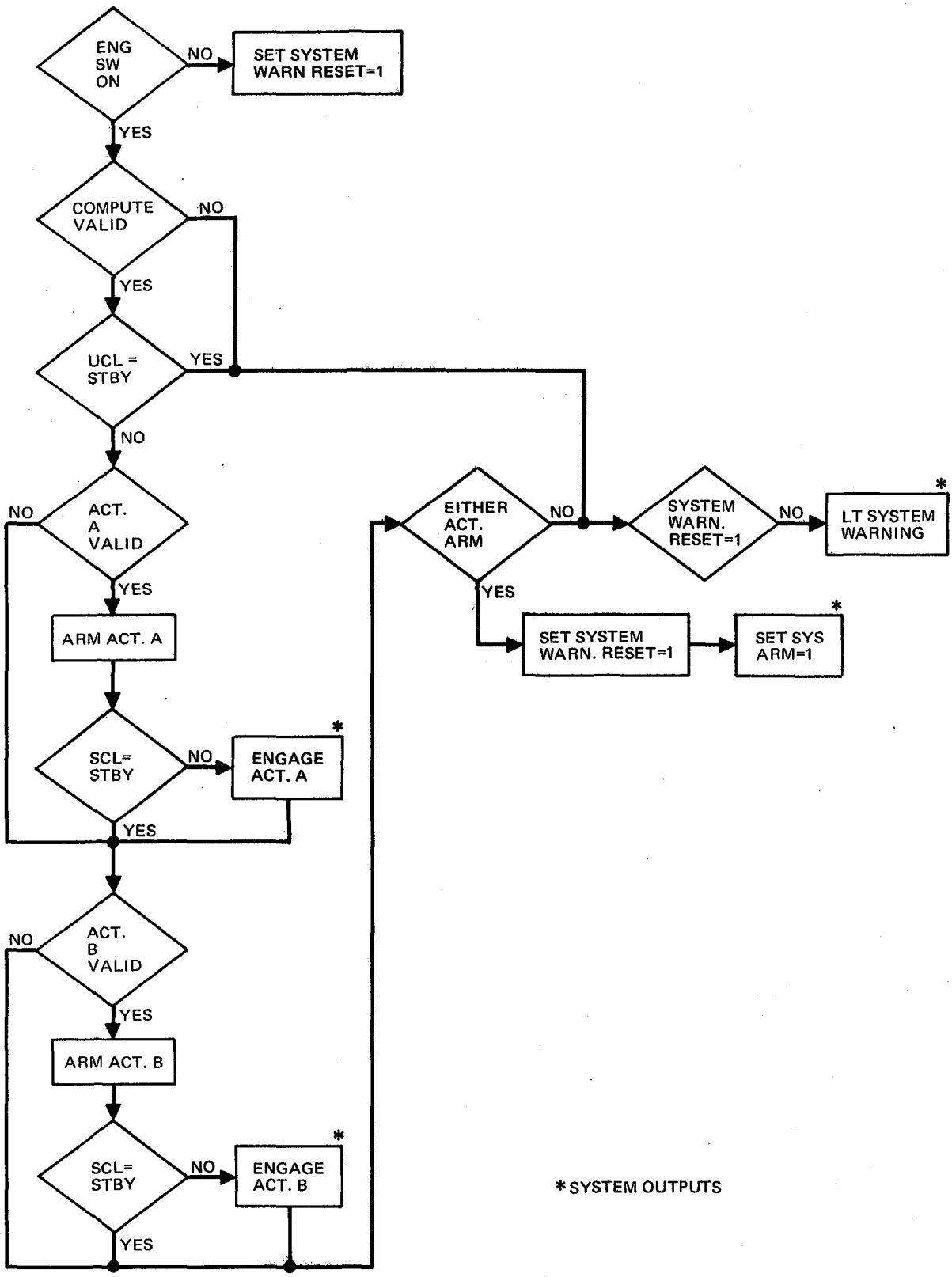

FIGURE 6-10. ACTUATOR ENGAGE AND SYSTEM WARNING

The most complex task of the executive function is to select the system control law. Figure 6-11 is the flow diagram for determining the highest-level control law available to a given computer — unit control law (UCL). This process determines from the monitor output which sensors are available. The UCL is then selected as the control law which uses the greatest number of sensors. This control law, however, may not be in agreement with the control law of the other computers due to tolerances or failure conditions. Common control laws, while not yet proven to be essential, do seem to be desirable for surface-to-surface tracking and total system performance. For this reason, each computer independently determines the system control law (SCL).

Figure 6-12 (a, b, c and d) shows the flow diagrams for the selection of the SCL (note that this diagram is for the No. 1 computer). In Figure 6-12a, the actuator arm/engage status of each computer is examined and, if OFF, all control law flags of that unit are set to "failed" for the purpose of selecting the SCL. In Figure 6-12b, the flags determined in 6-12a are counted and if all computers have common valid sensor arrays, the highest level (most sensors) control law is selected.

Figures 6-12c and 6-12d show the process followed to determine the SCL when all of the computers do not have a common control law available. The objective of this logic sequence is to determine if two computers have a valid, common control law and, if so, that SCL is selected and the computer that is not in agreement has its SCL put in standby (STBY). If no two computers agree, all computers revert to their UCL, which is considered the best decision available.

The thrust/pitch compensation function is also controlled by the executive as shown in Figure 6-13. Dual N_1 outputs for each engine are provided from the thrust-indicating system to each FAC. These N_1 signals are compared by the system monitor to determine the validity of the data and, if a failure is not detected, the thrust term used in the compensation calculation is N_1 = No. 1 N_1 + No. 2 N_1. If either engine datum is determined to be failed, N_1 is set

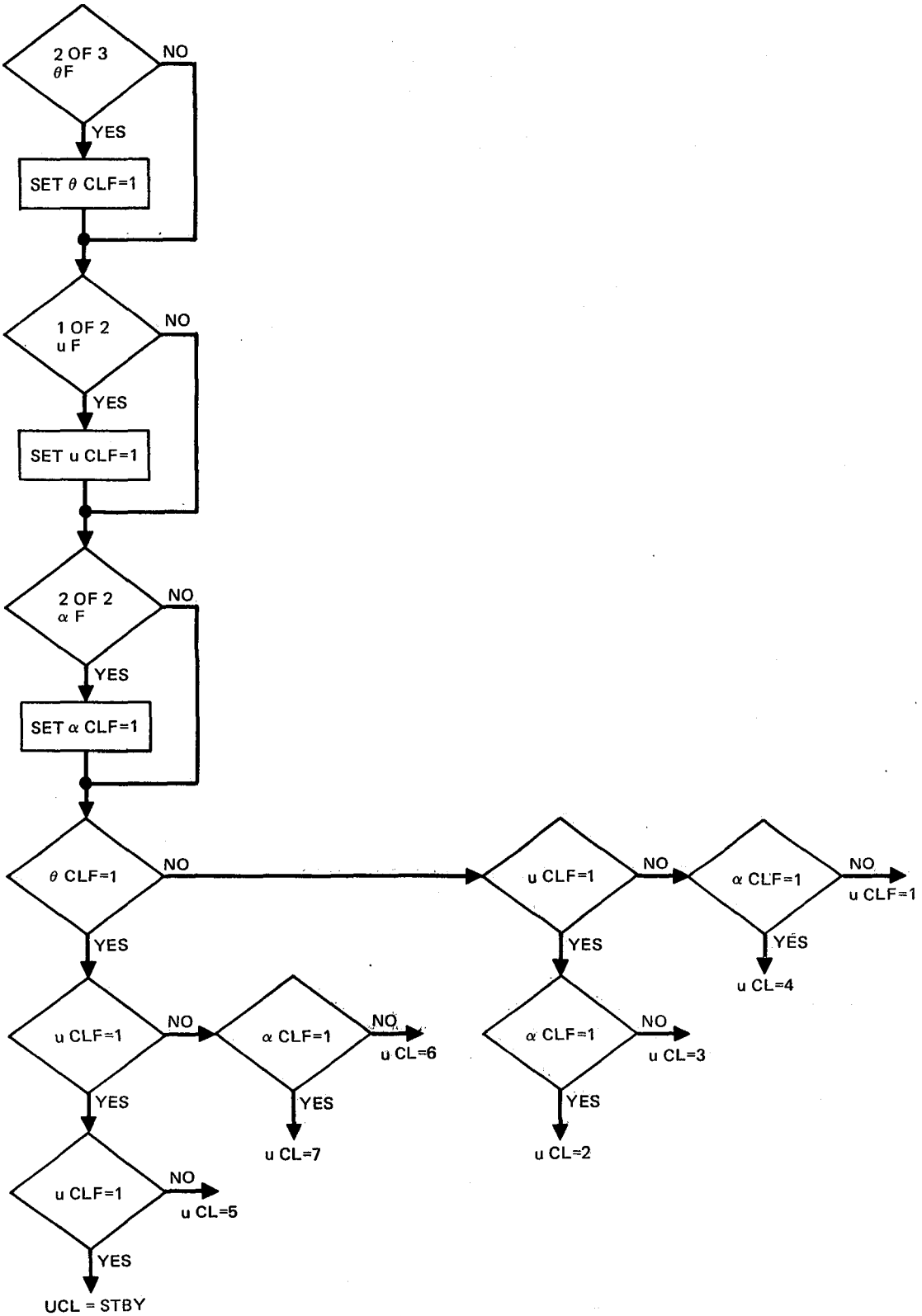

FIGURE 6-11. UNIT CONTROL LAW (UCL) SELECTION FLOW DIAGRAM

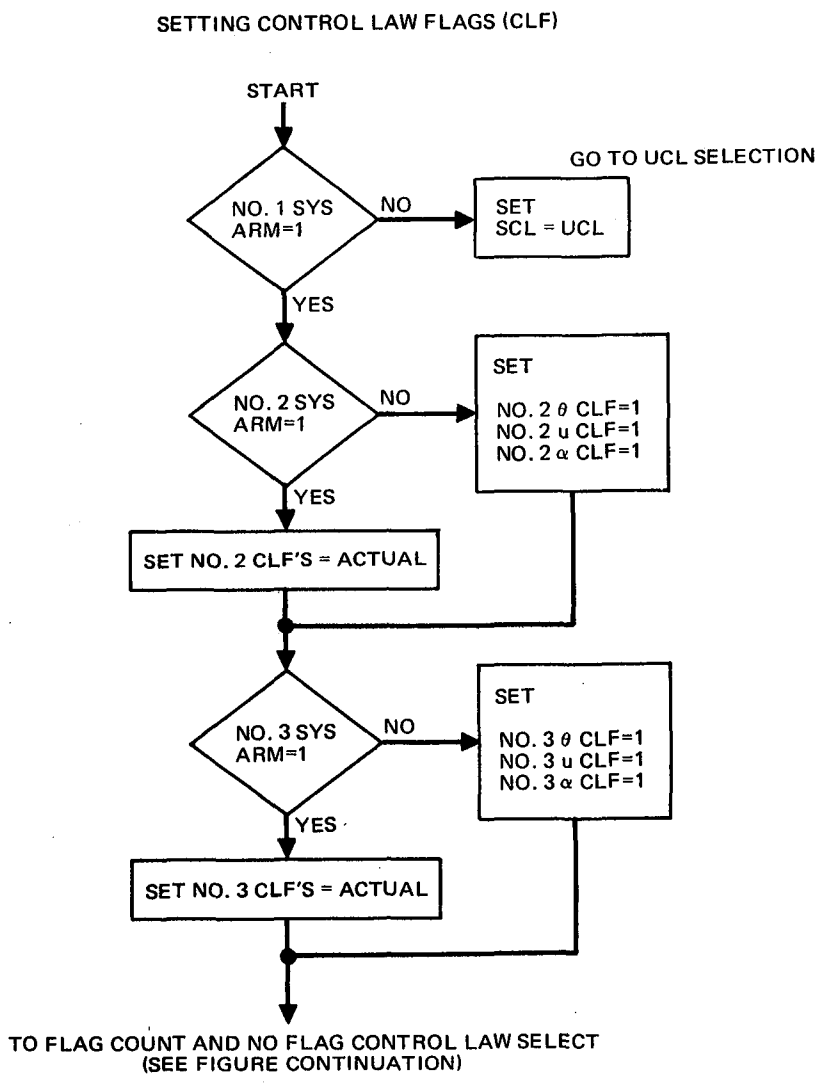

FIGURE 6-12a. SYSTEM CONTROL LAW (SCL) SELECTION FLOW DIAGRAM

equal to that of the valid datum. With both engines still operative, this will result in essentially half the required thrust-control gain with an accompanying caution annunciation. If both data sources fail, the thrust/compensation is put into hold and the appropriate warning light comes on.

(d) Monitoring System Functions. A variety of methods is used to detect failures within the computer and its associated components (sensors and actuators). Some of these techniques are aimed at specifically validating a hardware function. Others determine the system's health by evaluating its performance or potential performance ability. Such concepts are highly dependent upon the function, architecture, and intended performance of the system. The following discussion

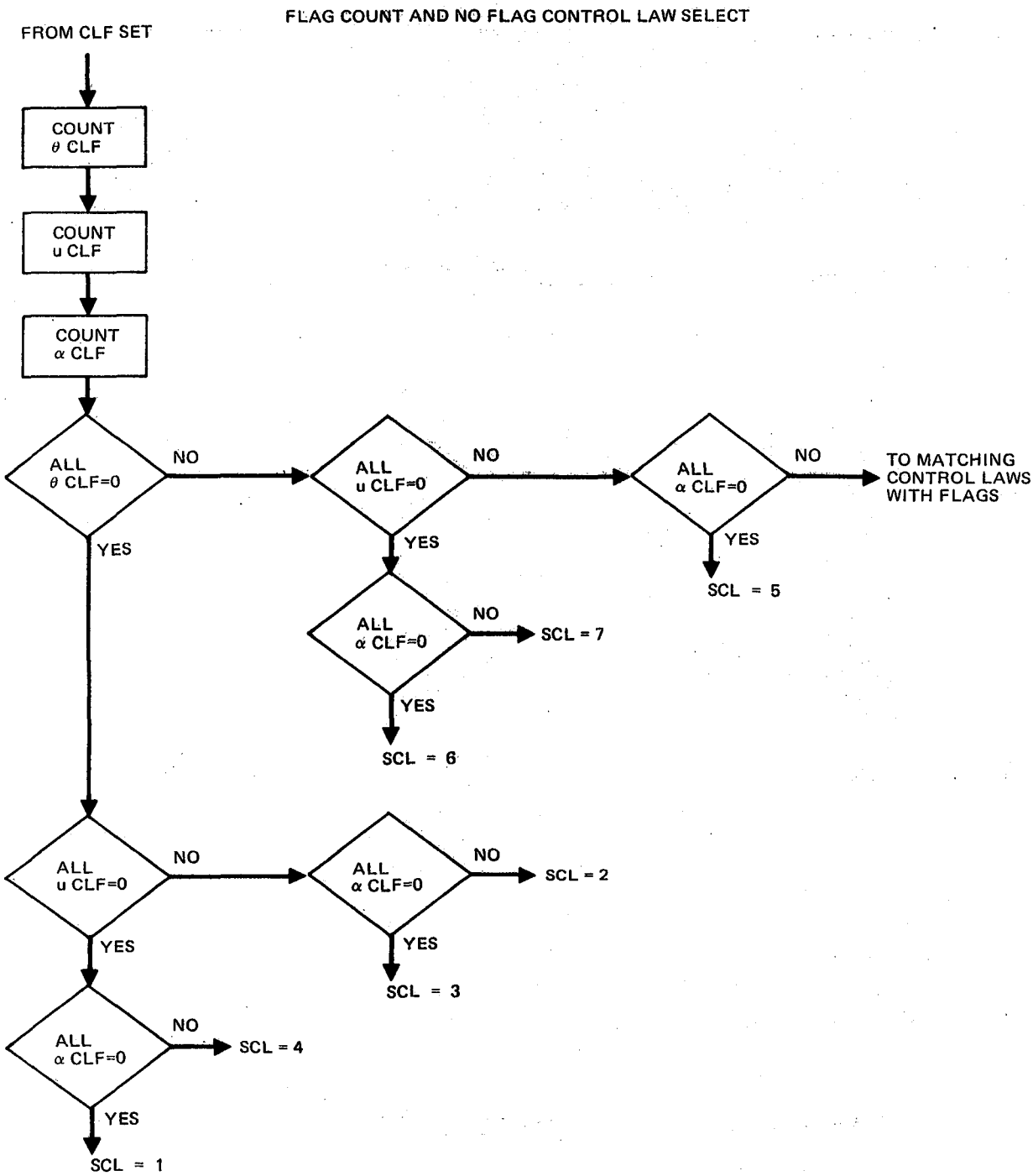

FIGURE 6-12b. SCL FLOW DIAGRAM (CONTINUED)

will highlight those monitor concepts intended for the RSSAS. Most of these are continuously functioning during flight or on the ground and are an integral part of both the monitoring and maintenance functions of the system.

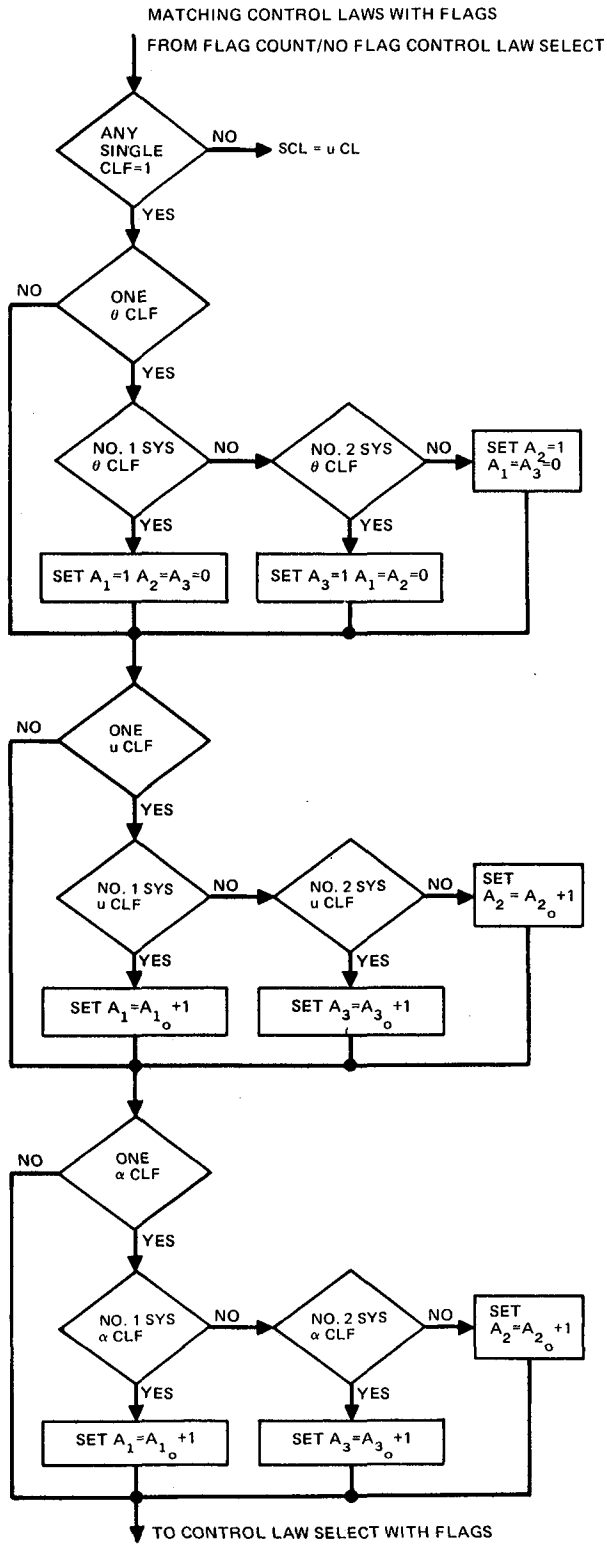

FIGURE 6-12c. SCL FLOW DIAGRAM (CONTINUED)

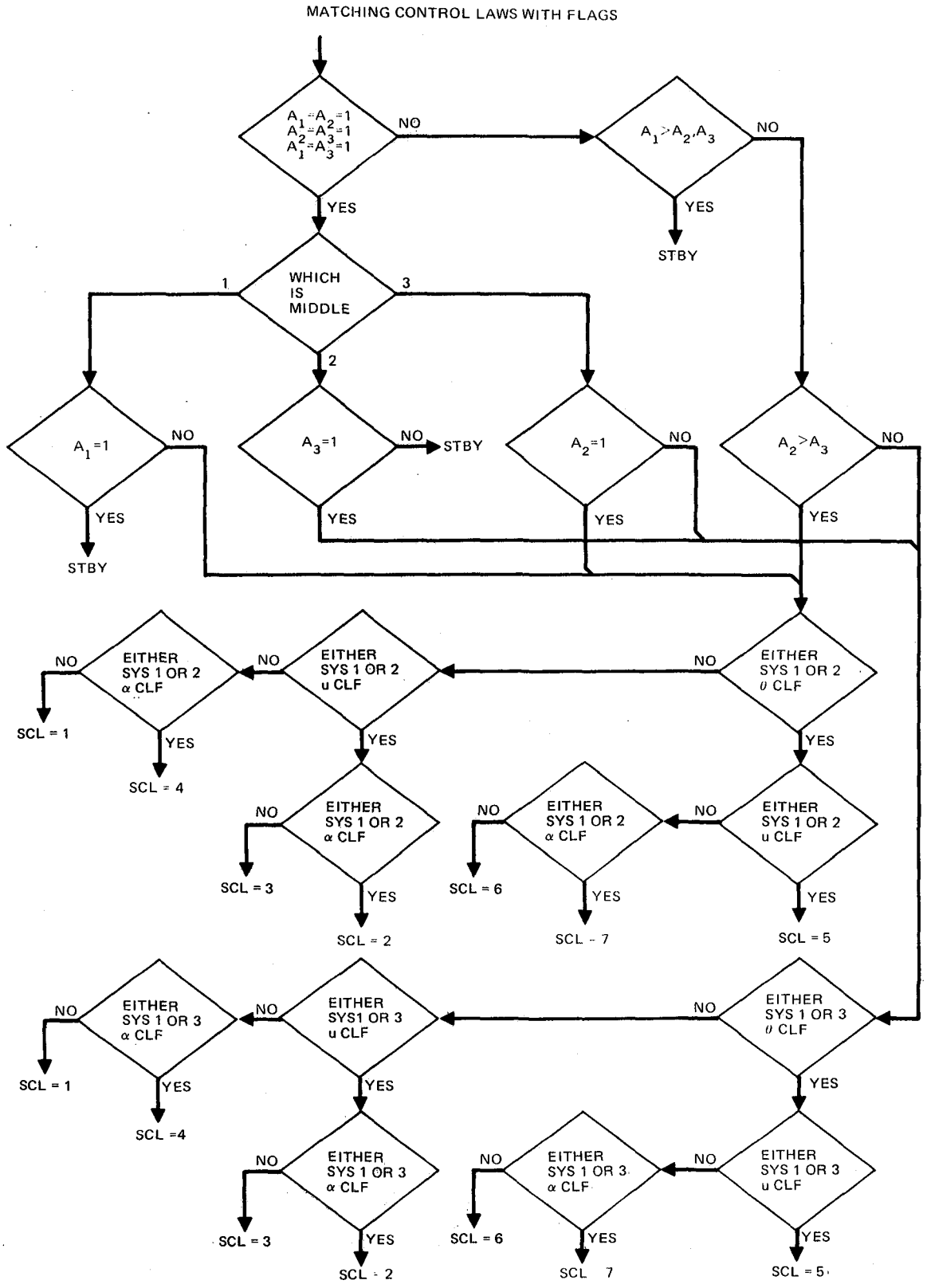

FIGURE 6-12d. SCL FLOW DIAGRAM (CONTINUED)

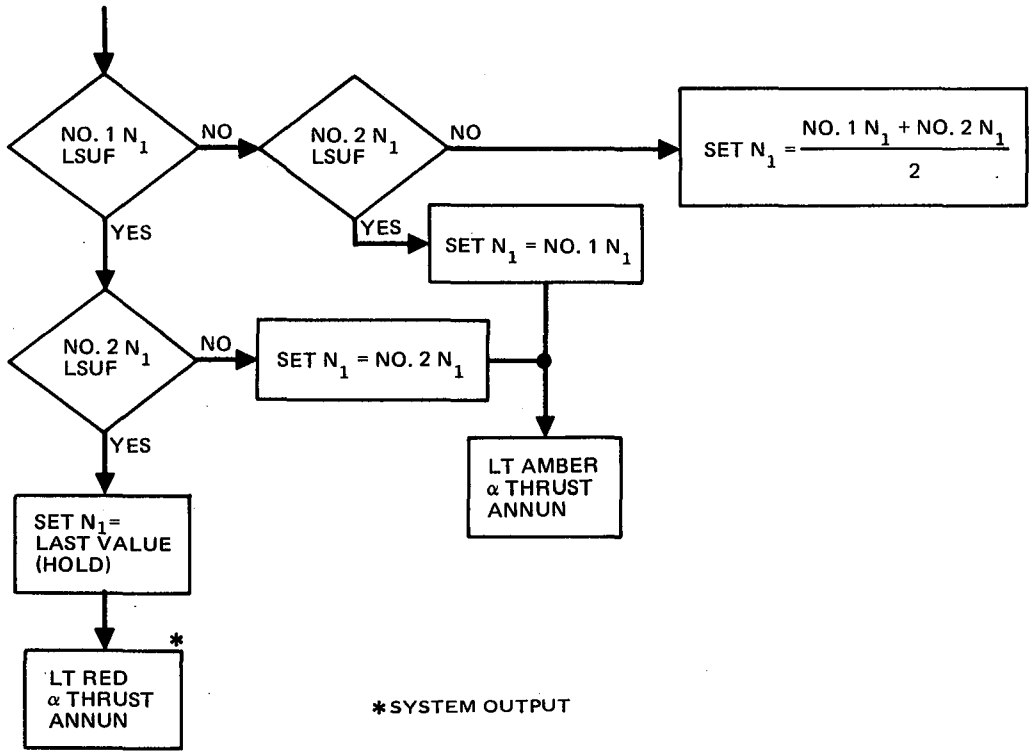

FIGURE 6-13. THRUST-COMPENSATION SIGNAL SELECT FLOW DIAGRAM

Computer Tests:

CPU Instruction Test — The CPU instructions can be exercised by performing arithmetic and logic operations by inserting known values, performing the functions, and comparing the answer with a known final result.

CPU Fixed Memory Tests — The permanent memory can be tested by a check routine which determines the number of 1's in data storage, and compares this number with a known result.

Scratch Pad Memory Test — The scratch pad memory can be tested by driving all locations in the memory to 1's, then to 0's, for read-in/out comparison, and verifying each bit is in the proper state. At the completion of the test, the original contents of the memory location are restored.

Analog/Digital (A/D) Test — A/D converter testing is accomplished by inserting a known reference voltage to the A/D converter, sampling the converted digital word, and then comparing it with the known value.

Computer Power Supply Test — The regulated power supplies can be tested by digitizing each voltage one at a time, through the A/D converter, and comparing them with known tolerances in the CPU.

Input Circuits Test — Analog input circuits can be tested by measuring two redundant channels for each input signal. The demodulator references are also converted to a known nominal value. The discrete input circuits are tested by applying logic stimuli to verify that the circuits are operational, by performing a decoder check, and by performing a stimulus removal check.

Output Circuit Test — All analog outputs can be tested by gating each back through the input analog multiplexer and the A/D converter, and then comparing this digital value with the known digital word which originally initiated the analog output. The computer discrete outputs are also reconverted into an input digital test word. This word is then compared with the known digital word which commanded the original discrete outputs.

Hardware Monitor — The preceding tests all require that the computer be running to be able to detect faults. It is also necessary to detect the fact that the computer stops functioning completely, such as in the absence of power or failure of the internal clock. This is accomplished by a square wave or "heartbeat" monitor. As the computer cycles through its program, it turns a signal on and off each cycle. The resulting square wave is monitored with hardware such that if the signal stops oscillating at the proper frequency (for example, 20 Hz), the engage solenoid of the actuator will disengage. Such a device is shown in Figure 6-14.

The above list does not presume to include all possible tests which are, or could be, included in the self-check routines of a specific digital computer mechanization; however, it does represent a general set which could apply to any machine. These kinds of tests, taken as a whole, are comprehensive in that they address all of the functional elements within the computer.

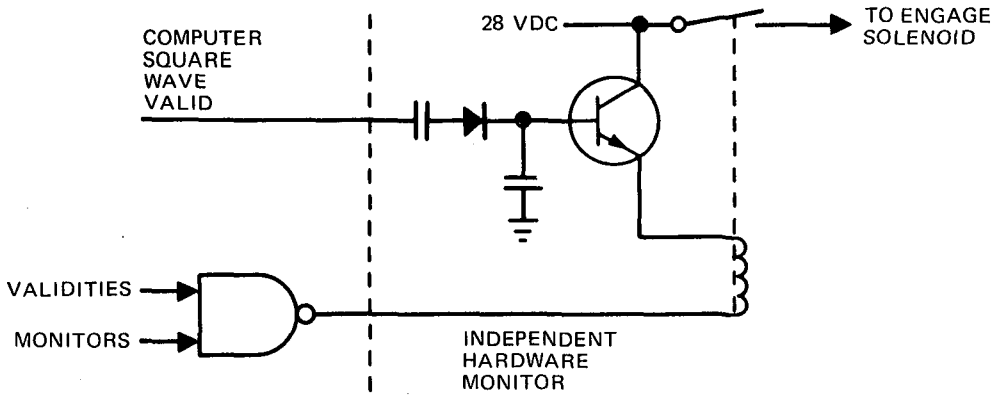

FIGURE 6-14. "HEARTBEAT" MONITOR

Sensor Tests:

Comparison and Voting — The RSSAS sensors will vary in degree of internal monitoring capability. Monitoring of these devices is accomplished by installing them in the vehicle in a way that makes each one completely independent of the other, and comparing (for two sensors) or voting (for more than two) the sensor outputs. Thresholds for the comparators are established by statistical models of the sensor and computer tolerances, and when the threshold is exceeded, both sensors are no longer used and the system shuts down or reverts to other modes of operation.

Sensors with digital outputs have validity incorporated in the word itself. The sign-status matrix, as it is called, dedicates 2 or 3 out of 32 bits to the validity of the signal. Some manufacturers feel, however, that there are failure modes in the sensor for which they cannot guarantee to set the digital word to a fail status. The alternative for the system designer then is to continue to look at the 28-VDC validity which does not properly reflect status, or ask the sensor supplier to remove the digital word altogether from the wire, which they agree they can do.

Parity Checks — For data transmitted on a digital bus, one bit of the 32-bit word is dedicated to parity. The bit indicates whether the total bit sum is even or odd, thus giving the user/flight control computer a way of establishing confidence in the transmitted signal. Parity is not a self-sufficient means of establishing validity,

since it will catch word errors only about half of the time. But since data rates are very high, parity errors will occur fast enough in a failed device to make the technique useful.

Reasonableness Check — The computer can assess a particular sensor's validity by comparing its data with data derived from an independent dissimilar sensor. Thus, if vertical speed, as measured by an air data sensor, makes a sudden change without a change in lagged normal acceleration, one would suspect either or both sources. Considerable effort is now being expended along these lines in an attempt to minimize the number of redundant sensors required aboard a vehicle.

Actuation Tests — Surface actuators are probably the most common devices to be modeled since they include several nonlinearities, or authority limits. Models are simply inserted into the comparator path before the comparison is made, and can detect such phenomena as hardovers, loss of hydraulic pressure, and servo-amplifier failures.

System Tests — Comparison and voting within the computer. The output commands of the several redundant, but uniquely different, control law computations have been demonstrated to track each other with a relatively high degree of accuracy. In the cases evaluated, a single control law was selected for augmentation control, while the others were being calculated but were in standby. In such a configuration, it appears that control-law-to-control-law comparisons can be used to validate the system performance. Failure of individual sensor elements could affect more than one control law type, which although detectable in the performance comparisons, would require several control law comparisons of dissimilar sensor arrays to provide fault isolation.

Mechanical or Aerodynamic Voting — Multiple channels of control and actuation are often tolerant of failures which result in errors of single-command elements. These failures are voted out in the mechanical system or if the erroneous command is transmitted to a single segment of a multiple segment surface, aerodynamic voting takes place. (The DC-10 autoland configuration with quad elevator and

aileron surface segments is an example of aerodynamic voting.) These failures must, of course, be quickly isolated and removed in anticipation of any subsequent fault.

Several of the RSSAS configurations which control a quad series elevator actuator arrangement can take advantage of similar voting characteristics. The quad-actuator, quad-surface configurations will vote aerodynamically. The quad-actuator configurations, with two actuators on each of two segments, can result in mechanical voting at the surface and then aerodynamic averaging of the two surfaces. This type of voting or averaging will be integral with RSSAS configurations regardless of whether the individual computers are operating with the same control laws (as was analyzed in this study) or whether each computer operates with a different control law which may be a desirable dissimilar computation configuration.

Performance Modeling — Modeling can be used to either measure or predict the system performance. For the RSSAS, the anticipated command of each control law in response to aircraft upsets and environment conditions can be predetermined and then compared with measured control-law performance. Another method might be to establish performance relationships between the various control laws as a function of the aircraft disturbance. These models could then be continuously evaluated in flight against the actual system performance. The statistical evaluation studies of Section 5 could provide the basis for this type of monitor function.

Figure 6-15 is a flow diagram of the RSSAS monitor function. The first step in this operation is to determine if the computer is correctly functioning. If the computer is failed, all further operations are in doubt; therefore, the executive is sent a message that flags all control functions. In addition, the computer flag is stored by the system maintenance function which accumulates all failure information. With the computer valid, the other control functions are sequentially checked. First, the actuator response is compared with the expected result determined with a model of the actuator. If two actuators are controlled, each is individually

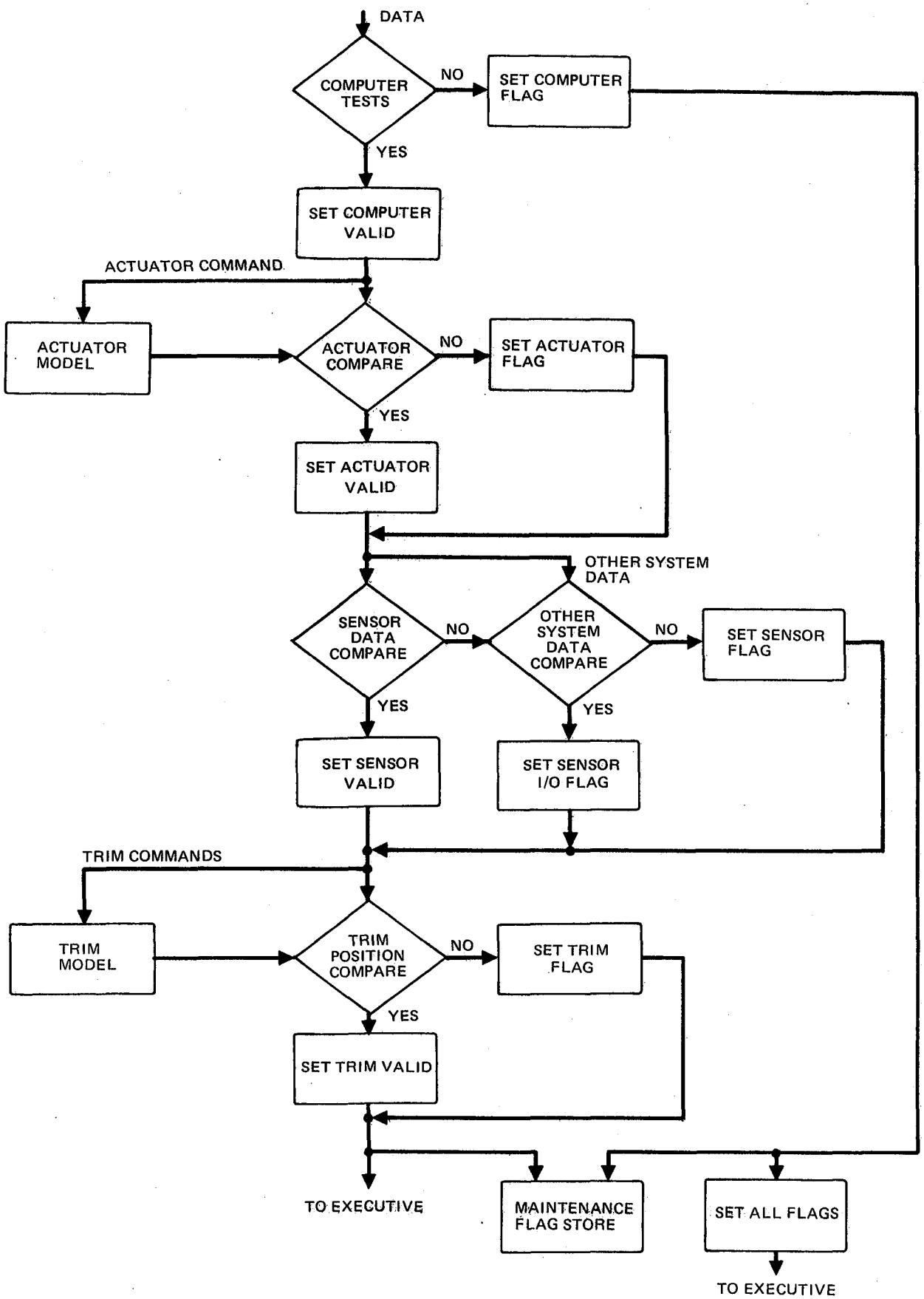

FIGURE 6-15. MONITOR FLOW DIAGRAM

monitored. Next, each set of sensors is compared. When a failure is detected, a second check of the same sensors is made using the data transferred from one of the other computers. If that comparison is also invalid, the sensor is determined to be failed; if not, the computer input port is probably failed. Finally, the trim system is monitored by putting all trim commands (pilot/autopilot and RSSAS) into a trim model and comparing this expected result with the actual horizontal stabilizer motion. All monitor data are then sent to the executive and maintenance functions for proper warning/status annunciation, control selection, engagement decision and data transfer.

Based upon the performance analyses reported in Section 5, two additional concepts not shown in Figure 6-15 may be employed in RSSAS monitoring. In one concept, control-law-command-to-control-law-command comparison monitoring appears useful for several but not all control laws. The other concept is to establish statistical performance models of the control laws which could be used in either of two ways. First, the control law performance model could be determined as a function of the environment. The monitoring task would then be to establish the environmental condition, call out the appropriate model, and compare it to the actual control law performance. The second method would be to determine a model which correlates the performance characteristics of two or more control laws. This model could then be used to continuously compare the real-time system performance. None of these techniques has yet been developed but now that the RSSAS control laws and performance have been established, future studies will be aimed specifically at improved monitoring concepts.

6.1.3 Actuation System. — Conventional commercial transport primary mechanical flight control systems operate in such a manner that as the pilot inputs move the control surfaces, this movement is fed back to reposition the pilot controls. When the automatic pilot operates in place of the pilot, it positions the surface by moving the primary control system with an auxiliary actuator. This mechanization is referred to as a parallel actuation system, since the autopilot input is essentially tied to the pilot controls and their

positions parallel each other. Augmentation systems which operate simultaneously with the primary flight controls and share the same control sufaces require an additional series actuator interface which causes the same control surface to respond to the sum of the control commands, but without the series input being reflected back into the pilot controls.

For the EET RSSAS, the elevator actuation system must be designed to provide this series and parallel operation. The baseline primary elevator control system is that of the DC-10 shown in Figure 6-16. Several alternative configurations which provide the required function have been qualitatively evaluated, along with the necessary hydraulic power interface using the baseline system shown in Figure 6-17.

6.1.3.1 Actuation Configurations and Operation. — Six basic elevator actuation systems have been considered. These are shown in Figures 6-18 through 6-23. The surface actuators incorporate tandem cylinders powered by two separate hydraulic systems, such that no single hydraulic failure can cause loss of any surface output. The auxiliary actuators for series and parallel commands, whether they are separate or incorporated within the surface actuators, are single cylinder units, each powered by one of the two hydraulic systems driving the associated surface actuator. The rationale behind elimination of the complexity of tandem cylinders for parallel and series actuators is that one parallel unit can drive the cruise autopilot and one pair of units is good for autoland, and loss of one or two series surface outputs is acceptable after a single hydraulic failure.

Configuration A, shown in Figure 6-18, is the basic configuration. In it, a series and a parallel actuator are added in the linkage path to each surface. The parallel mode actuator output rod is disengaged within the unit when hydraulic power is not applied, so that minimum friction is added to the system. The series mode actuator output rod is spring preloaded to the neutral position when hydraulic power is not applied, thus providing a reaction point for the summing link driving the surface actuator input. In this configuration, loss of hydraulic power to a series actuator causes loss of series outputs on its associated surface.

Figure 6-19 shows Configuration B, which combines a series and a parallel actuator into a single unit which also transmits mechanical commands. One of

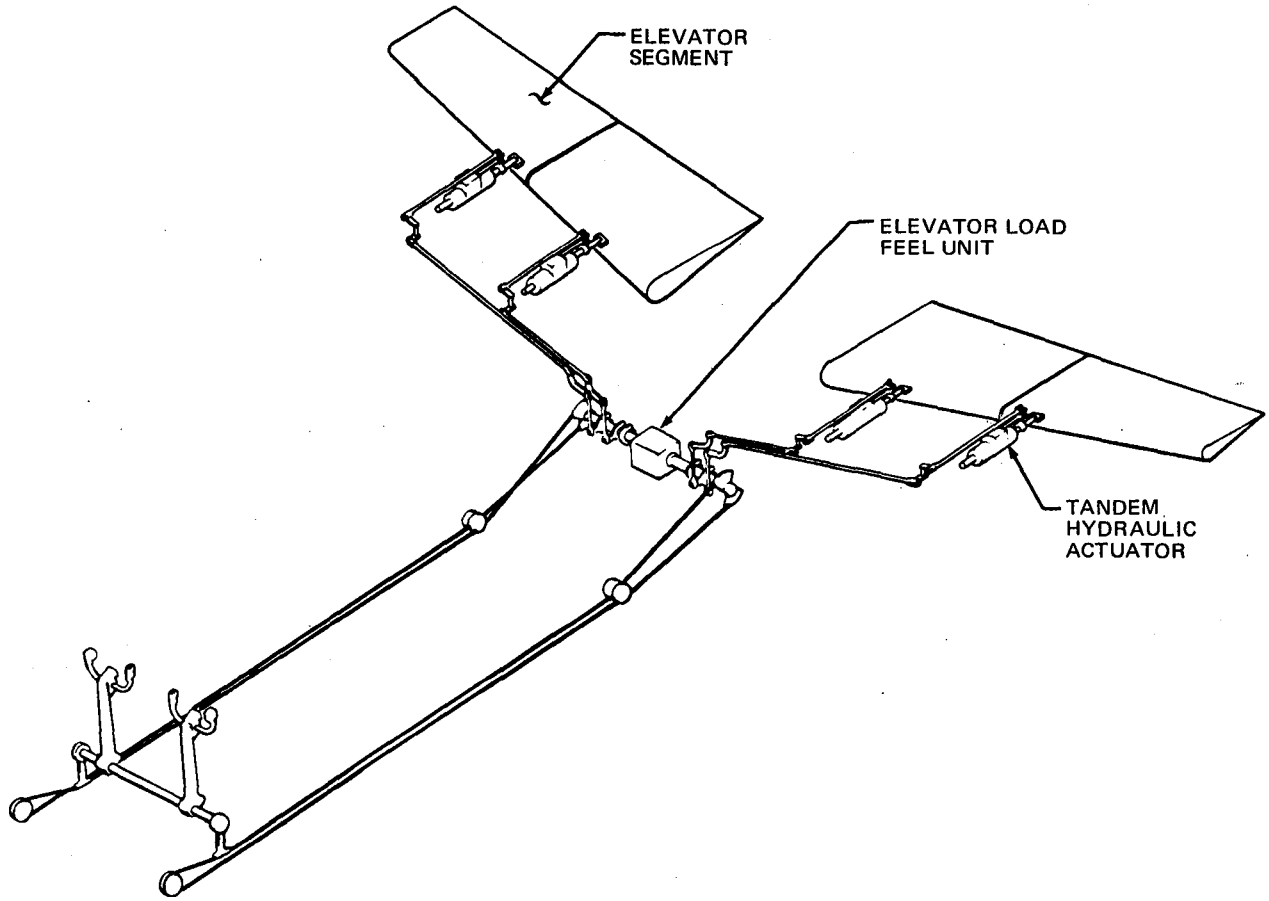

FIGURE 6-16. LONGITUDINAL PITCH MECHANICAL CONTROL

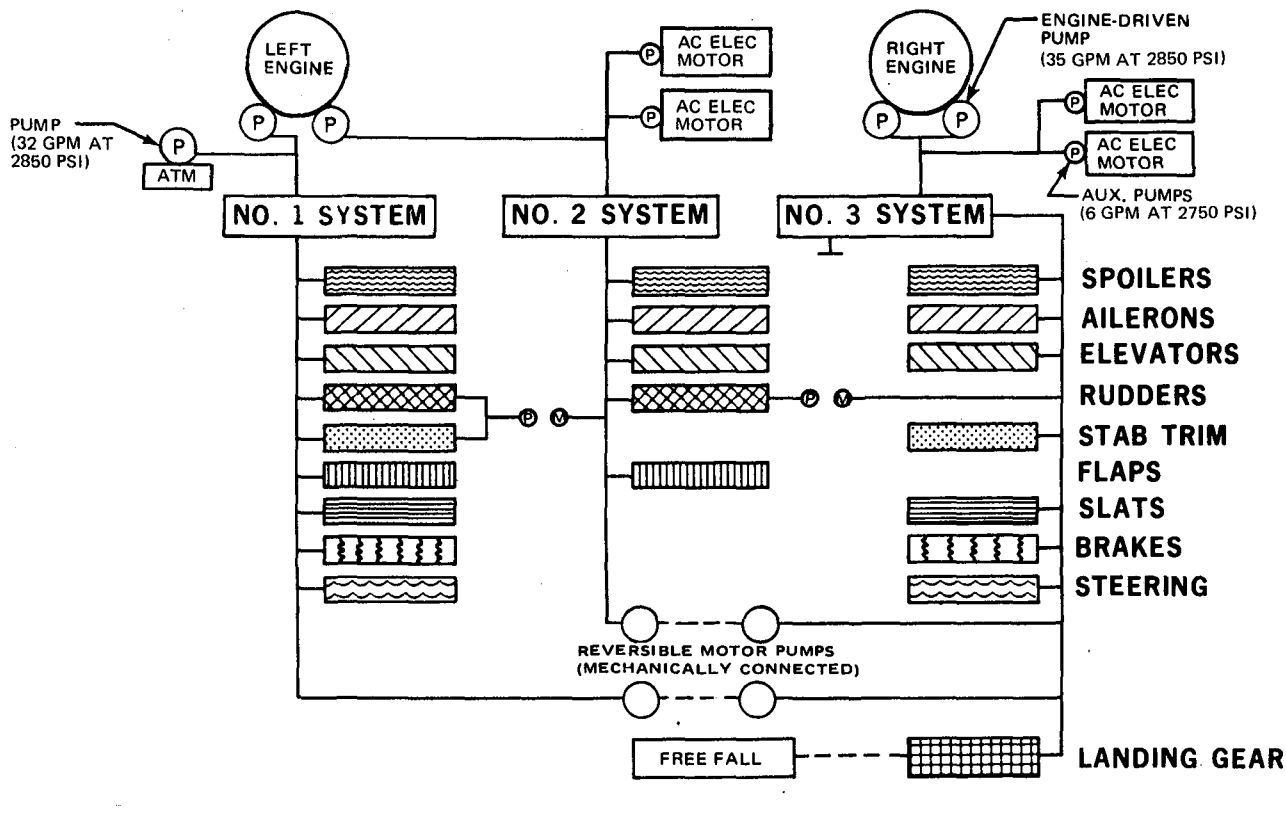

FIGURE 6-17. HYDRAULIC SYSTEM

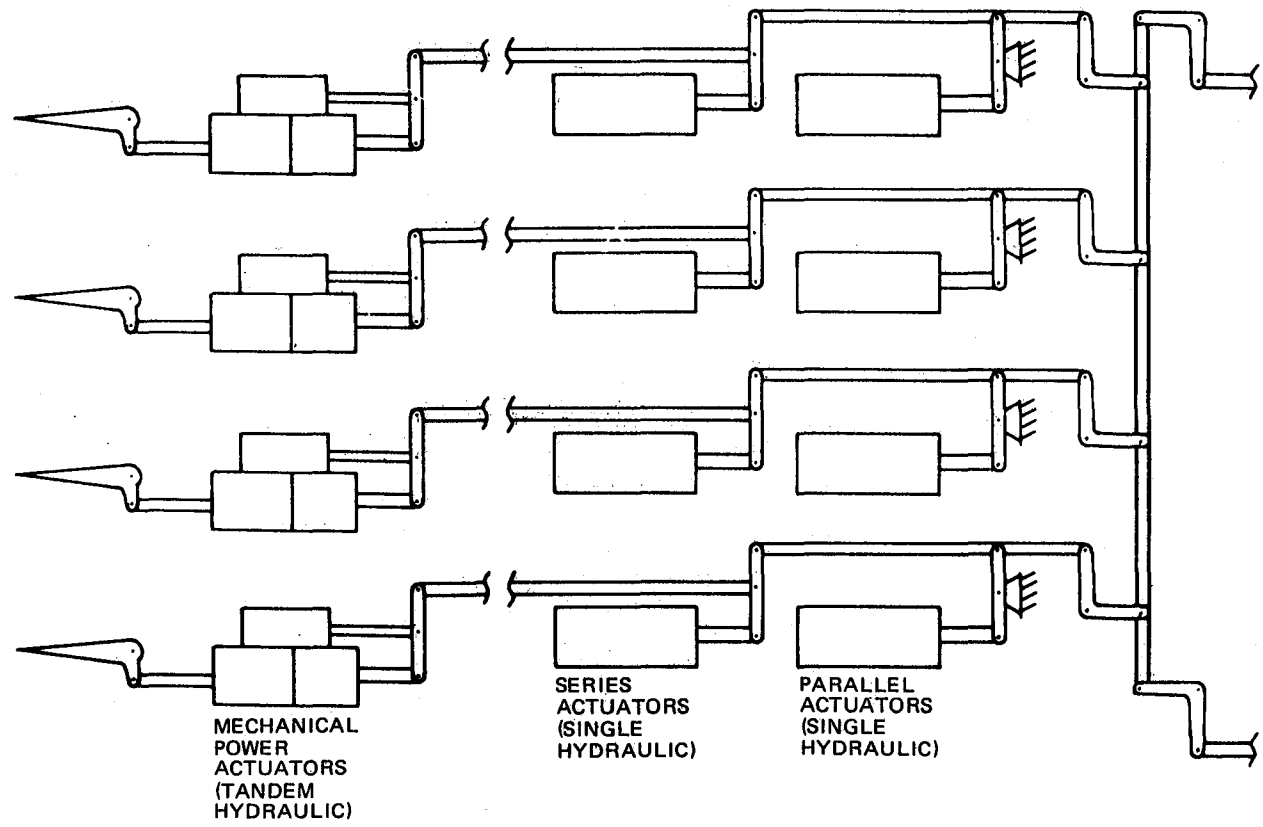

FIGURE 6-18. ACTUATION CONFIGURATION A

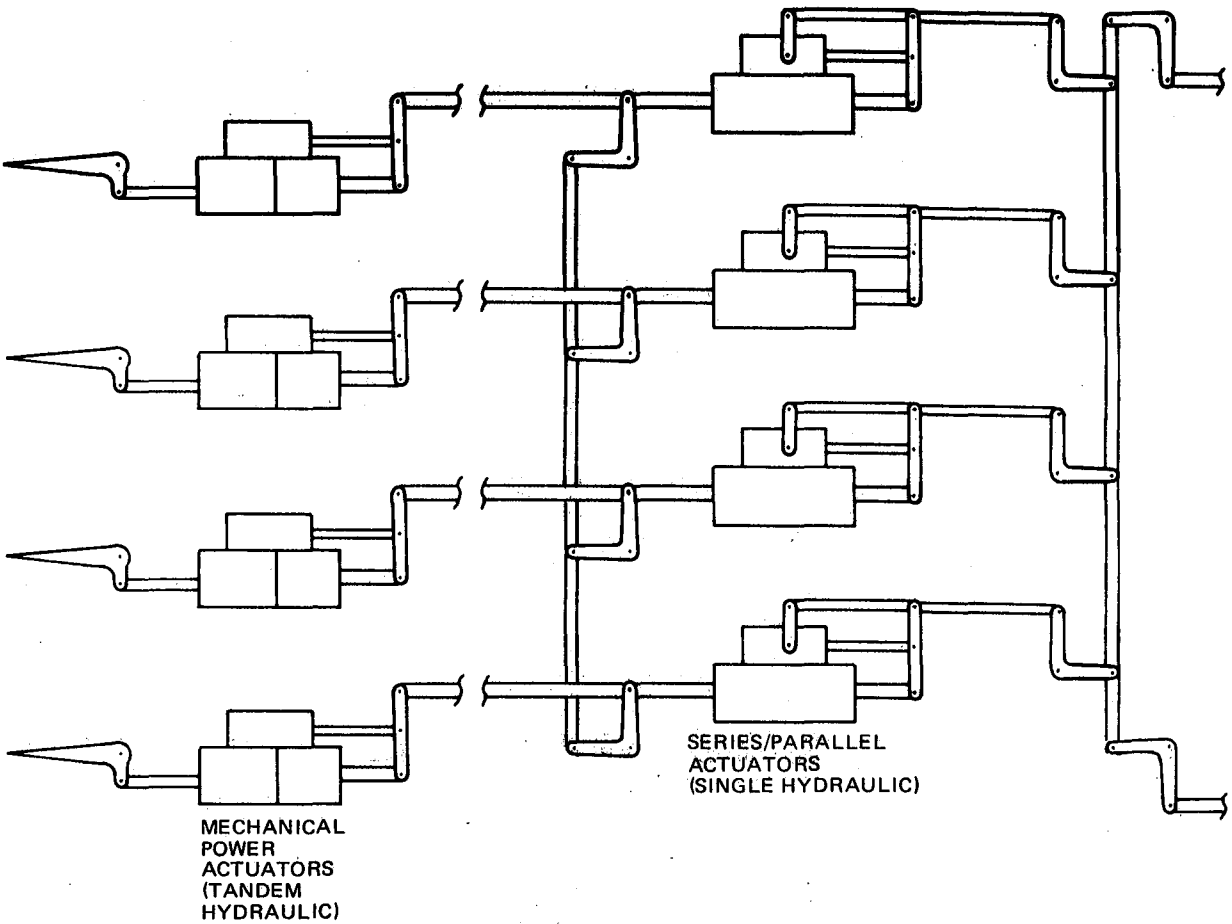

FIGURE 6-19. ACTUATION CONFIGURATION B

these units is incorporated in the linkage path to each surface. Since the actuators incorporate single hydraulic cylinders, the outputs must be bussed together to prevent loss of mechanical control of one or two surfaces after a single hydraulic failure. As a result, loss of hydraulic power to one, two, or even three of the series/parallel actuators causes no loss of series command to the surfaces. This is not as advantageous as it appears, however, since loss of two hydraulic systems also causes loss of output of at least one and possibly two surface actuators.

Configuration C, shown in Figure 6-20, combines three series and four parallel actuators into a single package located upstream of the control surface linkage bus. The individual actuators are identical to those of Configuration A. As in Configuration B, bussing of the series actuator outputs prevents loss of series commands after one or two hydraulic failures, although with two hydraulic failures one or two surfaces will also be inoperative.

Figure 6-21 shows Configuration D, an integrated series/parallel actuator located upstream of the control surface linkage bus. This unit accepts mechanical, series electrical, and parallel electrical inputs and provides dual mechanical outputs to the control surface bus. For reasons given subsequently, this configuration was quickly eliminated, so no further description is given.

Configuration E, shown in Figure 6-22, integrates the series actuators with the mechanical surface actuators. Units of this type are in common usage today, primarily in rudder actuators which incorporate yaw dampers. A parallel actuator, identical to those of Configuration A, is added in the linkage path to each actuator. As in Configuration A, loss of hydraulic power to the series portion of an actuator will cause loss of series output of that actuator.

Figure 6-23 shows Configuration F, which integrates both the series and parallel mode actuators into the surface actuators. As in the previous configuration, loss of hydraulic power to the series portion of the actuator causes loss of the series mode output of that actuator.

6.1.3.2 Actuation Configuration Evaluation. — The primary considerations in evaluating each of the proposed actuation configurations are discussed below:

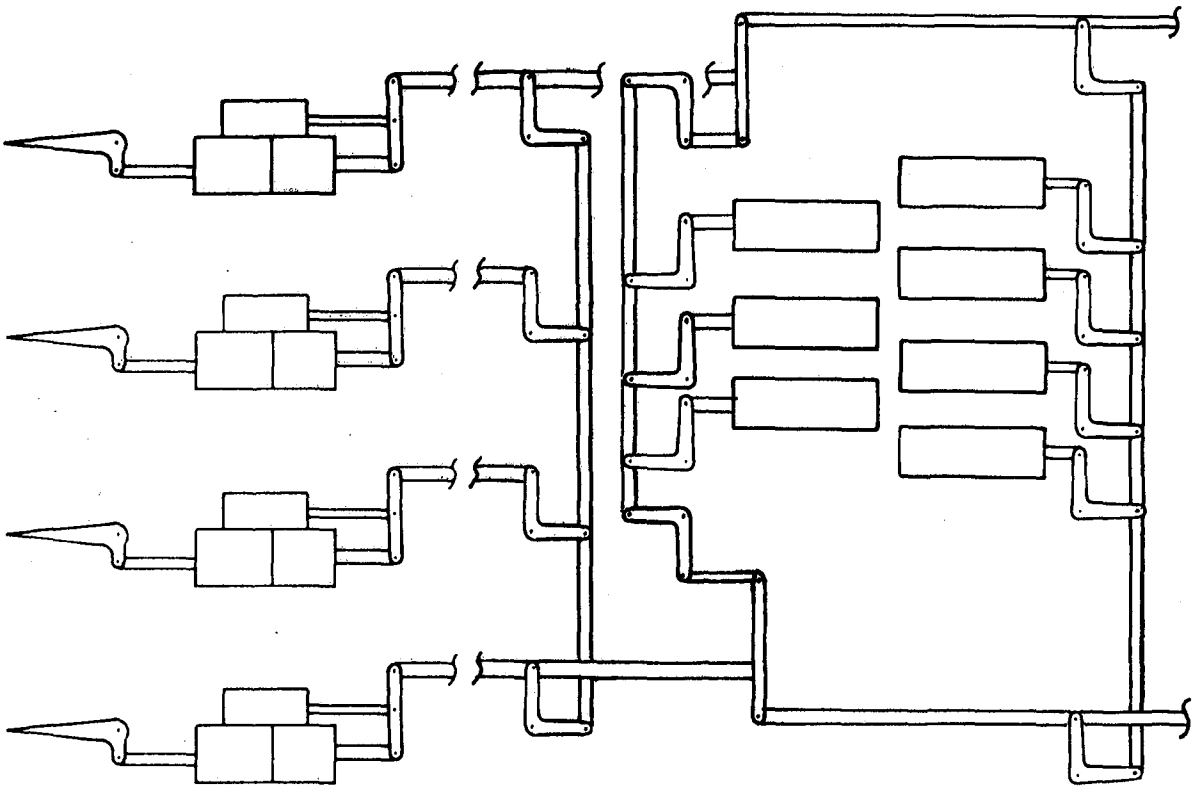

FIGURE 6-20. ACTUATION CONFIGURATION C

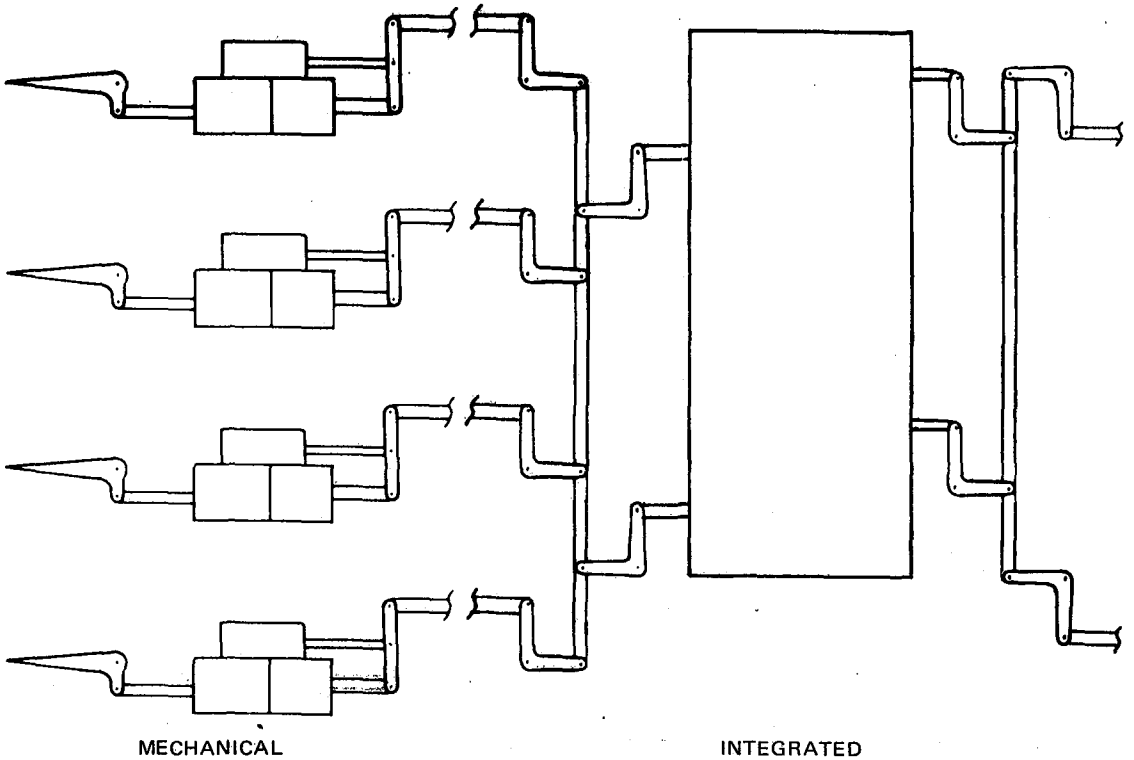

FIGURE 6-21. ACTUATION CONFIGURATION D

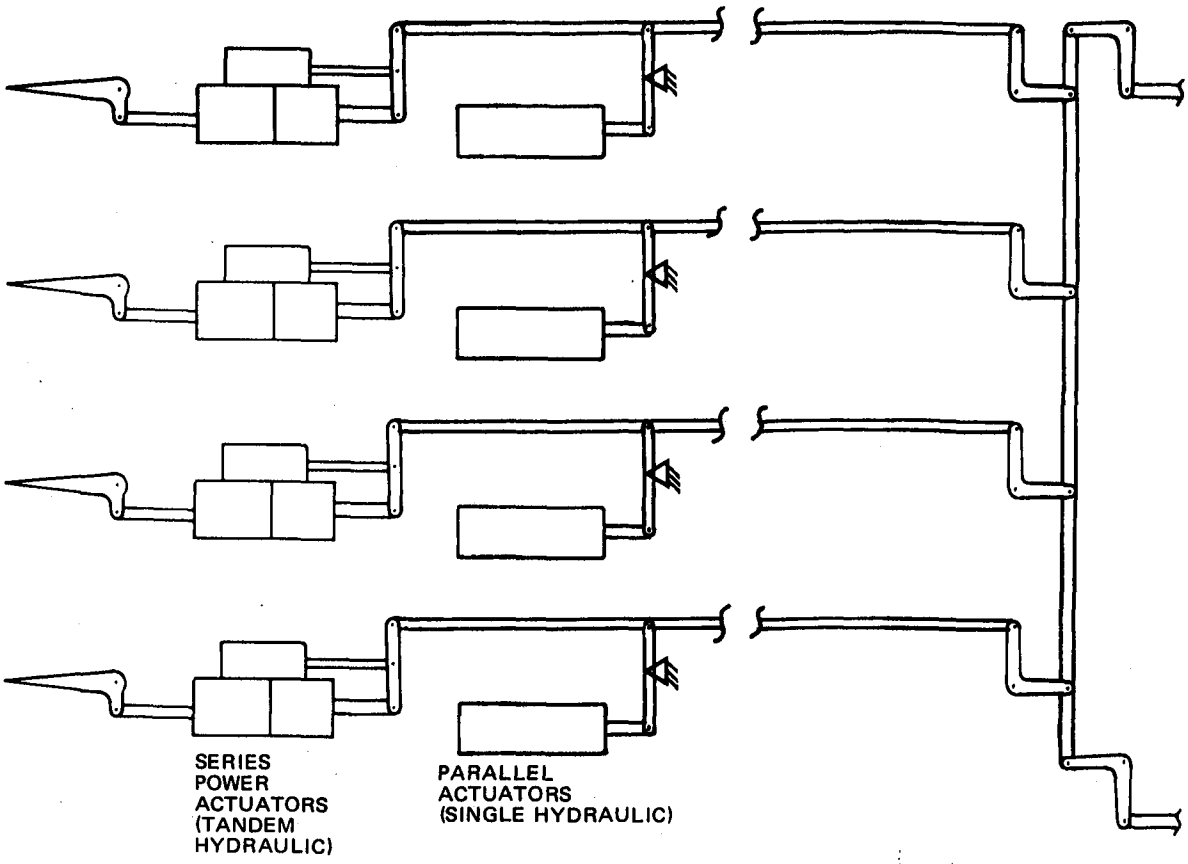

FIGURE 6-22. ACTUATION CONFIGURATION E

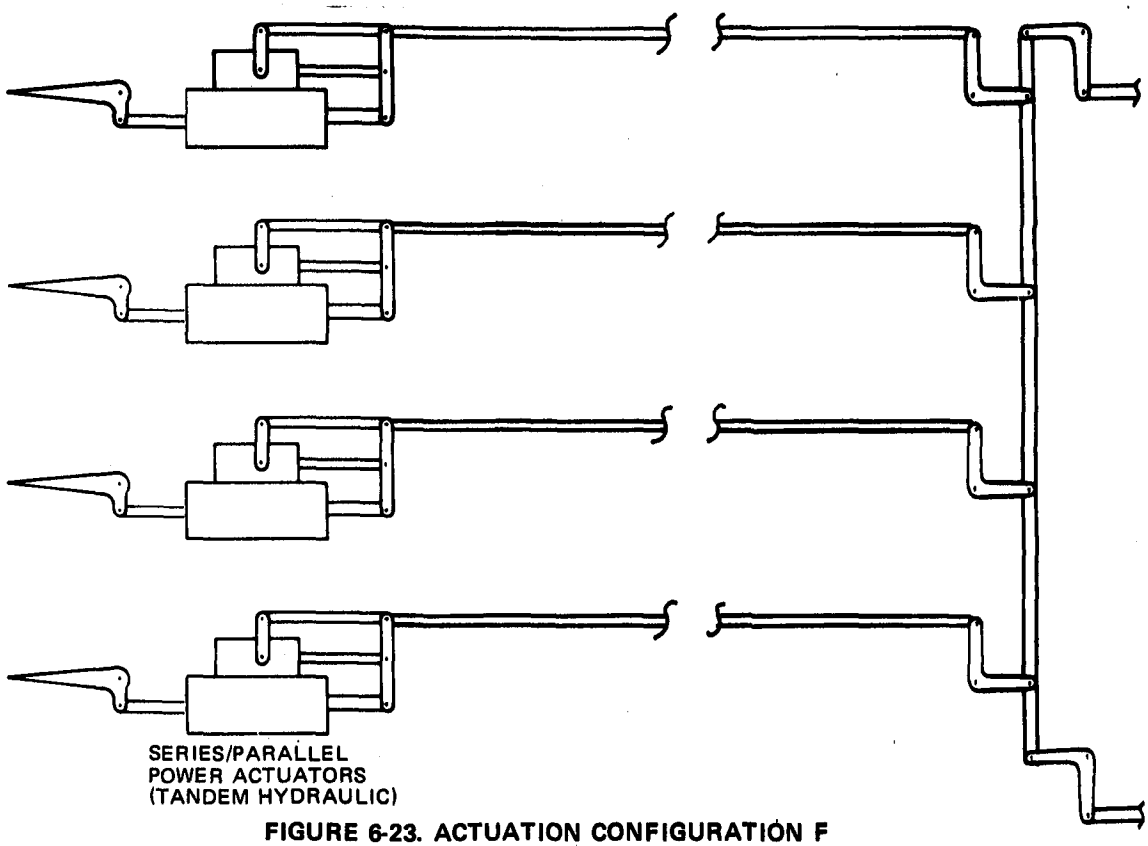

FIGURE 6-23. ACTUATION CONFIGURATION F

Configuration A

- Maximum number of actuators.
- Does not take advantage of existing unit capability.

Configuration B

- Primary pilot input linkage not direct to actuator — adds lag between pilot input and surface response.
- Added weight of additional bus system at output of series/parallel actuator.
- Does not take advantage of existing unit capability.

Configuration C

- Most flexible actuation arrangement — redundancy of autopilot and augmentation actuators easily changed to match reliability requirements.
- Large number of actuators.
- Does not take advantage of existing unit capability.

Configuration D

- Brings entire control system to a single, common point. Failure effects could be severe.
- Very complex pilot, autopilot, and augmentation interface. (Internals not shown in diagram.)

Configuration E

- Requires add-on of autopilot actuators to existing configuration.
- Existing actuators must be reworked (simple change) to provide series augmentation input rather than parallel autopilot input.

Configuration F

- Most adaptable to the existing mechanical configuration.
- Requires a one-for-one replacement of actuators.

To keep the RSSAS incorporation to a minimum risk and minimum change, Configurations E and F are the candidate selections. For the further RSSAS studies, these configurations are identical since both include the integration of the series augmentor actuator into the primary power actuator. In the total system architecture evaluations, two other variations to the selected configurations were considered. These were: (a) dual series command inputs into a single series actuator, and (b) actuation configurations which do not include a series input at each surface segment.

6.1.3.3 Hydraulic Arrangement.

(a) Control Surface Actuators. The surface actuators are tandem cylinder units, each utilizing two different hydraulic power supplies. For maximum reliability, all power supplies should be represented and they should be represented as equally as possible. With three supplies, the optimum combinations would be 1-2, 1-3, 2-3. Since there are four actuators to supply, the fourth must duplicate one of the other three. For purposes of the hydraulic arrangement study, the three supplies are considered identical, thus it is immaterial which actuator is duplicated. The actuator supplies have therefore been allocated as follows: 1-2, 1-2, 1-3, 2-3.

(b) Series Mode Actuators. Allocation of three hydraulic systems and/or three computer channels to three actuators is straightforward. How to optimize the allocation of three systems to four actuators is not immediately apparent. Several ground rules may be set up, however, for maximum reliability. First, a basic power source (i.e., engine, APU, etc.) will be used to generate both hydraulic power for the actuators and electrical power for the computer channels. These sources are designated as 1, 2, and 3, and hydraulic and electrical systems 1, 2, and 3 are each associated with the correspondingly numbered basic source. Thus, failure of a basic source will result

in loss of both the correspondingly numbered hydraulic system and electrical system. To prevent failure of a basic source from causing loss of more than one series mode channel, each channel (including the surface actuators) should utilize electrical and hydraulic power from a common basic source. A secondary source of hydraulic or electrical power may be used (as in the surface actuators) where its failure alone will not cause loss of that channel. If it is assumed that computation Channel 1 is supplied by electrical System 1, Channel 2 by electrical System 2, etc., the above ground rules may be stated more simply as follows:

- For a channel having one series mode actuator and one surface actuator, each actuator must utilize at least one hydraulic system numbered the same as the computation channel number.

- For a channel having two series mode actuators and two surface actuators, each series mode actuator must utilize one of the systems used by its associated surface actuator. At least one of the series mode actuators must utilize a hydraulic system numbered the same as the computation channel number.

Applying the above ground rules reduces the number of permutations of hydraulic systems and computer channels to a more manageable number. These cases were examined for the effects of all combinations of hydraulic and electrical failures up to the double-hydraulic, double-electrical level. Comparing the results on the basis of the number of surface actuators suffering a total loss of series commands, it is found that all cases fall into one of two groups. Configurations in which the two series mode actuators controlled by one computer are powered by the same hydraulic system, suffer complete loss of series mode capability for 12 failure cases. All other configurations suffer this same loss in only nine cases. Tables 6-1 and 6-2 show the analysis for two typical configurations, one for each of the two groups.

The configuration of the series mode actuators is such that they are readily adaptable to two inputs, one each from two different computer channels. In the event of a failure in one channel, the remaining

TABLE 6-1

COMPUTER CHANNEL/HYDRAULIC SYSTEM FAILURE MODE EFFECTS

FAILURE							X = LOSS OF SERIES CMD				CMDS LOST
COMPUTER			HYDRAULIC SOURCE				ACT. NO.				
1	2	3	1	2	3		1	2	3	4	
X							X				1
	X							X			1
		X							X	X	2
			X				X				1
				X				X			1
					X				X	X	2
X	X						X	X			2
X		X					X		X	X	3
	X	X						X	X	X	3
			X	X			X	X			2
			X		X		X		X	X	3
				X	X			X	X	X	3
			X	X			X	X			2
			X		X		X		X	X	3
				X	X			X	X	X	3

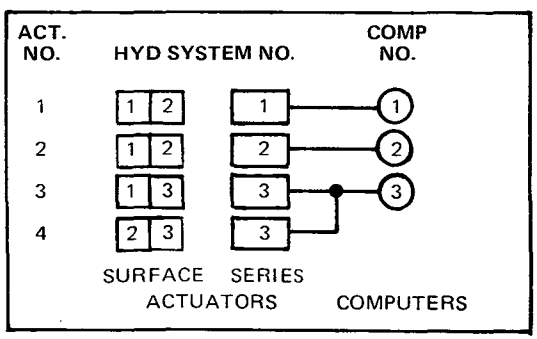

CONFIGURATION

FAILURE							X = LOSS OF SERIES CMD				CMDS LOST
COMPUTER			HYDRAULIC SOURCE				ACT. NO.				
1	2	3	1	2	3		1	2	3	4	
X			X				X				1
X				X			X	X			2
X					X		X		X	X	3
	X		X				X	X			2
	X			X				X			1
	X				X			X	X	X	3
		X	X				X		X	X	3
		X		X				X	X	X	3
		X			X				X	X	2
X			X	X			X	X			2
X			X		X		X		X	X	3
X				X	X		X	X	X	X	4
	X		X	X			X	X			2
	X		X		X		X	X	X	X	4
	X			X	X			X	X	X	3
		X	X	X			X	X	X	X	4
		X	X		X		X		X	X	3
		X		X	X			X	X	X	3

FAILURE							X = LOSS OF SERIES CMD				CMDS LOST
COMPUTER			HYDRAULIC SOURCE				ACT. NO.				
1	2	3	1	2	3		1	2	3	4	
X	X		X				X	X			2
X	X			X			X	X			2
X	X				X		X	X	X	X	4
X		X	X				X		X	X	3
X		X		X			X	X	X	X	4
X		X			X		X		X	X	3
	X	X	X				X	X	X	X	4
	X	X		X				X	X	X	3
	X	X			X			X	X	X	3
X	X		X	X			X	X			2
X	X		X		X		X	X	X	X	4
X	X			X	X		X	X	X	X	4
X		X	X	X			X	X	X	X	4
X		X	X		X		X		X	X	3
X		X		X	X		X	X	X	X	4
	X	X	X	X			X	X	X	X	4
	X	X	X		X		X	X	X	X	4
	X	X		X	X			X	X	X	3

TABLE 6-2

COMPUTER CHANNEL/HYDRAULIC SYSTEM FAILURE MODE EFFECTS

FAILURE							X = LOSS OF SERIES CMD				CMDS LOST
COMPUTER			HYDRAULIC SOURCE				ACT. NO.				
1	2	3		1	2	3	1	2	3	4	
X							X				1
	X							X			1
		X							X	X	2
				X			X				1
					X			X		X	2
						X			X		1
X	X						X	X			2
X		X					X		X	X	3
	X	X						X	X	X	3
				X	X		X	X		X	3
				X		X	X		X		2
				X			X				1

FAILURE						X = LOSS OF SERIES CMD				CMDS LOST
COMPUTER			HYDRAULIC SOURCE			ACT. NO.				
1	2	3		1	2	3	1	2	3	4	
X				X			X				1
X					X		X	X		X	3
X						X	X		X		2
	X			X			X	X			2
	X				X			X		X	2
	X					X		X	X		2
		X		X			X		X	X	3
		X			X			X	X	X	3
		X				X			X	X	2
X				X	X		X	X		X	3
X				X		X	X		X		2
X					X	X	X	X	X	X	4
	X			X	X		X	X		X	3
	X			X		X	X	X	X		3
	X				X	X		X	X	X	3
		X		X	X		X	X	X	X	4
		X		X		X	X		X	X	3
		X			X	X		X	X	X	3

FAILURE						X = LOSS OF SERIES CMD				CMDS LOST
COMPUTER			HYDRAULIC SOURCE			ACT. NO.				
1	2	3		1	2	3	1	2	3	4	
X	X			X			X	X			2
X	X				X		X	X		X	3
X	X					X	X	X	X		3
X		X		X			X		X	X	3
X		X			X			X	X	X	4
X		X				X		X	X	X	3
	X	X		X			X	X	X	X	4
	X	X			X			X	X	X	3
	X	X				X		X	X	X	3
X	X			X	X		X	X		X	3
X	X			X		X	X	X	X		3
X	X				X	X	X	X	X	X	4
X		X		X	X		X	X	X	X	4
X		X		X		X	X		X	X	3
X		X			X	X	X	X	X	X	4
	X	X		X	X		X	X	X	X	4
	X	X		X		X	X	X	X	X	4
	X	X			X	X		X	X	X	3

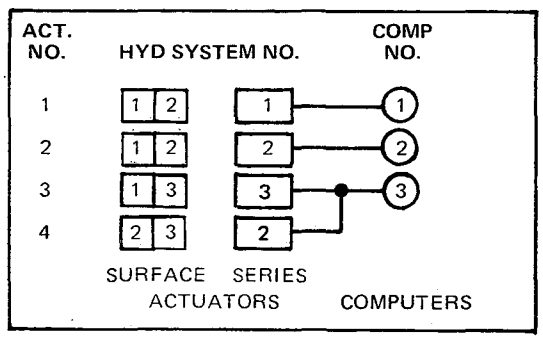

CONFIGURATION

channel would be capable of controlling the actuator within its normal authority, but at half-rate. This suggests the possibility of increasing reliability by applying commands from two different computer channels to each series mode actuator. An analysis, similar to that described above, was performed using this approach. Again, it was found that there is no real "optimum" arrangement

Tables 6-3 and 6-4 show two cases typical of the "worse" and "better" groups of configurations. A comparison of Table 6-2 with Table 6-4 (both representative of the "better" groups) shows that the dual inputs to the series mode actuators does result in fewer series command losses for the combined computer/hydraulic system failures. Although complete command losses are reduced, in most cases several or all of surfaces remaining active are operating at half-rate, thus reducing the servo-loop response and in some cases resulting in servo loops operating together but with different response characteristics.

The configuration of Table 6-4 is that currently being simulated. To avoid problems due to the rate limitation discussed above, the gain of the good input to an actuator is doubled when the other input fails.

(c) Parallel Mode Actuators. A study of hydraulic system allocation to the parallel mode actuators has not yet been accomplished. If a three-channel parallel mode were to be used, the series mode analysis would apply directly. If a four-channel mode should be selected, the DC-10 Automatic Flight Control System configuration would be directly applicable.

6.1.4 RSSAS Autotrim. — As the aircraft flight path or engine thrust changes, the RSSAS will command a steady-state elevator for these new conditions. To allow a retrim of the series elevator position and reestablish the range of authority for the RSSAS series actuator, an automatic trim feature is necessary to reposition the horizontal stabilizer an amount equivalent to that being maintained by the elevator. The autotrim system designed for the RSSAS performs this function with the use of the existing DC-10-type rate actuator horizontal stabilizer trim system shown in Figure 6-24, replacing the alternate trim with the RSSAS input.

TABLE 6-3

COMPUTER CHANNEL/HYDRAULIC SYSTEM FAILURE MODE EFFECTS

FAILURE							X = NO CMD • = 1/2 RATE				NO CMD / 1/2 RATE
COMPUTER			HYDRAULIC SOURCE				ACT. NO.				
1	2	3	1	2	3		1	2	3	4	
X							•	•	•		0/3
	X						•	•		•	0/3
		X							•	•	0/2
			X				X	X			2/0
				X						X	1/0
					X				X		1/0
X	X						X	X	•	•	2/2
X		X					•	•	X	•	1/3
	X	X					•	•	•	X	1/3
			X	X			X	X		X	3/0
			X		X		X	X	X		3/0
				X	X				X	X	2/0

ACT. NO.	HYD SYSTEM NO.	COMP NO.
1	1 2	1
2	1 2	1
3	1 3	3 → 2
4	2 3	2 → 3

SURFACE ACTUATORS — SERIES COMPUTERS

CONFIGURATION

FAILURE							X = NO CMD • = 1/2 RATE				NO CMD / 1/2 RATE
COMPUTER			HYDRAULIC SOURCE				ACT. NO.				
1	2	3	1	2	3		1	2	3	4	
X			X				X	X	•		2/1
X				X			•	•	•	X	1/3
X					X		•	•	X		1/2
	X		X				X	X		•	2/1
	X			X			•	•		X	1/2
	X				X		•	•	X	•	1/3
		X	X				X	X	•	•	2/2
		X		X					•	X	1/1
		X			X				X	•	1/1
X			X	X			X	X	•	X	3/1
X			X		X		X	X	X		3/0
X				X	X		•	•	X	X	2/2
	X		X	X			X	X		X	3/0
	X		X		X		X	X	X	•	3/1
	X			X	X		•	•	X	X	2/2
		X	X	X			X	X	•	X	3/1
		X	X		X		X	X	X	•	3/1
		X							X	X	2/0

FAILURE							X = NO CMD • = 1/2 RATE				NO CMD / 1/2 RATE
COMPUTER			HYDRAULIC SOURCE				ACT. NO.				
1	2	3	1	2	3		1	2	3	4	
X	X			X			X	X	•	•	2/2
X	X				X		X	X	•	X	3/1
X	X					X	X	X	X	•	3/1
X		X		X			X	X	X	•	3/1
X		X			X		•	•	X	X	2/2
X		X				X	•	•	X	•	1/3
	X	X		X			X	X	•	X	3/1
	X	X			X		•	•	•	X	1/3
	X	X				X	•	•	X	X	2/2
X	X			X	X		X	X	•	X	3/1
X	X			X		X	X	X	X	•	3/1
X	X				X	X	X	X	X	X	4/0
X		X		X	X		X	X	X	X	4/0
X		X		X		X	X	X	X	•	3/1
X		X			X	X	•	•	X	X	2/2
	X	X		X	X		X	X	•	X	3/1
	X	X		X		X	X	X	X	X	4/0
	X	X			X	X	•	•	X	X	2/2

TABLE 6-4

COMPUTER CHANNEL/HYDRAULIC SYSTEM FAILURE MODE EFFECTS

FAILURE						X = NO CMD • = 1/2 RATE				NO CMD / 1/2 RATE
COMPUTER			HYDRAULIC SOURCE			ACT. NO.				
1	2	3	1	2	3	1	2	3	4	
X						•	•	•		0/3
	X					•	•		•	0/3
		X						•	•	0/2
			X			X				1/0
				X			X		X	2/0
					X			X		1/0
X	X					X	X	•	•	2/2
X		X				•	•	X	•	1/3
	X	X				•	•	•	X	1/3
			X	X		X	X		X	3/0
			X		X	X		X		2/0
				X	X		X	X	X	3/0

FAILURE						X = NO CMD • = 1/2 RATE				NO CMD / 1/2 RATE
COMPUTER			HYDRAULIC SOURCE			ACT. NO.				
1	2	3	1	2	3	1	2	3	4	
X			X			X	•	•		1/2
X				X		•	X	•	X	2/2
X					X	•	•	X		1/2
	X		X			X	•		•	1/2
	X			X		•	X		X	2/1
	X				X	•	•	X	•	1/3
		X	X			X		•	•	1/2
		X		X			X	•	X	2/1
		X			X			X	•	1/1
X			X	X		X	X	•	X	3/1
X			X		X	X	•	X		2/1
X				X	X	•	X	X	X	3/1
	X		X	X		X	X		X	3/0
	X		X		X	X	•	X	•	2/2
	X			X	X	•	X	X	X	3/1
		X	X	X		X	X	•	X	3/1
		X	X		X	X		X	•	2/1
		X		X	X		X	X	X	3/0

FAILURE						X = NO CMD • = 1/2 RATE				NO CMD / 1/2 RATE
COMPUTER			HYDRAULIC SOURCE			ACT. NO.				
1	2	3	1	2	3	1	2	3	4	
X	X		X			X	X	•	•	2/2
X	X			X		X	X	•	X	3/1
X	X				X	X	X	X	•	3/1
X		X	X			X	•	X	•	2/2
X		X		X		•	X	X	X	3/1
X		X			X	•	•	X	•	1/3
	X	X	X			X	•	•	X	2/2
	X	X		X		•	X	•	X	2/2
	X	X			X	•	•	X	X	2/2
X	X		X	X		X	X	•	X	3/1
X	X		X		X	X	X	X	•	3/1
X	X			X	X	X	X	X	X	4/0
X		X	X	X		X	X	X	X	4/0
X		X	X		X	X	•	X	•	2/2
X		X		X	X	•	X	X	X	3/1
	X	X	X	X		X	X	•	X	3/1
	X	X	X		X	X	•	X	X	3/1
	X	X		X	X	•	X	X	X	3/1

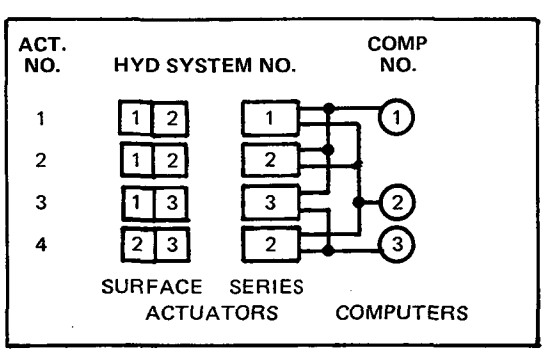

CONFIGURATION

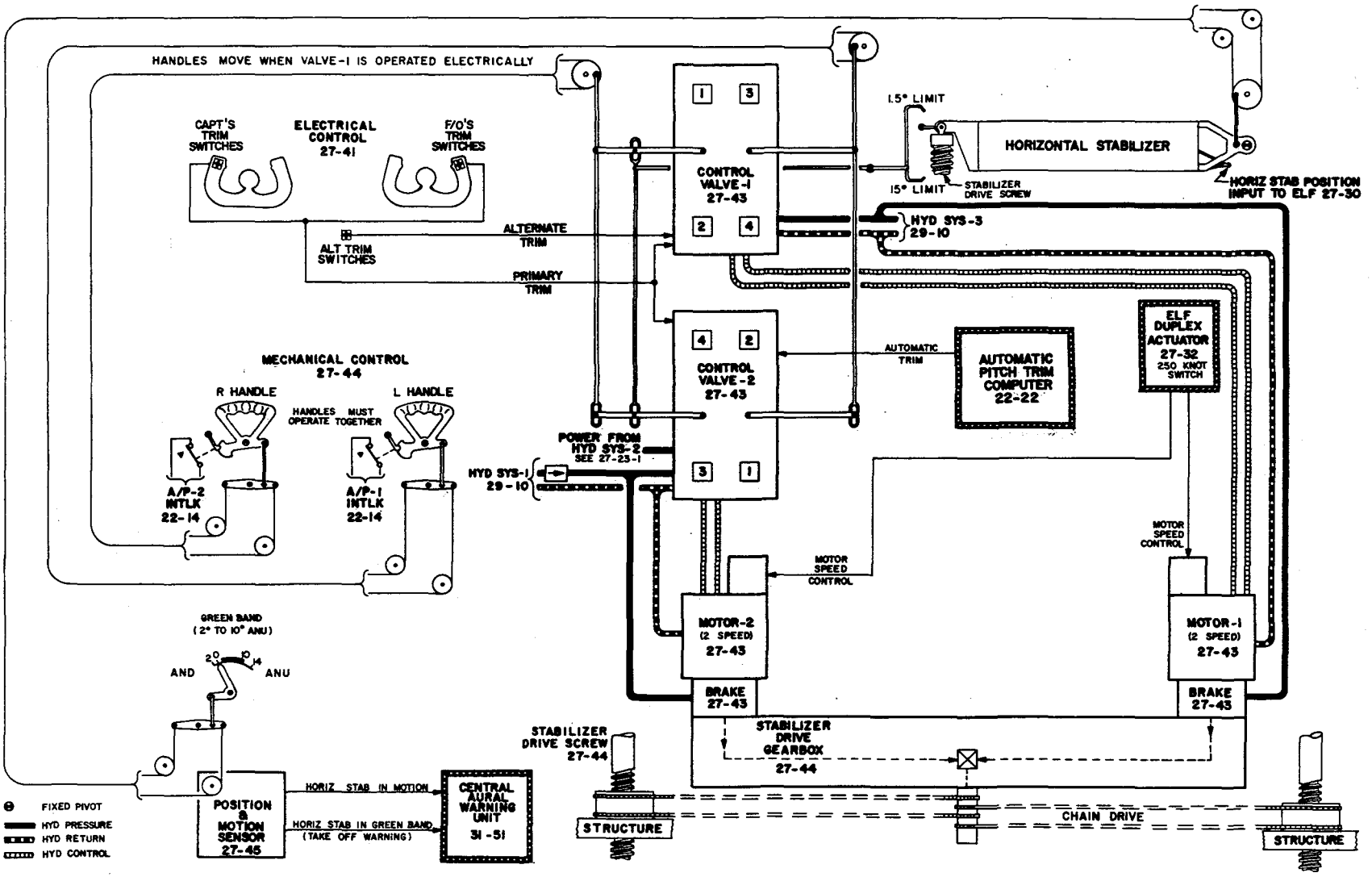

FIGURE 6-24. SYSTEM BLOCK DIAGRAM – HORIZONTAL STABILIZER TRIM

The block diagram shown in Figure 6-25 is a combination of RSSAS and autotrim concept. As the augmentor develops an elevator command, the threshold detectors sense this signal at Point A. The threshold detectors, in combination with the time delays, are set to minimize stabilizer motion resulting from transitory augmentation commands. A typical threshold detector characteristic is shown in Figure 6-26. The ON threshold is set at the minimum level above the average expected elevator displacement. This average may be established by evaluation of the augmentation commands in various levels of turbulence and/or during selected aircraft maneuvers. The OFF threshold is set at a position about which the augmentor may function without immediately requiring stabilizer motion. The OFF level must, however, be established so that it can be achieved during all flight conditions. If not, the autotrim will continuously drive the stabilizer. Both levels of the threshold detector must also be variable to correspond to the effectivity of the elevator. The time delays are set to complement the threshold detector such that transient elevator commands above the ON trim level do not result in stabilizer motion. The outputs of the threshold detector/time delays are fixed discrete commands to the stabilizer's actuation system.

The autotrim actuation consists of two dual electrohydraulic valves and motors which operate at fixed equivalent rates summing to drive the stabilizer. One of the valves combines the primary pilot input with the augmentation trim and the other valve combines the primary pilot input with the autopilot trim. A single motor operates the stabilizer at half the rate of the two combined. Therefore, under normal operation the primary pilot trim operates at twice the rate of either of the other two trim functions. Table 6-5 summarizes these rates. If the two inputs to a valve are opposing commands, the associated motor will not drive. If the two motors are driving in opposite directions, the stabilizer will not move.

To maintain consistent rates for the primary pilot trim function, the output of the threshold detector/time delays is inhibited as a function of pilot trim. Specifically, trim in the same direction is inhibited. In this way, the series elevator will not be retrimmed in a direction opposite to a pilot input which would effectively cut the pilot trim rate in half. Under all other conditions, the fixed RSSAS trim will be transmitted to the electrohydraulic valve. As the stabilizer moves in response to this command, the

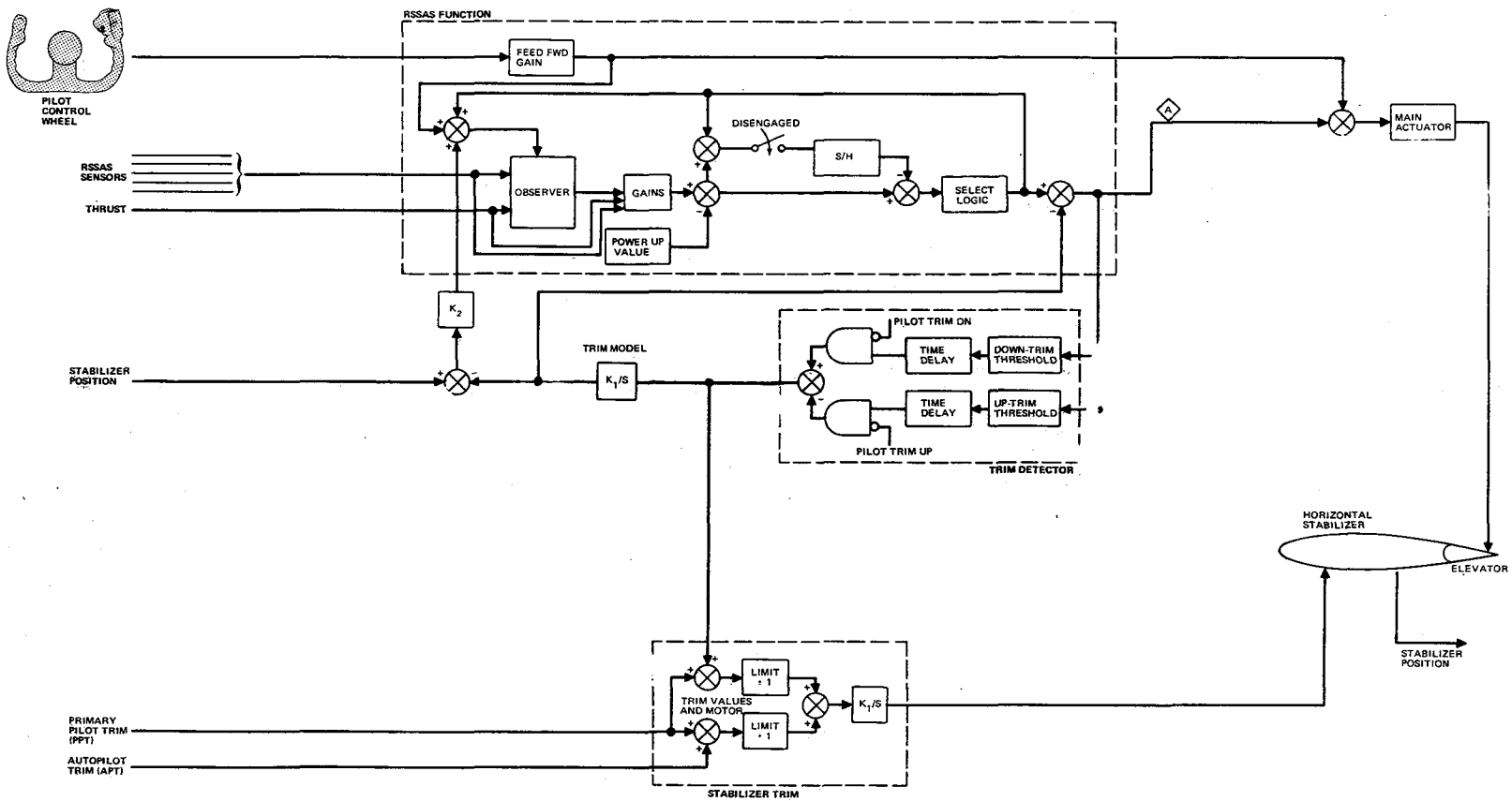

FIGURE 6-25. RSSAS BLOCK DIAGRAM WITH AUTOTRIM

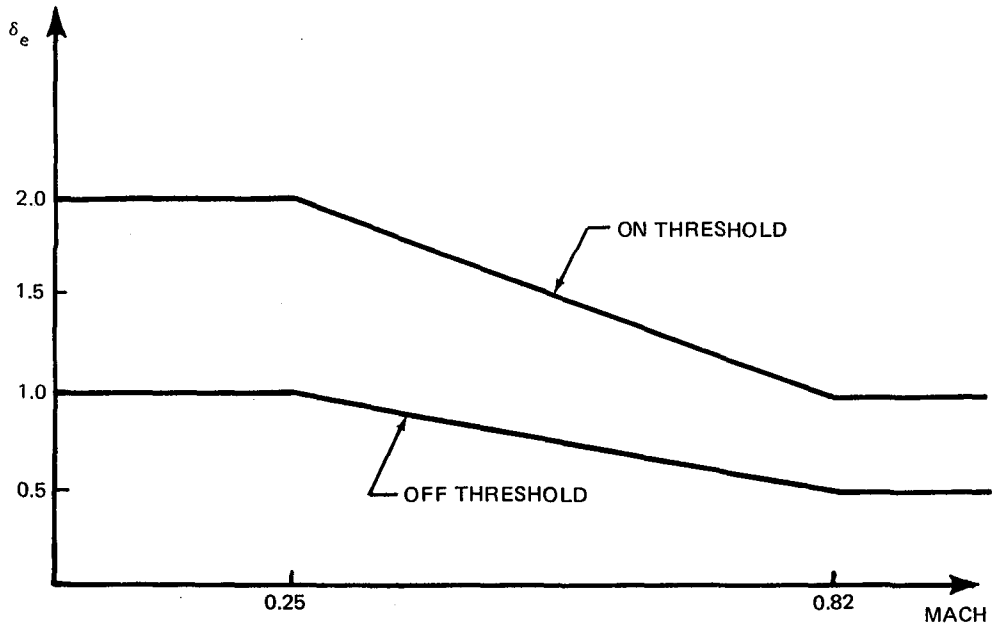

FIGURE 6-26. RSSAS AUTO TRIM THRESHOLD DETECTOR

TABLE 6-5
TRIM RATE SUMMARY

TRIM	TRIM RATE		MOTOR USED
	ABOVE 129 M/S (250 KN)	BELOW 129 M/S (250 KN)	
PRIMARY	0.0035 RAD/S (0.2°/SEC)	0.00873 RAD/S (0.5°/SEC)	–1 AND –2
RSSAS	0.00175 RAD/S (0.1°/SEC)	0.00436 RAD/S (0.25°/SEC)	–1
AUTOPILOT	0.00175 RAD/S (0.1°/SEC)	0.00436 RAD/S (0.25°/SEC)	–2

series elevator is repositioned an equivalent amount. Since the stabilizer position is a combination of all stabilizer commands, it is not used for this function. Instead, a model of the stabilizer motor provides the compensating signal which is summed with the series elevator command.

The output of this model is also used in subtraction from total stabilizer position to determine all motion used for flightpath guidance. This, in turn, is summed with primary elevator control and provided as an input to the RSSAS control.

Fault detection and isolation is an important consideration of the RSSAS trim function. Generally, two failure conditions can occur: (1) no trim action when required by the series elevator deflection, and (2) stabilizer motion does not agree with the elevator being off-loaded (i.e., the actuator model). Figure 6-27 expands the RSSAS autotrim diagram to include several

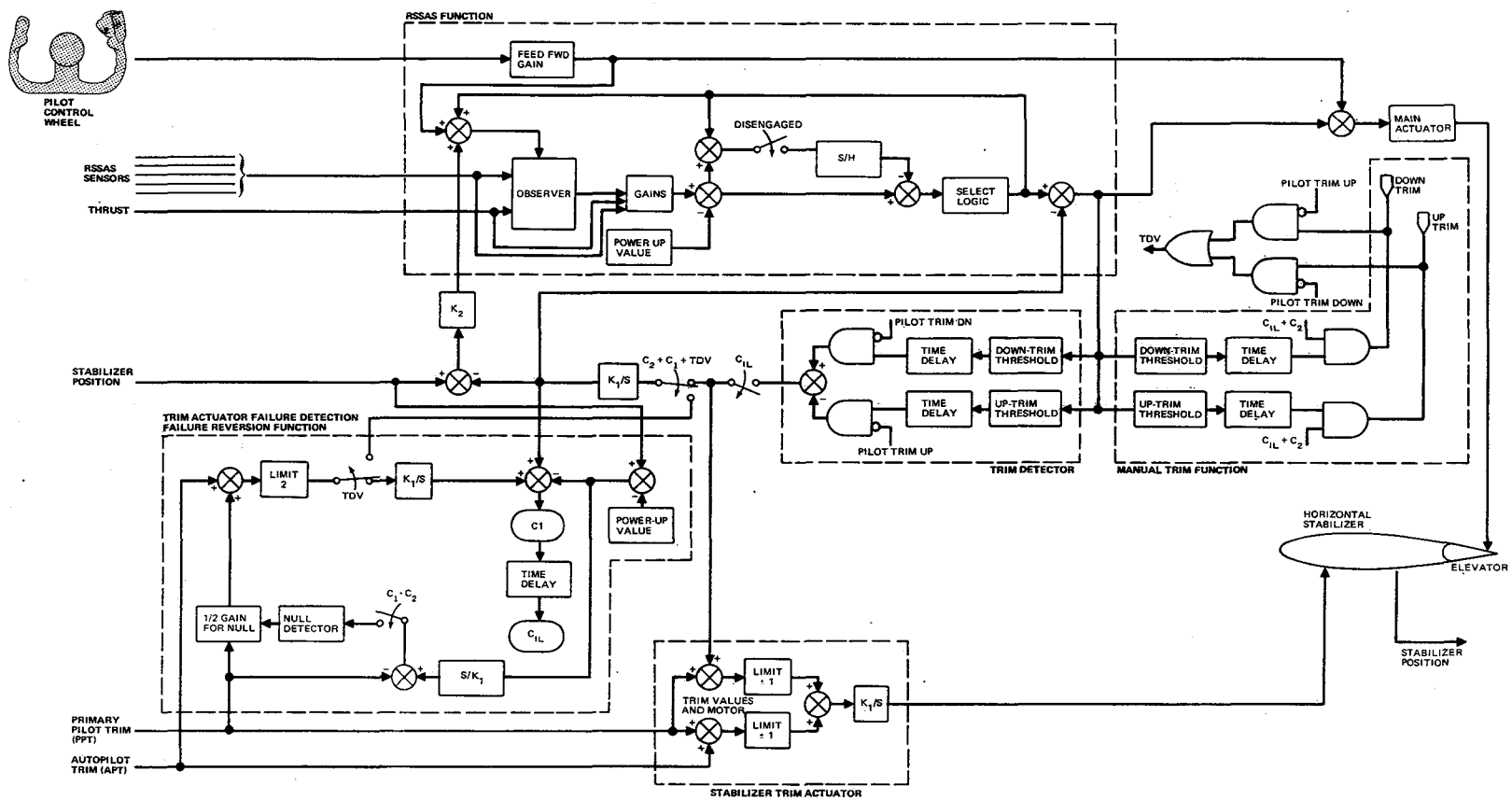

FIGURE 6-27. RSSAS BLOCK DIAGRAM WITH AUTOTRIM MONITORING

monitoring functions for these conditions. For the no-trim case, the C2 comparator is set to recognize an abnormally high series elevator deflection. The C1 comparator in turn sums all the trim inputs to determine agreement with the total stabilizer position. A failed condition sensed by either comparator set activates a manual trim director and allows primary pilot inputs to the actuator model to off-load the series elevator. A single electrohydraulic valve failure is also detectable by comparing the pilot trim input with the actual stabilizer rate at the actuator monitor null detector. Detection of mismatch at the null detector sets the model inputs to half value (half rate with only one valve operative).

A production installation of such a system would require further study into the criteria for failure warning and latching/resetting of internal monitoring functions. Faults must be promptly recognized, reacted to, and indicated, but the intelligence of the system may require a self-healing process. The design shown is a combination of self-healing monitors and a single-latching comparator intended to shut down the autotrim function for gross disagreements of trim actuation and elevator off-load.

6.1.4.1 Alternate RSSAS Autotrim Mechanization. — Another RSSAS autotrim mechanization considered was the use of a position (rather than rate) control system on the horizontal stabilizer with a fixed total travel capability. This concept, developed for the initial DC-10, was to be used with a mach/airspeed trim compensator. Early in the DC-10 development program, it was determined that this augmentation was not required so the position stabilizer control valve was not installed on the production aircraft.

This concept was not selected for the RSSAS, primarily for two reasons. First, a position system requires that the individual trim command of each FAC be synchronized or voted to establish a single stabilizer command. The resultant stabilizer position would then have to be fed back to the FACs in the correct proportion to the ratio of their desired displacement commands. An additional unit may be required to perform this trim drive. Second, and most significant, is the requirement that the RSSAS continuously control and position this actuation system properly for the flight regime. If the RSSAS is completely disengaged in flight and then subsequently engaged, the stabilizer actuation system may not be in the proper position to provide the range of stabilizer deflections necessary to off-load the

series elevator. This problem would not exist if the RSSAS was flight-crucial and it could be assured that full-time, continuous stabilizer control would be provided.

6.1.4.2 Autotrim Operation. — The RSSAS autotrim function has been analyzed for various primary pilot and autopilot trim demands. Several of these operations are presented here using the simplified trim schematic shown in Figure 6-28. Figures 6-29 through 6-32 show the altitude, elevator commands, and trim response corresponding to selected maneuvers. The actual values used are arbitrary and have been selected for convenience and proper direction of response but not assigned an absolute signal level. In Case 1, Figure 6-29, the pilot inputs a pitch-up command with nose-up elevator. The pilot input (δ_{ep}) is in one direction and the augmentation input (δ_{es}) may move in the opposite direction to stabilize the aircraft response (θ). After the appropriate time delay (TD) the augmentation trim command (δ_{TC}) turns on. The washout command (δ_{WD}) is summed with the augmentation command (δ_C) until the total (δ_{es}) is zero and the trim command (δ_{TC}) turns off. While δ_{TC} was on, the stabilizer (δ_{ST}) was moving at a fixed rate and has now established the required new setting. When the pilot returns the aircraft attitude to the original condition, the trim process is reversed.

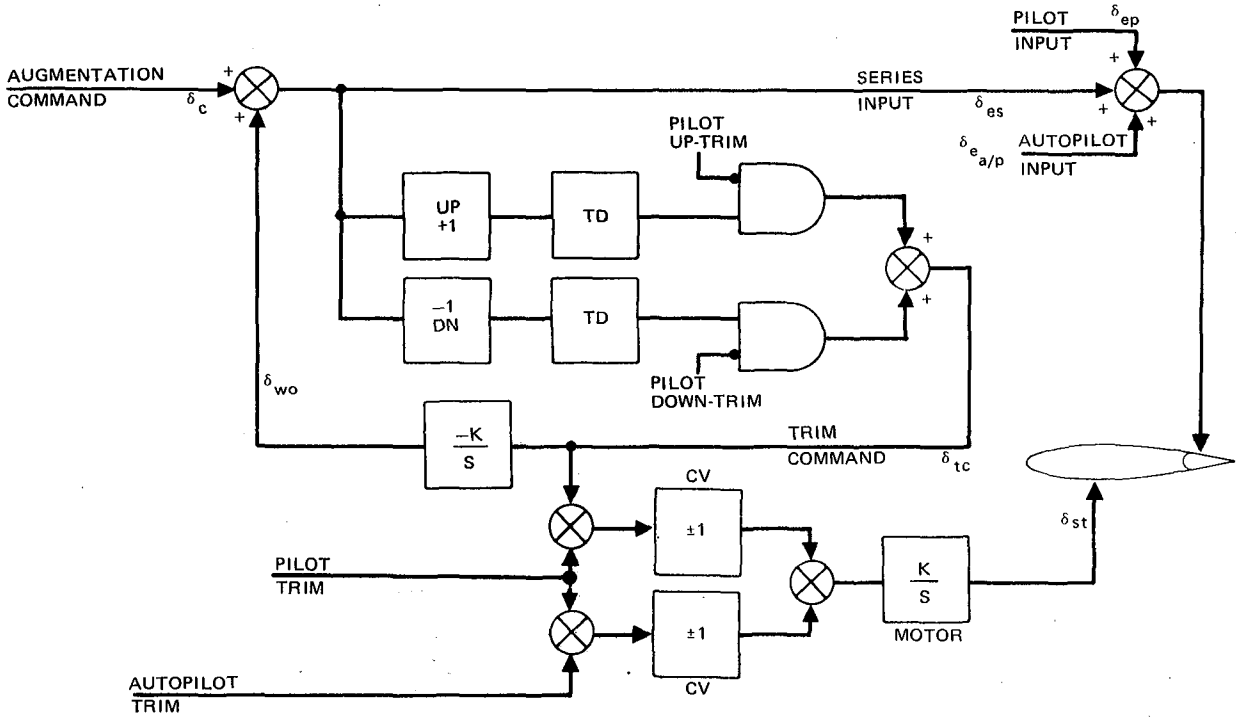

FIGURE 6-28. AUGMENTATION TRIM SCHEMATIC

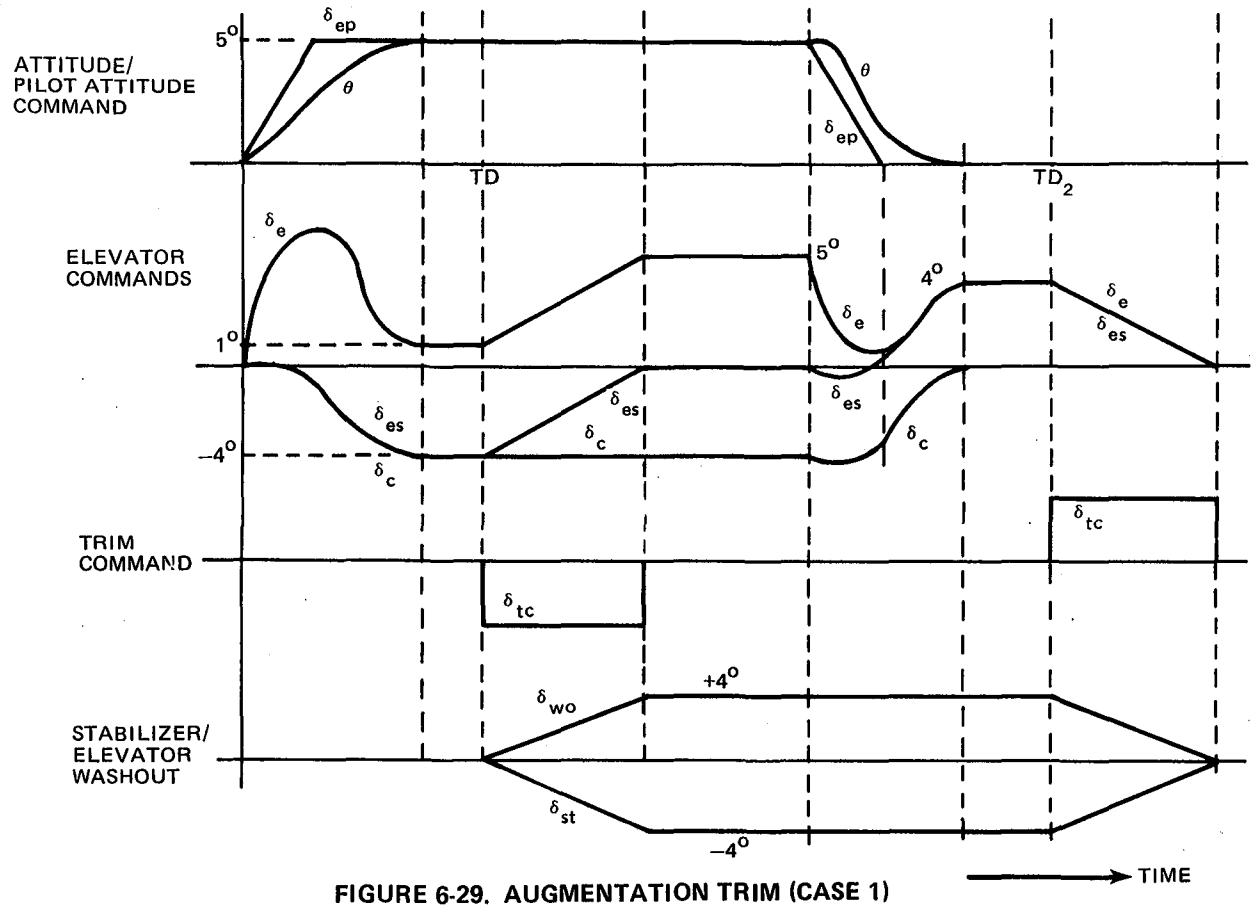

FIGURE 6-29. AUGMENTATION TRIM (CASE 1)

Figure 6-30 demonstrates a similar operation, but in this case the pilot has exercised his primary trim (δ_{PT}) to off-load his elevator displacement (δ_{ep}) prior to the operation of the augmentation trim. This leads to the next operational sequence with the pilot and RSSAS trim overlapping in time as shown in Figure 6-31. Note that the trim demands are in opposite directions, so the RSSAS trim-detector/time-delay output is not inhibited. If the trim demands were in the same direction, the RSSAS trim would be inhibited until the pilot trim is satisfied. The trim signals combine to turn off the upper control valve (CV) and the stabilizer runs at half rate. At the same time, the series elevator (δ_{es}) is reduced by the washout command (δ_{WO}) and this combines with the stabilizer motion (δ_{ST}) to provide an aircraft response identical to that resulting from full stabilizer rate.

The last example, shown in Figure 6-32, is the combined operation of autopilot and RSSAS trim responding to opposing commands. At time T_1, the autopilot trim (δ_{APT}) is initiated to off-load the autopilot elevator input ($\delta e_{A/P}$). At time TD, the RSSAS trim (δ_{TC}) turns on and, since the two trim commands are in opposition, the stabilizer motion (δ_{ST}) stops. The two

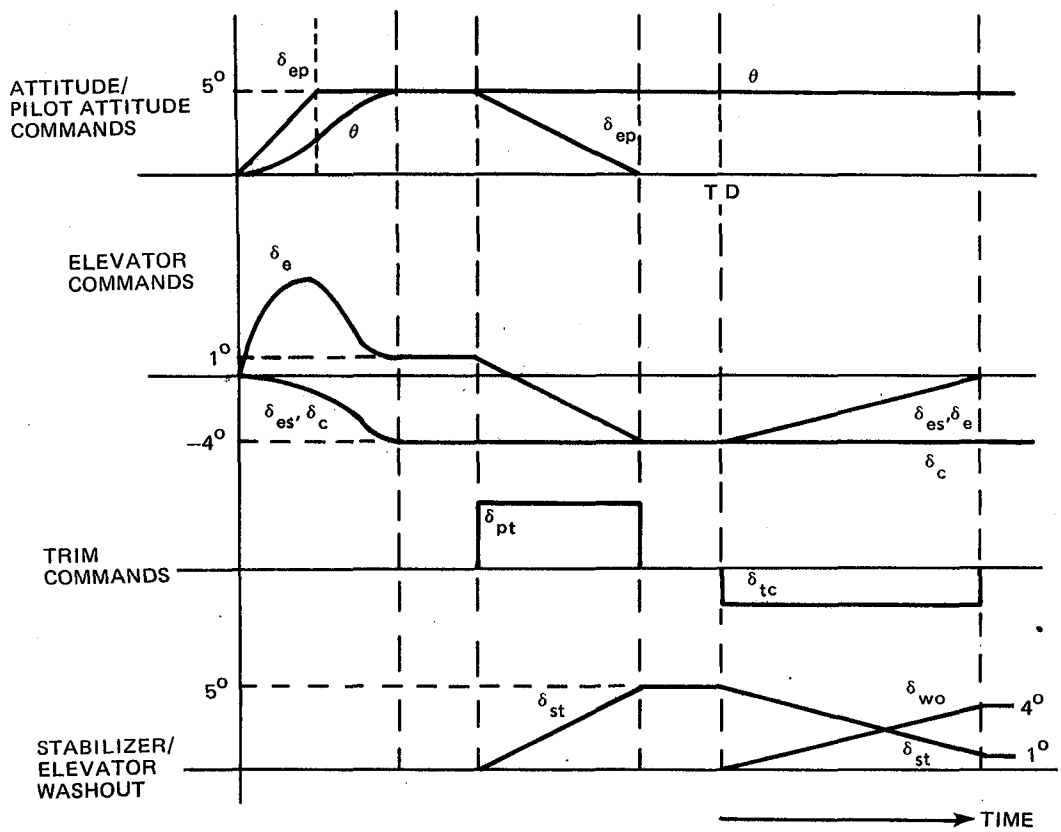

FIGURE 6-30. AUGMENTATION TRIM – CASE 2

elevator displacement commands ($\delta e_{A/P}$ and δ_{es}) continue to wash out at opposite equivalent rates. When either command error is nulled, the corresponding trim is turned off. In the example shown, the autopilot is satisfied first, and at this time the stabilizer begins to move in response to the existing RSSAS trim command.

6.1.5 Integration of Other Augmentation Functions. – Several other functions were considered for integration, together with the RSSAS function, into the FAC. These additional functions include:

- Yaw damping/turn coordination
- Elevator-load-feel programming (ELF)
- Flap-position limiting (FL)
- Stall warning.

Diagrams of the equivalent DC-10 systems are presented in Appendix 10.

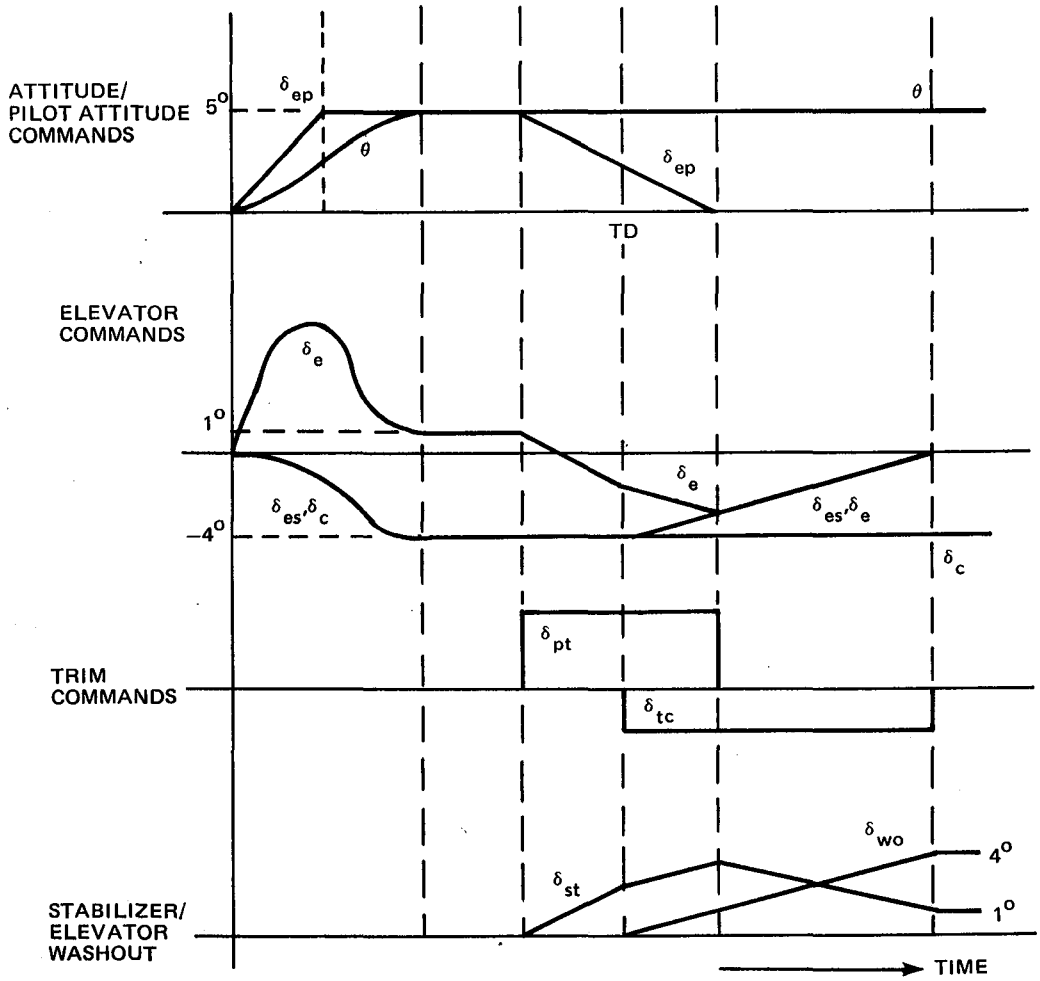

FIGURE 6-31. AUGMENTATION TRIM – CASE 3

There are two reasons for this integration. First, all of these functions are required for dispatch of the aircraft. Second, most of the required data to perform these calculations will normally be available to the RSSAS function. These signals include:

- Yaw rate – attitude heading reference system
- Roll attitude – attitude heading reference system
- Airspeed – air data computer
- Mach – air data computer
- Angle of attack – angle-of-attack vanes.

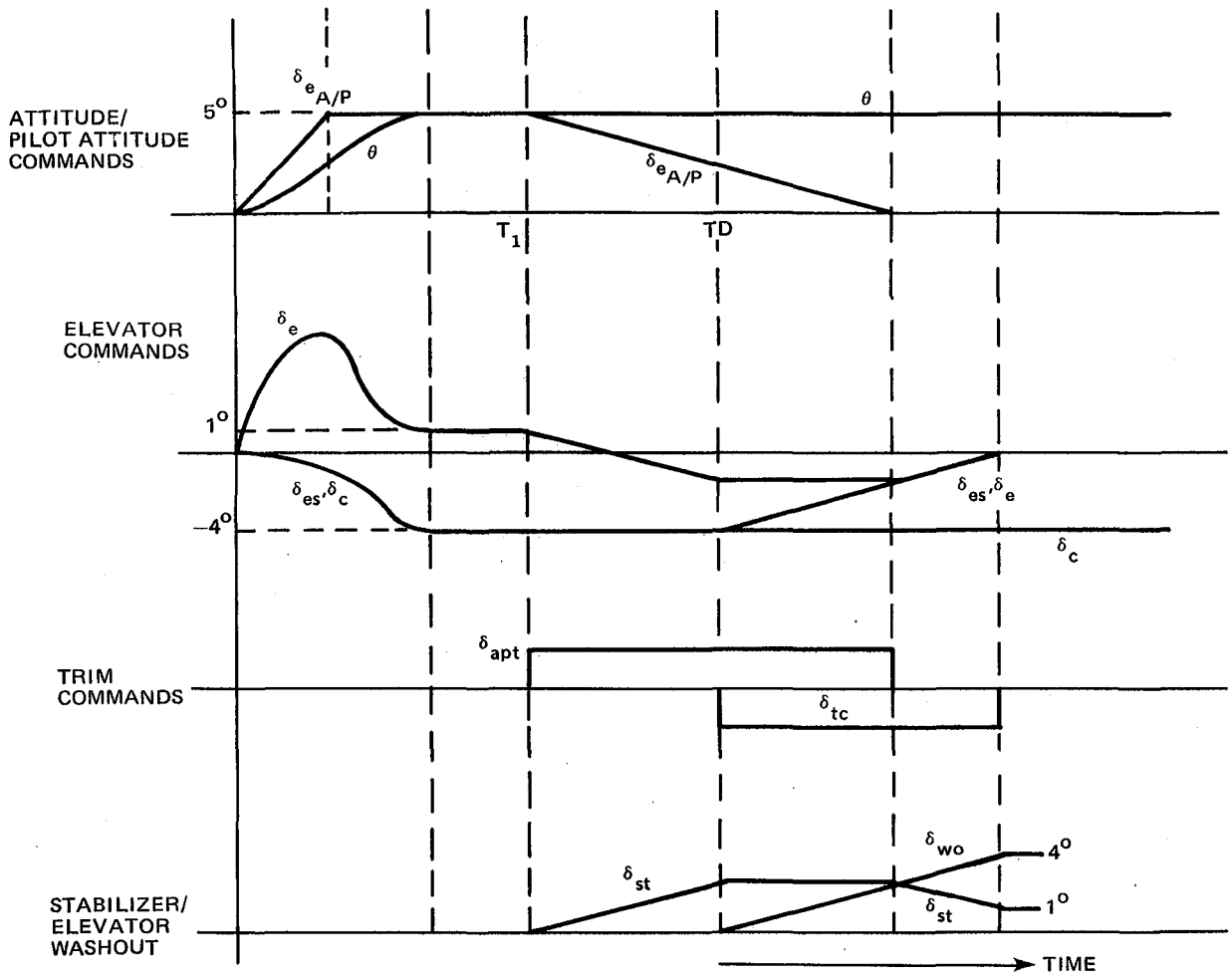

FIGURE 6-32. AUGMENTATION TRIM CASE 4

Additional sensor signals necessary to be provided to the FAC include:

- Flap position — FL and stall warning
- VCK position — stall warning
- Function-engage control — all functions
- Servo/actuator commands and feedback — all functions.

The effect on the computer architecture and system reliability of incorporating these functions is discussed in Paragraphs 6.1 and 4.2, respectively.

6.1.6 Electrical Power. — The EET basic aircraft flying qualities are such that an augmentor is not required for safety of flight. Thus, the augmentation system does not require a noninterruptable electrical power source, such as a battery. For this reason, a conventional electrical AC power system for the EET is acceptable. A description of the aircraft system is presented in Appendix 11.

6.1.7 Maintenance Concept. — Maintenance is the function performed by the user of a system to place that system in proper operating condition. To assist in that function, most avionics systems incorporate a certain amount of maintainability. The thoroughness and accuracy with which a system performs this function depends on the capabilities of the individual components and the complexity of its interfaces. The motivation for improving this capability is the cost of maintenance or possible lost revenues, as in the case of dispatch critical functions. All the functions (RSSAS, Yaw Damping, Elevator-Load-Feel/Flap-Limiting, and Stall Warning) proposed for integration into the FAC are in fact required for dispatch. Therefore, a complete and comprehensive built-in maintenance capability is desired. The three major tasks that this FAC maintenance function must perform are: (1) Fault Detection, (2) Fault Isolation, and (3) Functional Verification.

6.1.7.1 Fault Detection. — Fault detection is mostly performed continuously in flight by the system's monitors. Each FAC, of course, uses the data to make on-line control and/or configuration decisions. The data must also be transmitted to a central system maintenance unit and stored in a nonvolatile memory for subsequent recall. For the ground condition, a manually initiated, automatic test is required, which stimulates the system so that the monitors can perform their functions.

6.1.7.2 Fault Isolation. — The on-line system monitoring is primarily designed to isolate a fault to a function. In most cases, the fault is also isolated to a component failure or interface. Some faults, however, are not

easily isolated, such as different faults which produce the same effects. For these cases, the ground maintenance function must have the capability to sequentially stimulate the individual system elements. In other cases, an unusual combination of environmental conditions or control requirements may be the stimulus for the fault. Here the recorded data must be maintained and, upon recognition of the conditions or by recurrence of the event, the fault diagnosed.

6.1.7.3 Functional Verification. — There are two levels of functional verification of the system. The most complete is that verification necessary after installation of a system component — primarily a FAC. Using the central maintenance unit, all functions influenced by the newly installed component must be tested by the maintenance personnel for proper operation, including some level of performance capability. Besides being a function test, this procedure verifies the system to the component level. The other functional verification occurs during a normal preflight cockpit check and is performed by the flight crew. In this case, the maintenance unit is not used, but rather the test is initiated at the location of the normal cockpit controls for the function. Each function can be individually tested or performed as part of an integral test, depending on the cockpit layout and/or operation philosophy. The preflight test is intended to be solely a functional check, and verification to the flight crew is at a functional level.

To isolate a fault or verify a function while on the ground requires the capability to stimulate the sensors to known conditions. The FACs will in turn verify the sensor data, perform the necessary calculations for each of its functions, and provide an appropriate actuator command output. The actuation systems are checked by verifying the correct feedbacks. (Stall warning requires observation of the stick shaker.) All units of the FAC functions will have this capability.

6.1.7.4 The Maintenance Unit. — The maintenance unit is an integral part of the flight augmentation system design. It must interface with all FACs to issue maintenance test instructions and to interrogate the computer function. A single maintenance unit may perform the same function for other avionics systems such as the flight guidance systems (autopilot and flight

director), flight management systems (navigation and flight performance), and/or thrust management systems (autothrottle and thrust-rating). To assure that the maintenance unit does not become the limiting factor in the maintainability of these systems, a simple reliable device is required. The proposed unit would include a test-initiate pushbutton, a go/no-go annunciator, and select switch to allow individual system test or varying levels of functional test, depending upon the maintenance action required or aircraft configuration (hydraulic power available or surfaces locked). It is suggested that a microprocessor be included in the unit, with nonvolatile memory, to perform the necessary test data management and to record the inflight and test data. A multicharacter display also would be provided to convey the detailed performance information to the maintenance operator. The display also would be used by the system to request the maintenance operator to make aircraft configuration changes, verify display presentation, or to perform other functions not available to the maintenance unit. Verification or nonverification of the requested task would be signified through separate pushbutton inputs.

Due to the interaction of the maintenance unit and operator, it is suggested that the unit be located in the cockpit, convenient to the necessary aircraft controls and displays. A remote parallel unit may be considered for the avionics equipment compartment.

The maintenance unit required to perform these functions is similar to the DC-9 Series 80 Digital Flight Guidance System Maintenance Panel shown in Figure 6-33.

6.1.7.5 Preflight Tests. — The preflight tests of the augmentation system functions are initiated by the flight crew at the normal control location on the forward overhead control panel. The test-initiate signal is provided directly to the FAC which in turn sequences the proper system stimuli to verify the selected function. Initiation of the test will cause the appropriate function warning light to illuminate. Besides indicating the test in progress, this serves as a test of the warning light circuits. At the conclusion of the test, the warning light will extinguish if the

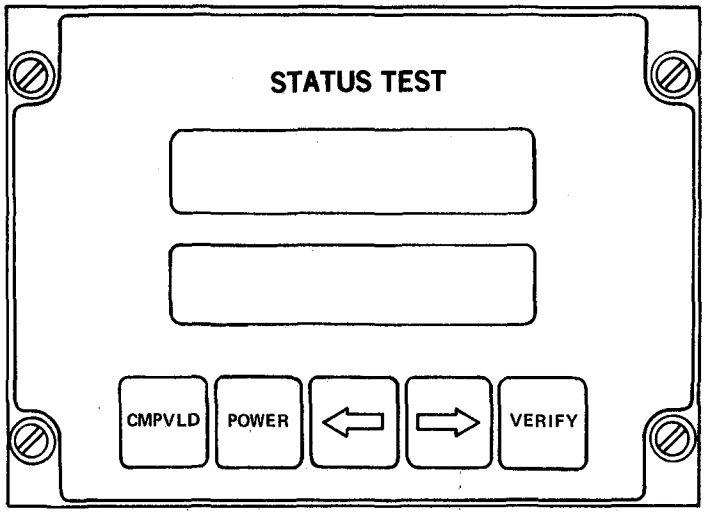

- PREFLIGHT/SEMIAUTOMATIC
- MAINTENANCE TESTING
- RECALL OF INFLIGHT FAILURES

8-DC9-91562

FIGURE 6-33. DC-9 SERIES 80 MAINTENANCE PANEL

function is satisfactory, but will remain illuminated if a fault is detected. The test results will also be monitored by the maintenance unit which may receive detailed component failure characteristics. Figure 6-34 shows the overhead instrument panel layout with appropriate augmentation function controls.

6.1.8 Fly-by-Wire Considerations. — The fly-by-wire (FBW) concept can be implemented as either hybrid nonflight crucial or as the total primary flight controls. The hybrid mechanization would require some level of mechanical capability as a backup to the electronic control, but the total system would not require such backing.

At first, FBW seems like an ideal candidate for integration with the RSSAS due to its high reliability and architecture (primarily actuator interface). After some consideration, however, many differences become apparent and these require significantly different design approaches. Some of these items are discussed below.

6.1.8.1 Reliability and Safety. — The loss of the RSSAS function must meet a $1x10^{-5}$ regulatory failure probability criterion, as interpreted in Figure 4-7, for a basic aircraft with Level 2 flying qualities which can

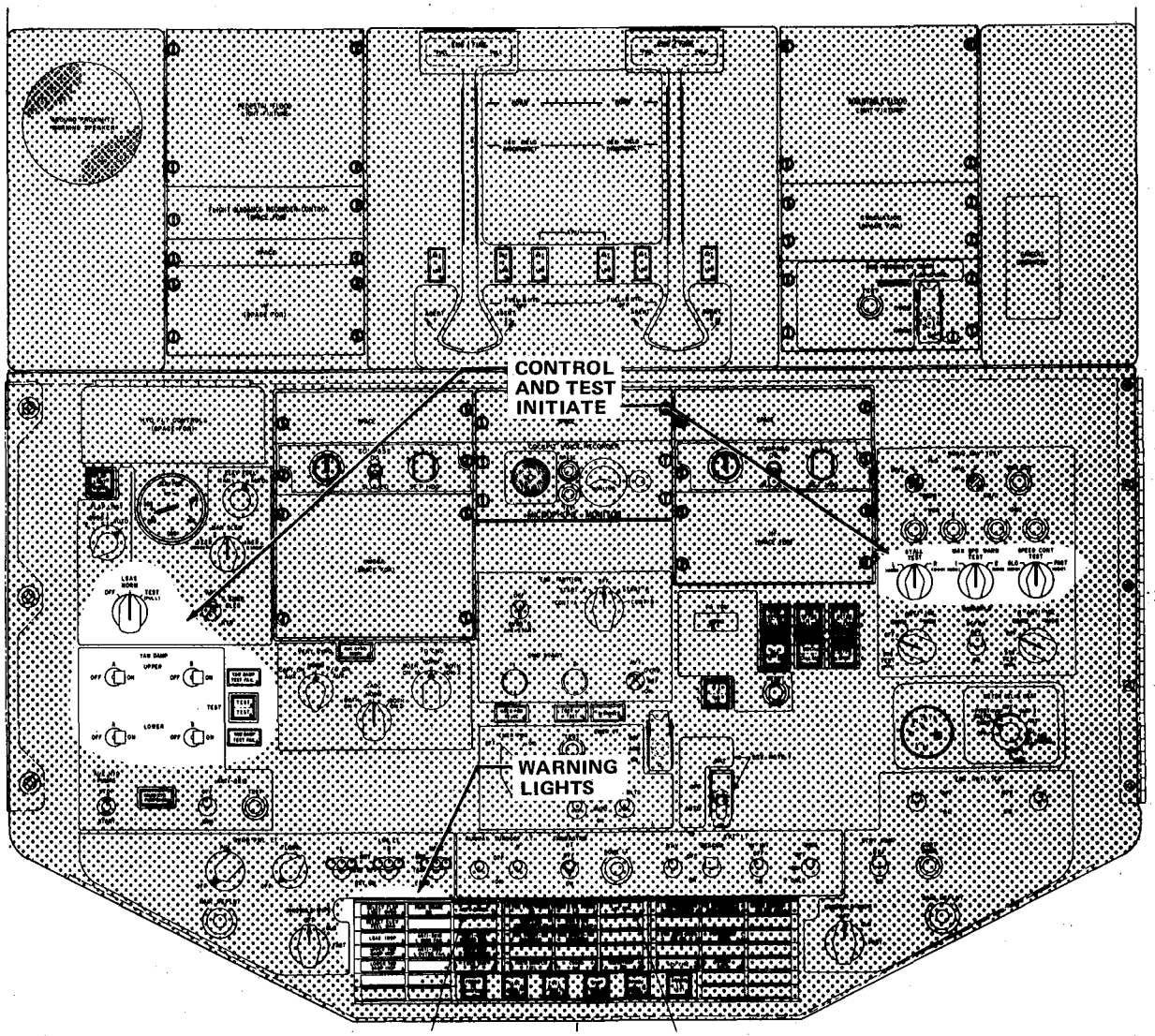

FIGURE 6-34. OVERHEAD PANEL PREFLIGHT TEST CONTROL

complete its mission or flight plan. The electronics of a hybrid FBW would probably have to satisfy the $1x10^{-7}$ probability requirement since the flight plan would be aborted with an immediate landing. This is a result of having only a single-string mechanical control system available, which may be a single failure away from loss of aircraft control. The full electronic FBW would, of course, require a maximum system failure probability of less than $1x10^{-9}$. Dispatch inoperative considerations would require an even greater level of redundancy than that required to meet the safety criteria.

6.1.8.2 Flying Qualities. — While the RSSAS is provided to maintain flying qualities, the FBW mechanizations are primarily a replacement for complex and heavy mechanical components.

6.1.8.3 Sensors. — The RSSAS requires several different types of aircraft sensors to describe the aircraft control and response. The FBW systems require only some type of pilot control sensors (control wheel or side-stick force or position), to determine the desired pilot input.

6.1.8.4 Computation. — The RSSAS function requires the processing of many inputs, a complex computation and logic operation, and a large degree of monitoring of different devices. The FBW function is a rather simple calculation with the minimum sensor input. Monitoring must be complete, but the task is relatively simple. The FBW systems will require control of many actuators (more than RSSAS) and, to keep the computation system simple, a fully monitored closed servo loop at each of these actuators may be required.

6.1.8.5 Actuation. — Static stability augmentation is accomplished through series elevator actuators which do not reflect back into the pilot control. The traditional commercial transport has used control systems which reflect the position of the control surfaces. For the hybrid FBW, this can be accomplished by using a parallel actuator at the surface and allowing this actuator to back-drive the control wheel/column through the backup cable system. The full electronic FBW would have no way of driving the control wheel/column through a mechanical system so that the surface actuator could be shared with other functions such as RSSAS. Either the control wheel/column would not be required to display the control surface position, or a separate actuator package would have to be installed at the pilot's position to move the control input in parallel with the surface.

6.1.8.6 Electrical Power. — Unlike the RSSAS, the FBW mechanization cannot be allowed to disconnect (even a temporary disconnect of the hybrid system would be a nuisance); therefore, a noninterruptible power source is required. The full electronic FBW requirement of the electrical system is more severe than any present electrical system requirement.

6.2 Architecture Formulation

Architecture formulation consists of defining the individual elements of the system, their level of redundancy, and the interconnection of the

devices. Based on individual design constraints and functional independence, it has been decided that the configurations for the relaxed static stability augmentation, pitch/thrust compensation, and automatic trim for the series elevator augmentation would be developed independently. Formulation of the relaxed static stability augmentation architecture has been initiated by first establishing the most demanding functional reliability requirements of the system. As shown in Figure 6-35, this can be based on the interpretation of the regulatory requirements, desired functional availability, or other criteria based on knowledge of, or experience with, such systems. In the reliability and safety section of this report, the regulatory requirement for the loss of augmentation for an aircraft with Level 2 flying qualities has been interpreted to specify a total RSSAS function failure probability of approximately $1x10^{-5}$ for one flight hour. The desired functional availability of the RSSAS is based on traditional capabilities of similar augmentation devices such as yaw damping. This allows one complete system loss per year for a fleet of 200 aircraft, each operating 1000 hours per year. This equals a failure rate of $2.5x10^{-6}$ failures/hour. The path through the design contingencies anticipates that as the aircraft aerodynamic definition progresses, it may be determined that there are isolated aircraft/envelope combinations in which the unaugmented aircraft flying qualities degrade to a Level 3. The regulatory requirements would then specify a total RSSAS failure probability $1x10^{-7}$ in these flight regimes. This most restrictive system failure probability has been established as the reliability requirement of the study. It is anticipated that this target, besides providing a margin for the specified flying qualities, will allow flexibility in operating and maintaining this dispatch-critical system.

The relaxed static stability augmentation has been partitioned into functional subsets as shown in Figure 6-36. These subsets include: (1) the sensors along with the data transmission to the computation; (2) the computation accepting the data input and providing control commands to the actuators, and (3) an actuation system which interfaces with the primary controls to drive the elevator surfaces and is powered by the hydraulic system. The existing conventional electrical system was assumed to be used for the power source and is described in Appendix 11.

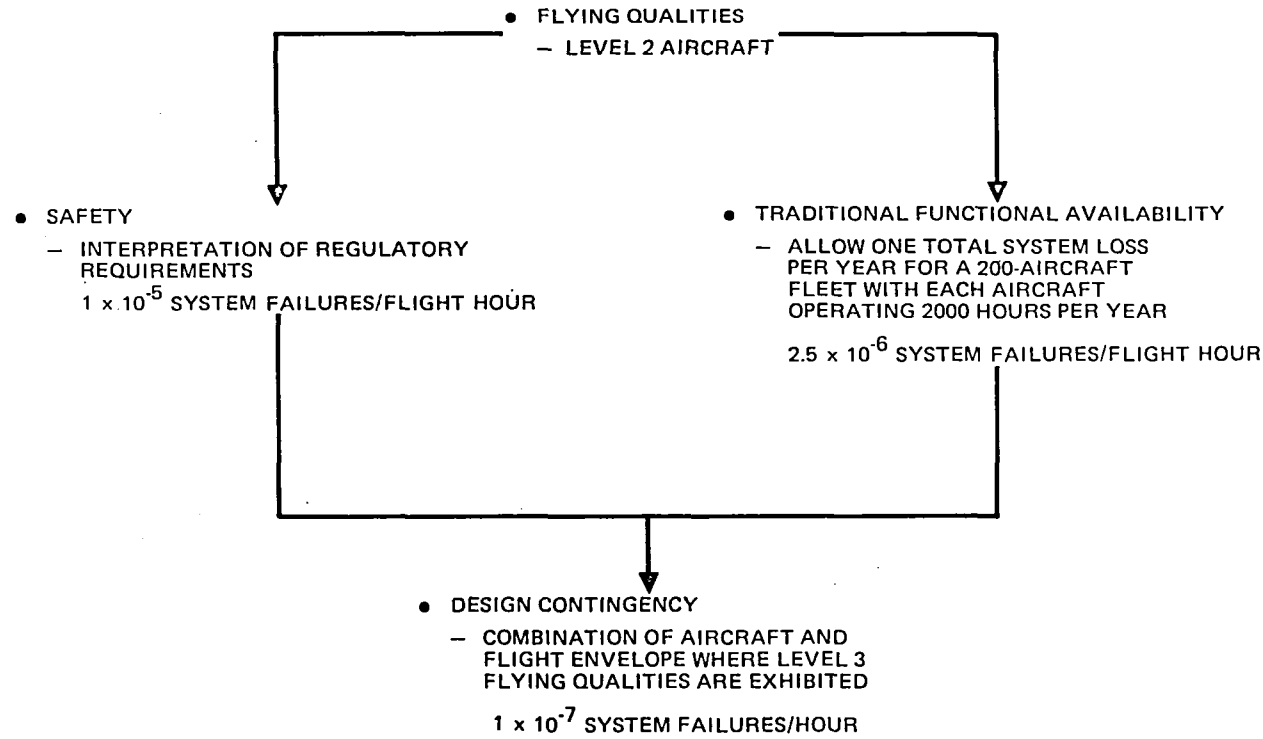

FIGURE 6-35. ARCHITECTURE FORMULATION RELIABILITY CONSIDERATIONS

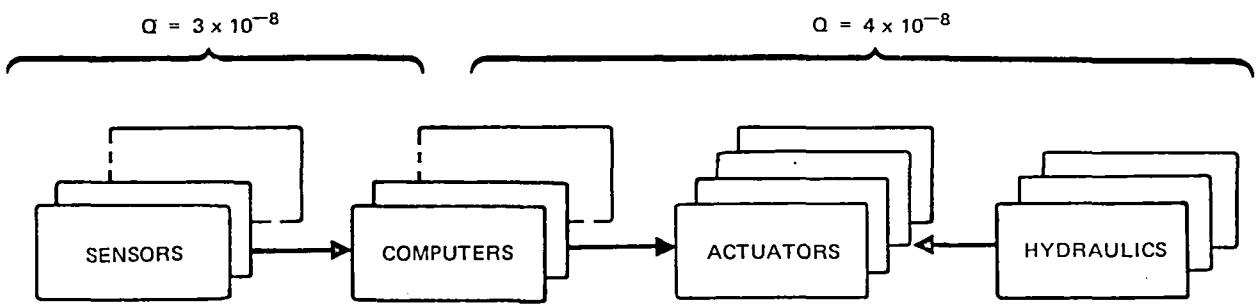

ELECTRICAL SYSTEM Q = 3×10^{-8}
Q = FAILURE PROBABILITY

FIGURE 6-36. RSSAS FUNCTIONAL PARTITION AND RELIABILITY ASSIGNMENT

Using this partitioning of function, the specified reliability has been allocated to the individual subsets proportionately to that system reliability experienced on the DC-10. As shown in Figure 6-36, the sensor system probability goals is $3x10^{-8}$ and the combined computer/actuation subsets goal is $4x10^{-8}$. The remaining $3x10^{-8}$ is allocated to the electrical system and any control devices. The computation and actuation subsets have been combined since an individual actuator system has a significantly lower failure probability than its corresponding computer drive, and the associated computer failure nearly always results in loss of the corresponding actuator control. This dependence of the actuation on the computation justifies combining the reliability requirement into a single subsystem goal.

Figure 6-37 is a system redundancy graph that relates the single system MTBF to the number of systems required to achieve a failure probability of $1x10^{-7}$ for one hour. All failures are assumed to be detected and isolated. This gives a first approximation of the level of redundancy needed in constructing a system architecture. For the partitioning assigned, this graph could have been constructed more accurately for the $3x10^{-8}$ and $4x10^{-8}$ failure probabilities of the subsystems. Based on avionics hardware experience which has shown typical component MTBF's in the 3000- to 5000-hour range, a redundancy level of two to no greater than three appears to satisfy the reliability requirement. In actuality, the curve differs from that shown when consideration is given to effects of failure modes and fault detection, isolation, and reconfiguration capabilities.

6.2.1 Sensor Array

6.2.1.1 Initial Component Redundancy Evaluation. — Prior to determination of acceptable control laws, a sensor reliability analysis was performed, assuming only a single control law capability would be attained. The failure probabilities of the sensor array related to each of the original 28 possible control law configurations have been calculated for various levels of component redundancy. This provides an insight into the sensor redundancy and/or sensor monitoring confidence required to satisfy the allotted failure probability of $3x10^{-8}$.

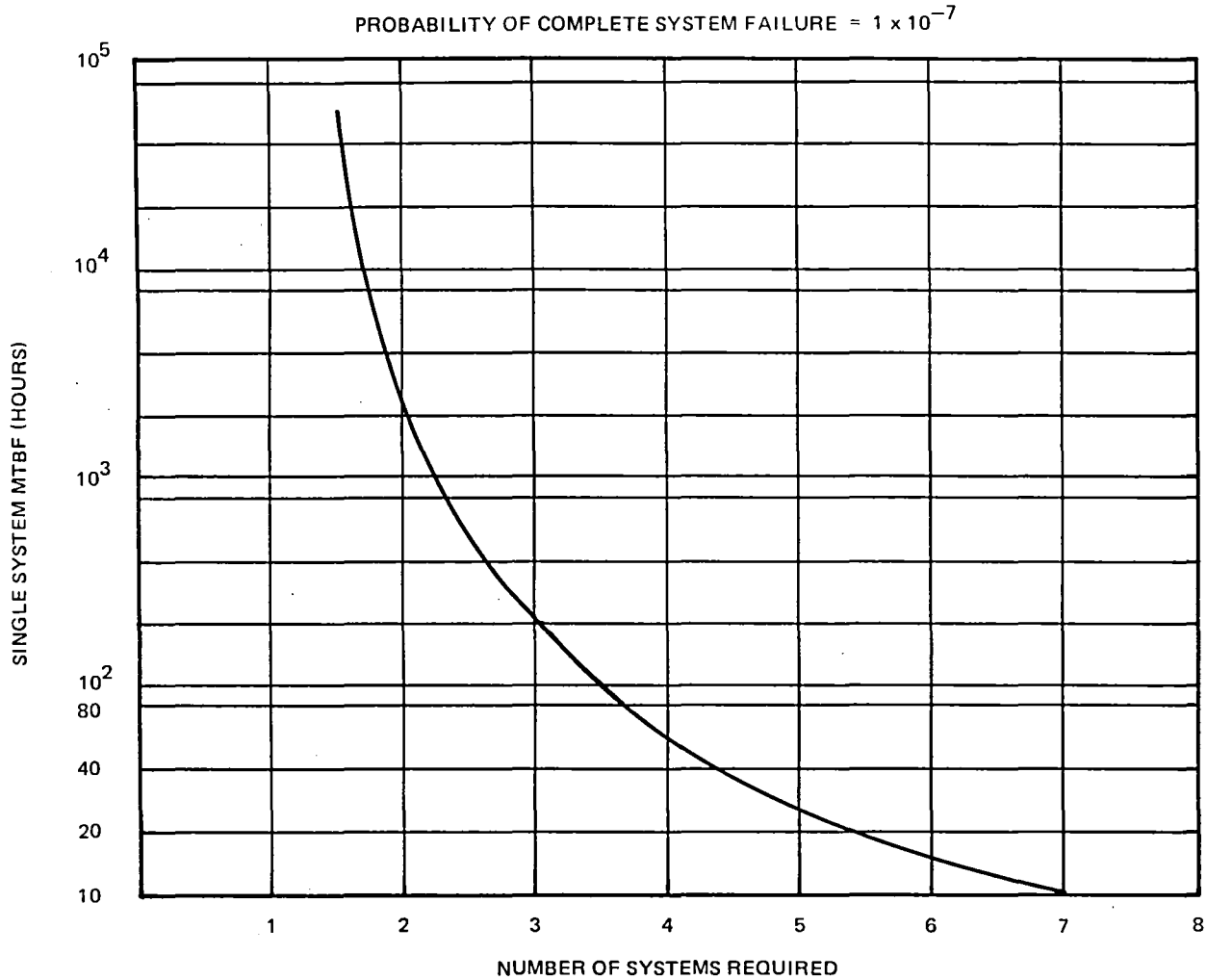

FIGURE 6-37. SYSTEM REDUNDANCY REQUIRED

Subsequent control law development has demonstrated that several control laws, each based on a unique sensor array, provide satisfactory augmentation. This allowed the use of a method of control law reversion (discussed in Paragraph 6.2.1.2) to meet the reliability criteria for sensor failures rather than "bulk sensor redundancy". A technique for selection of the required level of redundancy and monitoring for "bulk sensor redundancy" is presented in this section only as an example for the reader and was not used in the selection of the final system architecture.

Calculations have been made for redundancy levels of two, three, and four sensor systems. The MTBFs used for the various sensors are based on historical data available from DC-10 experience. These MTBFs are 3200 hours for the Vertical Gyro (θ), 6000 hours for the Air Data Computer (u, $\dot{h}$), 12,000 hours for the Accelerometer Unit (A_N, A_X), and 3000 hours for the Angle-of-Attack Sensor (α). Since there is no DC-10 sensor for pitch rate ($\dot{\theta}$), a MTBF of 5000 hours has been assigned; this value should be realistic whether the device is added circuitry to derive pitch rate from pitch attitude, or a separate rate sensor installed on the aircraft.

The study has assumed that the sensor-monitoring function would be such that with three or more operative units, a single failure would be detected by comparison-monitoring, isolated, and removed with 100-percent confidence. With two operative units of the same type, a failure would be detected by comparison-monitoring with 100-percent confidence but isolated and removed (such that the remaining unit can continue to operate) with a confidence factor, C, related to the capability of in-line monitoring of an individual sensor's data. Of course, when operating with a single-type sensor unit, all failures result in loss of function regardless of failure-detection capability. In the calculations performed, the confidence factor, C, is not assigned, but rather determined so that the reliability criteria are satisfied.

The reliability of the individual sensor units is $R_s = e^{-\lambda t}$ and the probability of failure is $Q_s = 1 - R_s = 1 - e^{-\lambda t}$. With λt very small, $Q = 1 - e^{-\lambda t} \approx \lambda t$. For a dual-sensor-type redundancy, the probability of total function failure due to the sensors, Q_{F_S}, is approximately the probability of failure of both devices of a type, $Q_{S_T}^2$, plus the probability of a failure in either single unit that can only be isolated at a probability of C, $2(1 - C_T)Q_{S_T}$. This gives the equation:

$$Q_{F_S} \approx \sum_{T=1}^{N} Q_{S_T}^2 + 2(1 - C_T)Q_{S_T}$$

where C_T = confidence of in-line fault detection and isolation of sensor type T.

In the triple redundancy sensor arrays, the probability of failure, Q_{F_S}, is approximately the probability of failure of all devices of a type, $Q^2_{S_T}$, plus the probability of two devices of a single type failing where the second failure can only be isolated at a probability of C, $3(1 - C_T)Q^2_{S_T}$. This gives the equation:

$$Q_{F_S} \approx \sum_{T=1}^{N} Q^3_{S_T} + 3(1 - C_T)Q^2_{S_T}$$

With quad-sensor redundancy, the probability of failure, Q_{F_S}, is approximately the probability of failure of all devices of a type, $Q^4_{S_T}$, plus the probability of three devices of a type failing where the third failure can only be isolated at a probability of C, $4(1 - C_T)Q^3_{S_T}$. This gives the equation:

$$Q_{F_S} \approx \sum_{T=1}^{N} Q^4_{S_T} + 4(1 - C_T)Q^3_{S_T}$$

The value of C has been calculated by setting $Q_{F_S} = 3\text{x}10^{-8}$. For those control laws with more than one sensor, C has been determined by allocating to each sensor type an equal probability of sensor function shutdown due to incomplete in-line monitoring of individual sensors ($C < 1$). As an example, for a triple-redundancy, three-sensor-type array:

$$Q_{F_S} = \sum_{T=1}^{3} Q^3_{S_T} + 3(1 - C_T)Q^2_{S_T}$$

$$= Q^3_{S_1} + Q^3_{S_2} + Q^3_{S_3} + 3(1 - C_1)Q^2_{S_1} + 3(1 - C_2)Q^2_{S_2} + 3(1 - C_3)Q^2_{S_3}$$

Equalizing the effect of the unmonitored failure terms gives:

$$3(1 - C_1)Q^2_{S_1} = 3(1 - C_2)Q^2_{S_2} = 3(1 - C_3)Q^2_{S_3}$$

$$= \frac{3 \times 10^{-8} - Q^3_{S_1} - Q^3_{S_2} - Q^3_{S_3}}{3}$$

Solving for the confidence terms gives:

$$C_1 = \frac{Q_{S_1}^3 + Q_{S_2}^3 + Q_{S_3}^3 - 3\times10^{-8}}{9Q_{S_1}^2} + 1$$

$$C_2 = \frac{Q_{S_1}^3 + Q_{S_2}^3 + Q_{S_3}^3 - 3\times10^{-8}}{9Q_{S_2}^2} + 1$$

$$C_3 = \frac{Q_{S_1}^3 + Q_{S_2}^3 + Q_{S_3}^3 - 3\times10^{-8}}{9Q_{S_3}^2} + 1$$

The required confidence level (or probability) of isolating faults with in-line monitoring for each sensor type is thus proportional to the probability of failure of the device. The higher the failure probability, the greater the necessary confidence that these failures will be isolated with in-line monitoring.

The results of the evaluation are presented in Table 6-6. For each of the candidate control law configurations, the following data is presented: Q_{F_S}(C'S = 100%) - failure probability of function with the confidence of in-line monitor fault detection and isolation set to 100 percent; Q_{F_S} (C'S = 0) - failure probability of function with zero confidence of in-line monitor fault detection; and then the calculated required confidence factors of each sensor element to achieve the desired 3×10^{-8} failure probability. In most cases the dual-redundant sensor array does not give the desired value of reliability even if the in-line monitoring detected and isolated 100 percent of all sensor failures. The triple-redundant sensor array exceeds the requirement for a 100-percent confidence factor and usually needs an in-line monitor confidence in excess of 90 percent to achieve the 3×10^{-8} failure probability. The quad-redundant sensor array would have sufficient reliability to achieve the desired value with zero-percent failure detection and isolation of an in-line monitor.

TABLE 6-6
EFFECT OF SENSOR REDUNDANCY

CONTROL LAW	TWO SENSORS	THREE SENSORS	FOUR SENSORS
1 $(\mu, \theta, \dot{\theta}, \alpha)$			
Q_{FS} (C'S = 100%)	2.765×10^{-7}	8.018×10^{-11}	2.425×10^{-14}
Q_{FS} (C'S = 0%)			3.208×10^{-10}
C_μ		91.02%	
C_θ		97.45%	
$C_{\dot{\theta}}$		93.77%	
C_α		97.76%	
2 $(\theta, \dot{\theta})$			
Q_{FS} (C'S = 100%)	1.377×10^{-7}	3.852×10^{-11}	1.114×10^{-14}
Q_{FS} (C'S = 0%)			1.541×10^{-10}
C_θ		94.89%	
$C_{\dot{\theta}}$		87.52%	
3 $(\theta, \dot{\theta}, \alpha)$			
Q_{FS} (C'S = 100%)	2.488×10^{-7}	7.555×10^{-11}	2.348×10^{-14}
Q_{FS} (C'S = 0%)			2.702×10^{-10}
C_θ		96.59%	
$C_{\dot{\theta}}$		91.88%	
C_α		97.08%	
4 $(\mu, \theta, \dot{\theta})$			
Q_{FS} (C'S = 100%)	1.654×10^{-7}	4.315×10^{-11}	1.191×10^{-14}
Q_{FS} (C'S = 0%)			4.316×10^{-11}
C_μ		88.02%	
C_θ		96.59%	
$C_{\dot{\theta}}$		91.68%	
5 (α)			
Q_{FS} (C'S = 100%)	1.111×10^{-7}	3.704×10^{-11}	1.235×10^{-14}
Q_{FS} (C'S = 0%)			1.482×10^{-10}
C_α		91.01%	
6 (μ, α)			
Q_{FS} (C'S = 100%)	1.389×10^{-7}	4.167×10^{-11}	1.312×10^{-14}
Q_{FS} (C'S = 0%)			1.667×10^{-10}
C_μ		82.02%	
C_α		95.56%	
7 (μ)			
Q_{FS} (C'S = 100%)	2.778×10^{-8}	4.63×10^{-12}	7.716×10^{-16}
Q_{FS} (C'S = 0%)			1.852×10^{-11}
C_μ	99.999%	64.01%	
8 $(\theta, \dot{\theta}, a_x, a_n)$			
Q_{FS} (C'S = 100%)	1.515×10^{-7}	3.967×10^{-11}	1.123×10^{-14}
Q_{FS} (C'S = 0%)			1.587×10^{-10}
C_θ		97.44%	
$C_{\dot{\theta}}$		93.76%	
C_{ax}		64.05%	
C_{an}		64.05%	

CONTROL LAW	TWO SENSORS	THREE SENSORS	FOUR SENSORS
9 $(\theta, \dot{\theta}\ a_x, \alpha)$			
Q_{FS} (C'S = 100%)	2.557×10^{-7}	7.613×10^{-11}	2.353×10^{-14}
Q_{FS} (C'S = 0%)			3.046×10^{-10}
C_θ		97.45%	
$C_{\dot{\theta}}$		93.77%	
C_{ax}		64.09%	
C_α		97.76%	
10 $(\theta, \dot{\theta}, a_x, \mu)$			
Q_{FS} (C'S = 100%)	1.724×10^{-7}	4.373×10^{-11}	1.196×10^{-14}
Q_{FS} (C'S = 0%)			1.749×10^{-10}
C_θ		97.44%	
$C_{\dot{\theta}}$		93.76%	
C_{ax}		64.05%	
C_μ		91.01%	
11 $(\theta, \dot{\theta}, a_x, \dot{h})$			
Q_{FS} (C'S = 100%)	1.724×10^{-7}	4.373×10^{-11}	1.196×10^{-14}
Q_{FS} (C'S = 0%)			1.75×10^{-10}
C_θ		97.44%	
$C_{\dot{\theta}}$		93.76%	
C_{ax}		64.05%	
$C_{\dot{h}}$		91.01%	
12 $(\theta, \dot{\theta}, a_n, \dot{h})$			
Q_{FS} (C'S = 100%)	1.724×10^{-7}	4.373×10^{-11}	1.196×10^{-14}
Q_{FS} (C'S = 0%)			1.75×10^{-10}
C_θ		97.44%	
$C_{\dot{\theta}}$		93.76%	
C_{an}		64.05%	
$C_{\dot{h}}$		91.01%	
13 $(\theta, \dot{\theta}, a_n, \alpha)$			
Q_{FS} (C'S = 100%)	2.557×10^{-7}	7.613×10^{-11}	2.353×10^{-14}
Q_{FS} (C'S = 0%)			3.046×10^{-10}
C_θ		97.45%	
$C_{\dot{\theta}}$		93.77%	
C_{an}		64.09%	
C_α		97.76%	
14 $(\theta, \dot{\theta}, a_n, \mu)$			
Q_{FS} (C'S = 100%)	1.724×10^{-7}	4.373×10^{-11}	1.196×10^{-14}
Q_{FS} (C'S = 0%)			1.75×10^{-10}
C_θ		97.44%	
$C_{\dot{\theta}}$		93.76%	
C_{an}		64.05%	
C_μ		91.01%	
15 $(\theta, \dot{\theta}, \mu, \dot{h})$			
Q_{FS} (C'S = 100%)	1.932×10^{-7}	4.778×10^{-11}	1.268×10^{-14}
Q_{FS} (C'S = 0%)			1.911×10^{-10}
C_θ		97.44%	
$C_{\dot{\theta}}$		93.76%	
C_μ		91.01%	
$C_{\dot{h}}$		91.01%	

TABLE 6-6
EFFECT OF SENSOR REDUNDANCY (CONTINUED)

CONTROL LAW	TWO SENSORS	THREE SENSORS	FOUR SENSORS
16 $(\theta, \dot{\theta}, \dot{h})$			
Q_{FS} (C'S = 100%)	1.654×10^{-7}	4.315×10^{-11}	1.191×10^{-14}
Q_{FS} (C'S = 0%)			4.316×10^{-11}
C_{θ}		96.59%	
$C_{\dot{\theta}}$		91.68%	
$C_{\dot{h}}$		88.02%	
17 $(a_x, a_n, \mu, \dot{h})$			
Q_{FS} (C'S = 100%)	6.944×10^{-8}	1.042×10^{-11}	1.64×10^{-15}
Q_{FS} (C'S = 0%)			1.042×10^{-11}
C_{ax}		64.01%	
C_{an}		64.01%	
C_{μ}		91%	
$C_{\dot{h}}$		91%	
18 $(a_x, a_n, \dot{h})$			
Q_{FS} (C'S = 100%)	4.167×10^{-8}	5.787×10^{-12}	8.681×10^{-16}
Q_{FS} (C'S = 0%)			2.315×10^{-11}
C_{ax}		52.01%	
C_{an}		52.01%	
$C_{\dot{h}}$		88%	
19 $(\mu, \dot{h})$			
Q_{FS} (C'S = 100%)	5.556×10^{-8}	9.26×10^{-12}	1.543×10^{-15}
Q_{FS} (C'S = 0%)			3.704×10^{-11}
C_{μ}		82%	
$C_{\dot{h}}$		82%	
20 $(\dot{h})$			
Q_{FS} ($C_{\dot{h}}$ = 100%)	2.778×10^{-8}	4.63×10^{-12}	7.716×10^{-16}
Q_{FS} ($C_{\dot{h}}$ = 0%)			1.852×10^{-11}
$C_{\dot{h}}$	99.999%	64.01%	
21 (a_x, a_n, μ)			
Q_{FS} (C'S = 100%)	4.167×10^{-8}	5.787×10^{-12}	8.681×10^{-16}
Q_{FS} (C'S = 0%)			2.315×10^{-11}
C_{ax}		52.01%	
C_{an}		52.01%	
C_{μ}		88%	

CONTROL LAW	TWO SENSORS	THREE SENSORS	FOUR SENSORS
22 (a_x, a_n, μ, α)			
Q_{FS} (C'S = 100%)	1.528×10^{-7}	4.282×10^{-11}	1.321×10^{-14}
Q_{FS} (C'S = 0%)			1.713×10^{-10}
C_{ax}		64.05%	
C_{an}		64.05%	
C_{μ}		91.01%	
C_{α}		97.75%	
23 (a_x, a_n, α)			
Q_{FS} (C'S = 100%)	1.25×10^{-7}	3.819×10^{-11}	1.244×10^{-14}
Q_{FS} (C'S = 0%)			1.528×10^{-10}
C_{ax}		52.06%	
C_{an}		52.06%	
C_{α}		97%	
24 (a_x, a_n)			
Q_{FS} (C'S = 100%)	1.389×10^{-8}	1.157×10^{-12}	9.645×10^{-17}
Q_{FS} (C'S = 0%)			4.63×10^{-12}
C_{ax}	99.99%	71.99%	
C_{an}	99.99%	71.99%	
25 (a_x)			
Q_{FS} (C_{ax} = 100%)	6.944×10^{-9}	5.787×10^{-13}	4.823×10^{-17}
Q_{FS} (C_{ax} = 0%)		2.083×10^{-8}	2.315×10^{-12}
C_{ax}	99.986%		
26 (a_n)			
Q_{FS} (C_{an} = 100%)	6.944×10^{-9}	5.787×10^{-13}	4.823×10^{-17}
Q_{FS} (C_{an} = 0%)		2.083×10^{-8}	2.315×10^{-12}
C_{an}	99.986%		
27 $(\mu, \dot{\theta})$			
Q_{FS} (C'S = 100%)	6.778×10^{-8}	1.263×10^{-11}	2.372×10^{-15}
Q_{FS} (C'S = 0%)			5.052×10^{-11}
C_{μ}		82.01%	
C_{θ}		87.51%	
28 $(\alpha, \dot{\theta})$			
Q_{FS} (C'S = 100%)	1.511×10^{-7}	4.504×10^{-11}	1.395×10^{-14}
Q_{FS} (C'S = 0%)			1.667×10^{-10}
C_{α}		95.51%	
C_{θ}		87.52%	

6.2.1.2 Alternate Sensor Configuration Flexibility. — The large number of acceptable control laws identified and verified using different sensor combinations provide considerable flexibility in reconfiguring the control law as a result of sensor failures. A reconfigured control law has a sensor combination that is a subset of the original (maximum) sensor array. Figure 6-38 shows the control law flexibility with sensor failures that allow reconfiguration to other available sensor sources. This type of control law reversionary scheme results in increased augmentation system availability without requiring addi-

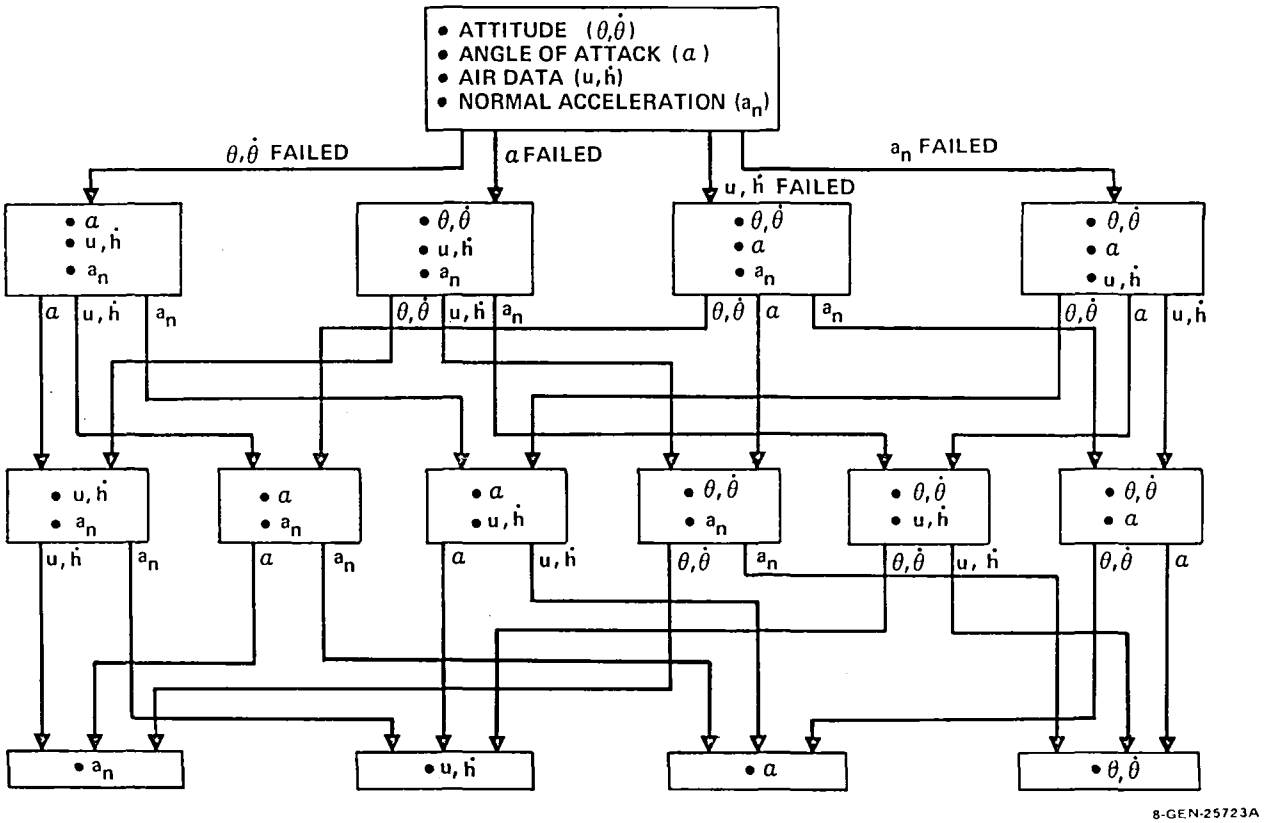

FIGURE 6-38. CONTROL LAW FLEXIBILITY

tional sensor hardware redundancy. The strategy followed is to operate with the control law having the highest-level sensor array (most unique parameters), thereby keeping all signals in the active computation rather than in a standby mode. If a sensor fails, the system is reconfigured, using the control law with the next highest sensor array.

6.2.2 Computer Architectures. — The computer architecture analysis considers a system which performs only the RSSAS function and a system which also performs the other augmentation functions described in Paragraph 6.1.5. The analysis evaluates and compares the reliabilities of each system.

In a digital computer, a large part of the total failure rate is independent of the functions performed. The processor, A/D converter, I/O control, and general purpose routines in memory are required regardless of the number of functions. Thus, memory growth as functions are added is minimal. The computer memory distribution is estimated for this study as:

Basic System	60 percent
Static Stability Augmentation	15 percent
Yaw Damper/Turn Coordination	10 percent
ELF/FL	6 percent
Stall Warning	9 percent

Figure 6-39 shows the computing subsystem elements. The basic system elements and their failure rates are given below. These element failure rates are independent of functions performed.

Basic System		$\lambda x10^{-6}$
Processor and Memory	=	28.4
Bus Interface and Control	=	21.3
Power Supply	=	8.3
A/D Converter and Control and MUX	=	25.4
I/O Discrete and Output Control	=	12.7
Total		95.9

The failure rate (in hours) for each function has then been determined assuming that static stability augmentation is first provided. Table 6-7 shows assignment of memory failure rate to the required analog and discrete inputs and outputs for each function. The total is $340.9x10^{-6}$ failures per hour including the basic system.

If the augmentation functions were to be provided by a separate digital computer, the basic core elements, as well as several data interfaces, must be added to each function as shown in Table 6-8. When these are added together, the total system failure rate is significantly higher as shown below:

Stability Augmentation	238.5
Yaw Damper	198.7
EFL/FL	192.9
Stall Warning	130.9
Total four independent units	$761x10^{-6}$ failures per hour

For subsequent calculations, the following FAC failure rates are used:

FAC with RSSAS only	250×10^{-6} failures per hour
FAC with all augmentation functions	340×10^{-6} failures per hour

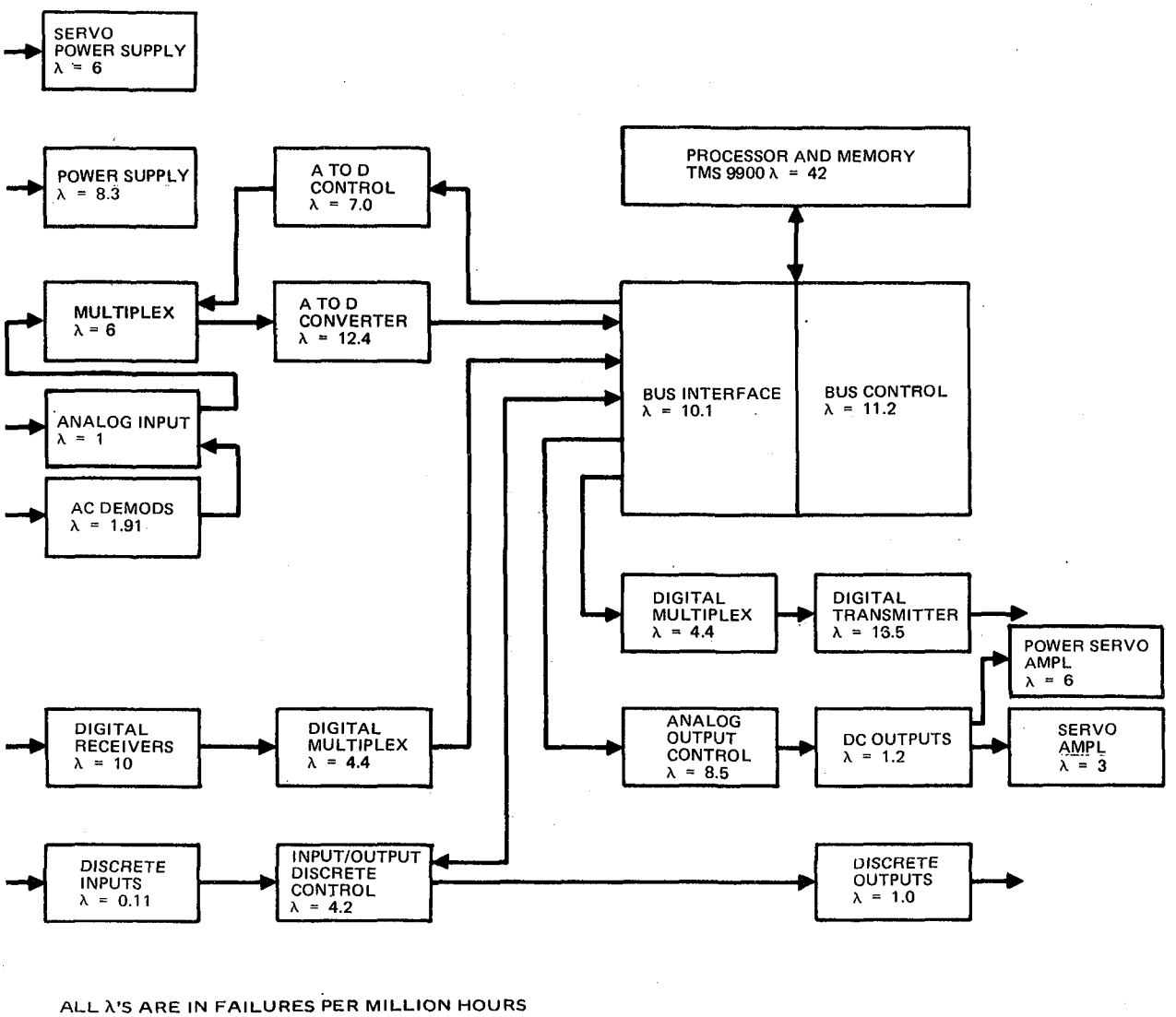

FIGURE 6-39. COMPUTER SUBSYSTEM ELEMENTS AND FAILURE RATES

TABLE 6-7
INTEGRATED FUNCTION RELIABILITY SUMMARY

	COMPONENT VALUE $\lambda \times 10^{-6}$ (EACH)	STABILITY AUGMENTATION		YAW DAMPER		ELF/FL		STALL WARNING	
		(NO.)	$\lambda \times 10^{-6}$	(NO.)	$\lambda \times 10^{-6}$	(NO)	$\lambda \times 10^{-6}$	(NO.)	$\lambda \times 10^{-6}$
MEMORY		(0.15)	5.1	(0.10)	3.4	(0.06)	2	(0.09)	3.1
SERVO AMPLIFIER	3.0	(2)	6	(2)	6				
AC INPUT	2.91	(13)	37.8	(6)	17.5	(6)	17.5	(1)	2.9
DC INPUT	1.0	(5)	5	(2)	2				
DISCRETE INPUT	0.11	(4)	0.5	(8)	0.9			(5)	0.6
DISCRETE OUTPUT	1.0	(10)	10	(17)	17	(4)	4	(8)	8
DC OUTPUT	1.2	(2)	2.4						
TRANSMITTER AND MULTIPLEXER	16.5	(1)	20.9*						
RECEIVER AND MULTIPLEXER	10.0	(5)	54.4*						
POWER SERVO AMPLIFIER PLUS POWER SUPPLY	6.0					(2)	18**		
TOTAL			142.1		46.8		41.5		14.6

*CONSTANT $\lambda \times 10^{-6}$ OF 4.4 ADDED TO THESE SUBSYSTEMS.
**CONSTANT $\lambda \times 10^{-6}$ OF 6.0 ADDED TO THIS SUBSYSTEM.

TABLE 6-8

INDIVIDUAL FUNCTION RELIABILITY SUMMARY

	COMPONENT VALUE $\lambda \times 10^{-6}$ (EACH)	STABILITY AUGMENTATION		YAW DAMPER		ELF/FL		STALL WARNING	
		(NO.)	$\lambda \times 10^{-6}$	(NO.)	$\lambda \times 10^{-6}$	(NO.)	$\lambda \times 10^{-6}$	(NO.)	$\lambda \times 10^{-6}$
BASIC CORE			95.9		95.9		95.9		95.9
MEMORY			5.6		3.7		2.2		3.3
SERVO AMPLIFIER	3.0	(2)	6	(2)	6				
AC INPUT	2.91	(13)	37.8	(6)	17.5	(6)	17.5	(3)	8.7
DC INPUT	1.0	(5)	5	(2)	2				
DISCRETE INPUT	0.11	(4)	0.5	(12)	1.3			(5)	0.6
DISCRETE OUTPUT	1.0	(10)	10	(17)	17	(4)	4	(8)	8
DC OUTPUT	1.2	(2)	2.4						
TRANSMITTER AND MULTIPLEXER	16.5	(1)	20.9*	(1)	20.9*	(1)	20.9*		
RECEIVER AND MULTIPLEXER	10.0	(5)	54.4*	(3)	34.4*	(3)	34.4*	(1)	14.4*
POWER SERVO AMPLIFIER PLUS POWER SUPPLY	6.0					(2)	18**		
TOTAL			238.5		198.7		192.9		130.9

*CONSTANT $\lambda \times 10^{-6}$ OF 4.4 ADDED TO THESE SUBSYSTEMS.
**CONSTANT $\lambda \times 10^{-6}$ OF 6.0 ADDED TO THIS SUBSYSTEM.

6.2.3 Sensor Computation Architectures. — Several alternative methods of transmitting data from the fixed DC-10-type sensor set to the computational elements have been considered. Shown in Figure 6-40, they include: (1) direct single sensor to corresponding computer signal conditioning data processor (SCDP); (2) data crossfed from each sensor to all computer SCDPs and between all computers; (3) data crossfed from each sensor to all computer SCDPs; and, (4) data crossfed between all computers.

Each of these methods was in turn coupled with triple- and dual-redundant computer configurations to form the architectures shown in Figures 6-41 to 6-43. All computers are assumed to be internally fully monitored either by in-line self-testing (triple computer configurations in Figure 6-41 and dual computer configuration in Figure 6-42), or by comparison of dual hardware channels (dual computer configuration in Figure 6-43). For the triple computer configurations in Figure 6-41, a direct dedicated sensor connection to each SCDP (Figure 6-40, configuration 1) is not possible since several of the sensor types (α, A_n, u, $\dot{h}$) are of a dual level of redundancy while the computers are triple-redundant. The sensors must therefore interface with more than single SCDP as in configurations 2 and 3 or the data must be crossfed between CPU's, as in configurations 2 and 4.

A reliability evaluation has been made of these candidate architectures using the DC-10 sensor failure rates previously listed in Paragraph 6.2.1.1 and the following representative computer reliability values, based on the previous computer discussion:

Computer MTBF

- Single-Channel Full In-Line Monitor — 4000 hours
- Dual-Channel Comparison-Monitor — 3200 hours

The corresponding internal function failure rates used are:

- SCDP (both type computers) — 62.5×10^{-6} failures/hour
- Remaining Electronics
  - Single-Channel Type — 187.5×10^{-6}
  - Dual-Channel Type — 125×10^{-6}/channel

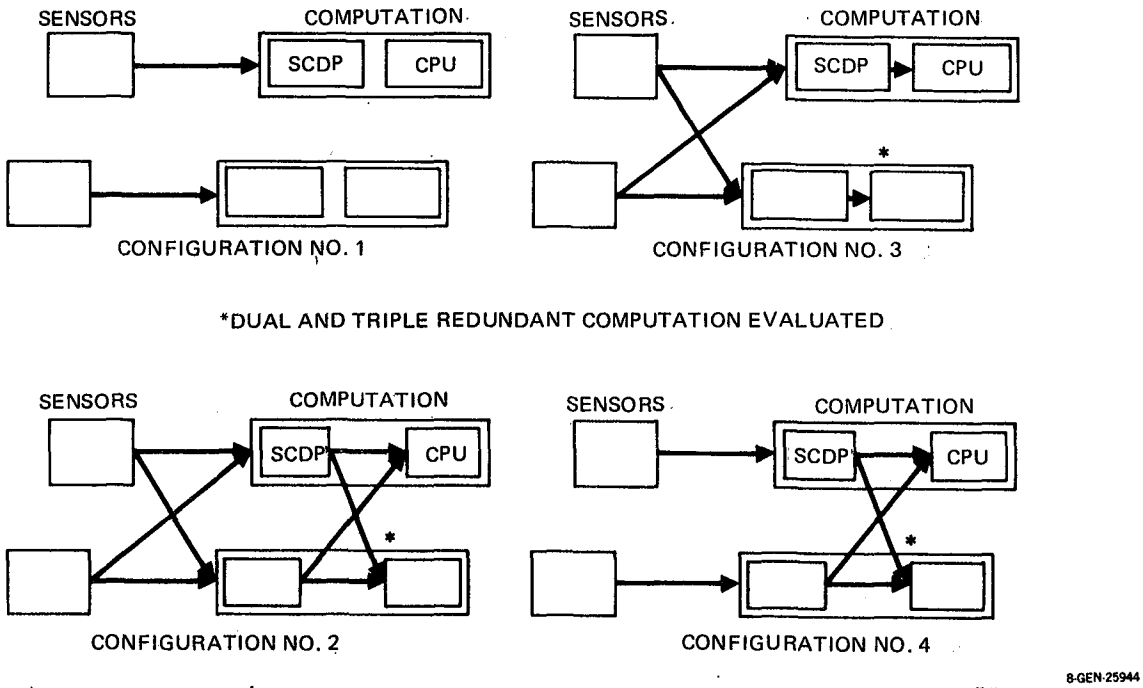

FIGURE 6-40. SENSOR/COMPUTATION INTERFACE – ARCHITECTURE FORMULATION

The results of the reliability calculations for each combination of computer, data transmission, and control law are summarized in Table 6-9. The probability of function loss calculated for each sensor combination assumes that all sensor subset combinations are also available and can provide satisfactory performance. As an example, the $\theta\dot{\theta}\alpha u$ control law failure probability includes the $\theta\dot{\theta}$, α, u, $\theta\dot{\theta}\alpha$, $\theta\dot{\theta}u$, and αu control laws and requires that all of these fail for loss of function. The allocated probability of failure for this portion of the system is 3×10^{-8}; therefore, all sensor combinations which do not exceed this probability limit describe a successful family of control laws. The combinations which do not satisfy the criteria are shown shaded in Table 6-9. (Note that the No. 1 method of data transmission was determined to exceed the probability limit and was not calculated for all combinations.) This table also shows the predominant contributor(s) to the failure probability, which can be the sensors (S), the computer SCDP (SC), the remaining computer function (CP), or the total computer (C). Probabilities are for one hour.

These data indicate that either triple- or dual-redundant computers, and several sensor families, can satisfy the reliability criteria. The sensor data must, however, be crossfed between the sensors and the computer. Use of the computer crosstalk data bus to crossfeed sensor cannot in itself satisfy the sensor data transmission requirements, but can be used to improve the data availability.

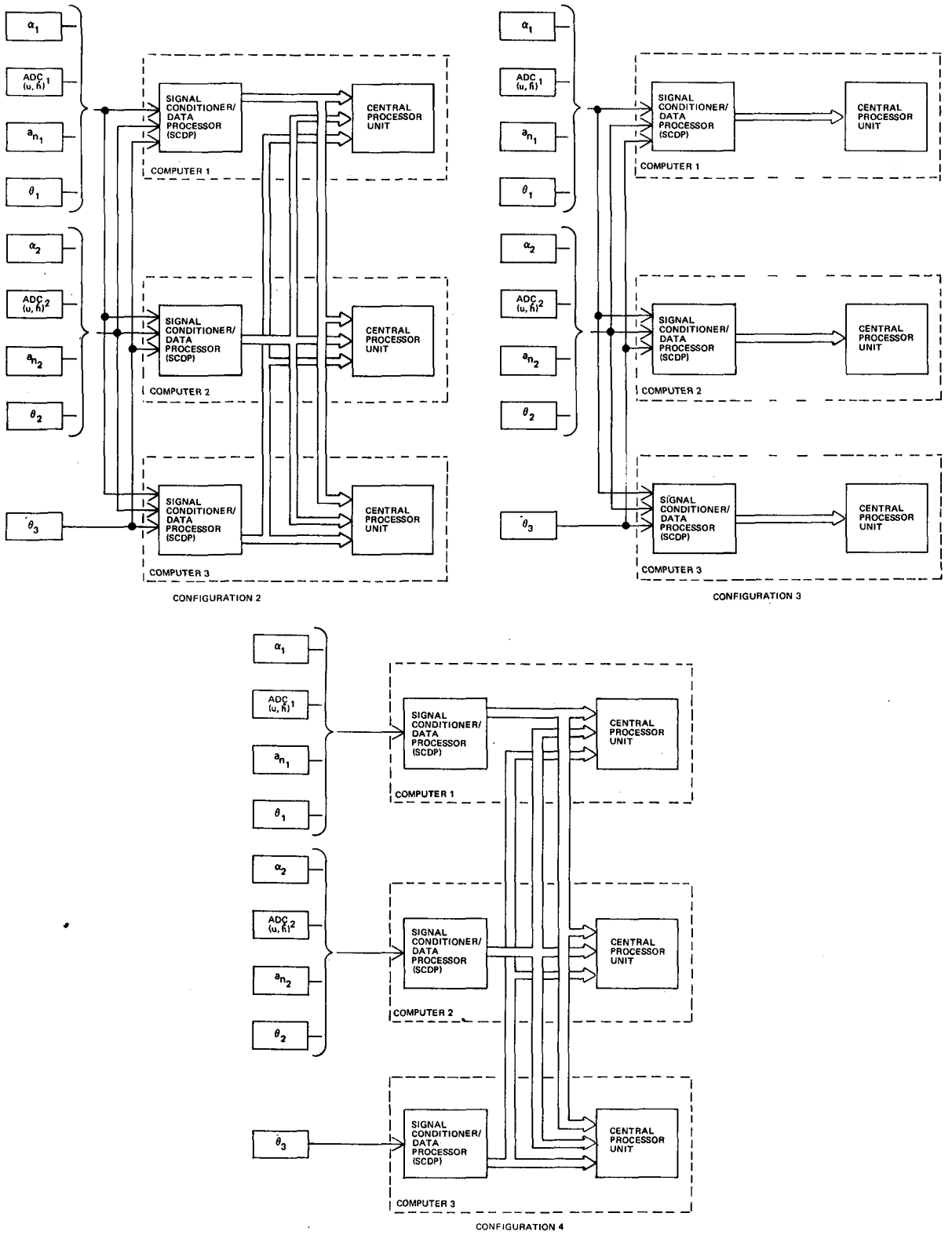

FIGURE 6-41. TRIPLE COMPUTER CONFIGURATION

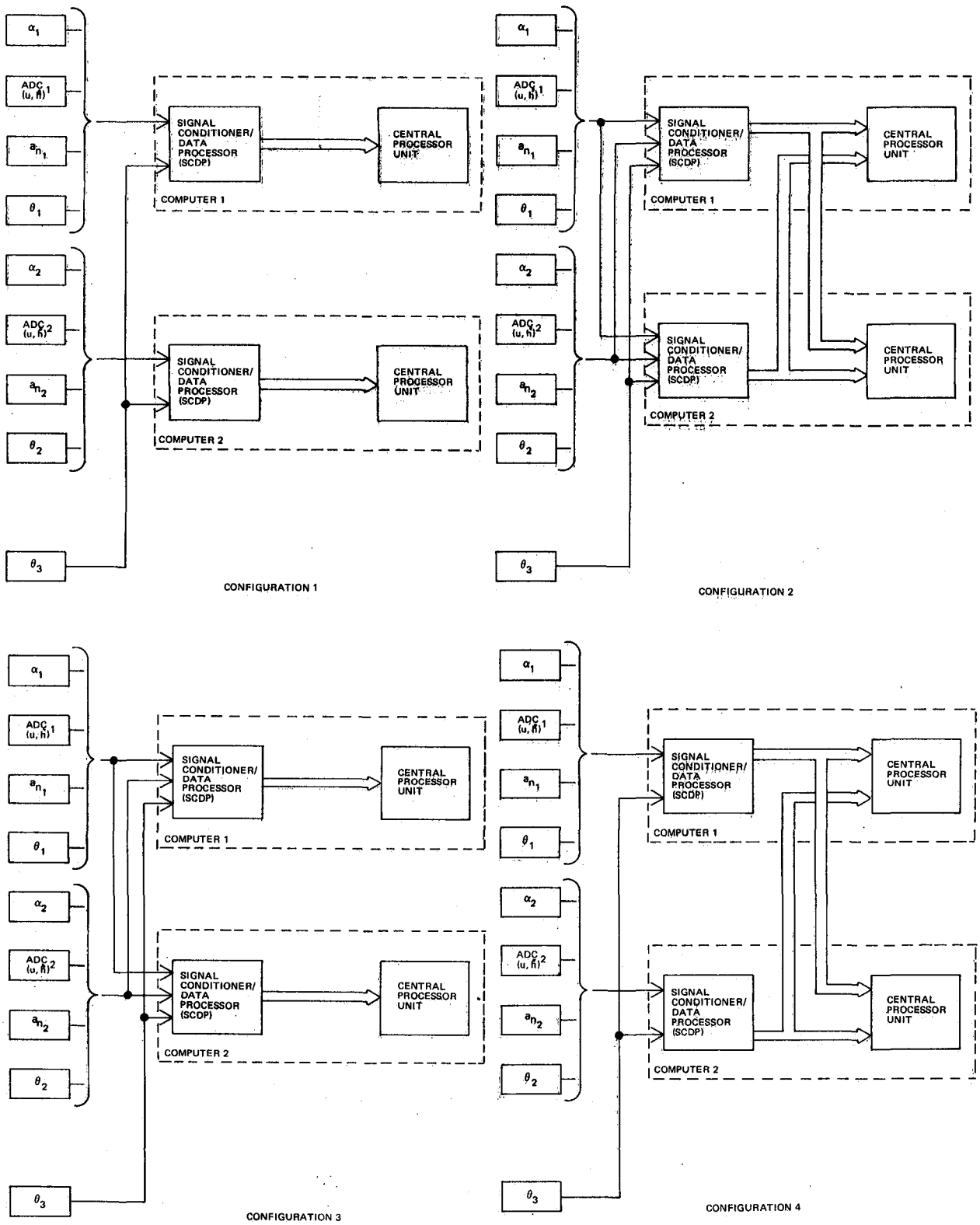

FIGURE 6-42. DUAL COMPUTER CONFIGURATION – SINGLE PROCESSOR

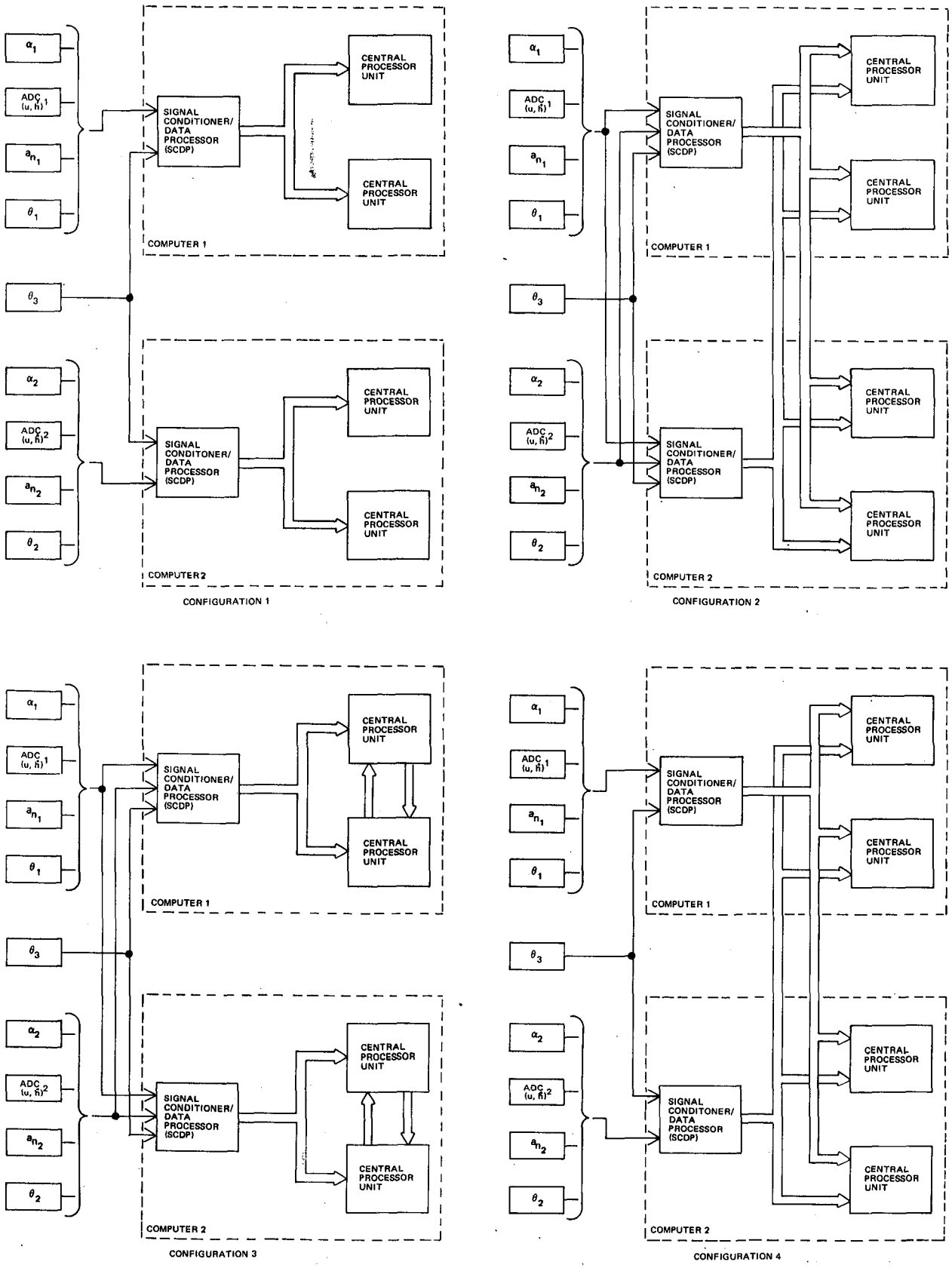

FIGURE 6-43. DUAL COMPUTER CONFIGURATION

TABLE 6-9
SENSOR/COMPUTATION INTERFACE – RELIABILITY ASSESSMENT

CONFIGURATIONS

CONTROL LAWS	TRIPLE 2	TRIPLE 3	TRIPLE 4	DUAL 1	DUAL 2	DUAL 3	DUAL 4	DUAL - DUAL 1	DUAL - DUAL 2	DUAL - DUAL 3	DUAL - DUAL 4
$u\ \alpha\ \dot{\theta}\ \theta$	7×10^{-12} CP	2×10^{-11} C	1×10^{-7} S SC		4×10^{-8} CP	6×10^{-8} C	2×10^{-7} S SC		4×10^{-9} SC	1×10^{-7} C	1×10^{-7} S SC
$\dot{\theta}\ \theta\ a_n\ \dot{h}$	7×10^{-12} CP	2×10^{-11} C	1×10^{-7} S SC		4×10^{-8} CP	6×10^{-8} C	2×10^{-7} S SC		4×10^{-9} SC	1×10^{-7} C	1×10^{-7} S SC
$\theta\ \dot{\theta}\ a_n\ \alpha$	7×10^{-12} CP	2×10^{-11} C	1×10^{-7} S SC		4×10^{-8} CP	6×10^{-8} C	2×10^{-7} S SC		4×10^{-9} SC	1×10^{-7} C	1×10^{-7} S SC
$\dot{\theta}\ \theta\ a_n\ u$	7×10^{-12} CP	2×10^{-11} C	1×10^{-7} S SC		4×10^{-8} CP	6×10^{-8} C	2×10^{-7} S SC		4×10^{-9} SC	1×10^{-7} C	1×10^{-7} S SC
$\dot{\theta}\ \theta\ \dot{h}\ u$	3×10^{-10} S	3×10^{-10} S	1×10^{-7} S SC		4×10^{-8} CP	6×10^{-8} C	2×10^{-7} S SC		4×10^{-9} SC	1×10^{-7} C	1×10^{-7} S SC
$\alpha\ \dot{\theta}\ \theta$	5×10^{-10} S	5×10^{-10} S	1×10^{-7} S SC		4×10^{-8} CP	6×10^{-8} C	2×10^{-7} S SC		4×10^{-9} SC	1×10^{-7} C	1×10^{-7} S SC
$u\ \dot{\theta}\ \theta$	3×10^{-10} S	3×10^{-10} S	1×10^{-7} S SC		4×10^{-8} CP	6×10^{-8} C	2×10^{-7} S SC		4×10^{-9} SC	1×10^{-8} C	1×10^{-7} S SC
$\dot{\theta}\ \theta\ \dot{h}$	3×10^{-10} S	3×10^{-10} S	1×10^{-7} S SC		4×10^{-8} CP	6×10^{-8} C	2×10^{-7} S SC		4×10^{-9} SC	1×10^{-7} C	1×10^{-7} S SC
$\theta\ \theta\ a_n$	7×10^{-12} S	2×10^{-11} S	1×10^{-7} S SC		4×10^{-8} CP	6×10^{-8} C	2×10^{-7} S SC		4×10^{-9} SC	1×10^{-7} C	1×10^{-7} S SC
$\theta\ \theta$	7×10^{-7} S	7×10^{-7} S	7×10^{-7} S		8×10^{-7} S	8×10^{-7} S	9×10^{-7} S SC		8×10^{-7} S	8×10^{-7} S	9×10^{-7} S SC
$u\ \alpha$	2×10^{-7} S	2×10^{-7} S	1×10^{-7} SC		3×10^{-7} S	3×10^{-7} S	1×10^{-4} SC		2×10^{-7} S	3×10^{-7} S	1×10^{-4} SC
$\dot{h}\ u$	3×10^{-4} S	3×10^{-4} S	5×10^{-4} S		3×10^{-4} S	3×10^{-4} S	5×10^{-4} S SC		3×10^{-4} S	3×10^{-4} S	5×10^{-4} S SC
$u\ \dot{\theta}$	3×10^{-10} S	3×10^{-10} S	1×10^{-7} S SC		4×10^{-8} CP	6×10^{-8} C	2×10^{-7} S SC		4×10^{-9} SC	1×10^{-7} C	1×10^{-7} S SC
$a_n\ u$	9×10^{-12} S	2×10^{-11} S	1×10^{-4} SC		4×10^{-8} S CP	6×10^{-8} S C	1×10^{-4} SC		4×10^{-9} S	1×10^{-7} S C	1×10^{-4} SC
$a_n\ \dot{h}$	9×10^{-12} S	2×10^{-11} S	1×10^{-4} SC		4×10^{-8} S CP	6×10^{-8} S C	1×10^{-4} SC		4×10^{-8} S	1×10^{-7} S C	1×10^{-4} SC
$a_n\ \alpha$	1×10^{-11} S	2×10^{-11} S	1×10^{-4} SC		4×10^{-8} S	6×10^{-8} S	1×10^{-4} SC		4×10^{-9} S	1×10^{-7} S C	1×10^{-4} SC
α	7×10^{-4} S	7×10^{-4} S	8×10^{-4} S SC		7×10^{-4} S	7×10^{-4} S	8×10^{-4} S SC		7×10^{-4} S	7×10^{-4} S	8×10^{-4} S SC
u	3×10^{-4} S	3×10^{-4} S	5×10^{-4} S SC		3×10^{-4} S	3×10^{-4} S	5×10^{-4} S SC		3×10^{-4} S	3×10^{-4} S	5×10^{-4} S SC
$\dot{h}$	3×10^{-4} S	3×10^{-4} S	5×10^{-4} S SC		3×10^{-4} S	3×10^{-4} S	5×10^{-4} S SC		3×10^{-4} S	3×10^{-4} S	5×10^{-4} S SC
a_n	7×10^{-9} S	7×10^{-9} S	2×10^{-4} S SC		4×10^{-8} S	7×10^{-8} S	1×10^{-4} S SC		1×10^{-8} S	1×10^{-7} S	2×10^{-4} S SC

✱DOES NOT MEET SUCCESS CRITERIA

PREDOMINANT CONTRIBUTORS TO FAILURE RATES

(CP) CPU (S) SENSOR (SC) SCDP (C) SCDP + CPU

8 GEN 2588

RELIABILITY GOAL: 3×10^{-8} FAILURE PROBABILITY FOR ONE HOUR

6.2.4 Computer/Actuation and Total System Architecture. — The computer-actuator configurations shown in Figures 6-44, 6-45, and 6-46 have been suggested as the architectures to interface with the sensor arrays concluded as successful in Paragraph 6.2.3. These configurations are based on dual- and triple-redundant computers interfacing with the DC-10-type split surface arrangement, using either two or four of the elevator segments (at least one surface on each side of the vertical tail). In addition, several of the configurations use dual series input actuators, allowing multiple computer control of a single elevator surface. The appropriate hydraulic system inputs to the series actuators have also been considered. The failure rates used for the actuation system are actuator = 0.02×10^{-3} and hydraulics = 0.09×10^{-3} failures per hour.

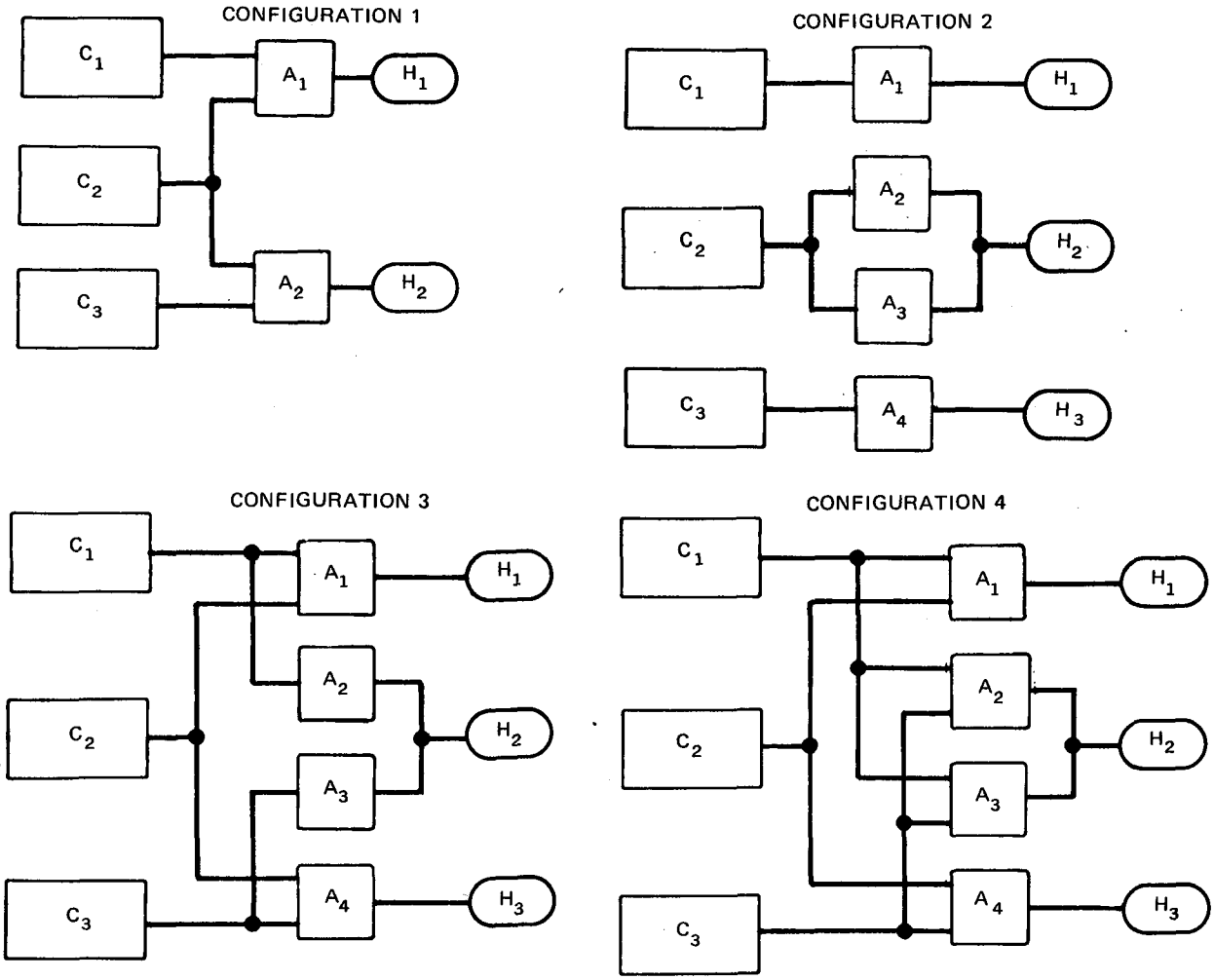

C — RSSAS FAC
A — SERIES ELEVATOR ACTUATOR
H — HYDRAULIC SYSTEM

FIGURE 6-44. TRIPLE-REDUNDANT COMPUTER/ACTUATOR CONFIGURATIONS

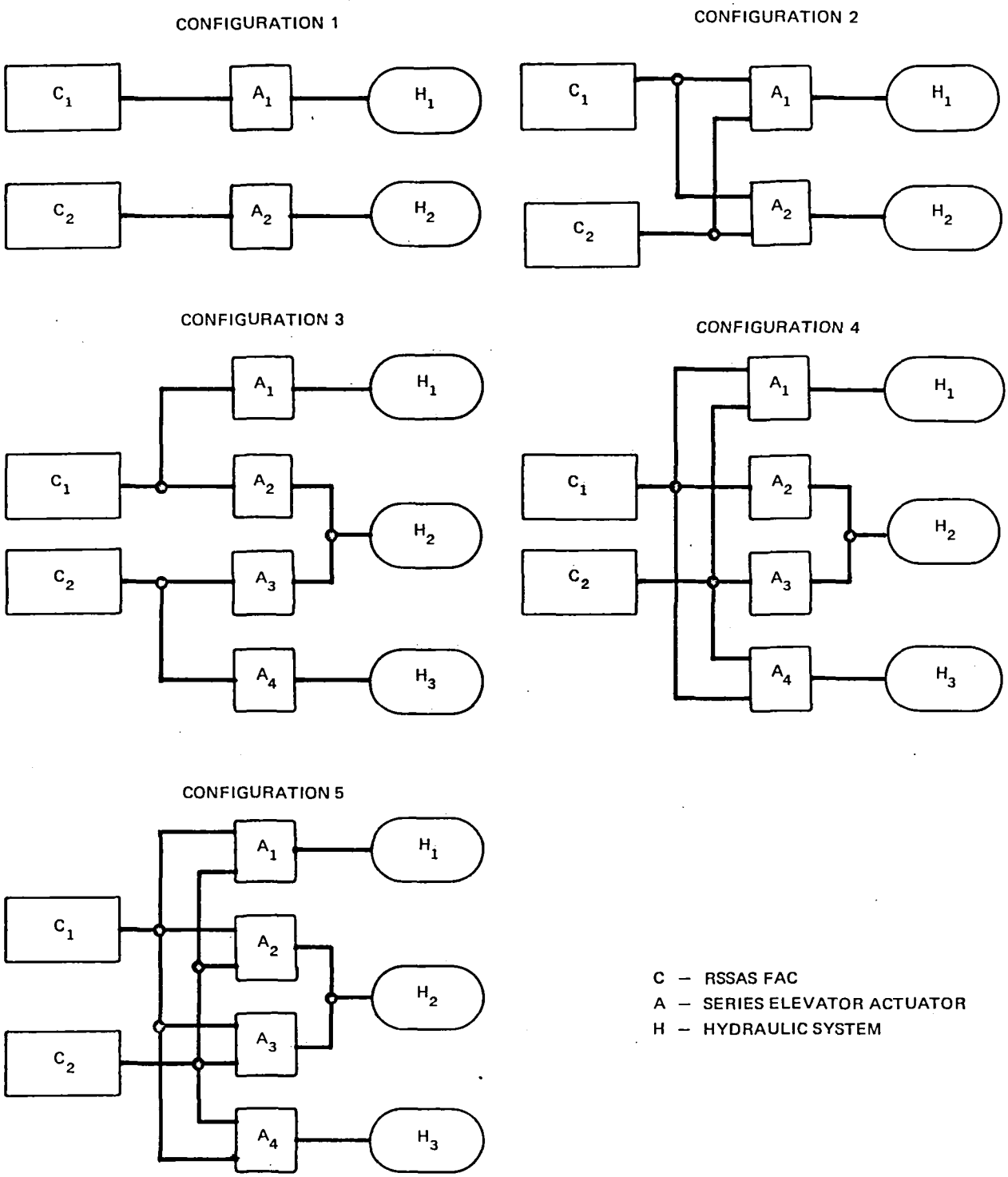

FIGURE 6-45. DUAL-REDUNDANT COMPUTER/ACTUATOR CONFIGURATIONS

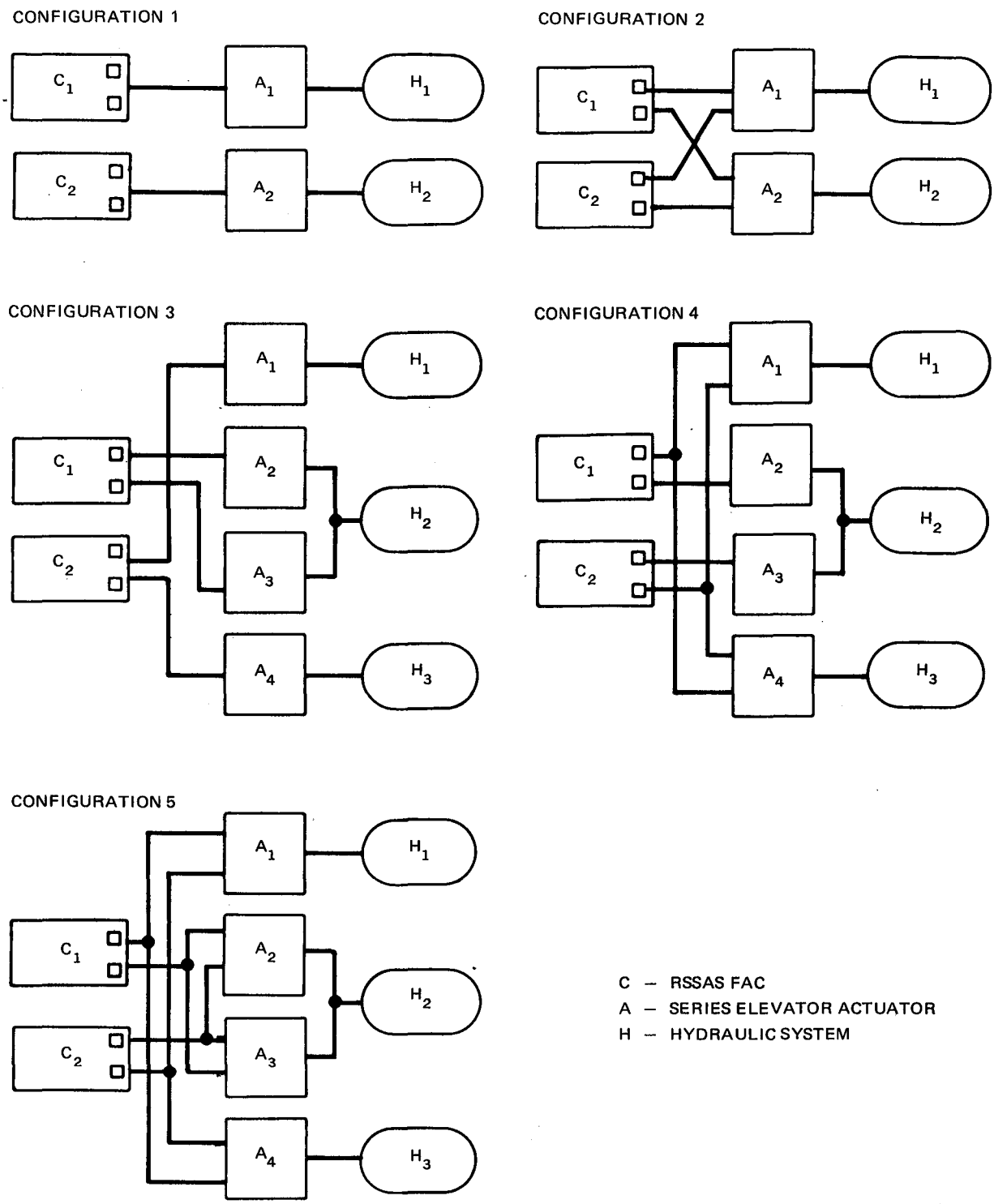

FIGURE 6-46. DUAL-DUAL COMPUTER/ACTUATOR CONFIGURATIONS

Table 6-10 is a summary of reliability calculations for the combined sensor, computer, and actuation architectures. For each combination of computer/sensor and computer/actuator configuration, a probability of loss-of-function is provided for each successful sensor array. Also provided is an indication of the predominant contributor to the failure which can be the sensors (S), the computers SCDP (SC), the total computer (C), the actuator (A), or the hydraulics (H).

From the data presented in Table 6-10, it is concluded that all configurations except Dual No. 1 computer/actuator satisfy the allotted probability of function loss of approximately 7×10^{-8} for one hour.

6.2.5 Candidate System Selection. — Several considerations enter into the final selection of the system architecture. It has previously been established that all sensor data must be crossfed to all computers. In addition, it is recognized that all computers must talk with each other with regard to control law selection, failure reversion, and probably even trim and normal augmentation control. Since an intersystem communication link is required, it should be used additionally to crossfeed sensor data. Also, while the system must satisfy the reliability design requirements, too much redundancy or complexity of interfaces is usually costly in terms of higher system purchase price and/or lower total system maintenance MTBF, which is reflected in higher maintenance costs. With these two considerations in mind, Figure 6-47 shows several sensor arrays combined with triple- and dual-redundant architectures as a function of their reliability potential. The legend in Figure 6-47 defines the level of computer redundancy, computer/actuation configuration, and sensor/computation interface. As an example, Triple 1.2 indicates triple-redundant computer/actuation configuration 1 (Figure 6-44) combined with sensor/computation configuration 2 (Figure 6-41).

As previously discussed, several other augmentation functions are candidates for integration into the FAC. This would result in lower computer MTBF and would effectively move all of the configurations shown in Figure 6-47

TABLE 6-10
SENSOR/COMPUTER/ACTUATOR RELIABILITY SUMMARY – TRIPLE-REDUNDANT COMPUTERS

COMPUTER/ ACTUATOR INTERFACE CONFIGURATIONS	COMPUTER/SENSOR INTERFACE CONFIGURATIONS													
	TRIPLEX CONFIGURATION 2													
	NO. 1 $\mu, \alpha, \dot{\theta}, \theta$	NO. 12 $\dot{\theta}, \theta, A_{N,h}$	NO. 13 $\dot{\theta}, \theta, A_N, \alpha$	NO. 14 $\dot{\theta}, \theta, A_N, \mu$	NO. 15 $\dot{\theta}, \theta, \dot{h}, \mu$	NO. 3 $\alpha, \dot{\theta}, \theta$	NO. 4 $\mu, \dot{\theta}, \theta$	NO. 16 $\dot{\theta}, \theta, \dot{h}$	NO. 29 $\dot{\theta}, \theta, A_N$	NO. 27 μ, θ	NO. 30 A_N, μ	NO. 31 $A_N, \dot{h}$	NO. 32 A_N, α	NO. 26 A_N
TRIPLE 1	1.2(A)(H) $\times 10^{-8}$	1.2(A)(H) $\times 10^{-8}$	1.2(A)(H) $\times 10^{-8}$	1.2(A)(H) $\times 10^{-8}$	1.2(A)(H) $\times 10^{-8}$	1.2(A)(H) $\times 10^{-8}$	1.2(A)(H) $\times 10^{-8}$	1.2(A)(H) $\times 10^{-8}$	1.2(A)(H) $\times 10^{-8}$	1.2(A)(H) $\times 10^{-8}$	1.2(A)(H) $\times 10^{-8}$	1.2(A)(H) $\times 10^{-8}$	1.2(A)(H) $\times 10^{-8}$	1.9(S)(A)(H) $\times 10^{-8}$
TRIPLE 2	1.9(C)(A)(H) $\times 10^{-11}$	1.9(C)(A)(H) $\times 10^{-11}$	1.9(C)(A)(H) $\times 10^{-11}$	1.9(C)(A)(H) $\times 10^{-11}$	2.7(S) $\times 10^{-10}$	5.1(S) $\times 10^{-10}$	2.7(S) $\times 10^{-10}$	2.7(S) $\times 10^{-10}$	1.9(C)(A)(H) $\times 10^{-11}$	2.7(S) $\times 10^{-10}$	2.1(S)(C)(A)(H) $\times 10^{-11}$	2.1(S)(C)(A)(H) $\times 10^{-11}$	2.4(S)(C)(A)(H) $\times 10^{-11}$	7.0(S) $\times 10^{-9}$
TRIPLE 3	8.1(CP)(A)(H) $\times 10^{-12}$	8.0(CP)(A)(H) $\times 10^{-12}$	8.0(CP)(A)(H) $\times 10^{-12}$	8.0(CP)(A)(H) $\times 10^{-12}$	2.5(S) $\times 10^{-10}$	5.1(S) $\times 10^{-10}$	2.5(S) $\times 10^{-10}$	2.5(S) $\times 10^{-10}$	7.9(CP) $\times 10^{-12}$	2.5(S) $\times 10^{-10}$	1.0(S)(CP) $\times 10^{-11}$	1.0(S)(CP) $\times 10^{-11}$	1.2(S)(CP) $\times 10^{-11}$	7.0(S) $\times 10^{-9}$
TRIPLE 4	8.1(CP)(A)(H) $\times 10^{-12}$	8.0(CP)(A)(H) $\times 10^{-12}$	8.0(CP)(A)(H) $\times 10^{-12}$	8.0(CP)(A)(H) $\times 10^{-12}$	2.5(S) $\times 10^{-10}$	5.1(S) $\times 10^{-10}$	2.5(S) $\times 10^{-10}$	2.5(S) $\times 10^{-10}$	7.9(CP) $\times 10^{-12}$	2.5(S) $\times 10^{-10}$	1.0(S)(CP) $\times 10^{-11}$	1.0(S)(CP) $\times 10^{-11}$	1.2(S)(CP) $\times 10^{-11}$	7.0(S) $\times 20^{-9}$
	TRIPLEX CONFIGURATION 3													
TRIPLE 1	1.2(A)(H) $\times 10^{-8}$	1.2(A)(H) $\times 10^{-8}$	1.2(A)(H) $\times 10^{-8}$	1.2(A)(H) $\times 10^{-8}$	1.2(A)(H) $\times 10^{-8}$	1.2(A)(H) $\times 10^{-8}$	1.2(A)(H) $\times 10^{-8}$	1.2(A)(H) $\times 10^{-8}$	1.2(A)(H) $\times 10^{-8}$	1.2(A)(H) $\times 10^{-8}$	1.2(A)(H) $\times 10^{-8}$	1.2(A)(H) $\times 10^{-8}$	1.2(A)(H) $\times 10^{-8}$	1.9(S)(A)(H) $\times 10^{-8}$
TRIPLE 2	2.8(C)(A)(H) $\times 10^{-11}$	2.8(C)(A)(H) $\times 10^{-11}$	2.8(C)(A)(H) $\times 10^{-11}$	2.8(C)(A)(H) $\times 10^{-11}$	2.7(S) $\times 10^{-10}$	5.2(S) $\times 10^{-10}$	2.7(S) $\times 10^{-10}$	2.7(S) $\times 10^{-10}$	2.8(C)(A)(H) $\times 10^{-11}$	2.7(S) $\times 10^{-10}$	2.8(C)(A)(H) $\times 10^{-11}$	2.8(C)(A)(H) $\times 10^{-11}$	3.2(C)(A)(H) $\times 10^{-11}$	7.0(S) $\times 10^{-9}$
TRIPLE 3	1.7(C) $\times 10^{-11}$	1.7(C) $\times 10^{-11}$	1.7(C) $\times 10^{-11}$	1.7(C) $\times 10^{-11}$	2.6(S) $\times 10^{-10}$	5.1(S) $\times 10^{-10}$	2.6(S) $\times 10^{-10}$	2.6(S) $\times 10^{-10}$	1.7(C) $\times 10^{-11}$	2.6(S) $\times 10^{-10}$	1.7(C) $\times 10^{-11}$	1.7(C) $\times 10^{-11}$	2.1(C) $\times 10^{-11}$	7.0(S) $\times 10^{-9}$
TRIPLE 4	1.7(C) $\times 10^{-11}$	1.7(C) $\times 10^{-11}$	1.7(C) $\times 10^{-11}$	1.7(C) $\times 10^{-11}$	2.6(S) $\times 10^{-10}$	5.1(S) $\times 10^{-10}$	2.6(S) $\times 10^{-10}$	2.6(S) $\times 10^{-10}$	1.7(C) $\times 10^{-11}$	2.6(S) $\times 10^{-10}$	1.7(C) $\times 10^{-11}$	1.7(C) $\times 10^{-11}$	2.1(C) $\times 10^{-11}$	7.0(S) $\times 10^{-9}$

PRIMARY CONTRIBUTORS TO FAILURE PROBABILITY (S) – SENSOR, (CP) – CPU, (C) – TOTAL COMPUTER, (A) – ACTUATOR, (H) – HYDRAULICS

TABLE 6-10

SENSOR/COMPUTER/ACTUATOR RELIABILITY SUMMARY – DUAL-REDUNDANT COMPUTERS

COMPUTER/ ACTUATOR INTERFACE CONFIGURATIONS	COMPUTER/SENSOR INTERFACE CONFIGURATIONS													
	DUAL CONFIGURATION 2													
	NO. 1 $\dot{\mu}, \alpha, \dot{\theta}, \theta$	NO. 12 $\dot{\theta}, \theta, A_{N,h}$	NO. 13 $\ddot{\theta}, \theta, A_N, \alpha$	NO. 14 $\ddot{\theta}, \theta, A_N, \mu$	NO. 15 $\ddot{\theta}, \theta, \dot{h}, \mu$	NO. 3 $\alpha, \dot{\theta}, \theta$	NO. 4 $\mu, \ddot{\theta}, \theta$	NO. 16 $\ddot{\theta}, \theta, \dot{h}$	NO. 29 $\ddot{\theta}, \theta, a_n$	NO. 27 μ, θ	NO. 30 A_N, μ	NO. 31 $A_N, \dot{h}$	NO. 32 A_N, α	NO. 26 A_N
DUAL 1	9.2 (C) (A) (H) $\times 10^{-8}$	9.2 (C) (A) (H) $\times 10^{-8}$	9.2 (C) (A) (H) $\times 10^{-8}$	9.2 (C) (A) (H) $\times 10^{-8}$	9.3 (C) (A) (H) $\times 10^{-8}$	9.3 (C) (A) (H) $\times 10^{-8}$	9.3 (C) (A) (H) $\times 10^{-8}$	9.3 (C) (A) (H) $\times 10^{-8}$	9.2 (C) (A) (H) $\times 10^{-8}$	9.3 (C) (A) (H) $\times 10^{-8}$	9.2 (C) (A) (H) $\times 10^{-8}$	9.2 (C) (A) (H) $\times 10^{-8}$	9.2 (C) (A) (H) $\times 10^{-8}$	9.9 (C) (A) (H) $\times 10^{-8}$
DUAL 2	5.1 (C) (A) (H) $\times 10^{-8}$	5.1 (C) (A) (H) $\times 10^{-8}$	5.1 (C) (A) (H) $\times 10^{-8}$	5.1 (C) (A) (H) $\times 10^{-8}$	5.1 (C) (A) (H) $\times 10^{-8}$	5.1 (C) (A) (H) $\times 10^{-8}$	5.1 (C) (A) (H) $\times 10^{-8}$	5.1 (C) (A) (H) $\times 10^{-8}$	5.1 (C) (A) (H) $\times 10^{-8}$	5.1 (C) (A) (H) $\times 10^{-8}$	5.1 (C) (A) (H) $\times 10^{-8}$	5.1 (C) (A) (H) $\times 10^{-8}$	5.1 (C) (A) (H) $\times 10^{-8}$	5.8 (C) (A) (H) $\times 10^{-8}$
DUAL 3	3.9 (C) $\times 10^{-8}$	3.9 (C) $\times 10^{-8}$	3.9 (C) $\times 10^{-8}$	3.9 (C) $\times 10^{-8}$	3.9 (C) $\times 10^{-8}$	3.9 (C) $\times 10^{-8}$	3.9 (C) $\times 10^{-8}$	3.9 (C) $\times 10^{-8}$	3.9 (C) $\times 10^{-8}$	3.9 (C) $\times 10^{-8}$	3.9 (C) $\times 10^{-8}$	3.9 (C) $\times 10^{-8}$	3.9 (C) $\times 10^{-8}$	4.6 (C) $\times 10^{-8}$
DUAL 4	3.9 (C) $\times 10^{-8}$	3.9 (C) $\times 10^{-8}$	3.9 (C) $\times 10^{-8}$	3.9 (C) $\times 10^{-8}$	3.9 (C) $\times 10^{-8}$	3.9 (C) $\times 10^{-8}$	3.9 (C) $\times 10^{-8}$	3.9 (C) $\times 10^{-8}$	3.9 (C) $\times 10^{-8}$	3.9 (C) $\times 10^{-8}$	3.9 (C) $\times 10^{-8}$	3.9 (C) $\times 10^{-8}$	3.9 (C) $\times 10^{-8}$	4.6 (C) $\times 10^{-8}$
DUAL 5	3.9 (C) $\times 10^{-8}$	3.9 (C) $\times 10^{-8}$	3.9 (C) $\times 10^{-8}$	3.9 (C) $\times 10^{-8}$	3.9 (C) $\times 10^{-8}$	3.9 (C) $\times 10^{-8}$	3.9 (C) $\times 10^{-8}$	3.9 (C) $\times 10^{-8}$	3.9 (C) $\times 10^{-8}$	3.9 (C) $\times 10^{-8}$	3.9 (C) $\times 10^{-8}$	3.9 (C) $\times 10^{-8}$	3.9 (C) $\times 10^{-8}$	4.6 (C) $\times 10^{-8}$
	DUAL CONFIGURATION 3													
DUAL 1	1.2 (C) $\times 10^{-7}$	1.2 (C) $\times 10^{-7}$	1.2 (C) $\times 10^{-7}$	1.2 (C) $\times 10^{-7}$	1.2 (C) $\times 10^{-7}$	1.2 (C) $\times 10^{-7}$	1.2 (C) $\times 10^{-7}$	1.2 (C) $\times 10^{-7}$	1.2 (C) $\times 10^{-7}$	1.2 (C) $\times 10^{-7}$	1.2 (C) $\times 10^{-7}$	1.2 (C) $\times 10^{-7}$	1.2 (C) $\times 10^{-7}$	1.2 (C) $\times 10^{-7}$
DUAL 2	7.5 (C) $\times 10^{-8}$	7.5 (C) $\times 10^{-8}$	7.5 (C) $\times 10^{-8}$	7.5 (C) $\times 10^{-8}$	7.5 (C) $\times 10^{-8}$	7.5 (C) $\times 10^{-8}$	7.5 (C) $\times 10^{-8}$	7.5 (C) $\times 10^{-8}$	7.5 (C) $\times 10^{-8}$	7.5 (C) $\times 10^{-8}$	7.5 (C) $\times 10^{-8}$	7.5 (C) $\times 10^{-8}$	7.5 (C) $\times 10^{-8}$	8.2 (C) $\times 10^{-8}$
DUAL 3	6.3 (C) $\times 10^{-8}$	6.3 (C) $\times 10^{-8}$	6.3 (C) $\times 10^{-8}$	6.3 (C) $\times 10^{-8}$	6.3 (C) $\times 10^{-8}$	6.3 (C) $\times 10^{-8}$	6.3 (C) $\times 10^{-8}$	6.3 (C) $\times 10^{-8}$	6.3 (C) $\times 10^{-8}$	6.3 (C) $\times 10^{-8}$	6.3 (C) $\times 10^{-8}$	6.3 (C) $\times 10^{-8}$	6.3 (C) $\times 10^{-8}$	6.9 (C) $\times 10^{-8}$
DUAL 4	6.3 (C) $\times 10^{-8}$	6.3 (C) $\times 10^{-8}$	6.3 (C) $\times 10^{-8}$	6.3 (C) $\times 10^{-8}$	6.3 (C) $\times 10^{-8}$	6.3 (C) $\times 10^{-8}$	6.3 (C) $\times 10^{-8}$	6.3 (C) $\times 10^{-8}$	6.3 (C) $\times 10^{-8}$	6.3 (C) $\times 10^{-8}$	6.3 (C) $\times 10^{-8}$	6.3 (C) $\times 10^{-8}$	6.3 (C) $\times 10^{-8}$	6.9 (C) $\times 10^{-8}$
DUAL 5	6.3 (C) $\times 10^{-8}$	6.3 (C) $\times 10^{-8}$	6.3 (C) $\times 10^{-8}$	6.3 (C) $\times 10^{-8}$	6.3 (C) $\times 10^{-8}$	6.3 (C) $\times 10^{-8}$	6.3 (C) $\times 10^{-8}$	6.3 (C) $\times 10^{-8}$	6.3 (C) $\times 10^{-8}$	6.3 (C) $\times 10^{-8}$	6.3 (C) $\times 10^{-8}$	6.3 (C) $\times 10^{-8}$	6.3 (C) $\times 10^{-8}$	6.9 (C) $\times 10^{-8}$

PRIMARY CONTRIBUTORS TO FAILURE PROBABILITY (C) – TOTAL COMPUTER, (A) – ACTUATOR, (H) – HYDRAULICS

TABLE 6-10
SENSOR/COMPUTER/ACTUATOR RELIABILITY SUMMARY – DUAL-DUAL COMPUTERS

COMPUTER/ ACTUATOR INTERFACE CONFIGURATIONS	COMPUTER/SENSOR INTERFACE CONFIGURATIONS													
	DUAL-DUAL CONFIGURATION 2													
	NO. 1 $\mu, \alpha, \dot{\theta}, \theta$	NO. 12 $\dot{\theta}, \theta, A_{N'} h$	NO. 13 $\dot{\theta}, \theta, A_{N'} \alpha$	NO. 14 $\dot{\theta}, \theta, A_{N'} \mu$	NO. 15 $\dot{\theta}, \theta, h, \mu$	NO. 3 $\alpha, \dot{\theta}, \theta$	NO. 4 $\mu, \dot{\theta}, \theta$	NO. 16 $\dot{\theta}, \theta, h$	NO. 29 $\dot{\theta}, \theta, a_n$	NO. 27 μ, θ	NO. 30 $A_{N'} \mu$	NO. 31 $A_{N'} h$	NO. 32 $A_{N'} \alpha$	NO. 26 A_N
DUAL-DUAL 1	1.6(A)(H) $\times 10^{-8}$	1.6(A)(H) $\times 10^{-8}$	1.6(A)(H) $\times 10^{-8}$	1.6(A)(H) $\times 10^{-8}$	1.6(A)(H) $\times 10^{-8}$	1.7(A)(H) $\times 10^{-8}$	1.6(A)(H) $\times 10^{-8}$	1.6(A)(H) $\times 10^{-8}$	1.6(A)(H) $\times 10^{-8}$	1.6(A)(H) $\times 10^{-8}$	1.6(A)(H) $\times 10^{-8}$	1.6(A)(H) $\times 10^{-8}$	1.6(A)(H) $\times 10^{-8}$	2.3(S)(SC)(A)(H) $\times 10^{-8}$
DUAL-DUAL 2	1.4(A)(H) $\times 10^{-8}$	1.4(A)(H) $\times 10^{-8}$	1.4(A)(H) $\times 10^{-8}$	1.4(A)(H) $\times 10^{-8}$	1.4(A)(H) $\times 10^{-8}$	1.5(A)(H) $\times 10^{-8}$	1.4(A)(H) $\times 10^{-8}$	1.4(A)(H) $\times 10^{-8}$	1.4(A)(H) $\times 10^{-8}$	1.4(A)(H) $\times 10^{-8}$	1.4(A)(H) $\times 10^{-8}$	1.4(A)(H) $\times 10^{-8}$	1.4(A)(H) $\times 10^{-8}$	2.1(S)(SC)(A)(H) $\times 10^{-8}$
DUAL-DUAL 3	3.9(SC) $\times 10^{-9}$	3.9(SC) $\times 10^{-9}$	3.9(SC) $\times 10^{-9}$	3.9(SC) $\times 10^{-9}$	4.2(SC) $\times 10^{-9}$	4.4(SC) $\times 10^{-9}$	4.2(SC) $\times 10^{-9}$	4.2(SC) $\times 10^{-9}$	3.9(SC) $\times 10^{-9}$	4.2(SC) $\times 10^{-9}$	3.9(SC) $\times 10^{-9}$	3.9(SC) $\times 10^{-9}$	3.9(SC) $\times 10^{-9}$	1.1(S)(SC) $\times 10^{-8}$
DUAL-DUAL 4	3.9(SC) $\times 10^{-9}$	3.9(SC) $\times 10^{-9}$	3.9(SC) $\times 10^{-9}$	3.9(SC) $\times 10^{-9}$	4.2(SC) $\times 10^{-9}$	4.4(SC) $\times 10^{-9}$	4.2(SC) $\times 10^{-9}$	4.2(SC) $\times 10^{-9}$	3.9(SC) $\times 10^{-9}$	4.2(SC) $\times 10^{-9}$	3.9(SC) $\times 10^{-9}$	3.9(SC) $\times 10^{-9}$	3.9(SC) $\times 10^{-9}$	1.1(S)(SC) $\times 10^{-8}$
DUAL-DUAL 5	3.9(SC) $\times 10^{-9}$	3.9(SC) $\times 10^{-9}$	3.9(SC) $\times 10^{-9}$	3.9(SC) $\times 10^{-9}$	4.2(SC) $\times 10^{-9}$	4.4(SC) $\times 10^{-9}$	4.2(SC) $\times 10^{-9}$	4.2(SC) $\times 10^{-9}$	3.9(SC) $\times 10^{-9}$	4.2(SC) $\times 10^{-9}$	3.9(SC) $\times 10^{-9}$	3.9(SC) $\times 10^{-9}$	3.9(SC) $\times 10^{-9}$	1.1(S)(SC) $\times 10^{-8}$
	DUAL-DUAL CONFIGURATION 3													
DUAL-DUAL 1	1.6(C)(A)(H) $\times 10^{-7}$	1.6(C)(A)(H) $\times 10^{-7}$	1.6(C)(A)(H) $\times 10^{-7}$	1.6(C)(A)(H) $\times 10^{-7}$	1.6(C)(A)(H) $\times 10^{-7}$	1.7(C)(A)(H) $\times 10^{-7}$	1.6(C)(A)(H) $\times 10^{-7}$	1.6(C)(A)(H) $\times 10^{-7}$	1.6(C)(A)(H) $\times 10^{-7}$	1.6(C)(A)(H) $\times 10^{-7}$	1.6(C)(A)(H) $\times 10^{-7}$	1.6(C)(A)(H) $\times 10^{-7}$	1.6(C)(A)(H) $\times 10^{-7}$	1.7(C)(A)(H) $\times 10^{-7}$
DUAL-DUAL 2	1.1(C) $\times 10^{-7}$	1.1(C) $\times 10^{-7}$	1.1(C) $\times 10^{-7}$	1.1(C) $\times 10^{-7}$	1.1(C) $\times 10^{-7}$	1.1(C) $\times 10^{-7}$	1.1(C) $\times 10^{-7}$	1.1(C) $\times 10^{-7}$	1.1(C) $\times 10^{-7}$	1.1(C) $\times 10^{-7}$	1.1(C) $\times 10^{-7}$	1.1(C) $\times 10^{-7}$	1.1(C) $\times 10^{-7}$	1.1(C) $\times 10^{-7}$
DUAL-DUAL 3	9.8(C) $\times 10^{-8}$	9.8(C) $\times 10^{-8}$	9.8(C) $\times 10^{-8}$	9.8(C) $\times 10^{-8}$	9.8(C) $\times 10^{-8}$	9.8(C) $\times 10^{-8}$	9.8(C) $\times 10^{-8}$	9.8(C) $\times 10^{-8}$	9.8(C) $\times 10^{-8}$	9.8(C) $\times 10^{-8}$	9.8(C) $\times 10^{-8}$	9.8(C) $\times 10^{-8}$	9.8(C) $\times 10^{-8}$	1.0(C) $\times 10^{-7}$
DUAL-DUAL 4	9.8(C) $\times 10^{-8}$	9.8(C) $\times 10^{-8}$	9.8(C) $\times 10^{-8}$	9.8(C) $\times 10^{-8}$	9.8(C) $\times 10^{-8}$	9.8(C) $\times 10^{-8}$	9.8(C) $\times 10^{-8}$	9.8(C) $\times 10^{-8}$	9.8(C) $\times 10^{-8}$	9.8(C) $\times 10^{-8}$	9.8(C) $\times 10^{-8}$	9.8(C) $\times 10^{-8}$	9.8(C) $\times 10^{-8}$	1.0(C) $\times 10^{-7}$
DUAL-DUAL 5	9.8(C) $\times 10^{-8}$	9.8(C) $\times 10^{-8}$	9.8(C) $\times 10^{-8}$	9.8(C) $\times 10^{-8}$	9.8(C) $\times 10^{-8}$	9.8(C) $\times 10^{-8}$	9.8(C) $\times 10^{-8}$	9.8(C) $\times 10^{-8}$	9.8(C) $\times 10^{-8}$	9.8(C) $\times 10^{-8}$	9.8(C) $\times 10^{-8}$	9.8(C) $\times 10^{-8}$	9.8(C) $\times 10^{-8}$	1.0(C) $\times 10^{-7}$

PRIMARY CONTRIBUTORS TO FAILURE PROBABILITY (S) – SENSOR, (SC) – SENSOR COMPUTER DATA PROCESSOR, (C) – TOTAL COMPUTER, (A) – ACTUATOR, (H) – HYDRAULICS

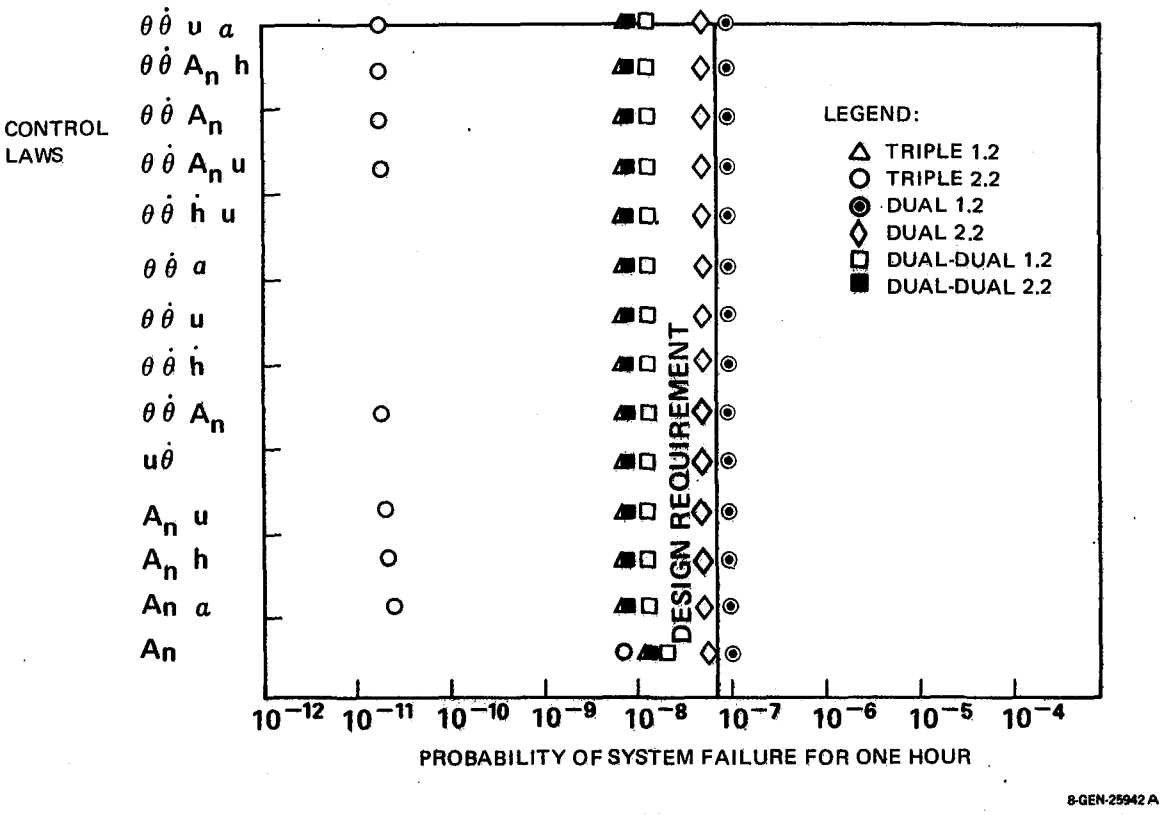

FIGURE 6-47. SYSTEM RELIABILITY ASSESSMENT (RELIABILITY GOAL: 7×10^{-8} FAILURE PROBABILITY)

toward the right with increased probability of system failure. Dual No. 1 would then be the first eliminated on the basis of not satisfying the reliability goal.

The lower MTBF of the DUAL-DUAL (dual CPU, dual computer) configurations tends to discourage its use. Assumming a 3200-hour dual CPU computer MTBF, the availability of two such computers with comparison monitoring is slightly higher than three 4000-hour MTBF in-line monitored computers. However, three computers provide a potential spare for possible in-service dispatchability requirements. With one computer inoperative, the system would revert to a dual configuration.

The RSSAS sensor array has more than the necessary redundancy and most of the components are required for dispatch as part of other systems so their availability is not chargeable to RSSAS alone. Two sources of θ (and $\dot{\theta}$) are required for dispatch by the attitude display system. Two sources of air data are also currently required and provide the u signal for RSSAS. The angle-of-attack transducers are required for dispatch by the stall warning system.

An aircraft is seldom dispatched without a fully operative actuation system (all hydraulics are mandatory). Thus, the minimum number of actuators required for safety is also adequate for RSSAS. For symmetry of control, however, it is important that a single computer control an elevator surface on each side of the vertical tail. Thus, a dual-actuator arrangement with dual inputs to each actuator is desired.

Based upon the considerations discussed above, the selected systems are those shown in Figure 6-48. These are Triple 1.2 with a reversion capability to Dual 2.2.

6.2.6 Thrust/Pitch Compensation Sensor Interface. — The need for automatic compensation of the pitching effects resulting from thrust changes is peculiar to aircraft with wing-mounted engines and not a requirement of the relaxed static stability concept. Pitch/thrust compensation will, however, be provided on the EET with nearly the same reliability of the static stability augmentation, since these two functions share computation and actuation devices. The only differences exist in the sensor interface. The pitch/thrust compensation interface with the engines is shown in Figure 6-49.

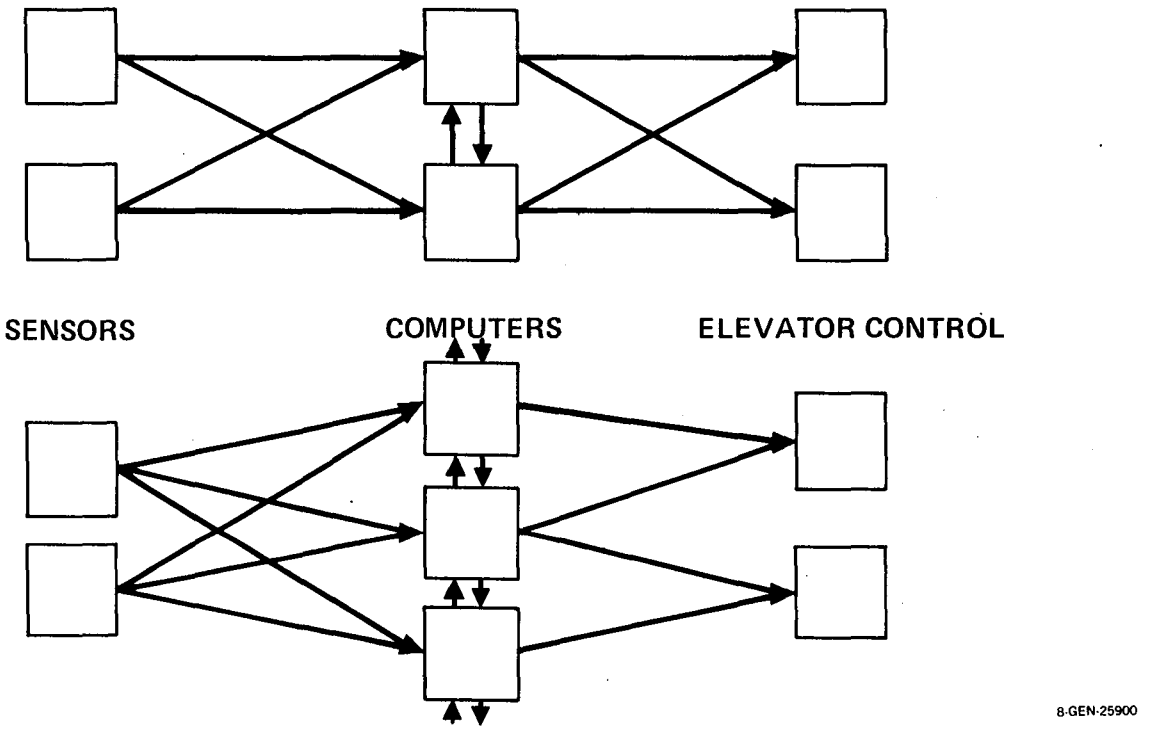

FIGURE 6-48. SELECTED SYSTEM ARCHITECTURES

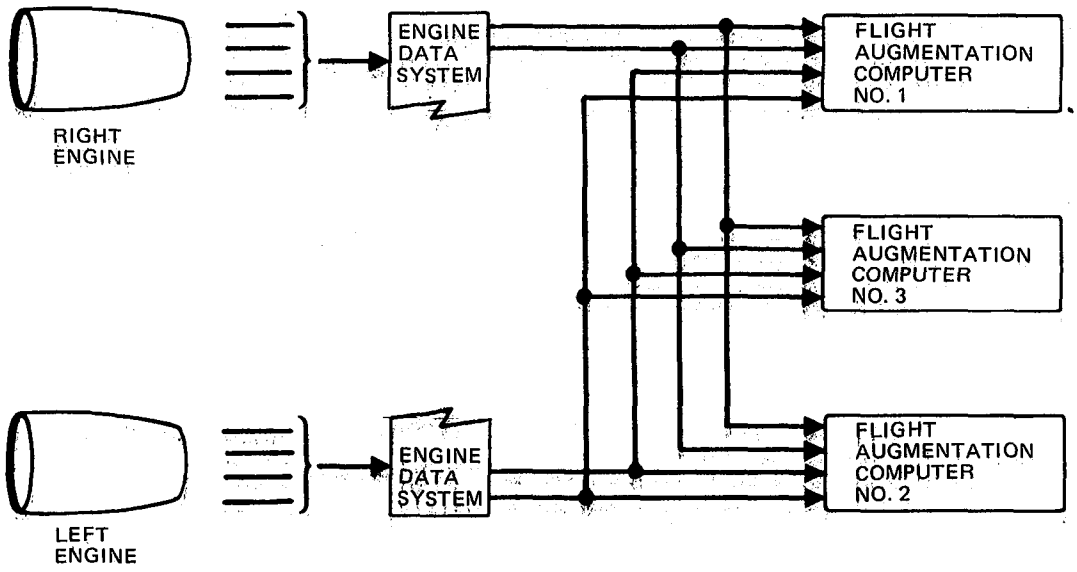

FIGURE 6-49. PITCH/THRUST COMPENSATION SENSOR INTERFACE

Loss of the thrust data from either engine results in the compensator providing only half the required thrust/pitch gain. Although degraded, significant compensation is still provided. Loss of both engine thrust data eliminates the thrust/pitch compensation. The probability of these two events are:

Loss of single engine thrust data

$$Q = 2(\lambda_{ET} + \lambda_{ED})t$$

$$Q = 2(100\times10^{-6} + 500\times10^{-6})(1)$$

$$Q = 1.2\times10^{-3}$$

where

ET = Engine transducer
ED = Engine data system
t = One hour
λ = Failures per hour

Loss of both engine thrust data

$$Q = (\lambda_{ET} + \lambda_{ED})^2(t)^2$$

$$Q = (100\times10^{-6} + 500\times10^{-6})^2(1)^2$$

$$Q = 3.6\times10^{-7}$$

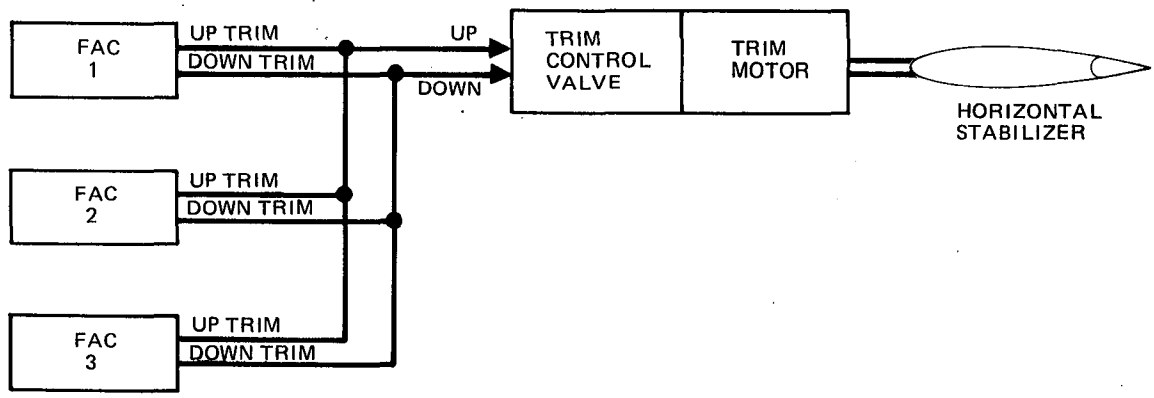

FIGURE 6-50. RSSAS AUTOTRIM INTERFACE

Failure rates are based on current DC-10 operational data.

6.2.7 RSSAS Auto Trim Interface. — The RSSAS autotrim function has been previously described in Paragraph 6.1.4. The interface of the discrete FAC trim outputs and the horizontal stabilizer trim system is relatively simple. As shown in Figure 6-50, each of the FACs, regardless of redundancy level, provides its discrete trim outputs, up-trim or down-trim, on separate signal paths. Then all of the up-trim wires are connected together and all of the down-trim wires are connected together. These separate trim commands are provided to the stabilizer trim control valve, which in turn commands the trim motor to drive the horizontal stabilizer at a fixed rate.

Although a simple mechanization, it is expected that the probability of loss of the autotrim will exceed that of the basic RSSAS function. Autotrim loss probability is calculated as:

$$Q = (\lambda_{\substack{\text{CONTROL} \\ \text{VALVE}}} + \lambda_{\substack{\text{TRIM} \\ \text{MOTOR}}})t = (28\text{x}10^{-6} + 38\text{x}10^{-6})(1)$$

$$Q = 6.6\text{x}10^{-5}$$

When this occurs, the manual RSSAS trim director is activated and the RSSAS series elevator displacements are off-loaded using the primary trim system as described in Paragraph 6.1.4. Again, the failure rates used in this calculation are based on DC-10 operational data.

SECTION 7
IMPACT OF RSSAS ON THE AIRCRAFT DESIGN AND CERTIFICATION

The incorporation of any or all systems on a commercial aircraft requires significant design, development, analysis, verification, and demonstration efforts. Although most systems must comply with specific regulatory requirements, satisfaction of these regulations is achieved through the normal design practices used by the airframe manufacturers and system/component suppliers to assure themselves of the quality and safety of their product. This section of the report provides an estimate of the effort in manpower and dollars required to incorporate relaxed static stability in an EET aircraft, with consideration of the FAA regulations for the aircraft certification which relate to this system.

7.1 Regulatory Requirements

An aircraft with relaxed static stability must comply with certain FAA requirements which specify performance for both the aircraft and augmentation system. The specific regulations which relate to the unique stability characteristics of the aircraft have been analyzed and are referenced and briefly discussed as follows:

Part 25 Airworthiness Standards: Transport Category Airplanes

25.21(c) The controllability, stability, trim, and stalling characteristics must be demonstrated for the unaugmented aircraft and every expected augmented aircraft configuration.

25.23(a) Ranges of acceptable centers of gravity may vary depending upon the configuration of the augmentation system. In practice, this dependency would have to be established with regard to the augmentation configuration at dispatch.

25.103 Most unfavorable center of gravity for stall may vary as a function of augmentation configuration.

25.105 Takeoff performance may be a function of augmentation configuration.
25.107
25.111 Ground-to-air cycle must be demonstrated.
25.115

25.143 Controllability and maneuverability must be considered for unaugmented and all augmented aircraft configurations.

25.161 The unaugmented aircraft may not be able to maintain a trim condition in a turbulent atmosphere.

25.171
25.173
25.175 The unaugmented aircraft would not be able to satisfy the stability requirements of these paragraphs. The unaugmented aircraft must, however, be considered the failed condition and an associated acceptable probability of occurrence established and demonstrated by analysis.

25.201
25.203
25.205 Stall characteristics may differ with augmentation configurations. Demonstration of all expected configurations is required.

25.671 Unaugmented and augmented aircraft configurations must be able to withstand primary flight control system failures and demonstrate satisfactory controllability. Failures critical to unaugmented and augmented aircraft may not be the same.

25.672 Failures of the augmentation system must be demonstrated to provide acceptable flying qualities, or shown to be sufficiently improbable.

25.1309 Critical failure conditions must be verified to be sufficiently improbable.

25.1503
25.1505 A speed limitation may be established if satisfactory performance cannot be achieved at high speeds.

7.2 System Validation

The validation of an avionics system is an integral part of the normal design process required to verify each element of the design, and it provides the data necessary to progress to the next step in the program. Figure 7-1 is a summary of a 42-month program for the validation of an RSSAS system on a new aircraft design. The subtasks of this program are classified as performance compliance, fault-related, or system description and design control. As noted in Figure 7-1, several data submittals to the FAA are anticipated and

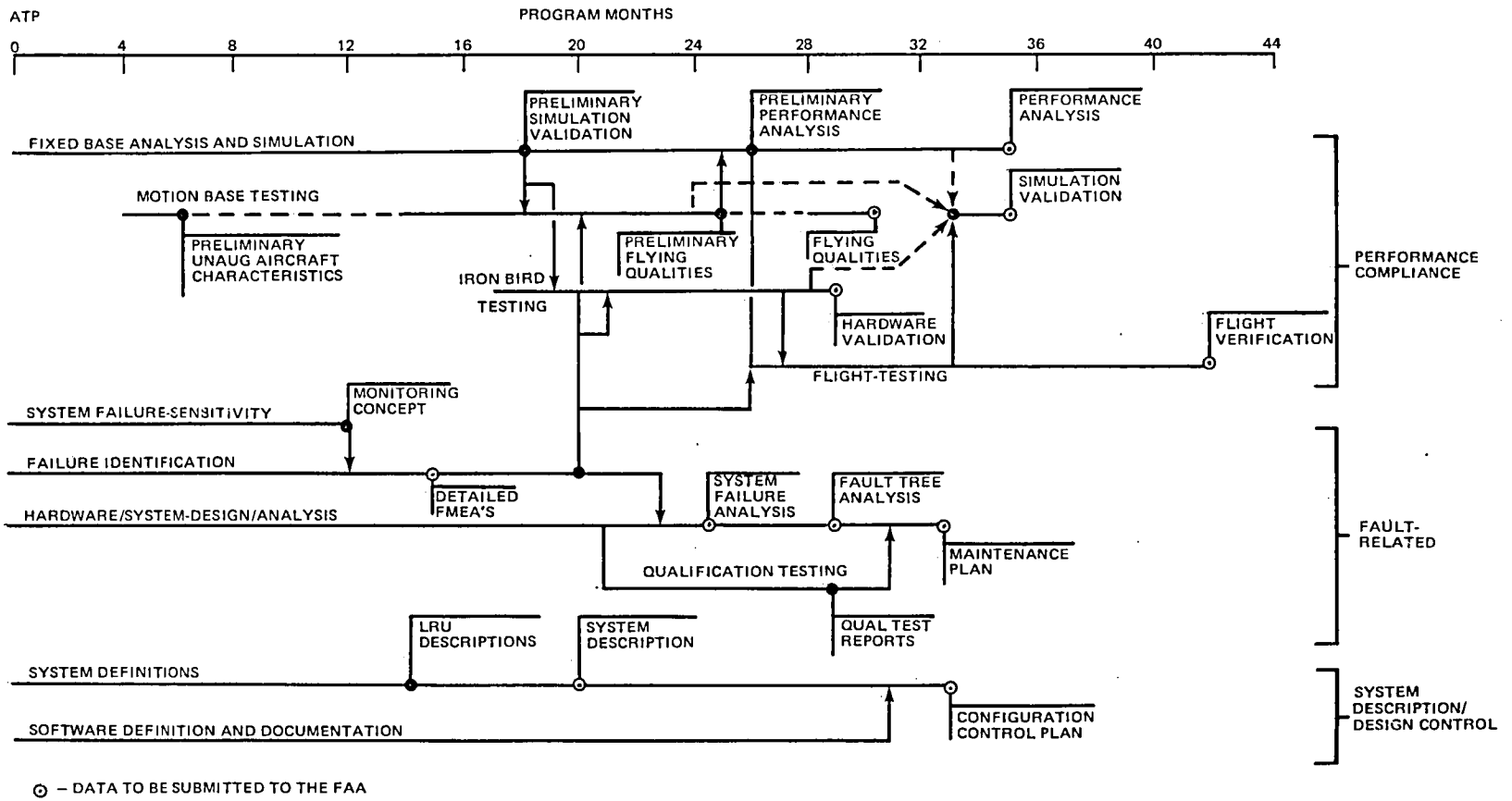

FIGURE 7-1. RSSAS VALIDATION SCHEDULE

although the form of the FAA reports may be unique, in most cases the requirement to collect these data is simply consistent with the design process. Exceptions exist only in the area of qualitative evaluations of the aircraft or RSSAS, which usually require additional testing to the motion base simulator and flight test program.

The performance compliance process begins with the aircraft simulation used to develop and analyze the RSSAS. This total simulation is then used to conduct motion base testing to evaluate the aircraft/system flying qualities. Iron bird* testing is used to validate the system hardware which is then demonstrated on the flight test vehicle. It should be noted that all performance verification includes both fault-free operation and failure configurations based upon the FMEA and fault analyses.

The fault analyses include determining the effects of system failures and formulation of the monitoring concepts. This usually includes detailed hardware FMEAs and system fault and fault tree analyses. These analyses contribute to aircraft and RSSAS maintenance plans and certification documentation.

System description and design control are essentials of the design, analysis, and verification tasks to assure a proper continuing understanding for both the designer and monitor (including the FAA) of the intended function of all elements of the hardware and system. The design control feature must be defined and maintained throughout the life of the aircraft/system.

7.3 RSSAS Implementation Cost

For the purpose of this study, the cost of incorporating the relaxed static stability concept in the EET is determined as the differential of the identical aircraft with and without RSSAS. This is somewhat different from the accumulated RSSAS implementation costs, since many of the required tasks are common to a conventional aircraft design. The primary contributors to the RSSAS cost are the airframe manufacturer and the suppliers of the primary components, the augmentation computers, and the new elevator actuators.

*A full-scale aircraft development fixture consisting of (1) the mechanical primary control and hydraulic supply systems duplicating the aircraft hardware and routing, (2) a cockpit simulation with pilot controls and displays, (3) test stations for installation and control of avionics systems, and (4) a computer simulation of the aircraft dynamics.

The following engineering disciplines and corresponding primary additional areas of effort would be required:

Aerodynamics

- Flying qualities criteria formulation and evaluation
- Stability and control analysis
  (Aerodynamic definitions, wind tunnel testing, etc., require the equivalent level of effort)

Avionics

- RSSAS hardware and system specification, system performance analysis, hardware verification, and vendor coordination

Electrical

- RSSAS electrical component and wiring installation

Flight Test

- Maintenance of the test aircraft and the conduct of RSSAS flight testing and certification demonstrations.

Laboratory

- Management of laboratory facilities and support engineering tests

Mechanical

- Elevator actuator specification, hardware verification, vendor coordination, and installation design

Reliability and Safety

- System reliability and safety analysis
- Monitoring of vendor reliability analyses

Structures

- Structure analysis with system operation (although wing and empennage position and sizing, landing gear, and door location may be different from conventional aircraft, the engineering tasks are assumed equivalent)

Other Departments

- Engineering System Compliance, Environmental, Human Factors, Operational Engineering and Flight Performance, Weights
  - Involved with assuring RSSAS/aircraft design but of significantly lower manpower level
- Product Support
  - Involved with maintaining the system in service
- Material
  - Performs purchasing, scheduling, and on-site inspection

The estimated manpower and flight test requirements for the most intensive Douglas design engineering effort are:

DEPARTMENT	MAN-HOURS
Aerodynamics	10,000
Avionics	92,000
Electrical	3,000
Flight Test	275,000
Laboratory	10,000
Mechanical	17,000
Reliability and Safety	18,000
Structures	2,000
Totals:	437,000
plus	275 aircraft flight hours

An additional factor of 25 percent of the design engineering (all of the above engineering except flight test and laboratory) must be included to cover drawing check, coordination, and other paper-processing requirements, bringing the total number of man-hours required to 475,000.

Assuming a representative aircraft industry cost of $40 per engineering man-hour and $10,000 per aircraft flight hour, the total nonrecurring airframe manufacturer's cost in 1979 dollars is $21.75 million.

The supplier costs are estimated from equivalent programs previously completed or currently in progress and assumes at least a 200-aircraft base over which to spread the nonrecurring charges.

Elevator Actuators	$60,000 per shipset
RSSAS Computers	$120,000 per shipset

Using the 200-aircraft base to establish the total result gives:

Airframe costs	$108,750
Supplier costs	$180,000
Total	$288,750* per aircraft

*in 1979 dollars

REFERENCES

1. Cooper, G.E. and Harper, R.P., "The Use of Pilot Rating in the Evaluation of Aircraft Handling Qualities," NASA TN D-5153, April 1969.

2. Anonymous, "Military Specification, Flying Qualities of Piloted Airplanes," MIL-F-8785B(ASG), 7 August, 1969.

3. Neal, T.P. and Smith, R.E., "An In-flight Investigation to Develop Control System Design Criteria for Fighter Airplanes," AFFDL-TR-70-74, Volume 1, December 1970.

4. Rickard, W.W., "Longitudinal Flying Qualities in the Landing Approach," Douglas Paper 6469, May 1976.

5. Wasserman, R. and Mitchell, J.F., "Inflight Simulation of Minimum Longitudinal Stability for Large Delta-Wing Transports in Landing Approach and Touchdown," AFFDL-TR-72-143, Volume 1, February 1973.

6. Barr, N.M., Gangsaas, D., and Schaffer, D.R., "Wind Models for Flight Simulator Certification of Landing and Approach Guidance and Control Systems," FAA-RD-74-206, December 1974.

7. Anonymous, "Proposals for Revising MIL-F-8785B, 'Flying Qualities of Piloted Aircraft,' Volume 1, Proposed Revisions," AFFDL-FGC Working Paper, August, 1977; Corrected February, 1978.

8. Markland, C.A., "Optimal Model-Following Control System Synthesis Techniques," Proceedings I.E.E., Volume 117, No. 3, March 1970

APPENDIX 1
BANDWIDTH MODEL

The Bandwidth Model is a pilot-in-the-loop analytical method which permits the estimation of the flying qualities rating a human pilot would give the pitch maneuvering characteristics of an arbitrary aircraft configuration. The airplane need not be built or flown; only a mathematical model of the pitch response (i.e., pitch transfer function) is needed. The rating is based on the closed-loop performance of a pilot model plus airplane system in a pitch-tracking task.

The method involves calculation of the optimal pilot model compensation for closed-loop pitch attitude tracking, as determined by using the adjustment rules of the Bandwidth Model. The method was originated by R. E. Smith and T. P. Neal of Cornell Aeronautical Laboratories in AFFDL-TR-70-74 (Reference 3).

The primary required information is the airplane-plus-control-system transfer function θ/F_s or θ/δ_e. Other inputs include desired bandwidth and droop, maximum allowable resonance, pilot transport delay, and maximum allowable pilot-lag-compensation angle. Primary outputs of the method are the computed pilot model parameters. Other outputs are the pilot model phase angle at the bandwidth frequency, the maximum closed-loop amplitude (resonant peak), and the low-frequency asymptotes of the transfer function. The method also yields the amplitude and phase angle versus frequency of the following transfer functions:

1. Open loop (θ/F_s)

2. Open loop plus delay $(\theta/\theta_c^* = e^{-\tau s}\ \theta/F_s)$

3. Open loop compensated $(\theta/\theta_c = K_p\ e^{-\tau s}\ \dfrac{(\tau_{p1}\ s+1)}{(\tau_{p2}\ s+1)}\ \theta/F_s)$

4. Closed loop compensated $(\theta/\theta_c = \dfrac{\theta/\theta_c}{1 + \theta/\theta_c})$

A chart is included in this report which permits the estimation of flying qualities ratings by use of the ouputs of the program.

APPENDIX 2
MOTION-BASE SIMULATOR FACILITY

Six-Axis Motion Base

Douglas has designed and fabricated a six-axis motion-simulation system capable of supporting a complete cockpit simulator and providing realistic motion cues (Figure A-1). The cockpit simulator is attached to a base supported by six hydraulic jacks arranged in the configuration developed by the Franklin Institute. The most important specifications are summarized below.

AXIS	EXCURSION	VELOCITY	ACCELERATION
Heave	1.07 m	0.99 m/s	1.65 g
Sway	1.71 m	1.70 m/s	2.43 g
Surge	1.65 m	1.80 m/s	1.50 g
Roll	0.54 Rad	0.62 Rad/s	7.8 Rad/s^2
Pitch	0.58 Rad	0.59 Rad/s	7.8 Rad/s^2
Yaw	0.68 Rad	0.63 Rad/s	7.9 Rad/s^2

These figures are for a payload of 44,000 kg. The figures for pitch and yaw refer to the platform axis. With the separation between aircraft center of gravity and the pilot's positon, the pitch and yaw motions appear primarily as heave and sway.

The motion system is controlled by a minicomputer which implements the geometric transformations, washout algorithms, and fail-safe features. The minicomputer is tied to the Sigma 5 computer via a digital data link. The minicomputer exercises servo valves and receives feedback data, via analog/digital converters, from Douglas-developed Linear Velocity Differential Transformers (LDVT). These transformers provide linear readout over the full travel of the hydraulic jacks. The motion system is currently equipped with a large-scale transport cockpit, and visual simulation is available from the Redifon visual flight attachment (Figure A-2).

Cockpit Interface Hybrid Satellite

Cockpit simulators are, as a matter of necessity, located some distance from the main Sigma 5 computer facility. The Interface Hybrid Satellites are

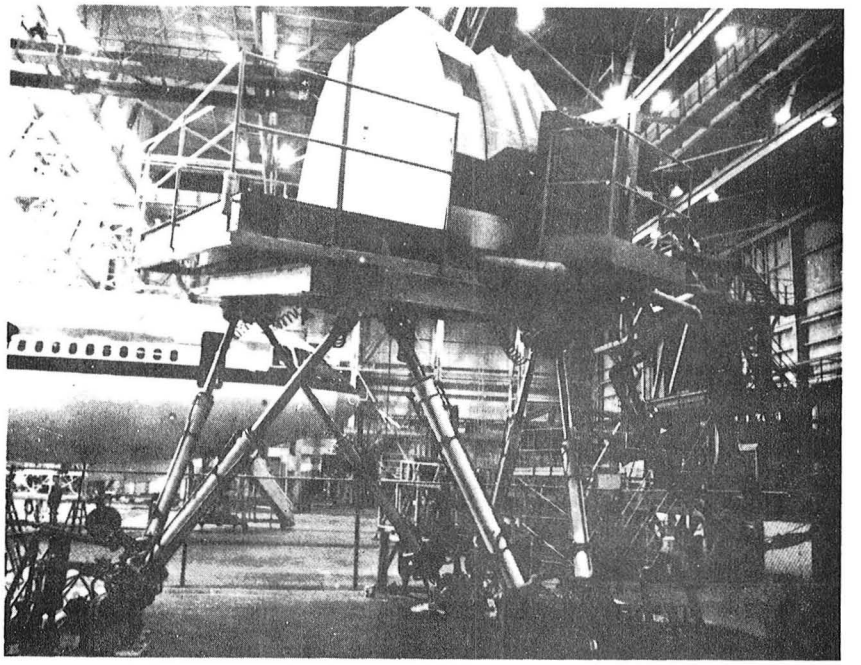

IRAD-96020-63

FIGURE A-1. SIX-AXIS MOTION-BASE SIMULATOR

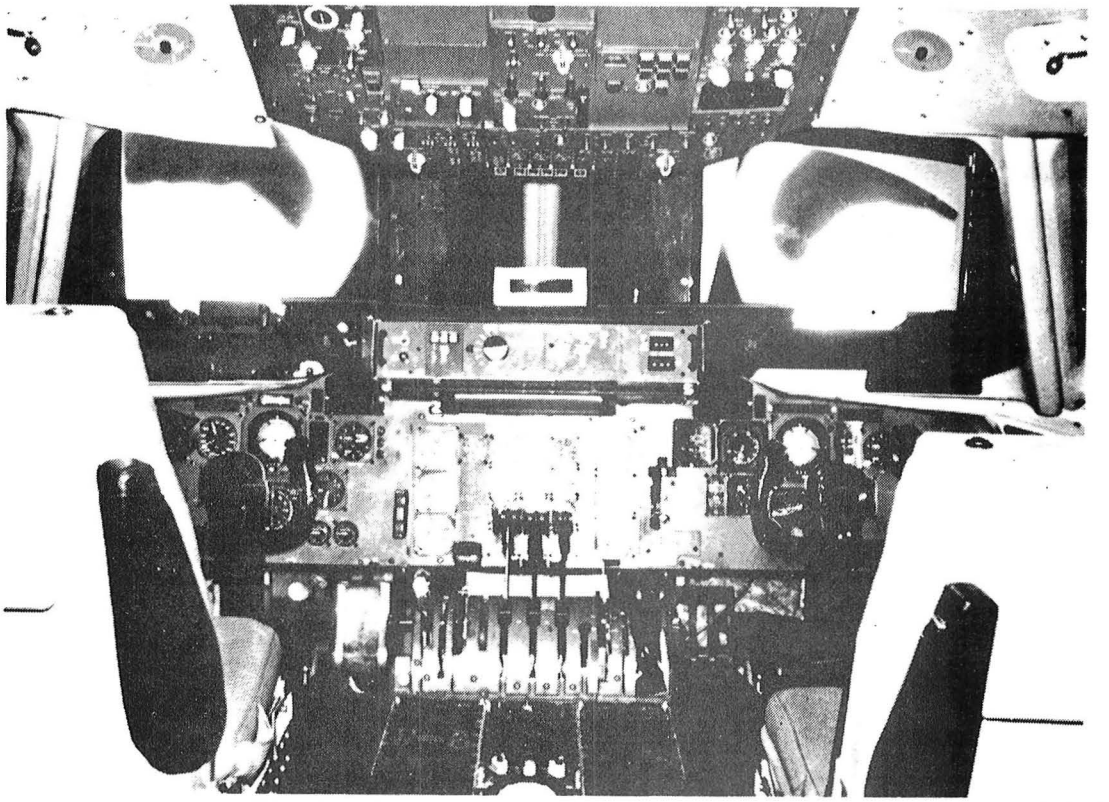

IRAD-96020-64

FIGURE A-2. LARGE-SCALE TRANSPORT COCKPIT

portable systems that may be located adjacent to a cockpit simulator and are designed to provide all of the necessary interfacing functions to the main computer system. The satellites contain up to 64 (A to D) and (D to A) channels, a small analog computer, and a PDP 11/40 digital computer. The systems are tied to the Sigma 5 through a digital link, ensuring noise-free communication. Patch boards are utilized to provide the necessary flexibility. In addition to providing the communication and conversion functions between the cockpit and the Sigma 5, the satellites possess substantial hybrid computing power that serves to unburden the Sigma 5 and reinforce its ability to accommodate real-time parallel tasks.

There is an advanced analog capability consisting of two Milgo 4100 computers. These very large solid-state systems contain in excess of 550 operational amplifiers each. They possess fully automatic programming features and are used extensively in supporting full cockpit simulators. These may include significant elements of the avionics systems.

Hybrid System

The largest and most sophisticated system in the laboratory is the XDS Sigma 5, Astrodata Ci-5000 hybrid. Their separate analog and digital capabilities are rendered compatible through a 32- by 32-channel system of Analog to Digital (A to D), and Digital to Analog (D to A) converters. These also provide the means of interfacing the digital computer with the parallel character of the real world as exemplified by pilots, cockpits, instruments, etc. The hybrid computer system represents the successful marriage of digital and analog techniques, and goes far in eliminating the inadequacies of either of the systems applied separately. Since its installation, this equipment has provided a full simulation of Douglas' commercial transport, the DC-10, and the Military STOL aircraft, the YC-15.

Hybrid System Software

Simulation programs are written in problem- or user-oriented languages such as FORTRAN, CSSL, and SL-1. Although not stated explicitly, every programmer writing in such languages assumes that the computer will properly understand the language in which he wrote his program and will faithfully follow

his instructions. However, the computer hardware alone cannot do this. There is resident in the computer a program or a set of programs that will interpret the programmer's instruction language, convert the programmer's instructions to machine directives, and cause the computer hardware to perform the desired acts.

Visual Flight Attachment (VFA)

One of the pilot's primary sources of data is the scene viewed from the forward window of the aircraft. This is particularly true during final approach where runway perspective, lighting, and landing aids provide significant data which can be critical to system performance.

Flight simulation aims at validating the design of a system, including the pilot, through study of the actual performance. If the pilot is to function in a normal and realistic fashion, he must be provided with data, including a visual scene, in as realistic a manner as possible. This is the purpose of the visual flight simulator at the Long Beach facility.

The visual simulator consists of two models, a servodriven television camera and the associated control electronics and lighting. The larger model, which consists of the airport, runway, and surrounding terrain, is three-dimensional (13 meters long by 4.6 meters high), with a scale of 750 to 1. A 3048-meter runway is located at the longitudinal center of the model. The runway is complete with approach lights, strobes, marker and threshold bars, touchdown zone, VASI, taxiway, edge, and centerline lights. The model is illuminated by a bank of fluorescent lights which can be controlled to provide daylight, dusk, or night conditions. The second model is 1.2 by 1.2 meters with a scale of approximately 1.6 kilometers to the inch. This model represents terrain and cloud cover as viewed from high altitude (Figure A-3).

A Phillips Plumbicon television camera is mounted on a gantry. The gantry travels on tracks parallel to the model to provide longitudinal motion. The camera carriage itself is driven in two directions to provide lateral motion and changes in altitude. Servodriven mirrors and prisms in the optics of the camera provide roll, pitch, and yaw.

Primary control signals from a cockpit simulator serve as inputs to a computer-mechanized math model of the airplane dynamics. This computer is linked to a control computer which converts aircraft center-of-gravity coordinates to pilot's eye coordinates and controls camera motion. The cameras then "flies" the approach as directed from the cockpit. The system can be used in simulation of any aircraft for which a computer model is available.

The video signal is sent to a television monitor which is viewed by the pilot through a collimating lens mounted approximately in the plane of the windscreen. MDC has undertaken a substantial amount of development in the area of these collimating lenses, and has produced the most advanced and distortion-free optical system available anywhere for simulator applications. Specifications of the VFA system are given in the following paragraph.

Maximum approach distance is 3.6 km. The eye altitude range of the airport model is from 221 m (maximum) to 4.6 m (minimum). Maximum longitudinal lateral velocities are 225 knots and maximum sink rate is 10.2 m/s. The maximum pitch is 0.43 rad; heading and roll are unlimited. Maximum angular velocities are 0.75 rad/s (heading), 0.5 rad/s (roll) and 1.5 rad/s (pitch). Maximum angular accelerations are 0.5 rad/s squared (heading), 1.0 rad/s squared (roll) and 3.5 rad/s squared (pitch). Angular field of view is 0.24 rad horizontal ($\pm$0.42 rad) and 0.63 rad vertical (+0.28 rad; $-$0.35 rad).

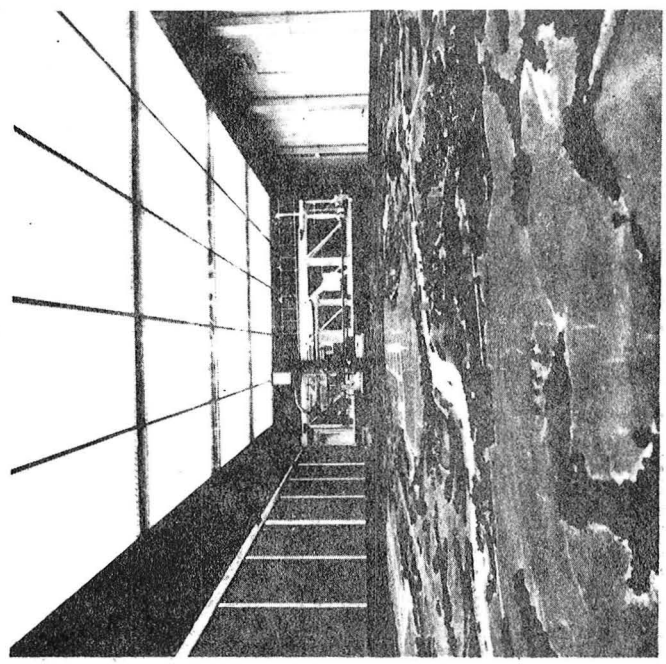

IRAD-96020-65

FIGURE A-3. VISUAL SIMULATOR

APPENDIX 3

COMPONENTS EVALUATED IN THE RELIABILITY ANALYSES AND CRITERIA BASELINE

COMPONENTS EVALUATED

ATA NO.	NAME
22-02-01	Sensing Unit, Wheel Spin-up
22-11-01	Computer, Flt Gdnc Pitch
22-11-02	Panel, Cont, Pitch Gdnc
22-11-03	LVDT, Average Elevator
22-12-01	Computer, Flt Gdnc Roll
22-12-02	Panel, Cont, Directional Gdnc
22-12-03	LVDT, Average Aileron
22-12-08	Sensor, Control Wheel
22-13-01	Computer, Flt Gdnc Yaw
22-13-02	Gyro, Rate, Yaw
22-13-03	Switch, Test, Yaw Damper
22-13-04	Detector, AC Current
22-15-20	Panel Assy, Flt Gdnc Cont
22-15-21	Rack, Flt Gdnc Cont Pnl
22-17-01	Unit, Mode Ann Logic
22-17-02	Annunciator, Mode, Flight
22-18-01	Annunciator, Warning, A/P
22-19-01	Accelerometer Unit, Linear
22-22-01	LVDT, Auto Pitch Trim
22-22-02	Computer, Auto Pitch Trim
22-31-02	Switch Assy, Throt Disc, Left
22-31-03	Switch Assy, Throt Disc, Rt
22-31-04	Panel, Cont, Auto Throttle
22-31-05	Switch, Limit, Min Authority
22-31-07	Computer, A/T Speed Cont
22-31-08	Servo, Duplex Throttle
22-31-09	Gearbox, Auto Throttle
22-31-10	Annunciator, Warning, ATS
22-31-11	Annunciator, Wrn, ATS (F.O.)
22-31-12	Switch, Test, Speed Control
22-33-01	Switch, Test, Stall Warning
22-33-02	Sensor, Angle of Attack
27-11-01	Regulator, Aileron
27-12-01	Actuator Assy, Aileron Trim

ATA NO.	NAME
27-12-02	Trim Assy, Aileron Ctr Wing
27-12-03	Control Assy, Trim
27-13-02	Valve, Check, -8
27-13-03	Valve, Check, -10
27-13-05	Restrictor, 2-Way Visc
27-13-20	Actuator Assy, Inbd Ail
27-13-21	Valve, Flow Cont, Elec-Hyd
27-13-23	Valve, SO, Sol Oper
27-13-24	LVDT, A/P Actuator
27-13-25	Filter, A/P Actuator
27-13-26	Valve, Main Control
27-13-30	Actuator Assy, Outbd Ail
27-13-31	Valve, Flow Cont, Elec-Hyd
27-13-33	Valve, SO, Sol Oper
27-13-34	LVDT, A/P Actuator
27-13-35	Filter, A/P Actuator
27-14-03	Indicator, Surface Pos
27-21-01	Regulator, Rudder
27-22-02	Actuator, Rudder Trim
27-23-02	Valve, Check, -6
27-23-20	Actuator Assy, Lower Rudder
27-23-21	Valve, Flow Cont, Elec-Hyd
27-23-23	Valve, SO, Sol Oper
27-23-24	LVDT, A/P Actuator
27-23-25	Filter, A/P Actuator
27-23-26	Valve, Main Control
27-23-30	Actuator Assy, Upper Rudder
27-23-31	2-Valve, Flow Cont, Elec-Hyd
27-23-33	3-Valve, SO, Sol Oper
27-23-34	3-LVDT, A/P Actuator
27-23-35	1-Filter, A/P Actuator
27-23-36	1-Valve, Main Control
27-26-01	Valve, Check
27-26-02	Valve, Check
27-26-04	Valve, Check

ATA NO.	NAME
27-26-05	Valve, Check
27-26-06	Valve, Shut-off, Motor Oper
27-26-07	Switch, Low Level, Comp
27-26-20	Pump, Motor, Alt Non Rev
27-26-21	Valve S/O, Pressure Oper
27-26-30	Sump, Alt Rud & HS
27-26-31	Sump, Alt Rud
27-26-31	Compensator, Motor Pump
27-31-03	Regulator, Elevator
27-31-04	Regulator, Elevator
27-32-01	Actuator, Duplex, ELF/FL
27-32-02	Programmer, ELF/FL
27-32-03	Indicator, Load Feel, Elev
27-32-05	Transmitter, Load Feel, Elev
27-32-06	Switch, Elev Feel
27-32-07	Switch, Manual Slew
27-33-02	Valve, Check, -12
27-33-03	Valve, Check, -10
27-33-04	Restrictor, 2-Way Visc, Elev
27-33-20	Actuator Assy, Inbd Elev
27-33-21	Valve, Flow Cont, Elec-Hyd
27-33-23	Valve, SO, Sol Oper
27-33-24	LVDT, A/P Actuator
27-33-25	Filter, A/P Actuator
27-33-26	Valve, Main Control
27-33-30	Actuator Assy, Outbd Elev
27-33-31	Valve, Flow Cont, Elec-Hyd
27-33-33	Valve, SO, Sol Oper
27-33-34	LVDT, A/P Actuator
27-33-35	Filter, A/P Actuator
27-33-36	Valve, Main Control
27-35-01	Shaker, Stick
27-41-07	Switch, Wheel, Horiz Stab
27-41-08	Switch, Alt Trim, Horiz Stab
27-43-02	Valve, Check, -8
27-43-04	Brake, Trim, Horiz Stab

ATA NO.	NAME
27-43-05	Valve, Check
27-43-06	Restrictor, 2-Way
27-43-07	Damper, Surge
27-43-30	Motor, Trim, Horiz Stab
27-43-31	Valve, So, Sol Oper
27-43-40	Valve, Control, Primary Trim
27-43-41	Valve, So, Sol Oper
27-43-42	Valve, Flow Cont, Horiz Stab
27-43-43	Valve, Check, -6
27-44-01	Gearbox, Horiz Stab Drive
27-44-04	Actuator Assy, Horiz Stab
27-44-08	Coupling, Torsional
27-45-01	Sensor, Horiz Stab Drum
27-45-02	Sensor, Horiz Stab Elec
27-52-01	Cylinder, Act, Inbd Wing Flap
27-52-02	Cylinder, Act, Outbd Wg Flap
27-52-03	Valve, Control, Wing Flap
27-52-05	Valve, Check, Press
27-52-07	Restrictor, 2-Way, Out Flap
27-52-08	Restrictor, 2-Way, O.R. Flap
27-52-09	Restrictor, 2-Way, Inbd Flap
27-52-10	Restrictor, 2-Way, I.R. Flap
27-52-11	Valve, Falp Lock
27-52-12	Restrictor, 2-Way
27-52-13	Manifold, Flap Up
27-52-14	Valve, Check
27-54-01	Indicator, Pos, Flap/Slat
27-54-02	Transmitter, Pos, Outbd Flap
27-54-03	Transmitter, Flap Handle
27-54-04	Transmitter, Pos, Inbd Flap
27-54-05	Switch, Arming, LDG Flap
27-54-07	Switch, Flap Intlk, G/A
27-56-01	Actuator, Duplex, ELF/FL
27-56-02	Programmer, ELF/FL
27-56-03	Switch, Limiter Cvrd, Flap

ATA NO.	NAME
27-61-20	Actuator Assy, Spoil Dr Svo
27-61-21	Valve, Spoil Dr Svo
27-62-01	Light, Speed Brake
27-63-01	Actuator, Elec, Spoiler Cont
27-63-02	Control Unit, Grd Spoiler
27-65-01	Actuator Assy, Spoiler Cont
27-65-02	Restrictor, 2-Way Visc
27-66-02	Transmitter, Pos, Spoiler
27-68-01	Sensor, Prox Spoiler A
27-68-02	Sensor, Prox Spoiler B
27-71-01	Damper, Buzz, Outbd Ail
27-71-02	Restrictor, Return, Filtered
27-73-01	Damper, Buzz, Elevator
27-73-02	Damper, Elevator
27-73-03	Restrictor, Return, Filtered
27-82-01	Cylinder, Slat
27-82-03	Valve, Control, Slat
27-82-03	Valve, Control, Slat
27-82-04	Valve, Two Speed, Slat
27-82-05	Valve, Check, Press
27-82-06	Restrictor, 2-Way, Ctr Slat
27-82-07	Restrictor, 2-Way, Cutbd Slat
27-82-08	Restrictor, Slat Ret, Outbd
27-82-09	Valve, Check, -6
27-82-11	Cylinder, Slat
27-83-01	Mech Assy, Outbd Slat Drive
27-83-02	Mech Assy, Outbd Slat Drive
27-83-03	Mech Assy, Indb Slat Drive
27-84-02	Sensor, Position, Slat
27-84-03	Indicator, Pos, Slat
27-85-01	Actuator, Elec, Slat Cont
32-24-01	Switch, Ground Sensing
34-11-01	Pitot Tube
34-11-02	Valve, Selector, Static
34-11-03	Plate Assembly, Static

ATA NO.	NAME
34-11-04	Ports, Alternate, Static
34-16-01	Computer, Central Air Data
34-16-02	Probe, Total Air Temp
34-16-03	Switching Unit, Air Data
34-18-01	Indicator, TAT & Thrust Rtg
34-18-03	Computer, Thrust Rtg
34-21-01	Gyro, Directional
34-21-02	Valve, Flux
34-21-03	Coupler, Compass
34-21-06	Controller, Compass
34-21-07	Switching Unit, Compass
34-23-01	Gyro, Vertical
34-23-02	Indicator, Attitude Director
34-23-03	Unit, Attd Mon/Switching
34-23-04	Rack, Gyro Mounting
55-21-01	Elevator Assy, Outbd LH
55-21-02	Elevator Assy, Outbd RH
55-22-01	Elevator Assy, Inbd LH
55-22-02	Elevator Assy, Inbd RH
55-22-03	Elevator Assy, Inbd Dtch LH
55-22-04	Elevator Assy, Inbd Dtch RH
55-41-01	Rudder Assy, Upper Fwd
55-41-02	Rudder Assy, Upper Aft
55-42-01	Rudder Assy, Lower Fwd
55-42-02	Rudder, Assy, Lower Aft
55-51-01	Bearing, Hinge, Horiz Stab
57-51-01	Aileron Assy, Outbd LH
57-51-02	Aileron Assy, Outbd RH
57-51-03	Aileron Assy, Inbd LH
57-51-04	Aileron Assy, Inbd RH
57-52-01	Flap Assy, Cutbd LH
57-52-02	Flap Assy, Outbd RH
57-52-03	Flap Assy, Inbd LH
57-52-04	Flap Assy, Inbd RH
57-53-01	Flap Vane Assy, Outbd LH
57-53-02	Flap Vane Assy, Outbd RH

ATA NO.	NAME
57-53-03	Flap Vane Assy, Inbd LH
57-53-04	Flap Vane Assy, Inbd RH
57-54-01	Spoiler Assy, #1 LH
57-54-02	Spoiler Assy, #1 RH
57-54-03	Spoiler Assy, #2 LH
57-54-04	Spoiler Assy, #2 RH
57-54-05	Spoiler Assy, #3 LH
57-54-06	Spoiler Assy, #3 RH
57-54-07	Spoiler Assy, #4 LH
57-54-08	Spoiler Assy, #4 RH
57-54-09	Spoiler Assy, #5 LH
57-54-10	Spoiler Assy, #5 RH
57-55-01	Slat Assy, #1 LH
57-55-02	Slat Assy, #2 LH
57-55-03	Slat Assy, #3 LH
57-55-04	Slat Assy, #4 LH
57-55-05	Slat Assy, #5 LH
57-55-06	Slat Assy, #6 LH
57-55-07	Slat Assy, #7 LH
57-55-08	Slat Assy, #8 LH
57-55-11	Slat Assy, #1 RH
57-55-12	Slat Assy, #2 RH
57-55-13	Slat Assy, #3 RH
57-55-14	Slat Assy, #4 RH
57-55-15	Slat Assy, #5 RH
57-55-16	Slat Assy, #6 RH
57-55-17	Slat Assy, #7 RH
57-55-18	Slat Assy, #8 RH
76-11-01	Switch Cam Assy, Throttle
76-11-02	Clutch Assy, A/T Drive
76-11-03	Switch Cam Assy, Throttle
76-11-04	Switch Cam Assy, Throttle
76-11-05	Switch Assy, Throt T/O & G/A
76-11-06	Switch, RTC #3 Eng 2
77-32-11	Cable Assy, Engine
77-32-12	Cable Assy, Wing Pylon
77-32-13	Cable Assy, Tail Pylon

APPENDIX 4
EXPOSURE TIME FOR PROBABILITY ANALYSIS

In the course of conducting the RSSAS study, several questions were raised on the intended meaning and interpretation of certain phrases used by the FAA and industry groups to describe the exposure parameter over which a particular risk probability applies. Two phrases that have caused some confusion when used as modifers to a probability value are "per flight or flight hour," and "for each trial or hour of exposure." These two phrases are synonomous when applied to aircraft, and the former is more commonly used for that purpose.

The following discussion attempts to accomplish three things:

1. Explain the prevailing interpretation of these phrases.

2. Point out that there is not international agreement on a standard-exposure-time parameter.

3. Discuss the implications of the lack of a standard on probabilistic risk analyses of complex aircraft systems.

To quantify the probability of an event occurring, one must define an exposure parameter (time, trials, cycles, etc.) over which the probability applies. For example, the probability that a coin will fall head-up in one toss is quite different from the probability that it will fall head-up once in 10 tosses. Although this appears obvious and almost trite, it can become a disturbing issue when exposure parameters are required for calculating the probability of specific functional fault conditions occurring in sophisticated aircraft systems.

It is necessary to first establish the exposure parameter for the undesired end-event of interest without regard for the elements that can contribute to causing the event. For aircraft, this parameter is usually expressed in terms of a flight or an increment of flight time. Regulatory agencies and industry groups worldwide have been, and still are, trying to reach agreement on a standard for end-event exposure parameters that can be used by all groups for validating system designs.

For systems that are critical for only a brief period during a flight, such as automatic landing systems, there is a consensus that the end-event exposure parameter is that brief time period during which the aircraft is at risk should certain functional fault conditions occur.

For active control systems such as RSSAS or load alleviation systems, which may in the future be critical to the airworthiness of the airplane throughout the flight duration, not all parties agree on a standard exposure time, or whether a standard is necessary. A currently active ICAO study group is attempting to develop guidance material on the certification of automatic landing systems and automatic flight control systems. The following is from the minutes of the group's August 1978 meeting:

> "It was proposed and agreed by the Study Group that the probability definitions used in the United States should be included in the draft material as an Appendix because they differ in detail from those presently in the text. The Study Group was, however, informed that firstly the material adopted contains intermediate levels which are not defined in the U.S. documents. Secondly, the numerical probability values are expressed 'per hour of flight determined for the expected mean flight time' whereas the U.S. values are expressed 'per flight or flight hour'. Thus there is only direct numerical equivalence for aeroplanes with an average flight time of one hour, although actual differences will be small for the normal range of flight times. Therefore, the use of other probability definitions in the U.S. does not affect the applicability of the material because the probability levels are similar in the actual certification of automatic landing systems."

A note to members subsequent to that meeting elaborated further for consideration by the members:

> "The meaning of the term 'expected mean flight time' . . . was considered to need some clarification and consequently:
>
> (i) The term was amended to read 'expected mean flight time,

i.e., duration of average individual flight for the type of aeroplane concerned'.

(ii) to further clarify this point, the second sentence of paragraph 1.4.1 of Appendix C was replaced by the following text (based on paragraph 2.8 of Attachment B to Study Note No. 15). 'The probabilities should be established as the risk per hour in a flight where the duration of the flight is equal to the expected mean flight time for type of aeroplane concerned. For example, in systems where the hazard results from multiple failure in the same flight, the numerical assessment must take account of the likelihood that this will occur in a flight of expected average duration. Similarly, in those cases where failures are only critical for a particular period of flight, the hazard may be averaged over the whole of the expected mean flight time.' "

For a function that is critical for the entire flight length, it is clear that the end-event exposure time is a variable, since not all flights of a typical airplane are the same length. One might calculate an average risk by using the average flight time, as is suggested by the ICAO Study Group, or a worst-case risk by using the longest flight time possible for the particular aircraft type. The current FAA view is understood to be that one hour is the longest end-event exposure time that must be used in risk analyses of this type, but if the actual critical exposure time is less than one hour, the actual value may be used. The ICAO Study Group seems to agree on the latter point. This actual lessor value comes from the words "per flight." The upper limit of one hour results from the words "per flight hour." The risk probability thus arrived at is for one hour of exposure to the end undesired event. It is important to recognize that a probability calculated for one hour cannot be linearly extrapolated to longer times even though the expression "per hour" is used, unless there is no redundancy and there are no latent undetected failure modes in the system.

The following simple example may serve to illustrate the implication of the current interpretation. For an event that occurs ramdomly in time at a reasonably constant rate (λ), the probability (Q) that the event will occur in a specified time space ($t = t_2 - t_1$) may be expressed as:

$$Q = 1 - e^{-\lambda t},$$

if it is known that the event has not occurred prior to t_1. For small values of λt, this expression may be closely approximated, for simplicity, by:

$$Q \approx \lambda t$$

If a device has a known failure rate of, say, nine failures per million hours, and two of these devices are used in parallel so that both must fail before a critical function is lost, the probability (Q_F) of losing the function is:

$$Q_F = Q_d \times Q_d = Q^2 = (\lambda_d t)^2 = (9 \times 10^{-6})^2 t^2 = (8.1 \times 10^{-11}) t^2$$

If this function is required for only a short time, such as during an automatic landing, and both devices have been verified operating prior to engaging the critical flight phase, then the value of t is quite small, say about 10 minutes. The probability of losing this function during the critical time period is then:

$$Q_F = (8.1 \times 10^{-11}) \left(\frac{10}{60}\right)^2 = 2.3 \times 10^{-12}.$$

Or, if this function is critical for one hour of the flight,

$$Q_F = (8.1 \times 10^{-11}) (1)^2 = 8.1 \times 10^{-11}.$$

For longer flight lengths, the probability will increase (in this example, as the square of the flight time), but the current FAA view is that such an increase for real systems will be well within the combined accuracy tolerances of the required probability and the data and assumptions used in the analysis, at least for values of t up to the average flight times of commercial aircraft.

The advantage of specifying allowable risk levels on a "per-flight-hour" basis is that it allows comparing, analyzing, and certifying various

system configurations to a common standard that is independent of the mission range of the vehicles they may eventually be used on. Also, within reasonable limits, if the risk requirement is achieved with some margin, the effect of some increase in exposure time does not usually increase the risk to a value greater than the required certification value. In the above example the value of t can go to 3.5 hours before the threshold of 1×10^{-9} is crossed.

$$1 \times 10^{-9} = (8.1 \times 10^{-11})t^2$$

$$t = 3.5 \text{ hours}$$

Or, to view it another way, the device failure rate could be as much as 3-1/2 times worse than was estimated for the one-hour case.

$$1 \times 10^{-9} = (\lambda)^2 (1)^2$$

$$\lambda = 32 \text{ failures per million hours}$$

Further, when analyzing actual systems with significant redundancies at various levels, and several states of degradation or reconfiguration, several different exposure times are almost always required for various system elements to account for latent failures in redundant or intermittently used functions. The exposure time for potential failures of such elements is always conservatively taken as the time from when the element was last known to be functioning, to the time its operation is again verified. Even for automatic landing systems, with an end-event exposure time of only a few minutes for a flight, some elements within the system may have exposure-to-failure times of hundreds or thousands of hours. These times are applicable, for example, to devices whose failure could remain undetected until certain special tests are performed. Often these devices become the final constraint on the system risk level, so that the difference in the end-event risk between a one-hour flight and one several hours long is relatively small.

The potential impact of latent failures is recognized by all regulatory groups and industry. Below is another quotation from the material being developed by the ICAO Study Group:

> "Dormant Failures (latent)
> When the failure of a device can remain undetected in normal operation, the frequency with which the device is checked will directly influence the probability that such a failure is present on any particular occasion. This should be taken into account when assessing the probabilities of any failure conditions which include the dormant failures of monitoring devices or unchecked redundant items."

There are, of course, many additional important factors that must be considered in conducting a comprehensive safety assessment of any aircraft system. The preceding discussion is intended only to clarify, and perhaps justify, the prevailing interpretation of the term "per flight or flight hour" as used by the FAA.

APPENDIX 5

NETWORK RELIABILITY ANALYSIS MODEL RESULTS FOR RSSAS

The methodology associated with the computer program results contained in this appendix is discussed in Paragraph 4.2.2.1.

Case 1

Triple-Redundant Computers

All elements operative at start of 1-, 2-, and 5-hour flights.

Case 2

Triple-Redundant Computers

Maximum number of elements inoperative at start of 1-, 2-, and 5-hour flights.

Case 3

Dual Computers

All elements operative at start of 1-, 2-, and 5-hour flights.

Case 4

Dual Computers

Maximum number of elements inoperative at start of 1-, 2-, and 5-hour flights.

N E T W O R K R E L I A B I L I T Y A N A L Y S I S P R O G R A M

RSSAS RELIABILITY ANALYSIS (CONF 1) MCDONNELL-DOUGLAS CORP.
FLIGHT TIME 1.00 HRS. RUN DATE 01/18/79

CODE	FUNCTION LOST	PROBABILITY OF FAILURE
A	RSSAS ONLY	0.259E-09
AA	RSSAS ALL FUNCTIONS	0.272E-09
B	YAW DAMPER	0.858E-07
C	STALL WARNING	0.258E-05
D	ELEVATOR LOAD FEEL	0.970E-07
E	FLAP LIMITING	0.970E-07
ALL	ALL FUNCTIONS	0.180E-10
AAB	RSSAS AND YAW DAMPER	0.245E-09

CASE 1, ONE HOUR

N E T W O R K R E L I A B I L I T Y A N A L Y S I S P R O G R A M

RSSAS RELIABILITY ANALYSIS (CONF 1) MCDONNELL-DOUGLAS CORP.
FLIGHT TIME 2.00 HRS. RUN DATE 01/18/79

CODE	FUNCTION LOST	PROBABILITY OF FAILURE
A	RSSAS ONLY	0.107E-08
AA	RSSAS ALL FUNCTIONS	0.118E-08
B	YAW DAMPER	0.343E-06
C	STALL WARNING	0.552E-05
D	ELEVATOR LOAD FEEL	0.388E-06
E	FLAP LIMITING	0.388E-06
ALL	ALL FUNCTIONS	0.144E-09
AAB	RSSAS AND YAW DAMPER	0.106E-08

CASE 1, TWO HOURS

N E T W O R K R E L I A B I L I T Y A N A L Y S I S P R O G R A M

RSSAS RELIABILITY ANALYSIS (CONF 1) MCDONNELL-DOUGLAS CORP.
FLIGHT TIME 5.00 HRS. RUN DATE 01/18/79

CODE	FUNCTION LOST	PROBABILITY OF FAILURE
A	RSSAS ONLY	0.737E-08
AA	RSSAS ALL FUNCTIONS	0.898E-08
B	YAW DAMPER	0.214E-05
C	STALL WARNING	0.165E-04
D	ELEVATOR LOAD FEEL	0.242E-05
E	FLAP LIMITING	0.242E-05
ALL	ALL FUNCTIONS	0.222E-08
AAB	RSSAS AND YAW DAMPER	0.810E-08

CASE 1, FIVE HOURS

N E T W O R K R E L I A B I L I T Y A N A L Y S I S P R O G R A M

RSSAS RELIABILITY ANALYSIS (CONF 1) MCDONNELL-DOUGLAS CORP.
FLIGHT TIME 1.00 HRS. RUN DATE 01/18/79

CODE	COMPONENT	PROBABILITY OF FAILURE
X1	VERTICAL GYRO1	0.510E-03
X2	VERTICAL GYRO2	0.510E-03
X3	VERTICAL GYRO3	0.510E-03
X4	ANGLE OF ATTACK 1	0.330E-03
X5	ANGLE OF ATTACK 2	0.330E-03
X6	AIR DATA COMPUTER 1	0.100E-03
X7	AIR DATA COMPUTER 2	0.100E-03
X8	YAW RATE GYRO 1	0.860E-04
X9	YAW RATE GYRO 2	0.860E-04
X10	FLAP POSITION 1	0.200E-05
X11	FLAP POSITION 2	0.200E-05
X12	SLAT POSITION 1	0.610E-04
X13	SLAT POSITION 2	0.610E-04
X14	SCDP1 (ALL FUNCTIONS)	0.800E-04
X15	SCDP2 (ALL FUNCTIONS)	0.800E-04
X16	SCDP3 (ALL FUNCTIONS)	0.800E-04
Y14	SCDP1 (RSSAS ONLY)	0.625E-04
Y15	SCDP2 (RSSAS ONLY)	0.625E-04
Y16	SCDP3 (RSSAS ONLY)	0.625E-04
X17	CPU1 (ALL FUNCTIONS)	0.260E-03
X18	CPU2 (ALL FUNCTIONS)	0.260E-03
X19	CPU3 (ALL FUNCTIONS)	0.260E-03
Y17	CPU1 (RSSAS ONLY)	0.188E-03
Y18	CPU2 (RSSAS ONLY)	0.188E-03
Y19	CPU3 (RSSAS ONLY)	0.188E-03
X20	STICK SHAKER	0.240E-05
X21	RUDDER ACTUATOR 1	0.500E-05
X22	RUDDER ACTUATOR 2	0.500E-05
X23	ELEVATOR ACTUATOR 1	0.500E-05
X24	ELEVATOR ACTUATOR 2	0.500E-05
X25	ELEVATOR LOAD FEEL ACTUATOR 1	0.351E-04
X26	ELEVATOR LOAD FEEL ACTUATOR 2	0.350E-04
X27	FLAP LIMITER ACTUATOR 1	0.350E-04
X28	FLAP LIMITER ACTUATOR 2	0.350E-04
X29	EHV,MOD,LVDT,AND S.O.V. 1	0.900E-05
X30	EHV,MOD,LVDT,AND S.O.V. 2	0.900E-05
X31	EHV,MOD,LVDT,AND S.O.V. 3	0.900E-05
X32	EHV,MOD,LVDT,AND S.O.V. 4	0.900E-05
X33	HYD. SYSTEM 1	0.150E-04
X34	HYD. SYSTEM 2	0.150E-04

COMPONENT HOURLY FAILURE PROBABILITIES

NETWORK RELIABILITY ANALYSIS PROGRAM

RSSAS RELIABILITY ANALYSIS (CONF 1) MCDONNELL-DOUGLAS CORP.
FLIGHT TIME 1.00 HRS. RUN DATE 01/18/79

CODE	FUNCTION LOST	PROBABILITY OF FAILURE
A	RSSAS ONLY	0.255E-06
AA	RSSAS ALL FUNCTIONS	0.294E-06
B	YAW DAMPER	0.366E-03
C	STALL WARNING	0.395E-03
D	ELEVATOR LOAD FEEL	0.295E-03
E	FLAP LIMITING	0.295E-03
ALL	ALL FUNCTIONS	0.740E-07
AAB	RSSAS AND YAW DAMPER	0.859E-07

CASE 2, ONE HOUR

NETWORK RELIABILITY ANALYSIS PROGRAM

RSSAS RELIABILITY ANALYSIS (CONF 1) MCDONNELL-DOUGLAS CORP.
FLIGHT TIME 2.00 HRS. RUN DATE 01/18/79

CODE	FUNCTION LOST	PROBABILITY OF FAILURE
A	RSSAS ONLY	0.102E-05
AA	RSSAS ALL FUNCTIONS	0.117E-05
B	YAW DAMPER	0.732E-03
C	STALL WARNING	0.791E-03
D	ELEVATOR LOAD FEEL	0.590E-03
E	FLAP LIMITING	0.590E-03
ALL	ALL FUNCTIONS	0.296E-06
AAB	RSSAS AND YAW DAMPER	0.344E-06

CASE 2, TWO HOURS

NETWORK RELIABILITY ANALYSIS PROGRAM

RSSAS RELIABILITY ANALYSIS (CONF 1) MCDONNELL-DOUGLAS CORP.
FLIGHT TIME 5.00 HRS. RUN DATE 01/18/79

CODE	FUNCTION LOST	PROBABILITY OF FAILURE
A	RSSAS ONLY	0.637E-05
AA	RSSAS ALL FUNCTIONS	0.734E-05
B	YAW DAMPER	0.183E-02
C	STALL WARNING	0.198E-02
D	ELEVATOR LOAD FEEL	0.148E-02
E	FLAP LIMITING	0.148E-02
ALL	ALL FUNCTIONS	0.185E-05
AAB	RSSAS AND YAW DAMPER	0.216E-05

CASE 2, FIVE HOURS

N E T W O R K R E L I A B I L I T Y A N A L Y S I S P R O G R A M

RSSAS RELIABILITY ANALYSIS (CONF 1) MCDONNELL-DOUGLAS CORP.
FLIGHT TIME 1.00 HRS. RUN DATE 01/18/79

CODE	COMPONENT	PROBABILITY OF FAILURE	
X1	VERTICAL GYRO1	0.510E-03	
X2	VERTICAL GYRO2	0.510E-03	
X3	VERTICAL GYRO3	0.510E-03	INOP
X4	ANGLE OF ATTACK 1	0.330E-03	
X5	ANGLE OF ATTACK 2	0.330E-03	INOP
X6	AIR DATA COMPUTER 1	0.100E-03	
X7	AIR DATA COMPUTER 2	0.100E-03	
X8	YAW RATE GYRO 1	0.860E-04	
X9	YAW RATE GYRO 2	0.860E-04	INOP
X10	FLAP POSITION 1	0.200E-05	
X11	FLAP POSITION 2	0.200E-05	INOP
X12	SLAT POSITION 1	0.610E-04	
X13	SLAT POSITION 2	0.610E-04	INOP
X14	SCDP1 (ALL FUNCTIONS)	0.800E-04	
X15	SCDP2 (ALL FUNCTIONS)	0.800E-04	INOP
X16	SCDP3 (ALL FUNCTIONS)	0.800E-04	
Y14	SCDP1 (RSSAS ONLY)	0.625E-04	
Y15	SCDP2 (RSSAS ONLY)	0.625E-04	INOP
Y16	SCDP3 (RSSAS ONLY)	0.625E-04	
X17	CPU1 (ALL FUNCTIONS)	0.260E-03	
X18	CPU2 (ALL FUNCTIONS)	0.260E-03	INOP
X19	CPU3 (ALL FUNCTIONS)	0.260E-03	
Y17	CPU1 (RSSAS ONLY)	0.188E-03	
Y18	CPU2 (RSSAS ONLY)	0.188E-03	INOP
Y19	CPU3 (RSSAS ONLY)	0.188E-03	
X20	STICK SHAKER	0.240E-05	
X21	RUDDER ACTUATOR 1	0.500E-05	
X22	RUDDER ACTUATOR 2	0.500E-05	INOP
X23	ELEVATOR ACTUATOR 1	0.500E-05	
X24	ELEVATOR ACTUATOR 2	0.500E-05	
X25	ELEVATOR LOAD FEEL ACTUATOR 1	0.351E-04	
X26	ELEVATOR LOAD FEEL ACTUATOR 2	0.350E-04	INOP
X27	FLAP LIMITER ACTUATOR 1	0.350E-04	
X28	FLAP LIMITER ACTUATOR 2	0.350E-04	INOP
X29	EHV,MOD,LVDT,AND S.O.V. 1	0.900E-05	
X30	EHV,MOD,LVDT,AND S.O.V. 2	0.900E-05	
X31	EHV,MOD,LVDT,AND S.O.V. 3	0.900E-05	
X32	EHV,MOD,LVDT,AND S.O.V. 4	0.900E-05	
X33	HYD. SYSTEM 1	0.150E-04	
X34	HYD. SYSTEM 2	0.150E-04	

COMPONENT HOURLY FAILURE PROBABILITIES WITH CASE 2 INOPERATIVE COMPONENTS NOTED

NETWORK RELIABILITY ANALYSIS PROGRAM

RSASS RELIABILITY ANALYSIS (CONF 2) MCDONNELL-DOUGLAS CORP.
FLIGHT TIME 1.00 HRS. RUN DATE 01/18/79

CODE	FUNCTION LOST	PROBABILITY OF FAILURE
A	RSSAS ONLY	0.414E-07
AA	RSSAS ALL FUNCTIONS	0.768E-07
B	YAW DAMPER	0.922E-07
C	STALL WARNING	0.259E-05
D	ELEVATOR LOAD FEEL	0.103E-06
E	FLAP LIMITING	0.103E-06
ALL	ALL FUNCTIONS	0.740E-07
AAB	RSSAS AND YAW DAMPER	0.742E-07

CASE 3, ONE HOUR

NETWORK RELIABILITY ANALYSIS PROGRAM

RSASS RELIABILITY ANALYSIS (CONF 2) MCDONNELL-DOUGLAS CORP.
FLIGHT TIME 2.00 HRS. RUN DATE 01/18/79

CODE	FUNCTION LOST	PROBABILITY OF FAILURE
A	RSSAS ONLY	0.166E-06
AA	RSSAS ALL FUNCTIONS	0.307E-06
B	YAW DAMPER	0.369E-06
C	STALL WARNING	0.555E-05
D	ELEVATOR LOAD FEEL	0.414E-06
E	FLAP LIMITING	0.414E-06
ALL	ALL FUNCTIONS	0.296E-06
AAB	RSSAS AND YAW DAMPER	0.297E-06

CASE 3, TWO HOURS

NETWORK RELIABILITY ANALYSIS PROGRAM

RSASS RELIABILITY ANALYSIS (CONF 2) MCDONNELL-DOUGLAS CORP.
FLIGHT TIME 5.00 HRS. RUN DATE 01/18/79

CODE	FUNCTION LOST	PROBABILITY OF FAILURE
A	RSSAS ONLY	0.103E-05
AA	RSSAS ALL FUNCTIONS	0.192E-05
B	YAW DAMPER	0.230E-05
C	STALL WARNING	0.167E-04
D	ELEVATOR LOAD FEEL	0.258E-05
E	FLAP LIMITING	0.258E-05
ALL	ALL FUNCTIONS	0.185E-05
AAB	RSSAS AND YAW DAMPER	0.186E-05

CASE 3, FIVE HOURS

N E T W O R K R E L I A B I L I T Y A N A L Y S I S P R O G R A M

RSASS RELIABILITY ANALYSIS (CONF 2) MCDONNELL-DOUGLAS CORP.
FLIGHT TIME 1.00 HRS. RUN DATE 01/19/79

CODE	FUNCTION LOST	PROBABILITY OF FAILURE
A	RSSAS ONLY	0.245E-06
AA	RSSAS ALL FUNCTIONS	0.281E-06
B	YAW DAMPER	0.366E-03
C	STALL WARNING	0.395E-03
D	ELEVATOR LOAD FEEL	0.295E-03
E	FLAP LIMITING	0.295E-03
ALL	ALL FUNCTIONS	0.740E-07
AAB	RSSAS AND YAW DAMPER	0.756E-07

CASE 4, ONE HOUR

N E T W O R K R E L I A B I L I T Y A N A L Y S I S P R O G R A M

RSASS RELIABILITY ANALYSIS (CONF 2) MCDONNELL-DOUGLAS CORP.
FLIGHT TIME 2.00 HRS. RUN DATE 01/19/79

CODE	FUNCTION LOST	PROBABILITY OF FAILURE
A	RSSAS ONLY	0.981E-06
AA	RSSAS ALL FUNCTIONS	0.112E-05
B	YAW DAMPER	0.732E-03
C	STALL WARNING	0.791E-03
D	ELEVATOR LOAD FEEL	0.590E-03
E	FLAP LIMITING	0.590E-03
ALL	ALL FUNCTIONS	0.296E-06
AAB	RSSAS AND YAW DAMPER	0.303E-06

CASE 4, TWO HOURS

N E T W O R K R E L I A B I L I T Y A N A L Y S I S P R O G R A M

RSASS RELIABILITY ANALYSIS (CONF 2) MCDONNELL-DOUGLAS CORP.
FLIGHT TIME 5.00 HRS. RUN DATE 01/19/79

CODE	FUNCTION LOST	PROBABILITY OF FAILURE
A	RSSAS ONLY	0.613E-05
AA	RSSAS ALL FUNCTIONS	0.701E-05
B	YAW DAMPER	0.183E-02
C	STALL WARNING	0.198E-02
D	ELEVATOR LOAD FEEL	0.148E-02
E	FLAP LIMITING	0.148E-02
ALL	ALL FUNCTIONS	0.185E-05
AAB	RSSAS AND YAW DAMPER	0.190E-05

CASE 4, FIVE HOURS

APPENDIX 6
AUGMENTATION BLOCK DIAGRAMS

This section contains block diagrams of all the initial control laws with the exception of those containing longitudinal acceleration. Material presented here is discussed in Section 5.

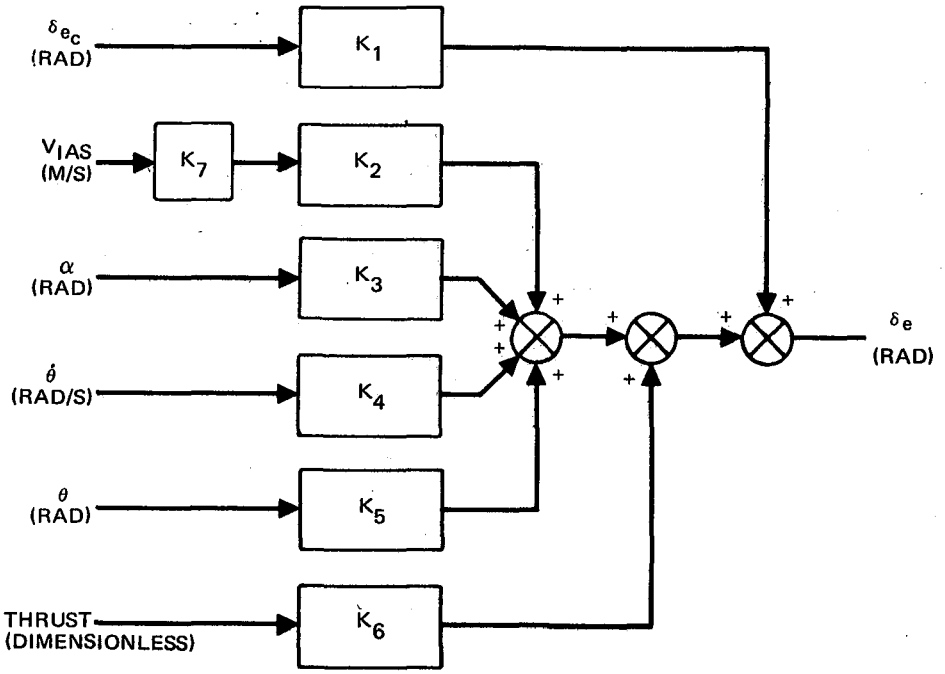

$K_1 = 0.5$
$K_2 = 0.63$
$K_3 = 0.1147$
$K_4 = 0.022876$
$K_5 = 0.009264$
$K_6 = 0.29$
$K_7 = 1.0/V_{TRIM}$

CONTROL LAW NO. 1 – CRUISE

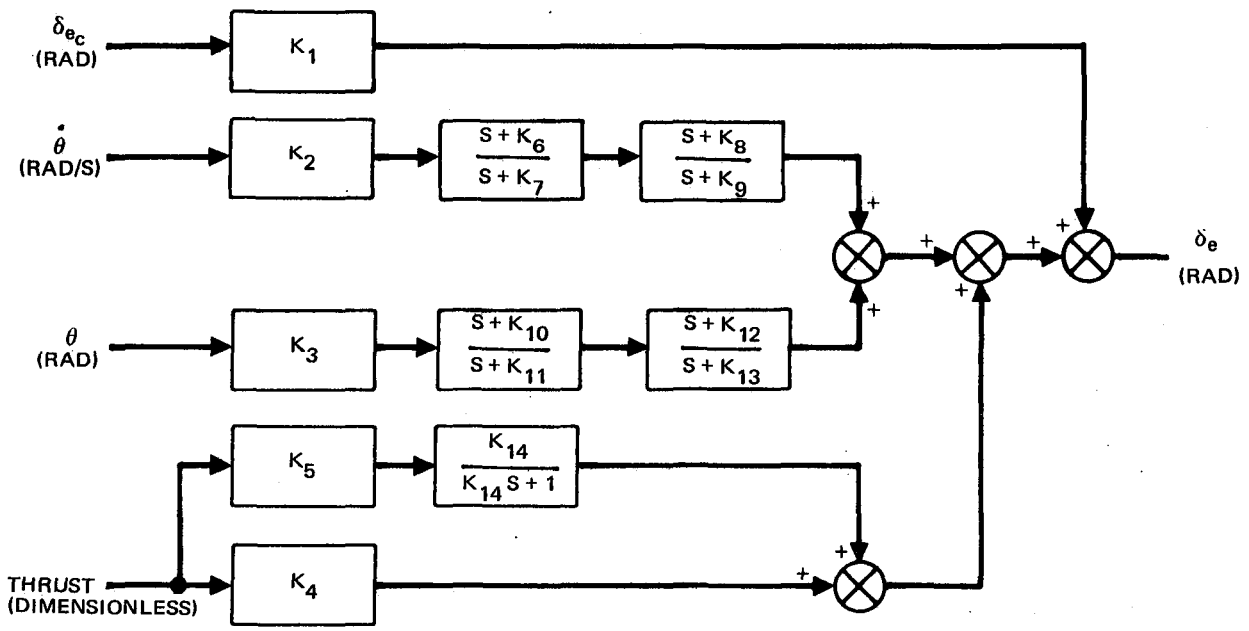

$K_1 = 0.4098$
$K_2 = 0.02289$
$K_3 = 0.009267$
$K_4 = 0.29$
$K_5 = 0.074$
$K_6 = 3.651$
$K_7 = 0.4963$
$K_8 = -0.1922$
$K_9 = 0.00559$
$K_{10} = 0.4498$
$K_{11} = 0.4963$
$K_{12} = -2.772$
$K_{13} = 0.00559$
$K_{14} = 178.0$

CONTROL LAW NO. 2 – CRUISE

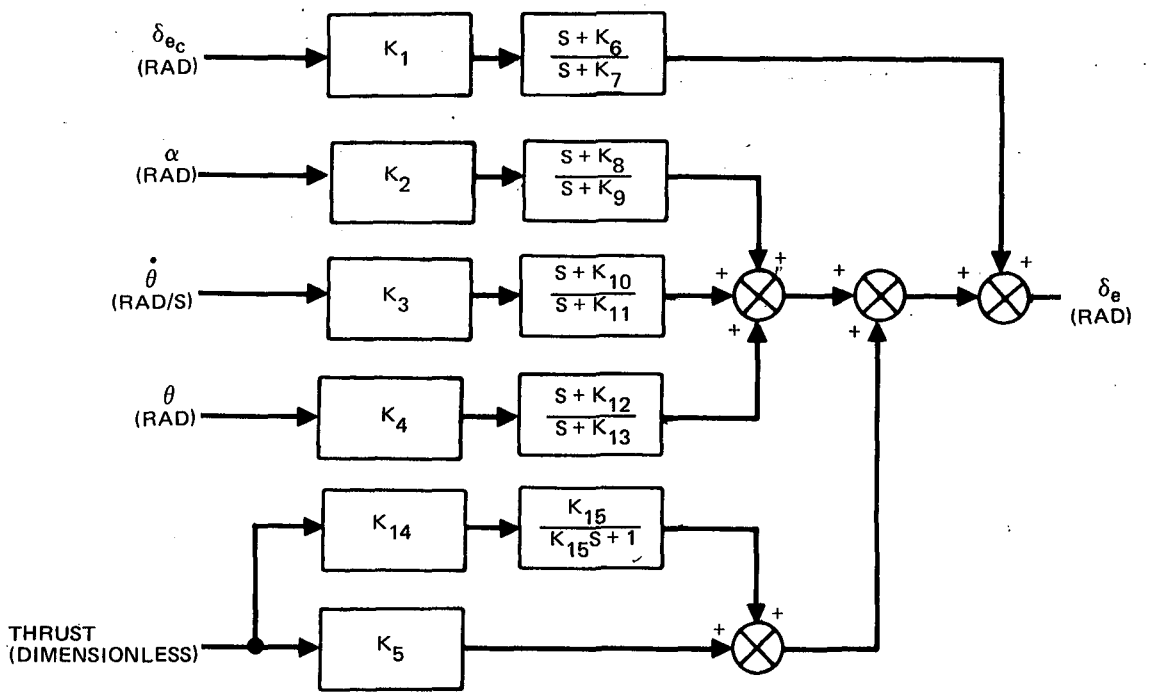

$K_1 = 0.4140$
$K_2 = 0.1147$
$K_3 = 0.02287$
$K_4 = 0.009262$
$K_5 = 0.29$
$K_6 = 0.00399$
$K_7 = 0.001728$
$K_8 = 0.03718$
$K_9 = 0.001728$
$K_{10} = -1.9899$
$K_{11} = 0.001728$
$K_{12} = -2.7979$
$K_{13} = 0.001728$
$K_{14} = 0.082$
$K_{15} = 565.0$

CONTROL LAW NO. 3 – CRUISE

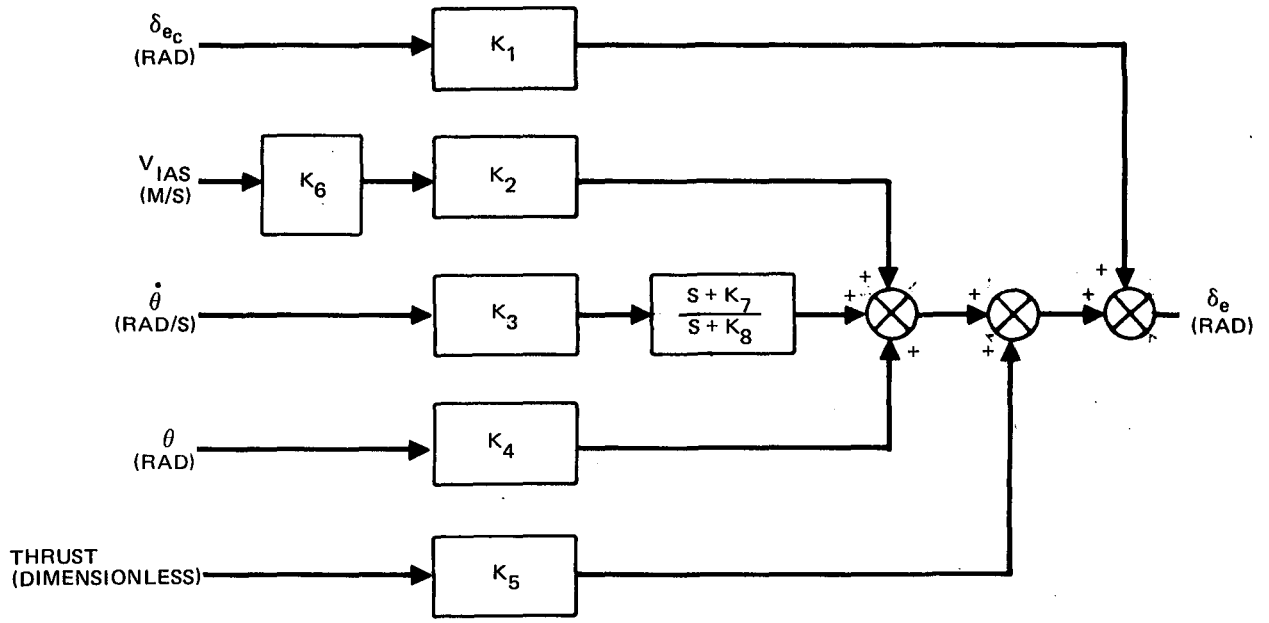

$K_1 = 0.6100$
$K_2 = 0.5621$
$K_3 = 0.02289$
$K_4 = 0.008814$
$K_5 = 0.29$
$K_6 = 1.0/V_{TRIM}$
$K_7 = 5.4485$
$K_8 = 0.5002$

CONTROL LAW NO. 4 – CRUISE

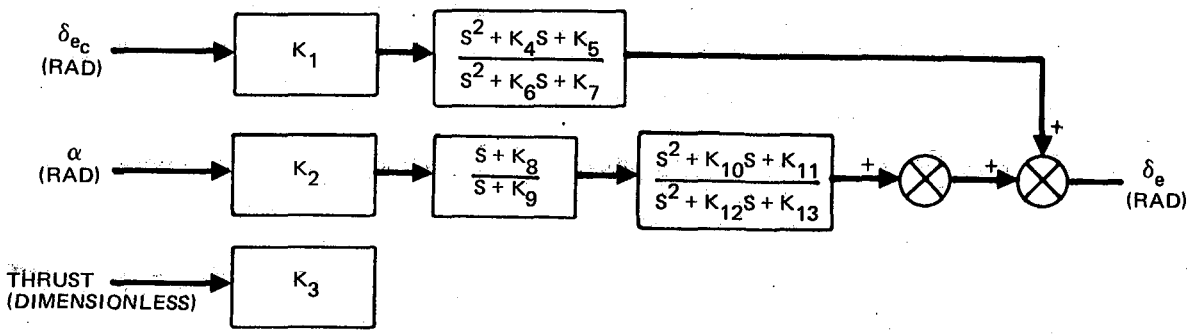

$K_1 = 0.51035$
$K_2 = 0.1195$
$K_3 = \text{NIL}$
$K_4 = 0.05$
$K_5 = 0.03338$

$K_6 = 0.02$
$K_7 = 0.004709$
$K_8 = 1.138$
$K_9 = 1.64$
$K_{10} = -0.2198$

$K_{11} = -0.02793$
$K_{12} = 0.02$
$K_{13} = 0.004709$

CONTROL LAW NO. 5 – CRUISE

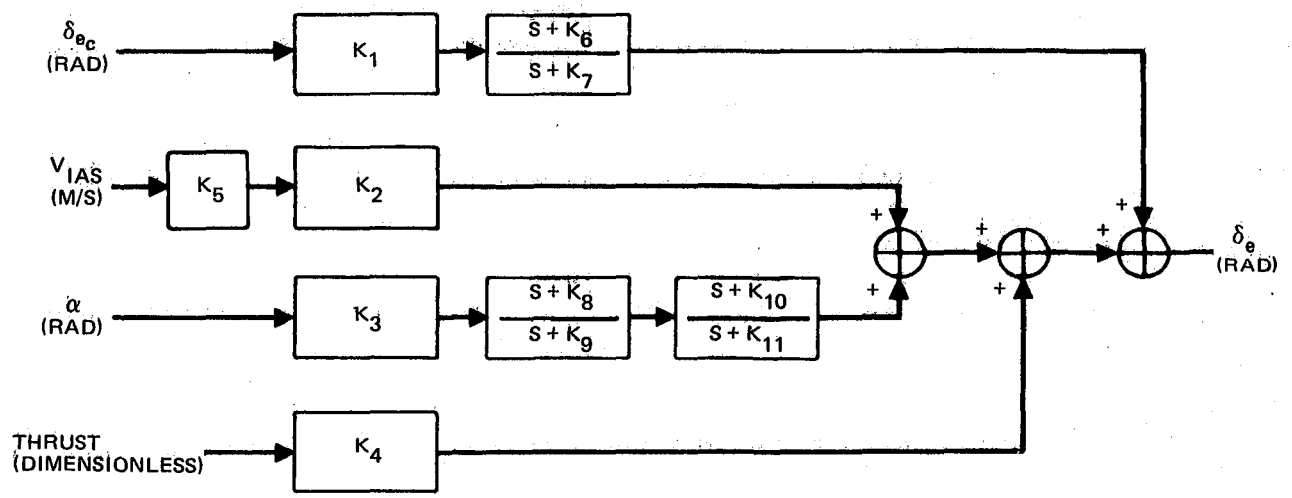

$K_1 = 0.522$
$K_2 = 0.5943$
$K_3 = 0.1148$
$K_4 = 0.29$
$K_5 = 1.0/V_{TRIM}$

$K_6 = 0.15$
$K_7 = 0.2$
$K_8 = 0.606$
$K_9 = 0.6939$
$K_{10} = 0.065$
$K_{11} = 0.2$

CONTROL LAW NO. 6 – CRUISE

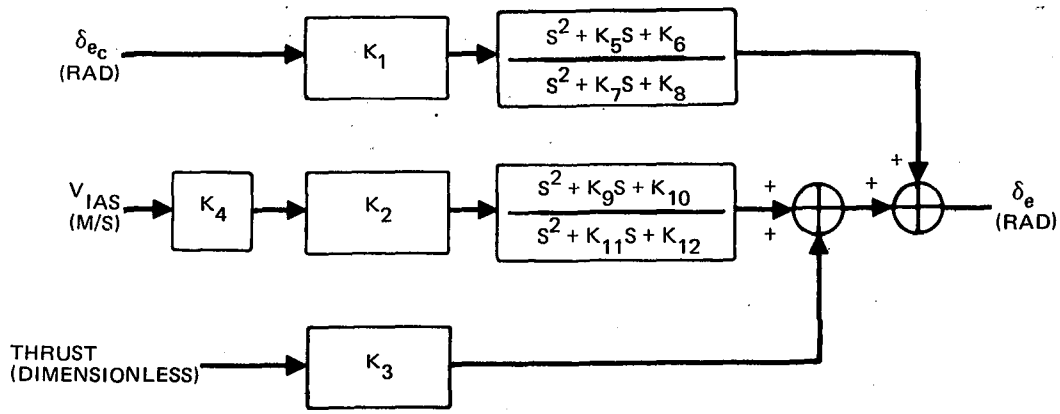

$K_1 = 0.5514$
$K_2 = 0.08297$
$K_3 = 0.31$
$K_4 = 1.0/V_{TRIM}$
$K_5 = 1.18$
$K_6 = 0.8086$
$K_7 = 1.242$
$K_8 = 1.1902$
$K_9 = 7.302$
$K_{10} = 8.2718$
$K_{11} = 1.242$
$K_{12} = 1.1902$

CONTROL LAW NO. 7 – CRUISE

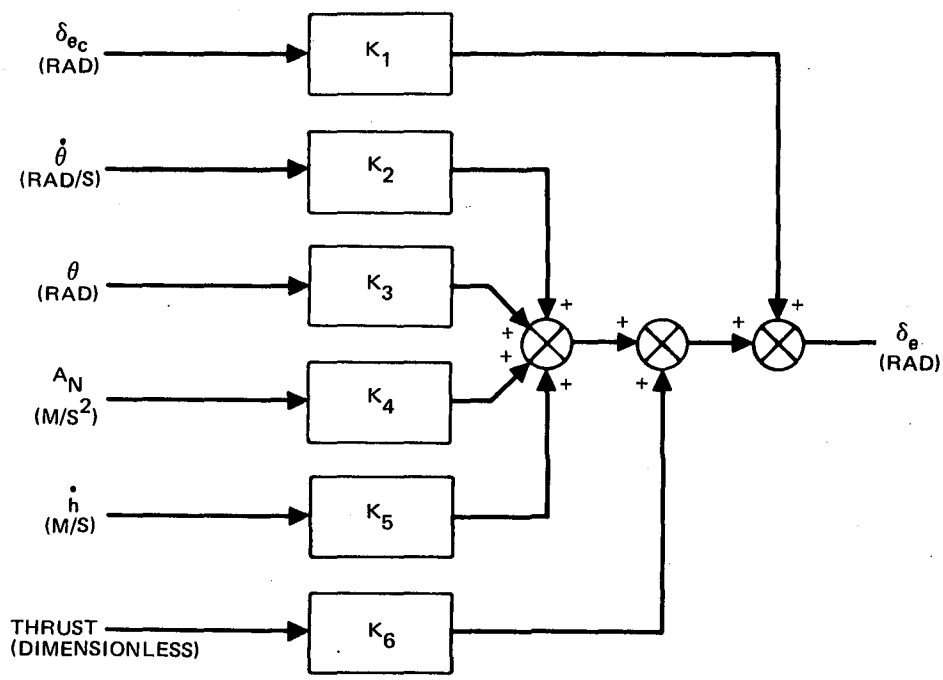

$K_1 = 0.6329$
$K_2 = 0.02413$
$K_3 = -0.929$
$K_4 = 0.0008611$
$K_5 = 0.000367$
$K_6 = 0.25$

CONTROL LAW NO. 12 – CRUISE

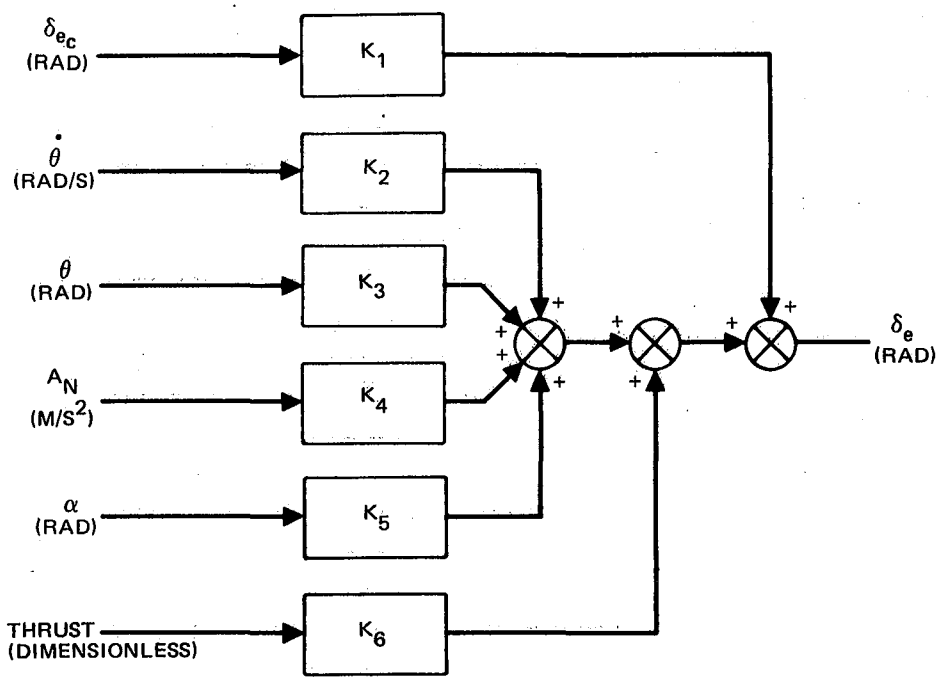

$K_1 = 0.6329$ $K_4 = 0.0008611$
$K_2 = 0.0241$ $K_5 = -0.9355$
$K_3 = 0.006599$ $K_6 = 0.25$

CONTROL LAW NO. 13 – CRUISE

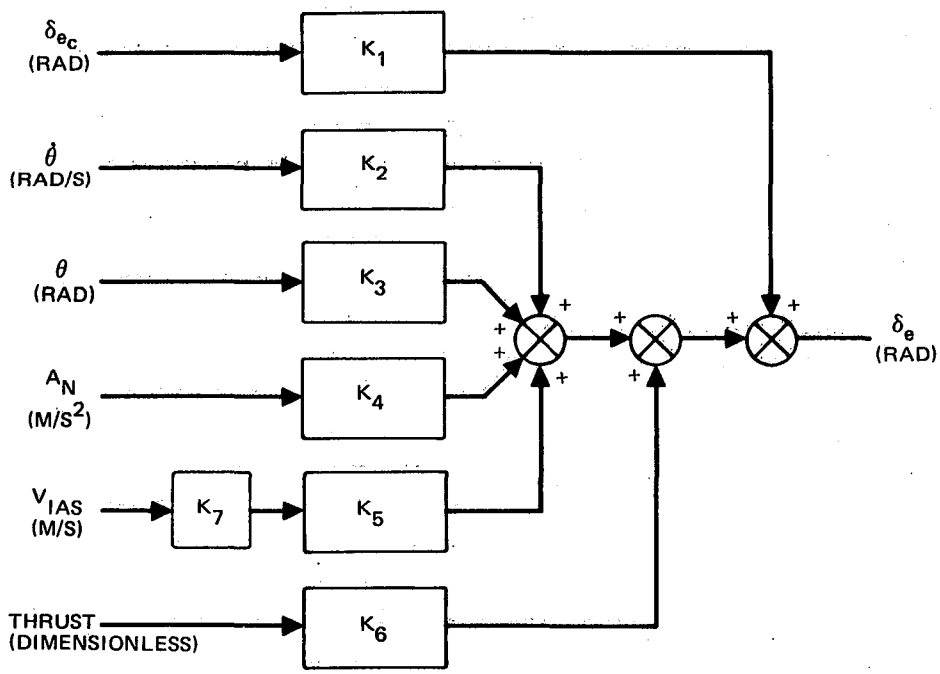

$K_1 = 0.5972$ $K_5 = 0.5612$
$K_2 = 0.02301$ $K_6 = 0.29$
$K_3 = 0.008966$ $K_7 = 1.0/V_{TRIM}$
$K_4 = 0.000094$

CONTROL LAW NO. 14 – CRUISE

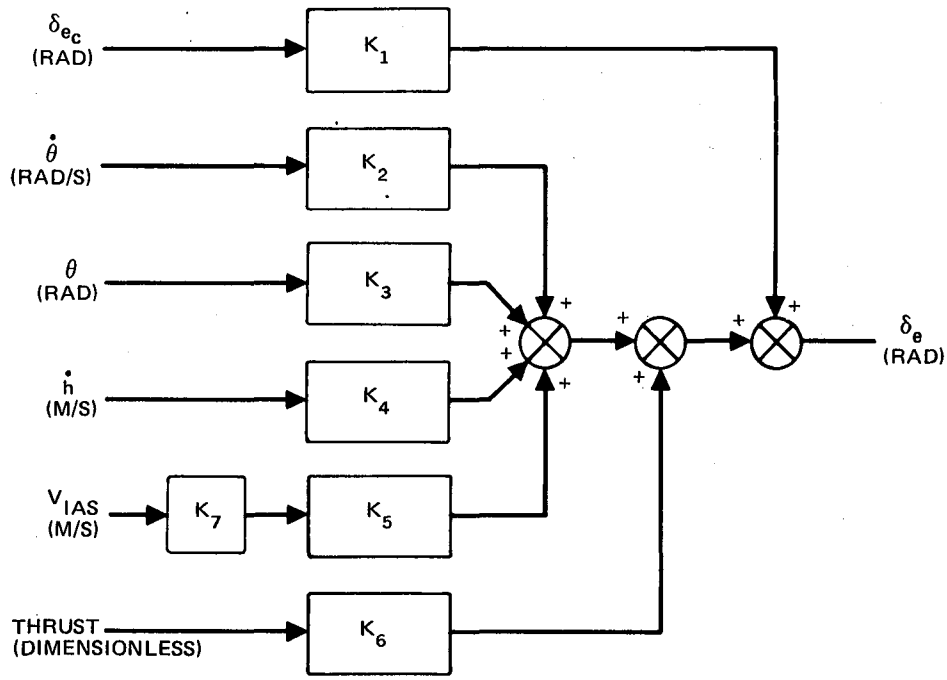

$K_1 = 0.5926$
$K_2 = 0.02288$
$K_3 = 0.124$
$K_4 = -0.00004499$
$K_5 = 0.63$
$K_6 = 0.29$
$K_7 = 1.0/V_{TRIM}$

CONTROL LAW NO. 15 – CRUISE

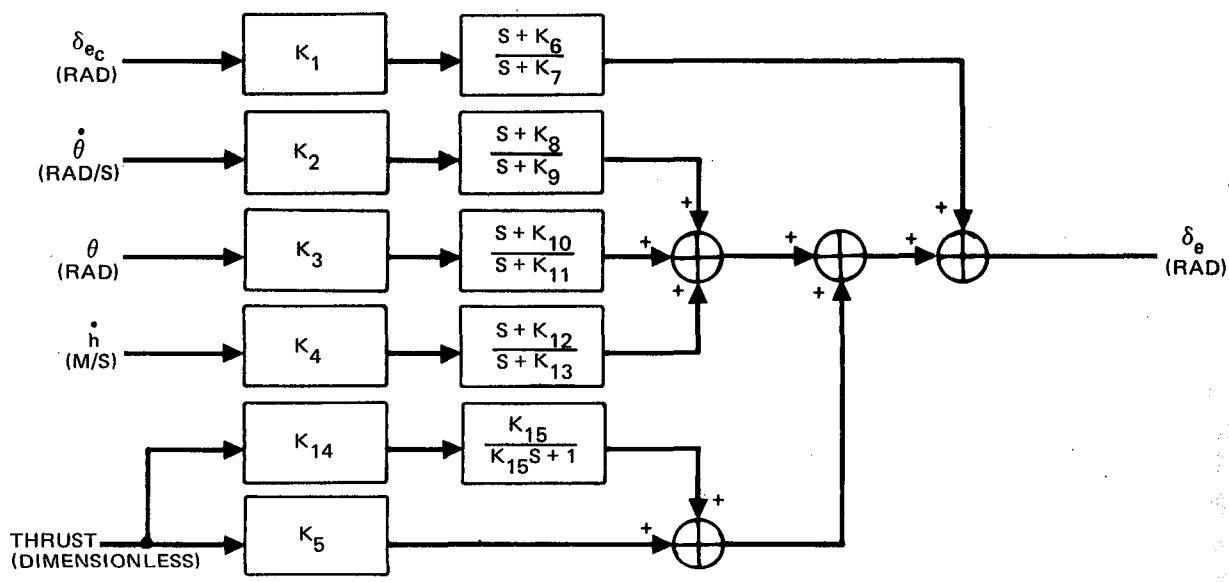

$K_1 = 0.5924$
$K_2 = 0.02287$
$K_3 = 0.1239$
$K_4 = -0.0000445$
$K_5 = 0.29$
$K_6 = 0.00391$
$K_7 = 0.001728$
$K_8 = -1.9899$
$K_9 = 0.001728$
$K_{10} = -0.1747$
$K_{11} = 0.001728$
$K_{12} = 0.03718$
$K_{13} = 0.001728$
$K_{14} = 0.082$
$K_{15} = 565.0$

CONTROL LAW NO. 16 – CRUISE

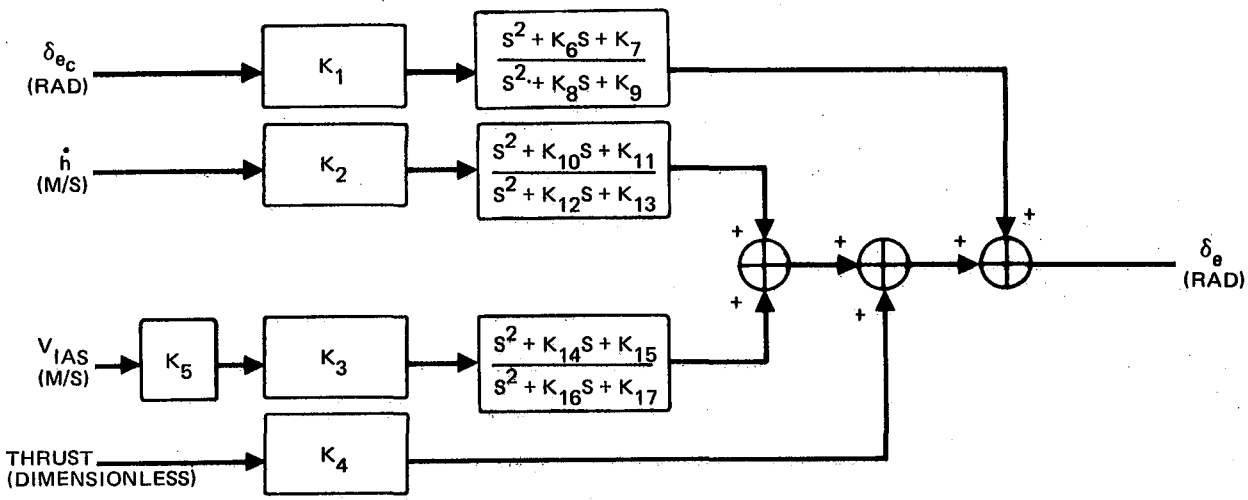

$K_1 = 0.5952$
$K_2 = -0.00004517$
$K_3 = 0.6327$
$K_4 = 0.29$
$K_5 = 1.0/V_{TRIM}$
$K_6 = 0.646$
$K_7 = 0.6465$
$K_8 = 0.6896$
$K_9 = 1.132$
$K_{10} = 0.5183$
$K_{11} = -0.051718$
$K_{12} = 0.6896$
$K_{13} = 1.132$
$K_{14} = 0.719$
$K_{15} = 1.0355$
$K_{16} = 0.6896$
$K_{17} = 1.132$

CONTROL LAW NO. 19 – CRUISE

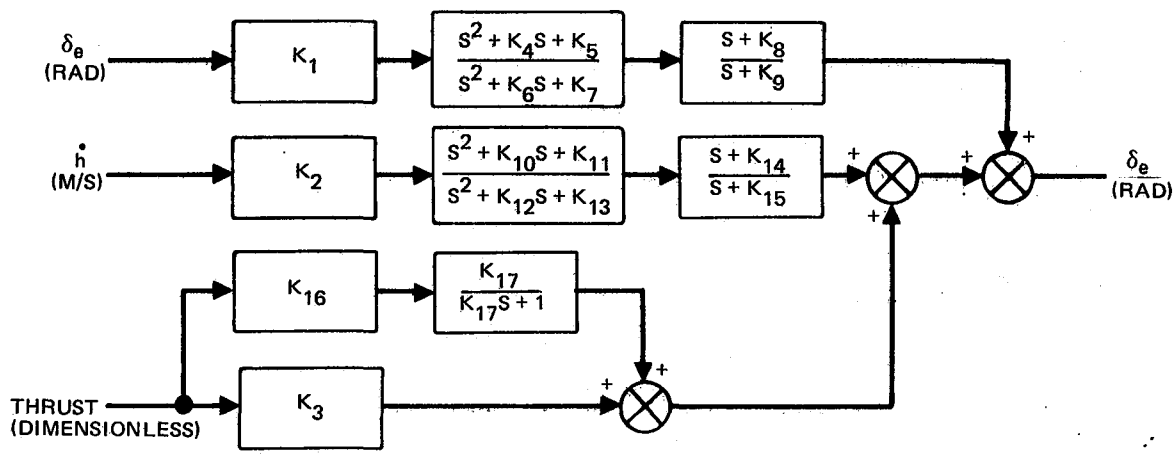

$K_1 = 0.5572$
$K_2 = 0.000353$
$K_3 = 0.29$
$K_4 = 0.4$
$K_5 = 1.0161$
$K_6 = 2.044$
$K_7 = 2.134$
$K_8 = 1.59$
$K_9 = 0.04998$
$K_{10} = 1.048$
$K_{11} = 1.172$
$K_{12} = 2.044$
$K_{13} = 2.134$
$K_{14} = -0.0289$
$K_{15} = 0.04998$
$K_{16} = 0.06$
$K_{17} = 10.0$

CONTROL LAW NO. 20 – CRUISE

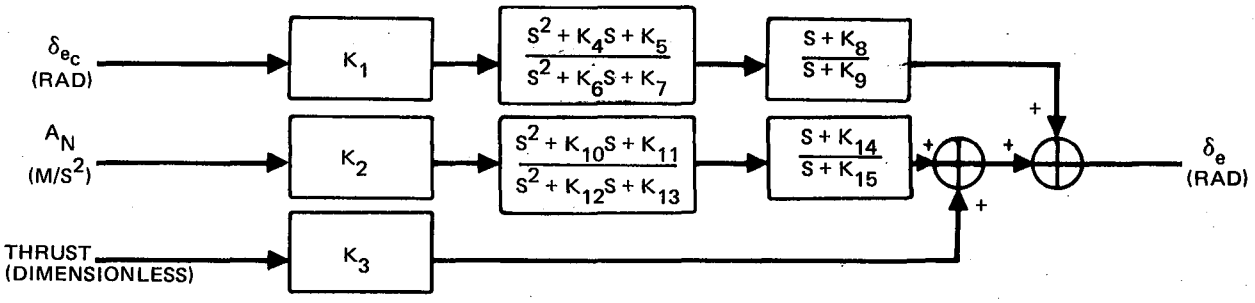

$K_1 = 0.587$
$K_2 = 0.0004032$
$K_3 = 0.37$
$K_4 = 1.08$
$K_5 = 0.5116$
$K_6 = 0.2$

$K_7 = 0.02134$
$K_8 = 1.144$
$K_9 = 2.327$
$K_{10} = 1.1$
$K_{11} = 0.844$
$K_{12} = 0.2$

$K_{13} = 0.02134$
$K_{14} = 0.466$
$K_{15} = 2.327$

CONTROL LAW NO. 26 – CRUISE

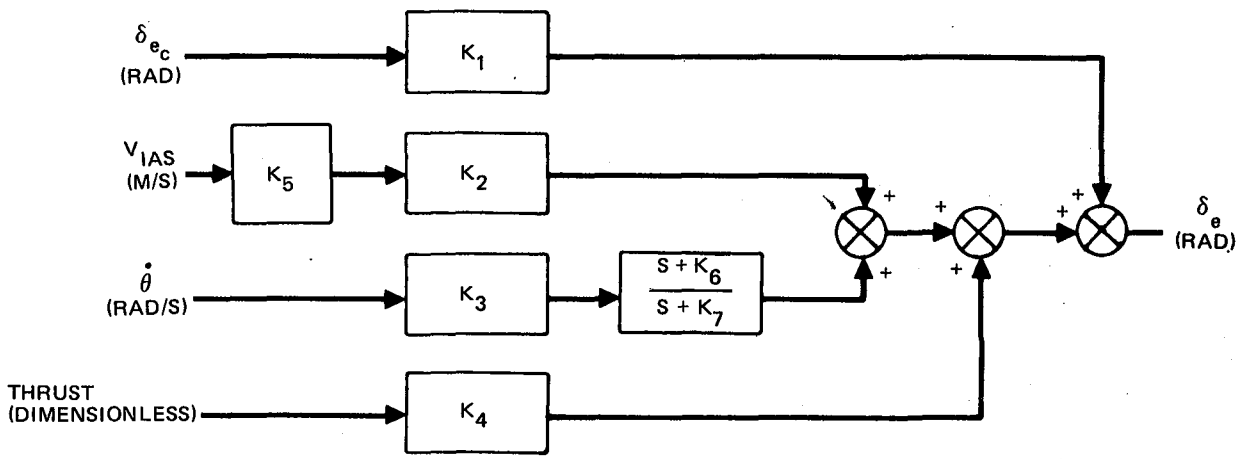

$K_1 = 0.5858$
$K_2 = 0.5623$
$K_3 = 0.02289$
$K_4 = 0.29$

$K_5 = 1.0/V_{TRIM}$
$K_6 = 5.82$
$K_7 = 0.5$

CONTROL LAW NO. 27 – CRUISE

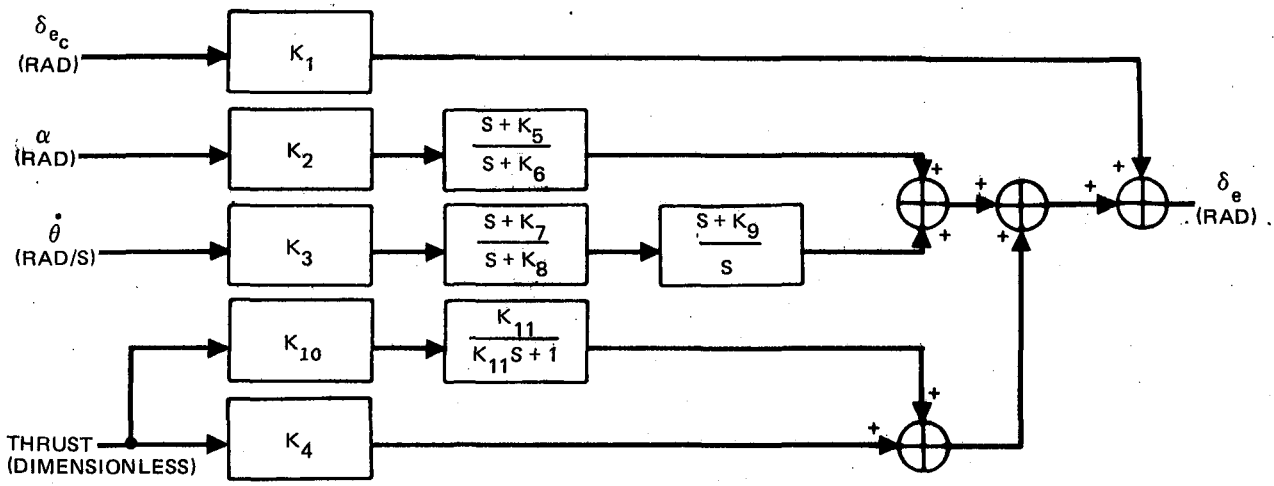

$K_1 = 0.4140$
$K_2 = 0.1147$
$K_3 = 0.02287$
$K_4 = 0.29$
$K_5 = 0.03718$

$K_6 = 0.001728$
$K_7 = -2.1195$
$K_8 = 0.001728$
$K_9 = 0.535$
$K_{10} = 0.082$

$K_{11} = 565.0$

CONTROL LAW NO. 28 – CRUISE

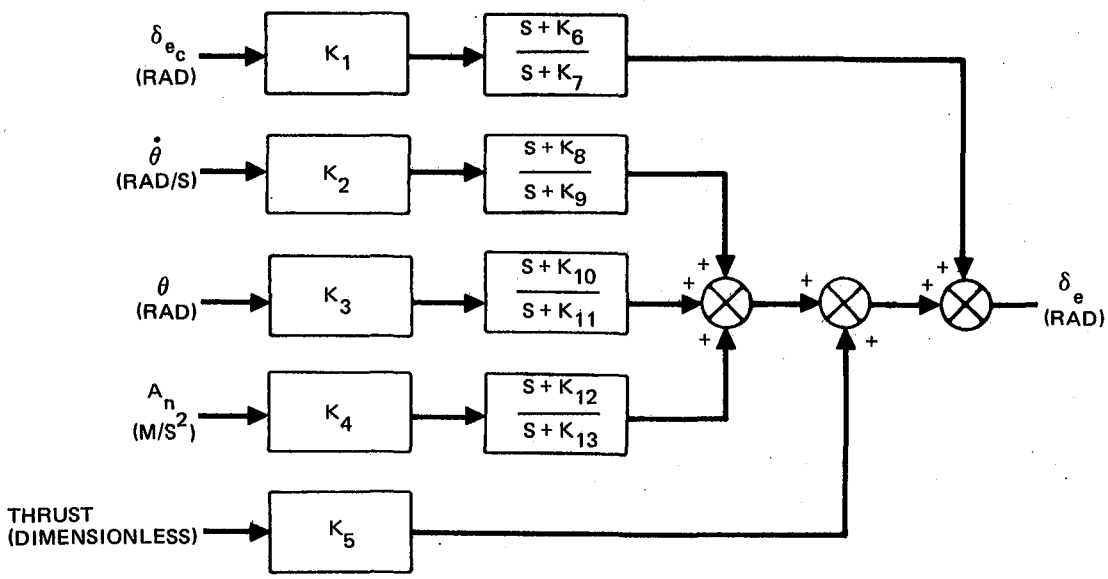

$K_1 = 0.628$
$K_2 = 0.02395$
$K_3 = 0.006549$
$K_4 = 0.000854$
$K_5 = 0.25$

$K_6 = 0.078$
$K_7 = 0.0067$
$K_8 = -38.23$
$K_9 = 0.0067$
$K_{10} = 0.1074$

$K_{11} = 0.0067$
$K_{12} = 0.446$
$K_{13} = 0.0067$

CONTROL LAW NO. 29 – CRUISE

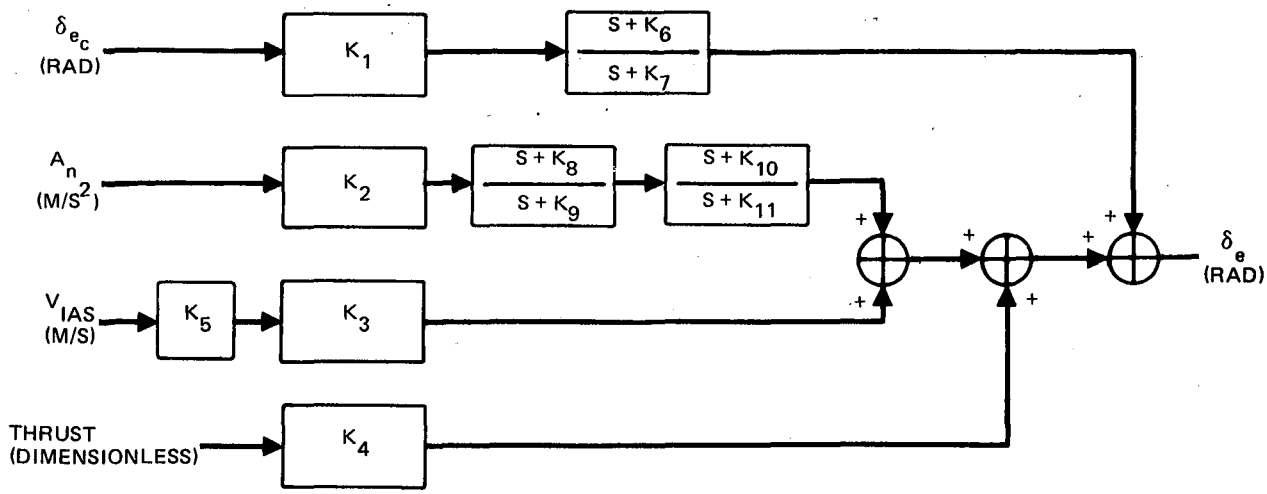

$K_1 = 0.569$
$K_2 = 0.0001008$
$K_3 = 0.564$
$K_4 = 0.29$
$K_5 = 1.0/V_{TRIM}$

$K_6 = 0.65$
$K_7 = 0.75$
$K_8 = 0.518$
$K_9 = 0.75$
$K_{10} = 0.185$
$K_{11} = 0.15$

CONTROL LAW NO. 30 – CRUISE

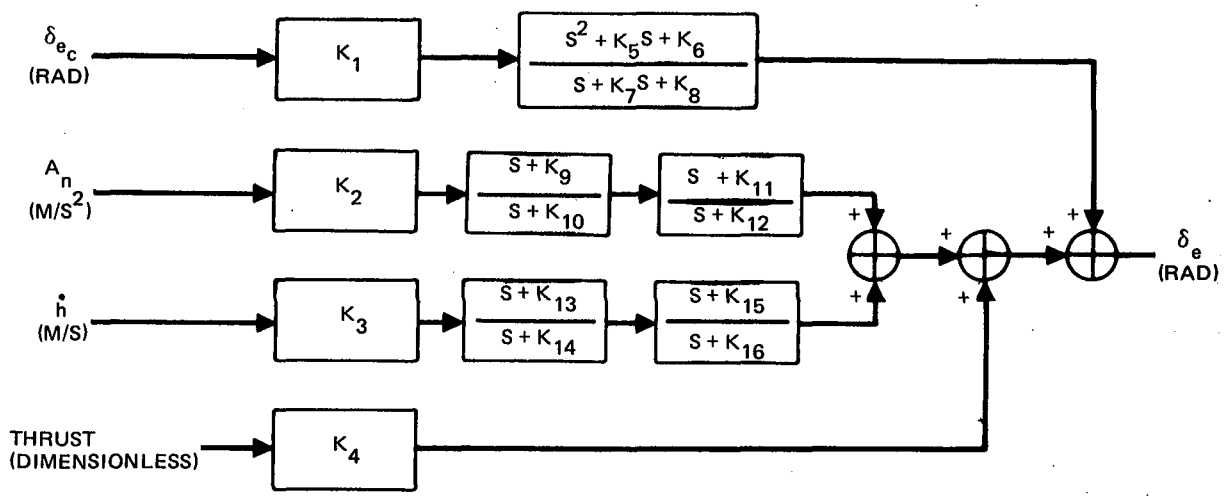

$K_1 = 0.5539$
$K_2 = 0.0003149$
$K_3 = -0.001653$
$K_4 = 0.25$
$K_5 = 0.808$
$K_6 = 0.8604$
$K_7 = 0.6$
$K_8 = 0.0675$

$K_9 = 6.528$
$K_{10} = 0.45$
$K_{11} = -0.237$
$K_{12} = 0.15$
$K_{13} = -0.435$
$K_{14} = 0.45$
$K_{15} = -0.0005$
$K_{16} = 0.15$

CONTROL LAW NO. 31 – CRUISE

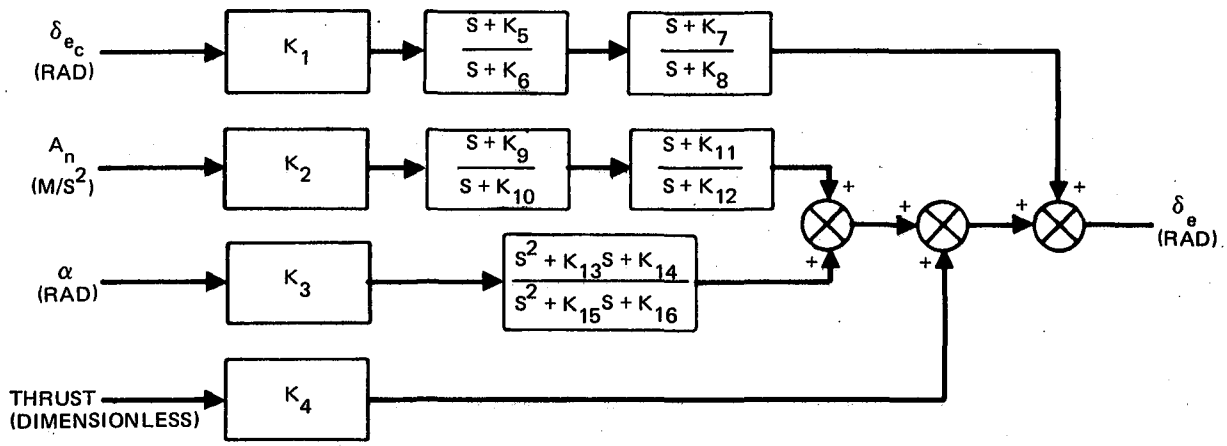

$K_1 = 0.5517$
$K_2 = 0.0007739$
$K_3 = -1.8317$
$K_4 = 0.255$
$K_5 = 5.55$
$K_6 = 3.5$

$K_7 = 0.5$
$K_8 = 1.934$
$K_9 = 1.5$
$K_{10} = 1.934$
$K_{11} = 4.196$
$K_{12} = 3.5$

$K_{13} = 3.2$
$K_{14} = 3.6478$
$K_{15} = 5.434$
$K_{16} = 6.769$

CONTROL LAW NO. 32 – CRUISE

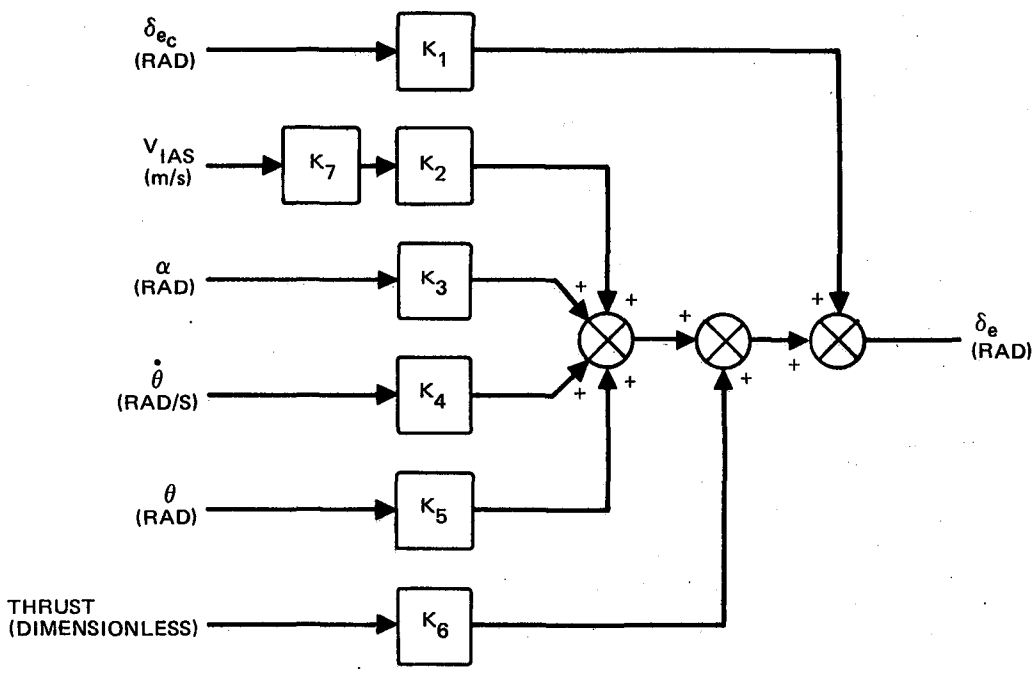

$K_1 = 0.674$
$K_2 = -0.07996$
$K_3 = 0.26831$

$K_4 = 0.11803$
$K_5 = 0.04004$
$K_6 = 0.31$

$K_7 = 1.0/V_{TRIM}$

CONTROL LAW NO. 1 – APPROACH

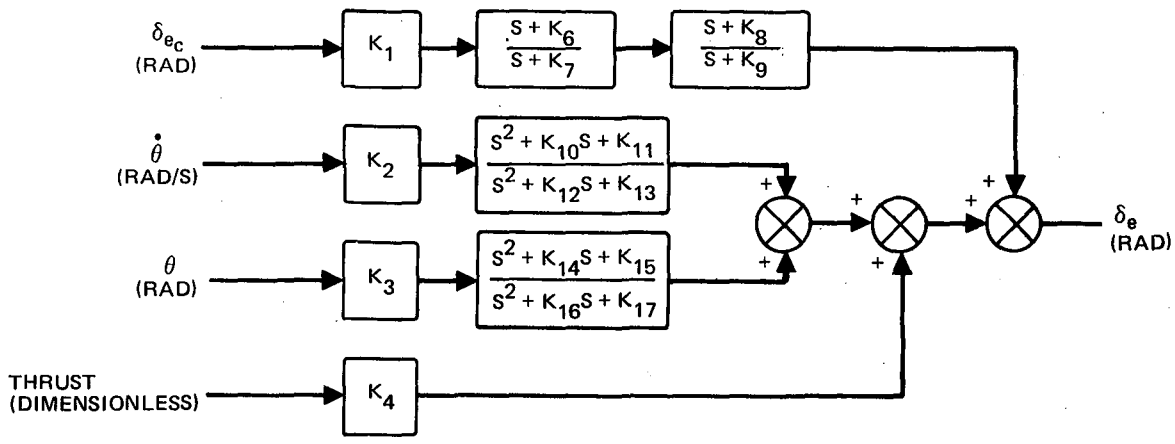

$K_1 = 0.674$
$K_2 = -4.7877$
$K_3 = 0.04$
$K_4 = 0.303$
$K_5 = \text{NOT USED}$
$K_6 = 0.58$
$K_7 = 5.7$
$K_8 = 0.15$
$K_9 = 0.415$
$K_{10} = 0.8354$
$K_{11} = 0.200717$
$K_{12} = 6.115$
$K_{13} = 2.366$
$K_{14} = 1.062$
$K_{15} = 0.5049$
$K_{16} = 6.115$
$K_{17} = 2.366$

CONTROL LAW NO. 2 – APPROACH

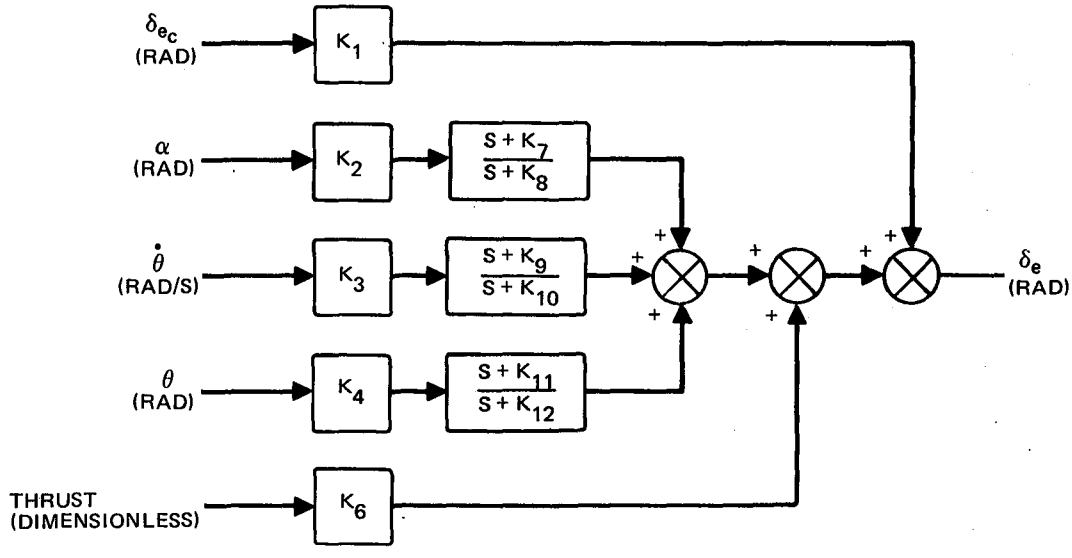

$K_1 = 0.674$
$K_2 = 0.2976$
$K_3 = 0.1172$
$K_4 = 0.04$
$K_5 = \text{NOT USED}$
$K_6 = 0.28$
$K_7 = 0.14$
$K_8 = 0.10$
$K_9 = -0.0717$
$K_{10} = 0.10$
$K_{11} = 0.36$
$K_{12} = 0.10$

CONTROL LAW NO. 3 – APPROACH

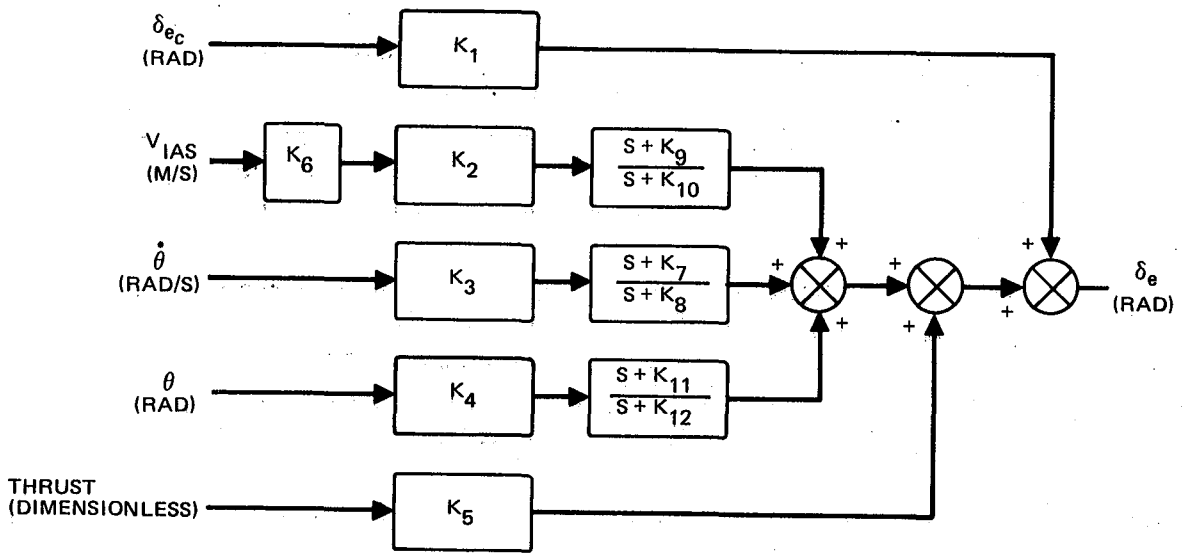

$K_1 = 0.6584$
$K_2 = -0.08$
$K_3 = 0.1182$
$K_4 = 0.04$
$K_5 = 0.29$
$K_6 = 1.0/V_{TRIM}$
$K_7 = 2.716$
$K_8 = 0.5246$
$K_9 = 1.447$
$K_{10} = 0.5246$
$K_{11} = 0.5799$
$K_{12} = 0.5246$

CONTROL LAW NO. 4 – APPROACH

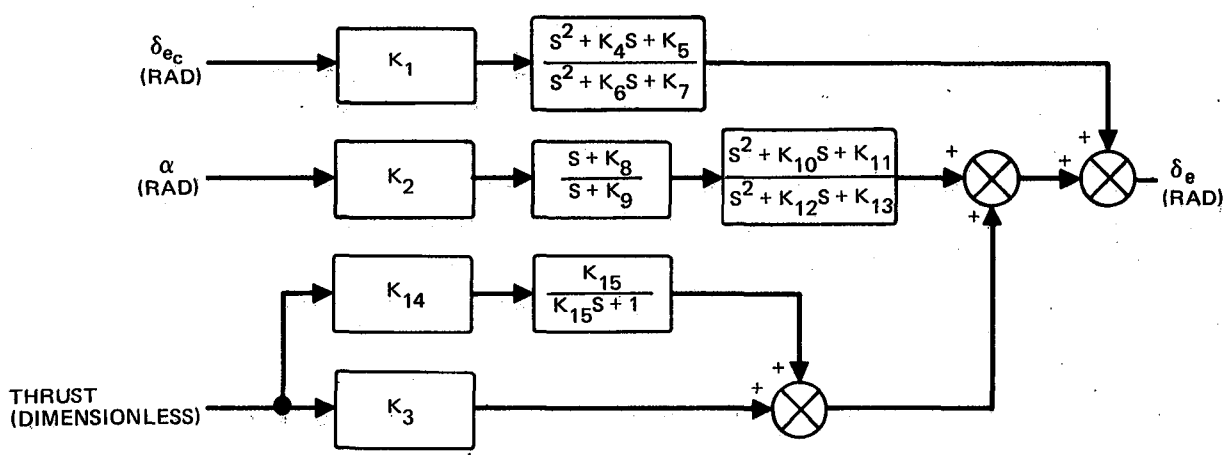

$K_1 = 0.6457$
$K_2 = 0.3816$
$K_3 = 0.20$
$K_4 = 0.0356$
$K_5 = 0.000318$
$K_6 = 0.07758$
$K_7 = 0.0227$
$K_8 = 1.385$
$K_9 = 1.80$
$K_{10} = 0.0478$
$K_{11} = -0.0008052$
$K_{12} = 0.07758$
$K_{13} = 0.0227$
$K_{14} = 0.0024$
$K_{15} = 50.0$

CONTROL LAW NO. 5 – APPROACH

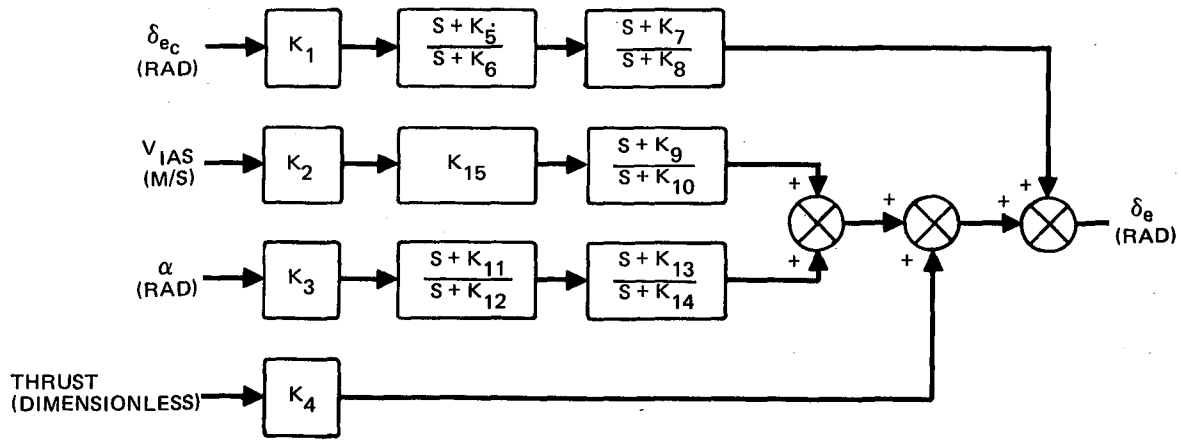

$K_1 = 0.6829$
$K_2 = 1.0/V_{TRIM}$
$K_3 = 0.194$
$K_4 = 0.32$
$K_5 = 1.0$
$K_6 = 0.8785$
$K_7 = 0.15$
$K_8 = 0.40$
$K_9 = 0.248$
$K_{10} = 0.8785$
$K_{11} = 1.085$
$K_{12} = 0.8785$
$K_{13} = 0.0637$
$K_{14} = 0.40$
$K_{15} = -0.255$

CONTROL LAW NO. 6 – APPROACH

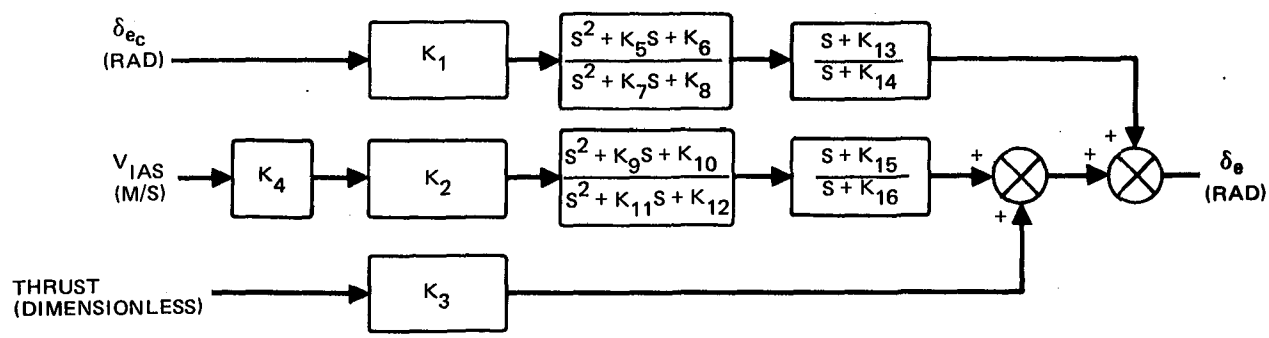

$K_1 = 0.6818$
$K_2 = -0.08089$
$K_3 = 0.31$
$K_4 = 1.0/V_{TRIM}$
$K_5 = 0.978$
$K_6 = 0.25376$
$K_7 = 1.05$
$K_8 = 0.61738$
$K_9 = 1.9164$
$K_{10} = 0.6872$
$K_{11} = 1.05$
$K_{12} = 0.61738$
$K_{13} = 0.000642$
$K_{14} = 0.042$
$K_{15} = -0.0034$
$K_{16} = 0.042$

CONTROL LAW NO. 7 – APPROACH

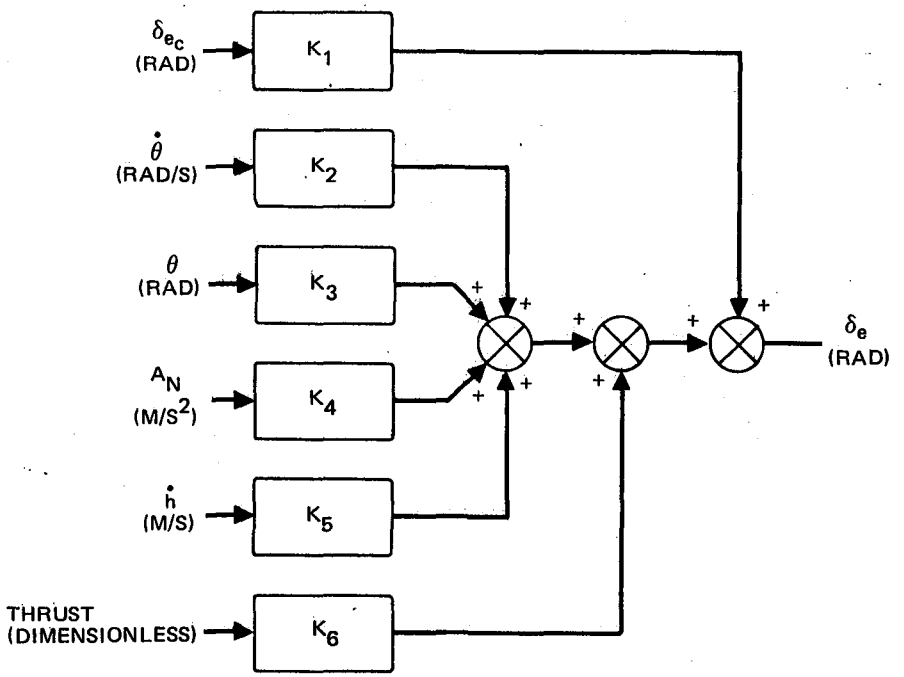

$K_1 = 0.6687$ $K_4 = -0.000359$
$K_2 = 0.1161$ $K_5 = -0.000529$
$K_3 = 0.4504$ $K_6 = 0.31$

CONTROL LAW NO. 12 – APPROACH

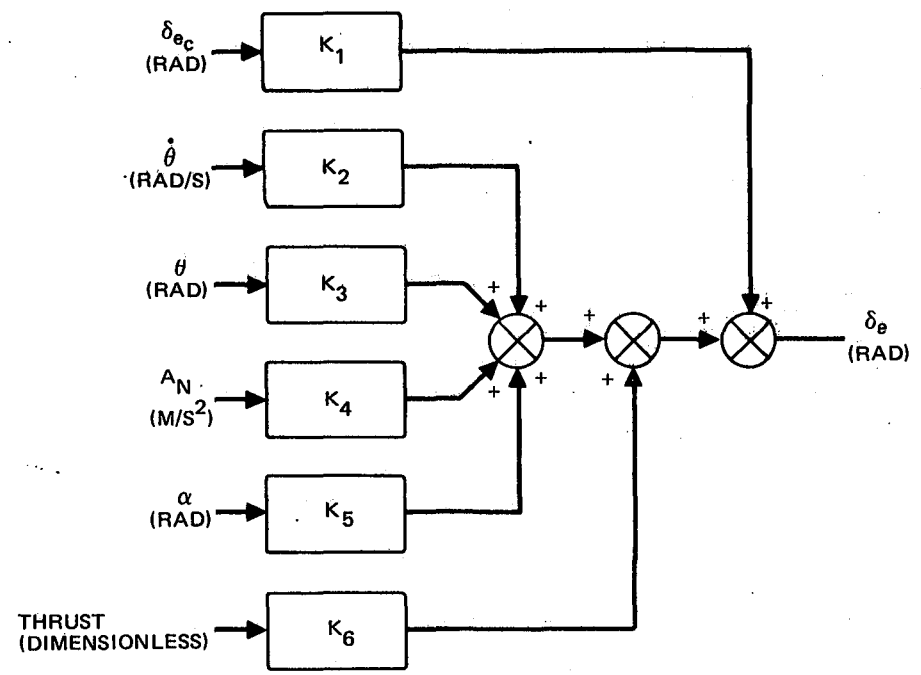

$K_1 = 0.6687$ $K_4 = -0.000359$
$K_2 = 0.1161$ $K_5 = 0.4116$
$K_3 = 0.03879$ $K_6 = 0.32$

CONTROL LAW NO. 13 – APPROACH

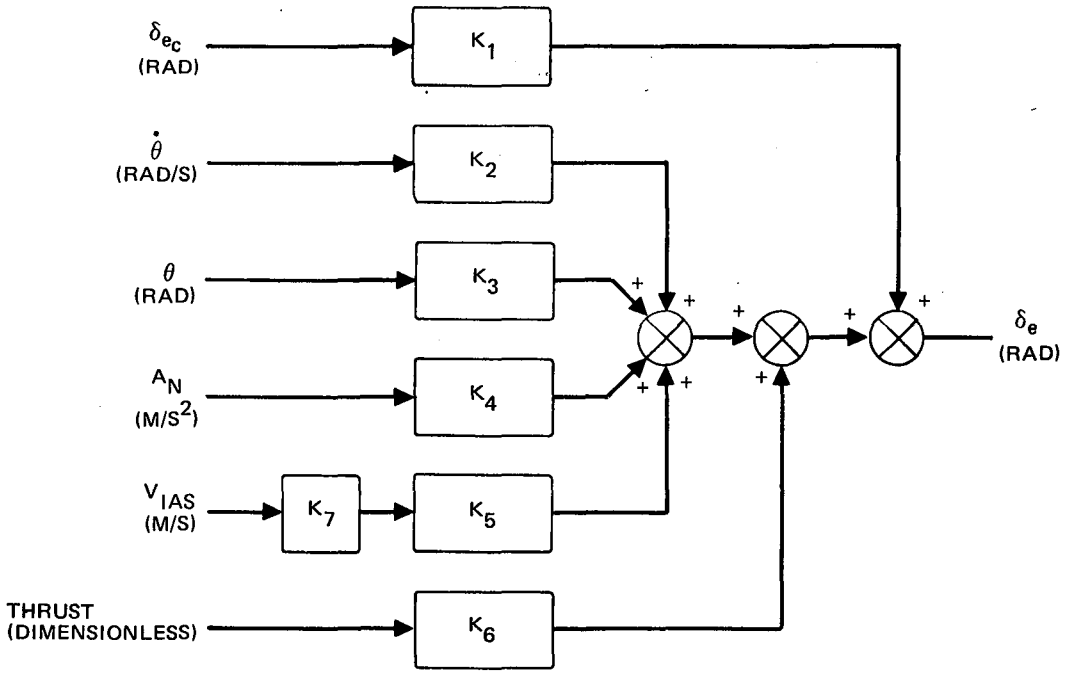

$K_1 = 0.684$ $K_4 = 0.0006827$ $K_7 = 1.0/V_{TRIM}$
$K_2 = 0.1216$ $K_5 = -0.2297$
$K_3 = 0.04230$ $K_6 = 0.32$

CONTROL LAW NO. 14 – APPROACH

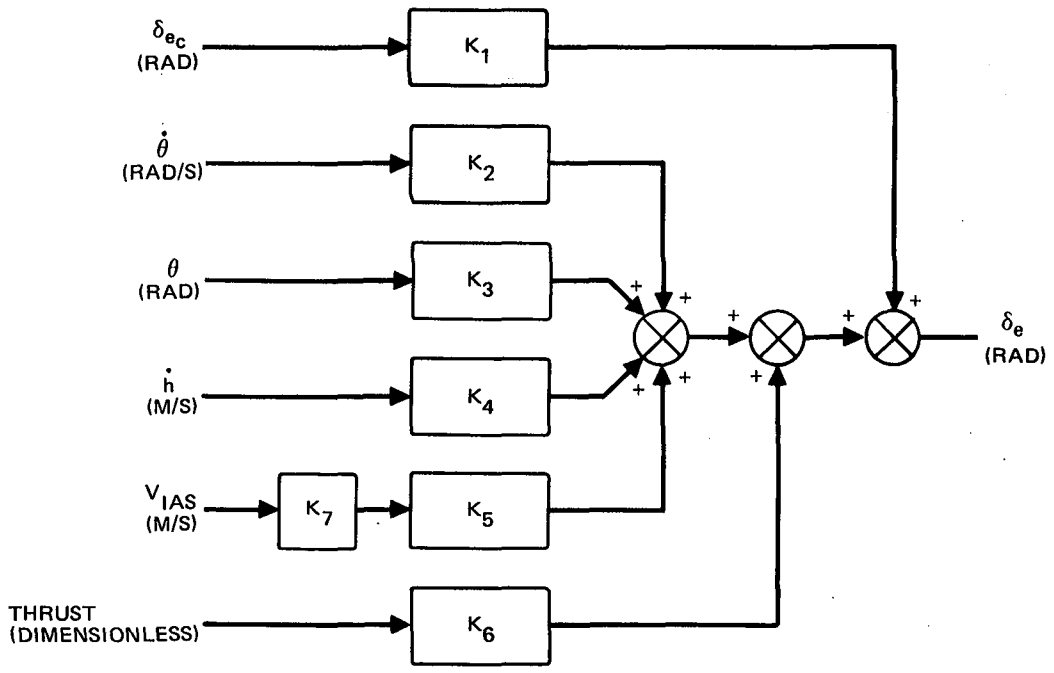

$K_1 = 0.674$ $K_4 = -0.000345$ $K_7 = 1.0/V_{TRIM}$
$K_2 = 0.118$ $K_5 = -0.07996$
$K_3 = 0.308$ $K_6 = 0.31$

CONTROL LAW NO. 15 – APPROACH

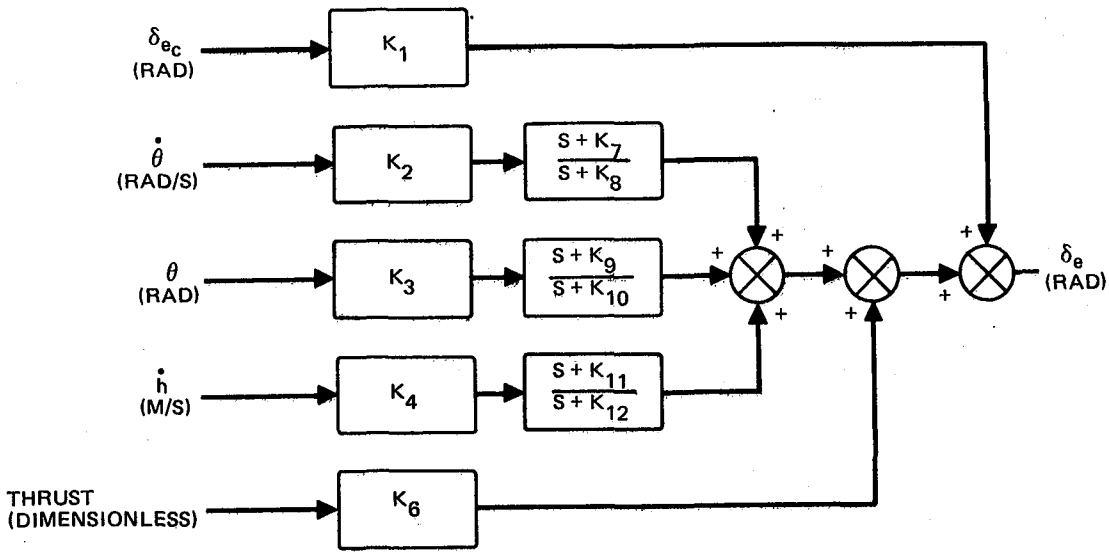

$K_1 = 0.674$
$K_2 = 0.116$
$K_3 = 0.3084$
$K_4 = -0.000419$

K_5 = NOT USED
$K_6 = 0.28$
$K_7 = 0.284$
$K_8 = 0.20$

$K_9 = 0.329$
$K_{10} = 0.20$
$K_{11} = 0.255$
$K_{12} = 0.20$

CONTROL LAW NO. 16 – APPROACH

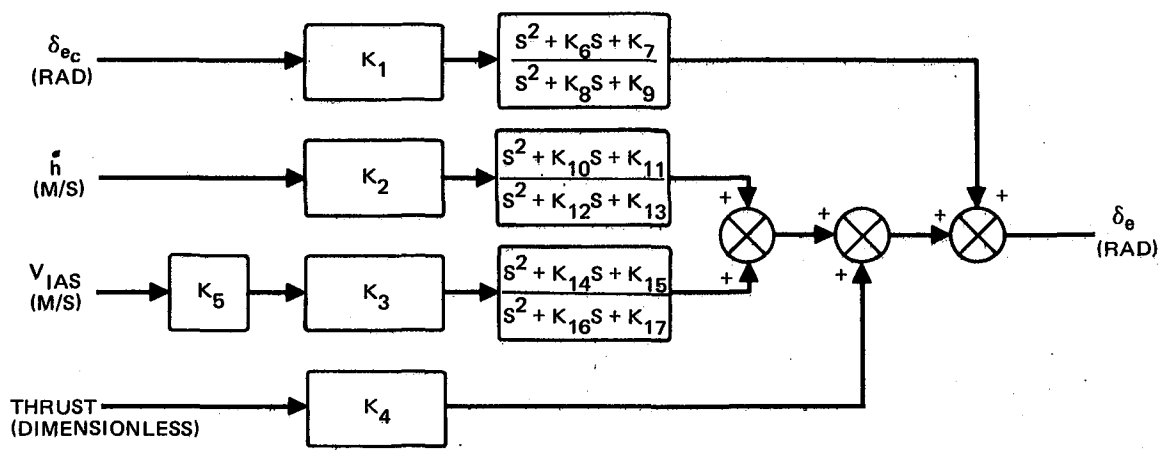

$K_1 = 0.6809$
$K_2 = -0.0003578$
$K_3 = -0.08078$
$K_4 = 0.313$

$K_5 = 1.0/V_{TRIM}$
$K_6 = 0.467$
$K_7 = 0.01603$
$K_8 = 0.568$

$K_9 = 0.3584$
$K_{10} = 0.46$
$K_{11} = -0.002325$
$K_{12} = 0.568$

$K_{13} = 0.3584$
$K_{14} = 0.4655$
$K_{15} = 0.01245$
$K_{16} = 0.568$

$K_{17} = 0.3584$

CONTROL LAW NO. 19 – APPROACH

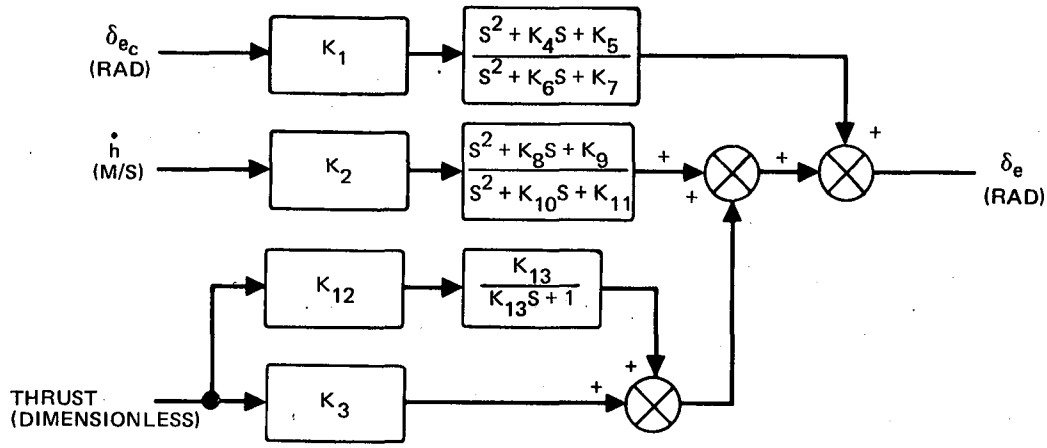

$K_1 = 0.6809$
$K_2 = -0.0003487$
$K_3 = 0.3$
$K_4 = 0.4382$
$K_5 = 0.003526$
$K_6 = 0.533$
$K_7 = 0.3488$
$K_8 = 0.4277$
$K_9 = -0.01664$
$K_{10} = 0.533$
$K_{11} = 0.3488$
$K_{12} = -0.0003$
$K_{13} = 10.0$

CONTROL LAW NO. 20 – APPROACH

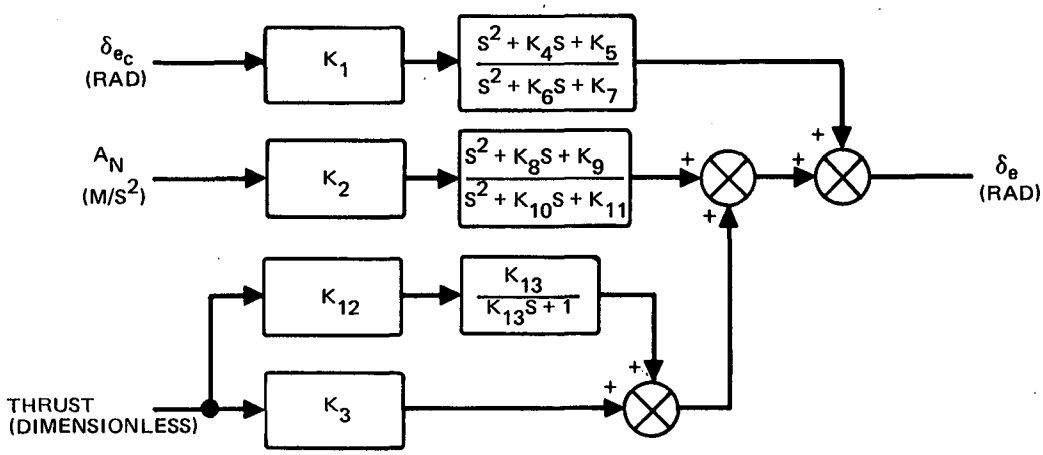

$K_1 = 0.6495$
$K_2 = 0.000326$
$K_3 = 0.3$
$K_4 = 0.10$
$K_5 = 0.006816$
$K_6 = 0.20$
$K_7 = 0.1757$
$K_8 = -0.659$
$K_9 = -0.1879$
$K_{10} = 0.20$
$K_{11} = 0.1757$
$K_{12} = 0.0005$
$K_{13} = 10.0$

CONTROL LAW NO. 26 – APPROACH

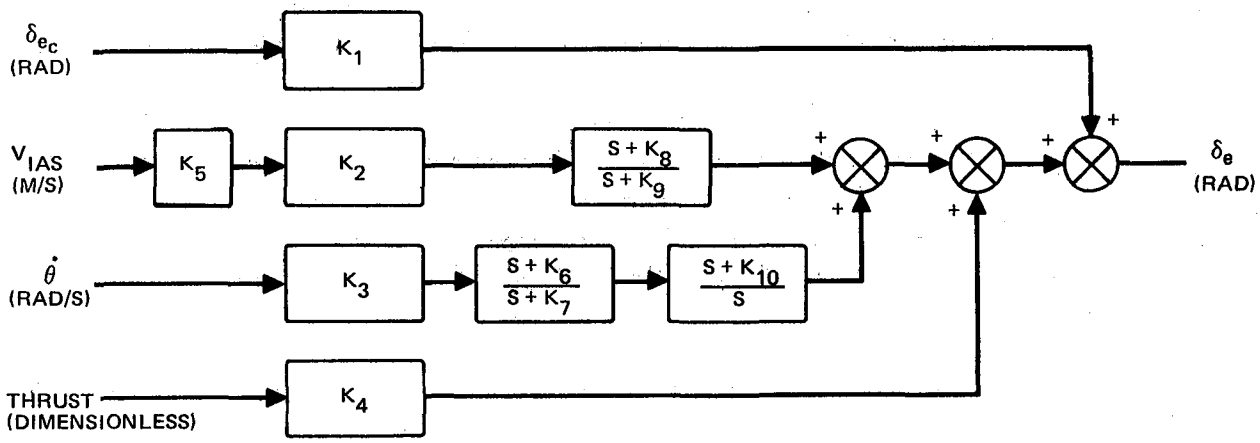

$K_1 = 0.6584$
$K_2 = -0.08007$
$K_3 = 0.11818$
$K_4 = 0.31$

$K_5 = 1.0/V_{TRIM}$
$K_6 = 2.9897$
$K_7 = 0.5246$
$K_8 = 1.4474$

$K_9 = 0.5246$
$K_{10} = 0.0658$

CONTROL LAW NO. 27 – APPROACH

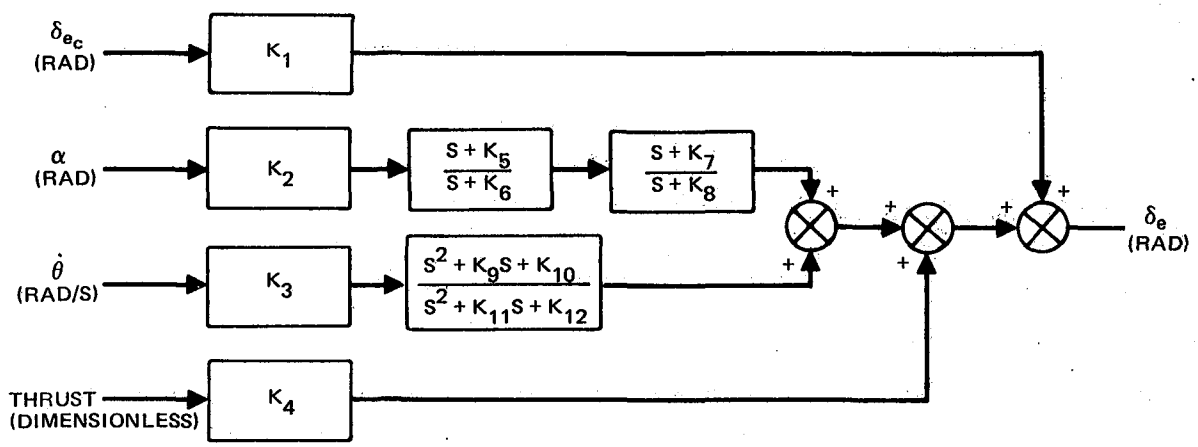

$K_1 = 0.6826$
$K_2 = 0.4524$
$K_3 = 0.1179$
$K_4 = 0.33$

$K_5 = 0.3942$
$K_6 = 0.2333$
$K_7 = 0.1205$
$K_8 = 0.2195$

$K_9 = -0.643$
$K_{10} = 0.1486$
$K_{11} = 0.4528$
$K_{12} = 0.0512$

CONTROL LAW NO. 28 – APPROACH

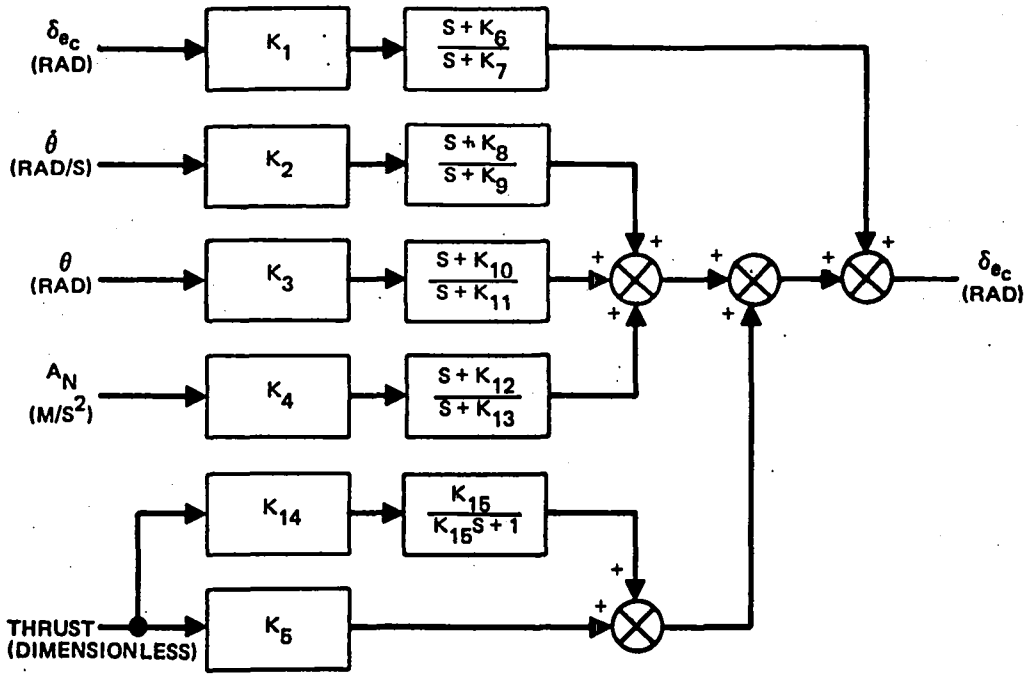

$K_1 = 0.6706$
$K_2 = 0.1164$
$K_3 = 0.03895$
$K_4 = -0.0003599$
$K_5 = 0.31$
$K_6 = 0.0005$
$K_7 = 0.0307$
$K_8 = 3.426$
$K_9 = 0.0307$
$K_{10} = 0.07515$
$K_{11} = 0.0307$
$K_{12} = 1.4474$
$K_{13} = 0.0307$
$K_{14} = -0.0105$
$K_{15} = 30.0$

CONTROL LAW NO. 29 – APPROACH

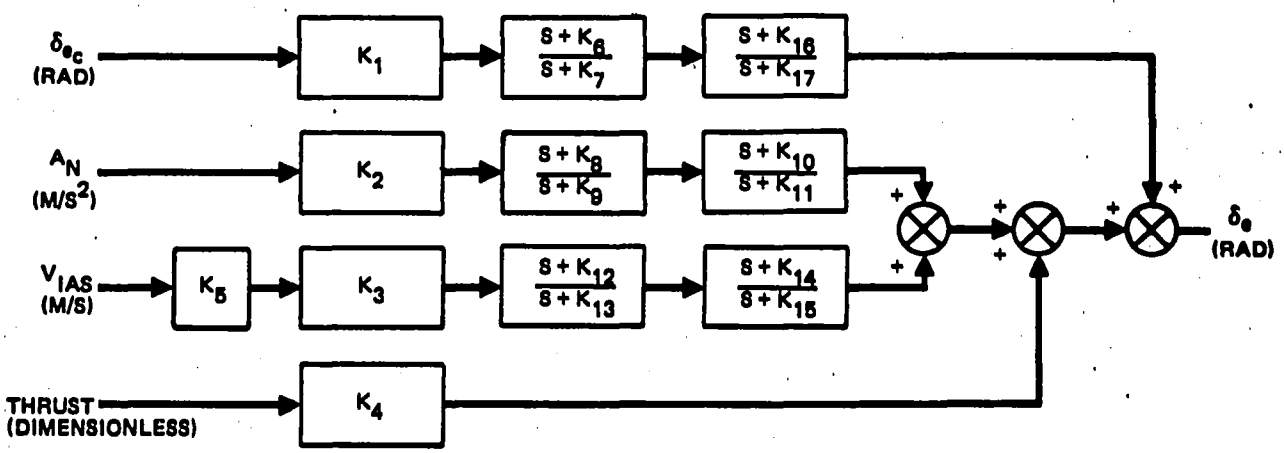

$K_1 = 0.6937$
$K_2 = 0.0006812$
$K_3 = -0.2329$
$K_4 = 0.31$
$K_5 = 1.0/V_{TRIM}$
$K_6 = 0.4669$
$K_7 = 0.5122$
$K_8 = 0.465$
$K_9 = 0.5122$
$K_{10} = -0.005145$
$K_{11} = 0.0924$
$K_{12} = 0.465$
$K_{13} = 0.5122$
$K_{14} = -0.0036$
$K_{15} = 0.0924$
$K_{16} = 0.0002$
$K_{17} = 0.0924$

CONTROL LAW NO. 30 – APPROACH

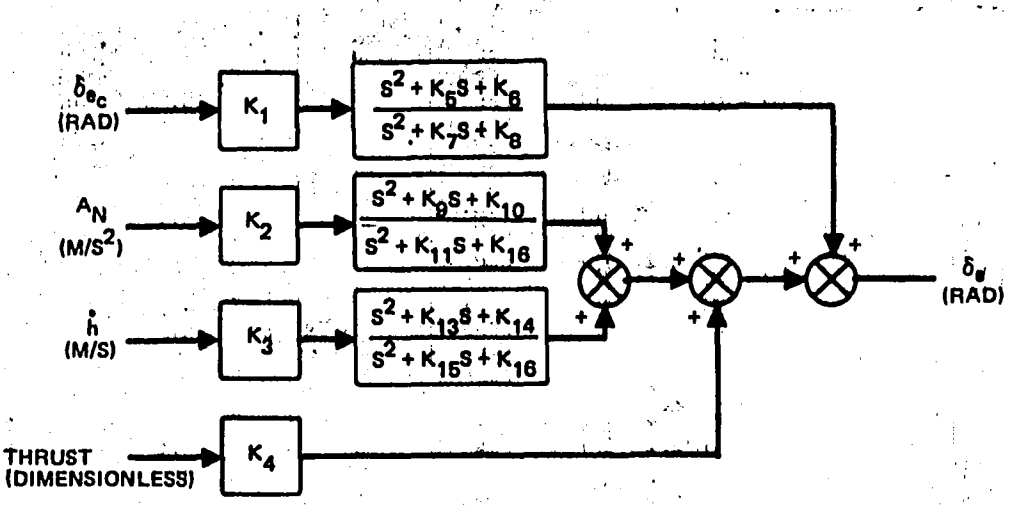

$K_1 = 0.6868$ $K_5 = 0.62$ $K_9 = 5.6419$ $K_{13} = 0.6591$
$K_2 = -0.0018$ $K_6 = 0.0736$ $K_{10} = 3.3$ $K_{14} = -0.00257$
$K_3 = 0.00806$ $K_7 = 1.20$ $K_{11} = 1.20$ $K_{15} = 1.20$
$K_4 = 0.26$ $K_8 = 1.17$ $K_{12} = 1.17$ $K_{16} = 1.17$

CONTROL LAW NO. 31 – APPROACH

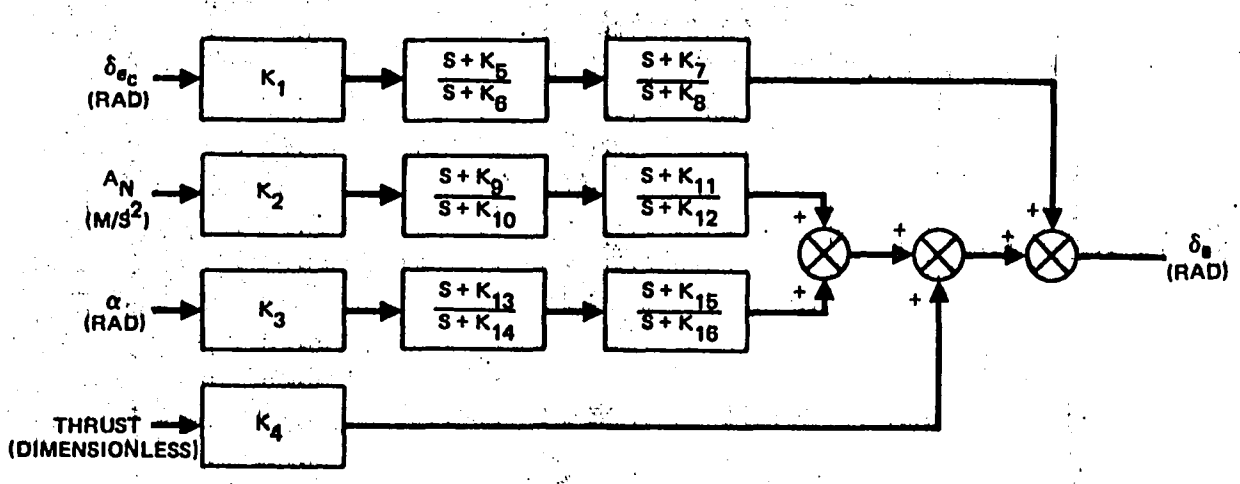

$K_1 = 0.6633$ $K_5 = 0.621$ $K_9 = 0.6257$ $K_{13} = 0.6215$
$K_2 = -0.00123$ $K_6 = 0.504$ $K_{10} = 0.504$ $K_{14} = 0.504$
$K_3 = 0.8412$ $K_7 = 0.703$ $K_{11} = 0.128$ $K_{15} = 0.3386$
$K_4 = 0.32$ $K_8 = 0.936$ $K_{12} = 0.936$ $K_{16} = 0.936$

CONTROL LAW NO. 32 – APPROACH

APPENDIX 7
FINAL AUGMENTATION CONTROL LAW EQUATIONS

This section contains the control laws expressed in difference equation form. The gain program for each control law used in the DETAC simulation is also provided. The rationale leading to the formulation of control laws in difference equation form is presented in Section 5.

Control Law Equations

The control law equations for all the final control laws are provided on the following pages.

FLIGHT CONDITION – CRUISE

$U = 0.0026545\,V + 0.114689\,\alpha + 0.022874\,\dot{\theta} + 0.009265\,\theta$

FEED FORWARD GAIN = 0.5 CROSSFEED GAIN = 0.29

APPROACH

$U = 0.0010931\,V + 0.268279\,\alpha + 0.118027\,\dot{\theta} + 0.04004\,\theta$

FEED FORWARD GAIN = 0.64 CROSSFEED GAIN = 0.31

UNITS: M/SEC, RADIANS

EET CONTROL EQUATIONS – LAW NO. 1

```
PX1 = EXP (–10.0 * DT)
PX2 = EXP (–0.1 * DT)

CRUISE
      U1 = 0.5 * PILOT COMMAND + U
      Z1 = Z1 * PX1 + U1 * (1 – PX1)
      Z2 = Z2 * PX2 + (–0.14514 * U1 + 1.27104 * THRUST – 1.36985 * α + 7.86 * θ̇ – 0.417 * θ ) * (1 – PX2)
      U = 0.00091 * Z1 + 0.63 * Z2 – 0.11387 * α + 0.02288 * θ̇ + 0.00926 * θ + 0.29 * THRUST
            FEED FORWARD = 0.5

APPROACH
      U1 = 0.674 * PILOT COMMAND + U
      Z1 = Z1 * PX1 + U1 * (1 – PX1)
      Z2 = Z2 * PX2 + (–0.11822 * U1 + 1.17898 * THRUST – 1.52104 * α + 2.477 * θ̇ – 1.303 * θ) * (1 – PX2)
      U = – 0.00009 * Z1 – 0.07996 * Z2 + 0.29757 * α + 0.11803 * θ̇ + 0.04 * θ + 0.31 * THRUST
            FEED FORWARD = 0.674
```

EET CONTROL EQUATIONS – LAW NO. 3

```
PX1 = EXP (–10.0 * DT)
PX2 = EXP (–0.3 * DT)
PX3 = EXP (–0.1 * DT)

CRUISE
      U1 = 0.5 * PILOT COMMAND + U
      Z1 = Z1 * PX1 + U1 * (1 – PX1)
      Z2 = Z2 * PX2 + (4.57327 * U1 + 0.15288 * THRUST + 3.7377 * θ̇ –0.49 * θ) * (1 – PX2)
      Z3 = Z3 * PX3 + (–5.25964 * U1 – 3.03405 * THRUST – 0.84122 *θ̇ +1.455 * θ) * (1 – PX3)
      U = –0.01503 * Z1 + 0.06645 * Z2 – 0.11245 * Z3 + 0.06119 *θ̇ + 0.00926 θ + 0.29 * THRUST
            FEED FORWARD = 0.5

APPROACH
      U1 = 0.674 * PILOT COMMAND + U
      Z1 = Z1 * PX1 + U1 * (1 – PX1)
      Z2 = Z2 * PX2 + (72.22104 * U1 – 21.81726 * THRUST + 15.23787 *θ̇ – 0.5876 θ) * (1 – PX2)
      Z3 = Z3 * PX3 + (143.577 * U1 – 42.22785 * THRUST + 50.72387 * θ̇ – 1.93338 θ) * (1 – PX3)
      U = – 0.17105 * Z1 + 0.29523 * Z2 – 0.3387 * Z3 + 1.54934 * θ̇ + 0.04 * θ + 0.31 * THRUST
            FEED FORWARD = 0.674
```

EET CONTROL EQUATIONS – LAW NO. 2

PX1 = EXP (−10.0 * DT)
PX2 = EXP (−0.3 * DT)

CRUISE
U1 = 0.5 * PILOT COMMAND + U
Z1 = Z1 * PX1 + U1 * (1 − PX1)
Z2 = Z2 * PX2 + (3.92 * U1 − 1.1792 * THRUST − 0.0122667 * V + 3.643 * $\dot{\theta}$ − 0.005 * θ) * (1 − PX2)
U = − 0.01349 * Z1 + 0.11471 * Z2 + 0.0026543 * V + 0.05766 * $\dot{\theta}$ +0.00926 * θ + 0.29 * THRUST
FEED FORWARD = 0.5

APPROACH
U1 = 0.674 * PILOT COMMAND + U
Z1 = Z1 * PX1 + 1.493 * U1 * (1 − PX1)
Z2 = Z2 * PX2 + (49.7775 * U1 − 15.03726 * THRUST − 0.0132705 * V + 10.586 * $\dot{\theta}$ + 0.034 θ) * (1 − PX2)
U = − 0.26831 * Z1 + 0.26831 * Z2 − 0.0011436 * V + 3.66227 * $\dot{\theta}$ + 0.04 θ + 0.31 * THRUST
FEED FORWARD = 0.624

EET CONTROL EQUATIONS − LAW NO. 4

PX1 = EXP (−10.0 * DT)
PX2 = EXP (−0.8 * DT)
PX3 = EXP (−0.25 * DT)
PX4 = EXP (−0.2 * DT)

CRUISE
U1 = 0.5 * PILOT COMMAND + U
Z1 = Z1 * PX1 + U1 * (1 − PX1)
Z2 = Z2 * PX2 + (−10.8726 * U1 + 2.05745 * THRUST − 1.83644 * α) * (1 − PX2)
Z3 = Z3 * PX3 + (−79.918 * U1 + 4.31615 * THRUST − 18.297 * α) * (1 − PX3)
Z4 = Z4 * PX4 + (79.777 * U1 − 1.38494 * THRUST + 22.18449 * α) * (1 − PX4)
U = 0.01501 * Z1 + 0.15802 * Z2 − 0.1778 * Z3 − 0.14585 * Z4 + 0.21952 * α + 0.29 * THRUST
FEED FORWARD = 0.5

APPROACH
U1 = 0.674 * PILOT COMMAND + U
Z1 = Z1 * PX1 + U1 * (1 − PX1)
Z2 = Z2 * PX2 + (−7.4035 * U1 + 2.0827 * THRUST − 0.71526 * α) * (1 − PX2)
Z3 = Z3 * PX3 + (−147.064 * U1 + 46.4056 * THRUST − 7.395 * α) * (1 − PX3)
Z4 = Z4 * PX4 + (157.61 * U1 − 50.7887 * THRUST + 9.20378 * α) * (1 − PX4)
U = 0.01519 * Z1 + 0.12673 * Z2 − 0.07174 * Z3 − 0.06469 * Z4 + 0.5598 * α + 0.31 * THRUST
FEED FORWARD = 0.674

EET CONTROL EQUATIONS − LAW NO. 5

PX1 = EXP (−10.0 * DT)
PX2 = EXP (−0.8 * DT)
PX3 = EXP (−0.25 * DT)

CRUISE
U1 = 0.5 * PILOT COMMAND + U
Z1 = Z1 * PX1 + U1 * (1 − PX1)
Z2 = Z2 * PX2 + (16.20791 * U1 − 8.026 * THRUST − 0.126874 * V + 2.279 * α) * (1 − PX2)
Z3 = Z3 * PX3 + (−49.0785 * U1 + 20.786 * THRUST + 0.1579 * V − 7.52138 * α) * (1 − PX3)
U = 0.00965 * Z1 − 0.00689 * Z2 + 0.00058 * Z3 + 0.0019674 * V + 0.11471 * α + 0.29 * THRUST
FEED FORWARD = 0.5

APPROACH
U1 = 0.674 * PILOT COMMAND + U
Z1 = Z1 * PX1 + U1 * (1 − PX1)
Z2 = Z2 * PX2 + (−1.28286 * U1 − 0.36578 * THRUST − 0.063231 * V − 0.00837 * α) * (1 − PX2)
Z3 = Z3 * PX3 + (−3.77418 * U1 + 1.35225 * THRUST + 0.0058868 * V − 0.05624 * α) * (1 − PX3)
U = 0.01322 * Z1 − 0.00804 * Z2 + 0.14885 * Z3 − 0.00246356 * V + 0.26831 * α + 0.31 * THRUST
FEED FORWARD = 0.674

EET CONTROL EQUATIONS − LAW NO. 6

```
PX1 = EXP (–10.0 * DT)
PX2 = EXP (–0.8 * DT)
PX3 = EXP (–0.3 * DT)
PX4 = EXP (–0.1 * DT)

CRUISE
   U1 = 0.5 * PILOT COMMAND + U
   Z1 = Z1 * PX1 + U1 * (1 – PX1)
   Z2 = Z2 * PX2 + (–1.96557 * U1 + 3.96326 * THRUST + 0.0888095 * V) * (1 – PX2)
   Z3 = Z3 * PX3 + (12.4322 * U1 – 19.8386 * THRUST – 0.1896362 * V) * (1 – PX3)
   Z4 = Z4 * PX4 + (–62.14339 * U1 + 31.32692 * THRUST + 0.203358 * V) * (1 – PX4)
   U = 0.01029 * Z1 + 0.13913 * Z2 + 0.02504 * Z3 – 0.00362 * Z4 – 0.00563762 * V + 0.29 * THRUST
      FEED FORWARD = 0.5

APPROACH
      U1 = 0.674 * PILOT COMMAND + U
      Z1 = Z1 * PX1 + U1 * (1 – PX1)
      Z2 = Z2 * PX2 + (–2.77793 * U1 – 0.90596 * THRUST – 0.146831 * V) * (1 – PX2)
      Z3 = Z3 * PX3 + (81.6286 * U1 – 31.22271 * THRUST – 0.236749 * V) * (1 – PX3)
      Z4 = Z4 * PX4 + (–220.68686 * U1 + 76.0263 * THRUST + 0.123556 * V) * (1 – PX4)
      U = 0.00783 * Z1 + 0.027712 * Z2 + 0.2725 * Z3 + 0.278 * Z4 + 0.0725686 * V + 0.31 * THRUST
            FEED FORWARD = 0.674
```

EET CONTROL EQUATIONS – LAW NO. 7

```
PX1 = EXP (–10.0 * DT)

CRUISE
      U1 = 0.5 * PILOT COMMAND + U
      Z1 = Z1 * PX1 + U1 * (1 – PX1)
      U = 0.00736 * Z1 + 0.02284 * θ̇ + 0.00891 * θ + 0.00101706 * (AN – 6.18744 * THRUST)
            + 0.00234827 * V + 0.29 * THRUST
            FEED FORWARD = 0.5

APPROACH
      U1 = 0.674 * PILOT COMMAND + U
      Z1 = Z1 * PX1 + U1 * (1 – PX1)
      U = 0.01464 * Z1 + 0.11981 * θ̇ + 0.04168 * θ + 0.0071194 * (AN – 1.92469 * THRUST)
            – 0.003096 * V + 0.31 * THRUST
            FEED FORWARD = 0.674
```

EET CONTROL EQUATIONS – LAW NO. 14

```
PX1 = EXP (–10.0 * DT)
PX2 = EXP (–0.8 * DT)
PX3 = EXP (–0.3 * DT)
PX4 = EXP (–0.1 * DT)

CRUISE
      U1 = 0.5 * PILOT COMMAND + U
      Z1 = Z1 * PX1 + U1 * (1 – PX1)
      Z2 = Z2 * PX2 + (–9.8747 * U1 + 1.67371 * THRUST – 0.145632 * (AN – 6.18744 * THRUST)) * (1 – PX2)
      Z3 = Z3 * PX3 + (–13.388 * U1 + 0.35893 * THRUST – 0.0241408 * (AN – 6.18744 * THRUST)) * (1 – PX3)
      Z4 = Z4 * PX4 + (9.00817 * U1 + 4.01193 * THRUST + 0.0714384 * (AN – 6.18744 * THRUST)) * (1 – PX4)
      U = 0.02528 * Z1 + 0.11535 * Z2 – 0.21582 * Z3 – 0.0949 * Z4 + 0.0016072 * (AN – 6.18744 * THRUST)
          + 0.29 * THRUST
          FEED FORWARD = 0.5

APPROACH
      U1 = 0.674 * PILOT COMMAND + U
      Z1 = Z1 * PX1 + U1 * (1 – PX1)
      Z2 = Z2 * PX2 + (45.476 * U1 – 12.35196 * THRUST + 0.11441 * (AN – 1.925 * THRUST)) * (1 – PX2)
      Z3 = Z3 * PX3 + (–181.178* U1 + 54.41 * THRUST – 0.20867 * (AN – 1.925 * THRUST)) * (1 – PX3)
      Z4 = Z4 * PX4 + (259.881 * U1 – 78.592 * THRUST + 0.882648 * (AN – 1.925 * THRUST)) * (1 – PX4)
      U = 0.11707 * Z1 – 0.13954 * Z2 – 0.18646 * Z3 – 0.20546 * Z4 + 0.043328 * (AN – 1.925 * THRUST)
          + 0.31 * THRUST
          FEED FORWARD = 0.674
```

EET CONTROL EQUATIONS – LAW NO. 26

PX1 = EXP (−10.0 * DT)
PX2 = EXP (−0.3 * DT)

CRUISE
U1 = 0.5 * PILOT COMMAND + U
Z1 = Z1 * PX1 + U1 * (1 − PX1)
Z2 = Z2 * PX2 + (−1.00934 * U1 + 0.19768 * THRUST + 3.226 * $\dot{\theta}$ + 0.0026 * θ − 0.0067568 * (AN − 6.189 * THRUST)) * (1 − PX2)
U = 0.03705 * Z1 − 0.876 * Z2 + 0.07379 * $\dot{\theta}$ + 0.00618 * θ + 0.008692 * (AN − 6.189 * THRUST) + 0.29 * THRUST
FEED FORWARD = 0.5

APPROACH
U1 = 0.674 * PILOT COMMAND + U
Z1 = Z1 * PX1 − 4.676 * U1 * (1 − PX1)
Z2 = Z2 * PX2 + (−15.33 * U1 + 14.38 * THRUST + 287.1 * $\dot{\theta}$ − 20.687 * θ − 1.788 * (AN − 1.925 * THRUST)) * (1 − PX2)
U = 0.4167 * Z1 + 0.41495 * Z2 + 0.11705 * $\dot{\theta}$ + 0.03914 * θ − 1.0404 * (AN − 1.925 * THRUST) + 0.31 * THRUST
FEED FORWARD = 0.674

EET CONTROL EQUATIONS — LAW NO. 29

PX1 = EXP (−10.0 * DT)
PX2 = EXP (−0.3 * DT)
PX3 = EXP (−0.1 * DT)

CRUISE
U1 = 0.5 * PILOT COMMAND + U
Z1 = Z1 * PX1 + U1 * (1 − PX1)
Z2 = Z2 * PX2 + (172.656 * U1 − 49.0487 * THRUST + 0.2597 * (AN − 6.189 * THRUST) − 0.43039 * V) * (1 − PX2)
Z3 = Z3 * PX3 + (−509.375 * U1 + 148.39 * THRUST − 0.9095 * (AN − 6.189 * THRUST) + 1.29456 * V) * (1 − PX3)
U = 0.01458 * Z1 + 0.0066 * Z2 + 0.00839 * Z3 + 0.0092 * (AN − 6.189 * THRUST) + 0.002348 * V + 0.29 * THRUST
FEED FORWARD = 0.5

APPROACH
U1 = 0.674 * PILOT COMMAND + U
Z1 = Z1 * PX1 + U1 * (1 − PX1)
Z2 = Z2 * PX2 + (31.072 * U1 − 9.436 * THRUST + 0.03431 * (AN − 1.925 * THRUST) − 0.003697 * V) * (1 − PX2)
Z3 = Z3 * PX3 + (−91.893 * U1 + 28.636 * THRUST − 0.2438 * (AN − 1.925 * THRUST) + 0.01126 * V) * (1 − PX3)
U = 0.02541 * Z1 + 0.02305 * Z2 + 0.03773 * Z3 + 0.0059368 * (AN − 1.925 * THRUST) − 0.003096 * V + 0.31 * THRUST
FEED FORWARD = 0.674

EET CONTROL EQUATIONS — LAW NO. 30

Gain Programs - DETAC Simulation Control Laws

The gain programs for the Control Laws 1 through 7 which were used in the DETAC Simulation are provided below:

Control Law No. 1

```
VES=778.3
P1=0.0001216*VES-0.04826
P2=-0.0002852*VES+0.33667
P3=-0.00005715*VES+0.053745
P4=-0.0001767*VES+0.1604
P5=-0.00212256*VES+18.272
P6=-0.00032312*VES+0.751484
```

Control Law No. 2

```
P1=1.0
P2=-1.2033662E-01*VES+105.23596
P3=2.3375975*VES-1810.5927
P4=-2.1355933E-02*VES+20.359
P5=1.8124419E-04*VES-0.63106235
P6=-0.27639125*VES+209.85567
P7=4.170175*VES-3419.4854
P8=-9.57568985-02*VES+73.686374
P9=6.2922562E-03*VES-3.442263
P10=2.89730735-04*VES-0.24052743
P11=-4.2484679E-04*VES+0.39710826
P12=4.2014856E-04*VES-0.43945162
P13=-2.7635097E-03*VES+2.2120296
P14=-5.1758774E-05*VES+0.053746674
P15=-2.11699165-03*VES+18.267654
P16=-3.2311977E-04*VES+0.75148412
```

Control Law No. 3

```
P1=1.0
P2=-4.9990714E-05*VES-0.10623222
P3=9.795077E-03*VES+65.201718
P4=2.8076137E-04*VES-1.5883665
P5=7.1164345E-04*VES+2.3066779
P6=1.6441225E-03*VES-1.6970705
P7=1.8570102E-06*VES-5.35311045-04
P8=1.3184215E-03*VES-0.39611748
P9=-7.6404828E-04*VES+0.48078877
P10=-1.7669452E-04*VES+0.16040134
P11=-5.7158774E-05*VES+0.053746674
P12=-2.1169916E-03*VES+18.267654
P13=-3.2311977E-04*VES+0.75148412
```

Control Law No. 4

P1=-9.16063135-04*VES+1.7129719
P2=-8.5157195E-02*VES+70.198205
P3=1.4744816*VES-1215.1522
P4=3.2548245E-05*VES-0.23968093
P5=-1.2893147E-02*VES+13.677756
P6=-7.2237697E-05*VES+0.051212599
P7=4.7320334E-04*VES-0.38178416
P8=-2.8523676E-04*VES+0.33670977
P9=1.2160471E-04*VES-4.82657755-02
P10=-6.69379755-03*VES+5.2674426
P11=-5.71587745-05*VES+0.053746674
P12=-2.11699165-03*VES+18.267654
P13=-3.23119775-04*VES+0.75148412

Control Law No. 5

P1=1.0
P2=(-0.0064421*VES-5.8587391)
P3=(-0.00004694*VES+2.094)
P4=(-0.0020818*VES-0.216036)
P5=(0.1246553*VES-176.9425)
P6=(-0.0781486*VES+65.1395)
P7=(-0.020233*VES-2.5418102)
P8=(-0.14449*VES+192.23915)
P9=(0.091731*VES-72.77957)
P10=(0.0240859*VES+3.42675)
P11=-0.0000003515*VES+0.01527859
P12=0.000057984*VES+0.112885
P13=-0.0001968869*VES-0.0245289
P14=-0.000150727*VES-0.028543
P15=-0.0006318477*VES+0.71129008
P16=-2.11699165-03*VES+18.267654
P17=-0.00032312*VES+0.75148

Control Law No. 6

P1=1.0
P2=3.2480538E-02*VES-9.0716931
P3=-0.81504921*VES+174.49115
P4=-2.0650175E-03*VES-0.60962817
P5=4.2475851E-03*VES-1.0270368
P6=-8.4130213E-02*VES+16.400245
P7=2.0677381*VES-418.36538
P8=4.9325143E-03*VES-1.0799593
P9=-1.3862841E-02*VES+3.2680693
P10=-6.6295264E-06*VES+1.480976E-02
P11=2.1355617E-06*VES-8.5521077E-03
P12=-2.7533895-04*VES+0.21487626
P13=1.43773255-04*VES-7.7522729E-02
P14=-2.8523676E-04*VES+0.33670977
P15=-2.1169916E-03*VES+18.267654
P16=-3.23119775-04*VES+0.75148412

Control Law No. 7

P1=1.0
P2=1.5085608E-03*VES-3.1396828
P3=0.51807939*VES-176.14312
P4=7.74553125-03*VES-4.4229271
P5=0.12849526*VES+112.44002
P6=0.2112531*VES-2079.388
P7=1.5288068E-03*VES-4.5033176
P8=0.29441684*VES-291.28801
P9=-4.7559634*VES-5496.4666
P10=2.58609215-03*VES+1.5387185
P11=4.56824515-06*VES+6.7345348E-03
P12=-2.5624883E-04*VES+0.33856847
P13=-4.5953574E-04*VES+0.38269667
P14=-5.2297121E-04*VES+0.40340849
P15=-2.5375425E-03*VES+1.8764645
P16=-2.1169916E-03*VES+18.267654
P17=-3.2311977E-04*VES+0.75148412

APPENDIX 8
AUGMENTED AIRCRAFT PERFORMANCE

This section contains data demonstrating the correlation of the Augmented EET aircraft response to that of the DC-10 model for elevator perturbations. Control laws 1 through 7 are shown for both approach and cruise flight conditions.

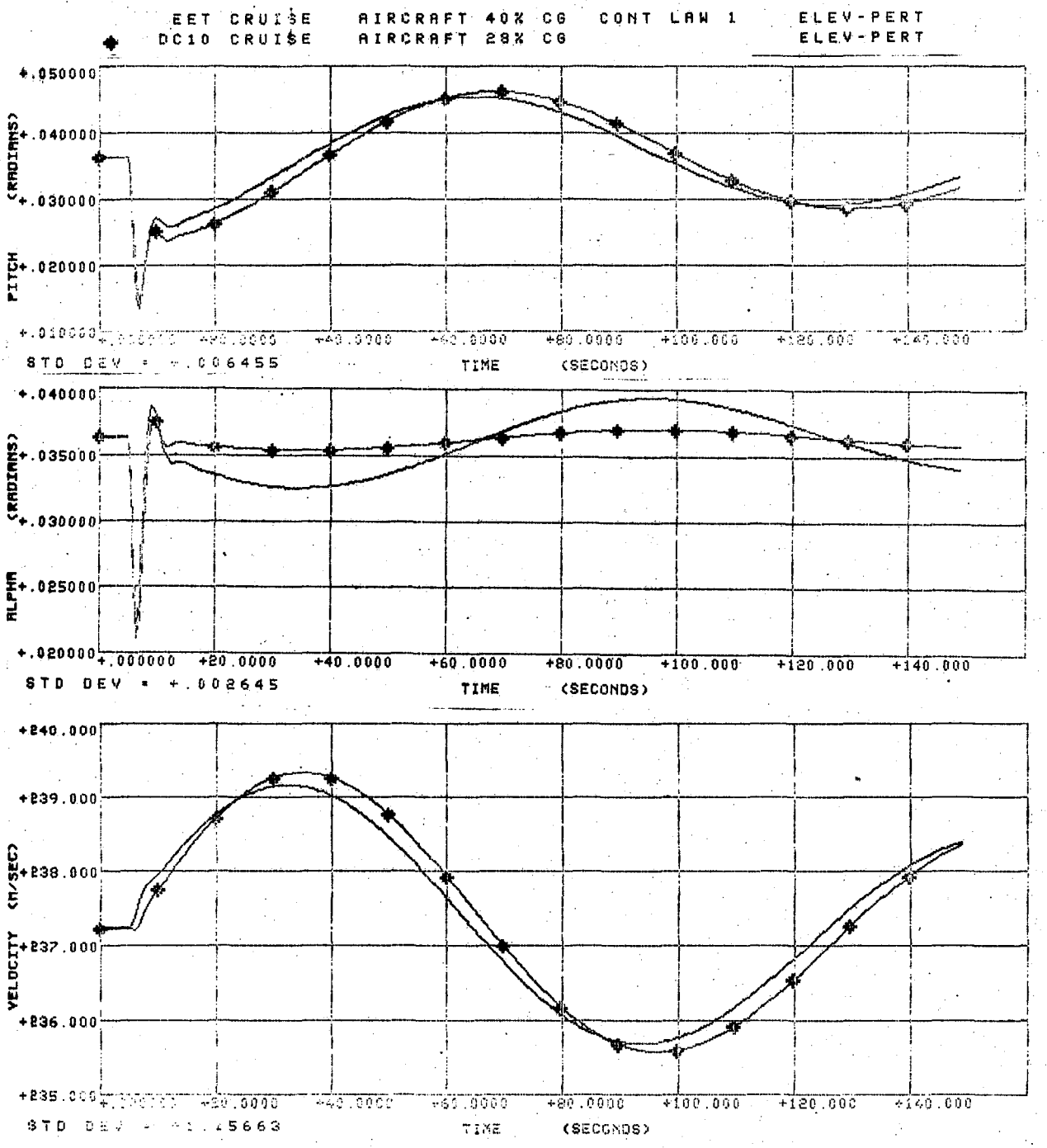

COMPARISON OF BASELINE AND AUGMENTED EET IN CRUISE – CONTROL LAW NO. 1

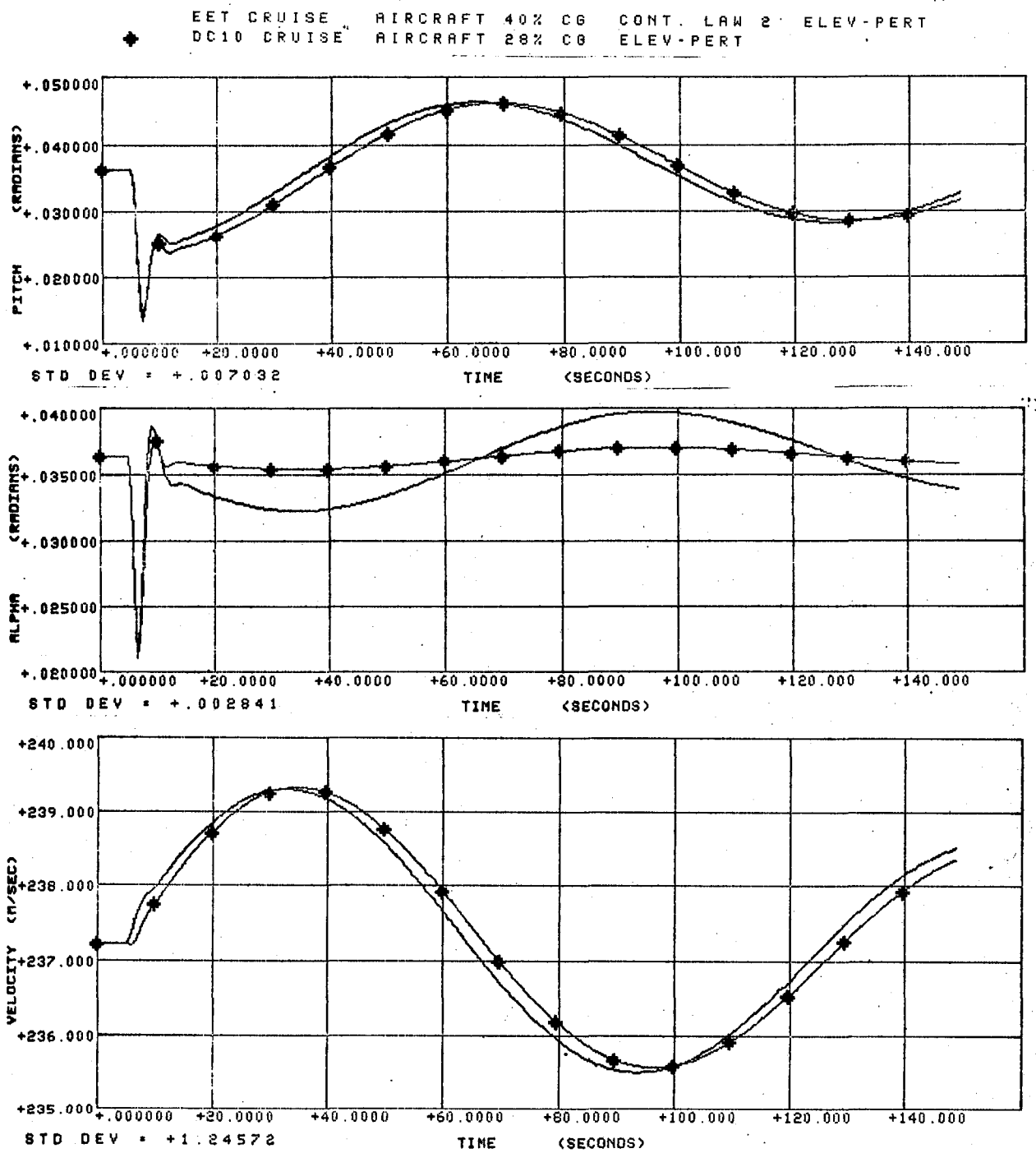

COMPARISON OF BASELINE AND AUGMENTED EET IN CRUISE – CONTROL LAW NO. 2

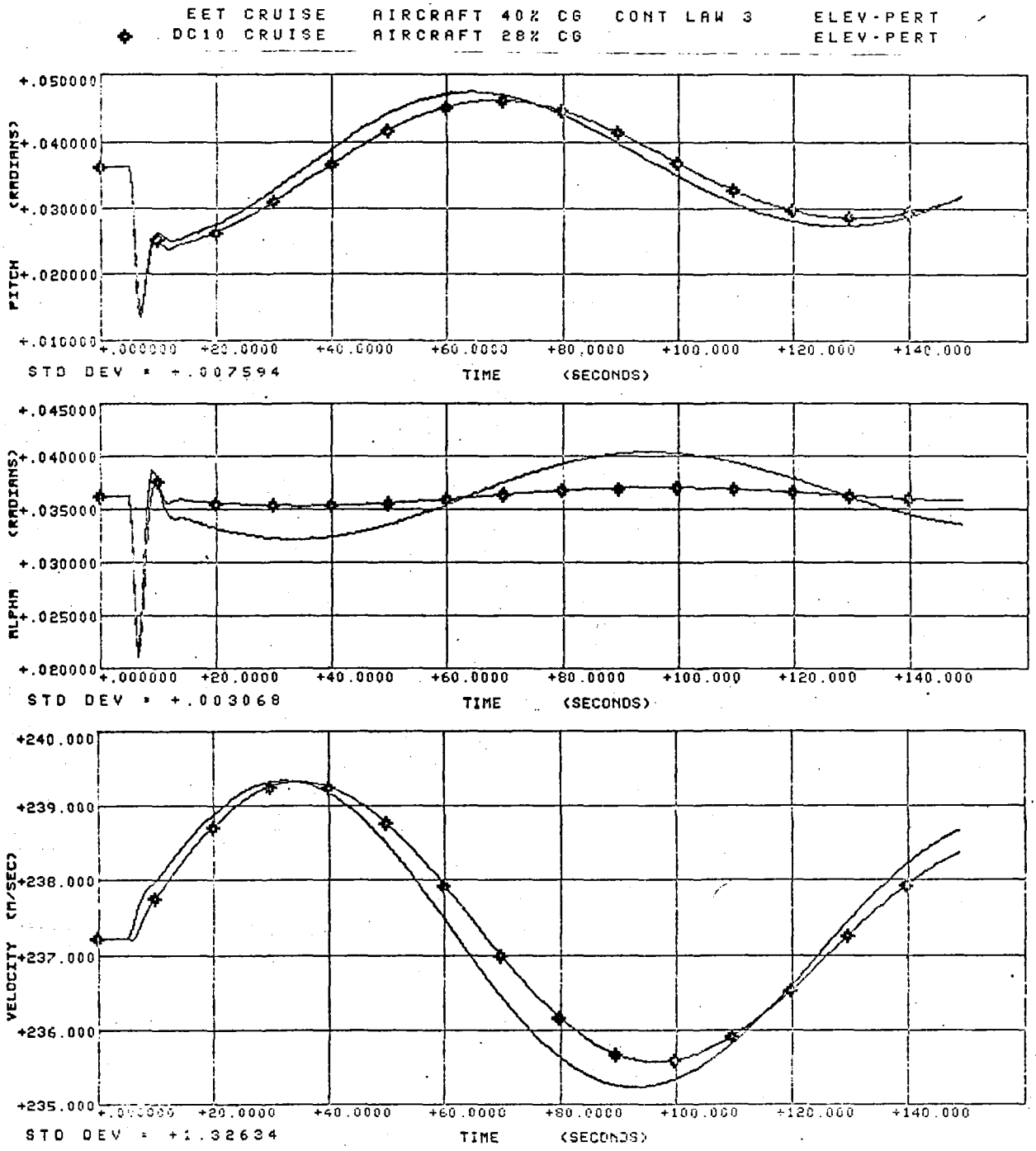

COMPARISON OF BASELINE AND AUGMENTED EET IN CRUISE – CONTROL LAW NO. 3

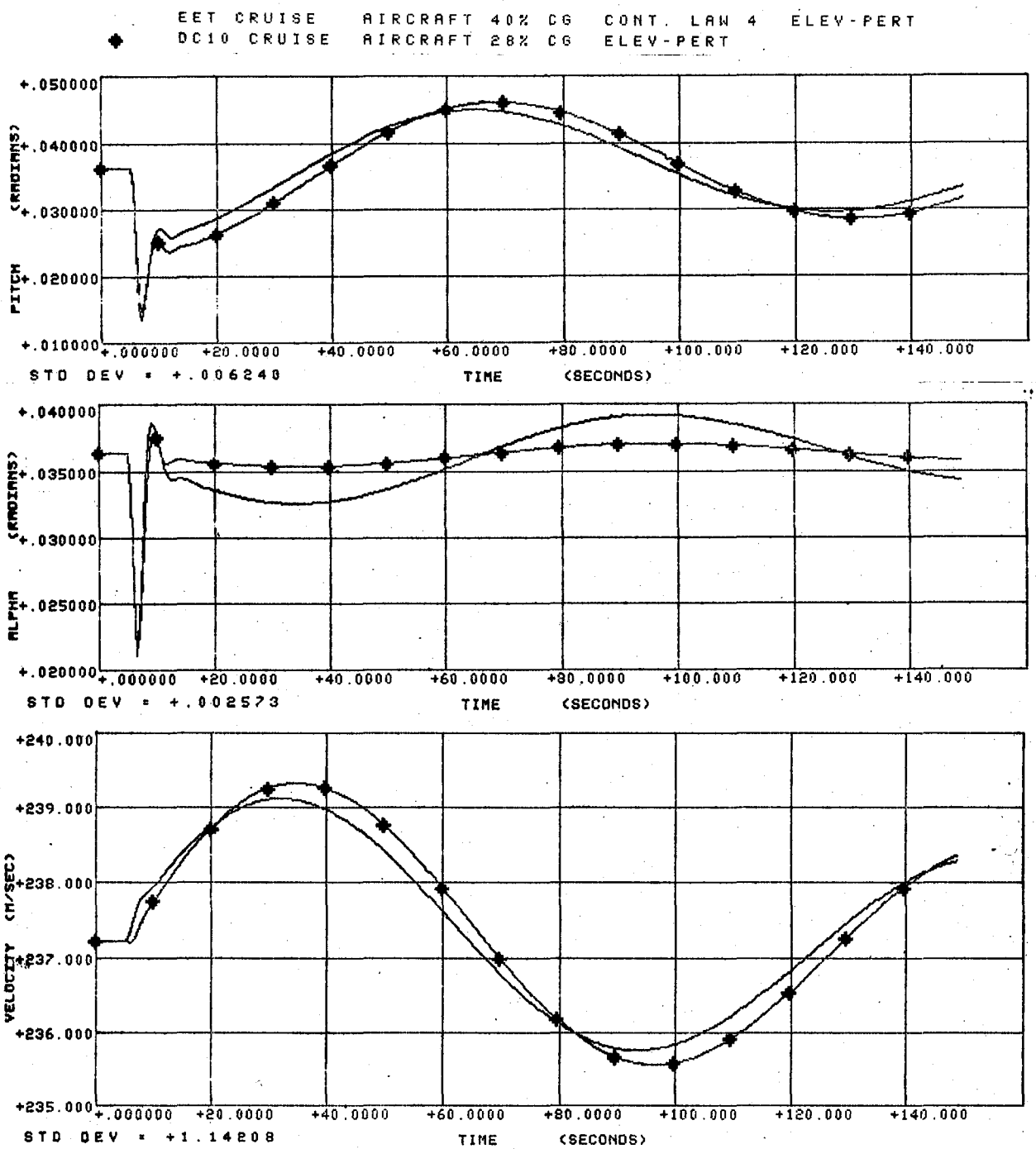

COMPARISON OF BASELINE AND AUGMENTED EET IN CRUISE – CONTROL LAW NO. 4

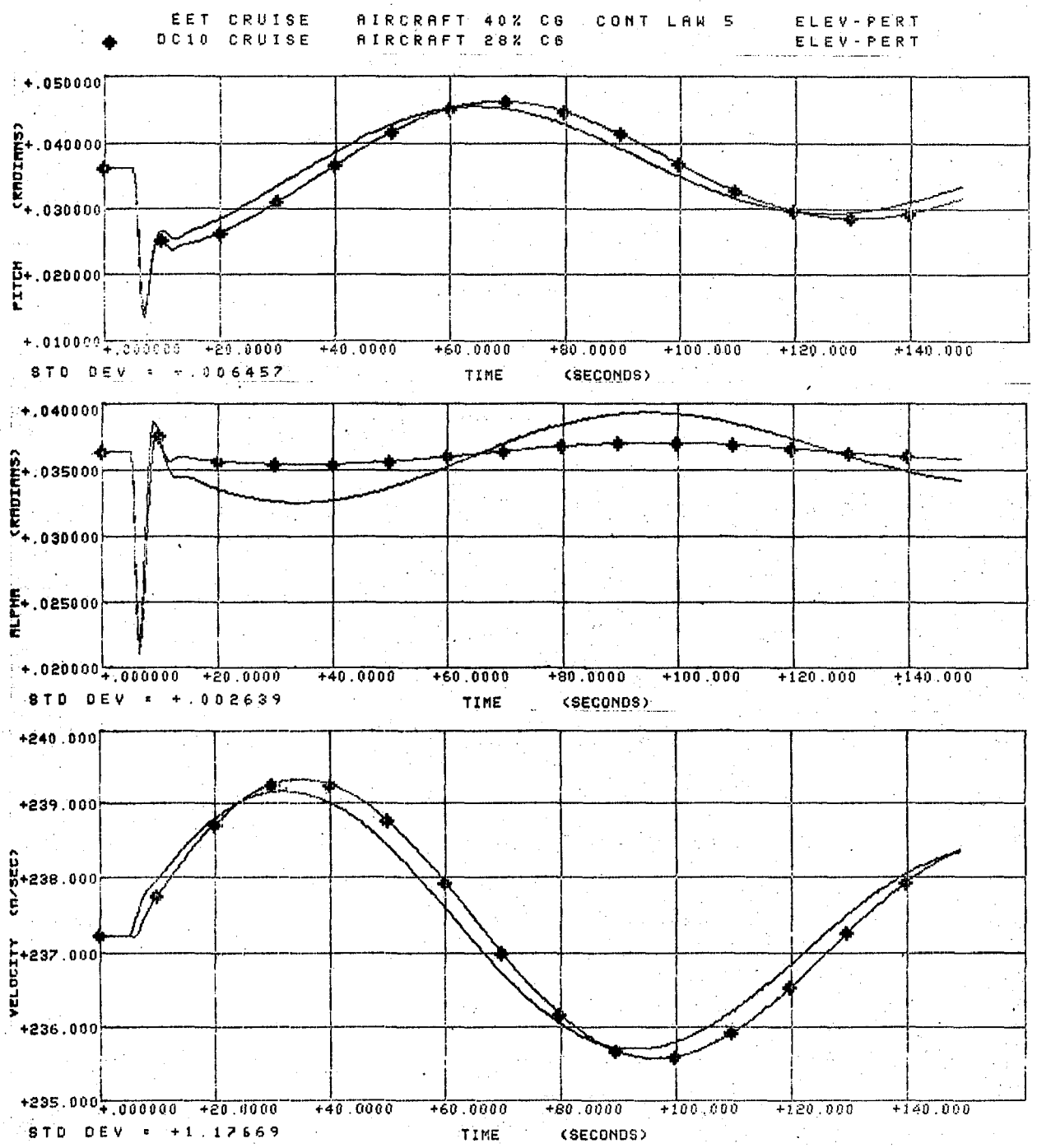

COMPARISON OF BASELINE AND AUGMENTED EET IN CRUISE – CONTROL LAW NO. 5

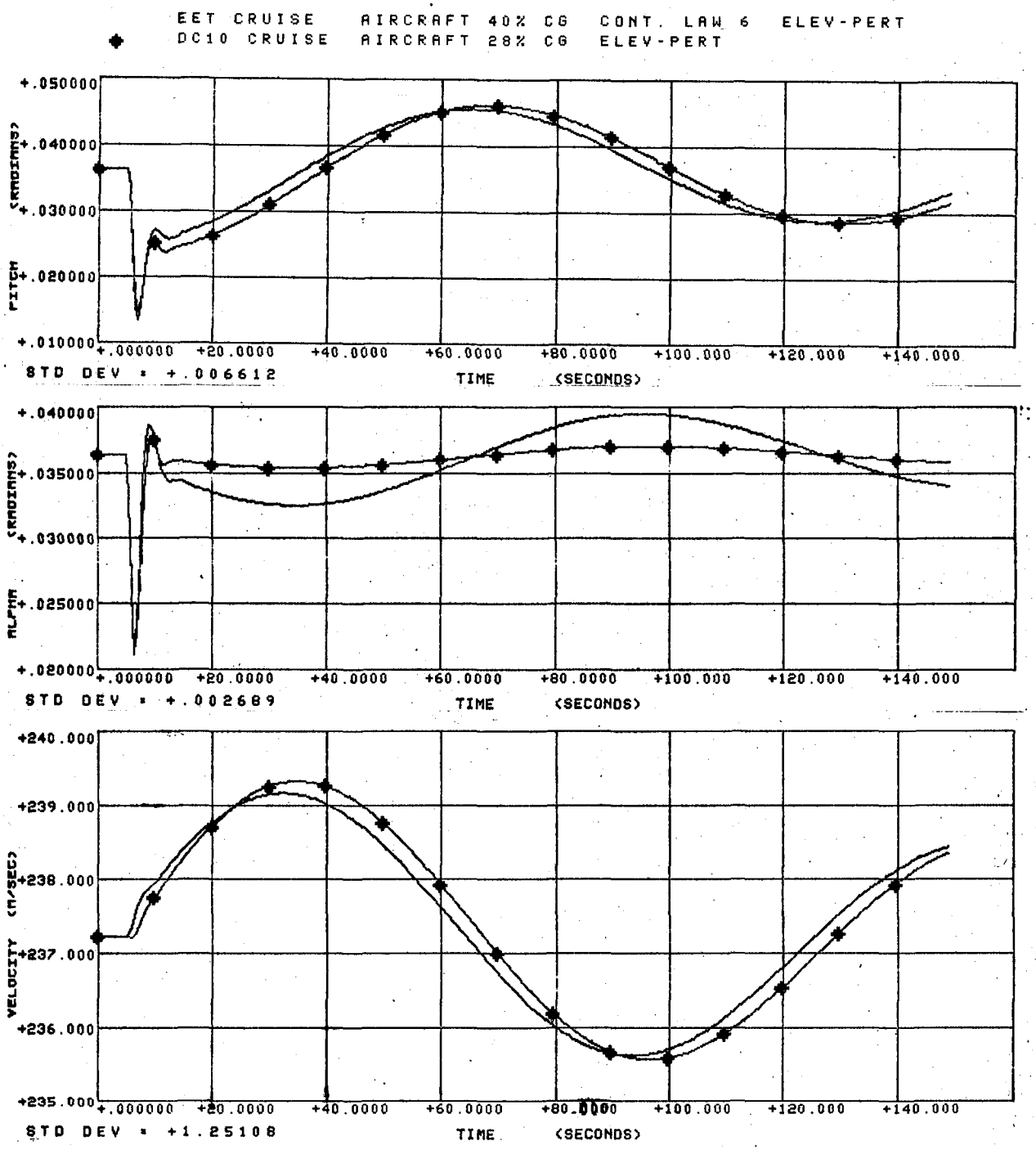

COMPARISON OF BASELINE AND AUGMENTED EET IN CRUISE – CONTROL LAW NO. 6

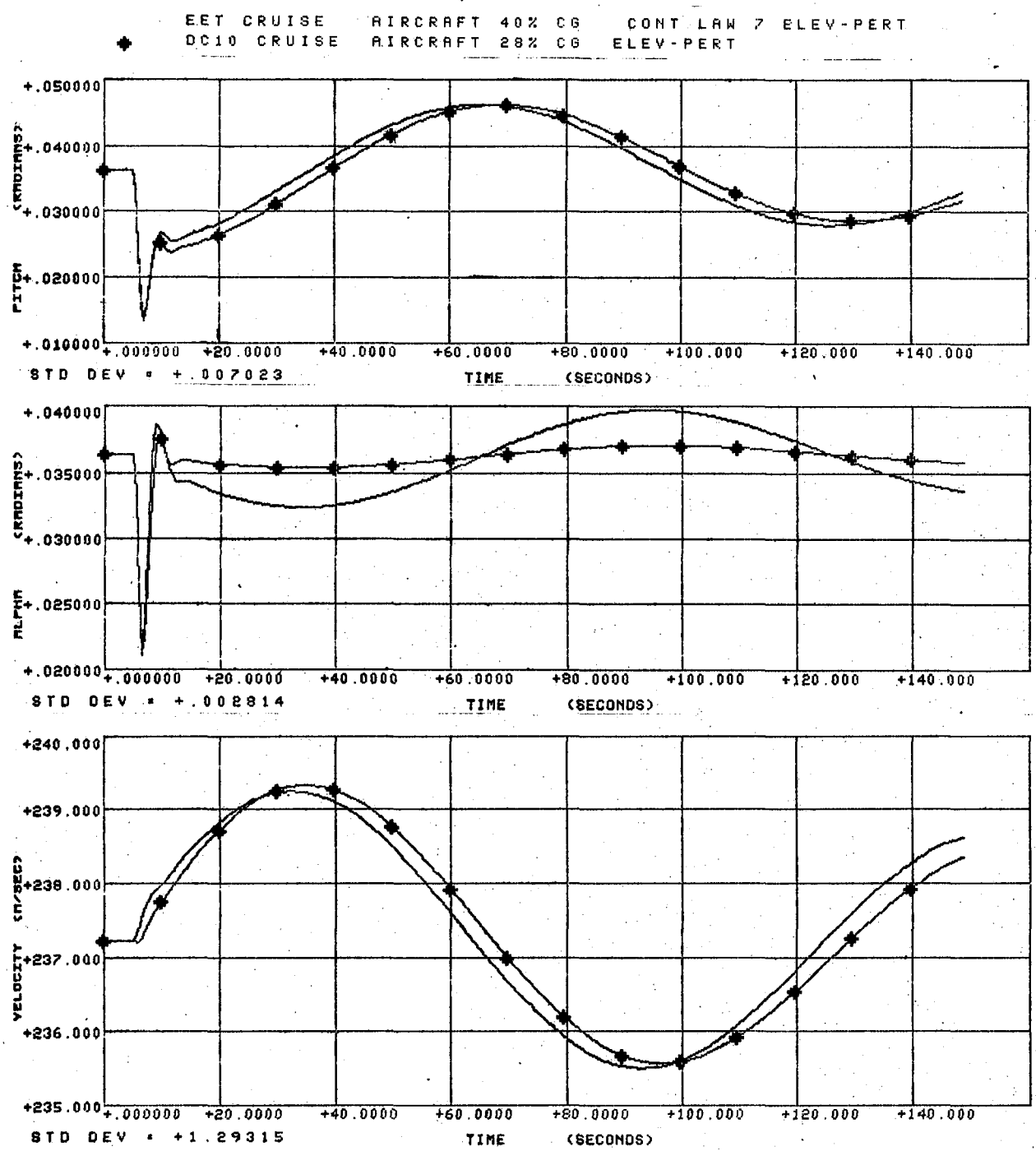

COMPARISON OF BASELINE AND AUGMENTED EET IN CRUISE – CONTROL LAW NO. 7

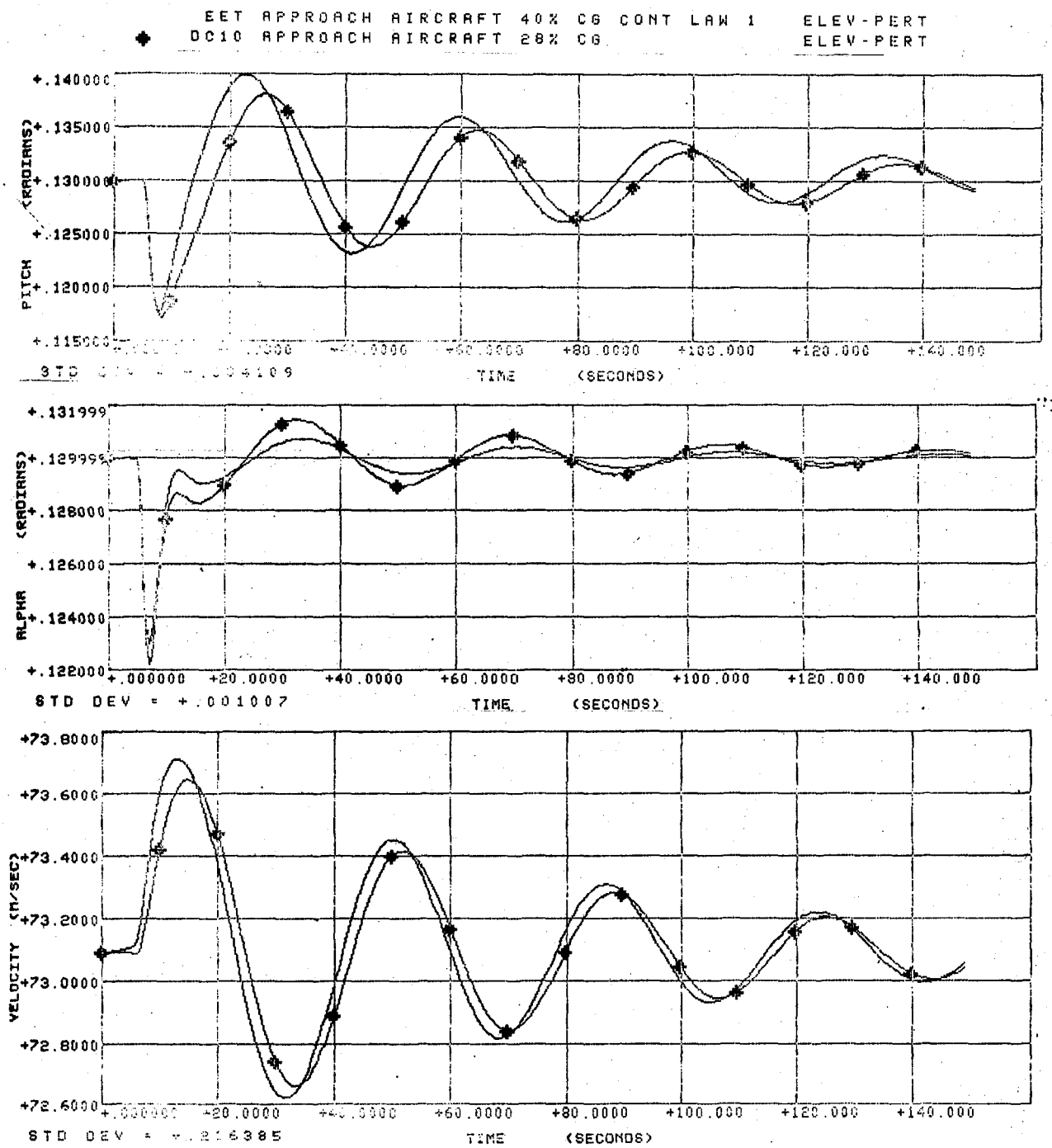

COMPARISON OF BASELINE AND AUGMENTED EET IN APPROACH – CONTROL LAW NO. 1

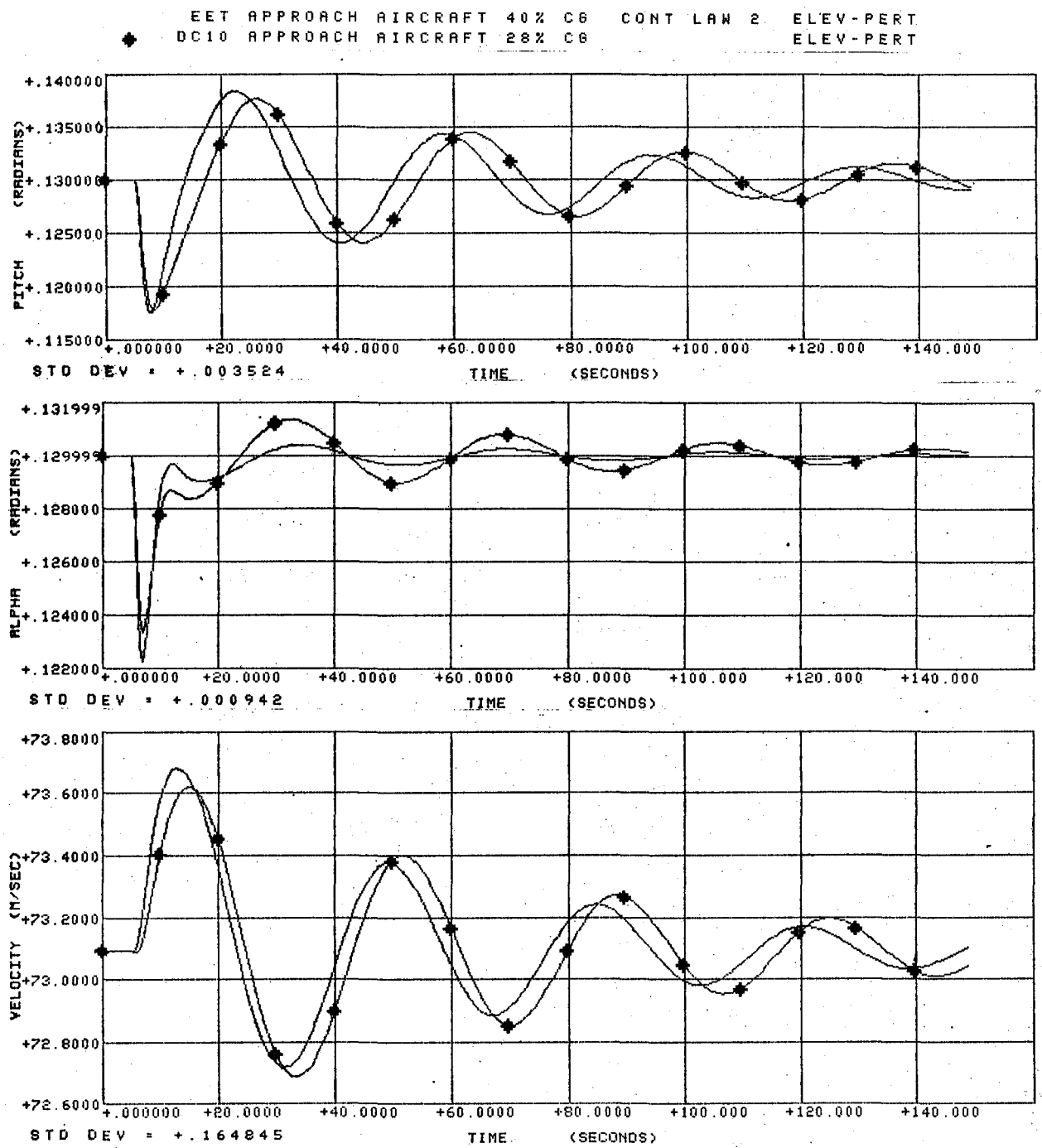

COMPARISON OF BASELINE AND AUGMENTED EET IN APPROACH – CONTROL LAW NO. 2

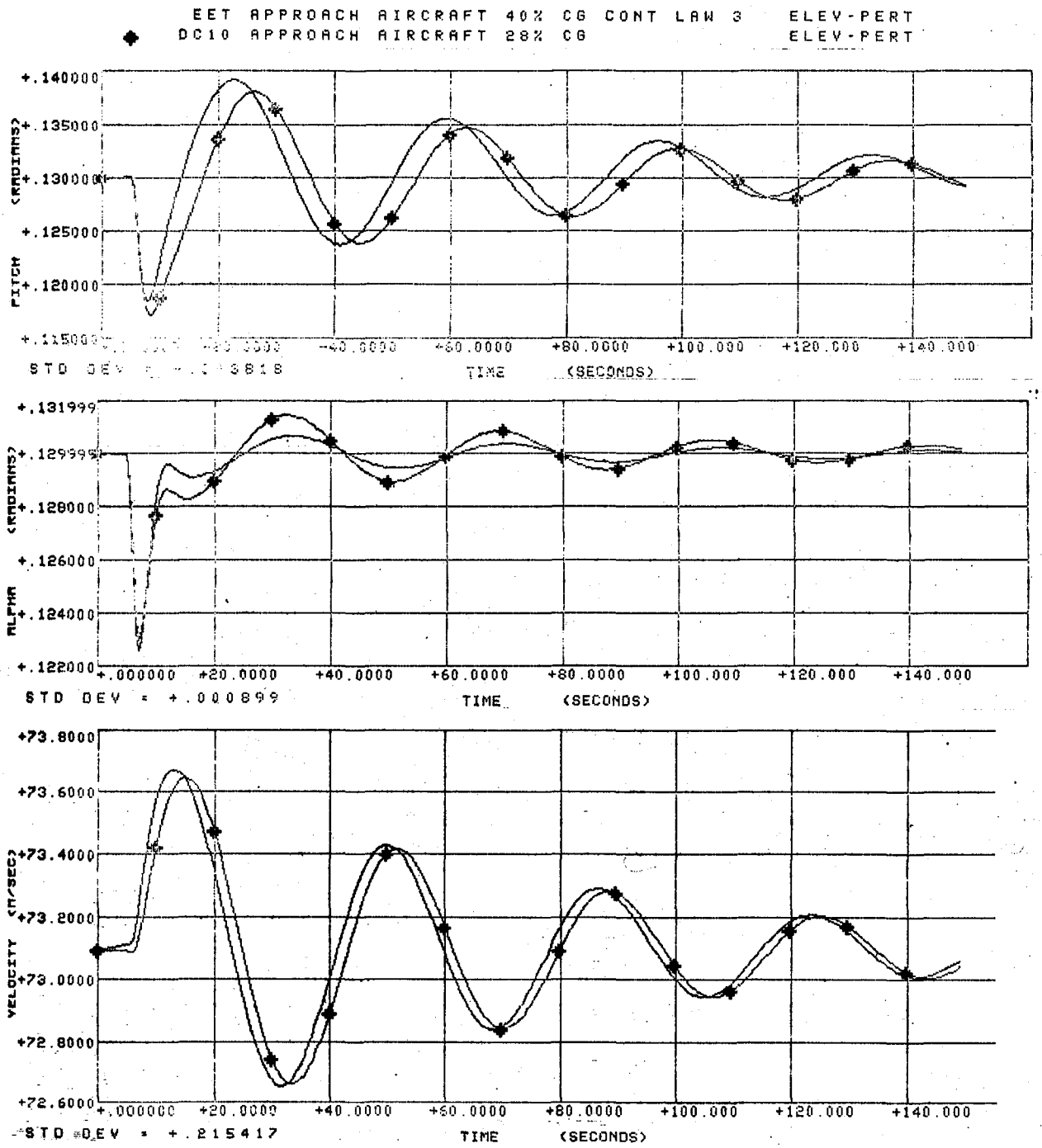

COMPARISON OF BASELINE AND AUGMENTED EET IN APPROACH – CONTROL LAW NO. 3

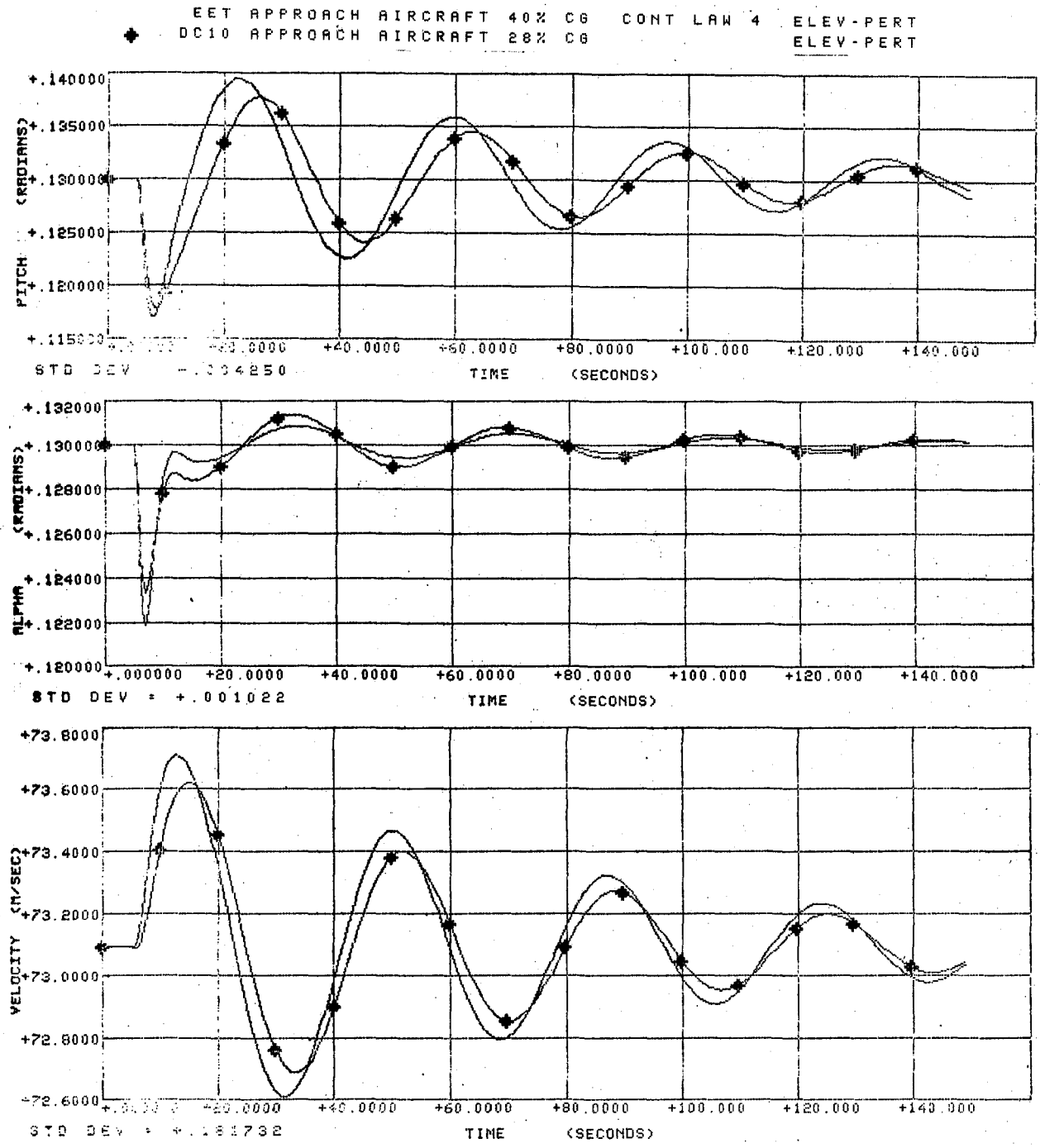

COMPARISON OF BASELINE AND AUGMENTED EET IN APPROACH – CONTROL LAW NO. 4

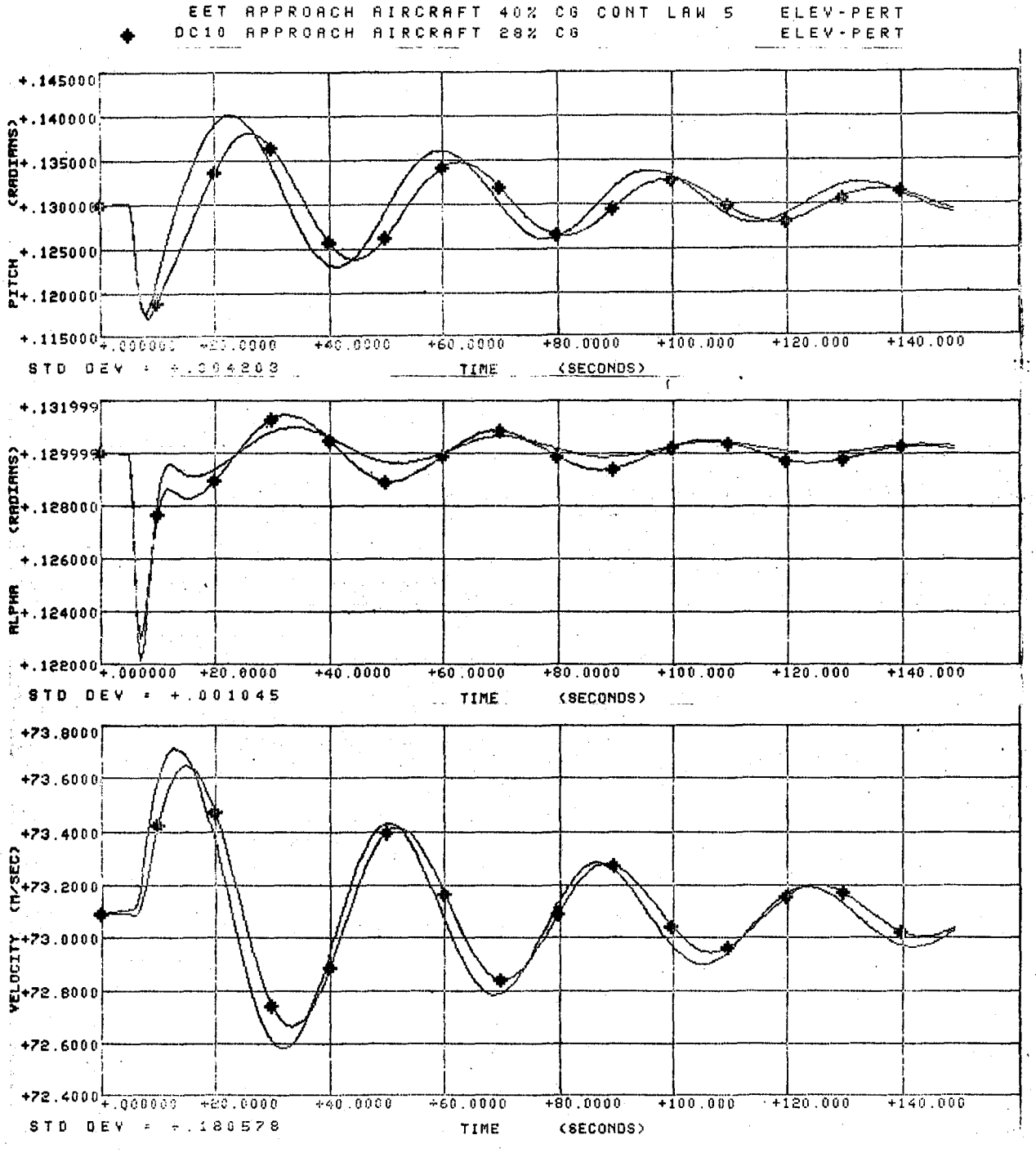

COMPARISON OF BASELINE AND AUGMENTED EET IN APPROACH – CONTROL LAW NO. 5

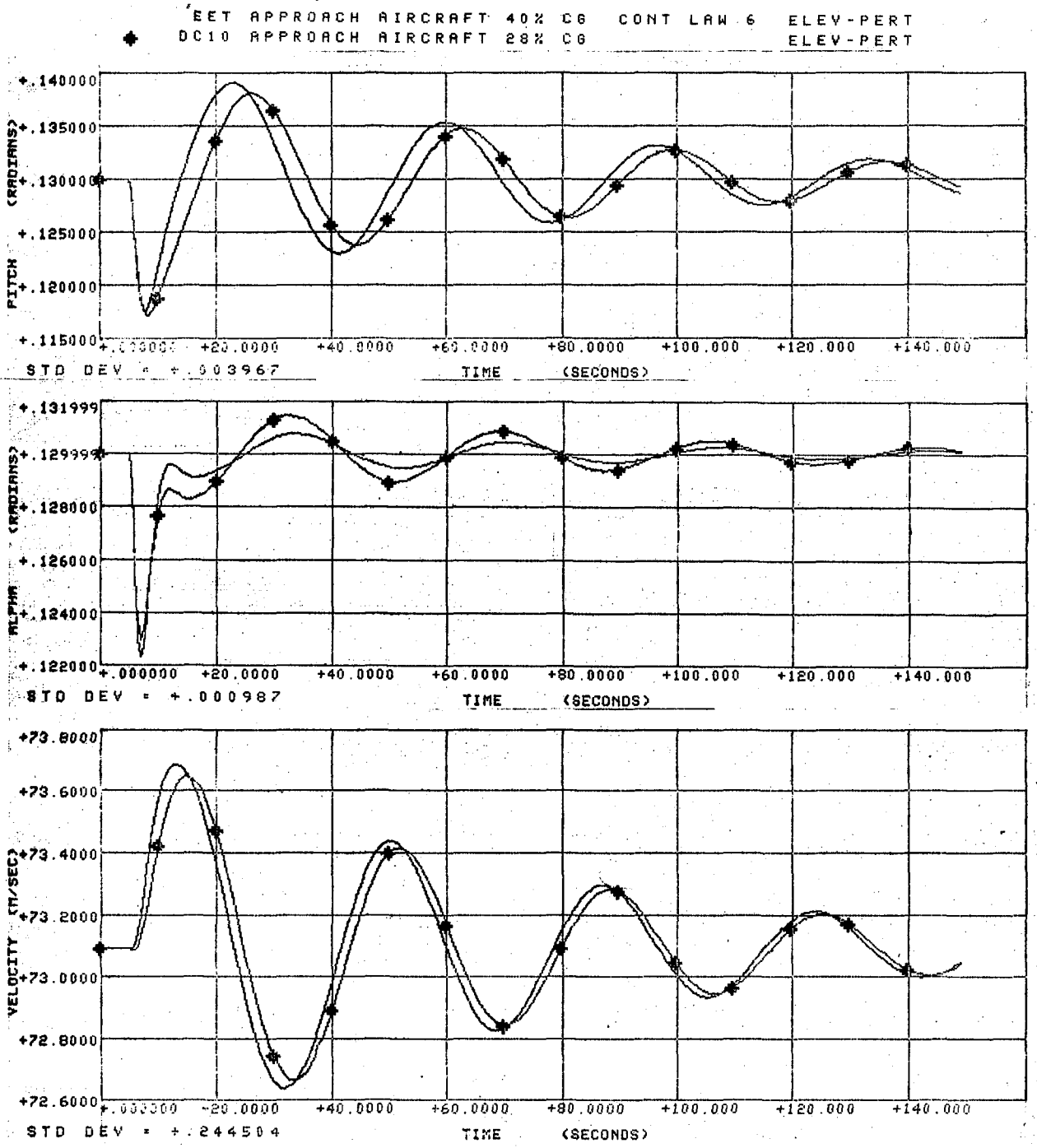

COMPARISON OF BASELINE AND AUGMENTED EET IN APPROACH – CONTROL LAW NO. 6

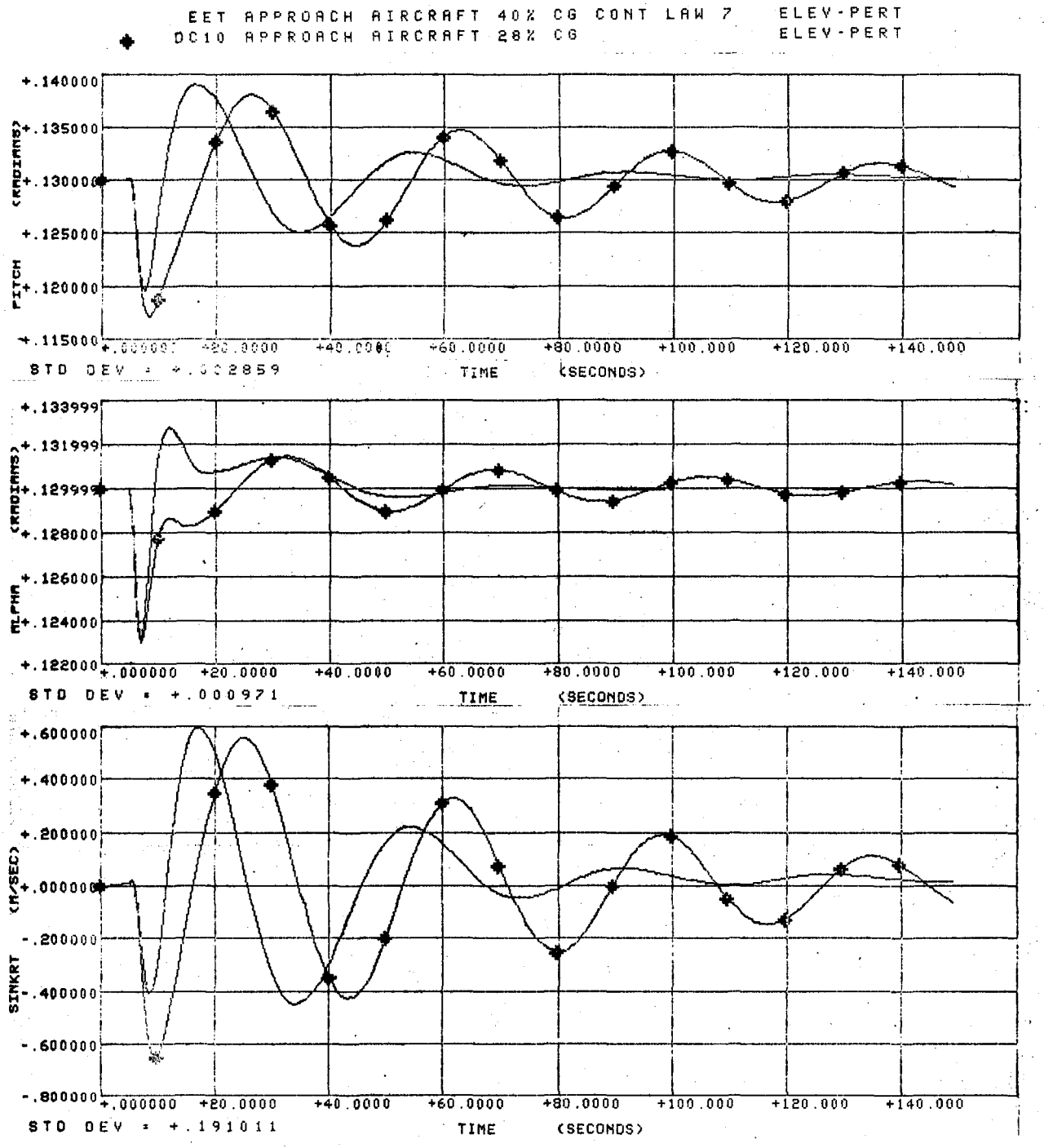

COMPARISON OF BASELINE AND AUGMENTED EET IN APPROACH – CONTROL LAW NO. 7

APPENDIX 9
CONTROL LAW SENSITIVITY

This section contains data showing control law sensitivity to sensor input parameters which have other than nominal tolerance values. The method for establishing worst-case sensor tolerance is discussed in Section 5.

DC10 CRUISE AIRCRAFT 28% CG ELEV-PERT
EET CRUISE AIRCRAFT 40% CG CL 1 MIN SENS TOL ELEV-PERT

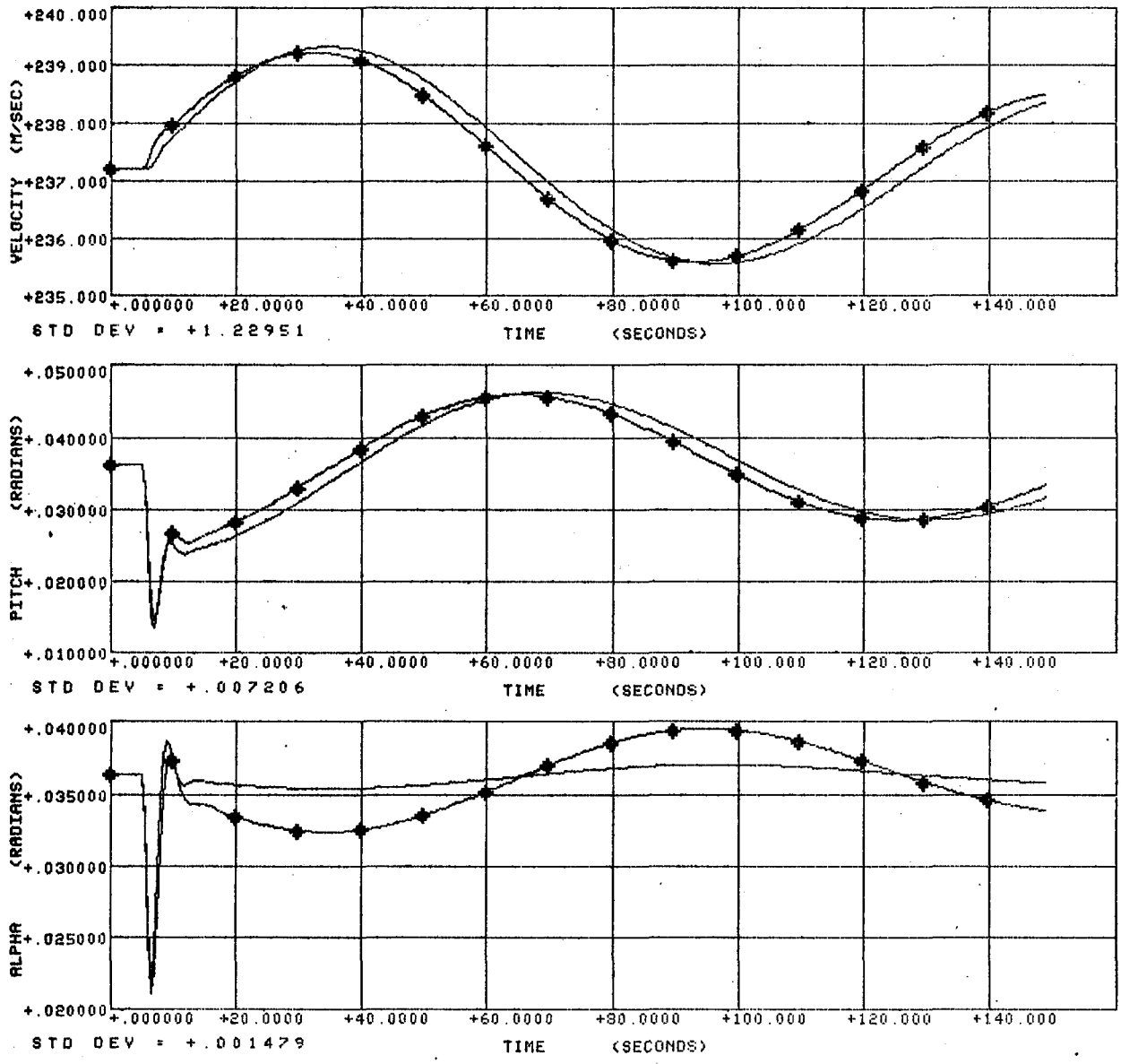

SENSOR TOLERANCE

DC10 CRUISE AIRCRAFT 28% CG ELEV-PERT
EET CRUISE AIRCRAFT 40% CG CL 2 MIN SENS TOL ELEV-PERT

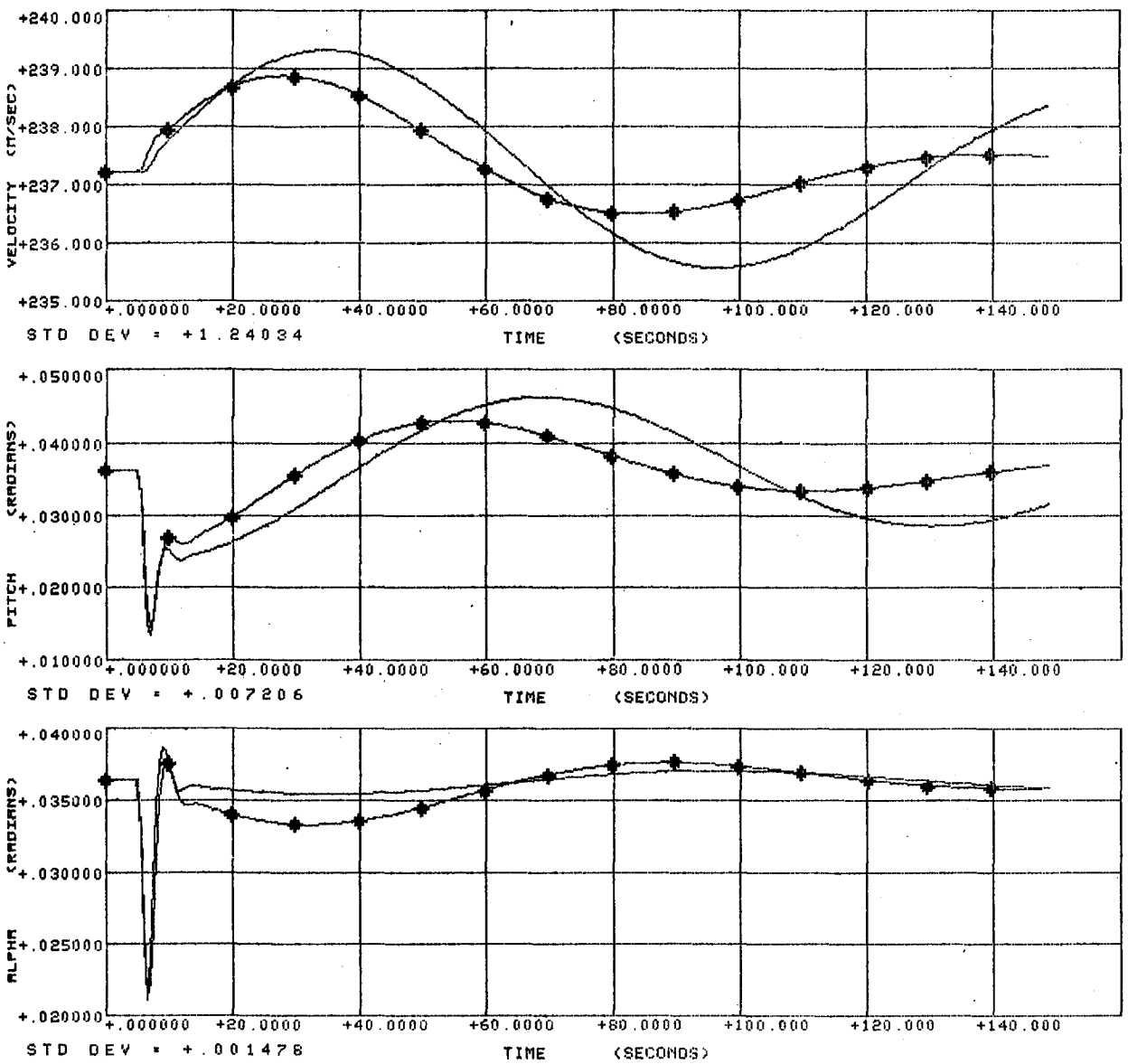

SENSOR TOLERANCE

DC10 CRUISE AIRCRAFT 28% CG ELEV-PERT
EET CRUISE AIRCRAFT 40% CG CL 3 MIN SENS TOL ELEV-PERT

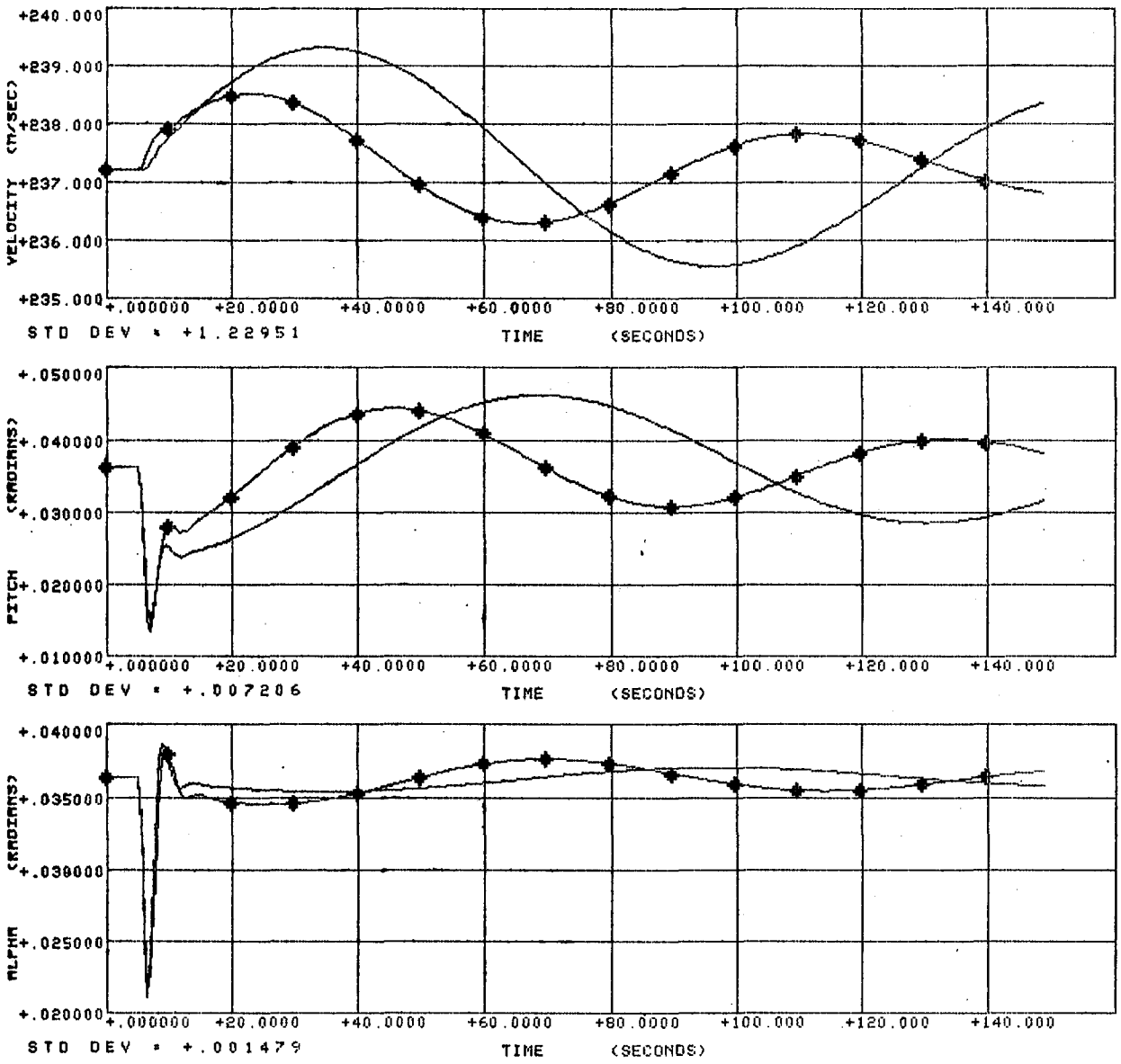

SENSOR TOLERANCE

EET CRUISE AIRCRAFT 40% CG CL 3 TH=1.0 ALP=1.0 ELEV-PERT

EET CRUISE AIRCRAFT 40% CG CL 3 TH=0.9 ALP=1.1 ELEV-PERT

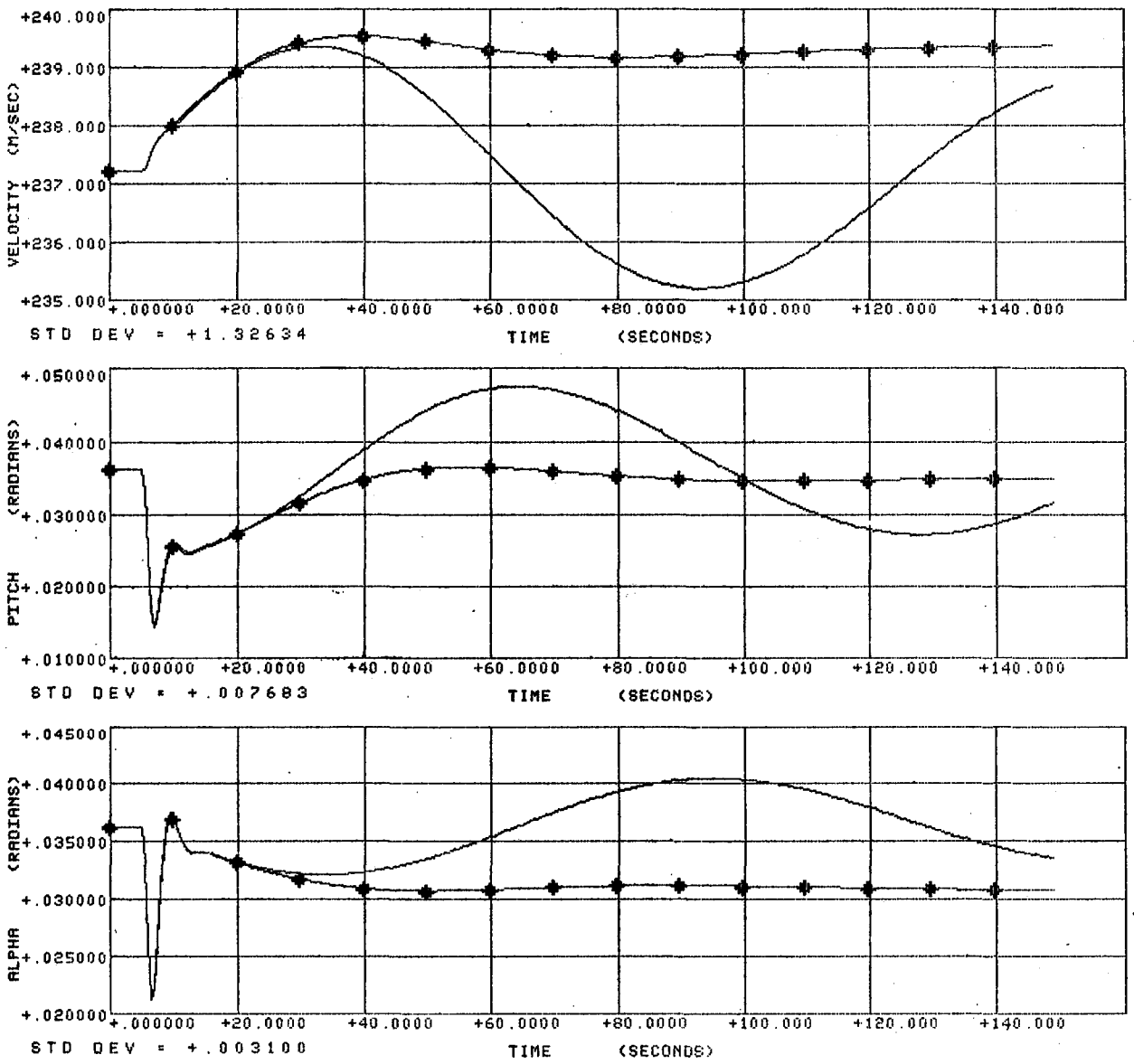

SENSOR TOLERANCE

EET CRUISE AIRCRAFT 40% CG CL 3 TH=1.0 ALP=1.0 ELEV-PERT
EET CRUISE AIRCRAFT 40% CG CL 3 TH=1.1 ALP=.9 ELEV-PERT

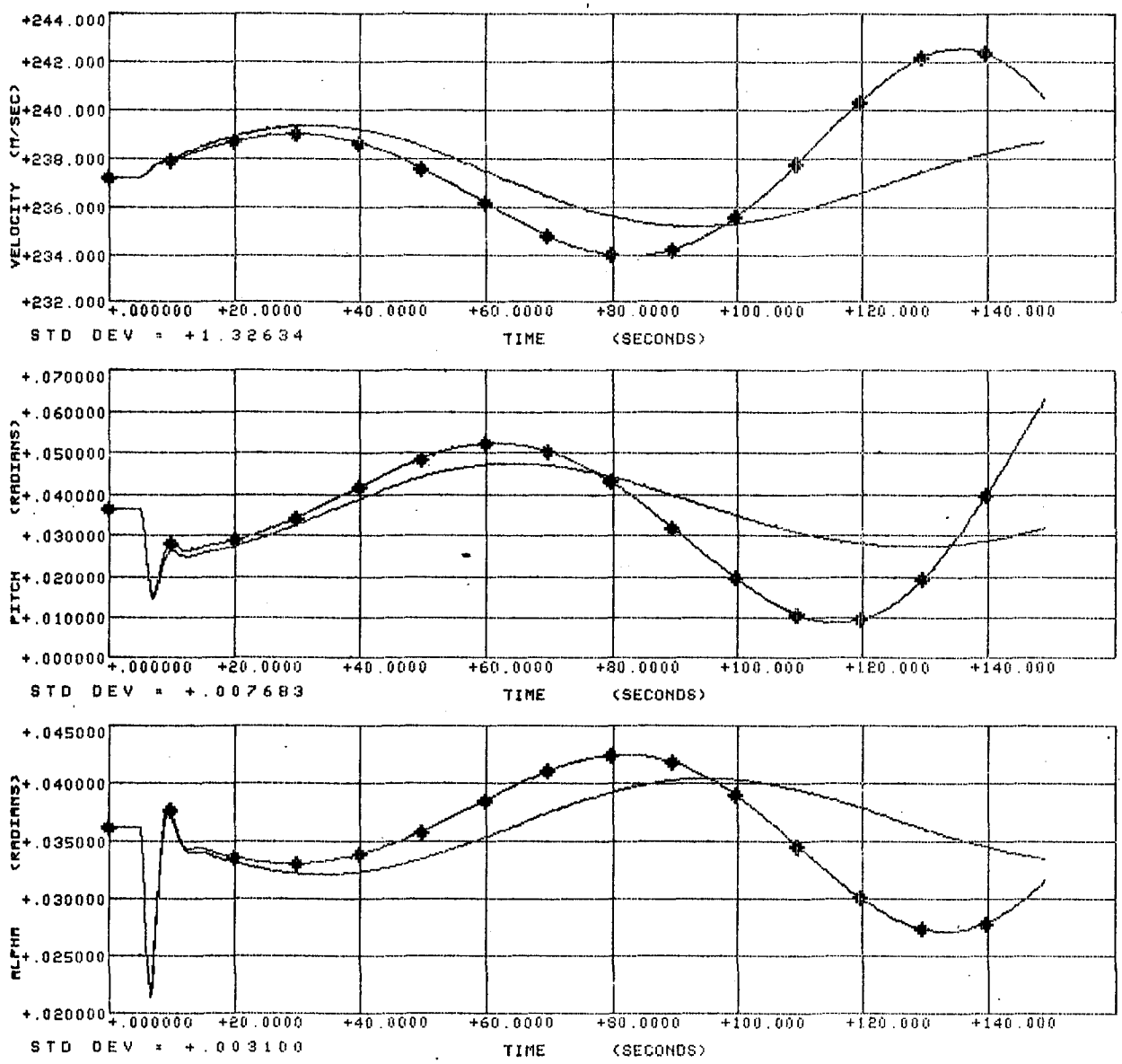

SENSOR TOLERANCE

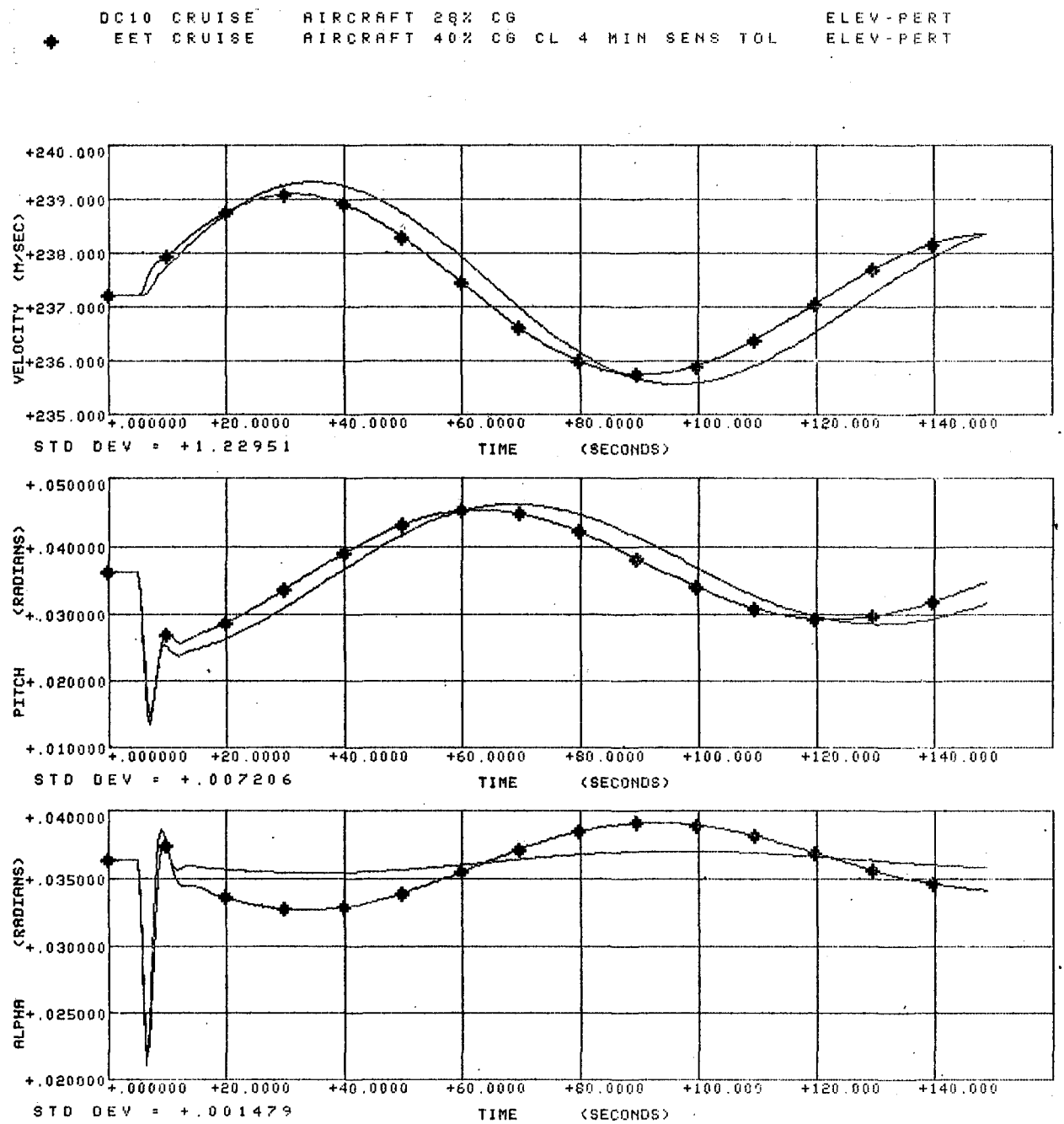

SENSOR TOLERANCE

DC10 CRUISE AIRCRAFT 28% CG ELEV-PERT
EET CRUISE AIRCRAFT 40% CG CL 5 MIN SENS TOL ELEV-PERT

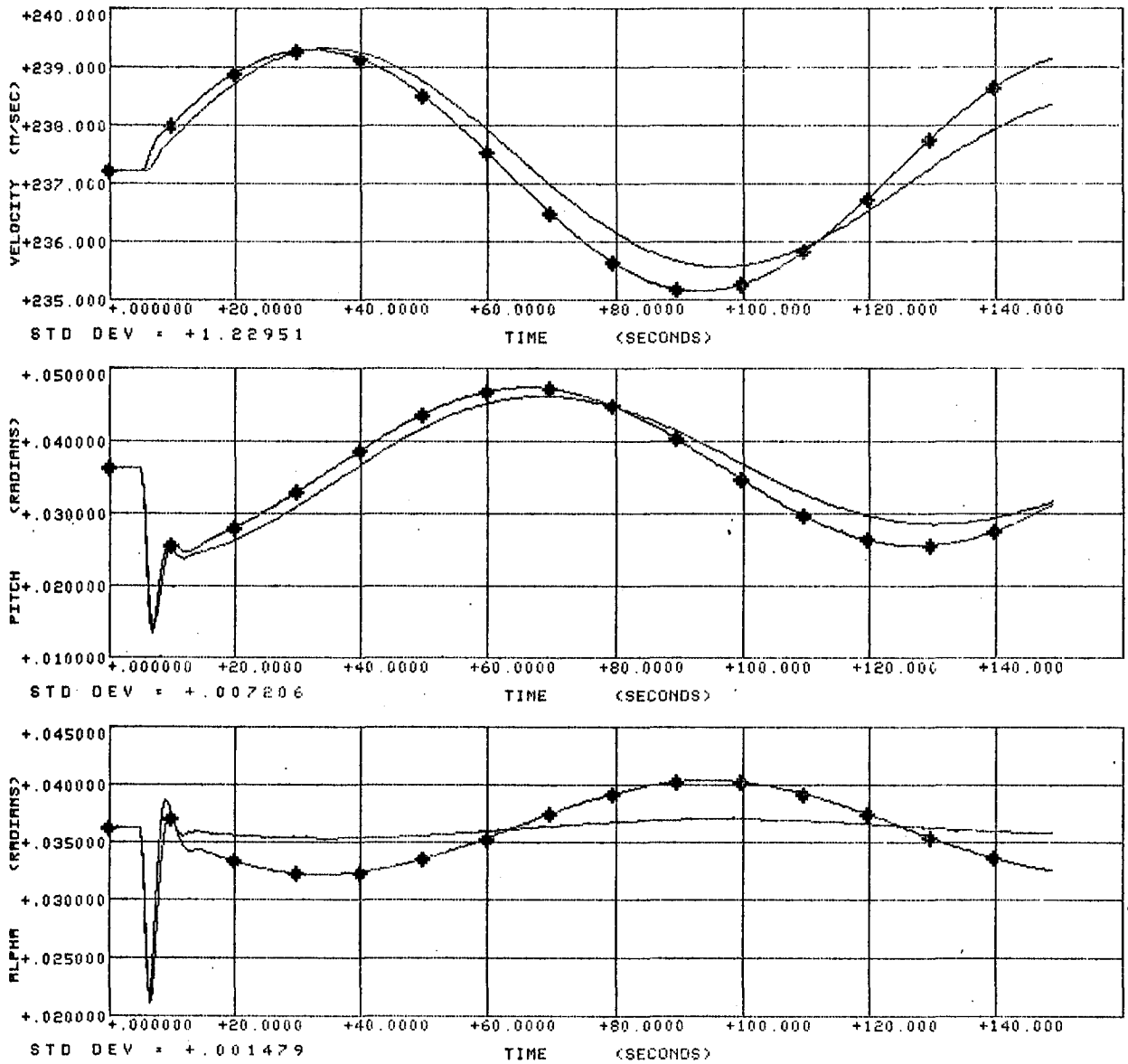

SENSOR TOLERANCE

DC10 CRUISE AIRCRAFT 28% CG ELEV-PERT
EET CRUISE AIRCRAFT 40% CG CL 6 MIN SENS TOL ELEV-PERT

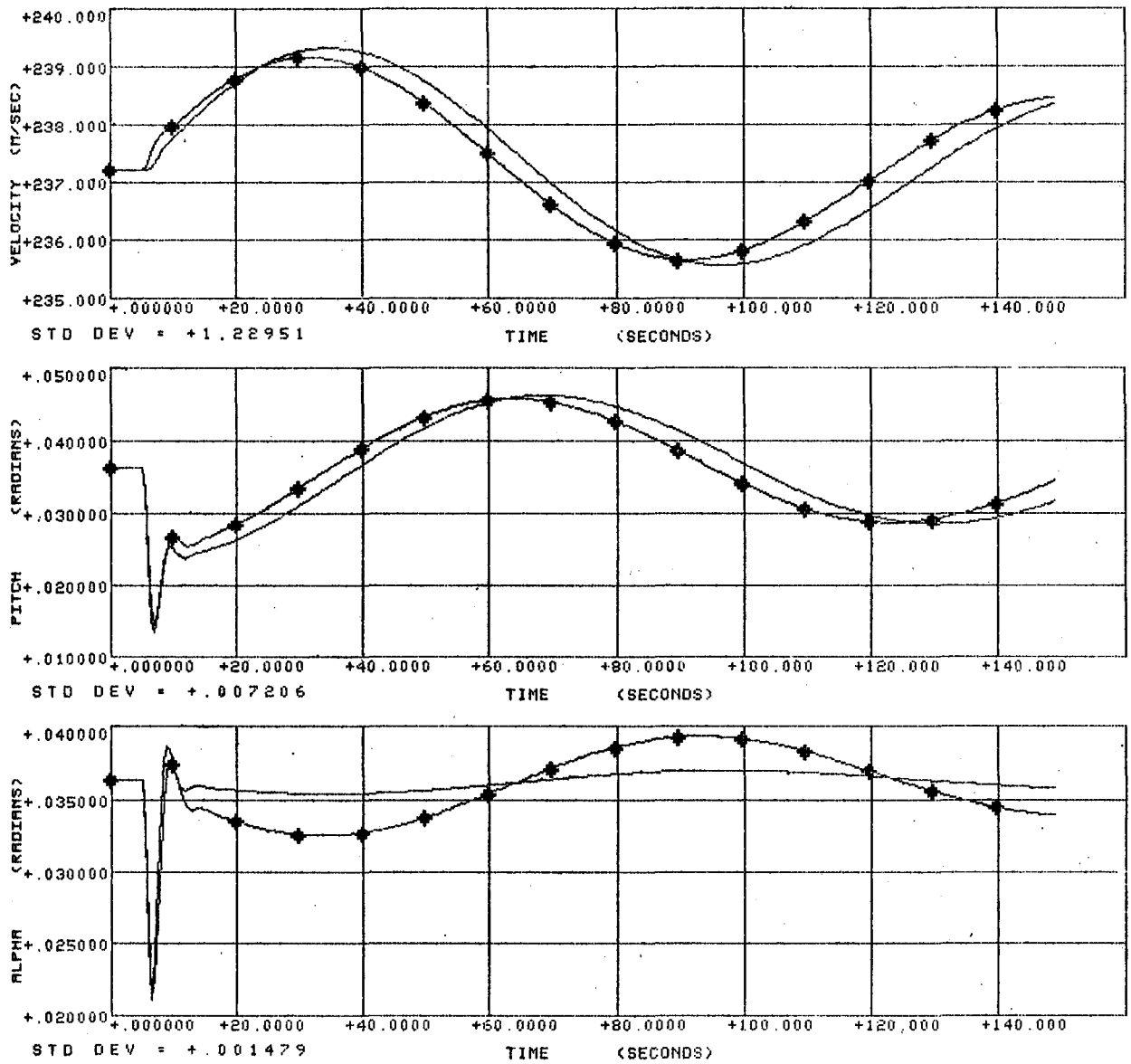

SENSOR TOLERANCE

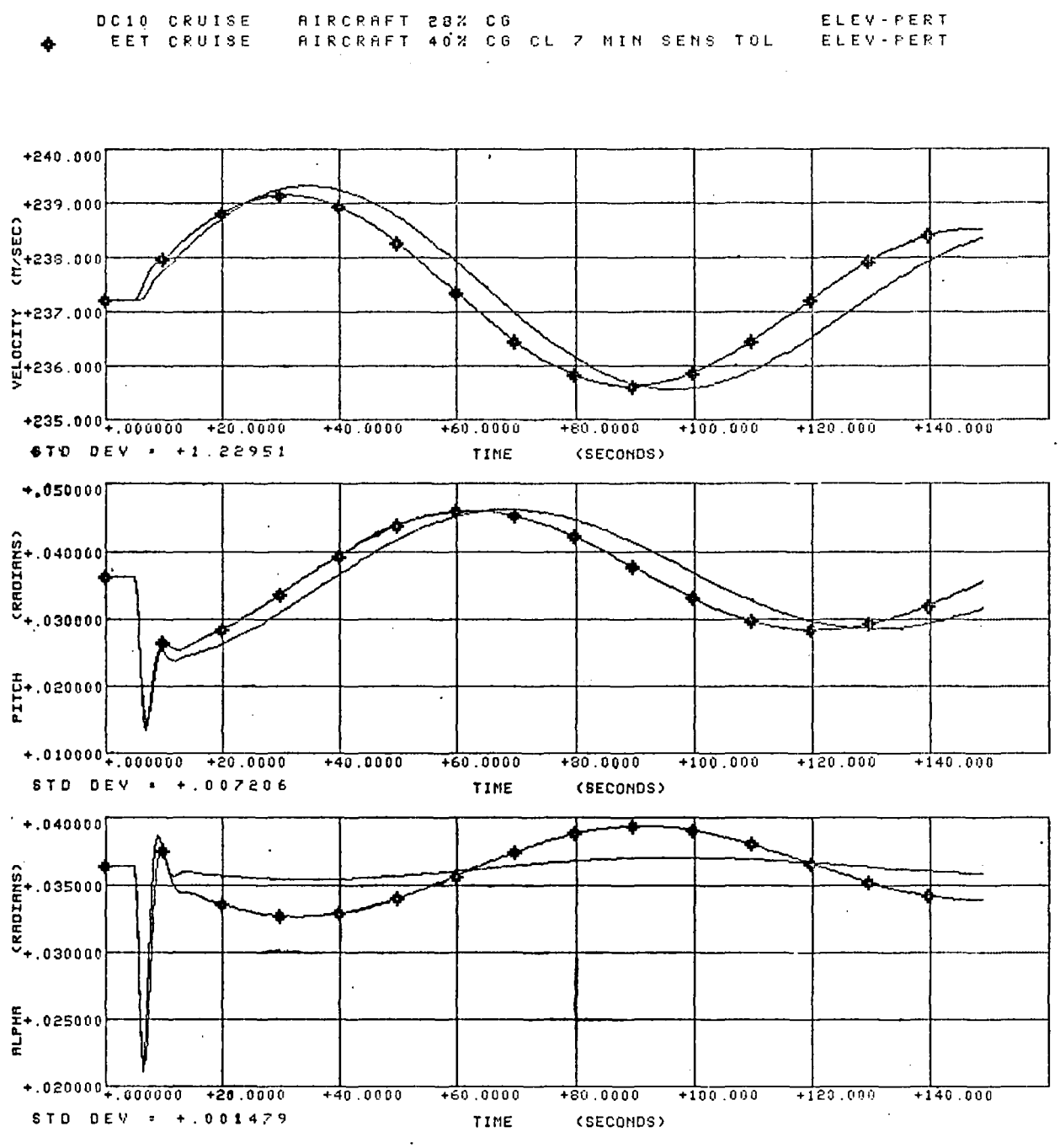

SENSOR TOLERANCE

APPENDIX 10
ADDITIONAL PROPOSED AUGMENTATION FUNCTION

This section contains diagrams of other augmentation functions proposed for integration with RSSAS into the Flight Augmentation Computer, as discussed in Section 6. These functions include Yaw Damping, Turn Coordination, Elevator Load Feel Programming, Flap Limiting, and Stall Warning. The figures shown describe the existing DC-10 system architectures.

YAW DAMPER INTERFACE TABLE

A. Inputs

Analog

2	Yaw Rate	DC
2	Roll Attitude	AC
2	Rudder Position	AC
2	T-Valve Position	AC

29 VDC

2	VG Valid
2	Land Interlock
2	On Ground
1	Inoperative
3	YRG BITE
2	Overhead Test

Digital

2	MACH (ADC)
1	Maintenance

B. Outputs

2	T-Valve Command
7	YRG BITE
2	Engage
6	Overhead Test
2	Engage Interlock
1	Inter-Computer

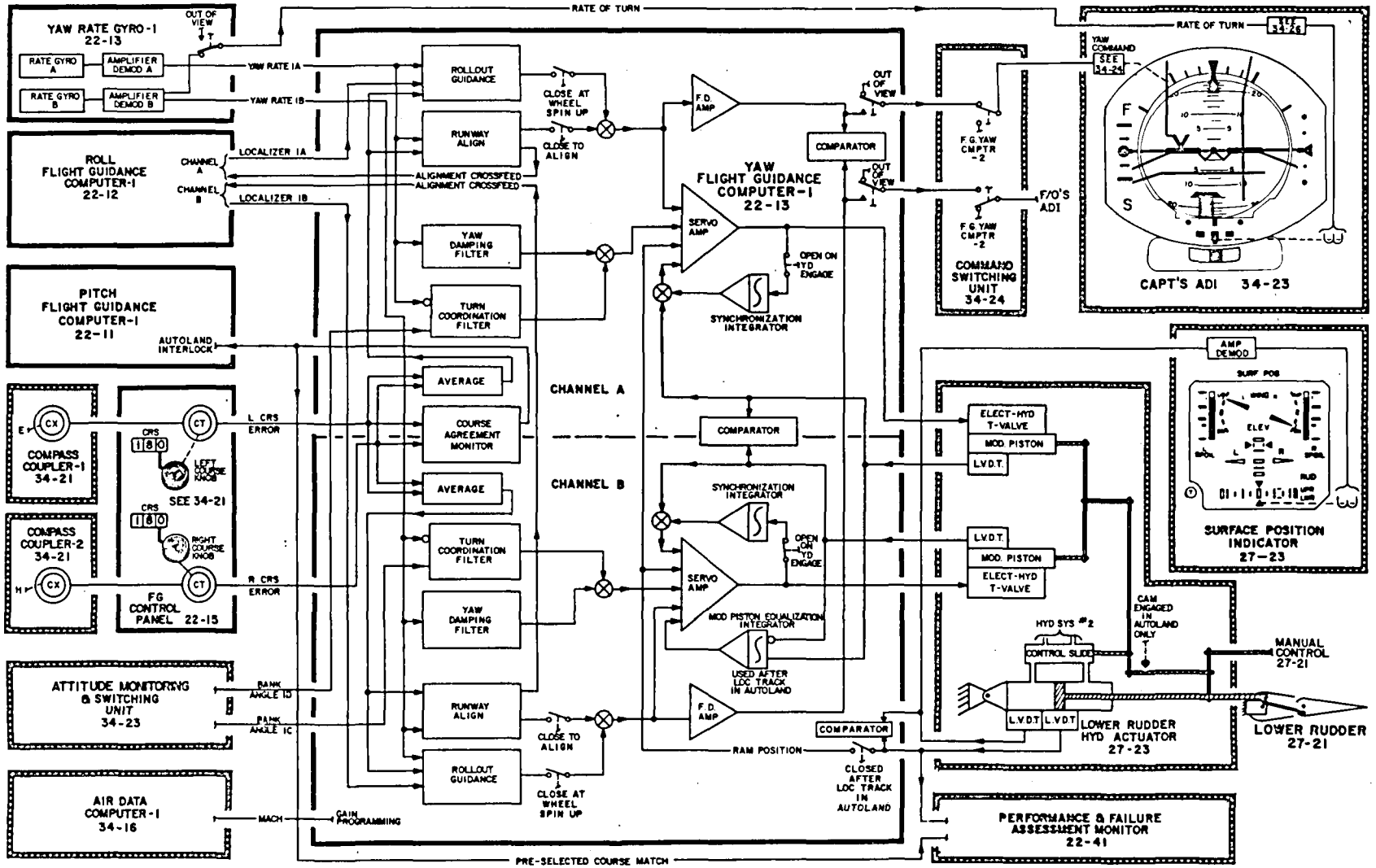

SIMPLIFIED SYSTEM SCHEMATIC – AUTOPILOT YAW AXIS

ELF/FL INTERFACE TABLE

A. Inputs		B. Outputs
Analog		
4 Tach FB	AC	
2 Position FB	AC	
28 VDC		
		2 Monitor
		2 Warning Lights
Digital		
2 Airspeed (ADC)		1 Inter-Computer
1 Maintenance		
Power Servo		
		2 Actuator

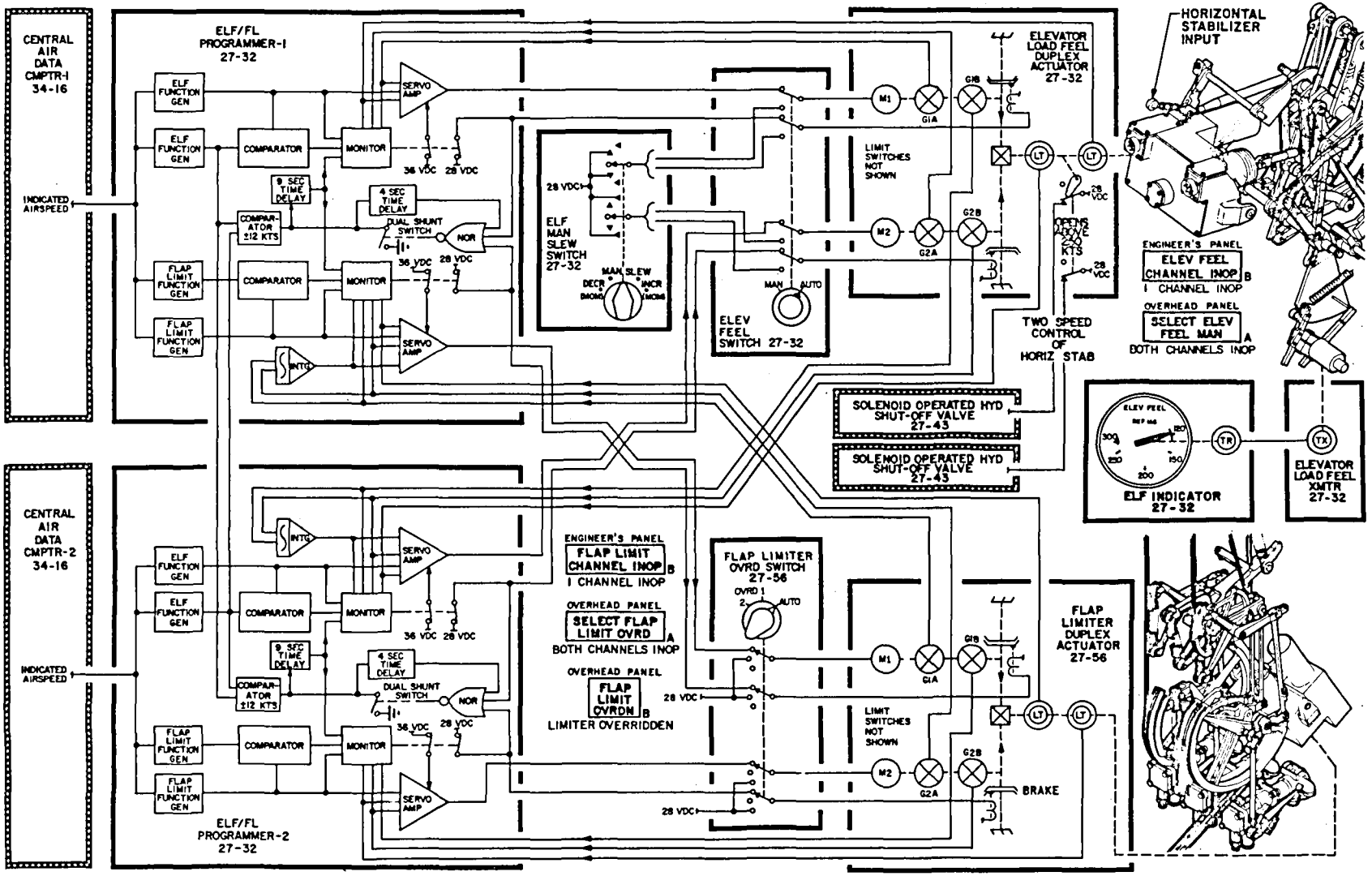

SIMPLIFIED SYSTEM SCHEMATIC – ELEVATOR VARIABLE LOAD FEEL AND FLAP LIMITER PROGRAMMER

STALL WARNING INTERFACE TABLE

A. Inputs

Analog

2 Angle of Attack	AC
1 Flaps	AC

28 VDC

2 Slats
2 AOA Valid
1 On Ground

Digital

1 Maintenance

B. Outputs

1 Slat
2 Stick Shaker
2 ADA Test
2 SW Test Overhead
1 Slat Test

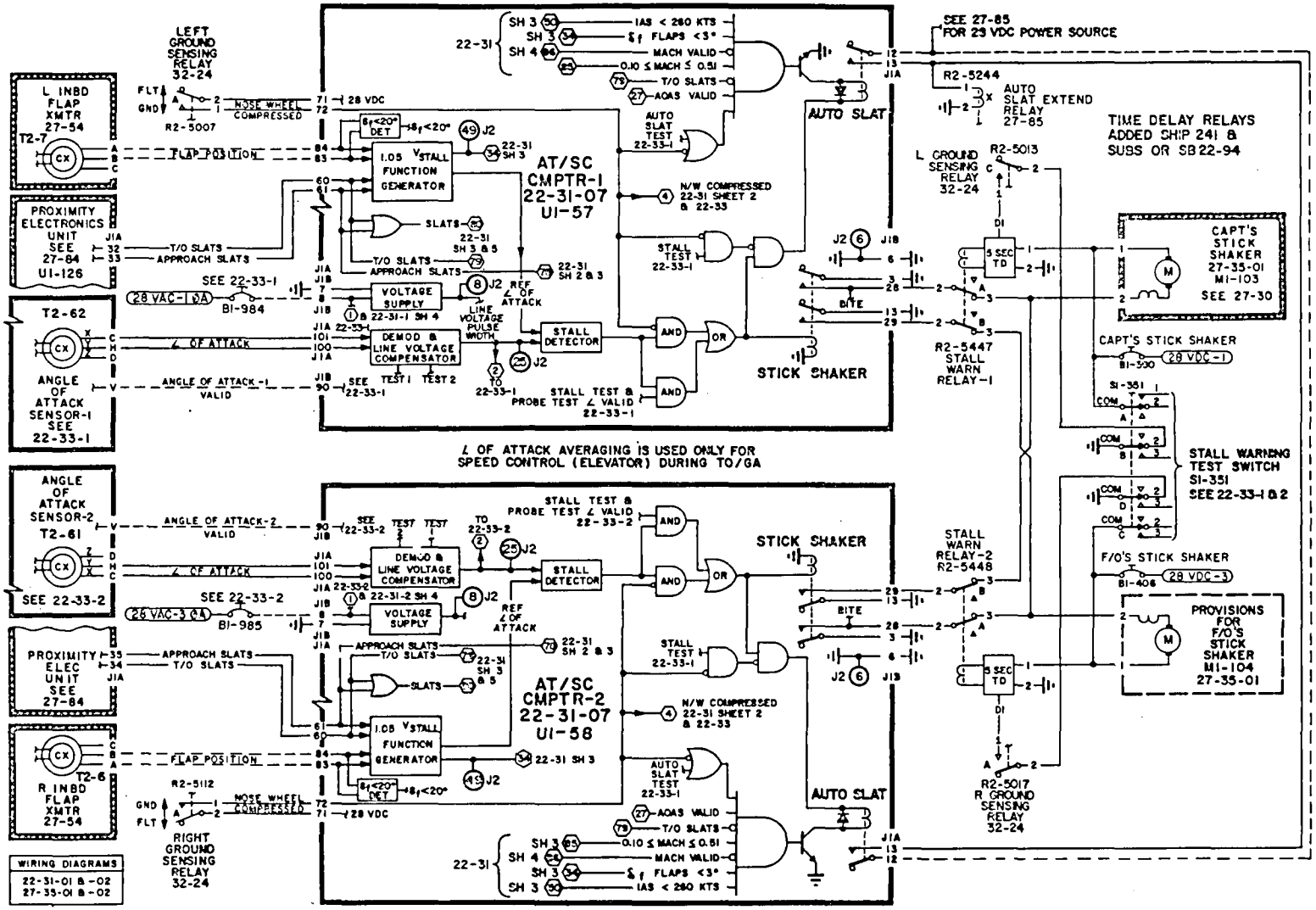

SYSTEM SCHEMATIC – STALL WARNING

APPENDIX 11
EET ELECTRICAL SYSTEM

The primary power system for the EET is a two-generator, 115/200-volt (at point of regulation in the electric power center), 3-phase (4-wire, grounded neutral), 400-Hz alternating current system. The two generators, one on each engine, are supplemented by an identical generator on the APU which is both ground and flight-operable. The main engine channels may be operated paralleled, unparalleled, or isolated. The system also provides emergency power, supplied by an air-driven generator and a battery. The APU generator or the external power supply is never paralleled with the main generators, or with each other. A 28-volt dc supply is derived from the ac system by transformer/rectifiers (see electrical system schematic).

The airplane can be dispatched with one main generator channel inoperative, providing the APU generator channel is operative.

The airplane can be dispatched with any one transformer/rectifier unit (except T/R-2) inoperative.

No single fault can cause the loss of more than one generator channel.

AC System Description

The EET derives its electrical power from 90-kva, 120/208-volt, 3-phase, 400-Hz, wye-connected brushless generators. The neutral of the wye connection is grounded to the airplane structure in each case.

The two main ac generating channels of the basic system are designed to operate equally well paralleled, unparalleled, or isolated. Design prevents these channels from being paralleled with the external ground supply or the APU generator.

The ac bus system is configured so that each main generator is connected through a generator relay to its own generator ac bus. The generator buses are used as load distribution buses for heavy 3-phase loads, including the ac buses and the emergency ac buses on the No. 1 and No. 2 systems. The ac buses are then used as load distribution buses for light 3-phase loads and single-phase loads.

Two bus tie relays, one for each main generator channel, are configured so that they connect the two generator buses through an ac tie bus. Both relays are closed during paralleled operation. Flight crew controls permit the bus tie

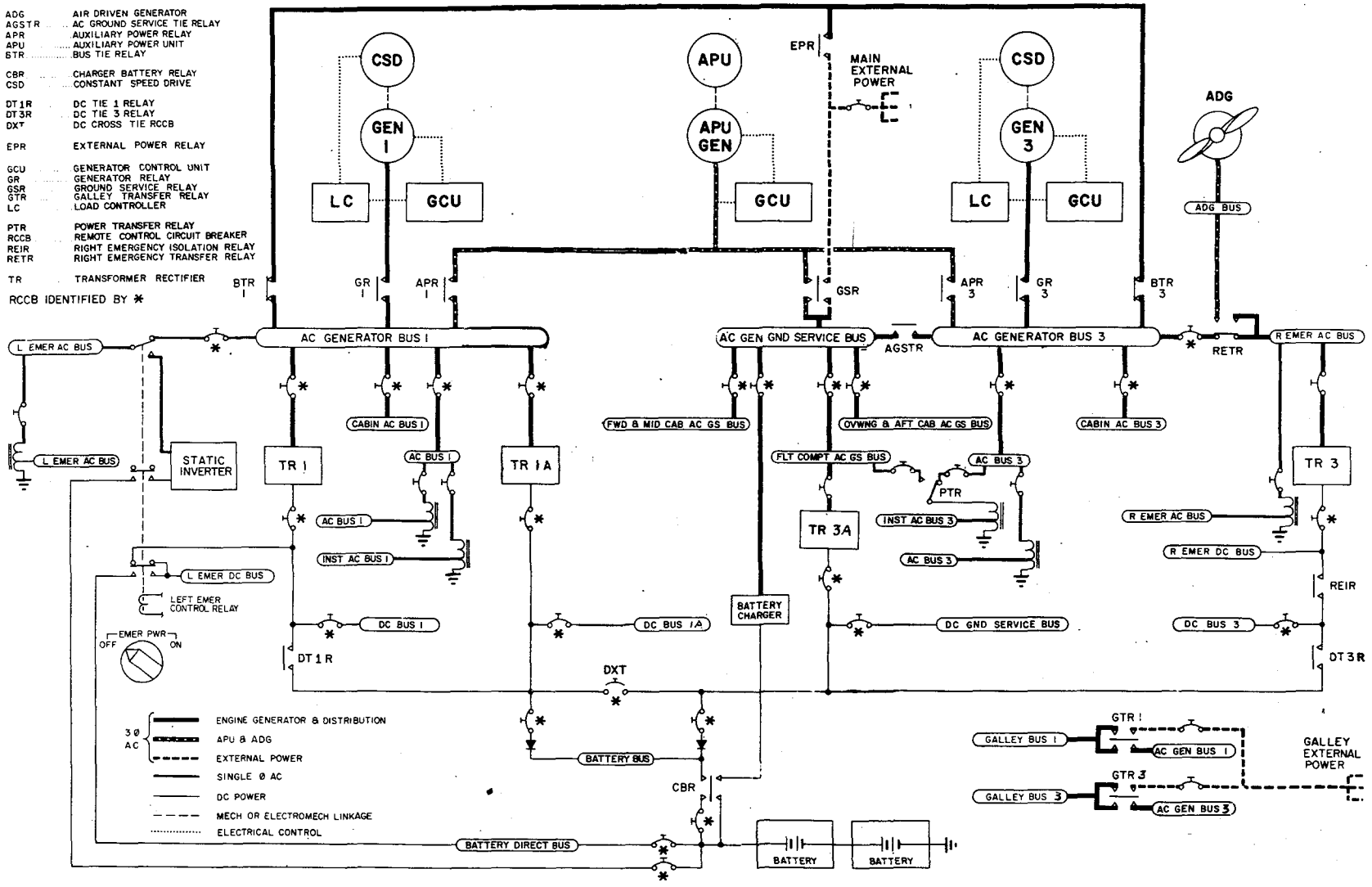

PR6-DC10-11111

EET ELECTRICAL SYSTEM

relays to be individually opened manually, thus isolating the two distribution systems.

Automatic circuits, when initiated by flight crew action, will parallel the two primary channels if system conditions are proper. If unparalleled operation is desired at startup, no action is required by the flight crew. If isolated operation is required, the bus tie relays can be manually switched open by the flight crew.

Auxiliary Power

Auxiliary power, derived from the generator driven directly by the onboard APU (located in the unpressurized portion of the aft fuselage), can be used to supplement the main system supply. The control arrangement allows connection of the APU generator output to a choice of one or both of the main distribution bus systems, or to the ac generator ground service bus only, without energizing any other ac bus.

DC System Description

The dc electrical power is derived from the ac system through four unregulated transformer/rectifier (T/R) units. Each unit is convection-cooled with a capacity of 75 amperes. The No. 1 and the No. 1A T/Rs receive power from the No. 1 generator bus. The No. 2 T/R receives power from the right ac emergency bus. The No. 2A T/R receives power from the ac generator ground service bus. Accordingly, during ground service operation, only the No. 2A T/R unit is energized. This provides power to the dc ground service bus and through a blocking diode to the battery bus. The four transformer/rectifier units are normally operated isolated, but can pick up another dc load bus through the manually controlled tie relays and cross-tie circuit breaker. Redundant power is provided to the battery bus from the No. 1A T/R. Blocking diodes are installed for power source isolation and to prevent the battery from supplying power to dc buses.

Electrical System Fault Tree

A fault tree for the loss of electrical power is shown in the following figure. The initial configuration assumed is for dual generators without an APU. The calculated probability of electrical power loss is shown to be $Q = 2.6 \times 10^{-8}$.

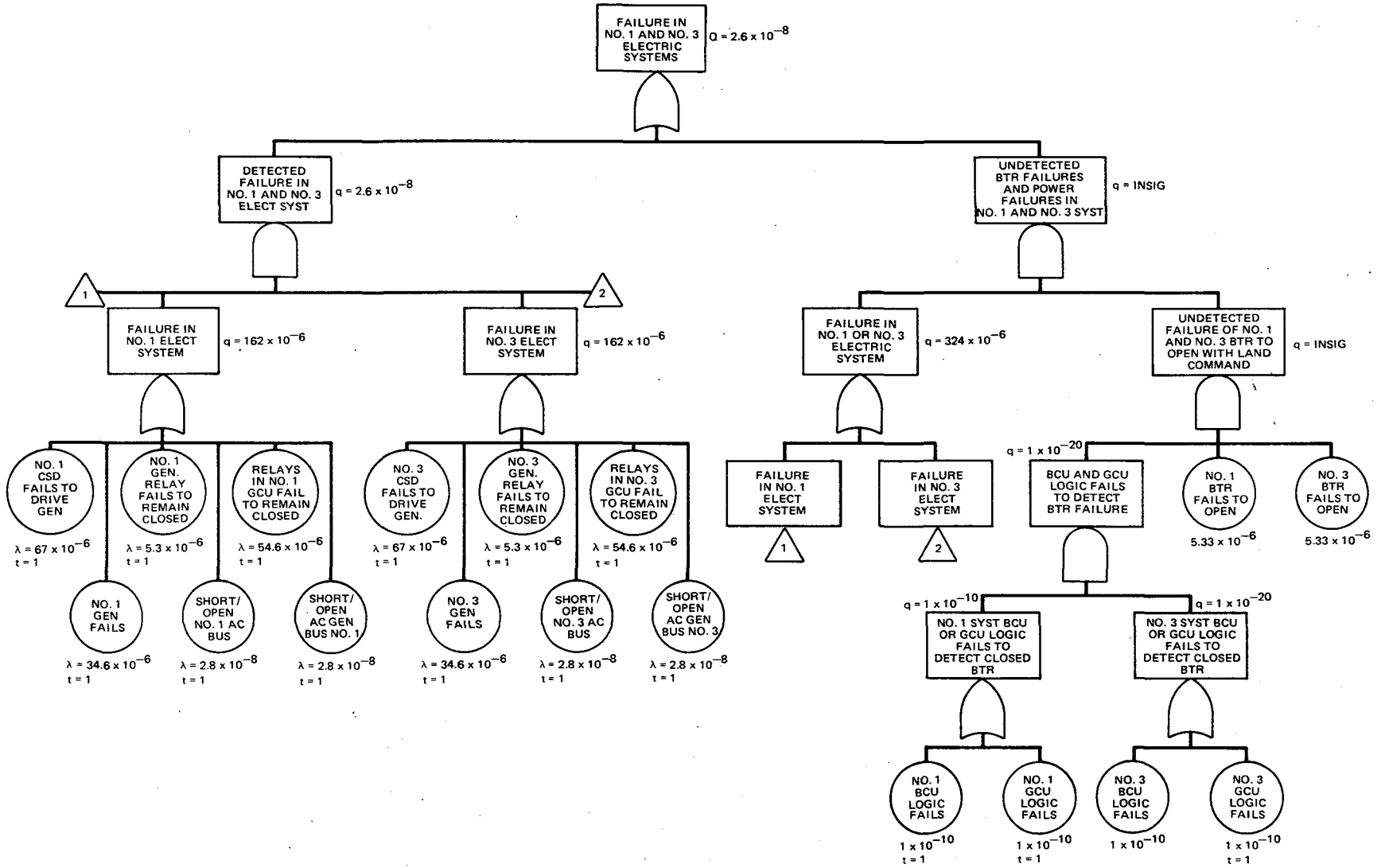

ELECTRICAL POWER FAULT TREE

1. Report No.	2. Government Accession No.	3. Recipient's Catalog No.
NASA CR-159166		

4. Title and Subtitle	5. Report Date
Development of a Low-Risk Augmentation System for an Energy-Efficient Transport Having Relaxed Static Stability	December 1979
	6. Performing Organization Code

7. Author(s)	8. Performing Organization Report No.
T. R. Sizlo, R. A. Berg, and D. L. Gilles	ACEE-06-FR-9679 (Rev. 10-79)
	10. Work Unit No.

9. Performing Organization Name and Address	11. Contract or Grant No.
Douglas Aircraft Company McDonnell Douglas Corporation 3855 Lakewood Boulevard Long Beach, California 90846	NAS1-14744
	13. Type of Report and Period Covered
12. Sponsoring Agency Name and Address	Contractor Report
National Aeronautics and Space Administration Washington, D.C. 20546	14. Army Project No.

15. Supplementary Notes

Project TRCO, D. L. Maiden, Energy-Efficient Transport Project
NASA Langley Research Center, Hampton, Virginia 23665

16. Abstract

This report describes the development of an augmentation system for a 230-passenger, twin-engine aircraft designed with a relaxation of conventional longitudinal static stability. The design criteria are established and candidate augmentation system control laws and hardware architectures are formulated and evaluated with respect to reliability, flying qualities, and flightpath tracking performance. The selected systems are shown to satisfy the interpreted regulatory safety and reliability requirements while maintaining the present DC-10 (study baseline) level of maintainability and reliability for the total flight control system. The impact of certification of the relaxed static stability augmentation concept is also estimated with regard to affected federal regulations, system validation plan, and typical development/installation costs.

17. Key Words (Suggested by Author(s))		18. Distribution Statement
Active Controls Flight Controls Flying Qualities	Relaxed Static Stability System Architecture Stability and Control	FEDD Distribution

19. Security Classif. (of this report)	20. Security Classif. (of this page)	21. No. of Pages	22. Price*
Unclassified	Unclassified	335	

* Available: NASA's Industrial Applications Centers